

Centre Eau Terre Environnement

**NOUVELLE APPROCHE DE PRÉTRAITEMENT DES BIOMASSES
LIGNOCELLULOSIQUES COMBINANT EXTRUSION ET BIODÉLIGNIFICATION
POUR AUGMENTER LA DIGESTIBILITÉ ENZYMATIQUE**

**NOVEL APPROACH OF LIGNOCELLULOSIC BIOMASS PRETREATMENT
COMBINING EXTRUSION AND BIODELIGNIFICATION TO INCREASE ENZYMATIC
DIGESTIBILITY**

Par

Béhibro Ange-Delon Konan

Thèse présentée pour l'obtention du grade de
Philosophiae Doctor (Ph.D.)
en sciences de l'eau

Jury d'évaluation

Président du jury et
examineur interne

Jean-François Blais
Centre Eau-Terre-Environnement (ETE)
Institut National de la Recherche Scientifique (INRS)

Examinatrice externe

Mariya Marinova
Department of Chemistry and Chemical Engineering
Royal Military College of Canada

Examineur externe

François Brouillette
Département de biochimie, chimie, physique et science forensique
Université du Québec à Trois-Rivières (UQTR)

Directeur de recherche

Kokou Adjallé
Centre Eau-Terre-Environnement (ETE)
Institut National de la Recherche Scientifique (INRS)

Co-directeur de recherche

Denis Rodrigue
Département de génie chimique
Université Laval (ULaval)

Co-directeur de recherche

Saïd Elkoun
Département de génie mécanique
Université de Sherbrooke (UdS)

REMERCIEMENTS

Le doctorat est une entreprise éprouvante, qui peut vite devenir très périlleuse pour des milliers de raisons possibles. Dans mon cas, ce fut une excellente expérience grâce au concours de plusieurs personnes clés que je voudrais prendre le temps de remercier ici. Habituellement, la section des remerciements c'est un peu du *free-style*. En fait, c'est le seul endroit de toute la thèse (plus de 200 pages) où l'on peut s'exprimer *normalement*, sans chiffres ni tests statistiques, et même avec des points d'exclamation ! Toutefois, compte tenu de la qualité des soutiens dont j'ai été l'objet tout au long de ma thèse, je voudrais garder un ton solennel, au moins jusqu'à l'avant-dernière phrase.

Je tiens à exprimer toute ma reconnaissance à mon Directeur de thèse, **Prof. Kokou Adjallé**. Les mots, si sophistiqués soient-ils, ne sauraient être à la hauteur pour exprimer ma profonde gratitude envers vous. Plus qu'un excellent directeur de thèse, vous avez été pour moi un mentor, un modèle d'excellence à suivre. Vous m'avez accordé votre confiance, formé à la recherche scientifique, ouvert de nombreuses opportunités, soutenu de plusieurs manières, encouragé, rassuré, etc. Je garde précieusement encore toute la sagesse de vos conseils. Si c'était à refaire, je referais le doctorat sous votre supervision. L'atmosphère de travail dans l'équipe est très agréable. Le bien fait à autrui n'étant jamais perdu, je vous souhaite tout le meilleur dans votre carrière et pour votre famille. Merci encore pour cette opportunité que vous m'avez offerte au sein de votre équipe de recherche.

Je voudrais remercier également mes co-directeurs. **Prof. Denis Rodrigue**, vous m'avez initié à l'utilisation des extrudeuses, à la fabrication de matériaux composites et au test de leurs propriétés. J'étais fasciné de voir tout ce qu'on peut fabriquer comme matériaux composites avec des résidus de biomasse. J'ai aussi beaucoup apprécié votre promptitude et votre méticulosité quant à la correction des articles que je vous soumettais. Votre collaboration fut d'une aide précieuse. **Prof. Saïd Elkoun**, vous m'avez accordé votre confiance et m'avez grandement ouvert votre laboratoire. Durant mon séjour à Sherbrooke, vous m'avez accueilli chaleureusement, accordé un bureau où travailler et aménagé un espace pour que j'utilise la mini-extrudeuse dans les meilleures conditions. Malgré votre horaire chargé, vous passiez régulièrement me voir au laboratoire pour discuter un peu, ou me téléphoniez pour savoir si je manquais de quelque chose et si tout se passait comme je voulais. Ce fut une excellente expérience. J'ai beaucoup appris du domaine des matériaux auprès de vous, de votre équipe et de celle du **Prof. Mathieu Robert**. Je voudrais aussi remercier **Prof. Koffi Ekoun** qui m'a

ouvert la voie pour le doctorat au Canada. Vous m'avez recruté dans votre équipe à l'Institut National Polytechnique Houphouët Boigny (INPHB). Vous m'avez ensuite apporté sans réserve votre soutien et avez donné toutes les autorisations nécessaires quand cette opportunité s'est offerte à moi.

Dr. Adana Ndao, je souhaite t'exprimer ma reconnaissance pour tout le soutien technique et moral que tu m'as apporté. Tu m'as fait gagner du temps précieux à maintes et maintes reprises par ton expérience et ta perspicacité. Il est inutile de mentionner que j'ai beaucoup apprécié de travailler avec toi. Je revois encore avec beaucoup de gratitude les temps de discussion avec toi sur divers sujets, dont la science, l'économie et la politique.

Je tiens également à remercier **Prof. Jean-François Blais**, **Prof. Mariya Marinova** et **Prof. François Brouillette** pour avoir accepté volontiers d'évaluer et corriger ce travail en tant que membres du jury d'évaluation. Merci beaucoup pour vos précieuses corrections, suggestions et commentaires.

Je voudrais adresser des remerciements spéciaux à mon père, **M. Kouassi Konan**, à ma mère **Mme Kouassi Alice**, à **Nova-Reine** ma petite sœur, à **Mickael** mon petit frère, à **Maryline** ma cousine et **M. Yoboué Serge**, mon oncle. Papa et maman, grâce à votre grande sagesse, j'ai passé 4 années à faire ce doctorat sans que jamais, pas même une seule fois, je n'ai été en souci ou stressé pour quelques raisons familiales que ce soit. Au contraire, vous m'avez encouragé, prié pour moi et soutenu dans toutes les difficultés par lesquelles je suis passé durant ces années. Cette thèse est sans aucun doute aussi la vôtre.

Tous mes remerciements aux membres de l'équipe de recherche avec qui j'ai pris plaisir à travailler (Daphné Brodeur, Linh Nguyen, Bennani Ghita, Danielle Niang, Soumaya Hammami, Ida Diribissakou, Mariya Malek et Azam Amini). Merci également au personnel du Laboratoire de Biotechnologie Environnementale du Labo Lourd (Dr Mathieu, Kevin, Marie-Kim, Amélie et François). Je ne saurais clore les remerciements sans adresser de vifs remerciements : (i) au personnel administratif de l'INRS et du Centre ETE avec lesquels j'ai collaboré dans le cadre des fonctions étudiantes que j'ai occupées, (ii) à tout le personnel technique des laboratoires de l'INRS, à tous les étudiants avec qui j'ai travaillé lors de mes mandats à la Fédération des Étudiants de l'INRS (FEINRS) et au Journal La Synthèse (JLS), ainsi qu'à tous mes amis et amies de l'INRS et en dehors. Souffrez que je ne vous nomme pas individuellement, la liste serait longue et je risquerais de me faire rappeler à l'ordre pour avoir pris plus de deux pages pour les remerciements ! Bon, j'arrête ici ; mais pour ceux que j'ai omis, je vous remercierai quand on se verra ! ☺

AVANT-PROPOS

Ce manuscrit présente les travaux de recherche réalisés en vue de l'obtention du grade de ***Philosophiae Doctor (Ph.D.)***. Il relève du domaine des **Biotechnologies** et s'inscrit dans le programme de doctorat en Sciences de l'Eau de l'Institut National de la Recherche Scientifique (Canada). Les travaux de recherche ont consisté à développer une approche novatrice de prétraitement des biomasses lignocellulosiques pour augmenter leur digestibilité enzymatique. Cette thèse est organisée en 9 chapitres, dont 6 articles. Les chapitres sont consécutivement liés les uns aux autres.

Le **chapitre 1** est une introduction générale du sujet de thèse. Dans un premier temps, ce chapitre présente le contexte du sujet, explore les technologies de prétraitement, puis débouche sur l'identification de l'extrusion et de la biodégradation comme des technologies prometteuses de prétraitement des biomasses lignocellulosiques. Dans un second temps, ce chapitre présente la problématique, les hypothèses et les objectifs de cette étude.

Le **chapitre 2** est consacré à la méthodologie générale qui a conduit à la réalisation des travaux de cette thèse.

Le **chapitre 3** (Article 1) répond à l'objectif 1. Il explore l'extrusion comme méthode de prétraitement des biomasses lignocellulosiques pour en identifier le potentiel, les paramètres de prétraitement et les relations qui existent entre eux.

Le **chapitre 4** (Article 2) répond à l'objectif 2. Il identifie et analyse les couplages de prétraitement existants et impliquant l'extrusion, afin de proposer une approche novatrice et adaptée de prétraitement au regard des résultats de cette analyse.

Le **chapitre 5** (Article 3) répond à l'objectif 3. Il explore la biodégradation par fermentation solide en tant que méthode de prétraitement des biomasses lignocellulosiques afin d'identifier son potentiel, les agents biologiques susceptibles de performer, les conditions de prétraitement et la compatibilité de cette technologie avec l'extrusion.

Le **chapitre 6** (Article 4) répond à l'objectif 4. Il consiste à analyser et optimiser les paramètres de prétraitement de deux biomasses lignocellulosiques (un résidu agricole et un résidu forestier) par extrusion pour enlever une fraction de lignine tout en réduisant la rigidité de leur structure sans générer d'inhibiteurs.

Le **chapitre 7** (Article 5) répond aux objectifs 5 et 6. Il consiste à analyser et optimiser les conditions de biodégradation par fermentation solide de deux biomasses lignocellulosiques prétraitées par extrusion, afin d'augmenter la digestibilité enzymatique de ces biomasses.

Le **chapitre 8** (Article 6) répond à l'objectif 7. Il consiste à effectuer une analyse technico-économique préliminaire afin d'identifier le potentiel et les conditions de rentabilité de l'approche de combinaison des deux prétraitements développés.

Le **chapitre 9** est consacré à la discussion générale de tous les travaux réalisés dans le cadre de cette thèse. Ce chapitre s'achève par des recommandations pour de futurs travaux.

PARCOURS HIVER 2021 – HIVER 2025

PRODUCTION SCIENTIFIQUE

ARTICLE DANS LA THÈSE (6)

1. **Konan, D.**, Koffi, E., Ndao, A., Peterson, E. C., Rodrigue, D., & Adjallé, K. (2022). An Overview of Extrusion as a Pretreatment Method of Lignocellulosic Biomass (review). *Energies*, 15(9), 3002. <https://doi.org/10.3390/en15093002> (Publié)
2. **Konan, D.**, Rodrigue, D., Koffi, E., Elkoun, S., Ndao, A., & Adjallé, K. (2024). Combination of Technologies for Biomass Pretreatment: A Focus on Extrusion (review). *Waste and Biomass Valorization*, 1-22. <https://doi.org/10.1007/s12649-024-02472-w> (Publié)
3. **Konan, D.**, Ndao, A., Koffi, E., Elkoun, S., Robert, M., Rodrigue, D., & Adjallé, K. (2024). Biodecomposition with *Phanerochaete chrysosporium*: A review. *AIMS Microbiology*, 10(4), 1068. <https://doi.org/10.3934/microbiol.2024046> (Publié)
4. **Konan, D.**, Ndao, A., Koffi, E., Elkoun, S., Robert, M., Rodrigue, D., & Adjallé, K. (2025). Optimization of Biomass Delignification by Extrusion and Analysis of Extrudate Characteristics. *Waste*, 3(2), 12. <https://doi.org/10.3390/waste3020012> (Publié)
5. **Konan, D.**, Ndao, A., Koffi, E., Elkoun, S., Robert, M., Rodrigue, D., & Adjallé, K. (2025). Extrusion-Biodelignification Approach for Biomass Pretreatment. *Waste*, 3(3), 21. <https://doi.org/10.3390/waste3030021>.
6. **Konan, D.**, Ndao, A., Koffi, E., Elkoun, S., Robert, M., Rodrigue, D., & Adjallé, K. (2025). Technico-economic analysis of a novel pretreatment approach for a large-scale production of second-generation bioethanol. (En rédaction)

ARTICLES HORS-THÈSE (2)

7. Bennani, G., Ndao, A., **Konan, D.**, Brassard, P., Le Roux, É., Godbout, S., & Adjallé, K. (2023). Valorisation of Cranberry Residues through Pyrolysis and Membrane Filtration for the Production of Value-Added Agricultural Products. *Energies*, 16(23), 7774. <https://doi.org/10.3390/en16237774>
8. Ndao, A., Bennani, G., **Konan, D.**, Diop, A., & Adjallé, K. (2025). Production and Valorization of Acetic Acid from Lignocellulosic Biomass Pyrolysis: Influence of Operational Conditions and Membrane Separation Processes. *Sustainable Chemistry for the Environment*, 100268. <https://doi.org/10.1016/j.scenv.2025.100268>

AUTRES (2)

9. **Poster : Konan, D.**, Ndao, A., Rodrigue, D., Koffi, E., Elkoun, S., & Adjallé, K. Nouvelle approche de prétraitement des résidus de biomasse pour la production de composés à

hautes valeurs ajoutées. [2022](#). 36ème symposium de l'est du Canada sur la recherche sur la qualité de l'eau.

10. **Article de vulgarisation scientifique** : Konan D., et Adjallé K. [2025](#). Le casse-tête des résidus agricoles et forestiers. *Journal La Synthèse*.

SERVICES À LA COMMUNAUTÉ ET ENGAGEMENTS

1. INRS - Institut National de la Recherche Scientifique
Ambassadeur ([2023](#))
2. Journal la Synthèse – Journal étudiant de vulgarisation scientifique
Président ([2024 – 2025](#))
3. Journal la Synthèse – Journal étudiant de vulgarisation scientifique
Éditeur en chef ([2023 – 2024](#))
4. FEINRS - Fédération des Étudiants de l'Institut National de la Recherche Scientifique
Président ([2022 – 2023](#))
5. FEINRS - Fédération des Étudiants de l'Institut National de la Recherche Scientifique
Secrétaire ([2021 – 2022](#))
6. Colloque Étudiant 2023 du CRIBIQ - Consortium de recherche et innovations en bioprocédés industriels au Québec
Co-organisateur de colloque scientifique ([2023](#))
7. Projet CRFQ - Cartographie des Résidus Fermentescible du Québec
Développeur de cartographie interactive en ligne ([2023](#), [2025](#))
8. Pôle Géoscientifique du Québec (PGQ)
Développeur du site web ([2023](#), [2025](#))
9. CINÉIAG - Consortium intersectoriel en écologie industrielle et agroalimentaire
Développeur du site web ([2025](#))

BOURSES ET CONFÉRENCES

1. Bourse d'excellence en reconnaissance de l'implication étudiante ([2024](#))
Programme des ambassadeurs de l'INRS
Québec, Qc, Canada.
2. Bourse de séjour - PRISM ([2024](#))
PRISM – Stanford Postdoctoral Recruitment Initiative in Sciences and Medicine
Stanford University, CA, USA.

3. Bourse de voyage TD Assurance pour participation à une conférence (2023)
TD Assurance
Massachusetts Institute of Technology (MIT) - Woods Hole Oceanographic Institution (WHOI)
Falmouth, MA, USA.
4. Présentation orale (2023)
A novel approach to lignocellulosic biomass pretreatment for biofuel production.
World Congress of Smart Materials 2023
Barcelone, Espagne.
5. Présentation d'affiche scientifique (2022)
Nouvelle approche de prétraitement des résidus de biomasse pour la production de composés à hautes valeurs ajoutées.
36ème symposium de l'est du Canada sur la recherche sur la qualité de l'eau
Québec, QC, Canada.
6. Bourse de développement web (2024)
Pôle Géoscientifique du Québec (PGQ)
Québec, QC, Canada.
7. Bourse de formation à l'entrepreneuriat scientifique (2023)
Programme QcES – V1 Studio
Québec, QC, Canada.

RÉSUMÉ

On estime à 181 milliards de tonnes, la quantité globale de biomasses lignocellulosiques disponible chaque année et prête à être valorisée. Cependant, cette biomasse est sous-exploitée du fait de la difficulté à retirer la lignine du complexe lignocellulosique, afin de récupérer les composés d'intérêt (cellulose et hémicellulose). Cette thèse a eu pour objectif de développer une approche novatrice de prétraitement des biomasses lignocellulosiques. Il s'agissait d'un couplage séquentiel de deux technologies prometteuses : l'extrusion (Ex) et la biodégradation (SSF). L'approche Ex-SSF a été développée sur des résidus de maïs (RMA) et sur des résidus d'épinette noire (REN).

L'étape d'extrusion s'est faite avec une extrudeuse bis-vis de 11 mm de diamètre. Les résultats ont montré qu'en optimisant les conditions d'extrusion par analyse de surfaces de réponse (RSA), les taux de dégradation étaient significativement améliorés. Les taux augmentaient de 2,3 % à 27,4 % pour les RMA, ainsi que de 1 % à 25,3 % pour les REN. Les taux de dégradation étaient reproductibles à $\pm 1,2$ %. Les deux modèles d'optimisation développés étaient capables de prédire les résultats de dégradation avec une précision de 0,8 % pour les RMA et de 3 % pour les REN. Les températures d'extrusions optimisées étaient relativement faibles, soit 50°C (REN) et 65°C (RMA). De plus, l'analyse des caractéristiques des extrudats a montré une réduction significative de la taille des particules, de 1 mm à 55 μm pour les REN, ainsi que de 1 mm à 204 μm pour les RMA. Quant à la surface spécifique des extrudats, on a enregistré une augmentation de 4 fois la surface spécifique initiale des RMA (512 à 2402 cm^2/cm^3) et une augmentation de 50 % de celles des REN (399 à 597 cm^2/cm^3). De plus, les analyses GC/MS n'ont révélé aucun inhibiteur (furfural ou hydroxyméthylfurfural).

Ces extrudats ont ensuite été prétraités pour une deuxième fois par un procédé de fermentation solide pour enlever le reste de la lignine (biodégradation). La souche utilisée était *Phanerochaete chrysosporium*. Les résultats ont montré un maximum de 17 % de biodégradation avec les contrôles négatifs (fermentation avec les biomasses brutes) pour un taux de dégradation final de 65,4 % avec les RMA extrudés, ainsi que de 59,1 % avec les REN extrudées. La lignine peroxydase (LiP) était la principale enzyme responsable de la biodégradation dans les contrôles négatifs avec $53,7 \pm 2,7$ U/l (REN) et $16,4 \pm 0,8$ U/l (RMA), tandis que la manganèse peroxydase (MnP) était la principale enzyme responsable de la biodégradation dans les extrudats, avec 13,8 U/l pour les REN et 32,0 U/l pour les RMA. L'hydrolyse enzymatique des biomasses prétraitées à l'extrudeuse (Ex) et la fermentation solide (SSF) (Ex-SSF) a permis de récupérer

7,6 mg/l de sucre avec les REN, soit 2,3 fois la concentration de sucre obtenue avec les REN brutes. Quant aux RMA prétraités à l'Ex-SSF, on a récupéré 17,0 mg/l de sucre, ce qui représentait une amélioration de 44 % par rapport aux RMA bruts.

Ces résultats ont conduit à une analyse technico-économique de la production de bioéthanol de seconde génération (2G) intégrant le prétraitement Ex-SSF. Trois scénarios de départ ont été identifiés (S1, S2 et S3). Les coûts d'investissement (CAPEX) par tonne de biomasses étaient de 1154 \$/t pour S1, de 825 \$/t pour S2, et de 739 \$/t pour S3. Quant aux coûts d'exploitation (OPEX), ils étaient de 57,7 \$/t pour S1, de 41,3 \$/t pour S2 et de 151,6 \$/t pour S3. Ces résultats ont permis d'identifier les conditions minimales de rentabilité d'une bioraffinerie intégrant le prétraitement Ex-SSF. Dans le cas d'une exploitation agricole dans les conditions de S1, il s'agissait d'une capacité minimale de 2 458 tonnes de biomasses par an, soit l'équivalent de la production de résidus lignocellulosiques de 345 ha de culture de maïs. Dans le cas d'une association d'exploitants agricoles dans les conditions de S2, il s'agissait d'une capacité de 3 522 tonnes de biomasse par an, soit l'équivalent de la production de résidus lignocellulosiques de 495 ha de culture de maïs.

Mots-clés : Biomasse lignocellulosique, extrusion, fermentation, biodégradation, hydrolyse enzymatique, analyse technico-économique, prétraitement, enzymes lignolitiques, *Phanerochaete chrysosporium*, plans d'expériences, résidus de maïs, épinette noire.

ABSTRACT

It is estimated that 181 billion tonnes of lignocellulosic biomass are available each year, ready for valorization. However, this biomass is under-exploited due to the difficulty of removing lignin from the lignocellulosic complex to recover the compounds of interest (cellulose and hemicellulose). The aim of this thesis was to develop an innovative approach to biomass pretreatment. It is based on a sequential coupling of two promising technologies: extrusion (Ex), and biodelignification (SSF). The Ex-SSF approach was developed on corn stover (CS) and black spruce residues (BS).

Extrusion was carried out using an 11 mm diameter twin-screw extruder. The results showed that by optimizing the extrusion conditions using response surface analysis (RSA), delignification yields were significantly improved. The yields increased from 2.3% to 27.4% for CS, and from 1% to 25.3% for BS. Delignification yields were reproducible to within $\pm 1.2\%$. Both optimization models developed were able to predict delignification results with an accuracy of 0.8% for CS, and 3% for BS. The optimized extrusion temperatures were relatively low: around 50°C (BS) and 65°C (CS). In addition, analysis of the extrudate characteristics showed a significant reduction in particle size, from 1 mm to 55 μm for BS, and from 1 mm to 204 μm for CS. As for the specific surface area of the extrudates, a 4-fold increase was recorded for CS (512 to 2402 cm^2/cm^3), while a 50% increase was observed for BS (399 to 597 cm^2/cm^3). GC/MS analysis revealed no inhibitors (furfural and hydroxymethylfurfural).

The extrudates were then pretreated by fermentation. *Phanerochaete chrysosporium* was the strain selected. The results showed a maximum of 17% biodelignification with the negative controls (fermentation with raw biomass); while the yield was 65.4% with extruded CS, and 59.1% with extruded BS. Lignin peroxidase (LiP) was the main enzyme responsible for biodelignification in the negative controls with 53.7 ± 2.7 U/l (BS) and 16.4 ± 0.8 U/l (CS); while manganese peroxidase (MnP) was the main enzyme in the extrudates with 13.8 ± 0.7 U/l (BS) and 32.0 ± 0.7 U/l (CS). Enzymatic hydrolysis of extruded BS pretreated with Ex-SSF recovered 7.6 mg/l of sugar; i.e. 2.3 times the sugar concentration obtained with raw BS. As for CS pretreated with Ex-SSF, 17.0 mg/l of sugar was recovered which represents a 44% improvement over the raw CS.

These results led to a techno-economic analysis of 2G bioethanol production integrating Ex-SSF pretreatment. Three initial scenarios were identified (S1, S2 and S3). The capital expenditures (CAPEX) per tonne of biomass were 1154 \$/t for S1, 825 \$/t for S2, and 739 \$/t for S3. The operation expenditure (OPEX) were \$57.7/t for S1, \$41.3/t for S2 and \$151.6/t for S3. These

results led to the identification of the minimum conditions for the profitability of a biorefinery integrating Ex-SSF pretreatment. In the case of a farm under S1 conditions, the condition was a minimum capacity of 2,458 tonnes of biomass per year, equivalent to the production of lignocellulosic residues from 345 ha of corn crops. In the case of a farmers' association under S2 conditions, the condition was a capacity of 3,522 tonnes of biomass per year, equivalent to the production of lignocellulosic residues from 495 ha of corn crops.

Keywords: Lignocellulosic biomass, extrusion, fermentation, biodelignification, enzymatic hydrolysis, technol-economic analysis, pretreatment, lignolytic enzymes, *Phanerochaete chrysosporium*, experimental designs, corn stover, black spruce.

TABLE DES MATIÈRES

REMERCIEMENTS	I
AVANT-PROPOS	III
PARCOURS HIVER 2021 – HIVER 2025	V
RÉSUMÉ	VIII
ABSTRACT	XI
TABLE DES MATIÈRES	XIII
LISTE DES FIGURES.....	XXI
LISTE DES TABLEAUX.....	XXIII
MATÉRIEL SUPPLÉMENTAIRE.....	XXIV
APPENDICES.....	XXIV
LISTE DES ÉQUATIONS	XXV
LISTE DES ABRÉVIATIONS.....	XXVII
1 INTRODUCTION GÉNÉRALE	1
1.1 CONTEXTE	1
1.2 VALORISATION DES BIOMASSES LIGNOCELLULOSIQUES	3
1.2.1 <i>Voies de valorisation physique</i>	3
1.2.2 <i>Voies de valorisation chimique</i>	4
1.2.3 <i>Voies de valorisation biologique</i>	5
1.3 DÉFIS ET PERSPECTIVES DE VALORISATION DES BIOMASSES LIGNOCELLULOSIQUES	6
1.4 MÉTHODES DE PRÉTRAITEMENT DES BIOMASSES LIGNOCELLULOSIQUES.....	7
1.4.1 <i>Méthodes physiques</i>	7
1.4.2 <i>Méthodes chimiques</i>	8
1.4.3 <i>Méthodes physico-chimiques</i>	9
1.4.4 <i>Méthodes biologiques</i>	9
1.5 HYPOTHÈSES, OBJECTIFS ET ORIGINALITÉ.....	10
1.5.1 <i>Problématique</i>	10
1.5.2 <i>Originalité de la recherche</i>	11
1.5.3 <i>Hypothèses</i>	12
1.5.4 <i>Objectifs</i>	14
2 MATÉRIEL ET MÉTHODES	16
2.1 BIOMASSES.....	16
2.1.1 <i>Biomasses lignocellulosiques</i>	16
2.1.2 <i>Préparation des biomasses pour l'extrusion</i>	17

2.2	PLAN D'EXPÉRIENCE D'EXTRUSION	18
2.2.1	<i>Utilité des plans d'expériences</i>	18
2.2.2	<i>Choix du plan d'expérience</i>	19
2.3	EXTRUSION	21
2.3.1	<i>Mélange de biomasses et d'additif chimique</i>	21
2.3.2	<i>Conduite des extrusions</i>	22
2.3.3	<i>Lavage des extrudats</i>	23
2.4	CARACTÉRISATION DE LA BIOMASSE APRÈS L'EXTRUSION.....	24
2.4.1	<i>Taille des particules</i>	24
2.4.2	<i>Taux d'humidité de la biomasse</i>	24
2.4.3	<i>Composition de la biomasse et taux de délignification</i>	25
2.4.4	<i>Spectroscopie infrarouge à transformation de Fourier (FTIR)</i>	25
2.4.5	<i>Microscopie électronique à balayage (MEB)</i>	25
2.4.6	<i>Chromatographe en phase gazeuse/spectromètre de masse (GC/MS)</i>	26
2.5	BIODÉLIGNIFICATION	26
2.5.1	<i>Choix des souches</i>	26
2.5.2	<i>Culture des souches</i>	27
2.5.3	<i>Préparation des substrats</i>	27
2.5.4	<i>Préparation de l'inoculum</i>	27
2.5.5	<i>Conduite des fermentations</i>	28
2.5.6	<i>Centrifugation</i>	28
2.5.7	<i>Caractérisation des biomasses et taux de délignification</i>	28
2.6	HYDROLYSE ENZYMATIQUE	28
2.7	ANALYSE TECHNICO-ÉCONOMIQUE PRÉLIMINAIRE	29
3	PREMIER ARTICLE	30
3.1	ABSTRACT.....	31
3.2	GRAPHICAL ABSTRACT	32
3.3	INTRODUCTION	32
3.4	LIGNOCELLULOSIC BIOMASS	34
3.4.1	<i>Biomass composition</i>	34
3.4.2	<i>Crystallinity</i>	37
3.4.3	<i>Particle size</i>	39
3.4.4	<i>Morphology</i>	39
3.4.5	<i>Moisture</i>	40
3.4.6	<i>Biomass preparation before pretreatment</i>	40
3.5	EXTRUDER	42
3.5.1	<i>Screw type</i>	43

3.5.2	<i>Screw configuration</i>	45
3.5.3	<i>Screw elements</i>	46
3.5.4	<i>Forward screw element</i>	47
3.5.5	<i>Reverse screw element</i>	48
3.5.6	<i>Kneading element</i>	48
3.5.7	<i>Die Shape</i>	50
3.5.8	<i>Torque</i>	51
3.5.9	<i>Specific Mechanical Energy</i>	51
3.6	ADDITIVES.....	54
3.6.1	<i>Addition before extrusion</i>	54
3.6.2	<i>Addition during extrusion</i>	55
3.7	WORKING PARAMETERS	56
3.7.1	<i>Temperature</i>	56
3.7.2	<i>Residence Time</i>	57
3.7.3	<i>Screw Speed</i>	58
3.8	CHALLENGES, LIMITATIONS, AND FUTURE PROSPECTS	59
3.9	CONCLUSIONS.....	60
3.10	ACKNOWLEDGEMENT	61
4	DEUXIÈME ARTICLE	62
4.1	ABSTRACT.....	63
4.2	INTRODUCTION	64
4.3	PRETREATMENT TECHNOLOGIES	65
4.4	EXTRUSION PRETREATMENT.....	66
4.4.1	<i>Extrusion design and principle</i>	66
4.4.2	<i>Extrusion attractivity</i>	68
4.5	COMBINATION OF EXTRUSION WITH OTHER PRETREATMENTS	69
4.5.1	<i>Reactive extrusion</i>	69
4.5.2	<i>Alkaline extrusion</i>	69
4.5.3	<i>Bioextrusion</i>	70
4.5.4	<i>Extrusion and liquid hot water</i>	71
4.5.5	<i>Extrusion and steam explosion</i>	73
4.5.6	<i>Extrusion and ultrasonication</i>	75
4.5.7	<i>Extrusion and microwave</i>	77
4.5.8	<i>Extrusion and ionic liquid</i>	78
4.5.9	<i>Extrusion and deep eutectic solvent</i>	80
4.5.10	<i>Extrusion and organosolv/clean fractionation</i>	81
4.5.11	<i>Extrusion and ammonia fiber explosion</i>	83

4.6	SUMMARY OF EXTRUSION-BASED PRETREATMENT RESULTS	84
4.7	COMBINATION CHALLENGES	85
4.7.1	<i>Couplings optimization</i>	86
4.7.2	<i>Substrate supply</i>	86
4.7.3	<i>Energy consumption</i>	86
4.7.4	<i>Scaling up</i>	87
4.8	RECOMMENDATIONS	89
4.9	CONCLUSION.....	91
5	TROISIÈME ARTICLE	92
5.1	ABSTRACT.....	93
5.2	INTRODUCTION	94
5.3	CLASSIFICATION IN THE FUNGI KINGDOM	95
5.4	GENETIC IDENTITY	96
5.5	NATURAL HABITAT	98
5.6	ISOLATION TECHNIQUE AND NATURAL SUBSTRATE	99
5.7	ENZYMATIC SYSTEM.....	102
5.7.1	<i>Key enzyme</i>	102
5.7.2	<i>Manganese peroxidases</i>	103
5.7.3	<i>Lignin peroxidases</i>	104
5.7.4	<i>Laccases</i>	105
5.8	CULTURE IN SOLID FERMENTATION	106
5.8.1	<i>Inoculum preparation</i>	106
5.8.2	<i>Solid fermentation</i>	107
5.8.3	<i>Bioreactors</i>	108
5.8.4	<i>Solid state fermentation parameters</i>	112
5.9	APPLICATIONS	115
5.9.1	<i>Biodelignification</i>	117
5.9.2	<i>Decolorization</i>	118
5.9.3	<i>PAH Biomemediation</i>	119
5.9.4	<i>Production of ligninolytic enzymes</i>	120
5.10	PERSPECTIVES.....	121
5.11	CONCLUSION.....	122
5.12	ACKNOWLEDGEMENT	122
6	QUATRIÈME ARTICLE	123
6.1	ABSTRACT.....	124
6.2	INTRODUCTION	125
6.3	MATERIALS AND METHODS	127

6.3.1	<i>Raw biomasses and characterization</i>	127
6.3.2	<i>Parameter screening</i>	127
6.3.3	<i>Reactive extrusion</i>	127
6.3.4	<i>Experimental plan</i>	128
6.3.5	<i>Preparation of biomass</i>	130
6.3.6	<i>Moisture content</i>	131
6.3.7	<i>Particle size and specific surface</i>	131
6.3.8	<i>Delignification percentage</i>	131
6.3.9	<i>Optimization</i>	132
6.3.10	<i>Scanning Electron Microscopy (SEM)</i>	133
6.3.11	<i>Fourier Transformed Infrared Spectroscopy (FTIR) analysis</i>	133
6.3.12	<i>Gas chromatography/mass spectrometry (GC/MS)</i>	133
6.4	RESULTS AND DISCUSSION	133
6.4.1	<i>Biomass characteristics</i>	133
6.4.2	<i>Extrusion conditions</i>	135
6.4.3	<i>Extrudate characteristics</i>	138
6.4.4	<i>Statistical analysis</i>	141
6.4.5	<i>Effect of the parameters on delignification percentage</i>	145
6.4.6	<i>Response optimization</i>	147
6.4.7	<i>Effect of extrusion on the biomass structure</i>	149
6.4.8	<i>Energy consumption and pretreatment cost</i>	154
6.4.9	<i>Perspective for future work</i>	155
6.4.10	<i>Conclusion</i>	156
6.4.11	<i>Acknowledgement</i>	157
6.4.1	<i>Supplementary material</i>	157
6.4.2	<i>Appendixes</i>	158
7	CINQUIÈME ARTICLE	160
7.1	ABSTRACT	161
7.2	INTRODUCTION	162
7.3	MATERIALS AND METHODS	164
7.3.1	<i>Raw biomass</i>	164
7.3.2	<i>Extrusion</i>	164
7.3.3	<i>Substrate for semi solid fermentations</i>	165
7.3.4	<i>Fungal strains, inoculum and maintenance</i>	165
7.3.5	<i>Flask fermentations (250 ml)</i>	165
7.3.6	<i>Bioreactor fermentations (5 L glass tank)</i>	166
7.3.7	<i>Enzyme extraction</i>	167

7.3.8	<i>Enzymatic essays</i>	167
7.3.9	<i>Delignification</i>	168
7.3.10	<i>Fourier Transform Infrared Spectroscopy (FTIR)</i>	169
7.3.11	<i>Enzymatic hydrolysis</i>	169
7.4	RESULTS AND DISCUSSION	170
7.4.1	<i>Lignocellulosic biomass recalcitrance</i>	170
7.4.2	<i>Extrusion</i>	171
7.4.3	<i>Flask fermentations (250 ml)</i>	172
7.4.4	<i>Bioreactor fermentations (5 L glass tank)</i>	175
7.4.5	<i>Effect of Ex-SSF pretreatment</i>	175
7.4.6	<i>Enzymatic digestibility</i>	183
7.4.7	<i>Effect of enzyme load on enzyme digestibility</i>	186
7.4.8	<i>Overview of Ex-SSF techno-economic potential</i>	187
7.5	CONCLUSION.....	189
7.6	ACKNOWLEDGEMENT	189
8	SIXIÈME ARTICLE	190
8.1	ABSTRACT.....	190
8.2	INTRODUCTION	191
8.3	MATERIEL AND METHODS	192
8.3.1	<i>Context</i>	192
8.3.2	<i>Study background</i>	193
8.3.3	<i>Feedstocks</i>	193
8.3.4	<i>Scenarios</i>	193
8.3.5	<i>Ex-SSF model</i>	194
8.3.6	<i>Process technical design</i>	195
8.3.7	<i>Project economics</i>	200
8.4	RESULTS AND DISCUSSION	201
8.4.1	<i>Scenarios implications</i>	201
8.4.2	<i>Capital expenditure comparison</i>	202
8.4.3	<i>Operation expenditure comparison</i>	204
8.4.4	<i>Product value comparison</i>	207
8.4.5	<i>Economic profitability scenario</i>	208
8.4.6	<i>Conclusion</i>	208
9	DISCUSSION GÉNÉRALE, CONCLUSION, RECOMMANDATIONS.....	210
9.1	DISCUSSION GÉNÉRALE	210
9.1.1	<i>Évaluation du potentiel de l'extrusion et détermination des principaux paramètres de prétraitement</i>	212

9.1.2	<i>Analyse des couplages de prétraitement impliquant l'extrusion et proposition d'une nouvelle approche de prétraitement.</i>	215
9.1.3	<i>Optimisation des paramètres d'extrusion et analyse des caractéristiques des extrudats</i>	219
9.1.4	<i>Optimisation des conditions de biodégradation par fermentation solide des biomasses prétraitées par extrusion et hydrolyse enzymatique des préhydrolysats.</i>	224
9.1.5	<i>Analyse technico-économique de la production de bioéthanol 2G avec le prétraitement Ex-SSF</i>	227
9.2	CONCLUSION GÉNÉRALE	229
9.3	RECOMMANDATIONS	231
10	BIBLIOGRAPHIE	233
11	ANNEXE I	282
12	ANNEXE II	284
13	ANNEXE III	286

LISTE DES FIGURES

FIGURE 1.1	CHAMPIGNONS DE LA POURRITURE BLANCHE (BASIDIOMYCÈTES).....	10
FIGURE 2.1	COPEAUX D'ÉPINETTE NOIRE (A) ET RÉSIDUS DE MAÏS (B).....	17
FIGURE 2.2	BROYEUR (A), TAMIS DE 1 MM (B) ET TAMIS DE 1,5 MM (B).....	18
FIGURE 2.3	EXTRUDEUSE BIS-VIS DE 11 MM DE DIAMÈTRE.....	22
FIGURE 2.4	BIOMASSE À LA SORTIE DE L'EXTRUDEUSE : (A) RÉSIDUS DE MAÏS ET (B) ÉPINETTE NOIRE.....	23
FIGURE 2.5	DISPOSITIF DE LAVAGE.....	24
FIGURE 3.1	ESSENTIAL COMPONENTS OF A LIGNOCELLULOSIC MICROFIBER.....	35
FIGURE 3.2	COMPOSITION OF SOME LIGNOCELLULOSIC BIOMASS.....	36
FIGURE 3.3	ILLUSTRATION OF A TWIN-SCREW EXTRUDER WITH THE MAIN PARTS.....	43
FIGURE 3.4	ONE-PIECE SCREW.....	44
FIGURE 3.5	MODULATED SCREW.....	44
FIGURE 3.6	CO-ROTATIVE AND COUNTER-ROTATIVE EXTRUDER SCREWS.....	45
FIGURE 3.7	SIDE VIEW OF INTERMESHING FORWARD/REVERSE TWIN-SCREW ELEMENTS.....	47
FIGURE 3.8	KNEADING BLOCKS (FRONT-FACING AND LATERAL VIEW).....	49
FIGURE 3.9	SPECIFIC MECHANICAL ENERGY FOR SOME LIGNOCELLULOSIC BIOMASS EXTRUSION (Wh/kg).....	53
FIGURE 4.1	ILLUSTRATION OF A TYPICAL EXTRUDER WITH THE MAIN COMPONENTS.....	68
FIGURE 4.2	REACTOR DESIGN FOR LIQUID HOT WATER PRETREATMENT.....	72
FIGURE 4.3	LABORATORY SCALE SET FOR ULTRASONICATION PRETREATMENT.....	76
FIGURE 4.4	ORGANOSOLV PRETREATMENT.....	82
FIGURE 5.1	<i>P. CHRYSOSPORIUM</i> ON PETRI DISH STARTED WITH A PIECE OF MYCELIUM AS INOCULUM.....	100
FIGURE 5.2	STRUCTURE OF A LIGNOCELLULOSE MICROFIBER.....	101
FIGURE 5.3	TRANSFORMATION MECHANISM OF Mn^{2+} INTO Mn^{3+} BY MANGANESE PEROXIDASES STRUCTURE OF A LIGNOCELLULOSE MICROFIBER.....	104
FIGURE 5.4	SOLID STATE FERMENTATION WITH <i>P. CHRYSOSPORIUM</i> ON CORN STOVER AND BLACK SPRUCE CHIPS IN FLASKS AND PETRI DISHES.....	108
FIGURE 5.5	TRAY BED REACTORS IN AN INCUBATOR.....	110
FIGURE 5.6	FIXE REACTOR LABFORS (5 L) AND ROTATIVE DRUM TERRAFORS (15 L).....	111
FIGURE 6.1	SCREW CONFIGURATION FOR THE EXTRUSION STEP (T = TRANSPORT ZONE, F = FORWARD SCREW ELEMENT AND K = KNEADING ELEMENTS BLOCK).....	128
FIGURE 6.2	ELEMENTAL COMPOSITION OF BLACK SPRUCE CHIPS AND CORN STOVER.....	135
FIGURE 6.3	BLACK SPRUCE CHIPS (BS) AND CORN STOVER (CS) CHARACTERIZATION.....	135
FIGURE 6.4	CORN STOVER OF 1 MM PARTICLE SIZE EXTRUDED: (A) WITH A DIE IN DIFFERENT CONDITIONS OF TEMPERATURE AND SCREW SPEED, AND (B) WITHOUT A DIE IN DIFFERENT CONDITIONS OF TEMPERATURE AND SCREW SPEED.....	137
FIGURE 6.5	DISTRIBUTION OF THE EXTRUDATE PARTICLE SIZE (BLACK SPRUCE CHIPS AND CORN STOVER).....	140

FIGURE 6.6	COMPARISON OF THE PARTICLE SIZE DISTRIBUTION BETWEEN THE EXTRUDATES AND MILLED RAW BIOMASSES: A) BLACK SPRUCE CHIPS (BS), AND B) CORN STOVER (CS).	141
FIGURE 6.7	MODEL PREDICTIONS AS A FUNCTION OF THE EXPERIMENTAL DELIGNIFICATION PERCENTAGE.	145
FIGURE 6.8	2D AND 3D RESPONSE SURFACE OF THE OPTIMUM EXTRUSION CONDITIONS FOR BLACK SPRUCE CHIPS (A AND C: 0% NaOH; B AND D: 15% NaOH).	146
FIGURE 6.9	2D AND 3D RESPONSE SURFACE OF THE OPTIMUM EXTRUSION CONDITIONS FOR BLACK SPRUCE CHIPS AND CORN STOVER (A AND C: 0%NaOH; B AND D: 15%NaOH).	147
FIGURE 6.10	SCANNING ELECTRON MICROSCOPE IMAGES OF BLACK SPRUCE CHIPS (BS) AND CORN STOVER (CS) BEFORE AND AFTER EXTRUSION.	152
FIGURE 6.11	FTIR SPECTRA OF BLACK SPRUCE CHIPS (A) AND CORN STOVER (B) BEFORE AND AFTER EXTRUSION.	153
FIGURE 7.1	COMPOSITION OF THE RAW BLACK SPRUCE CHIPS (BS) AND RAW CORN STOVER (CS).	171
FIGURE 7.2	COLONIZATION OF EXTRUDED BLACK SPRUCE CHIPS (BSE) AND CORN STOVER (CSE) BY PHANEROCHAETE CHRYSOSPORIUM DURING FLASK SOLID STATE FERMENTATION.	174
FIGURE 7.3	TYPE OF WATER SUPPLY AVAILABLE IN BIOMASS FOR MICROBIAL DEVELOPMENT.	174
FIGURE 7.4	EVOLUTION OF LACCASE, MANGANESE PEROXIDASE AND LIGNIN PEROXIDASE ACTIVITIES DURING 24 DAYS OF SEMI SOLID FERMENTATION (SSF) WITH EXTRUDED BLACK SPRUCE CHIPS (BS) AND CORN STOVER (CS).	179
FIGURE 7.5	BIOMASS DELIGNIFICATION RATE DURING THE TANK FERMENTATION OF BLACK SPRUCE CHIPS AND CORN STOVER.	181
FIGURE 7.6	FTIR SPECTRA OF THE RAW AND Ex-SSF PRETREATED BLACK SPRUCE CHIPS (BS) AND CORN STOVER (CS).	183
FIGURE 7.7	REDUCING SUGAR CONCENTRATION AS A FUNCTION OF HYDROLYSIS TIME WITH AN ENZYME CONTENT OF 0.25 ML/G OF BIOMASS.	185
FIGURE 7.8	SUGAR CONCENTRATION REDUCTION AS A FUNCTION OF HYDROLYSIS TIME WITH AN ENZYME CONTENT OF 0.50 AND 0.75 ML/G OF BIOMASS.	187
FIGURE 8.1	OVERALL PROCESS OF THE Ex-SSF PLANT BASED MODEL.	195
FIGURE 8.2	EVOLUTION OF THE AVERAGE FARMLAND SIZE (HA) AND THE NUMBER OF FARMS FROM 1951 TO 2021. DATA SOURCE (CANADA, 2021).	202
FIGURE 8.3	CAPEX COMPOSITION AND CAPEX/PLANT CAPACITY.	204
FIGURE 8.4	OPEX COMPOSITION AND OPEX/FEEDSTOCK QUANTITY.	207
FIGURE 9.1	CHEMINEMENT DE LA THÈSE.	211
FIGURE 13.1	ETHANOL PRICE EVOLUTION OVER THE PAST FIVE YEAR (JAN 2020 TO DEC 2024) FROM (ECONOMICS, 2025).	289

LISTE DES TABLEAUX

TABLEAU 2.1	ESPACE EXPÉRIMENTAL DES EXTRUSIONS DES RÉSIDUS DE MAÏS ET D'ÉPINETTE NOIRE.	20
TABLEAU 2.2	TABLE DES TESTS DES RÉSIDUS DE MAÏS POUR 1 MM DE TAILLE DE PARTICULE.	21
TABLEAU 3.1	LIGNOCELLULOSIC BIOMASS COMPOSITION BEFORE AND AFTER EXTRUSION.	37
TABLEAU 3.2	CRYSTALLINITY INDEX.	38
TABLEAU 3.3	PRACTICES OF BIOMASS PREPARATION BEFORE EXTRUSION.	41
TABLEAU 4.1	SUMMARY OF EXTRUSION-BASED PRETREATMENT RESULTS.	85
TABLEAU 4.2	UPSCALING CHALLENGES ASSOCIATED WITH THE SECOND PRE-TREATMENT IN A TWO-STEP COUPLING WITH EXTRUSION.	89
TABLEAU 5.1	APPLICATION OF <i>PHANEROCHAETE CHRYSOSPORIUM</i> FOR BIODECOMPOSITION IN DIVERSE INDUSTRIES.	116
TABLEAU 5.2	SOME RESULTS OF BIODELIGNIFICATION WITH <i>P. CHRYSOSPORIUM</i>	118
TABLEAU 6.1	EXPERIMENTAL SPACE FOR THE EXTRUSION CONDITIONS.	129
TABLEAU 6.2	EXPERIMENTAL TRIALS FOR BLACK SPRUCE CHIPS (BS) AND CORN STOVER (CS).	129
TABLEAU 6.3	EXTRUSION EXPERIMENTAL SPACE CODES.	137
TABLEAU 6.4	SUMMARY OF THE RESPONSES.	139
TABLEAU 6.5	PEARSON CORRELATION COEFFICIENTS.	139
TABLEAU 6.6	RESPONSES OF THE STATISTICAL ANALYSES.	143
TABLEAU 6.7	SUMMARY OF THE ANOVA ANALYSIS FOR BS AND CS.	144
TABLEAU 6.8	OPTIMIZATION CONSTRAINTS IMPOSED OF THE MODELS.	149
TABLEAU 6.9	FUNCTIONAL GROUPS DETECTED IN THE BIOMASS SAMPLES BY FTIR SPECTROSCOPY.	154
TABLEAU 7.1	PROCESS 11 EXTRUDER SPECIFICATIONS.	164
TABLEAU 7.2	EXPERIMENTAL SPACE SELECTED FOR THE STUDY.	166
TABLEAU 7.3	EXPERIMENTAL CONDITIONS FOR CORN STOVER AND BLACK SPRUCE.	166
TABLEAU 7.4	GROWTH ASSESSMENT OF <i>PHANEROCHAETE CHRYSOSPORIUM</i> ON EXTRUDED BLACK SPRUCES CHIPS (BSE) AND CORN STOVER (CSE).	173
TABLEAU 7.5	CRYSTALLINITY INDEX OF THE SAMPLES.	183
TABLEAU 8.1	EX-SSF WORKING CONDITION FOR CORN STOVER AND BLACK SPRUCE CHIPS.	197
TABLEAU 8.2	SIMULTANEOUS SACCHARIFICATION AND FERMENTATION CONDITIONS.	198
TABLEAU 8.3	TOTAL INSTALLED EQUIPMENT COSTS PER AREA.	204
TABLEAU 8.4	RESULTS OF EQUATIONS 8.1 TO 8.15.	206
TABLEAU 8.5	ECONOMICS OF THE MINIMUM PROFITABILITY SCENARIOS.	208
TABLEAU 9.1	POTENTIEL DES COUPLAGES ET DÉFIS ASSOCIÉS À LEUR IMPLÉMENTATION.	218
TABLEAU 9.2	OPTIMIZATION CONSTRAINTS IMPOSED OF THE MODELS.	223
TABLEAU 9.3	CONDITIONS OPTIMISÉES D'EXTRUSION.	224
TABLEAU 11.1	REVUE SUR LES EXTRUSIONS DE BIOMASSE LIGNOCELLULOSIQUES.	282

TABLEAU 12.1	DELIGNIFICATION MODEL RESULTS FOR EX-SSF PRE-TREATED BLACK SPRUCE CHIPS.....	284
TABLEAU 12.2	DELIGNIFICATION MODEL RESULTS FOR EX-SSF PRE-TREATED CORN STOVER.....	285
TABLEAU 13.1	LIST OF EQUIPMENT PER AREA AND THEIR RESPECTIVE ESTIMATED COST ADAPTED FROM ADEN ET AL. (2002).....	286
TABLEAU 13.2	ESTIMATED PRE-CONSTRUCTION AND UTILITIES COSTS ADAPTED FROM ADEN ET AL. (2002)..	288

MATÉRIEL SUPPLÉMENTAIRE

SUPPLEMENTARY MATERIALS 1. PARAMETER SCREENING.....	157
---	-----

APPENDICES

APPENDIX A. GAS CHROMATOGRAPHY/MASS SPECTROMETRY (GC/MS) RESULTS OF BLACK SPRUCE EXTRUDATE.	158
APPENDIX B. GAS CHROMATOGRAPHY/MASS SPECTROMETRY (GC/MS) RESULTS OF CORN STOVER EXTRUDATE.	159

LISTE DES ÉQUATIONS

ÉQUATION 2.1 - HUMIDITÉ.....	25
ÉQUATION 2.2 – TAUX DE DÉLIGNIFICATION	25
ÉQUATION 3.1 – CRISTALLINITY INDEX (CRI).....	37
ÉQUATION 3.2 – OPTIMUM OFFSET ANGLE (A).....	49
ÉQUATION 3.3 – SPECIFIC MECHANICAL ENERGY (SME).....	52
ÉQUATION 5.1 – REACTIONS CYCLE OF MANGANESE PEROXIDASE.....	103
ÉQUATION 5.2 – REACTIONS CYCLE OF LIGNIN PEROXIDASE.....	105
ÉQUATION 6.1 – MOISTURE.....	131
ÉQUATION 6.2 – DELIGNIFICATION PERCENTAGE.....	132
ÉQUATION 6.3 – GENERAL EQUATION FOR A QUADRATIC MODEL WITH N INDEPENDENT VARIABLES.....	132
ÉQUATION 6.4 – CALORIFIC ENERGY.....	134
ÉQUATION 6.5 – CLAUSIUS-CLAPEYRON EQUATION.....	137
ÉQUATION 6.6 - REGRESSION EQUATION OF DELIGNIFICATION PERCENTAGE FOR BLACK SPRUCE.....	142
ÉQUATION 6.7 - REGRESSION EQUATION OF DELIGNIFICATION PERCENTAGE FOR CORN STOVER.....	143
ÉQUATION 7.1 – ENZYMATIC ACTIVITY.....	168
ÉQUATION 7.2 – DELIGNIFICATION PERCENTAGE.....	169
ÉQUATION 7.3 – REACTIONS CYCLE OF MANGANESE PEROXIDASE.....	177
ÉQUATION 8.1 – PLANT CAPACITY (P).....	196
ÉQUATION 8.2 – FEEDSTOCK QUANTITY (M).....	196
ÉQUATION 8.3 – TRANSPORTATION COST (T).....	196
ÉQUATION 8.4 – TOTAL VOLUME OF THE SEMI SOLID FERMENTATION TANKS (Vt).....	196
ÉQUATION 8.5 – NUMBER OF TANKS (N).....	197
ÉQUATION 8.6 – TOTAL VOLUME OF THE VESSEL (Vtsf).....	198
ÉQUATION 8.7 – TOTAL VOLUME OF BIOETHANOL (VEtOH).....	198
ÉQUATION 8.8 – TOTAL VOLUME OF THE STORAGE (Vst).....	199
ÉQUATION 8.9 – TOTAL VOLUME OF THE DIGESTOR (Vdigestor).....	199
ÉQUATION 8.10 – BIOMETHANE PRODUCTION (VCH4).....	200
ÉQUATION 8.11 – ELECTRICITY PRODUCTION FROM BIOMETHANE (E).....	200
ÉQUATION 8.12 – CAPITAL EXPENDITURE (CAPEX).....	200
ÉQUATION 8.13 – INSTALLATION COST (CInst).....	200
ÉQUATION 8.14 – OPERATION EXPENDITURE (OPEX).....	201
ÉQUATION 8.15 – FEEDSTOCK COST (CFeed).....	201

LISTE DES ABRÉVIATIONS

A – C		
ABTS	:	2,2'-azino-bis(3-ethylbenzothiazoline-6-sulfonic acid)
ADF	:	Acid Detergent Fiber
AFEX	:	Ammonia Fiber Explosion
ANOVA	:	Analysis Of Variance
BLC	:	Biomasses Lignocellulosiques
BRF	:	Brown Rot Fungi
BS	:	Black Spruce
BSE	:	Extruded Black Spruce
CAPEX	:	Capital Expenditure
CCD	:	Central Composite Design
CEC	:	Capacité d'Échange de Cations
CHNS	:	Carbon Hydrogen Nitrogen Sulfur
CINEAG	:	Consortium Intersectoriel en Écologie Industrielle et Agroalimentaire
CITE	:	Center for Innovation in Technological Ecodesign
COL	:	Catalog Of Life
CRFQ	:	Cartographie des Résidus Fermentescibles du Québec
CRIBIQ	:	Consortium de Recherche et Innovations en Bioprocédés Industriels au Québec
CS	:	Corn Stover
CSE	:	Extruded Corn Stover
CV	:	Calorific Value
D – F		
DES	:	Deep Eutectic Solvent
DMF	:	2,5-Diméthylfurane
DMSO	:	Dimethyl Sulfoxide
DNA	:	Deoxyribonucleic Acid
DNS	:	Dinitrosalicylic Acid
DSC	:	Differential Scanning Calorimetry
DSMZ	:	Deutsche Sammlung von Mikroorganismen und Zellkulturen
EHT	:	Extra High Tension
EMF	:	5-Éthoxyméthylfurfural
ETE	:	Eau Terre Environnement
EV	:	Electric Vehicle

Ex-SSF	:	Extrusion – Semi Solid Fermentation
FEINRS	:	Fédération des Étudiants de l'INRS
FSE	:	Forward Screw Element
FTIR	:	Fourier Transformed Infrared Spectroscopy
G – J		
GC/MS	:	Gas Chromatography/Mass Spectrometry
GES	:	Gaz à Effet de Serre
GIEC	:	Groupe d'Experts Intergouvernemental sur l'Évolution du Climat
GNL	:	Gaz Naturel Liquéfié
GVL	:	γ -Valérolactone
HBA	:	Hydrogen Bond Acceptor
HBD	:	Hydrogen Bond Donor
HBT	:	1-Hydroxybenzotriazole
HMF	:	Hydroxyméthylfurfural
INPHB	:	Institut National Polytechnique Félix Houphouët Boigny
INRS	:	Institut National de la Recherche Scientifique
JLS	:	Journal la Synthèse
K – N		
KE	:	Kneading Element
LBE	:	Lignocellulosic Biomass Extrusion
LCB	:	Lignocellulosic Biomass
LDPE	:	Low Density Polyethylene
LHW	:	Liquid Hot Water
LOI	:	Lateral Order Index
MEB	:	Microscopie Électronique à Balayage
MHQ	:	Methoxyhydroquinone
MIBK	:	Methyl Isobutyl Ketone
MIT	:	Massachusetts Institute of Technology
NADES	:	Natural Deep Eutectic Solvent
NCYC	:	National Collection of Yeast Cultures
NDF	:	Neutral Detergent Fiber
NMMO	:	N-Methylmorpholine N-Oxide
NREL	:	National Renewable Energy Laboratory
NSC	:	Non-Structural Component
NSERC	:	National Science and Engineering Research Council of Canada
O – R		
O&M	:	Operation And Maintenance

OPEX	:	Operation Expenditure
PAH	:	Polyaromatic Hydrocarbons
PGQ	:	Pôle Géoscientifique du Québec
PRISM	:	Postdoctoral Recruitment Initiative in Sciences and Medicine
PVC	:	Polyvinyl Chloride
REN	:	Résidus d'Épinette Noire
RMA	:	Résidus de Maïs
RSA	:	Analyse de Surfaces de Réponse
RSE	:	Reverse Screw Element
RSM	:	Response Surface Method
RT	:	Room Temperature
S – W		
SEM	:	Scanning Electron Microscopy
SESE	:	Screw Extrusion Steam Explosion
SIFBI	:	Singapore Institute of Food and Biotechnology Innovation
SME	:	Specific Mechanical Energy
SPORL	:	Sulfite Pretreatment to Overcome Recalcitrance of Lignocellulose
SRF	:	Soft Rot Fungi
SSF	:	Solid-State Fermentation
SUV	:	Sport Utility Vehicle
TGA	:	Thermogravimetric Analysis
TMPD	:	N,N,N',N'-Tetramethyl-1,4-Phenylenediamine
WHOI	:	Woods Hole Oceanographic Institution
WRF	:	White Rot Fungi

1 INTRODUCTION GÉNÉRALE

1.1 Contexte

Depuis plusieurs décennies, le contexte environnemental mondial se dégrade d'année en année. Ce constat est particulièrement alarmant ([Hennessy et al., 2022](#)). En effet, dès le XVIII^e siècle, les sociétés modernes ont développé une dépendance aux matières fossiles d'abord pour des besoins énergétiques ; mais ensuite pour des applications très diversifiées grâce à l'essor de la pétrochimie. La dépendance vis-à-vis des matières fossiles s'est maintenue depuis lors. Pour preuve, dans le secteur de l'énergie par exemple, le pétrole et le gaz naturel liquéfié (GNL) restent les principales sources d'énergie et surtout des atouts géopolitiques importants.

Pourtant, il est maintenant bien établi que l'exploitation des ressources fossiles est la principale source d'émission de gaz à effet de serre. La Conférence de Paris de 2015 avait abouti à un engagement des parties prenantes à réduire les émissions de gaz à effet de serre (GES) pour contenir le réchauffement climatique à 1,5 °C. Dix ans plus tard, nous sommes bien loin de la trajectoire requise pour atteindre ces objectifs. Bien que les émissions de CO₂ aient été réduites de 5,2 % au plus fort moment de la pandémie de COVID-19 en 2020, elles ont repris à la hausse en 2021 avec plus de 6 % ([IEA, 2022](#)). Or, si la tendance actuelle à la consommation d'énergie fossile est maintenue, il est certain (95 % de certitude selon le GIEC) que la limite critique des 1,5 °C sera largement dépassée et ce, avant la deuxième moitié du siècle. La persistance des matières fossiles dans les habitudes de consommation peut s'expliquer par plusieurs raisons, mais l'une des principales est l'immaturation technique et économique des énergies renouvelables au regard des énergies fossiles ([Kempa et al., 2021](#)).

De toutes les alternatives renouvelables disponibles, la biomasse est celle qui est la plus susceptible de se substituer aux ressources fossiles, tant pour les besoins énergétiques (biodiesel, bioéthanol, etc.) que pour des produits pétrochimiques (résines, adhésifs, pesticides, détergents, etc.) ([Sun et al., 2024](#); [Wang et al., 2018a](#)). Cela fait d'elle une matière première « spéciale ». En ce qui concerne la production d'énergie par utilisation de la biomasse, il s'est développé au fil des années un nouveau concept de raffinerie : la bioraffinerie. Selon [Clark and Deswarte \(2015\)](#), une bioraffinerie est une installation ou un réseau d'installations qui convertit la biomasse, y compris les déchets, en divers produits chimiques, biomatériaux et énergie, en maximisant la valeur de la biomasse et en minimisant les déchets. La première génération de bioraffinerie (bioraffinerie 1G) utilise comme intrant les cultures dites énergétiques telles que le maïs, le colza et la betterave. Les productions de ces cultures (grains, fruits, etc.) sont

transformées en sucres simples (glucose), puis converties en bioéthanol par l'entremise de microorganismes lors d'une fermentation éthanolique. Cependant, l'utilisation même des produits agricoles destinés à la consommation humaine et animale pour produire de l'énergie pose des problèmes d'éthique et de sécurité alimentaire. La bioraffinerie 1G a eu pour préjudice majeur de rajouter une pression supplémentaire sur les terres arables et d'entrer en compétition directement ou indirectement avec l'alimentation humaine et animale (Naqvi & Yan, 2015). Ce désavantage critique de la bioraffinerie 1G a été le moteur du changement de paradigme vers la deuxième génération de bioraffinerie (Bioraffinerie 2G). En théorie, le concept est simple : utiliser les résidus (déchets) agricoles non comestibles (branche, feuille, paille, tige, tronc, etc.) à la place des parties comestibles (grains, graines, fruits, etc.). Dans la pratique, la complexité de la tâche requiert des recherches avancées. Les résidus non-comestibles visés sont des biomasses lignocellulosiques (BLC). La biomasse lignocellulosique est abondante et peu coûteuse en comparaison des cultures énergétiques (WSP, 2021a). On estime à plus de 180 milliards de tonnes par an, la quantité de BLC disponible mondialement (Dahmen et al., 2019). Elle se compose essentiellement de résidus agricoles et forestiers. En revanche, bien qu'elle soit attractive, l'utilisation de la biomasse lignocellulosique requiert une étape supplémentaire pour sa transformation en bioénergie : le prétraitement. En effet, la lignocellulose contenue dans les biomasses lignocellulosiques, est un composé complexe et récalcitrant formé par de la cellulose, de l'hémicellulose et de la lignine. Cette dernière sert naturellement de système de défense aux plantes contre les agressions microbiologiques, physiques et chimiques. Plusieurs études ont montré que l'étape de prétraitement représente le facteur de coût le plus élevé dans les procédés de valorisation de biomasses lignocellulosiques (BLC). L'efficacité du prétraitement et son coût affectent la valorisation des BLC en bioénergie. On estime que l'étape de prétraitement compte pour plus de 40 % du coût total de valorisation de ces biomasses (Sindhu et al., 2016).

À ce jour, des prétraitements de BLC existent, mais des défis sont reliés à leurs efficacités, leurs coûts et leurs impacts sur l'environnement. Toutefois, certains de ces prétraitements sont prometteurs. Ces méthodes de prétraitement nécessitent d'être améliorées et développées avec de nouvelles approches. L'un des moyens d'y arriver est de combiner (par complémentarité) des prétraitements de sorte à maximiser leurs avantages respectifs tout en minimisant les inconvénients associés à chacun d'eux pris individuellement. Ce projet de thèse a eu pour principal objectif d'adresser le sujet en développant une approche novatrice de prétraitement des BLC en vue d'augmenter leurs digestibilités enzymatiques et d'accroître leur potentiel de valorisation. Les sections suivantes présentent : (i) les concepts essentiels du sujet de recherche et (ii) la démarche pour atteindre les objectifs.

1.2 Valorisation des biomasses lignocellulosiques

On distingue trois voies de valorisation des biomasses lignocellulosiques (BLC). Il s'agit des voies de valorisations physiques, des voies de valorisation chimiques et des voies de valorisation biologiques.

1.2.1 Voies de valorisation physique

La valorisation physique des BLC se fait par combustion, par pyrolyse ou par gazéification.

La combustion survient lorsque la BLC sèche est mise au contact d'une source de chaleur en milieu aérobie. Bien souvent, la combustion est précédée par une étape de compression ou de pelletisation; le but étant la densification de la biomasse et l'augmentation de sa capacité calorifique (Bajwa et al., 2018). La combustion est une voie de valorisation répandue. En effet, elle est utilisée prioritairement pour des besoins de chauffage domestique et de cuisson dans les zones rurales à travers le monde (Heltberg, 2003). Au niveau industriel, la combustion des BLC sert à produire de la chaleur ou de la vapeur qui sera ensuite utilisée pour faire tourner des systèmes mécaniques pour la production d'électricité (Caposciutti et al., 2022; McKendry, 2002). Sous certaines configurations, il est possible de produire simultanément de la chaleur et de l'électricité : on parle de cogénération (Abbas et al., 2020). Les inconvénients liés à la combustion sont la consommation d'énergie, ainsi que les émissions de CO₂ et de CO. Ces deux gaz participent à l'effet de serre en plus de la toxicité du CO.

La pyrolyse consiste à la combustion de la biomasse à de très hautes températures allant de 300 à plus de 1100 °C en absence d'oxygène (Yogalakshmi et al., 2022). Selon les conditions, on obtient une fraction solide (bio-charbon), une fraction liquide (bio-huile) et une fraction gazeuse constituée de H₂ et de CO. Dans la pratique, on distingue la pyrolyse lente et la pyrolyse rapide. La première aboutit essentiellement à la production de bio-charbon (biochar) et dure plusieurs heures, voire plusieurs jours. Quant à la seconde, elle permet en quelques minutes la production principalement de bio-huile et de gaz de synthèse (syngaz) en sus du biochar. De plus en plus, il est mentionné de « pyrolyse flash » dans la littérature (Yang et al., 2022). Ce type de pyrolyse désigne une pyrolyse ultra rapide de l'ordre d'une à cinq secondes. Elle aboutit à une production d'environ 60 % de biochar et 40 % de bio-huile et syngaz. De façon générale, le type, la qualité et la quantité de produits obtenus dépendent de plusieurs facteurs, tels que la température, la durée de traitement, le type de BLC, la taille des particules de biomasse, l'humidité de la BLC, la quantité et la nature du catalyseur (Wang et al., 2022).

La gazéification utilise la technique de l'oxydation partielle à plus de 1600 °C pour transformer la biomasse en un mélange de composés gazeux (CO, CO₂, H₂ et CH₄) duquel est extrait le syngaz. En pratique, la gazéification implique quatre phases dont une phase de pyrolyse (Molino et al., 2016). Le procédé aboutit également à la production de petites quantités de biochar et de composés condensés. Son inconvénient majeur est similaire aux précédentes voies de valorisation : la consommation d'énergie liée aux très hautes températures requises (Lam et al., 2016; Puig-Arnavat et al., 2010).

Ainsi, les produits des voies de valorisation physique sont essentiellement la chaleur, le biochar, les bio-huiles et le syngaz. La chaleur est utilisée comme source d'énergie ou de chauffage résidentiel. Le biochar est composé en grande partie de carbones chimiquement très stables. Il est utilisé comme moyen de séquestration de carbone atmosphérique, car il possède la capacité de capter et de fixer le carbone atmosphérique. Il agit ainsi comme un puits de carbone. Cependant, c'est plutôt en agriculture que l'utilisation du biochar est répandue comme amendement : amélioration de la capacité de rétention de l'eau dans le sol, source de carbone pour les plantes et les microorganismes, augmentation de la capacité d'échange de cations (CEC), amélioration du pouvoir fertilisant, etc. (Ippolito et al., 2011). Les bio-huiles peuvent être utilisées soit directement comme combustibles énergétiques ou servir à la production de produits variés, tels que des biocarburants, de l'hydrogène, des liants pour asphalte, des pesticides et de la mousse polyuréthane (Hu & Gholizadeh, 2020). Quant au syngaz, il peut être utilisé comme carburant ou être transformé en carburant synthétique liquide par la méthode Fischer-Tropsch. Après purification, le syngaz peut servir de combustible pour les turbines à gaz (Kobayashi, 2021).

1.2.2 Voies de valorisation chimique

La cellulose et l'hémicellulose contenues dans les BLC sont composées d'oses (glucose, xylose, galactose, etc.). La lignine, quant à elle, est constituée de composés aromatiques (essentiellement des motifs phénylpropane). La valorisation chimique de la BLC a pour but d'extraire ces molécules d'intérêt. Pour cela, divers types de procédés et de réactions chimiques sont employés selon le type de molécule d'intérêt qu'on souhaite obtenir. Par exemple, le procédé d'organosolvation est utilisé pour le fractionnement de la biomasse en ses différents constituants de base (cellulose, hémicellulose et lignine). L'industrie du papier utilise ce procédé pour l'extraction de la cellulose pour la fabrication du papier. La cellulose peut être aussi convertie en éthylène glycol (polyester, antigels, etc.) par une réaction catalysée en milieu aqueux ; en sorbitol

(laxatif, édulcorant, pâte dentifrice, humectant, etc.) par hydrogénation hydrolytique; en acide lactique par hydrolyse suivie d'aldolisation; en acide lévulinique (produits pharmaceutiques et aromatisants, solvants, plastifiants, agents antigel, etc.) par déshydratation catalysée par un acide suivie d'hydrolyse ; etc. (Godswill, 2017; Guleria *et al.*, 2020; Marianou *et al.*, 2019; Rackemann & Doherty, 2011). L'hémicellulose est généralement hydrolysée par voie enzymatique pour la récupération de monosaccharides qui peuvent être utilisés comme tels ou servir de précurseurs pour divers composés à hautes valeurs ajoutées, tels que l'acide citrique, l'acide butyrique, l'acétaldéhyde, l'acétone, l'acide succinique et l'isopropanol (Dulie *et al.*, 2021). Quant à la lignine, sa conversion catalytique permet la récupération de divers composés aromatiques, tels que des composés phénoliques, des hydrocarbures cycliques et des aldéhydes aromatiques (Wang *et al.*, 2019). Ces composés entrent dans la composition de résines, de biopesticides, d'adhésifs et de nombreux autres produits d'usage quotidien.

Les molécules d'intérêt sont aussi les composés chimiques qui résultent de la dégradation directe ou indirecte des constituants de base des BLC. De nombreux composés à hautes valeurs ajoutées peuvent être ainsi obtenus. Par exemple, le furfural et l'hydroxyméthylfurfural (HMF) sont des produits de la déshydratation (sous condition acide) de pentoses et d'hexoses respectivement (Xu *et al.*, 2020a). Ces deux composés peuvent à leur tour subir des réactions de condensation pour produire d'autres types de composés furanes à hautes valeurs ajoutées tels que le DMF (2,5-diméthylfurane), le 2-MF (2-méthylfurane), l'EMF (5-éthoxyméthylfurfural) et le GVL (γ -valérolactone). Ces furanes sont vus aujourd'hui comme des alternatives renouvelables aux dérivés pétroliers, notamment pour la production de carburant grâce à leur forte densité énergétique et leur haut indice d'octane (Bohre *et al.*, 2015). Ainsi, les possibilités de valorisation chimique de la BLC sont innombrables et les applications potentielles très diversifiées.

1.2.3 Voies de valorisation biologique

Les voies de valorisation biologique sont celles qui impliquent l'utilisation des microorganismes. Les produits les mieux connus des voies de valorisation biologique des BLC sont entre autres, le bioéthanol, le biogaz (essentiellement CH₄ et CO₂) et les enzymes. Le bioéthanol est obtenu par la transformation métabolique des sucres (monosaccharides) par des ferments micro-organismes (levures) en milieu liquide anaérobie : c'est la fermentation alcoolique. Cette fermentation est précédée d'une étape de prétraitement et d'hydrolyse pour permettre l'accès des sucres aux microorganismes (Sofokleous *et al.*, 2022). Le bioéthanol est mélangé avec l'essence et utilisé comme carburant pour les engins motorisés. Plusieurs types de mélanges existent, dont

les plus connus sont E5 (5% bioéthanol et 95% essence), E10, E15 et E85. Le biogaz aussi est obtenu par la fermentation en milieu liquide anaérobie des sucres par des bactéries spécialisées (méthanogènes) : c'est la fermentation méthanique. Tout comme pour le bioéthanol, une étape de prétraitement des BLC est nécessaire. La conversion de la BLC en biogaz suit les étapes d'hydrolyse, d'acidogénèse, d'acétogénèse et de méthanogénèse. C'est à cette dernière étape que le biogaz est produit à partir de l'acide acétique, du dihydrogène et du dioxyde de carbone rendus disponibles par les étapes précédentes. Le biogaz est utilisé comme combustible pour divers besoins en énergie, tels que le chauffage résidentiel, la production d'électricité, la cuisson d'aliments et le transport. La production des enzymes, quant à elle, est rendue possible grâce à des champignons et des bactéries soit par voie de fermentation en milieu liquide ou par fermentation solide. Les enzymes pouvant être obtenues sont des cellulases, des hémicellulases et des ligninases (Ravindran & Jaiswal, 2016). L'intérêt pour les enzymes est sans cesse croissant au fil des années. Pour preuve, le marché mondial des enzymes étaient de 9,9 milliards de dollars en 2019 et une croissance totale de 7,1 % est attendu d'ici 2027 (Easwaran *et al.*, 2022).

1.3 Défis et perspectives de valorisation des biomasses lignocellulosiques

Le potentiel de la biomasse lignocellulosique est considérable et les possibilités de sa valorisation semblent inépuisables. Pourtant, elle est sous-exploitée. Les deux principales raisons sont : (1) les défis technologiques et (2) la rentabilité financière de leur valorisation (Kempa *et al.*, 2021). Le prétraitement est le défi technologique majeur de la valorisation de la biomasse lignocellulosique. En effet, contrairement aux cultures énergétiques, la biomasse lignocellulosique doit subir un ou plusieurs prétraitements. L'imbrication complexe et robuste de la lignine autour de la cellulose et de l'hémicellulose, empêche l'utilisation directe de la biomasse lignocellulosique dans les procédés de bioraffinerie. L'objectif de l'étape de prétraitement est donc de déstructurer les composants de la biomasse, afin de permettre l'accès aux composés d'intérêt (cellulose et hémicellulose). Les moyens pour y arriver sont très divers et définissent le type de prétraitement (physique, chimique, physico-chimique ou biologique). Bien que plus d'une dizaine de méthodes de prétraitement aient été développées, elles sont encore loin de répondre aux exigences du prétraitement adéquat (Sindhu *et al.*, 2016). Le prétraitement idéal devrait au moins :

- a) Être économiquement rentable;

- b) Ne pas générer d'inhibiteurs pour les activités de fermentation subséquentes (biodégradation, fermentation éthanolique, etc.);
- c) Être assez flexible pour prétraiter tout type de biomasse lignocellulosique (résidus forestiers, agricoles, agro-industriels, etc.);
- d) Utiliser très peu ou pas d'additifs chimiques, surtout ceux dont la fabrication est peu respectueuse de l'environnement (liquides ioniques, etc.);
- e) Consommer très peu ou pas d'eau;
- f) Être simple d'utilisation et ne pas nécessiter un suivi permanent;
- g) Être capable de fonctionner en *Fed-batch* ou en continu;
- h) Pouvoir être mis à l'échelle.

À ce jour, il n'existe pas de méthodes de prétraitement qui satisfassent toutes ces exigences, mais certaines d'entre elles sont assez prometteuses du point de vue de l'efficacité, de l'accessibilité de la technologie, de la flexibilité et de la consommation d'énergie. Quant à l'aspect économique, c'est un paramètre majeur et déterminant pour l'utilisation des biomasses lignocellulosiques et le développement de la bioraffinerie de deuxième génération. Il est intrinsèquement lié aux défis technologiques énoncés plus haut.

1.4 Méthodes de prétraitement des biomasses lignocellulosiques

Plusieurs méthodes ont été développées pour le prétraitement des BLC. On les classe en prétraitements physiques, chimiques, physico-chimiques et biologiques (Haghighi Mood *et al.*, 2013). Les méthodes de prétraitement des biomasses diffèrent des voies de valorisation en ce sens qu'elles regroupent les techniques utilisées pour rendre accessible les principales composantes des biomasses dans le but d'une utilisation de ces composés dans des étapes de conversion ultérieures ; tandis que les voies de valorisation aboutissent directement aux produits finis ou semi-finis en utilisant directement les biomasses sans les fractionner en leur principaux constituants. Chacune de ces classes de prétraitement possède des avantages et des inconvénients.

1.4.1 Méthodes physiques

Les méthodes physiques utilisent des systèmes mécaniques, des ondes ou des champs électriques pour prétraiter les BLC. Certaines d'entre elles associent des températures élevées

pour améliorer leur efficacité sur la biomasse. L'extrusion, le broyage, l'ultrasonication et le champ électrique pulsé sont parmi les méthodes de prétraitement physique.

Les méthodes physiques possèdent des particularités intéressantes. Elles peuvent être utilisées sur tous les types de BLC. Elles réduisent la taille des particules du matériel prétraité et sont généralement beaucoup plus rapides que les autres types de prétraitement. De plus, leur principe de fonctionnement est simple et facile à maîtriser. Elles ne génèrent ni inhibiteurs ni effluents en bout de prétraitement. Compte tenu de ces caractéristiques, elles sont un excellent choix comme premier prétraitement dans le cadre de couplage de technologie de prétraitement (Amin *et al.*, 2017). Cependant, il est difficilement possible de mettre à l'échelle ce type de méthodes. Elles consomment relativement d'importantes quantités d'énergie (Jędrzejczyk *et al.*, 2019). Le transfert de chaleur et l'action sur la biomasse sont difficilement uniformes à grandes échelles (pilote et industrielle). Elles ne sont pas sélectives, c'est-à-dire ne permettent pas de cibler un composé d'intérêt particulier que l'opérateur souhaiterait valoriser. **De toutes les méthodes physiques, l'extrusion est l'une des plus prometteuses pour plusieurs raisons dont la rapidité, la flexibilité et la relative faible consommation d'énergie en plus des avantages communs aux méthodes de prétraitement physique en général** (Duque *et al.*, 2017; Guiao *et al.*, 2022a).

1.4.2 Méthodes chimiques

Les méthodes chimiques utilisent les composés chimiques sous forme liquide pour dépolymériser les biopolymères en brisant les liaisons (covalentes ou autres) contenues dans la biomasse. Les méthodes chimiques sont généralement plus efficaces et consomment très peu d'énergie électrique. L'hydrolyse acide ou alcaline, l'ozonolyse, l'organosolvation, les traitements par liquides ioniques et par solvants eutectiques profonds sont autant d'options de prétraitements chimiques disponibles (Hassan *et al.*, 2018). Bien qu'efficaces, les méthodes chimiques possèdent de nombreux inconvénients. Les coûts d'investissement sont souvent relativement moins élevés, mais les coûts de fonctionnement sont importants à cause des produits chimiques (achat, gestion, recyclage, etc.). Les méthodes chimiques utilisent des produits chimiques souvent très coûteux et potentiellement toxiques comme les liquides ioniques, les solvants eutectiques profonds et les solvants organiques (Elgharbawy *et al.*, 2020; Ghandi, 2014). Ces solvants ne sont pas toujours recyclables et génèrent des effluents en fin de prétraitement. De plus, dans la majorité des cas, avant l'étape d'hydrolyse enzymatique, les BLC prétraitées chimiquement doivent subir une étape de neutralisation ou de rinçage. De grandes quantités

d'eau sont alors utilisées. Elles sont en revanche quasi inefficaces sur les particules de grande taille ; d'où la nécessité de les précéder d'une étape de réduction de la taille des particules.

1.4.3 Méthodes physico-chimiques

Les méthodes physico-chimiques utilisent les propriétés physico-chimiques et l'action mécanique de certaines molécules pour prétraiter les BLC. On distingue les prétraitements hydrothermaux et les non-hydrothermaux. Les premiers regroupent les prétraitements utilisant les propriétés de la molécule d'eau à hautes températures et pressions. Les plus utilisées sont l'explosion à la vapeur et l'eau chaude liquide (LHW). Dans les seconds on retrouve le SPORL (*Sulfite Pretreatment to Overcome Recalcitrance of Lignocellulose*), l'explosion au CO₂, l'AFEX (*Ammonia Fiber Explosion*) et l'oxydation humide (Jin & Dale, 2024; Li *et al.*, 2024a). Les méthodes physicochimiques aboutissent à la destruction des microfibrilles, à la réduction de la taille des particules et à la solubilisation d'une partie de l'hémicellulose. Elles utilisent des produits chimiques peu coûteux et en moins grande quantité que les méthodes chimiques. Elles ont comparativement aussi un faible coût environnemental. L'hydroxyde de sodium, l'acide sulfurique et l'ammoniac sont les plus utilisées. Les avantages des méthodes physico-chimiques sont spécifiques à chaque prétraitement, mais de manière générale, des problèmes de corrosion sont présents pour les réacteurs dans lesquels le prétraitement se fait. Un des principaux avantages de ces méthodes est la possibilité de leur mise à l'échelle. Cependant, on observe une dilution excessive des produits (xylose, galactose, etc.), la condensation de la lignine et la formation d'inhibiteurs. Le facteur de sévérité basé sur le pH, la température et le temps de résidence de la biomasse est une notion particulièrement importante pour ce type de prétraitement (Merklein *et al.*, 2016).

1.4.4 Méthodes biologiques

Les méthodes biologiques de prétraitement des BLC utilisent des micro-organismes. Leur action consiste à dégrader la lignine par des métabolites secondaires. Certaines bactéries, telles que *Cupriavidus basilensis* B-8 (Yan *et al.*, 2017), sont capables de jouer ce rôle, mais les meilleurs délignificateurs connus sont les champignons de la pourriture blanche et spécialement ceux de la division (phylum) des basidiomycètes. Il s'agit par exemple d'espèces de *Phanaerochate chryso sporium*, *Trametes versicolor*, *Lentinula edodes* et *Pleurotus ostreatus*. Les champignons de la pourriture blanche produisent des enzymes capables de délignifier les BLC pour faciliter l'accès aux carbohydrates (cellulose et hémicellulose). Ce processus de délignification s'observe

dans la nature sur le bois mort (**Figure 1.1**). Les méthodes biologiques sont très peu coûteuses, respectueuses de l'environnement, n'utilisent pas de produits chimiques, ne produisent pas d'inhibiteurs pour l'hydrolyse enzymatique subséquente, n'émettent pas d'effluents en fin de prétraitement et consomment peu d'énergie. C'est le cas de la biodégradation en fermentation solide. **Pour ces raisons, la biodégradation en milieu solide est considérée comme l'une des plus prometteuses de toutes les méthodes biologiques de prétraitement des BLC** (Ejaz & Sohail, 2021; Hadj Saadoun *et al.*, 2021; Karimi *et al.*, 2021). Les enzymes produites pendant le prétraitement peuvent être purifiées et commercialisées. Cependant, les méthodes biologiques sont celles qui ont les temps de prétraitement les plus longs (plusieurs jours, voire semaines). De plus, sous certaines conditions, les micro-organismes consomment pour leur métabolisme primaire, une partie des carbohydrates libérés par l'action des enzymes lignolitiques. La conséquence est la réduction des taux de récupération des carbohydrates.



Figure 1.1 Champignons de la pourriture blanche (basidiomycètes).

(A) *Phanerochaete chrysosporium*; (B) *Trametes versicolor*; (C) *Lentinula edodes*; (D) *Pleurotus ostreatus*; (E) *Pleurotus pulmonarius*; (F) *Inonotus hispidus*; (G) *Phellinus igniarius*; (H) *Ganoderma lucidum*; (I) *Ganoderma applanatum*; (J) *Bjerkandera adusta*; (K) *Irpex lacteus*; (L) *Phlebia radiata*.
(Peralta *et al.*, 2017).

1.5 Hypothèses, objectifs et originalité

1.5.1 Problématique

Le rapport 2021 sur l'inventaire des biomasses du ministère québécois de l'Énergie et des ressources naturelles fait état de 6 800 000 tonnes de bois et de 549 000 tonnes de biomasses agricoles végétales qui ne trouvent pas preneur chaque année (WSP, 2021b). Ces statistiques

portent uniquement sur la province de Québec. Au niveau du Canada, la quantité de ces résidus s'évaluerait à plusieurs dizaines de millions de tonnes. Pourtant, la biomasse lignocellulosique possède un potentiel énorme en termes de produits et sous-produits qu'il est possible d'en tirer. Résines, éthanol, bioplastiques, aérogels, composites fonctionnels et absorbants sont quelques-uns des nombreux produits et sous-produits qui peuvent être produits à partir des biomasses lignocellulosiques (Liu *et al.*, 2019). Le fait est que ce paradoxe (disponibilité en grande quantité d'une ressource très importante, mais sous-exploitée) cache une réalité sous-jacente. En effet, la valorisation de ce type de résidus, essentiellement lignocellulosique, est à peine, voire pas du tout économiquement rentable. La difficulté se situe au niveau de l'ajout indispensable de l'étape de prétraitement qui à elle seule monopolise environ 40% du coût total de la valorisation (Sindhu *et al.*, 2016). De ce point de vue, les cultures énergétiques demeurent toujours beaucoup plus attractives que les résidus lignocellulosiques. Cependant, les problèmes d'éthiques et de sécurité alimentaire que l'utilisation des cultures énergétiques pose interpellent sur la nécessité de changer de paradigme et d'opter pour les résidus lignocellulosiques plutôt que les cultures énergétiques. Cela exige de réduire les coûts et d'augmenter l'efficacité des méthodes de prétraitement des biomasses lignocellulosiques. En réalité, les coûts élevés de prétraitement sont directement liés à la récalcitrance du complexe lignocellulosique (cellulose-hémicellulose-lignine). À ce jour, des technologies de prétraitement des biomasses lignocellulosiques existent. Le fait est qu'elles allient rarement les quatre aspects essentiels suivant : **efficacité du traitement, faible coût, possibilité de mise à l'échelle et aspect écologique**. Par exemple, les liquides ioniques sont une technologie nouvelle et attractive du point de vue de l'efficacité du prétraitement pour la récupération des carbohydrates, mais sont coûteux et leur récupération après prétraitement requiert un lavage excessif à l'eau (Ovejero-Pérez *et al.*, 2021). La méthode de l'explosion à la vapeur améliore l'hydrolyse enzymatique des biomasses prétraitées, mais libère des composés toxiques, tels que le furfural et l'hydroxyméthylfurfural, qui sont des inhibiteurs des levures durant la fermentation éthanolique (Hoang *et al.*, 2023). C'est dans ce contexte que s'inscrit cette thèse dont l'objectif est de développer une **nouvelle approche de prétraitement des biomasses lignocellulosiques en combinant deux technologies prometteuses et complémentaires que sont l'extrusion et la biodégradation**.

1.5.2 Originalité de la recherche

L'originalité de la recherche réside dans le concept suivant : plutôt que d'utiliser un prétraitement unique, il s'agit dans cette thèse du couplage de deux technologies prometteuses sélectionnées sur la base de leur complémentarité et qui permettrait après couplage, de répondre aux questions

liées aux quatre (4) aspects essentiels du prétraitement évoqué plus haut à savoir **l'efficacité du prétraitement**, le **faible coût de prétraitement**, la **possibilité de la mise à l'échelle** et le **respect de l'environnement**. Le couplage consiste au prétraitement des BLC par la combinaison du prétraitement par extrusion suivi de la biodégradation par fermentation solide (Ex-SF). Ces deux technologies n'ont jamais fait l'objet de couplage pour le prétraitement de la biomasse lignocellulosique (cf. §4.8).

1.5.3 Hypothèses

1.5.3.1 Extrusion

Hypothèse 1 : L'optimisation des conditions d'extrusion devrait permettre une meilleure dégradation, une réduction significative de la taille des particules et une augmentation de leurs surfaces spécifiques ; l'hypothèse nulle (H_{1_0}) étant que l'optimisation des conditions d'extrusion n'a aucune incidence sur ces paramètres (taille, surface, dégradation).

L'[ANNEXE I](#) est une investigation de 20 travaux de référence utilisant l'extrusion comme une méthode de prétraitement des biomasses lignocellulosiques. Le tableau montre le potentiel de l'extrusion pour la récupération des sucres sur différentes biomasses et dans différentes conditions. L'efficacité du traitement à l'extrusion variait significativement entre les travaux selon les caractéristiques d'extrusion et les caractéristiques de la biomasse ([ANNEXE I](#)). Plusieurs études, dont celles de [Karunanithy and Muthukumarappan \(2010\)](#) et [Duque et al. \(2013\)](#), suggèrent que la capacité de l'extrusion à dégrader la biomasse lignocellulosique dépendrait de plusieurs paramètres dont la configuration des vis, la vitesse de rotation des vis, la température d'extrusion, la taille des particules de biomasse, le type et la quantité d'additif chimique. Certains paramètres seraient plus importants que d'autres. Ainsi, l'optimisation des conditions d'extrusion devrait permettre une meilleure dégradation des biomasses. De plus, l'extrusion est une méthode de prétraitement physique de la biomasse. L'optimisation des conditions d'extrusion devrait permettre d'améliorer significativement la réduction des tailles des particules de biomasse et augmenter leurs surfaces spécifiques (comparé aux extrusions sans optimisation).

Pour ce qui est du choix des biomasses lignocellulosiques, un résidu agricole (résidus de récolte de maïs) et un résidu forestier (résidus d'épinette noire non exploités de scierie) ont été considérés pour les travaux de cette thèse. La raison est que les résidus agricoles et les résidus forestiers possèdent des comportements rhéologiques différents durant l'extrusion. Elles possèdent des différences importantes dans leur structure lignocellulosique. Les résidus

forestiers sont généralement plus riches en lignine que les résidus agricoles. De ce fait, les résidus agricoles possèdent une structure moins rigide (c'est-à-dire plus flexible) que les résidus forestiers, mais sont plus volumineux.

1.5.3.2 Biodélicnification

Hypothèse 2 : L'optimisation des paramètres de fermentation et le choix d'espèces spécialisées dans la délicnification des BLC devraient permettre d'améliorer significativement la délicnification de la biomasse et ainsi améliorer l'hydrolyse enzymatique des bouillons de fermentation ; l'hypothèse nulle (H_{2_0}) étant que l'optimisation des paramètres de fermentation et le choix d'espèces n'a pas d'incidence sur la délicnification.

La biodélicnification par fermentation solide est une technologie prometteuse de prétraitement des biomasses lignocellulosiques pour les raisons énoncées au § 1.4.4. Toutefois, le succès de la biodélicnification est lié aux : (i) caractéristiques des biomasses dont la taille des particules et leur surfaces spécifiques et (ii) les conditions de fermentation (Suryadi *et al.*, 2022). L'étape d'extrusion devrait permettre de réaliser une délicnification partielle de la biomasse tout en réduisant significativement la taille des particules et en augmentant leurs surfaces spécifiques. Quant aux conditions de fermentation, l'optimisation des paramètres de fermentation et le choix de espèces spécialisées dans la délicnification des BLC devraient permettre d'améliorer significativement la délicnification de la biomasse et ainsi augmenter l'hydrolyse enzymatique des bouillons de fermentation. Les champignons de la pourriture blanche, spécialement ceux de la division des basidiomycètes, regroupent à ce jour les meilleures souches pour la biodélicnification (Blanchette, 1991; Li *et al.*, 2022). Ainsi, l'utilisation dans des conditions optimales de basidiomycètes ayant un fort potentiel de délicnification devrait améliorer l'efficacité de la biodélicnification sur une biomasse extrudée ; l'extrusion ayant pour effet d'augmenter significativement la surface spécifique de la biomasse pour permettre un accès maximal aux enzymes lignolitiques.

1.5.3.3 Mise à l'échelle

Hypothèse 3 : Il serait possible de mettre à l'échelle le couplage extrusion-fermentation solide (Ex-SSF) pour la délicnification des BLC. L'hypothèse nulle (H_{3_0}) étant que le procédé Ex-SSF ne peut pas être mis à l'échelle de manière efficace (viabilité technologique et économique) pour la délicnification des biomasses lignocellulosiques (BLC).

Il existe dans le commerce des extrudeuses et des fermenteurs de différentes tailles. Pris individuellement, l'extrusion et la fermentation solide sont deux méthodes qui sont possibles de mettre à l'échelle (Balakrishnan *et al.*, 2021) (Nastaj & Wilczyński, 2021). La littérature regorge d'études de mise à l'échelle d'extrusion pour diverses applications, telles que la production de produits pharmaceutiques (Wesholowski *et al.*, 2019). Il n'existe pas spécifiquement à ce jour d'études de mise à l'échelle de l'extrusion avec pour objectif la délignification de BLC. La mise à l'échelle reste faisable sur la base des modèles existants. Pour la biodégradation, on retrouve aussi dans la littérature des mises à l'échelle de fermentation solide pour divers objectifs, tels que la production d'enzymes, de PHA (polyhydroxyalkanoate), etc. (Martínez-Avila *et al.*, 2022). De plus, il n'existe pas spécifiquement d'études de mise à l'échelle de la fermentation solide comme méthode de délignification des biomasses lignocellulosiques, la mise à l'échelle reste faisable (au moins extensivement avec plusieurs réacteurs de faible volume). Il serait ainsi possible de mettre à l'échelle le couplage extrusion-fermentation solide (Ex-SSF) pour la délignification des BLC.

1.5.4 Objectifs

L'objectif général de cette thèse est d'augmenter la digestibilité enzymatique des biomasses lignocellulosiques (agricoles et forestières) avec une approche combinant deux procédés de prétraitement des biomasses, économiques et respectueux de l'environnement.

Cette thèse poursuit sept (7) objectifs consécutifs qui sont :

- ❖ **Objectif 1** : Explorer l'extrusion comme méthode de prétraitement des biomasses lignocellulosiques pour : (1) identifier le potentiel, (2) étudier les paramètres de prétraitement et les relations qui existent entre elles (Article 1) ;
- ❖ **Objectif 2** : Identifier et analyser les couplages de prétraitement existants et impliquant l'extrusion afin de proposer une approche novatrice et adaptée de prétraitement au regard des résultats de cette analyse (Article 2) ;
- ❖ **Objectif 3** : Explorer la biodégradation par fermentation comme méthode de prétraitement des biomasses lignocellulosiques afin de : (1) identifier son potentiel, (2) étudier les agents biologiques susceptibles de performer et (3) déterminer les conditions de prétraitement (Article 3) ;
- ❖ **Objectif 4** : Analyser et optimiser les paramètres de prétraitement de deux biomasses lignocellulosiques (un résidu agricole et un résidu forestier) par extrusion pour enlever une

fraction de la lignine tout en réduisant la rigidité de la structure des biomasses sans générer d'inhibiteurs (Article 4) ;

- ❖ **Objectif 5** : Optimiser les conditions de biodégradation par fermentation solide en fioles et en bioréacteurs de 5 litres des différentes biomasses prétraitées par extrusion (Article 5) ;
- ❖ **Objectif 6** : Réaliser des essais d'hydrolyse enzymatique des préhydrolysats (BLC prétraitée) obtenus après le couplage de prétraitements (Article 5) ;
- ❖ **Objectif 7** : Effectuer une analyse technico-économique afin d'identifier sommairement le potentiel et les conditions de rentabilité de l'approche de prétraitement développée dans le contexte canadien (en général) et québécois (en particulier) (Article 6).

2 MATÉRIEL ET MÉTHODES

Ce chapitre présente la méthodologie suivie pour effectuer les recherches expérimentales de cette thèse. Elle est divisée en 6 sections consécutives. La première section (cf. § 2.1) est axée sur les biomasses brutes. Elle présente l'origine des **biomasses** et les préparations qu'elles ont subies avant utilisation. La deuxième section (cf. § 2.2) traite des **plans expérimentaux**. Les plans expérimentaux sont essentiels dans cette thèse. Ils sont utilisés tout au long de la thèse pour optimiser les conditions de prétraitement des biomasses. Dans cette section, l'utilité des plans d'expérience est présentée, suivi de la méthodologie de construction des plans d'expériences utilisés dans cette thèse. La troisième section (cf. §2.3) concerne les opérations réalisées étape par étape pour prétraiter les biomasses à l'**extrusion**. Elle couvre les opérations sur la biomasse avant extrusion, les opérations réalisées pendant la conduite des extrusions et les opérations post-extrusion. La quatrième section (cf. § 2.4) regroupe les **méthodes analytiques** qui ont permis d'analyser les caractéristiques des biomasses brutes et les biomasses extrudées. Ce sont au total six analyses. La cinquième section (cf. § 2.5) est celle qui regroupe toutes les opérations et analyses effectuées dans le cadre de la **biodélicnification** des extrudats de biomasse. Tout comme la troisième section, les méthodologies de cette section sont présentées par ordre d'opérations depuis le choix des souches jusqu'à la caractérisation des biomasses fermentées. La sixième section (cf. § 2.4) présente la méthodologie employée pour effectuer les **hydrolyses enzymatiques** des biomasses après prétraitement. La dernière section (cf. § 2.7) présente la démarche suivie pour l'analyse technico-economique succincte du procédé développé dans cette thèse.

2.1 Biomasses

2.1.1 Biomasses lignocellulosiques

Les biomasses lignocellulosiques utilisées dans cette étude sont : (1) les résidus secs de récolte de maïs constitués d'un mélange de feuilles, tiges et épis fournis par la compagnie Agrosphère Inc et (2) les résidus (copeaux) secs d'épinette noire fournis par la scierie Savard et fils. Le maïs est la principale culture produite au Québec, tandis que l'épinette noire (*Picea mariana*) est l'une des principales espèces d'arbres de la forêt boréale du Québec. À la réception, ces résidus avaient des tailles de particules comprises entre 2 et 5 mm (**Figure 2.1**).



Figure 2.1 Copeaux d'épinette noire (A) et résidus de maïs (B).

2.1.2 Préparation des biomasses pour l'extrusion

Les biomasses reçues ont été réduites en taille de particule de 1 mm et de 1,5 mm à l'aide d'un broyeur Cutting Mill Pulverisette 15 (Fritsch, Allemagne) équipé de différents types de tamis (Figure 2.1). Les tailles de particule de 1 mm et de 1,5 mm ont été obtenues respectivement à l'aide des tamis de 1 mm et 1,5 mm.

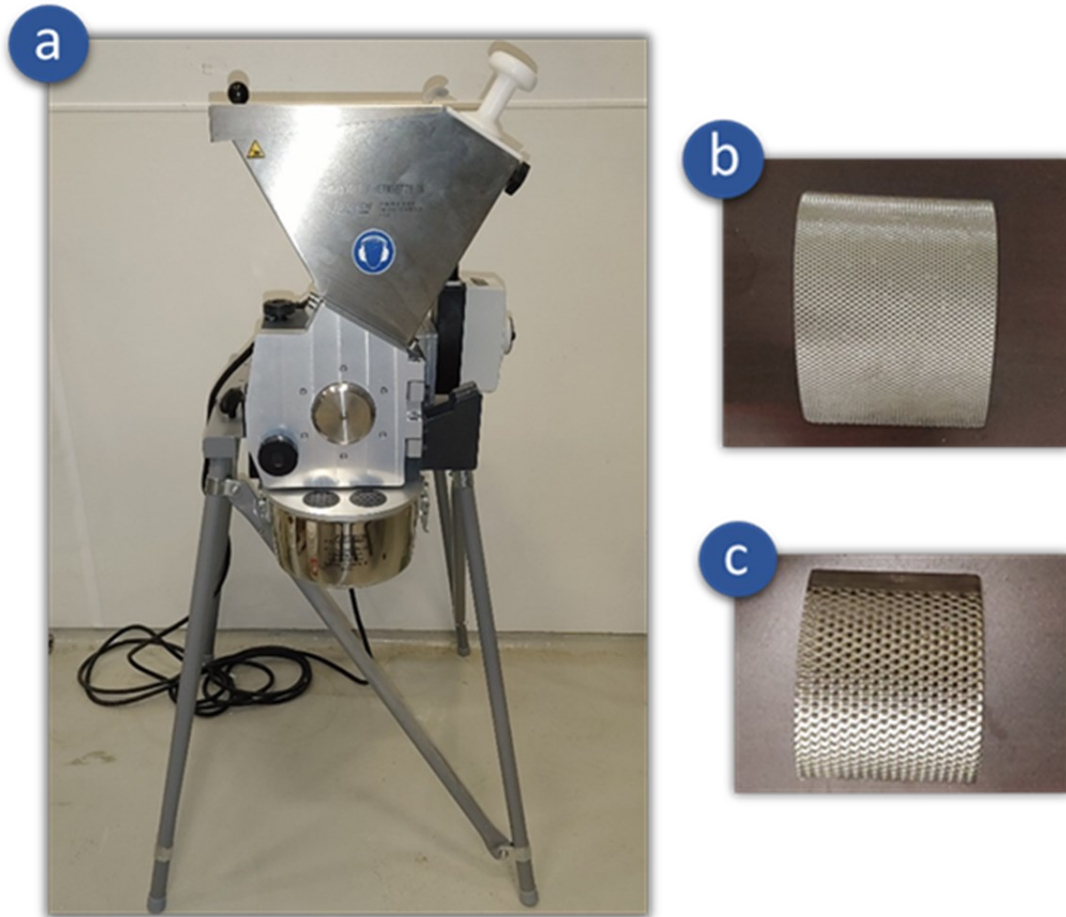


Figure 2.2 Broyeur (a), tamis de 1 mm (b) et tamis de 1,5 mm (c).

2.2 Plan d'expérience d'extrusion

2.2.1 Utilité des plans d'expériences

Les plans d'expériences permettent de modéliser de manière fiable et robuste un phénomène, un processus, un procédé ou une réponse sur la base d'un nombre réduit d'essais. L'avantage associé est l'économie de temps, d'énergie et d'argent. Les plans d'expérience sont beaucoup utilisés dans l'industrie. On utilise généralement un plan d'expérience pour l'une ou l'autre des trois raisons suivantes : (i) la comparaison ou la caractérisation, (ii) le *screening* et (iii) l'optimisation. On utilise un plan de comparaison ou de caractérisation lorsqu'on souhaite prouver ou démontrer l'importance qu'un paramètre possède sur la réponse indépendamment de l'existence d'autres paramètres importants. Le *screening* sert à identifier parmi un grand nombre de paramètres, les paramètres qui ont la plus grande influence sur la réponse. L'optimisation est de loin la plus répandue de toutes, car elle permet de trouver le ou les configurations optimales

des paramètres en fonction du niveau de réponse voulu. Dans la pratique, l'optimisation est souvent précédée d'un *screening*.

2.2.2 Choix du plan d'expérience

Il existe plusieurs types de plan d'expérience qui permettent d'optimiser une réponse, mais le plan central composé (CCD) et le Box-Behnken, tous deux basés sur la méthodologie des surfaces de réponse (RSM), sont les plus utilisés. Le CCD est utilisé dans le cadre de cette thèse. Il offre la possibilité de rajouter par la suite, en fonction des résultats obtenus, plusieurs niveaux par facteur et la possibilité d'explorer au-delà de l'espace expérimental initial.

2.2.2.1 Identification des paramètres et espace expérimental

A) Identification des paramètres

Le Chapitre 3 va permettre d'identifier les quatre paramètres majeurs qui influencent l'efficacité de l'extrusion sur la lignine dans les biomasses. Il s'agit de trois paramètres numériques (c'est-à-dire pouvant prendre des valeurs numériques continues) et d'un paramètre catégorique ordinal (c'est-à-dire prenant des valeurs numériques discrètes). Ce sont : (i) la température, (ii) la vitesse de rotation des vis et (iii) la concentration de NaOH pour les paramètres numériques, ainsi que (iv) la taille des particules pour le paramètre catégorique.

B) Détermination de l'espace expérimental

Pour chacun des paramètres numériques, il a été déterminé un niveau haut (maximum ou +1) et un niveau bas (minimum ou -1) (**Tableau 2.1**). Ces limites inférieures et supérieures déterminent **l'espace expérimental**. **Cet espace a été déterminé à la suite de plusieurs séries d'essais préliminaires d'extrusion. De ces essais préliminaires, il en est ressorti les observations suivantes :**

- Les conditions d'extrusion des résidus de maïs différaient de celles des résidus d'épinettes noires notamment au niveau des limites de **vitesse de rotation des vis** et de la **température** ; d'où la différence d'espace expérimental observée pour les deux biomasses dans le **Tableau 2.1**.

- L'extrusion avec une filière¹ était impossible avec les résidus d'épinette en raison du blocage de la biomasse au niveau de la filière. Les extrusions ont donc toutes été conduites sans filière par la suite.
- Pour l'extrusion avec la mini-extrudeuse utilisée, l'alimentation manuelle était préférable à l'alimentation automatique pour deux raisons principales : (i) pour avoir plus de contrôle sur la stabilité de l'extrusion et (ii) pour minimiser le nombre de tests car la vitesse d'alimentation de la biomasse deviendrait un paramètre à part entière à investiguer or moins important sur la réponse (la délignification) (Chapitre 3).
- Le rapport biomasse:solution (2:1) fut le mélange optimal pour les extrusions des deux types de biomasses. Au-delà, il était difficile d'extruder la biomasse soit parce que le torque excédait la limite de l'extrudeuse quand la biomasse est trop consistante, soit la biomasse se comportait comme un liquide et ne pouvait être extrudée.

Tableau 2.1 Espace expérimental des extrusions des résidus de maïs et d'épinette noire.

Paramètres	Dimension	Niveau bas (-1)	Niveau haut (+1)
Résidus de maïs			
Taille des particules	mm	1	1,5
Température	°C	40	110
Vitesse de rotation	rpm	80	300
[NaOH]	%	0	15
Épinette noire			
Taille des particules	mm	1	1,5
Température	°C	50	100
Vitesse de rotation	rpm	150	300
[NaOH]	%	0	15

2.2.2.2 Table des essais

Sur la base de l'espace expérimental, le logiciel Design Expert 13 a permis de générer la table randomisée des essais par type de biomasse (2 types) et par taille des particules (2 tailles). Pour

¹ Filière : Pièce placée au bout de l'extrudeuse pour forcer la forme de l'extrudat à la sortie.

chaque biomasse, deux (2) tables de 17 essais ont été générées. Les 17 essais sont répartis comme suit : 8 essais factoriels, 6 essais axiaux et 3 essais centraux soit 68 tests au total pour les deux biomasses. Le **Tableau 2.2** présente la table des tests des résidus de maïs pour 1 mm de taille de particule. La concentration de NaOH à 0% dans la table correspond à de l'eau.

Tableau 2.2 Table des tests des résidus de maïs pour 1 mm de taille de particule.

Test	Type d'essai	Vitesse de rotation	Température	NaOH
		rpm	°C	% m/m
1	Centre	190	80	7,5
2	Axial	190	110	7,5
3	Factoriel	300	110	15
4	Centre	190	80	7,5
5	Axial	190	50	7,5
6	Axial	300	80	7,5
7	Factoriel	80	110	0
8	Axial	190	80	0
9	Centre	190	80	7,5
10	Factoriel	300	50	0
11	Axial	190	80	15
12	Factoriel	80	110	15
13	Factoriel	80	50	15
14	Factoriel	300	110	0
15	Axial	80	80	7,5
16	Factoriel	300	50	15
17	Factoriel	80	50	0

2.3 Extrusion

2.3.1 Mélange de biomasses et d'additif chimique

L'extrudeuse ne possédant pas de pompe/port pour l'injection de liquide, l'additif (les solutions d'hydroxyde de sodium) a été mélangé à la biomasse peu avant l'extrusion dans la proportion biomasse:additif de 2:1 (m/m). Par exemple, 500 g de biomasses étaient mélangés à 250 g de solution d'hydroxyde de sodium (7,5 % ou 15 %). Afin d'éviter des biais, la quantité de biomasses nécessaire à une série d'extrusion étaient calculée et préparée en une seule fois. De plus, les essais ont été conduits dans un ordre aléatoire. Après un essai, les paramètres étaient ajustés pour l'essai suivant. Après que les paramètres de l'extrudeuse avaient été stabilisés, il était laissés pour 1 à 3 min d'extrusion selon la vitesse de rotation des vis avant de commencer à collecter l'extrudat.

2.3.2 Conduite des extrusions

Les essais d'extrusion ont été réalisés à dans les laboratoires de l'UdS à l'aide d'une mini-extrudeuse bis-vis de 11 mm de diamètre (Process 11, Thermo Scientific™, MA, USA) équipée d'un panneau de contrôle numérique facilitant le contrôle des paramètres de température et de vitesse de rotation (**Figure 2.3**). Les biomasses ont été soumises à différentes conditions de prétraitement à l'extrusion avec et sans ajout d'une solution d'hydroxyde de sodium (NaOH) à différentes concentrations conformément au **Tableau 2.2**. Le choix de NaOH se justifie par le fait qu'il est plus accessible, moins coûteux que les autres alternatives, facilement neutralisable au besoin, ne produit pas d'inhibiteurs et est efficace pour solubiliser la lignine. Avant de procéder aux tests d'extrusion, les vis et le baril de l'extrudeuse étaient nettoyés avec du polyéthylène de basse densité (LDPE) dans le but d'éliminer toutes contaminations éventuelles qui pourraient résulter de précédentes utilisations de l'extrudeuse. Les biomasses ont ainsi été extrudées dans différentes conditions suivant un plan d'expérience. Les extrudats ont ensuite fait l'objet de différentes analyses en vue d'étudier l'impact de l'extrusion sur les biomasses et d'optimiser l'efficacité de cette première étape de prétraitement.

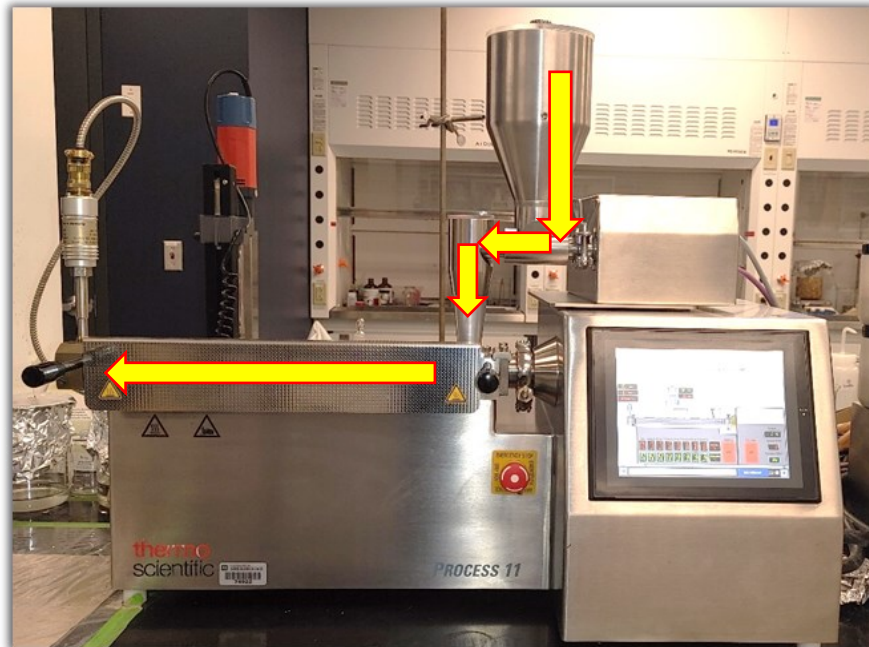


Figure 2.3 Extrudeuse bis-vis de 11 mm de diamètre.

Au cours des extrusions, le torque et la pression étaient surveillés. Les extrudats des résidus de maïs étaient recueillis sous la forme de filons à cause de la filière, tandis que les résidus d'épinette noire étaient recueillis sous la forme de fine poudre (**Figure 2.4**). Quand survenait un arrêt de

l'extrudeuse lors d'un essai (souvent par suite d'une surcharge des vis), le collecteur d'échantillon était immédiatement retiré. L'extrudeuse était remise en route avec les paramètres de l'essai et laissée en fonctionnement jusqu'à stabilisation pour évacuer la biomasse restée à l'intérieur du baril. La collecte de l'échantillon reprenait ensuite. Une fois que la quantité d'échantillons voulue était collectée, les paramètres étaient ajustés pour le prochain essai et l'opération reprenait.

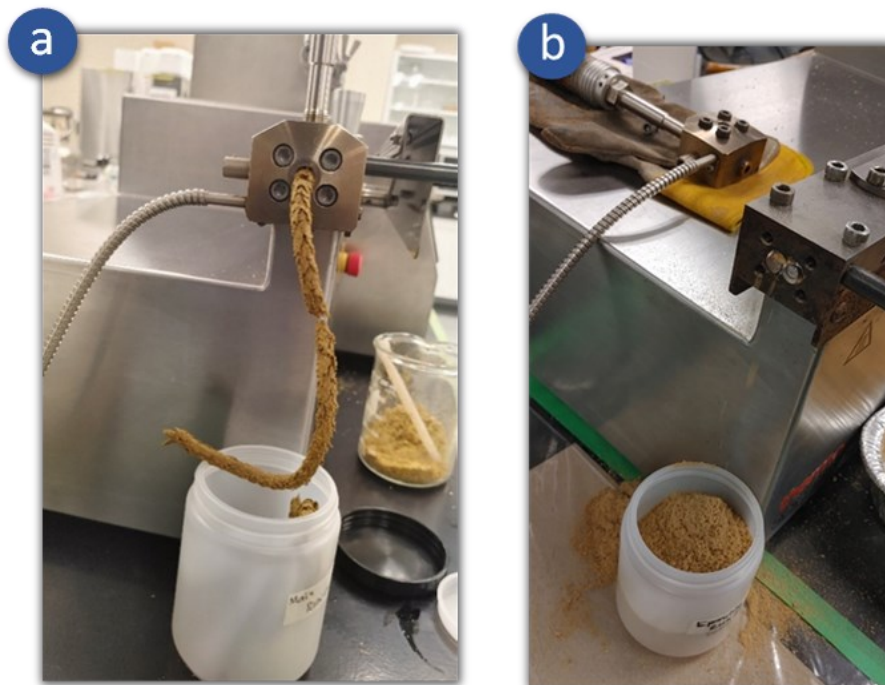


Figure 2.4 Biomasse à la sortie de l'extrudeuse : (a) résidus de maïs et (b) épinette noire.

2.3.3 Lavage des extrudats

L'objectif de cette étape était double. Il s'agissait d'une part de réduire la concentration de NaOH qui, à forte dose, peut influencer négativement la fermentation. D'autre part, l'objectif du lavage était d'extraire les produits de la dégradation de la lignine (les monolignols et leurs dérivés).

Pour chaque type de biomasse (résidus de maïs et résidus d'épinette), vingt échantillons ont été lavés. Il s'agissait des 17 extrudats du plan expérimental, d'un échantillon de biomasse brute, d'un échantillon de biomasse brute préparé avec la solution NaOH à 7,5 % et d'un échantillon de biomasse brute préparée avec la solution NaOH à 15 %. Pour chaque échantillon, 5 g de biomasse ont été imprégnés dans 50 ml d'eau distillée. Durant cette étape, une partie de la lignine est solubilisée. Le mélange était ensuite lavé à l'aide d'un dispositif à pompe et le filtrat était recueilli dans un flacon pour être conservé à -4°C (Figure 2.5). Quant à la fraction solide, elle

était recueillie dans un bécher et séchée à l'étuve à 60 °C pendant plusieurs heures avant d'être collectée dans des sacs plastiques et conservée à température ambiante.



Figure 2.5 Dispositif de lavage.

2.4 Caractérisation de la biomasse après l'extrusion

2.4.1 Taille des particules

La distribution de la taille des particules a été obtenue à l'aide de l'analyseur de taille de particule LA950 (HORIBA, Kyoto, Japon). Cet analyseur utilise la diffraction laser pour caractériser la distribution granulométrique d'une large gamme de produits dont les sédiments, les poudres, des suspensions et des émulsions. Les particules diffusent la lumière selon un angle qui est inversement proportionnel à leur taille. Pour analyser les tailles des particules de biomasses, 2 g de biomasse sont introduits dans l'équipement qui contient de l'eau en circulation. L'eau permet de mettre les particules de biomasse en mouvement. Des rayons laser sont projetés sur les particules en mouvement et des capteurs permettent de recueillir la lumière diffractée. Cette information est traduite en signal lisible par le logiciel intégré, puis convertie en donnée de distribution des tailles de particule. Des étapes intermédiaires, comme l'ultrasonication pour la dispersion efficace des particules, permet d'assurer la qualité des résultats.

2.4.2 Taux d'humidité de la biomasse

L'humidité des biomasses brutes et des extrudats a été déterminée à l'aide d'un analyseur d'humidité (HR83 Halogen, Mettler Toledo, USA). Environ 0,5 g de biomasse était introduit dans

l'appareil et chauffé à 105 °C jusqu'à ce que la masse de l'échantillon soit constante. L'humidité est alors calculée selon la formule suivante :

Équation 2.1 - Humidité

$$\%Humidité = \frac{100 (0,5 - m_{105})}{0,5}$$

m_{105} = masse de l'échantillon à 105 °C.

2.4.3 Composition de la biomasse et taux de délignification

La caractérisation de la composition de la biomasse, c'est-à-dire la détermination des pourcentages en cellulose, hémicellulose, lignine, extractibles et cendres, a été réalisée selon la méthode globale gravimétrique de Van Soest ([Van Soest et al., 1991a](#)). Les analyses étaient réalisées en dupliqua. Le taux de délignification est calculé à partir de la différence entre le pourcentage de lignine de la biomasse brute, ainsi que le pourcentage de lignine de l'extrudat après lavage. L'équation du taux de délignification est donnée par :

Équation 2.2 – Taux de délignification

$$\% \text{ délignification} = 100 \left(1 - \frac{\% \text{ lignine de l'extrudat après filtration}}{\% \text{ lignine avant extrusion}} \right)$$

2.4.4 Spectroscopie infrarouge à transformation de Fourier (FTIR)

La FTIR a été utilisée dans le but d'étudier les changements dans la composition des biomasses avant et après les prétraitements. Un appareil Nicolet iS50 FT-IR (Jasco, OK, USA) a servi pour l'acquisition des spectres dans la plage de longueur d'onde 400 – 4 000 cm^{-1} et les données ont été analysées dans le logiciel Origin.

2.4.5 Microscopie électronique à balayage (MEB)

L'aspect des biomasses prétraitées a été examiné avant et après extrusion à l'aide d'un microscope électronique à balayage (MEB) Zeiss EVO® 50 smart SEM (Allemagne), permettant une observation micrométrique de la morphologie des échantillons grâce à un faisceau d'électrons. Avant l'analyse, les échantillons ont été recouverts d'une fine couche de platine par pulvérisation cathodique sous vide (Leica Microsystems, Canada) afin d'améliorer leur conductivité et d'éviter l'accumulation de charges électrostatiques, garantissant ainsi des images

nettes et précises. L'observation a été effectuée sous différents grossissements et distances de travail, en utilisant un détecteur d'électrons secondaires 1 (SE 1) pour capturer les détails topographiques avec un contraste optimal. Une tension extra-haute (EHT) de 10 kV a été appliquée afin d'améliorer la pénétration du faisceau d'électrons et d'optimiser la résolution des images, facilitant ainsi l'analyse des modifications structurales des biomasses avant et après extrusion.

2.4.6 Chromatographe en phase gazeuse/spectromètre de masse (GC/MS)

L'objectif du GC/MS était d'identifier la présence d'inhibiteurs potentiellement générés par le prétraitement à l'extrusion. Il s'agissait principalement du furfural et de l'hydroxyméthylfurfural (HMF). Ces deux composés proviennent de la dégradation (déshydratation) sous hautes températures de pentoses et d'hexoses respectivement. La recherche de furfural et de HMF dans les filtrats obtenus après lavage s'est faite au GC/MS à l'aide d'un Clarus 500 (Perkin Elmer, USA). Après l'optimisation des conditions d'extrusion, 2 g de biomasse ont été prélevés de l'extrudat et mélangés avec 40 g d'eau déionisée dans un bécher de 250 mL. Le mélange a été soigneusement homogénéisé et légèrement chauffé pendant 5 minutes sur une plaque chauffante équipée d'un agitateur magnétique. Après 5 minutes, le mélange a été filtré à l'aide d'un papier filtre Whatman de 45 µm. Le filtrat a été recueilli puis injecté dans un chromatographe en phase gazeuse couplé à un spectromètre de masse Clarus 500 (Perkin Elmer, Shelton, CT, USA). L'injection de l'échantillon a été réalisée en mode splitless, avec une température de l'injecteur de 250 °C, une durée splitless de 0,75 minute, et un volume d'injection de 0,7 µL. L'eau a été utilisée comme solvant de rinçage pour les injecteurs A et B. La séparation chromatographique a été effectuée sur une colonne RTX-WAX (30 m × 0,25 mm × 0,25 µm), avec un débit constant d'hélium de 1,5 mL/min utilisé comme gaz vecteur. La température initiale du four a été fixée à 70 °C. La détection des composés a été réalisée en mode SCAN, avec une gamme de masse de 35 à 350 m/z, une température de ligne de transfert de 250 °C, et une température de la source d'ions de 260 °C.

2.5 Biodégradation

2.5.1 Choix des souches

Phanerochaete chrysosporium (souche *P. chrysosporium* A-381 ATCC 48746) a été choisie sur la base de son potentiel pour la dégradation. Cette souche est parmi les rares à posséder un système lignolitique complet composé des trois enzymes majeures (lignine peroxidases,

manganèse peroxydases et laccases). C'est une souche disponible commercialement et relativement tolérante aux contaminations. C'est aussi une des principales espèces de biodégradeurs pour lesquelles on dispose de données dans la littérature.

2.5.2 Culture des souches

Dès réception des ampoules contenant les souches de *Phanerochaete chrysosporium* A-381 (ATCC 48746), elles ont été conservées à 4 °C. La revitalisation des souches s'est faite de la manière suivante : un volume d'un ml d'eau distillée stérilisée est introduit dans l'ampoule et mélangé pour former une suspension. La suspension est transvasée dans 3 tubes Eppendorf contenant quelques millilitres d'eau distillée stérile. Les tubes sont conservés à température ambiante pendant 4 heures pour permettre la réhydratation des souches. Une fois cette étape complétée, les souches sont cultivées d'abord sur milieu PD (Potato Dextrose) pendant 4 à 7 jours dans un incubateur agitateur à 180 rpm et 30 °C. Une partie du mycélium obtenu est déposée sur un milieu gélosé en boîte de pétri. Le milieu gélosé comprenait 3 g d'extrait de levure, 3 g extrait de malt, 10 g de dextrose, 5 g peptone, 20 g agar et 1000 ml eau distillée. Après 2 à 3 jours de croissance du mycélium, il est recueilli dans des tubes Eppendorf contenant du glycérol et conservés à -4 °C.

2.5.3 Préparation des substrats

La préparation des substrats a consisté à les stériliser à l'autoclave avant le démarrage des fermentations. Quoique les deux souches soient relativement résistantes aux contaminations, la stérilisation des substrats permet d'éviter les risques ou variations liés à des effets de synergisme, de symbiose ou de commensalisme avec des contaminants biologiques (bactéries, champignons, etc.).

2.5.4 Préparation de l'inoculum

Le mycélium d'un tube Eppendorf est cultivé sur boîte de pétri pendant 5 jours pour la germination des spores. La récolte des spores s'est faite comme suit : 20 ml d'eau distillée stérilisée sont déposés sur la surface des boîtes de pétri. La surface est ensuite délicatement ratissée pour décoller les spores. La quantité de spores dans la suspension est estimée entre 2×10^6 et 5×10^6 spores/ml.

2.5.5 Conduite des fermentations

L'étape de biodégradation s'est déroulée dans des bioréacteurs de 250 ml, puis de 5 litres. La biomasse stérilisée était introduite dans le bioréacteur et inoculée selon les conditions du plan d'expérience. Tout au long de la fermentation, on prélève régulièrement des échantillons pour la détermination de la composition de la biomasse (taux de cellulose, d'hémicellulose et de lignine), le calcul du taux de dégradation et pour évaluer l'activité des enzymes lignolitiques.

2.5.6 Centrifugation

L'objectif de la centrifugation était de séparer les phases solides et liquides d'échantillons. Dans le cas de la préparation d'échantillons pour les analyses au spectrophotomètre par exemple, la biomasse fermentée était transférée dans une fiole agitée de 250 ml de volume contenant 35 ml d'eau distillée et placée dans un incubateur à agitation à 37 °C et 180 rpm pendant 24 h. Le contenu était ensuite filtré avec un papier Whatman 45 µm, puis centrifugé à 3000 rpm et 10 °C pendant 10 min à l'aide d'une centrifugeuse (Allegra 6R Centrifuge, Beckman Coulter, USA).

2.5.7 Caractérisation des biomasses et taux de dégradation

Les échantillons fermentés ont été séchés au four à 60 °C pendant 4 heures avant d'être soumis à l'extraction Soxhlet pendant 12 cycles pour éliminer le mycélium. Le solvant utilisé était un mélange d'éthanol et de benzène à un ratio 2:1 v/v. La fraction solide après extraction a été laissée à température ambiante pour séchage et évaporation du solvant. La biomasse a ensuite été lavée avec de l'eau chaude du robinet par filtration pour éliminer le solvant restant. La caractérisation et le calcul du taux de dégradation après ces étapes étaient les mêmes que celles décrites au cf. § 2.4.3.

2.6 Hydrolyse enzymatique

Des tests d'hydrolyse enzymatique ont été réalisés sur les biomasses brutes et les biomasses soumises à une extrusion suivie de fermentation. Le protocole d'hydrolyse enzymatique était basé sur ceux de [Danisco \(2007\)](#) et [Miller \(1959b\)](#). Un échantillon de 15 g de biomasse était séché au four à 50 °C pendant 24 h pour obtenir une siccité supérieure à 95 %. Une quantité de 12,5 g de cet échantillon était placée dans une fiole de 500 ml contenant 3,125 ml d'enzyme, 100 ml de tampon citrique (0,05 M), 0,5 ml de tétracycline et 0,4 ml de cycloheximide. Le pH du mélange était de 4,8. Un cocktail enzymatique, l'Accellerase Duet (Danisco, Danemark), était ajouté au mélange et introduit dans un incubateur-agitateur à 55 °C et 180 rpm pendant 96 h. Une aliquote

était prélevée toutes les 24 h et conservée à -4 °C. Les analyses de sucres réducteurs dans les échantillons se sont faites suivant la méthode de [Miller \(1959b\)](#) utilisant du DNS (acide dinitrosalicylique) et la lecture au spectrophotomètre à 540 nm.

2.7 Analyse technico-économique préliminaire

L'analyse technico-économique réalisée dans le cadre de cette étude est basée sur le guide technique du NREL sur l'analyse technico-économique de la production du bioéthanol à partir des biomasses lignocellulosiques ([Aden et al., 2002](#)). Bien que des co-produits autres que le bioéthanol puissent être intégrés dans le processus de bioraffinage, dans le cadre de cette étude préliminaire, seul le bioéthanol est envisagé comme bioproduit. Les résidus de maïs et les résidus d'épinette noire constituaient les matières premières. L'étude a été circonscrite à la province du Québec. Le procédé Ex-SSF a été introduit dans un modèle classique d'une plateforme de production de bioéthanol à partir des résidus lignocellulosiques. Ce modèle comprenait sept (7) zones différentes à savoir : réceptions et stockage des matières premières (zone 100), prétraitement des biomasses par le procédé Ex-SSF (zone 200), saccharification et fermentation éthanolique (zone 300), distillation et déshydratation (zone 400), stockage du bioéthanol (zone 500), traitement des effluents (zone 600) et production d'électricité et de vapeur (zone 700). Pour évaluer la rentabilité d'une telle plateforme, trois scénarios réalistes d'exploitation d'une bioraffinerie dans le contexte Québécois ont été identifiés. Le premier scénario (S1) était celui d'un producteur de grain de maïs. Le deuxième scénario (S2) était celui d'une coopérative agricole de maïs, et le troisième (S3) celui d'un entrepreneur indépendant. Pour chaque scénario, le choix des installations et le dimensionnement de ces installations ont été effectués à partir des données du guide NREL (listes d'équipements, formules, coefficients, etc.) et des données de littérature. Les coûts d'investissement (CAPEX) et de fonctionnement (OPEX) ont été évalués à partir de prix actualisés disponibles en ligne et/ou provenant de catalogues spécialisés. L'analyse économique des différents scénarios s'est faite en étudiant le coût d'investissement par unité de capacité de la bioraffinerie (CAPEX/Plant capacity) et les coûts de fonctionnement par unité de matière première (OPEX/Feedstock quantity).

3 PREMIER ARTICLE

An overview of extrusion as a pretreatment method of lignocellulosic biomass

Un aperçu de l'extrusion comme méthode de prétraitement des biomasses lignocellulosiques

Delon Konan ¹, Ekoun Koffi ², Adama Ndao ¹, Eric Charles Peterson ^{1,3}, Denis Rodrigue ⁴ and Kokou Adjallé ^{1,*}

1. Centre Eau, Terre, Environnement (ETE), Institut National de la Recherche Scientifique (INRS), 490 Rue de la Couronne, Québec City, QC G1K 9A9, Canada; behibro_angedelon.konan@inrs.ca (D.K.); adama.ndao@inrs.ca (A.N.); eric.peterson@sifbi.a-star.edu.sg (E.C.P.)

2. Département de Génie Mécanique et Énergétique, Institut National Polytechnique Felix Houphouët Boigny (INPHB), Yamoussoukro, P.O. Box 1093 Yamoussoukro, Côte d'Ivoire; ekoun.koffi@inphb.ci

3. Singapore Institute of Food and Biotechnology Innovation (SIFBI), Agency for Science Technology and Research (A*STAR), 31 Biopolis Way, Singapore 138669, Singapore.

4. Département de Génie Chimique, Université Laval, Pavillon Adrien-Pouliot, 1065 Avenue de la Médecine, Québec City, QC G1V 0A6, Canada; denis.rodrigue@gch.ulaval.ca

*Correspondence: kokou.adjalle@inrs.ca

***Energies*, 2022, 15(9), 3002.**

Submission received: 26 March 2022 / Revised: 13 April 2022 / Accepted: 18 April 2022 / Published: 20 April 2022

DOI : <https://doi.org/10.3390/en15093002>

Contribution des auteurs :

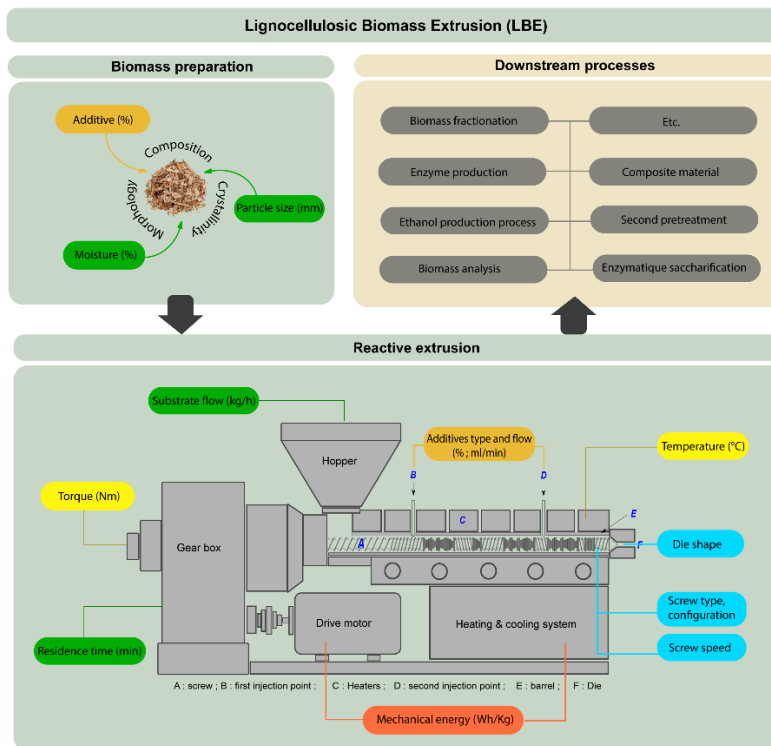
Conceptualization, Writing-Original Draft: Delon Konan; Writing-Review & Editing: Delon Konan, Ekoun Koffi, Adama Ndao, Eric Charles Peterson, Denis Rodrigue, Kokou Adjallé; Supervision: Kokou Adjallé.

3.1 Abstract

Lignocellulosic biomass is both low cost and abundant, and unlike energy crops, can escape associated ethical dilemmas such as arable land use and food security issues. However, their usage as raw material in a biorefinery implies an inherent upstream pretreatment step to access compounds of interest derived from lignocellulosic biomass. Importantly, the efficiency of this step is determinant for the downstream processes, and while many pretreatment methods have been explored, extrusion is both a very flexible and promising technology. Extrusion is well-known in both the polymer and pharmaceutical industries and has been used since the 18th century. However, as a pretreatment method for lignocellulosic biomass, extrusion is relatively new. The first use for this purpose dates back to the 1990s. Extrusion enjoys a high degree of flexibility due to the many available parameters, but an understanding of extrusion requires a knowledge of these parameters and the different relationships between them. In this paper, we present a concise overview of lignocellulosic biomass extrusion by reviewing key extrusion parameters and their associated extruder design components and operating conditions.

Keywords: biomass pretreatment; lignocellulosic biomass; extrusion; reactive extrusion

3.2 Graphical abstract



3.3 Introduction

Petroleum, its derivatives, and more generally fossil materials, have found deep-rooted applications in all sectors of modern life. Gasoline, kerosene, sanitizers, fertilizers, asphalt, textiles, cosmetics, pharmaceuticals, solvents, diluents, plastics, printing inks, vaseline, and rust removers are some of the products that have become an integral part of today's lifestyles (Al-Samhan et al., 2022; Gupta et al., 2022). Among all these products, those with energy applications (fuels) are of particular importance because they enter into the production process of almost everything produced on an industrial scale.

The problems associated with the use of fossil fuels are well known and their consequences on the environment are increasingly obvious. However, getting out of this dependence on fossil fuels means finding competitive alternatives. Among the renewable energies available today, lignocellulosic biomass is one of those capable of replacing fossil materials in many applications, including energy production (Braga & Faria, 2022; Liu et al., 2021; Peter et al., 2022; Reshmy et al., 2022). Long considered useless or of little interest, lignocellulosic biomass (LCB) is one of the most abundant resources on earth. Global lignocellulosic biomass production is estimated at

several billion dry tons per year. In Canada, lignocellulosic residues (forest and agricultural) are estimated between 64 and 561 million dry tons per year, and less than 30 million tons are used in the industry (Antar *et al.*, 2021).

LCB is an important source of renewable energy. However, many difficulties hinder its use as a raw material in the industry. LCBs must be pretreated before their utilization in a biorefinery process. The goal of this step is to deconstruct the lignocellulosic structure to get access to the desired compound (i.e., glucose, xylose, etc.). It is well documented that pretreatment is the limiting step in the biorefinery context (Hoang *et al.*, 2021; Xu *et al.*, 2021; Zhang *et al.*, 2021c), at least for two reasons. First, LCBs are recalcitrant to pretreatment. Lignocellulose is a complex matrix, and as the main constituent of plants cells walls, lignocellulose acts in nature as a defense system against microbial, chemical, and physical attacks. This matrix is mainly comprised of cellulose, hemicellulose, and lignin linked to each other by a diversity of strong and weak bonds (ester, ether, hydrogen, Van der Waals, etc.). The second reason is a corollary of the first since several pretreatments methods have been developed to address the complex nature of LCBs, but still need improvements regarding efficiency, cost, and environmental aspects.

LCB pretreatments are classified into four classes: (a) chemical, (b) physical, (c) biological, and (d) physicochemical (Galbe & Zacchi, 2007; Kumar *et al.*, 2009) (Kumar *et al.*, 2009). Class (a) pretreatments include acid hydrolysis, alkaline hydrolysis, ozonolysis, organosolvation, oxidative delignification, ionic liquids, deep eutectic solvents, and natural deep eutectic solvents. Class (b) includes physical treatments such as extrusion, milling, irradiation, microwave, ultrasound, pyrolysis, and pulsed electric fields. Biological pretreatments (i.e., class (c)) are named according to the type of organism involved: fungi, bacteria, and archaea. Class (d) includes physicochemical treatment methods such as steam explosion, liquid hot water, SPORL (sulfite pretreatment to overcome recalcitrance of lignocellulose), AFEX (ammonia fiber explosion), CO₂ explosion, and wet oxidation.

Extrusion, from class (b), is a promising pretreatment method. It presents many key advantages for biomass pretreatment in a biorefinery context and is a complex technology with a simple core principle. It consists of destructuring LCB under high shearing forces through contact with one or two rotative screws into a barrel, or more specifically, an extruder. This technology is particularly adaptable, can be used for diverse purposes outside biomass pretreatment, and possesses several parameters that can be modified according to the desired goal (Pérez-Rodríguez *et al.*, 2017). Short residence time is another advantage of extrusion, usually requiring only a few minutes (Gatt *et al.*, 2018). Concerning operating conditions, extrusion can be run in batch, fed-

batch, and continuous processing, and can be run at a mild temperature with low energy consumption and high solid loadings. This technology is also known for rapid heat transfer and effective mixing. Moreover, extrusion offers the possibility to be coupled with other pretreatments methods, and is also a scalable technology possible to achieve comparable results when transferring from a laboratory scale to pilot and industrial scales (Zhang *et al.*, 2012c). Extrusion has been used in food, polymer, and many other industries for a long time (since 1797), but as a pretreatment method for LCB, extrusion is quite recent (the 1990s), and is receiving increasing attention (Morales-Huerta *et al.*, 2021).

The great flexibility of Lignocellulosic Biomass Extrusion (LBE) is an advantage. However, at the same time, this flexibility adds a layer of complexity because of the great number of parameters available. Those parameters are important to better understand how LBE works and for scaling up purposes. Thus, the main purposes of this paper are to present an overview of relevant LBE parameters, to show the influence of extrusion setups on the efficiency of the pretreatment, to give core information about typical operational practices, and to highlight R&D needs.

3.4 Lignocellulosic biomass

3.4.1 Biomass composition

Since the beginning of biomass extrusion, it has been used for various purposes such as furfural recovery (Zhang *et al.*, 2019a), lipid extraction (with microalgae) (Li *et al.*, 2020), pigment extraction (Pan-Utai & lamtham, 2019), torrefaction/pelletization (Sarker *et al.*, 2022), biomass briquettes making (Ahiduzzaman & Islam, 2013), and composite materials formation (Rowell, 2007a). For lignocellulosic biomass pretreatment, sugars recovery (monosaccharides, oligosaccharides, and polysaccharides) remains the preponderant goal so far (Guiao *et al.*, 2022b; Zhang *et al.*, 2021c; Zhang *et al.*, 2022). The reasons are that sugars (cellulose and hemicellulose) represent 50 to 80% of LCB and also because downstream processes utilizing sugar are well mastered today as they have been studied since the beginnings of first-generation biorefinery.

Figure 3.1 illustrates lignocellulose. Cellulose is the principal constituent of plant cells wall and the most abundant polymer from living organisms (Li *et al.*, 2021). It is a linear D-glucose polymer with $\beta(1-4)$ glycosidic bonds. In LCB, cellulose occupies between 20% and 50% of all components (Kumar & Singh, 2019). Hemicellulose, like cellulose, is a biopolymer. It consists of about 15–35% of LCB on a dry basis (Kumar & Singh, 2019). While cellulose is a hexose polymer composed

of only one type of monomer, hemicellulose is a heteropolymer (mixtures of pentoses and hexoses). The most abundant monomers in hemicellulose by order are xylose and arabinose for pentoses and mannose, glucose, and galactose for hexoses. Hemicellulose is also a nonlinear polymer with significant short branching sidechains that contribute to the overall cohesion of lignocellulosic structures. This biopolymer is embedded between cellulose fibers and lignin and plays the role of a binder via covalent bonds. Compared to cellulose, the molecular weight of hemicellulose is low, and its structure is easily hydrolyzed.

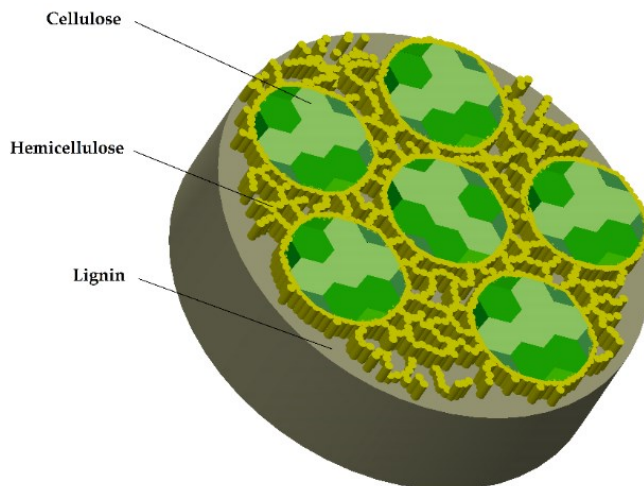


Figure 3.1 Essential components of a lignocellulosic microfibril (Cellulose, Hemicellulose and Lignin).

After cellulose, lignin is the most abundant biopolymer on earth and is counted for about 5% to 30% in the composition of LCB (Niu *et al.*, 2020). Lignin is a three-dimensional aromatic biopolymer (Fernández-Rodríguez *et al.*, 2017). It is also a plant cell wall component like hemicellulose and cellulose in woody plant tissues. The main role of lignin is to prevent the cell from exterior threats such as microorganism attacks. It is made of three monomers (monolignols): *p*-coumaryl alcohol, coniferyl alcohol, and sinapyl alcohol, which respectively appear in the lignin polymer as Hydroxyphenyl (H lignin), Guaiacyl (G lignin), and Syringyl (S lignin). Softwood is mainly composed of G lignin units while hardwood has essentially both S and G lignin units (Ahvazi *et al.*, 2011). Monolignols are linked one to another by alkyl-aryl, alkyl-alkyl, and aryl-aryl bonds. The relative abundance of one of these linkages over the others determines the physicochemical and biological properties of the lignin (Garlapati *et al.*, 2020). Lignin and cellulose are linked both by hydrogen (weak) and covalent (strong) bonds. **Figure 3.2** shows an overview of some LCB compositions. Cellulose, hemicellulose, and lignin form a complex and resistant material (i.e., lignocellulose) whose structure can vary depending on many factors (type of

biomass, sources, stage of maturity, plant part, etc.). Generally, agricultural residues require less harsh pretreatment conditions than forest residues. During lignocellulosic biomass extrusion (LBE), the mechanical action of the screws on the extrudate disrupts the lignocellulose material. Covalent and hydrogen bonds are altered and weakened, while the degree of polymerization of cellulose is technically reduced and a part of the lignin layer is removed. As [Tableau 3.1](#) shows, so far, studies do not permit to state clearly whether or not there is a significant difference between biomass composition before and after extrusion. The differences observed can be for diverse reasons: A structural change in the biomass during extrusion, the denaturation of certain compound according to the severity of the pretreatment conditions, the fact of bias related to precision and accuracy of the protocol used for biomass composition estimation, etc.

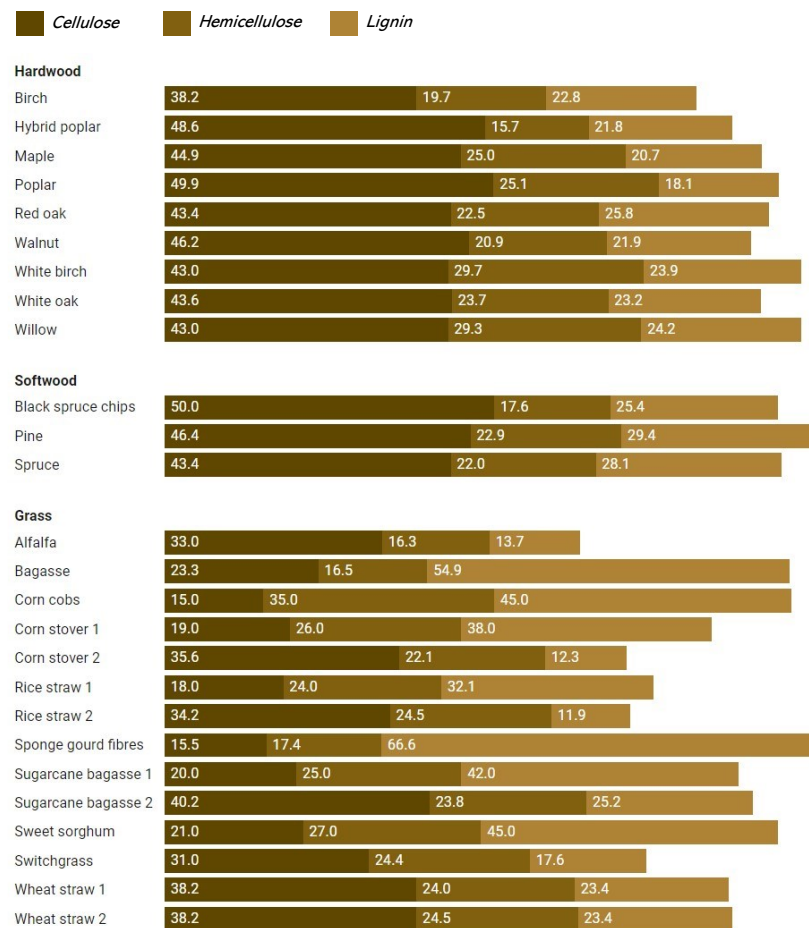


Figure 3.2 Composition of some lignocellulosic biomass.

Tableau 3.1 Lignocellulosic biomass composition before and after extrusion.

Biomass	Compounds	Composition (%)		References
		Before extrusion	After extrusion	
Bulgur bran	Glucose	36.38 ± 0.32	30.86 ± 0.64	(Yağcı <i>et al.</i> , 2022b)
	Hemicellulose	29.42 ± 0.13	33.18 ± 0.53	
	Total lignin	12.54 ± 0.14	16.24 ± 0.31	
Eucalyptus	Cellulose	46.90 ± 1.21	44.90 ± 1.86	(Duque <i>et al.</i> , 2018b)
	Hemicellulose	12.87 ± 0.35	13.71 ± 0.32	
	Lignin	31.15 ± 0.40	32.97 ± 0.86	
	Ash	0.86 ± 0.00	0.57 ± 0.05	
Olive stove	Cellulose	20.8 ± 0.2	18.3 ± 2.8	(Doménech <i>et al.</i> , 2020)
	Hemicellulose	25.9 ± 0.1	22.4 ± 0.4	
	Lignin	35.5 ± 0.6	39.0 ± 0.2	
Barley straw	Glucose	32.9	32.80	(Duque <i>et al.</i> , 2020)
	Hemicellulose	26.1	15.53	
	Lignin	18.8	15.71	
	Ash	3.9	2.17	
Corn stover	Cellulose	32.75 ± 0.32	33.98 ± 0.14	(Wang <i>et al.</i> , 2020)
	Hemicellulose	31.08 ± 0.57	30.20 ± 0.28	
	Lignin	10.07 ± 0.91	9.89 ± 0.43	
Oat hull	Cellulose	31.16 ± 1.15	34.32 ± 2.06	(Debiagi <i>et al.</i> , 2021)
	Hemicellulose	28.72 ± 0.25	26.40 ± 0.53	
	Lignin	18.12 ± 0.63	15.00 ± 1.30	
Wheat straw	Cellulose	37.8 ± 1.9	46.9 ± 0.1	(Coimbra <i>et al.</i> , 2016)
	Hemicellulose	28.2 ± 0.5	28.7 ± 0.1	
	Lignin	19.8 ± 0.3	15.4 ± 0.1	
	Ash	3.7 ± 0.0	3.3 ± 0.0	
Corn cob	Cellulose	42.0 ± 0.15	34.8 ± 0.23	(Pérez-Rodríguez <i>et al.</i> , 2017)
	Hemicellulose	45.9 ± 0.90	38.9 ± 0.52	
	Neutral detergent soluble	9.3 ± 0.95	19.0 ± 0.60	

3.4.2 Crystallinity

Usually, in LBE, crystallinity refers to cellulose. Natural cellulose polymers contain both crystalline (d-glucose monomers ordered) and amorphous (d-glucose monomers disordered) sequences (Chen *et al.*, 2019; Park *et al.*, 2010), and the crystallinity index is the overall percentage of the crystalline fraction. That is, it is the relative quantity of crystalline sequence in cellulose. Crystallinity is determined by X-ray diffraction and the following formula:

Équation 3.1 – Crystallinity index (CrI)

$$CrI = \frac{I_{200} - I_{am}}{I_{200}}$$

where I_{200} represent the height of the (200) peak and I_{am} is the minimum intensity between the (200) and the (110) peaks (Lee *et al.*, 2009).

Hemicellulose and lignin are considered non-crystalline polymers (amorphous polymers) and are both heteropolymers. However, hemicellulose can also be highly crystalline because of multiple ramifications of homopolymers with a crystalline structure (xylans, mannans, arabinans, and galactans) attached to the principal heteropolymer chain (Ansell & Mwaikambo, 2009). The crystallinity of cellulose is particularly important in LBE when enzymes are involved before, during, or after the processing for enzymatic hydrolysis. This is because the amorphous part of cellulose is more susceptible to saccharification compared to the crystalline part, and can be degraded between five and thirty times more quickly (Ghaemi *et al.*, 2019; Zhao *et al.*, 2012).

Kuster Moro *et al.* (2017) recorded a decrease from 57% to 54% of the crystallinity index after extrusion of sugarcane bagasse. It could be obvious that the crystallinity index might decrease after extrusion, but many studies showed that it is not always so. For example, Vandenbossche *et al.* (2014) extruded four types of biomass (i.e., barley straw, sweet corn, blue agave, and oil palm empty fruit bunch) and found that the crystallinity of all extrudates was higher than for the raw materials (Tableau 3.2). Marone *et al.* (2018) came to the same conclusion with corn stover. Fu *et al.* (2018) observed the crystallinity of Douglas fir residuals and found that after extrusion, the crystallinity index slightly increased, which was attributed to effects from both heat and moisture content. Recrystallization can occur in cellulose because, under high temperatures, hydrogen atoms in the amorphous region undergo a realignment (Gu *et al.*, 2019).

As an indicator of enzymatic hydrolysis yield, cellulose crystallinity is also controversial. Some authors reported a strong correlation between crystallinity and glucose and xylose/mannose yield, while others showed that crystallinity index is not accurate to predict sugar yield (Gu *et al.*, 2019; Zhang *et al.*, 2012d).

Tableau 3.2 Crystallinity index.

Biomass	Substrate crystallinity (%)	Extrudate crystallinity (%)	References
Banana fibers	39	-	(Guimarães <i>et al.</i> , 2009)
Sugarcane bagasse	48	-	(Guimarães <i>et al.</i> , 2009)
Sponge gourd fibers	50	-	(Guimarães <i>et al.</i> , 2009)
Sweet corn	41 ± 3	47 ± 6	(Vandenbossche <i>et al.</i> , 2014)
Barley straw	44 ± 8	46 ± 2	(Vandenbossche <i>et al.</i> , 2014)
Blue agave bagasse	27 ± 7	52 ± 1	(Vandenbossche <i>et al.</i> , 2014)
OPEFB	50 ± 8	51 ± 7	(Vandenbossche <i>et al.</i> , 2014)
Corn stover	48 ± 4	51.2 ± 3.4	(Marone <i>et al.</i> , 2018)
Sugarcane bagasse	57.3 ± 1.3	54.0 ± 0.23	(Kuster Moro <i>et al.</i> , 2017)

3.4.3 Particle size

Usually, biomass will undergo a size reduction before its application to the extrusion process. A grinder is used in that case, and this step involves energy consumption and must be included in the energy balance of LBE process. At pilot and industrial scales, biomass size reduction can seriously affect the economic profitability of the LBE. However, particle size plays an important role in lignin removal, reaction kinetics, hydrolysis rate, rheological properties of the substrate inside the barrel, and sugar yield. A strong correlation between the particle size and the extrusion Specific Mechanical Energy (SME) (-0.786), the torque (-0.788), the glucose recovery yield (-0.813), and the xylose/mannose recovery yield (-0.787) has been observed during extrusion of Douglas-fir forest residuals, all with p -value inferior to 0.01 (Gu *et al.*, 2019). This means that when the particle size decreased, the SME, torque, glucose recovery yield, and xylose-mannose recovery yield increased. Additionally, many authors reported a size reduction of the extrudate relatively to the substrate after the extrusion process (Kang *et al.*, 2013; Zhang *et al.*, 2020; Zheng *et al.*, 2015). The reduction of the extrudate particle size increases their specific surface, which has clear advantages with respect to improvements in enzymatic saccharification.

3.4.4 Morphology

After extrusion, a visual inspection of the extrudate allows a first appreciation of the impact of the extrusion pretreatment on the biomass. Particle size is reduced, the extrudate looks rough, crumbly, and has a broken surface to the touch (Marone *et al.*, 2018; Rashed *et al.*, 2021). LCBs' microstructure can be observed by Scanning Electron Microscopy (SEM). Usually, extrudates show a disruptive surface with a lot of clear exfoliations compared to substrates which are compact (bundled) and have smooth surfaces. Important fibrillation in the extrudate has also been reported in the literature. Extrudate microfibrils are twisted, untied, and untangled (Byun *et al.*, 2020; Debiagi *et al.*, 2019; Senturk-Ozer *et al.*, 2011; Vaidya *et al.*, 2016). The disruptive and fibrillation effect of extrusion can be remarkably enhanced when chemicals are used during the extrusion process (reactive extrusion). For example, (Han *et al.*, 2020) observed a significant disruption and fibrillation in the microstructure of the extrudate (wood powder of pussy willow) when [EMIM]Ac (1-ethyl-3-methylimidazolium acetate) and DMSO (dimethyl sulfoxide) were used as additive during the extrusion process. The chemicals reacted with the water molecules inside the substrate and then created voids (porosity) in the biomass. Byun *et al.* (2020) experienced a similar microstructure with Amur silvergrass. Porosity is also created by water evaporation under mild and high-temperatures extrusion (above 100 °C), but this effect is significantly enhanced with

hydrophilic chemical additives. The increase in porosity results in an increase in the specific surface of the extrudate, which is highly beneficial for enzymatic hydrolysis (Zhang *et al.*, 2020). Karunanithy and Muthukumarappan (2013) demonstrated that the efficiency of enzymatic hydrolysis strongly depends on the accessibility of sugars to the enzymes. The greater the accessible surface, the higher the rate of enzymatic hydrolysis. Size reduction also participates in the increase of the specific surface, as highlighted in the preview section. Cellulose microfibrils in Han's extrudate were less than 500 nm in diameter (Han *et al.*, 2020).

3.4.5 Moisture

Substrate moisture is a key parameter for LBE. Most of the time, LCBs after harvest are not immediately pretreated, but rather undergo preparation before extrusion. The storage conditions (i.e., temperature and time) determine the biomass moisture content. Ambient temperature is preferred for storage to reduce energy consumption, and storage can last from a few hours to many months. The biomass is stored until the desired moisture for extrusion is reached. This moisture ranges from 6% to 50% according to the type of biomass (Tableau 3.3). It is important to note that materials above 50% are not sufficiently consistent to be extruded and behave more like a liquid than a solid. Moisture content around 25% seems to be an optimum for high (above 70%) sugar recovery from barley and wheat straw (Coimbra *et al.*, 2016; Duque *et al.*, 2013), but more investigations are required.

3.4.6 Biomass preparation before pretreatment

Biomass preparation is a necessary step for successful extrusion. We investigated twenty-seven LBE studies in order to identify common practices during biomass preparation before extrusion (Tableau 3.3). Biomass preparation steps consist of [a] sorting/washing, [b] drying, [c] grinding/milling, [d] sieving, [e] mixing with additives, [f] storing, and [g] extrusion. The first step (sorting) is an inspection of the sample collected, to remove contaminants (plastic, sand, etc.). Sometimes washing is necessary to remove the contaminants (Zhang *et al.*, 2020). The drying step has at least two goals. The first one is to restrict microbial activity in the biomass, especially if the biomass is very wet, while the second is to lower the moisture content of the raw material (Kuster Moro *et al.*, 2017). Grinding/milling steps are for the size reduction of the substrate, and sieving ensures a desired particles size for the substrate (Pérez-Rodríguez *et al.*, 2017). There are two ways to use additives in LBE: after and during the extrusion process. Some prefer the

former and run step [e] (Han *et al.*, 2020). Then, the biomass is directly extruded or stored until extrusion (Duque *et al.*, 2018a).

Authors freely adapt these steps to their material and their goal. **Tableau 3.3** shows that some omit certain steps or change the order. For example, Liu *et al.* (2013) used only [d] (milling) for corn stover preparation; Kuster Moro *et al.* (2017) used steps [b] (drying), [c] (milling), [d] (sieving), and [e] (mixing with additive) to prepare sugarcane bagasse and sugarcane straw for extrusion; while for eucalyptus tree, Duque *et al.* (2018a) opted for a [c]-[b]/[f]-[d] sequence. However, generally speaking, all the above steps mentioned remain important for best practices for biomass preparation before extrusion.

Tableau 3.3 Practices of biomass preparation before extrusion.

Substrate	Source	Steps	Size (mm)	Storage time	T (°C)	Moisture (%)	Additives (before extrusion)	Reference
Barley straw	Research centre	[b]-[c]-[d]-[g]	5	-	-	-	No	(Vandenbossche <i>et al.</i> , 2014)
Barley straw	Research centre	[c]-[d]-[f]-[g]	5	Stored until use	-	6	No	(Duque <i>et al.</i> , 2013)
Big bluestem	Farm	[c]-[d]-[f]-[g]	0.4–0.8	Stored until use	RT*	-	-	(Karunanithy <i>et al.</i> , 2014)
Big bluestem	Farm	[c]-[d]-[e]/[f]-[g]	2, 4, 6, 8, 10	~8 h	RT*	10, 20, 30, 40, 50	Water	(Karunanithy & Muthukumarappan, 2011a)
Blue agave	Manufacture	[b]-[c]-[d]-[g]	2	-	-	-	No	(Vandenbossche <i>et al.</i> , 2014)
Corn cob	Farm	[b]-[c]-[d]-[g]	2	-	RT*	-	No	(Pérez-Rodríguez <i>et al.</i> , 2017)
Corn stover	Farm	[c]-[b]-[e]-[g]	2	-	RT*	22.5, 25, 27.5	No	(Zhang <i>et al.</i> , 2012d)
Corn stover	Farm	[c]-[b]-[e]-[f]-[g]	2	8 h	RT*	50	NaOH	(Zhang <i>et al.</i> , 2012c)
Corn stover	Farm	[c]-[g]	2–5	0 h	-	-	No	(Liu <i>et al.</i> , 2013)
Corn stover	Farm	[c]-[d]-[e]/[f]-[g]	2, 4, 6, 8, 10	~8 h	RT*	10, 20, 30, 40, 50	Water	(Karunanithy & Muthukumarappan, 2011a)
Eucalyptus trees	Research centre	[c]-[b]/[f]-[d]-[g]	60–190	2 months	-	20	No	(Duque <i>et al.</i> , 2018a)
Hardwood biomass (oak, fir, and pine sawdust)	-	[e]-[g]	1	-	RT*	21–28	NaOH	(Senturk-Ozer <i>et al.</i> , 2011)
Miscanthus	Farm	[c]-[d]-[g]	3	-	7	-	No	(Cha <i>et al.</i> , 2016)
Olive tree pruning	Farm	[b]-[c]-[e]-[g]	1–4	-	RT*	10	No	(Negro <i>et al.</i> , 2015)
OPEFB	Manufacture	[b]-[c]-[d]-[f]	2	-	-	-	No	(Vandenbossche <i>et al.</i> , 2014)
Prairie cordgrass	Farm	[c]-[d]-[e]/[f]-[g]	2, 4, 6, 8, 10	~8 h	RT*	10, 20, 30, 40, 50	Water	(Karunanithy & Muthukumarappan, 2011a)
Rape straw	Research centre	[c]-[d]-[g]	1.4–2.36	24 h	45 ± 5	6.44	No	(Choi & Oh, 2012b)
Rice hull	Manufacture	[a]-[b]-[c]-[d]-[g]	25.4	24 h	60	-	No	(Zhang <i>et al.</i> , 2020)
Soybean hulls	Manufacture	[b]-[d]-[g]	1.041	24 h	RT*	40, 45, 50	No	(Yoo <i>et al.</i> , 2011)

Substrate	Source	Steps	Size (mm)	Storage time	T (°C)	Moisture (%)	Additives (before extrusion)	Reference
Sugarcane bagasse	Mill	[b]-[c]-[d]-[e]-[f]-[g]	0.2–2	24 h	Cold room	10.4 ± 0.36 8.9 ± 0.30	Water, Glycol, Ethylene glycol, Tween 80	(Kuster Moro <i>et al.</i> , 2017)
Sugarcane bagasse	Manufacture	[c]-[d]-[e]-[g]	0.425–1.000	-	40	10	[EMIM]Ac	(Da Silva <i>et al.</i> , 2013b)
Sugarcane straw	Mill	[b]-[c]-[d]-[e]-[f]-[g]	0.2–2	24 h	Cold room	12.05 ± 0.36 10.34 ± 0.26	Water, Glycol, Ethylene glycol, Tween 80	(Kuster Moro <i>et al.</i> , 2017)
Sweet corn	Manufacture	[b]-[c]-[d]-[g]	6	-	-	-	No	(Vandenbossche <i>et al.</i> , 2014)
Switchgrass	Farm	[c]-[d]-[e]/[f]-[g]	2, 4, 6, 8, 10	~8 h	RT*	10, 20, 30, 40, 50	water	(Karunanithy & Muthukumarappan, 2011a)
Switchgrass (matured)	Farm	[c]-[d]-[f]-[g]	0.3–1.2	Stored until use	RT*	-	-	(Karunanithy <i>et al.</i> , 2014)
Wheat straw	-	[c]-[f]-[g]	5	Stored until use	40	6	No	(Coimbra <i>et al.</i> , 2016)
Wood powder of pussy willow	-	[d]-[b]-[f]-[e]-[g]	25.4	24 h	40	-	[EMIM]Ac, DMSO, [EMIM]Ac/DMSO	(Han <i>et al.</i> , 2020)

*RT : Room temperature

3.5 Extruder

An extruder is a thermomechanical device composed of different parts, with the most important being the barrel (inside which are one or more screws) and the die. These two parts are generally temperature controlled by a system of heating and cooling. Most often, extruders are equipped with one or more liquid injection points (**Figure 3.3**). The first patent of an extruder was filed by Joseph Bramah in 1797. Today, several types of extruders are available according to the number of screws. However, single-screw extruders and twin-screw extruders are both widely used for LBE, although twin-screw designs are more common. These screws rotate around their axis thanks to a drive motor and exert a significant mechanical force on the biomass, which is caught between the screws and between the screws and the wall.

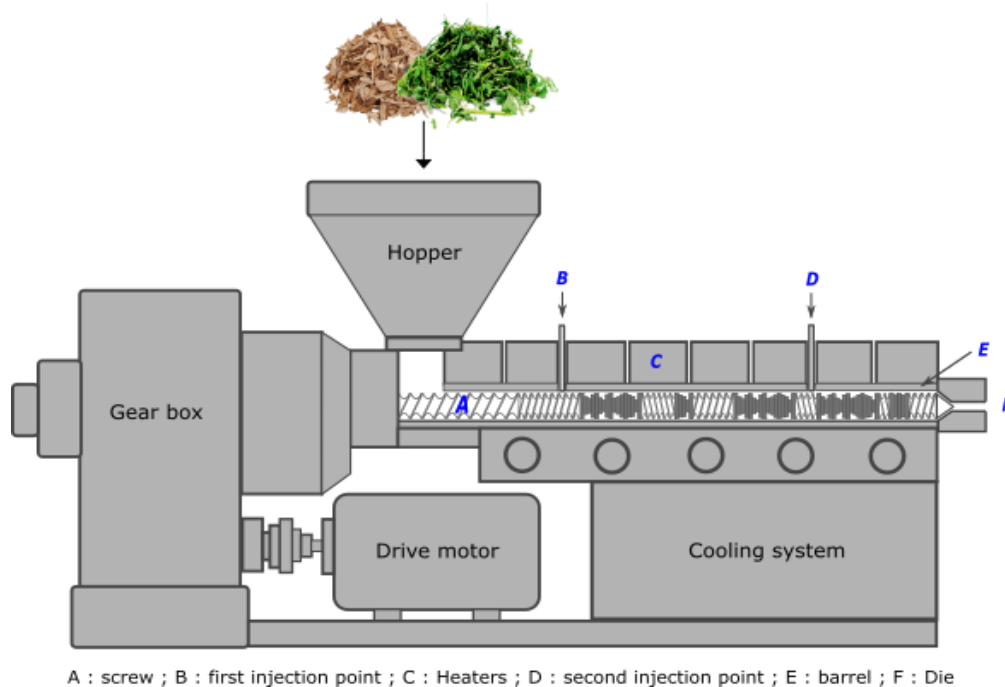


Figure 3.3 Illustration of a twin-screw extruder with the main parts (screws, injection points, heaters, barrel and die).

3.5.1 Screw type

Screws have two principal functions: convey and disrupt. The lignocellulosic substrate is conveyed from the feeding zone (zone under the hopper) to the die. During transport, the substrate undergoes high shearing forces as a consequence of protrusions of the screws, which results in the disorganization of the lignocellulose complex, with a part of the lignin layer removed while the cellulose crystallinity is technically assumed to decrease.

An extruder screw is made of a non-corrosive and resistant (high shearing forces) metal (Choi & Oh, 2012a), and consists of a shaft surmounted by different shapes of protrusion, with two typical screw types: the one-piece screw and the modulated screw. The one-piece screw is a full bar on which protrusions are made directly on the shaft (Figure 3.4). In the case of a modulated screw, this consists of a bar ridged lengthwise on which modules (screw elements) are mounted (Figure 3.5). Contrary to one-piece screws, modulated screws offer more flexibility because the configuration of the screw can be changed by using different modules (Senturk-Ozer *et al.*, 2011). In the case of LBE, modulated screws are better suited, as most of the time the screw configuration must be changed according to the type of biomass.

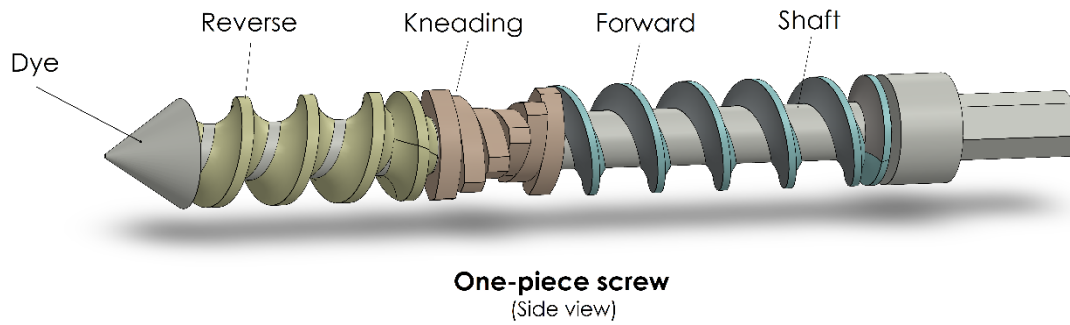


Figure 3.4 One-piece screw.

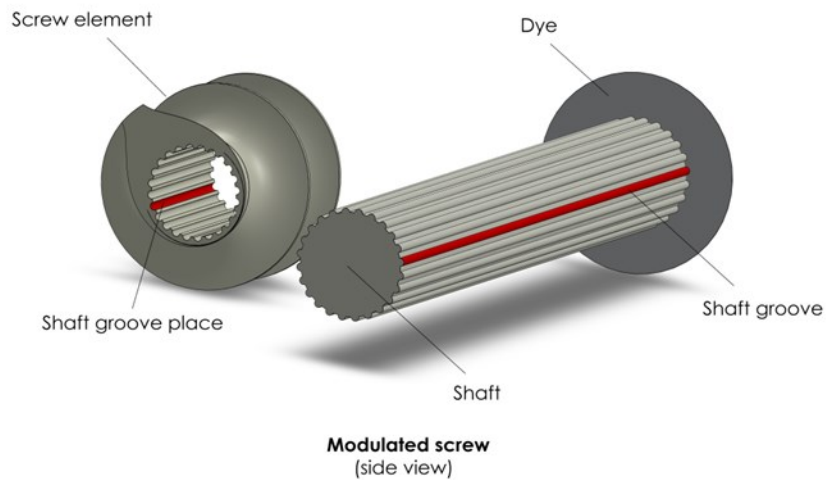


Figure 3.5 Modulated screw.

Similarly, twin-screws have more than one configuration and can be co-rotative (turn in the same direction) or counter-rotative (turn in opposite directions). Furthermore, counter-rotative screws can be intermeshing or non-intermeshing (**Figure 3.6**). Conversely, co-rotative screws are always intermeshing and provide better mixing than counter-rotative configurations ([Cantine, 2017](#); [Gupta, 2004](#)).

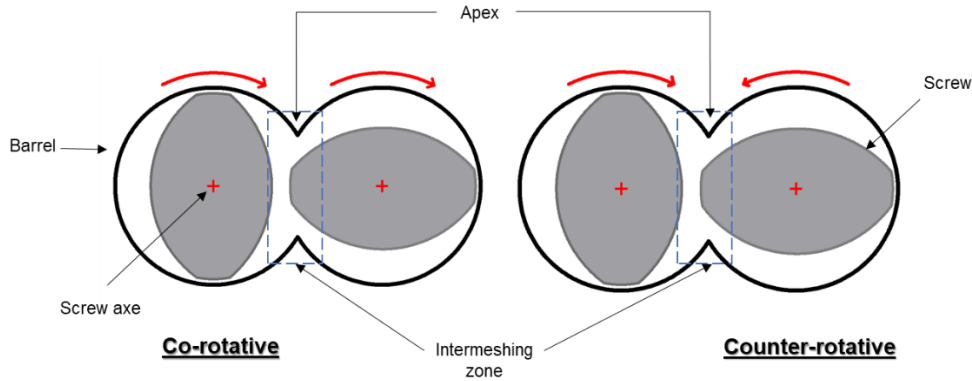


Figure 3.6 Co-rotative and counter-rotative extruder screws.

Screws can also take different longitudinal geometries. Cylindrical, conical, and mixed-shape screw configurations are the best known. For a typical cylindrical screw design, the diameter is the same along the screw from the beginning to the end of the screw, and this is the most common design for LBE. For conical screw designs, the diameter constantly decreases (or increases) from one end to the other, and this kind of design is used for biomass briquetting (Solano *et al.*, 2016). Mixed-shape screw designs feature two different screw diameters linked by a conical compression zone, which facilitates a transition from one diameter to the next. Such compression zone designs can be both considered soft (long) or strong (short). Conical and mixed-shape screws have been explored in studies for materials such as thermoplastic polyurethane, polyvinyl chloride (PVC), and plastic composites (Leng *et al.*, 2019; Vera-Sorroche *et al.*, 2014; Zhang *et al.*, 2014b).

The choice of the screw type is made when the extruder is purchased, and generally, the operators do not have much freedom for modification afterwards.

3.5.2 Screw configuration

Lignocellulosic Biomass Extrusion (LBE) efficiency is strongly dependent on the screw configuration (Kelly *et al.*, 2006). Screw configuration is the final layout obtained from the arrangement of screw elements on the shaft. Contrary to screw type, authors have full control of overall screw configuration.

LBE screw configuration is formed by transport elements (forward and reverse) and mixing elements (kneading). Gatt *et al.* (2018) proposed the following screw configuration for LBE: F-T-M-R-M-R-M-T; where F = forward transport element (with more spaced spirals than T), T = transport element (forward), M = mixing element (kneading), and R = reverse transport element.

Although screw configuration differs from one user to another, the T-M pattern is almost always present at the beginning of a screw configuration (Duque *et al.*, 2014; Gatt *et al.*, 2018; Lamsal *et al.*, 2010; Zheng *et al.*, 2016).

Wahid *et al.* (2015) investigated the effect of screw configuration on the pretreatment of wheat straw and deep litter in order to produce biogas. They tested many screw configurations by using a starting screw configuration only composed of forward screw elements, and they changed some of these forward screw elements by kneading or reverse screw elements to get a new configuration. Five screw configurations were then obtained. These are (a) mild kneading (medium length kneading block replacing some forward screw elements); (b) long kneading (a long block of kneading screw elements replacing some forward screw elements); (c) reverse (a block of reverse screw elements replacing some forward screw elements); (d) kneading and reverse (a block of kneading screw element and a block of reverse screw elements replacing some forward screw element on the same shaft. However, these two blocks are separated from each other by some forward screw elements; and (e) kneading with reverse (the same configuration as the previous but here the two blocks are contiguous). Configuration (a) was found suitable for deep litter (soft texture) and configuration (d) for wheat straw because they gave the best compromise between energy consumption, sugar availability, and methane yield. As for configuration (b), it was found unproductive because of important energy consumption for both LCBs. The authors have also demonstrated that the energy consumption increases as reverse and/or kneading elements are added to the screw configuration and at the same time, these elements enhance the disruptive effect of the screw on the biomass (like with the (d) configuration). In the same perspective, Kuster Moro *et al.* (2017) pre-treated sugarcane biomass and observed that the glucose recovery yield was improved when reverse elements are placed just after the last kneading zone. With a similar screw configuration, Negro *et al.* (2015) reported an increase in the overall sugar yield with olive-tree prunings.

Thus, a screw configuration starting with T-M followed by a reverse element after one or two kneading elements, including the last kneading element, should be optimal to improve the sugar recovery yield. However, more investigations are required to confirm this assertion.

3.5.3 Screw elements

Each screw element type has a geometry that defines its function, and this geometric variation will systematically affect extrusion performance. Furthermore, lignocellulose composition differs from one type of biomass to another (wood, agricultural residues, etc.) as well as variability within

a specific biomass type according to different factors (age, maturity stage, etc.), and this also affects screw element selection. Thus, an ideal geometry exists according to each specific biomass to be pre-treated. However, from a practical perspective, this can prove to be difficult because of downtime associated with reconfiguration, which can limit productivity.

3.5.4 Forward screw element

The Forward Screw Element (FSE) is an elliptical screw element designed to convey the substrate forward while turning around its axis on a rotor force. It appears at the beginning of the screw, under the feeding zone of the extruder. FSE are selected for extrusion processing according to their depth, length of the pitch, and flight angle. **Figure 3.7** shows a side view of FSE. The geometry and orientation of the design is important for performance. For instance, as the tip angle increases, the speed at which the substrate is conveyed also increases. Similarly, increasing pitch, in turn, translates to a larger available volume in the FSE. Finally, increasing the screw tip width increases the clearance surface (between tip and barrel) and reduces the available volume in the FSE.

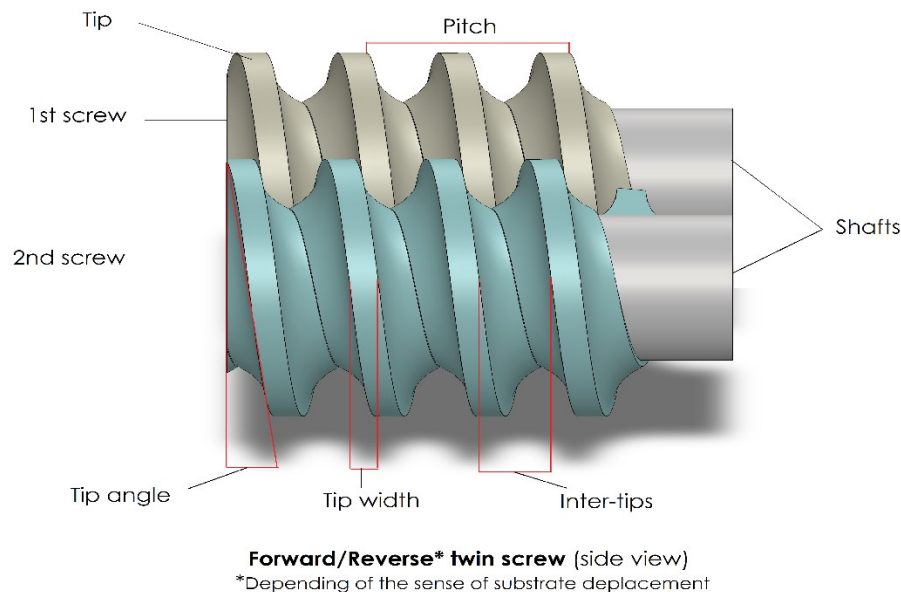


Figure 3.7 Side view of intermeshing forward/reverse twin-screw elements.

FSE has an impact on the resulting extrudate properties, and this was demonstrated by [Djuric and Kleinebudde \(2008\)](#) wet granulation of lactose monohydrate with a twin-screw extruder. Wet granulation is one of the ways to make solid oral forms (tablets, capsules) in the pharmaceutical industry ([Fülöp et al., 2021](#)), where fine powder particles are agglomerated together to form larger compounds. [Djuric and Kleinebudde \(2008\)](#) tested the porosity and the friability of the extrudate

obtained after using different FSE pitches and found that the friability of the extrudate increased with the pitch length. With respect to LBE, depending on the rheological behavior of the substrate, excessively small pitches can lead to extra flow resistance in the barrel, while increasing the FSE pitch may lead to substrate friability; the substrate has insufficient viscosity to ensure a suitable fluidity inside the barrel. Usually, FSE with greater pitch are set directly under the feeding zone, while those with lower pitch are placed downstream from the feeding zone. [Kohlgrüber *et al.* \(2008\)](#) considered a pitch range 1.5–2 times that of the screw diameter as the most suitable for FSE under the feeding zone.

3.5.5 Reverse screw element

A Reverse Screw Element (RSE) has the same design as a FSE, but with opposite flights (**Figure 3.7**). Set together on the same shaft as an FSE, an RSE is an obstacle to the forward displacement of the substrate, and thus an RSE represents a high zone of resistance. The goal of RSE in LBE is to increase pressure on the substrate and also to reach a steady state, especially with small pitches ([Vandenbossche *et al.*, 2015](#)). Similar to FSE, a side view section of an RSE shows the same behavior with respect to tip angle and tip width, with an additional particularity: as the pitch decreases, the resistance generated by RSE highly increases, which controls the back pressure and increases the specific mechanical energy.

RSE has an impact on the LBE efficiency, as [Gu *et al.* \(2019\)](#) have shown through their investigation of glucose and xylose/mannose yield obtained during an LBE of Douglas-fir residues. Using a twin-screw divided into six zones, they found a significant increase in the glucose and xylose/mannose yield next to the RSE due to high shearing forces. [Kuster Moro *et al.* \(2017\)](#) reported similar results on sugarcane biomass, with the insertion of a RSE increasing the yield of lignocellulose hydrolysis. [Zheng *et al.* \(2016\)](#) investigated height screw configuration to find the best one for xylose separation from steam-exploded corncobs and found that xylose recovery was higher using configurations containing one or more RSE. They also found that while xylose yield varied with configurations containing RSE, these outcomes were always superior to a configuration without RSE. However, regardless of how a RSE improves LBE pretreatment, attention must be paid to the specific mechanical energy.

3.5.6 Kneading element

Kneading elements (KE) play a disruptive and distributive effect on the substrate, and can also act as mild flow-restricting elements ([Choudhury & Gautam, 1999](#); [Gatt *et al.*, 2018](#)). A screw

configuration for LCB pretreatment will typically contain at least one kneading block comprised of two or more juxtaposed KE. During LBE a kneading block is ideally set immediately downstream of the first FSE (Duque *et al.*, 2014; Gatt *et al.*, 2018; Zheng *et al.*, 2016). Furthermore, Kuster Moro *et al.* (2017) demonstrated that the best place for a RSE is just after a kneading block because of the additional back pressure and resistance provided by the RSE.

Kneading blocks geometry depends on the angles between KE, KE staggering, tip thickness, and clearance. **Figure 3.8** presents both facing and lateral views of a kneading block. As KE tip thickness increases, the kneading surface also increases, while reducing the available volume in the kneading block. Furthermore, creating an offset angle between the KE will improve the distributive function of the kneading block. The optimum offset angle (α) as a function of the number of KE (nKE) is given by:

Équation 3.2 – Optimum offset angle (α)

$$\alpha = \frac{180}{nKE}$$

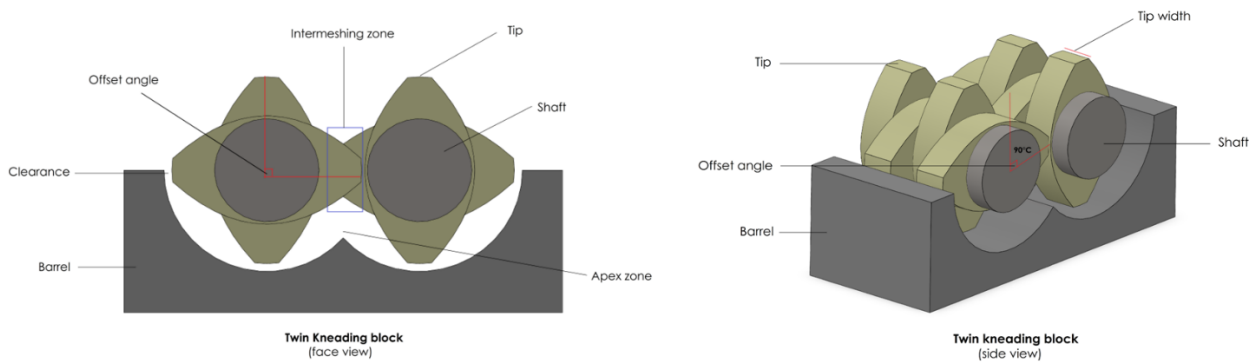


Figure 3.8 Kneading blocks (front-facing and lateral view).

All the KE presented in **Figure 3.8** are vertical and then have no conveying function, only disruptive and distributive function. However, sometimes a KE is staggered either because a conveying function or an increase or decrease of shearing forces on the substrate in the kneading zone is needed. Shearing forces increase when the staggering of the kneading block is opposite to the displacement direction of the substrate and decrease when the staggering is in the same direction (Duque *et al.*, 2017; Senturk-Ozer *et al.*, 2011). The choice of the staggering angle of the kneading block should be related to the extrusion purpose (Kuster Moro *et al.*, 2017).

Usually, kneading blocks are composed of 4–8 KE. The length of a kneading block influences the LBE. During their experiment on wheat straw and deep litter, [Wahid et al. \(2015\)](#) found that a longer kneading block improved the biodegradability of the extruded biomass better than a shorter one. As for [Fu et al. \(2018\)](#), they recorded a 7% increase in the glucose yield when the number of KE was increased. Therefore, it may seem interesting to lengthen the kneading block to maximize the biodegradability of the extrudate. However, the authors pointed out that long kneading blocks increase the temperature, the residence time, and the specific mechanical energy, and this must be taken into consideration before lengthening the kneading block, especially for bioextrusion, as enzyme degradation can result in excessive kneading effects or a rise in temperature. A good alternative is to use both KE and RSE instead of a long kneading block, which is more favorable. The first solution is better than the second in terms of temperature control (due to reduced shearing forces), specific mechanical energy saving, and screw length shortening ([Wahid et al., 2015](#)).

3.5.7 Die Shape

The die is the end of the screw through which the substrate exits the extruder, and its diameter is consistently lower than the inner barrel diameter. Similar to the screws and the barrel, the die is generally heated. It is an important part of the extruder because it influences the back pressure inside the barrel and in turn the overall efficiency of the LBE process ([Gu et al., 2019](#)). The die entry is a high-pressure zone, as the substrate inside the barrel is conveyed by the screws and forced to pass through the die which has a smaller diameter ([Abeykoon et al., 2016](#); [Vera-Sorroche et al., 2014](#)).

Different shapes of dies are available, but a typical common design for a LBE is a cone entry followed by a cylinder at the end ([Figure 3.3](#)). [Patil et al. \(2006\)](#) studied the influence of this shape over the pressure in the barrel, and both the entry angle (2α) and the length-to-die diameter ratio (L/D_{die}) were found to be correlated with the internal pressure. For entry angles (2α) up to 30° , the pressure linearly increased with a slope of 0.5. With respect to L/D_{die} ratio, the relation has a slope of 0.6. Understanding this relationship, a given die design can be used to regulate the extrusion pressure ([Senturk-Ozer et al., 2011](#)). Moreover, a larger die requires a lower specific mechanical energy than a smaller one because the pressure at the die entry for a larger die entry is lower and requires less mechanical energy.

Sometimes extrusion is run without a die for many different reasons. The principal reason for LBE operation without a die is reports of serious packing at the die entrance due to insufficient fluidity of the substrate (lack of solvent or catalyst) (Ai *et al.*, 2020; Han *et al.*, 2020).

3.5.8 Torque

The torque (i.e., moment or moment of a force) is the capacity of a force to turn an object around its axis. For an extruder, the torque is the aptitude of the screws to turn around their axis, and it is an indicator of the efficiency of the extruder (Guha *et al.*, 1997). Torque also plays a role in the determination of the specific mechanical energy and is correlated to other extrusion parameters. For example, substrate moisture is inversely correlated with torque (Yoo *et al.*, 2011). The torque increases when the barrel temperature and the screw speed are lowered (Akdogan, 1996; Chen *et al.*, 2011; Duque *et al.*, 2017). Adding Reverse Screw Elements (RSE) to the screw configuration tends to increase the torque (Harmann & Harper, 1973; Lei *et al.*, 2005). Concerning the particle size of the substrate, there is no evidence about its impact on the torque (Karunanithy & Muthukumarappan, 2011a).

Importantly, torque influences the sugar recovery yield. Higher torque leads to sugar recovery improvement. Gu *et al.* (2019) recorded an increase from 27% up to 43% of glucose yield and from 13% to 21% for xylose/mannose yield when the torque was increased from 15 Nm to 70 Nm. However, there is no specific torque range for LBE extrusion because it can differ from one extruder to another, according to the type of biomass and the extrusion conditions (Duque *et al.*, 2017). However, one approach to lower the torque and still reach good sugar recovery yield is to use additives (solvent or catalyst), especially those with a great affinity towards cellulose such as ethylene glycol and glycerol (Lee *et al.*, 2009).

3.5.9 Specific Mechanical Energy

The specific mechanical energy (SME) is an input parameter that is expressed in Watt-hour per kilogram (Wh/kg) or Joule per kilogram (J/kg). The SME is the energy supplied for one kilogram of extrudate obtained. It is an indicator of the stability and capacity of the extrusion process, as a rapid change of the SME usually relates to instability in the flow (Duque *et al.*, 2018a; Gatt *et al.*, 2018).

SME is a function of the torque, the mass flow, the power of the extruder motor, and the screw speed, as outlined in the following formula:

Équation 3.3 – Specific mechanical energy (SME)

$$SME = \frac{(Total\ torque - Friction\ torque) \times N \times (P_m)}{(max_t) \times (max_{ss}) \times m_f}$$

where N is the screw speed (rev/min), m_f is the mass flow rate (kg/s), max_t is the maximum allowable torque, max_{ss} is the maximum allowable screw speed, and P_m is the power of the drive motor at a rated speed of max_{ss} . [Gu et al. \(2019\)](#) found that the SME is correlated with the median particles size and the crystallinity of the substrate respectively with $r = -0.79$ and $r = -0.87$. Furthermore, it has been reported that the viscosity of the substrate influences the SME as less viscous substrates require higher SME ([Godavarti & Karwe, 1997](#)).

[Zheng et al. \(2016\)](#) studied the role of the SME in xylose recovery yields and found that mass flow higher than 1.45 kg/h negatively affected the xylose recovery yield. However, when the additive flow (water) was increased, they recorded an improvement in the xylose recovery yield while the SME decreased concurrently, which was attributed to lower friction in the barrel due to increased moisture content. These results show that additives can be used to lower the SME in LBE and improve the sugar recovery results.

Energy consumption is one of the main concerns of biomass pretreatment. The goal is to recover the highest amount of the desired compound under the least energy consumption possible. Thus, the SME should be set in the optimum range for a given LBE. For example, [Lamsal et al. \(2010\)](#) tested SME values from 222 to 639 Wh/kg and found that 416.6 Wh/kg was optimum for wheat bran. **Figure 3.9** gives an overview of some SME for LBE. In cases where the SME is an output, the value can be predicted with a highly accurate model ($R^2 = 0.978$) developed by [Lei et al. \(2005\)](#) for a twin-screw extruder.

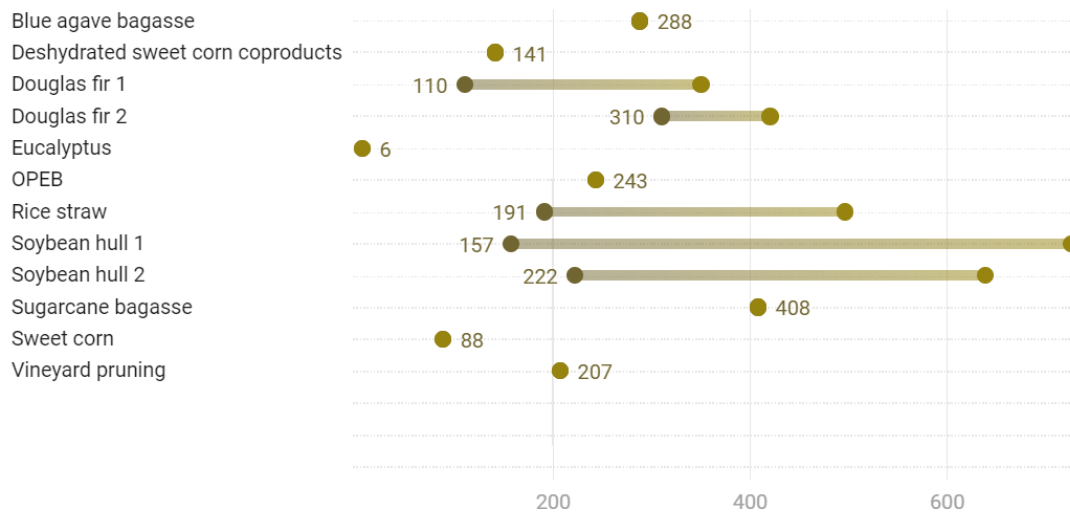


Figure 3.9 Specific mechanical energy for some lignocellulosic biomass extrusion (Wh/kg).

Comparing power consumption between pretreatment methods is complicated and somewhat unnecessary. Indeed, the pre-treatment method must be evaluated with regard to the profitability of the product which allows it to manufacture at the end of the chain (ethanol, biogas, biodiesel, enzymes, resin, etc.). [Kazi et al. \(2010\)](#) used an ASPEN Plus model to simulate the profitability (on short-term economic viability) of four LCB pretreatment methods for ethanol production. The pretreatment methods were dilute acid, 2-stage dilute acid, ammonia fiber explosion (AFEX), and hot water. Corn stover was the raw biomass for all of them. Results showed the dilute acid pretreatment as the best pretreatment method as it gave the lowest product value (1.36 dollars of gasoline-equivalent). On the other hand, [Yoo \(2011\)](#) compared the profitability (for a year) of dilute acid and extrusion pretreatment in the production of ethanol. The Monte Carlo model was used for this purpose and soybean hulls were the substrate. Extrusion pretreatment was the best pretreatment as it produced 23.4% more ethanol than the dilute acid pretreatment. The main reason was the high conversion of cellulose to glucose, achieved with extrusion pretreatment ([Zheng & Rehmann, 2014](#)).

In practice, in order to lower the energy balance of the whole extrusion pretreatment, good practices are:

- Avoid the use of a thermal source during biomass preparation, instead privilege room temperature or solar heat.
- Use kneading screw elements and reverse screw elements sparingly in the screw configuration. As highlighted in § 3.2, these two elements enhance the disruptive effect of

screws on biomass, but at the same time, they increase the energy consumption (Negro *et al.*, 2015; Wahid *et al.*, 2015). The operator must find a compromise according to the objectives of their extrusion pretreatment.

- Select continuous extrusion to avoid unnecessary energy consumption and also because starting up the extruder is time-consuming and energy-intensive. Therefore, plan each extrusion well and prepare everything before starting.
- Make sure the moisture of the substrate is sufficient to ensure smooth transport of the substrate in the barrel, as dry matter content and extruder electricity consumption are strongly linked ($R^2 = 0.73$) (Hjorth *et al.*, 2011). This practice also helps to avoid the overloading of the barrel and the jamming of the screws.
- Limit to the strict minimum the number of passes of the biomass in the extruder. This number may vary from one type of biomass to another. For this, preliminary tests are necessary. As highlighted in § 3.5.2, several studies have shown that beyond a certain number of passes, there is no longer any significant improvement in the sugar recovery rate (Da Silva *et al.*, 2013b; Kuster Moro *et al.*, 2017).

3.6 Additives

Reactive extrusion is performed in an extruder where one or more additives chemically react with the biomass to achieve a change in composition and structure of the lignocellulose. Reactive extrusion is very common in LBE. Usually, the additive is a catalyst, a solvent, an enzyme (bioextrusion), or a combination of them. Additives can also be acid, alkali, organosolv, mineral, etc. Water, sodium hydroxide (NaOH), ethylene glycol, lime (CaOH), sulphuric acid (H₂SO₄), Tween 80 (polysorbate 80) as surfactant, and [EMIM]Ac (1-ethyl-3-methylimidazolium acetate) as ionic liquid are the most used. Reactive extrusion presents a key advantage because LCBs have poor flow capabilities. The aim of using additives is to enhance the flowability of the substrate in the barrel and facilitate saccharification via hydrolysis of the chemicals over the substrate. Reactive extrusion can be performed via two methods: mixing the additive with the substrate during the preparation step or adding the additive during the extrusion process.

3.6.1 Addition before extrusion

Adding additives to the biomass before extrusion (i.e., during biomass preparation) modifies the biomass moisture and this has certain advantages for reactive extrusion. In particular, this

approach allows for a more precise control of the moisture content and mixing is optimal for maximum contact with the additive. Furthermore, when the mixture is stored in the presence of reactive additives, delignification can start during this period, weakening the lignocellulose structure and subsequently facilitating extrusion flow. Many studies have demonstrated that using additives before the extrusion process can be a very good practice, and the application of different kinds of additives has been investigated. [Kuster Moro *et al.* \(2017\)](#) studied the effect of water, glycerol, Tween 80, and ethylene glycol on sugar recovery with sugarcane bagasse and sugarcane straw, and water was found to be the best additive for both biomasses as evidenced by sugar recovery yield. However, this also led to problems with flow during extrusion. Under the pretreatment conditions tested (i.e., long residence time of the substrate inside the barrel, high shearing forces, and temperature), the substrate began to dry and then blocked the screws. Glycerol, as an additive, achieved a slightly lower glucose recovery yield, but substantially improved the flow conditions. On the other hand, with willow and [EMIM]Ac as additives, [Han *et al.* \(2020\)](#) achieved recovery yield for glucose and xylose of 99% and 99.5%, respectively. [Da Silva *et al.* \(2013b\)](#) applied the same solvent on sugarcane bagasse, and achieved 90% glucose recovery yield at 25 wt.% for 8 min extrusion. [Zhang *et al.* \(2012c\)](#) obtained 86.8% of glucose recovery yield and 50.5% of xylose recovery yield with dry corn stover combined with NaOH.

3.6.2 Addition during extrusion

Adding reagents during extrusion involves the use of a pump with a controllable flow rate. Some extruders are equipped with one or two additive pumps, wherein a first additive is injected in the screw zone located after the biomass hopper (**Figure 3.3**). Subsequently, another reagent is added downstream in the extruder to neutralize the first additive (in the case of alkali). The two flows and their respective concentration must be correctly adjusted. If not, the first additive action will not be optimal, or a poor neutralization can occur, negatively affecting further treatment of the extrudate. Extrusion performed this way saves time and energy compared to the case when the biomass and additives are mixed before extrusion and is well adapted to continuous extrusion. These advantages are crucial, especially at pilot and industrial scales. However, the mixing time for biomass and additive is reduced, and the sugar recovery yield can be affected ([Duque *et al.*, 2014](#); [Han *et al.*, 2020](#); [Montiel *et al.*, 2016](#)). [Choi and Oh \(2012b\)](#) pretreated ripe straw with sulphuric acid without a neutralization reagent. Only 43% of glucan (glucose) at 3.5% w/v H₂SO₄ was recovered. Thus, the application of additives before or during the extrusion process must consider the objectives of the experiments, as well as energy consumption, and scale up implications. Sometimes, LBE is coupled with other pretreatments methods ([Beisl *et al.*, 2017](#)). In

that case, the second pretreatment method must be taken into account during the decision-making process.

3.7 Working Parameters

3.7.1 Temperature

Extrusion is defined as a high-temperature technology (Merci *et al.*, 2015). In fact, there are three ranges of temperature for LBE: under 100 °C (low temperatures), between 100 °C and 150 °C (mild temperatures), and above 150 °C (high temperatures) (Appels *et al.*, 2010; Fu *et al.*, 2018).

The temperature inside the extruder barrel results from the heat generated by both external and internal sources. The external source is coming from the heating system of the extruder, while the internal source is the heat generated by the effect of shear forces inside the extruder (viscous dissipation) (Formela *et al.*, 2018). Some extruders offer the possibility to impose a temperature profile along the screw. For example, Montiel *et al.* (2016) pretreated blue agave bagasse using an extruder with four screw sections with different temperatures: 22 °C in the feeding zone, 50 °C in deconstruction zone, 25 °C in the neutralization zone, and 25 °C in the filtration zone. In this case, a higher temperature in the neutralization zone, such as 50 °C in the deconstruction zone, can denature the neutralization agent. This is a good example of how a temperature profile across the extruder design is advantageous for setting the optimum temperature for each screw zone.

It is unclear which temperature range (low, mild, or high) is suitable for a better sugar recovery. For Karunanithy *et al.* (2012a), single-extruded pine wood ran at different temperatures (100 °C, 150 °C, and 180 °C) achieved best recovery results at 180 °C with 66.1% of total sugar recovery. Zheng *et al.* (2016) experienced similar results after a twin-screw extrusion of sweet corn, with xylose recovery yield increasing with temperature (65–100 °C). At higher temperatures, biomass moisture loss is important, which can cause a powerful disturbance in the biomass structure due to shearing forces and elevated thermal action. Higher temperatures can have additional negative impacts on the extrusion process, as the substrate releases volatile organic compounds which can hinder downstream processes (enzymatic saccharification, fermentation, etc.) (Espert *et al.*, 2005; Formela *et al.*, 2016; Formela *et al.*, 2018). Gu *et al.* (2019) used a twin-screw extruder to pre-treat Douglas fir residuals. The screws had five sections (T1 to T5) along with the screws, with the following temperature profile: T1 and T2 (25 °C), T3 (50 °C), T4 and T5 (50, 100, or 150 °C). The results showed that glucose and xylose/mannose yield decreased when the temperature increased in sections T4 and T5, where the conditions ranged from 50 °C to 150 °C. They

attributed this result to the fact that moisture evaporation is pronounced in T4 and T5 at high temperatures, leading to particle agglomeration, an increase in particle size, and cellulose recrystallization.

3.7.2 Residence Time

The biomass residence time in extrusion is considered a particular advantage for this process, as it is very short compared to other pretreatment methods. For LBE, the timespan is on the scale of minutes, with residence times around 1 min 30 s being achieved by [Karunanithy *et al.* \(2012a\)](#) and [Vaidya *et al.* \(2016\)](#). However, there are no standard residence times for laboratory studies, as residence times between 1 and 10 min are common ([Duque *et al.*, 2017](#)). On the other hand, a short residence time could be a problem, especially in the case of bioextrusion (extrusion with enzymes) or in reactive extrusion, when additives are added during the processing, both of which would require longer times for the necessary reactions to take place.

The residence time is the consequence of many factors. For example, screw design can play a role, as cylindrical screws generate longer residence time than conical screws for the same screw length ([Seifert, 2013](#)). Depending on screw speed and the screw configuration, the residence time can be lengthened or shortened. Screw configurations containing more KE, RSE, and short pitches elements lengthen the residence time, while more FSE and larger pitches elements tend to shorten the residence time ([Gogoi *et al.*, 1996](#); [Raquez *et al.*, 2008](#); [Wahid *et al.*, 2015](#)). On the other hand, many authors found that the screw speed is inversely proportional to the residence time ([da Silva *et al.*, 2013a](#); [Duque *et al.*, 2018b](#); [Gu *et al.*, 2019](#)). Generally speaking, flow resistance inside the barrel translates into longer residence times. Furthermore, an extruder without a die at the end of the barrel results in shortened residence times. The length to diameter ratio (L/D) of the screws also influences the residence time, with higher ratios increasing the residence time ([Duque *et al.*, 2017](#)).

So far, there is no evidence about the role of other parameters such as liquid/solid ratio on the residence time. Based on current knowledge, it can be assumed that a higher ratio will shorten the residence time because adding additives enhances the substrate flowability.

It has been reported that long residence times enhance sugar recovery yield as the effects of the shearing forces and all the other pretreatment conditions over the substrate are exerted over a longer period. However, long residence times also raise the SME ([Duque *et al.*, 2021](#); [Zheng *et al.*, 2016](#)). Usually, operators increase the residence time by recirculating the extrudate into the extruder as many times as needed (i.e., number of passes). The number of passes can be up to

ten or more. [Da Silva *et al.* \(2013b\)](#) investigated the effect of the number of passes on saccharification yield for sugarcane bagasse with an ionic liquid as the additive. The results showed that the glucose and xylose recovery increased after the first pass, but additional passes did not significantly increase the yields of glucose and xylose recovery compared to the first pass. [Kuster Moro *et al.* \(2017\)](#) experimented with 10 extrusion passes with both sugarcane bagasse and straw. As previously mentioned, a slight improvement of the glucose recovery yield was observed for each pass (after the first). However, for bagasse after 3 passes and 7 for straw, no improvement was recorded. Additionally, multi passes did not affect the crystallinity index, as no significant variation of the index was observed after the first pass.

3.7.3 Screw Speed

From the initial development of extrusion as a processing step, even in the case of LCB pretreatment, screw speed has been considered as an important parameter ([Chung, 1975](#); [Guo & Chung, 1989](#); [Wahid *et al.*, 2015](#)). Screw speed is measured in rotations per minute (rpm) and usually ranges from 30 to 200 rpm in laboratory LBE settings. Screw speeds less than 100 rpm are considered low and those above 120 rpm are considered high. In particular cases, it can be set very low (down to 5 rpm), or very high (up to 420 rpm) ([Choi *et al.*, 2014](#); [Endersen, 2012](#); [Han *et al.*, 2020](#); [Yoo *et al.*, 2011](#)). As noted in the previous sections, screw speed influences the torque, the SME, the barrel temperature, the residence time, and the substrate flow rate.

Screw speed is one of the most documented parameters in LBE. Like temperature, screw speed alone cannot guarantee the efficiency of the extrusion pretreatment ([Duque *et al.*, 2017](#); [Lamsal *et al.*, 2010](#); [Zhang *et al.*, 2012d](#)). It must be related to other extrusion parameters. For example, [Karunanithy and Muthukumarappan \(2010\)](#) extruded switchgrass, while [Heredia-Olea *et al.*, 2015](#)) extruded Brewers' spent grain. Both studies recorded opposite behavior about screw speed over the glucose recovery yield. While [Karunanithy and Muthukumarappan \(2010\)](#) found the best result by decreasing the screw speed from 150 to 50 rpm, [Heredia-Olea *et al.* \(2015\)](#) obtained their best results by increasing the screw speed from 100 up to 200 rpm. However, it is important to notice that [Heredia-Olea *et al.* \(2015\)](#) ran the extrusion under 20% moisture at 50 °C, while [Karunanithy and Muthukumarappan \(2010\)](#) worked at 15% moisture content and 150 °C. It is also possible to vary the screw speed between high and low settings during the extrusion process. In that case, a way to overcome the rise of the SME is to lower the torque at high screw speeds ([Karunanithy & Muthukumarappan, 2011a](#); [Zheng *et al.*, 2016](#)). Nevertheless, this processing requires more complex design and controls to operate.

3.8 Challenges, limitations, and future prospects

Reactive extrusion is an interesting technology due to the advantages it has over other pretreatment methods, and the traditional disadvantages from which it is freed. These are: the high risk of corrosion of the equipment, the use of large quantities of water during or after pretreatment, the appearance of inhibitors, the pollution and toxicity linked to the use of certain chemical products, and the length of the pre-treatment time which can last several days for example in the case of biological pre-treatments (fungi, bacteria, termites, etc.) (Zhang *et al.*, 2022; Zhao *et al.*, 2022). On the other hand, the challenges related to extrusion as a method of LCB pretreatment can essentially be summarized in four points: the initial investment cost, the energy consumption, the post-purchase flexibility of the design parameters, and the process scale-up.

Although on a medium and long-term basis extrusion is a commercially attractive solution and far better than many other pretreatment methods, the investment costs in this technology are high (Yoo, 2011; Zheng & Rehmann, 2014). The high prices of extruders hinder the democratization of their use. In this case, it might be interesting to diversify the use of the extruder. For example, the same extruder could be used to manufacture composite materials whose commercialization could allow a faster return on investment. Concerning energy consumption, extruders need a heat source and a cooling system in addition to a power supply. These are made possible through the use of electricity. The consequence is a non-negligible energy consumption. It is possible from several practical techniques, such as those presented in § 3.6, to save energy or improve the energy efficiency of the extruder, but less energy-consuming extruders are of essential needs to accelerate the return on investment in the case where the extruder is exclusively used for LCB pretreatment. Another important aspect is the relatively small leeway of the extruder holders for the modification of the screw elements. Extruder owners in most cases have to refer to the equipment supplier for modifications, which add delays and affect the productivity of the extruder. Although technically very difficult, the design of adaptable screw elements according to the desired shapes, inclinations, and diameters or the development of an extruder capable of variably housing one, two, or three screws could revolutionize the use of extruders for maximum destruction of the lignocellulosic complex but also for many other applications. The limits of extrusion are those of mechanical pretreatments in general. They necessarily require an external energy source. Moreover, with mechanical pretreatments, it is impossible to be selective and to target, for example, the types of chemical bonds in the biomass that we would like to break, as this is the case with most chemical pretreatments. Thus, biomass fractionation (separation into

its three major components) with extrusion requires coupling with another pretreatment method such as Organosolv (Brudecki *et al.*, 2013).

Regarding future prospects, in addition to solving the challenges mentioned above, it is about finding an interesting coupling of extrusion with another method of pretreatment. The idea would be to benefit from the many advantages offered by extrusion while mitigating its disadvantages. So far, several coupling ideas have been studied in the literature. For example, extrusion has been coupled with liquid hot water for eucalyptus and aspen pretreatment (Tian *et al.*, 2019), with Steam explosion for corncob pretreatment (Zhang *et al.*, 2014a), Ultrasonication for rice hull pretreatment (Zhang *et al.*, 2020), Ionic Liquid (IL) for pussy willow and sugar bagasse pretreatment (Han *et al.*, 2020), and with Organosolv method for prairie cordgrass pretreatment (Brudecki *et al.*, 2013). As extrusion is one of the most used methods in pretreatment couplings, it is of great interest to investigate, in a review, each of the couplings extrusion has been implicated in, in order to highlight their efficiency, their advantages and disadvantages, their need for improvement, and if possible to advise possible interesting coupling ideas based on lessons learned from existing couplings.

Extrusion optimization and scaling up is also an aspect that is attracting more and more interest. Indeed, experimental designs with response surfaces have been and continue to be used for optimization. The problem is that they take time and are sometimes very expensive. Today, new computational techniques (therefore faster and less expensive) are in development. A genetic algorithm method is one that currently focuses attention. Nastaj and Wilczyński (2021)'s work entitled "optimization and scale-up for polymer extrusion" is a rich source of information on this subject.

3.9 Conclusions

Extrusion is a very flexible method of lignocellulosic biomass pretreatment due to the many parameters available, with optimal conditions for a given process, and can include extruder design, biomass type, additives, and operating conditions. While some parameters related to the extruder design are limited to initial design plans, several other parameters can be adopted as needed by operators to customize for a process' given needs. Most of these parameters are correlated, and clear identification of the purpose of the extrusion and the downstream treatments, as well as the possibility to scale up the process, are important when selecting the extrusion settings. Particular attention should be paid to the energy consumption during the biomass

preparation and the extrusion process, with settings leading to satisfactory sugar recovery with the lowest energy consumption as a focus.

3.10 Acknowledgement

This work was supported by Institut National de la Recherche Scientifique (INRS) (Grant No. 121486) and the Natural Sciences and Engineering Research Council of Canada (NSERC) (Grant No. RGPIN-2020-05720).

4 DEUXIÈME ARTICLE

Combination of technologies for biomass pretreatment: a focus on extrusion

Combinaison de technologies pour le prétraitement de la biomasse : cas de l'extrusion

Delon Konan ¹, Denis Rodrigue ², Ekoun Koffi ³, Saïd Elkoun ⁴, Adama Ndao ¹, and Kokou Adjallé ^{1,*}

1. Laboratoire de Biotechnologies Environnementales, Institut National de la Recherche Scientifique (INRS), 2605, boulevard du Parc-Technologique, G1P 4S5, Québec (Québec), Canada.

2. Département de génie chimique, Université Laval, 1065 Avenue de la Médecine, G1V0A6, Québec (Québec), Canada.

3. Département de génie mécanique et énergétique, Institut National Polytechnique Felix Houphouët Boigny (INPHB), Yamoussoukro, Côte d'Ivoire.

4. Département de génie mécanique, Université de Sherbrooke, 2500, boulevard de l'Université, Sherbrooke (Québec) J1K 2R1.

*Correspondence: kokou.adjalle@inrs.ca

***Waste and Biomass Valorization*, 2024, Volume 15, pages 4519–4540.**

Received: 5 July 2023 / Accepted: 13 February 2024 / Published online: 25 March 2024

DOI : <https://doi.org/10.1007/s12649-024-02472-w>

Contribution des auteurs :

Conceptualization, Writing - Original Draft: Delon Konan; Writing - Review & Editing: Denis Rodrigue, Ekoun Koffi, Saïd Elkoun, Adama Ndao, Kokou Adjallé; Supervision: Kokou Adjallé.

Lien entre l'article ou les articles précédents et le suivant :

L'article précédent (Article 1) répondait à l'objectif 1 qui était d'explorer l'extrusion en tant que méthode de prétraitement des biomasses lignocellulosiques pour en identifier le potentiel, les paramètres de prétraitement et les relations qui existent entre eux. Il en est ressorti principalement quatre leçons :

- (i) l'extrusion est une technologie d'une grande flexibilité pour le prétraitement de tout type de biomasses lignocellulosiques.
- (ii) l'extrusion possède plus d'une vingtaine de paramètres liés à l'extrudeuse, à la biomasse, aux additifs chimiques et aux conditions d'extrusions. Certains de ces paramètres sont corrélés.
- (iii) le succès de l'extrusion passe par l'optimisation de cinq (5) principaux paramètres que sont : la configuration des vis, la vitesse de rotation des vis, la température d'extrusion, la taille des particules et la quantité d'additif utilisé.
- (iv) l'extrusion du fait de ces caractéristiques ferait un excellent prétraitement préliminaire dans le cadre d'un couplage de prétraitement.

Cette dernière leçon a conduit à identifier et analyser les couplages de prétraitements existants et impliquant l'extrusion, afin d'en tirer une expérience et proposer une approche novatrice et adaptée de prétraitement (Objectif 2). C'est le but de ce deuxième article.

4.1 Abstract

Lignocellulosic biomasses, mainly forestry and agricultural residues, are inexpensive, available and attractive to reduce the dependence of the world on fossil fuels. However, before their processing in biorefineries, they must undergo a pre-treatment to allow access to the desired compounds of interest (cellulose, hemicellulose, or lignin). However, the pretreatment step significantly reduces and affects the profitability of the biorefinery process. Several pretreatment technologies have been developed so far. However, taken individually, these methods do not make lignocellulosic biomass a fully cost-effective input for biorefineries, hence the current trend to combine technologies. Extrusion is currently one of the most attractive technologies. Despite reactive extrusion is relatively new, it has been combined with many other methods to pretreat various types of biomasses with interesting benefits and results. This article provides a critical review of pretreatment combinations involving extrusion and discusses the challenges, solutions, and R&D needs for these combinations.

Keywords: lignocellulosic biomass, biomass pretreatment, extrusion, biorefinery.

Highlights

- Extrusion is a promising pretreatment for lignocellulosic biomass.
- Sugar recovery yields from residues are usually close to 80%.
- Extrusion mitigates the disadvantages of other technologies.
- Optimization, throughput, energy consumption, and scaling up are the main challenges.
- Coupled pretreatments suffer from a lack of techno-economic analysis.

4.2 Introduction

Sustainable development, economic decarbonization, and green policy are concepts that cannot be effective if alternatives to unsustainable energies are not found. Over the years, the energy consumption in our society has continuously grown. For example, the global energy consumption (oil, gas, coal, and nuclear) in 1865 was less than 4 000 million tons of oil equivalent, while in 2018 the value was over 12 000 million tons of oil equivalent (Rodrigue, 2020). This represents a 300% increase over a period of only 53 years. The related environmental consequences are now very well-known, especially in terms of increased average temperature. Current global energy demand suggests that fossil energy will continue to be one of the leading sources of energy for many years to come, especially for two reasons. On one side, it is because the modern economic system is deeply based on fossil energy. On the other hand, renewable energies are not sufficiently developed to compete or replace fossil energies in the short term. About the first point, economic policies are changing over the year with introduction of new orientations such as green finance. However, for the second point, active research to find new and sustainable sources of energy is mandatory.

Lignocellulosic biomass is considered as one of the most important alternatives to eliminate our fossil energy dependence (Dong *et al.*, 2021; Zhao *et al.*, 2021). Available in high amount (about 181.5 billion tons/year), lignocellulosic biomass is also cheaper and renewable. This makes it attracting more and more attention (Dahmen *et al.*, 2019). Bioproducts from lignocellulosic materials find applications in diverse domains such as automotive, food industry, agriculture, medicine, cosmetics, energy, and a several new applications are under development. Lignocellulosic biomass is mainly made of lignin, cellulose, and hemicellulose, which bond to each other in a complex and strong three-dimension structure. Before being used as a raw material for

biorefinery, lignocellulosic biomass must be pretreated. The goal of this pretreatment is to weaken or disrupt the lignocellulosic structure to extract/recover the compounds of interest. Most of the time, recovering sugars (cellulose, hemicellulose, and their oligosaccharide or monosaccharides) is the target. But lignin prevents the access of those compound. Over the years, several lignocellulosic biomass pretreatments have been proposed such as reactive extrusion, microwave, ultrasound, pyrolysis, liquid hot water (LHW), ammonia fiber explosion (AFEX), sulfite pretreatment to overcome recalcitrance of lignocellulose (SPORL), and biological pretreatments (Agbor *et al.*, 2011b; Arora *et al.*, 2020; Prasad *et al.*, 2015; Taherzadeh & Karimi, 2008). However, their results remain limited in terms of efficiency, economics, or scaling up (Banu J *et al.*, 2021; Zabed *et al.*, 2019). It is difficult to remove a high percentage of lignin from lignocellulosic biomass in a single pretreatment step, hence the need to explore the combination of two (or even more) pretreatments becomes interesting (Chen *et al.*, 2022b). So, many authors proposed to combine extrusion with other pretreatments, as extrusion is attractive in many ways (Karunanithy *et al.*, 2014; Zhang *et al.*, 2020). Thus, this article provides a critical review of pretreatment combinations involving extrusion and discusses the challenges, solutions, and R&D needs for these combinations.

4.3 Pretreatment technologies

Pretreatments for lignocellulosic biomass are generally classified into four groups, as to date biomass pretreatment has been largely dominated by single-stage pretreatment (Baksi *et al.*, 2023). The four groups are: (i) physical pretreatment (milling, extrusion, microwave, pyrolysis, ultrasonication, etc.), (ii) chemical pretreatment (acid, alkali, oxidative, ionic liquid, organosolv), (iii) physico-chemical pretreatment (steam explosion, wet oxidation, ammonia fiber explosion, CO₂ explosion and (iv) biological pretreatment (enzymatic or microbial) (Akram *et al.*, 2023). Documentation on most of these pre-treatments abounds in the literature. Biological pretreatments involve microorganisms and/or enzymes to deconstruct the lignocellulosic complex. Used for delignification (lignin removal), there are considered environmentally friendly but on the other hand, they are the slowest pretreatment method. This is a major concern for the profitability of the whole valorization process. Nevertheless, they might have a positive effect on the subsequent enzymatic hydrolysis step has reported by some author (Suhara *et al.*, 2012). However, the amount of chemicals used in physico-chemical pretreatment is much lower (no chemicals in hydrothermal pretreatment) than in chemical pretreatment, where the cost of chemicals is one of the main problems, with an additional washing step required. In physico-chemical and chemical pretreatments, furfural and hydroxymethylfurfural (HMF), two of the most

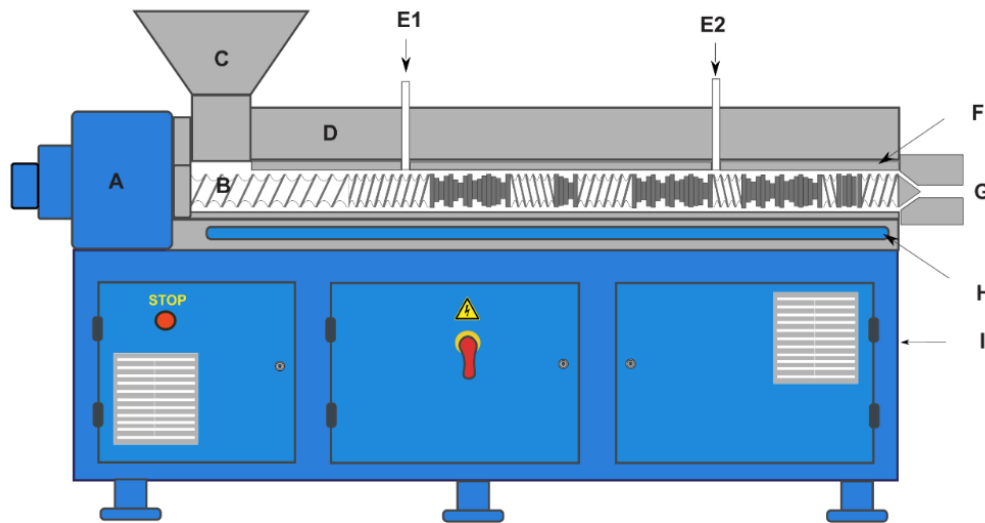
common inhibitors of enzymatic hydrolysis, are produced. Furfural comes mainly from the degradation of hemicellulose, and HMF from cellulose (Dedes *et al.*, 2020; He *et al.*, 2021). Carbohydrate degradation occurs easily under difficult pretreatment conditions, as is the case with physico-chemical and chemical pretreatments. Nevertheless, chemical pretreatment is highly effective for sugar recovery from lignocellulosic biomass (Yao *et al.*, 2021). Many ionic liquids and deep eutectic solvents have been successfully used for lignocellulosic biomass pretreatment. However, the cost of pretreatment remains an almost unavoidable problem. If we consider the ecological aspect of chemical pretreatment (physico-chemical and chemical pretreatment), a major effort is needed here, as most of these chemicals are not environmentally friendly. As for physical pretreatment, to which extrusion belongs, it is highly effective in reducing biomass size and increasing particle surface area. Physical pretreatments use mechanical forces, heat and/or waves to defibrillate the lignocellulosic complex. This makes them an appropriate choice as the first step in a multi-stage pretreatment. Some of them, such as extrusion, are even capable of delignification of lignocellulosic biomass (Konan *et al.*, 2022b). All these pretreatments are carried out and integrated as a step in the process of valorization of lignocellulosic biomass. They must be inexpensive. It has been reported that pretreatment must be less than 40% of the total cost of the valorization process to be profitable. The valorization of lignocellulosic biomass is highly diversified, but most routes lead to bioenergies (bioethanol, biofuel, renewable hydrogen, etc.) or functional materials (bioplastics, optical and flexible devices, functional membranes, hydrogels, foams, etc.) (Sugiarto *et al.*, 2022). Pretreatment is currently the limited step to all those applications. By studying pretreatment technologies, it appears that a new paradigm of pretreatment should be implemented, i.e. capitalizing on the advantages of several technologies by combining those that are complementary. Hence, among the pretreatment combinations that have been explored to date, extrusion (although relatively new as a pretreatment method) has been involved in many of them because of its interesting characteristics.

4.4 Extrusion pretreatment

4.4.1 Extrusion design and principle

Extrusion is a thermo-mechanical process carried out in an extruder where a material (polymer, biomass, etc.) undergoes high shearing forces for different purposes such as blending, compounding, mixing, disruption, compaction, pelletization and shaping. A typical extruder is composed of a feed hopper, a barrel, one or more screws, a die, a drive motor, and a heating and cooling system for temperature control (**Figure 4.1**). The most common extruders so far are single

screw and twin-screw extruders. Other extruder designs including triple screws (Xin *et al.*, 2020; Xue *et al.*, 2018), quadruple screws and even more are in development (Zhu *et al.*, 2018). An extruder screw is either in a single piece or is composed of modules. Modular screws consist of a shaft on which different screw elements are nested depending on the task to be performed. The screws are placed inside the barrel and rotate around their axes thanks to the drive motor. Along a typical screw, three zones can be distinguished: the conveying zone, the mixing zone, and the compressing zone. Each of these functions is ensured by a specific kind of screw element design (Konan *et al.*, 2022b). Generally, extrusion pretreatment for lignocellulosic biomass involves three types of screw elements: forward elements (conveying function), kneading elements (mixing and compression function), and reverse elements (compressing and mixing function) (Guihao *et al.*, 2022a). The distance between the tip of the screw elements and the barrel is usually very tight to limit back flow. During extrusion, the material (substrate) is fed into the barrel through the hopper with a controlled flow rate. The substrate, in contact with the screws, is conveyed by rotation of the screws from the beginning of the screw (feed zone) to the end (die) (Duque *et al.*, 2017). During this transport, the substrate is sheared between the barrel and the screws. Shear forces are controlled through various factors such as the number of screws, screw diameter, screw configuration, the type of elements composing the screw configuration, the space between the screw and the barrel (clearance), the type of screw rotation (corotative or counter-rotative), the intermeshing of the screws, the substrate flow rate, the screw rotational speed, the residence time of the substrate inside the barrel, the die dimensions and geometry (Konan *et al.*, 2022b). All these parameters are related to the extruder. Other parameters are related to the substrate itself such as the particle size distribution, the substrate viscosity, the concentration/formulation rate, and the rheological behavior of the substrate (Mankar *et al.*, 2021).



A: Drive motor, B: Screw, C: Hopper, D: Heating system, E1: First injection point, E2: Second injection point, F: Barrel, G: Die, H: Cooling system, I: Gear box

Figure 4.1 Illustration of a typical extruder with the main components.

4.4.2 Extrusion attractivity

Extrusion has several advantages that make it very attractive for industrial production. It can be operated in batch, fed-batch and continuous processes over a wide range of conditions and materials. It can also be used for process intensification; perform several operations in a single step. For example, in a biorefinery context, the same extruder can be used for both biomass pretreatment and biomass pelletization. Compared to other physical pretreatments, extrusion is considered a low-energy consumption technology (Gu *et al.*, 2018; Hjorth *et al.*, 2011). First of all, depending on the size of the extruder, a significant amount of biomass (several Kg) can be pretreated during one extrusion passage which generally lasts from a few seconds to no more than 5 minutes. As a matter of fact, the energy consumption per biomass pretreated is significantly reduced compared for example to milling technology (Kapoor *et al.*, 2018). Moreover, extrusion does not require important downstream operations because it does not generate inhibitors and does not use high water amounts as hydrothermal pretreatments do (Haghighi Mood *et al.*, 2013). The short pretreatment time is one of the main advantages of extrusion; while biological, chemical and some physico-chemical pretreatments may take from 30 min to several days, one extrusion pretreatment takes a few minutes (usually around 2-3 min). Another interesting advantage is the flexibility of this technology. Extrusion also involves a wide range of parameters (more than 20) that the operator can use to reach his goal. These parameters are related to the biomass, the extruder design, and the extrusion conditions (Konan *et al.*, 2022b). Another important advantage

is that contrary to some pretreatment methods such as ammonia fiber explosion (AFEX) which is only efficient on low lignin biomass (Bals *et al.*, 2010), extrusion has been reported to be effective on all kinds of lignocellulosic biomass. Moreover, extrusion is a scalable technology and extruders are already available on the market for laboratory scale, as well as for pilot and industrial scales. Finally, extruders are usually equipped with one or more secondary injection point for liquids and solids which offers more possibilities.

4.5 Combination of extrusion with other pretreatments

Despite relatively new in biomass pretreatment, extrusion has been combined with several other pretreatments methods for different purposes such as sugar recovery optimization, to overcome other pretreatments technical and economical disadvantages and for scaling-up purposes. To date, extrusion has been combined with physico-chemical pretreatments like steam explosion, liquid hot water, and ammonia fiber explosion; with physical pretreatments such as ultrasonication and microwave; and with chemical pretreatments such as Ionic Liquid (IL), Deep Eutectic Solvent (DESs), and organosolvation.

4.5.1 Reactive extrusion

Reactive extrusion is a process involving chemical additives into standard extrusion processing. It combines the advantages and drawbacks of extrusion as noted in § 4.4 and those of chemical pretreatments stated in § 1.4.2. Raw biomasses without any preparation step are difficult to be processed in an extruder because of their poor rheological behavior (Senturk-Ozer *et al.*, 2011). So, prior to be used in the extruder, raw biomass must be humidified enough by a liquid to improve their rheological behavior. Water addition, in non-optimal condition and ratio (solid/liquid), result in biomass compaction problems inside the barrel because of evaporation and low viscosity. Thermostable additives are then preferred instead of water (Lamsal *et al.*, 2010). The chemical additive can be a catalyst, a solvent, an enzyme, or a binder. However, their concentration must be optimized to provide good fluidity while keeping the shear stresses high on the biomass (Duque *et al.*, 2017).

4.5.2 Alkaline extrusion

Generally, extruders are equipped with a dedicated pump where chemicals are injected inside the barrel with controlled flow rates. For a long time, alkali was considered more suitable for this kind of pretreatment, not only because of good sugar recovery yield, but also because they

generate a better fluidity of the biomass inside the barrel compared to acidic chemicals. Among the alkali used for extrusion, sodium hydroxide (NaOH) is popular because it is relatively cheap, highly efficient, and less damaging to the environment. Sodium hydroxide is able to break ether-ester bonds links in hemicellulose and lignin, as well as to enhance their solubilization during the pretreatment. It is also efficient for breaking ether and carbon-carbon links inside lignin. It is also well-known for its deacetylation effect. However, the effect of NaOH, and alkali in general, on cellulose is weak. This is attributed to the crystalline structure of cellulose which is difficult to amorphized under alkaline conditions (Xu & Cheng, 2011). Duque *et al.* (2018a) run reactive extrusion with NaOH as additive to pretreat Eucalyptus biomass and proposed information/conditions for high sugar recovery yield. These are: low screws speed, a liquid/solid ratio higher than 1, and the NaOH/dry matter ratio must be higher than 8%. The cellulose fraction was not affected by the amount of NaOH within the limit tested (5%, 10%, and 20%). On the other hand, during alkali extrusion, an acid is generally used as an alkali-neutralization agent in case of enzymatic saccharification. Sodium hydroxide is giving way to new chemicals with interesting properties such as ionic liquids and deep eutectic solvents (see § 4.5.8 and 4.7).

4.5.3 Bioextrusion

Enzymes are also used for reactive extrusion (bioextrusion). In this case, the enzymes (α -amylases, glucoamylases, pectinases, etc.) are used as catalysts directly inside the extruder. Among bioextrusion applied to carbohydrates, starch bioextrusion is well-studied; but as a method for lignocellulosic biomass pretreatment bioextrusion was presented recently (Gatt *et al.*, 2018). It may be interesting to study starch bioextrusion to understand the basics of lignocellulosic biomass bioextrusion. But even if the processes are similar, starch bioextrusion and lignocellulosic biomass bioextrusion are different. Starch is a homopolysaccharide and its bioextrusion is run for liquefaction (increase or decrease viscosity) (Mesa-Stonestreet *et al.*, 2012; Xu *et al.*, 2018). On the other hand, lignocellulosic biomass bioextrusion is run for biomass pretreatment which means disrupt the material to enhance the recovery of compounds of interest (sugar, aromatic compounds, etc.). Basically, bioextrusion is like alkali extrusion with a particular attention to extrusion temperatures as enzymes are sensitive to temperature. In fact, due to friction and viscous dissipation during the process, the internal temperature of the barrel can drastically raise and degrade the enzymes. Fortunately, for most extruders available in the market, the temperature can be controlled by a heating and cooling system. Temperatures under 50°C are optimal for biomass bioextrusion. Nevertheless, partial enzymes inactivation can be observed for reasons not yet fully understood (Montiel *et al.*, 2016), thus limiting the efficiency of

this process. The good mixing provided by extrusion is an advantage to generate high specific surface for the enzymes. On the other hand, the short residence time of the substrate inside the barrel is a challenge. Usually, enzymes are used in batch reactors with long residence times between a few hours to several days. For extrusion, the residence time is about a few minutes (2-3) and rarely above 5 min. But it is possible to recirculate the bio-extrudate as many times as needed inside the extruder with or without new enzymes addition (make-up). The motor torque of the extruder can be monitored and usually decreases as the number of passes increase, but the total energy consumption must be considered.

Enzymes and alkali can also be combined in a single extrusion method since enzymes have low efficiency on the raw materials. The complex formed by lignin and hemicellulose hinders the access of enzymes to cellulose (Sinitsyn & Sinitsyna, 2021). The goal of the alkali is to deconstruct this complex to give more accessibility to cellulose fibers. A study of the literature about biomass bioextrusion shows the following facts : (1) there is a significant solubilization of organic matters after the bioextrusion process (more than 2 times the amount without enzymes), (2) above 70% of cellulose fraction is recovered, (3) saccharification starts during the short residence time (few minutes), and (4) the enzymes activity continue after the bioextrusion process (Duque *et al.*, 2020; Gatt *et al.*, 2018; Montiel *et al.*, 2016; Vandenbossche *et al.*, 2016). Vandenbossche *et al.* (2016) observed that after bioextrusion, an increase of two, five, and thirteen-fold the amount of water-soluble organic compounds for blue agave bagasse, sugarcane bagasse, and sawdust of eucalyptus respectively, with a cellulose recovery up to 89% and cellulose saccharification up to 31% (sawdust of eucalyptus) and hemicellulose solubilization up to 45% (sugarcane bagasse). Montiel *et al.* (2016) has showed that the efficiency of the treatment depends on the type of enzyme. The development of low-cost enzymes less sensitive to temperature variations could raise bioextrusion among the methods of choice for the pretreatment of biomass on an industrial scale.

4.5.4 Extrusion and liquid hot water

Liquid hot water (LHW) technology uses the acidic properties of water at high temperatures and pressure to pretreat lignocellulosic biomasses. LHW take place in a dedicated reactor under temperatures between 130 and 400°C, pressure above 5 MPa and biomass residence times from a few minutes to an hour (Figure 4.2) (Li *et al.*, 2017; Refaat, 2012; Talebnia *et al.*, 2010). LHW was reported to enhance enzymatic saccharification yield and lower cellulose polymerization by up to 65% (Li *et al.*, 2017). On the other hand, according to the severity of the LHW pretreatment,

undesirable compounds, such as furfural, acetic acid, 5-hydroxymethylfurfural (HMF), and formic acid, might appear. A way to overcome this issue is to control the pH between 5 and 7 as in the patented process “pH-controlled liquid hot water” (Ladisch *et al.*, 1998). This technology has some advantages and disadvantages. LHW is a simple, cost-effective, and low inhibitor production method. It is cost-effective for two reasons: it does not require any chemicals in the process, only water is added limiting the costs of raw materials. Also, low-cost material can be used to build the reactor as limited corrosion is expected, thus limiting the capital costs (Refaat, 2012; Tomás-Pejó *et al.*, 2011; Yang *et al.*, 2019). However, the large amounts of water (above 80% of the total volume) are involved in the process leading to significant energy consumption (heating) and downstream recovery of the desirable compounds (high dilution). Now, LHW is still at the laboratory and pilot scale and the main limitation for an industrial scale is the economics: high water input and high energy consumption. It also has low production rates in a batch process.

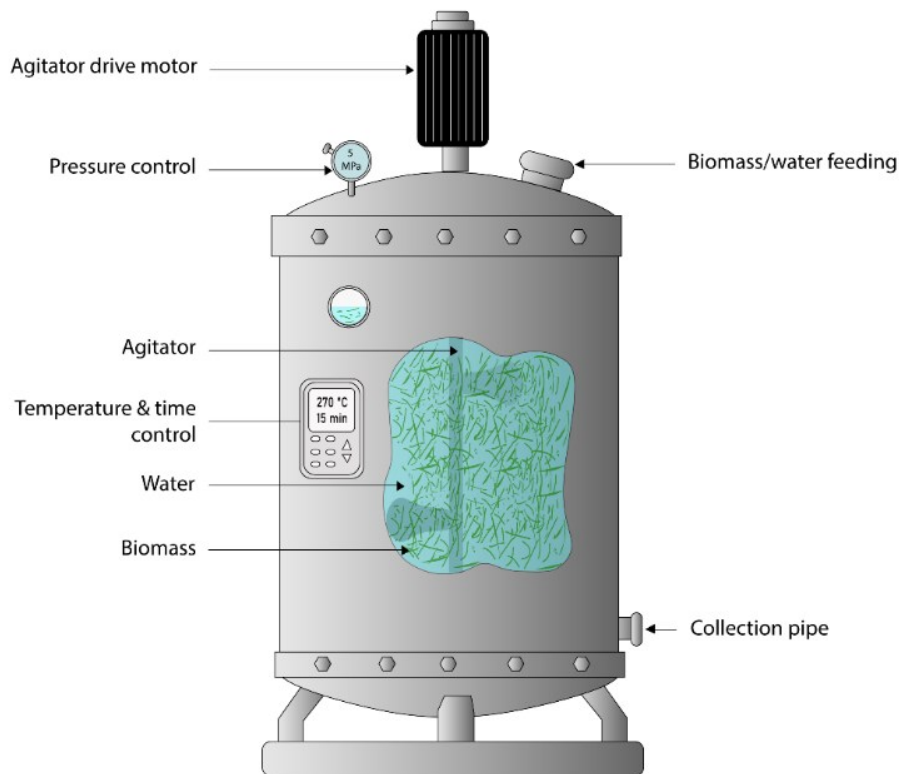


Figure 4.2 Reactor design for Liquid hot water pretreatment.

Based on the advantage of LHW and extrusion, Tian *et al.* (2019) combined both technologies for Eucalyptus and Aspen pretreatment (both hardwood). LHW was the first step followed by extrusion. The idea was that LHW at mild temperature (170°C for 45 and 90 min) should solubilize a high fraction of cellulose and hemicellulose (mainly xylans) and soften the woody biomass.

Then, the extrusion step with high shear stresses should be more efficient to break-up the remaining lignocellulose complex and improve the sugar recovery yield during enzymatic saccharification. The results showed that during LHW, cellulose was hydrolyzed into glucose by up to 98.4%. Beyond 45 min of processing, the xylans underwent degradation and up to 17.8% of lignin was removed. But one interesting observation was the structural change in lignin. For 45 min at 170°C, significant structural change and negligible lignin condensation was observed. This structural change is useful for the downstream pretreatment, but lignin condensation is not desired because it may require harsher conditions during downstream processing. Lignin condensation generally occurs under high temperatures and long residence times for hydrothermal pretreatments (Sun *et al.*, 2021). In the second step (extrusion), Tian *et al.* (2019) reported a significant disruption, size reduction, and fibril exposure of both biomass (Eucalyptus and Aspen). Cellulose hydrolysis yield was above 80% after 72 h.

These results can be extended to some point to softwood, but not for agricultural residues. The fact is that hardwood and agricultural residues are structurally different. The former is composed of more rigid structures (branches, barks, roots, etc.), while the latter regroup all the residues coming from agricultural harvest like straw, husk, stover, bagasse, pruning, fibers, shells, hulls, etc. (Adhikari *et al.*, 2018; Badgujar & Bhanage, 2018). So, further investigation should be made to confirm whether LHW-extrusion technology is an interesting method for agricultural residues pretreatment. About the scale-up of LHW-extrusion, it is technically possible as LHW and extrusion are individually scalable. The challenge is to handle their coupling (rate of production) to get a fully continuous process. Thus, an economical and eco-friendly solution must be found to overcome the issues related to huge amounts of water and energy consumed during the LHW step.

4.5.5 Extrusion and steam explosion

Steam explosion is an old technology. The patent for this pretreatment was filed by Mason in 1926 (Mason, 1926). Similar to LHW, steam explosion is a hydrothermal pretreatment. Both methods present similarities, but their effect on the lignocellulosic material is different. LHW uses liquid water under high pressure and temperature, while steam explosion uses water steam (vapor) under high pressure and temperature. The steam generated comes from the water supply and the biomass moisture. Among all the hydrothermal pretreatments, steam explosion is the most used (Bhutto *et al.*, 2017).

In this process, the lignocellulosic material is placed in an airtight reactor containing liquid water. Then it is heated (140 – 260°C) and kept under pressure (1 and 3.5 MPa) for a relatively short residence time (1 to 20 min). The temperature must be high enough to turn the liquid water into steam in the reactor. After a specific residence time, the pressure is rapidly dropped in the reactor causing explosive decompression. The effects are very fast, and the lignocellulose material is broken down into fibers. Cellulose remains essentially intact, while hemicellulose is degraded and solubilized. The main effect on lignin is the cleavage of β -O-4 ether links and C_α - C_β bonds leading to significant lignin depolymerization (Ahmad & Pant, 2018; Bandyopadhyay-Ghosh *et al.*, 2015; Chung & Washburn, 2016; Shrotri *et al.*, 2017). Sometimes, a catalyst is involved to enhance the explosion effect. The most common are sulfuric acid (H_2SO_4) for liquid catalysts, and sulfur dioxide (SO_2) or carbon dioxide CO_2 for gas-phase acid catalysts. Sulfuric acid is relatively cheaper and has a good disrupting effect (Keskin *et al.*, 2019; Shrotri *et al.*, 2017). The main parameters for steam explosion are temperature, pressure, residence time and the liquid-solid ratio of the catalyst. Steam explosion has a relatively low environmental impact (Hamawand *et al.*, 2020) and is cost-effective as it requires less energy and lower concentration of cheaper catalysts (Pereira Marques *et al.*, 2021). Steam explosion can be applied in different areas such as biogas production, bioethanol, etc. However, as for LHW, furfural, hydroxymethylfurfural, and acetic acid are more likely to be released during steam explosion according to the severity of the treatment. This is one of the main drawbacks.

So far in the literature, there are two sorts of combination of extrusion and steam explosion: continuous Screw Extrusion Steam Explosion (SESE), and the two-step coupling. SESE technology is similar to extrusion pretreatment of biomass, except that the pressure and temperature inside the extruder are higher than in conventional extrusion. At the die exit, the substrate undergoes a sudden drop in pressure. Pressure drops from 2.5 MPa to atmospheric pressure (0.1 MPa). Then the explosive decompression is triggered. Authors using this pretreatment method reported interesting results in terms of sugar recovery. Zhang *et al.* (2014a) pretreating corncob reached 90% of hemicellulose saccharification into monomeric compounds for 5.5 min of SESE pretreatment and after enzymatic hydrolysis. For Chen *et al.* (2014) with corn stover, it was 89% for 2 min processing followed by 70 hours of enzymatic hydrolysis. The morphology comparison between pretreated and raw biomass revealed that SESE increases the specific surface of the extruded material and then enhances hydrolysis efficiency (Feng *et al.*, 2016; Liang *et al.*, 2016). The crystallinity of the substrate increases significantly after the SESE pretreatment. This may be due to structural change occurring in the amorphous region of the cellulose chain (Rashed *et al.*, 2021). Two-step coupling technology consists of steam explosion

pretreatment followed by extrusion, or extrusion followed by steam explosion (less often). Steam explosion and extrusion are run separately, and the solid fraction obtained in the first pretreatment becomes the substrate for the second pretreatment. [Oliva \(2017\)](#) used this method to pretreat barley straw. Steam explosion was the first step followed by extrusion. Results showed high content of lignin and glucan in the solid fraction and significant hemicellulose in the liquid fraction with low inhibitory compounds.

Extruders specially designed for SESE are available on the market. There are capable of processing large quantities of biomass per hour. Regarding the result obtained with this technology, it is obvious that it is a promising technology. However, more investigation is required to lower the energy input and overcome issues related to undesirable compounds such as furfural, HMF, and acetic acid, which are released under harsh pretreatment conditions.

4.5.6 Extrusion and ultrasonication

Ultrasounds are acoustic waves above 20 kHz ([Bhargava et al., 2021](#)). They are not audible to humans and possess interesting properties. When ultrasounds evolve in water, bubbles (4 – 300 μm diameter) are instantly created and collapse just after nanoseconds: It is cavitation. The forced-out air releases locally an extremely high pressure up to 50 MPa and temperatures up to 5000°C (**Figure 4.3**) ([Luo et al., 2014](#)). Ultrasound pretreatment is based on the effect of cavitation on the submerged biomass. Acoustic waves for this purpose range between 16 kHz and 20 kHz ([Flores et al., 2021](#)). Commonly ultrasonication is used with chemicals to enhance the effect of the pretreatment (Assisted-ultrasonication).

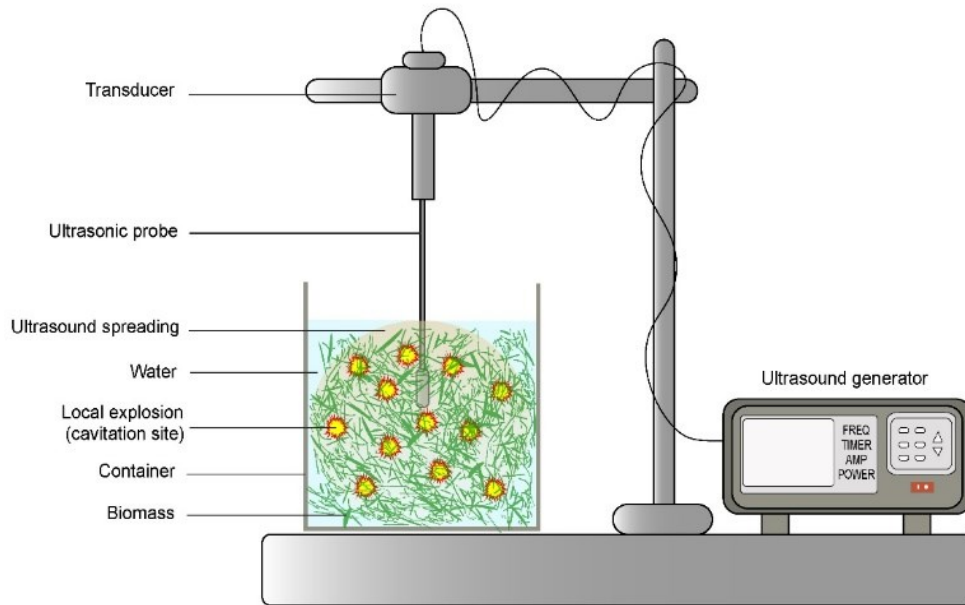


Figure 4.3 Laboratory scale set for ultrasonication pretreatment.

Ultrasound has a variety of effects on biomass. They modify the physico-chemical structure of wood. The pretreated biomass contains fewer alkali metals such as potassium, calcium, and magnesium than the substrate (He *et al.*, 2017). Cellulose fibrillation during an alkali-assisted ultrasonication has also been reported on garden biomass (Gabhane *et al.*, 2014). Saratale *et al.* (2020) obtained 90%, 70%, and 65% for respectively glucose yield, delignification, and xylose yield with NaOH-assisted ultrasonication. Another important fact about the ultrasound effect is its proven ability to increase cellulase activity under frequencies between 18 and 24 kHz. Many authors results confirm this assumption. Wang *et al.* (2012) recorded up to 24.67% cellulase activity improvement after 10 min of pretreatment with 24 kHz. Luzzi *et al.* (2017) obtained 47% increase in cellulase activity with 18 kHz after 15 min of exposition. On the other side, both studies stated that severe pretreatment, meaning high frequency or long residence time, tends to decrease cellulases activities. Crystallinity index is also a parameter affected by ultrasonication pretreatment as highlighted by He *et al.* (2017) after pretreated eucalyptus by ultrasonication. They reported an increase in crystallinity from 31.8 to 35.5%. There is a lack of data to better understand the impact of ultrasound frequency over the efficiency of the pretreatment, but it can be hypothesized that the higher the frequency, the more important efficient is the pretreatment in term of biomass disruption. In fact, higher frequencies carry more energy which is required to vibrate atomic nuclei in lignocellulose and break α -O-4 and β -O-4 ether bonds in lignin and hemicellulose (Sidana & Yadav, 2022). But on the other hand, increase the frequency implies to

increase the energy consumption. The challenge will be making a trade-off between the energy consumption and the maximization of the disruption effect of the pretreatment.

Extrusion-Ultrasound association for lignocellulosic biomass pretreatment is recent. It has been performed for this purpose (sugar recovery) for the first time in 2020 by [Zhang *et al.* \(2020\)](#) and [Byun *et al.* \(2020\)](#). The former pretreated rice hull. No chemical was used either in the ultrasonication process or during extrusion. Extrusion was the first step and ultrasonication the second. A Response surface method (RSM) was used to operate the extrusion process under optimum conditions. Then ultrasonication was run for 1.5 h at 40 kHz and 500 W with the extrudate. Results showed cellulose and hemicellulose conversion of about 77.5%. [Byun *et al.* \(2020\)](#) obtained 83.1% with Amur silvergrass (*Miscanthus sacchariflorus*) by using alkaline extrusion (0.2 M NaOH) followed by one hour of ultrasonication (14.8 kHz, 1.2 kW). These yields are interesting but are less than what some authors, such as [Saratale *et al.* \(2020\)](#) found with only ultrasonication. Many reasons can explain this situation. Some substrates are more recalcitrant than others even from the same plant because of many factors such as the maturity stage of the plant and the substrate preparation conditions. The microstructure and macrostructure of the biomass are affected during those processes. Leaves, trunks, hulls, and straws from the same plant are all lignocellulosic materials but possess different structures. But apart from this, despite extrusion parameters have been optimized, the particle size of the extrudate is not necessarily the optimum size for ultrasonication. Parameter optimization should take into consideration both extrusion and ultrasonication; not just only extrusion parameters but also those of ultrasonication which are ultrasound frequency, temperature, and power consumption ([Methrath Liyakathali *et al.*, 2016](#)). The attractive results obtained with ultrasonication involved the use of chemicals. This can be a problem especially if downstream treatments involve microorganisms or enzymes. Also, there is a lack of evidence about if the pretreatment order (extrusion before ultrasonication or ultrasonication before extrusion) affects the sugar recovery yield.

4.5.7 Extrusion and microwave

Microwaves correspond to frequencies between 300 MHz and 300 GHz with wavelengths from 1mm to 1m ([Huang *et al.*, 2016](#)). Microwave is one of the most documented lignocellulosic biomass pretreatments. The principle of microwaves pretreatment is the same as for home microwaves. For many laboratories scale studies, a home microwave is used. The lignocellulosic raw material is irradiated for less than 30 min in a microwave device with or without chemicals at

a wave frequency generally about 2.5 GHz. Contrary to ultrasonication, microwave pretreatment severity is expressed in terms of power. It ranges between 60 W and 1000 W. There is a correlation between power and biomass heated temperature. The higher the power is, the higher the temperature. The temperature inside the biomass can easily reach 800°C. Today microwave for lignocellulosic biomass pretreatment is a simple and well-mastered technology. It ensures rapid heating and demonstrates its effectiveness for pyrolysis with relatively low energy consumption (Lo *et al.*, 2017).

To enhance the efficiency (in terms of sugar recovery yield) of extrusion, Karunanithy and Gibbons (Karunanithy *et al.*, 2014) developed the sequential-extrusion-microwave process to pretreat switchgrass and bluestem. The setup consisted of two devices: a single screw extruder and a microwave. The biomasses were first pretreated by extrusion and the extrudate was submitted to microwave under power going from 180 W to 720 W for 2.5 to 10 min. Results showed that the microwave step was efficient to enhance the total sugar recovery yield of at least 19.7% compared to extrusion only. They found that, regardless of the type of biomass, the main microwave parameters were moisture content, temperature, and residence time. The optimum moisture content was 25%. Beyond 25%, there is no significant improvement in the sugar recovery yield (Wang *et al.*, 2013). The effect of microwaves on the extrudate is mainly due to the dielectric properties of water. Water absorbs the radiation, and the vibration of the water molecules inside the extrudate ensures a better heat transfer and then the deconstruction of the lignocellulose complex (Aguilar-Reynosa *et al.*, 2017). Chemicals with high dielectric constants such as polar solvents (organic preferably) can be used to enhance this effect. The problem with the coupling extrusion-microwaves is primarily a matter of scale-up as it involves important energy consumption, essentially due to microwaves (Mitani, 2018); and subsequently, there is no guarantee of effectiveness of the pretreatment at a large scale. In fact, energy transfer is a serious problem for the large application of microwaves as pretreatment method. Microwaves are not enough powerful to penetrate deeply and uniformly in massive biomass quantity. In this way, a temperature gradient is created in the biomass from outside to inside, with the outer zones directly exposed to microwaves being the most irradiated.

4.5.8 Extrusion and ionic liquid

Ionic Liquids (ILs) are liquids composed exclusively of ions linked to each other by different kinds of bonds. They are salts. ILs are liquid at ambient temperature and their melting point is under 100°C while conventional salts have a very high melting point (Lei *et al.*, 2017). For example

ethylammonium nitrate melting point is around 13°C while sodium chloride (NaCl) melting point is 803°C (Tadesse & Luque, 2011). ILs are considered an alternative to organic and aqueous solvents with low vapor pressure and relatively low viscosity (Singh & Savoy, 2020). There are more stable and less likely to evaporate compared to organic solvents (MacFarlane *et al.*, 2014). The other interesting characteristics making them unique and attractive are their non-flammability, their thermal stability, and their good conductivity for electrochemical purposes (Patel & Lee, 2012). ILs are proved their capability for diverse kinds of reactions such as depolymerization, polymerization, alkylation, acidic hydrolysis, Beckmann rearrangement, carbonization, esterification, and pre-extraction (Acharya *et al.*, 2021; Huang *et al.*, 2021; Mehta *et al.*, 2021; Wu *et al.*, 2021; Zhang *et al.*, 2013).

Despite ILs show interesting properties, their “greenness” is controversial. Not all ILs can be considered green solvents (Ghandi, 2014). However, recently ILs have been used for lignocellulosic biomass pretreatment. Many studies have demonstrated the effectiveness of ILs on cellulose and lignin and both for forestry and agricultural residues (An *et al.*, 2015; Tadesse & Luque, 2011). Concerning cellulose, the main effect observed is the break of intramolecular hydrogen bonds that lead to enhance the hydrolysis yield. After ILs pretreatment, the cellulose obtained is highly amorphous (Li *et al.*, 2010). This pretreatment is also effective for lignin solubilization.

ILs pretreatment has been combined with extrusion by Han *et al.* (2020) and Da Silva *et al.* (2013b). Both studies used [Emim][Ac] (1-methylimidazolium acetate). Wood powder of pussy willow and sugar bagasse was merged first in the ILs, mixed, and then fed into the extruder for processing. The residence time (number of passes), the effect of barrel temperature, the biomass loading, and the biomass morphology were investigated. The results of both studies showed that the number of passes had no significant impact on total sugar recovery. The optimal temperature is around 150°C depending on the biomass loading. About the morphology analysis of the extruded materials, both studies reported a significant disruption and fibrillation effect in the biomass. Cellulose microfibrils diameter was less than 500 nm. This led to an increase of more than 100-fold of the cellulose specific surface area. The enzymatic saccharification yield was improved under these conditions. Han *et al.* (2020) reported glucose and xylose recovery of respectively 99.0% and 99.5% under 160°C, 5 rpm, and 15% solid loading after 72 h of enzymatic saccharification. As for Da Silva *et al.* (2013b), they obtained more than 90% of glucose after 24 h of enzymatic saccharification under 25% solid loading, 140°C, 15 rpm, and 8 min residence time (two passes). So, very high sugar recovery can be obtained with ILs-Reactive extrusion

technology. However, ILs are expensive. It is possible to recycle and reuse them but they remain costly compared to many other pretreatment methods (An *et al.*, 2015; Bernal *et al.*, 2014; Groff *et al.*, 2013). On this subject, research investigations are promising. George *et al.* (2015) for example synthesized a relatively low-cost IL (triethylammonium hydrogen sulfate) and used it for switchgrass pretreatment and compared the saccharification yield to a well-known commercial IL [Emim][Ac]. The low cost-cost IL was 75% as effective as [Emim][Ac]. While solving the economic aspect of ILs, the environmental impact of their production must also be considered.

4.5.9 Extrusion and deep eutectic solvent

Deep eutectic solvents (DESs) have been and continue to be considered by many authors as a special category of ILs. But even if they share similarities, these two types of chemicals are different. DESs are liquids obtained from a mixture of two or more constituents (usually solid at room temperature) in a certain relative proportion. The resulting body should have a unique melting point lower than those of each constituent taken separately (Guthrie, 2010; Zhang *et al.*, 2012a).

DESs involve at least one Hydrogen Bond Donor (HBD) and one Hydrogen Bond Acceptor (HBA) (Kalhor & Ghandi, 2019). As for ILs, there are composed only of ions (one discrete anion and cation) (Smith *et al.*, 2014; Zhao & Anderson, 2012). Compared to ILs they possess the following advantages: non-flammability, ease of preparation (simple mixing, moderate heating), low production cost (20% of ILs cost), and large-scale application. On the other hand, cellulose is poorly soluble in DESs. They are less chemically inert, and information about their toxicity is missing (Elgharbawy *et al.*, 2020; Smith *et al.*, 2014; Zhang *et al.*, 2012a). However, DESs are generally admitted being less toxic than ILs because they can be produced from natural primary metabolites (Natural Deep Eutectic Solvent (NADES) (Kalhor & Ghandi, 2019; Paiva *et al.*, 2014).

Since their appearance, DESs have been used for lignocellulosic biomass pretreatment. DESs can break carbon-carbon and aryl ether bonds and can be used as solvents, co-solvents, or catalysts. Chlorine-based DESs are the most widespread. Factors affecting the efficiency of DES pretreatment include biomass composition, biomass crystallinity, particle size, the effect of HBD and HBA, molar ratio of each other, and reaction conditions of the pretreatment (Elgharbawy *et al.*, 2020; Xu *et al.*, 2020b).

DESs has been combined to extrusion for lignocellulosic biomass pretreatment. The advantage of this combination is the possibility to load up to 50% of biomass and still have important sugar recovery yield. This advantage has been put in evidence by Ai *et al.* (2020). They ran experiments

to compare batch pretreatment (with DES) and DES-Continuous extrusion pretreatment. The DES was Choline Chloride: Glycerol (ChCl:Gly). Results obtained at 10% of biomass loading rate after 2 hours of residence time in the batch pretreatment were similar to that obtained with 30% biomass loading rate after only 16 min at the same temperature. In addition, with a continuous extrusion at 50% biomass loading, up to 87% and 86.5% of glucose and xylose respectively were obtained. However, more experiments should be run on different biomasses to confirm the effectiveness of this pretreatment.

Extrusion and DESs are in their early stages. There is a lack of studies about their coupling and techno-economic analysis. Even if it is well assumed that DES is promising in lignocellulosic biomass pretreatment, there are a couple of unexplored fields to be covered to enable broader use of DESs like in the coupling Extrusion-DES. So far, the reaction mechanism of DESs is unclear and DESs are highly moisture-sensitive. This can be a major problem in biomass pretreatment since generally, pretreatment must be flexible for diverse biomasses. A clear understanding of this mechanism may help to develop a computer model and design less moisture-sensitive DES.

4.5.10 Extrusion and organosolv/clean fractionation

Organosolv pretreatment is a well know technology in the paper industry. It is used during the pulping process. It presents many drawbacks but possesses interesting advantages that keep it still using until now. Organosolv pretreatment consists of the use of organic solvent to separate the principal constituents of the biomass. Organic solvents break α -O-4 and β -O-4 aryl ether linkages within lignin, and covalent bonds between lignin and hemicellulose (mostly α -ether bond) (Nishimura *et al.*, 2018; Wei Kit Chin *et al.*, 2020; Zhao *et al.*, 2009). However, the lignin initial structure is not altered. Lignin and hemicellulose are solubilized whereas cellulose remains solid. With simple filtration and precipitation, nearly pure lignin and cellulose can be recovered at the end of the process: lignin from the black liquor and cellulose from the solid fraction. **Figure 4.4** illustrates an organosolv pretreatment. This pretreatment seems to be effective on diverse types of lignocellulosic biomass, from hardwood chips to agricultural residues such as husk, straw, and bagasse (Joseph *et al.*, 2021). For a long time, it was admitted that the delignification effect of this pretreatment was the main reason for the enzymatic hydrolysis improvement. But now we know that even if delignification contributes to enhance saccharification yield, the decreasing of the cellulose polymerization degree is the main reason (Zhang *et al.*, 2016). Another advantage of the organosolv process is the possibility for the solvent to be recycled by distillation.

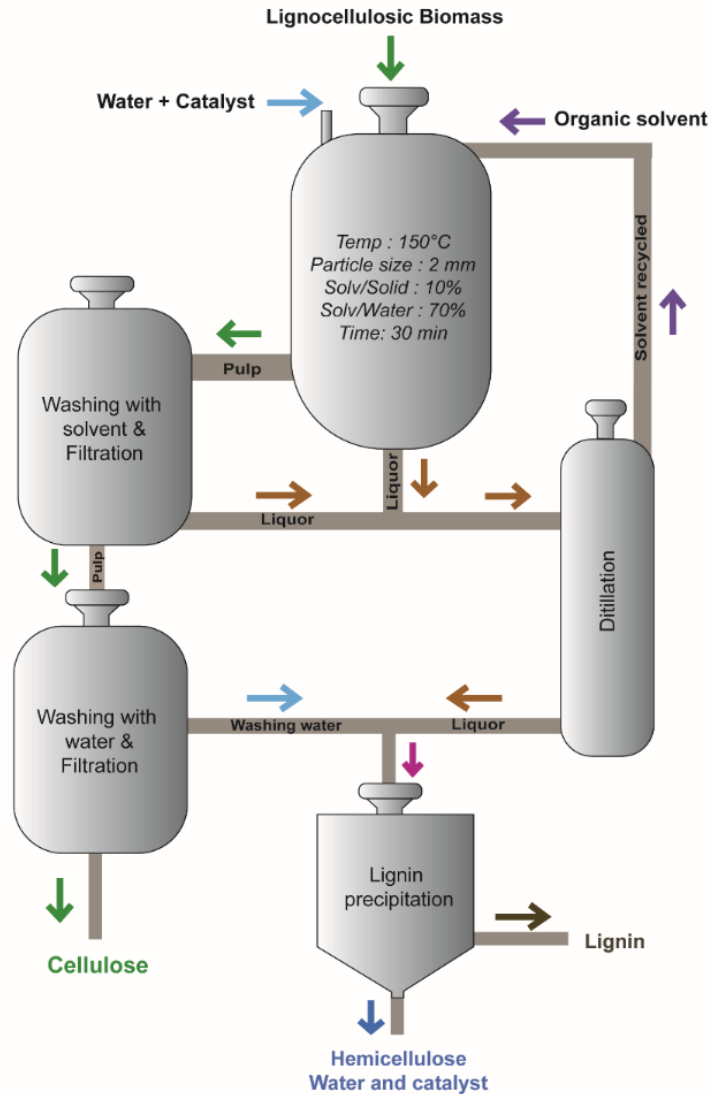


Figure 4.4 Organosolv pretreatment.

At a laboratory scale, the reaction usually takes place in a batch reactor. The main operating parameters are temperature (100 – 220°C), solvent concentration (60 – 100%), biomass/solvent ratio (5 – 10%), particles size (a few μm to 8 mm), and the pretreatment duration (15 minutes to hours). Inorganic salts or acids such as sulfuric acid (H_2SO_4) or hydrogen chloride (HCl) can be used as a catalyst to enhance delignification (Alio *et al.*, 2019; Zhou *et al.*, 2018). In that case, the catalyst concentration (0.05 – 2%) is a key parameter. Harsh organosolv pretreatment i.e. high temperature, long residence time, and solvent concentration near 90% usually lead to poor fractionation results and the appearance of furfural and 5-hydroxymethylfurfural (Pathak *et al.*, 2020). Mild operation conditions are then advised. There is a large number of organic solvents but the most used are methanol, ethanol, acetic acid, ethylene glycol, glycerol, formic acid,

acetone, phenol, MIBK (methyl isobutyl ketone), and NMMO (N-Methylmorpholine N-oxide). The choice of the solvent is based on the price of the solvent, its boiling point, and its efficacy. Low boiling point solvents consume less energy during distillation and primary alcohols have a better delignification effect than second and tertiary alcohols (Zhao *et al.*, 2009). The toxicity and flammability of organic solvent are important drawbacks of organosolv pretreatment.

As far as we know, organosolv has been combined two times with extrusion for biomass pretreatment. The first extrusion-organosolv coupling was performed by Brudecki *et al.* (2013) and Beisl *et al.* (2017). Single screw extrusion (90°C at 65 rpm) was the first step followed by organosolv pretreatment. They investigated the influence of time, temperature, and the concentration of catalyst and solvents on prairie cordgrass fractionation. Sulfuric acid (H₂SO₄) was the catalyst, and the solvent was a mixture of water and two organosolvents (methyl isobutyl ketone (MIBK) and ethanol) at different concentrations each. Results indicated that at optimum conditions (by Response Surface Methodology), the combined pretreatment was significantly more effective than organosolv pretreatment only. Glucose, lignin, and xylose recovery yields were respectively 92, 87, and 95%. The extrusion step was significantly effective to improve the xylan and lignin removal during organosolv. However, they recorded the formation of hydroxymethyl furfural coming from up to 4% of the initial glucose. The second extrusion-organosolv coupling was performed by Beisl *et al.* (2017) with a conical twin-screw extruder. The first step was extrusion followed by organosolv with water and ethanol as solvents without catalyst. The raw material was wheat straw. The results showed non-significant improvement in lignin and carbohydrates recovery yield with relatively low formation of inhibitors such as furfural (0.25%), HMF (less than 0.8%), and acetic acid (less than 3%). Unfortunately, enzymatic hydrolysis was not performed to go deeper in the analysis. However, the non-improvement of the compound recovery yield may be due to screw configuration, which plays an important role in the disruption effect of the raw material but is not taken into consideration during optimization. At this stage, no conclusion can be made about the efficiency of the organosolv-extrusion coupling. More investigations are needed to figure out whether the efficiency depends on the type of solvent, catalyst, biomass, and/or the extruder. In case of important sugar recovery yields a scale-up and technical-economic analysis will be useful.

4.5.11 Extrusion and ammonia fiber explosion

Ammonia Fiber Explosion (AFEX) is a method that uses ammonia (NH₃) in specific conditions of temperature (60 – 140°C), time (5–45 min), pressure (17 – 20 bar), and concentration (0.3–2/kg

dry matter) to pretreat lignocellulosic biomass. AFEX does not produce downstream effluent as it is a dry-to-dry process. This method is effective for lignin deacetylation, cellulose crystallinity reduction, and breaking the α -ether bond between lignin and carbohydrates. However, it has been reported several times that AFEX is less effective on biomass with high lignin content like woods and some agricultural residues (Zhao *et al.*, 2020). Besides good carbohydrate conversion yield, AFEX is famous for its relatively low temperature (60 – 140°C) and the ammonia can be recycled (97%) at the end of the process (Chundawat *et al.*, 2010; Stoklosa *et al.*, 2017). In a biorefinery concept, AFEX is also interesting as it preserves lignin and protein from denaturation so that they can be valued for diverse purposes (Saville *et al.*, 2016). However, AFEX can be less attractive in terms of capital cost compared to many other pretreatment methods. For example, Nieder-Heitmann *et al.* (2019) ran a scenario with Aspen Plus for succinic acid production and electricity production with lignocellulosic biomass. Among the seven profitable pretreatment methods, AFEX had the highest total capital cost (CAPEX).

Apart from biomass densification (pelletization and briquetting), the only study reported in the literature that couples AFEX and extrusion for biomass pretreatment was performed by Dale *et al.* (1999). Their goal was to improve the digestibility of corn stover in ruminants by combining the advantages of extrusion (temperature control, good mixing, low cost, high throughput) and those of AFEX mentioned above. The AFEX pretreatment was carried out directly inside the extruder so that the two pretreatments were carried out simultaneously. Results were satisfactory. Compared to the untreated material, enzymatic digestibility was enhanced by 3.5 times, and the ruminant digestibility was increased up to 32%. However, no more studies are available to compare the result and to assess the technical and economic feasibility of this pretreatment combination in the biorefinery industry.

4.6 Summary of extrusion-based pretreatment results

Tableau 4.1 summarizes the results of extrusion pretreatment. Glucose yields more than 90% can be achieved with many extrusion combination pretreatments, such as Bioextrusion, Extrusion-ionic liquid and Extrusion-organosolv. Most existing extrusion-based pretreatments focus on agricultural residues, and to date, there are few studies on wood or forest residues. This may be explained by the poor rheological behavior of wood inside the extruder barrel. In this case, the extrusion step must be preceded by a pretreatment capable of reducing the hardness of the wood ("chips") and/or significantly reducing the size of the chips. In addition, reactive extrusion can be

carried out to increase the viscosity of the material in the extruder, using a suitable quantity of ionic liquid or deep eutectic solvent, for example.

Tableau 4.1 Summary of extrusion-based pretreatment results.

Pretreatment	Biomass	Results	References
Alkaline extrusion	Eucalyptus	Glucan conversion: 40%; Xylans conversion: 75%	(Duque <i>et al.</i> , 2018a)
Bioextrusion	Sweet corn, sugar cane bagasse, Eucalyptus, Vineyard pruning, blue agave bagasse, Oil palm empty fruit bunch (OPEFB)	Hemicellulose extraction: 18 – 54%; Lignin extraction: 9 – 41%; Cellulose conversion into glucose: 39 – 85 %	(Vandenbossche <i>et al.</i> , 2016)
	Blue agave bagasse	Glucose yield: 96%; Sugar concentration: 69.5 g/L	(Montiel <i>et al.</i> , 2016)
Extrusion - Liquid hot water	Eucalyptus, aspen wood	Xylans conversion: 54% for eucalyptus and 38.1% for aspen wood; Cellulose hydrolysis: 79.6% for eucalyptus and 100% for aspen wood	(Tian <i>et al.</i> , 2019)
Extrusion - Steam explosion	Corn cob	Hemicellulose conversion: 90%	(Zhang <i>et al.</i> , 2014a)
	Corn stover	Sugar recovery yield: 89%	(Chen <i>et al.</i> , 2014)
	Hazelnut skin	Lignin reduction from 35% to 29.4%; methane production 310.6 ml CH ₄ /g VS	(Oliva, 2017)
Extrusion - Ultrasonication	Rice hull	Carbohydrates conversion: 77.7%; Sugar reducing yield: 381.59 mg/g (sugar), 291.59 mg/g (glucose), and 88.87 mg/g (xylose) of rice hull	(Zhang <i>et al.</i> , 2020)
	Miscanthus sacchariflorus	Sugar recovery: 83.1%	(Byun <i>et al.</i> , 2020)
Extrusion - Microwave	Switchgrass (SG) and Big bluestem (BB)	Sugar recovery: 59.2% (SG) and 68.1% (BB); glucose recovery: 52.6% (SG), 83.2%; xylose recovery: 75.5% (SG), 92.1% (BB)	(Karunanithy <i>et al.</i> , 2014)
Extrusion - Ionic liquid	Wood powder of pussy willow	Glucose yield: 99%; xylose yield: 99.5%	(Han <i>et al.</i> , 2020)
	Sugarcane bagasse	Glucose yield: 92.2%; xylose yield: 85.9%	(Da Silva <i>et al.</i> , 2013b)
Extrusion - Deep eutectic solvent	Sorghum bagasse	Glucose yield: 87.0%; xylose yield: 86.5%	(Ai <i>et al.</i> , 2020)
Extrusion - Organosolv	Prairie cordgrass	Glucose yield: 92%; lignin removal: 87% xylan removal: 95%	(Brudecki <i>et al.</i> , 2013)
	Wheat straw	Lignin extraction: 22.3%	(Beisl <i>et al.</i> , 2017)
Extrusion - AFEX	Corn stover	Enzymatic hydrolysis increased by 3.5 times compare to untreated	(Dale <i>et al.</i> , 1999)

4.7 Combination challenges

As seen above, some couplings are promising. However, they face important challenges that may affect their attractiveness if those challenges are not addressed properly. This section presents an overview of major coupling challenges.

4.7.1 Couplings optimization

Extrusion couplings are of two kinds: either single-step or two-step processes. These couplings involve not only challenges related to each pretreatment method but also challenges of the combination of the two pretreatments (extrusion being the first or the second pretreatment). To be efficient, extrusion parameters and the parameters of the other pretreatment must be optimized together for the goal of the pretreatment which can be substrate deconstruction, biomass fractionation, sugar recovery, etc. (Yağcı *et al.*, 2022a). In fact, optimizations can be performed separately in the case of two-stage coupling, but this may not be the best way to proceed. For example, in a two-step coupling with extrusion as a first pretreatment, the extrudate particle size with the optimum extrusion parameters is not necessarily the optimum particle size for the second pretreatment. If possible, the two pretreatment methods should not be optimized separately but rather as a whole. In that case, a design of experiment with a response surface methodology can be suitable to find the optimum setup with the least experiment to run. Central Composite Design is widely used for extrusion optimization but the choice of the design of experiment for the coupling must consider both extrusion and the other pretreatment method (Mota *et al.*, 2021; Zheng *et al.*, 2016).

4.7.2 Substrate supply

Extrusion has a short residence time and can be carried out in a batch, fed-batch, or a continuous process. This is not the case for all pretreatment methods (Ruiz *et al.*, 2020). An extrusion combination with a pretreatment method with a long residence time, like AFEX and clean fractionation, should deal with the mass flow. Extruders are designed for a relatively narrow range of mass flows. The more the screw diameter is, the higher the mass flow is. The choice of the desired mass flow is made only at the time to purchase the extruder. In practice, the mass flow varies according to the properties of the substrate and the extrusion parameters. So, when choosing an extruder for coupling purposes, the decision must take into account the rheological behavior of the biomass to be pretreated and the desired mass flow rate.

4.7.3 Energy consumption

Energy consumption is of great concern. In single-step extrusion combination such as alkaline extrusion, extrusion-DESs, or extrusion-ILs, the specific energy consumption is lower compared to extrusion. These chemicals improve the fluidity of the biomass in the barrel, then lower the specific mechanical energy by lowering the torque. Contrary to single-step extrusion, the specific

energy consumption increases with two-step processes when the second pretreatment method use energy (microwave, ultrasonication, etc.). The profitability of the pretreatment is affected because more energy is consumed in the pretreatment combination to pretreat the same amount of biomass than when only extrusion is carried out. It is particularly true for hydrothermal pretreatments due to a large amount of energy they involve (Agbor *et al.*, 2011a). However, this must be balanced with the extra sugar recovery yield allowed by the efficiency of the pretreatment. On the other hand, biomass pretreatment may not be profitable as a step, but due to its effectiveness, it should make profitable the entire process in which it is integrated (Zhao *et al.*, 2020).

4.7.4 Scaling up

Despite extrusion is a scalable process, it still faces many scaling-up challenges. Extrusion scaling studies has been performed the most for the polymer industry, and up to date, there is a lack of information about the scaling up of extrusion as a pretreatment method of lignocellulosic biomass. Nastaj and Wilczyński (2021) pointed out some general important scaling up challenges. Among them, there is the improvement of the extrusion model which can be considered the first step toward the scaling up. In fact, due to the broad number of extrusion parameters, scaling up based on experimental tests can be expensive and time-consuming. Modeling/simulation as an alternative has been found to be more efficient. Genetic algorithms are getting attention for this purpose. So far, various models have been developed with more or less success for basic operations. These models do not integrate, or difficulty simulate complex operations during extrusion such as a combination of flood and starve-fed extrusion with non-conventional screw configuration. Extrud, REX, SSEM, NEXTRUCAD, Akro-Co-Twin, SIGMA, LUDOVIC, TXSTM, TSEM, and GEM are some of the well-known models (Nastaj & Wilczyński, 2021).

Lignocellulosic biomasses have different flow behavior (particulate solid) inside the extruder compared to polymers such as thermoplastics for which extrusion scaling up has been most studied. Thus, specific investigations into lignocellulosic biomass extrusion are required to develop a model first and explore scaling up perspectives. Some authors are interested in this topic, and they have made progress in the development of a model. For instance, Karunanithy and Muthukumarappan (2011a) developed a quadratic model for single-screw extrusion by investigating the effect of many extrusion parameters on the torque. The mathematical model was able to predict the torque requirement of four biomasses: Switchgrass, prairie cordgrass, corn stover, and big bluestem. As for Mikulandrić *et al.* (2016), after some simplification of the

assumptions, they developed a model for heat transfer in the biomass and on the barrel wall. The accuracy of the model to predict the temperature was $R^2 = 0.82$, which can be considered a good result regarding the complexity of the relationships between parameters influencing temperature during lignocellulosic biomass extrusion. Recently, an important breakthrough was made by [Morales-Huerta *et al.* \(2020\)](#) with twin-screw extruders. They designed and tested a model of a reactive extrusion (NaOH and H₂SO₄) of lignocellulosic biomass. The model was an integration of four sub-models (one flow model and three biopolymer degradation models) and aimed to predict sugars recovery yields. Despite the prediction was relatively accurate on the whole basis, the model was not reliable in many aspects. For example, hemicellulose predictions were in agreement with what was experienced only when NaOH concentration was 4 wt %; beyond the model failed to predict the results. Despite LBE modeling is getting more and more attention, there are important gaps to fill in the literature. Extrusion couplings should deal with these difficulties regardless of whether it is a single step or a two-step coupling. In fact, apart from reactive extrusion where various chemicals additives can be used inside the extruder to improve the pretreatment, extrusion couplings are two-step couplings. It means that the first step is extrusion, and the second step is the other pretreatment or vice versa. Those two-step couplings bring challenges related to the upscaling of the other pretreatment. For example, in case of extrusion-ultrasonication coupling, in addition to the upscaling challenges of extrusion discussed above, ultrasonication brings its own upscaling challenges which are: (i) the optimization of energy consumption, (ii) the uniformity of cavitation activity within the biomass for high volume, and (iii) the reactor design to avoid biomass compaction [HYPERLINK "bookmark://_ENREF_166" Flores *et al.*, 2021; Ong & Wu, 2020a](#)). Tableau 4.2 below lists the upscaling challenges associated with the second pre-treatment method with which extrusion is combined.

Tableau 4.2 Upscaling challenges associated with the second pre-treatment in a two-step coupling with extrusion.

Pretreatment	Challenges	References
Hydrothermal (liquid hot water, steam explosion)	Reactor design, kinetic model, heat transfer model, reactor corrosion, water consumption, energy consumption, large scale studies, continuous reactor	(Chen <i>et al.</i> , 2022b; Heidari <i>et al.</i> , 2019; Li <i>et al.</i> , 2013; Pavlovic <i>et al.</i> , 2013; Ruiz <i>et al.</i> , 2020)
Ultrasonication	Energy wastage, optimization of energy consumption, reactor design, economic profitability, uniformity of cavitation activity	(Flores <i>et al.</i> , 2021; Ong & Wu, 2020a)
Microwave	Fundamental understanding of microwaves heating system, the penetration depth of the waves inside the biomass, dielectric properties of different biomass, uneven distribution of microwave energy, inhomogeneity of reaction temperature, missing technical information for commercial design and development, need for electrical energy, risk of overheating (degradation of compounds)	(Kostas <i>et al.</i> , 2017; Mitani, 2018; Puligundla <i>et al.</i> , 2016; Robinson <i>et al.</i> , 2022)
Ionic liquid	Toxicity, stability, moisture sensibility, high viscosity, solvent regeneration and recycling, reaction kinetic and parameters, development of biobased ILs, costliness, lack of scale-up studies	(Amini <i>et al.</i> , 2021; Asim <i>et al.</i> , 2019; Badgujar <i>et al.</i> , 2019; Chen <i>et al.</i> , 2022a; Zhang <i>et al.</i> , 2021b)
Deep eutectic solvent	Thermal stability, high viscosity, lack of life cycle analysis and techno-economic studies, inhibitor generation, contaminant susceptibility, recycling, clarifying reaction mechanism, thermodynamic models, computer simulation, the influence of water molecule in DES	(Chen <i>et al.</i> , 2021a; Chen <i>et al.</i> ; Florindo <i>et al.</i> , 2019; Sandlewal <i>et al.</i> , 2018; Tang <i>et al.</i> , 2017)
Organosolv/clean fractionation	Corrosivity, high volatility, flammability, toxicity, the large amount of water used in the process, high process cost, energy consumption, compounds recovery (solvent and catalyst), high temperature, continuous organosolv process	(Vaidya <i>et al.</i> , 2022; Wei Kit Chin <i>et al.</i> , 2020; Zhang <i>et al.</i> , 2022; Zhao <i>et al.</i> , 2022)
Ammonia fiber explosion	High temperature and pressure, energy consumption, environment pollution, partial lignin removal, ineffectiveness on high-lignin biomass, cost of ammonia	(Wagle <i>et al.</i> , 2022; Zhao <i>et al.</i> , 2022)

4.8 Recommendations

Recommendations for successful extrusion pretreatment can focus on the four main combination challenges described above. Regarding combination optimization, firstly, given that different biomasses have different rheological behaviors, extrusion pretreatment optimization must be carried out for each biomass. It has been shown that separate optimization of the pretreatment involved in the combination does not necessarily result in optimization of the combined pretreatment (§ 4.7.1). Consequently, optimization must be carried out, regardless of the number of steps involved. When considering optimization, it is always a good idea not to rely solely on the literature, but to carry out a screening design to select the most critical parameters, as these may differ from those in the literature depending on numerous parameters such as biomass type and maturity, and extruder type. Most of the time, the configuration and arrangement of the extruder screws are not defined in articles, even though they are very important parameters. Wahid *et al.* (2015), and Duque *et al.* (2018b) have clearly demonstrated the role of these important but

neglected parameters on sugar recovery yield. The main disadvantage of extrusion is the cost of capital expenditure (CAPEX). In combination with other technologies, the extruder is more likely to be used for a short period than the pretreatment it is combined with, as extrusion is a very fast technology. Thus, the discontinuity in substrate supply can be turned into an attractive advantage by using the extruder for other value-added purposes during this time. We therefore recommend using the extruder not only for biomass pretreatment, but also for many other complementary tasks to improve the profitability of the pretreatment. This may require the purchase of specific additional accessories to be added to the extruder but will result in reduced operating costs (OPEX) and lower energy consumption costs. For example, the extruder can be used to manufacture bio-based plastic films, pellets for 3D printing, biomass pelletizing, and so on (La Fuente *et al.*, 2022; Singamneni *et al.*, 2019). If well-chosen and diversified, these secondary uses can be as profitable, or even more profitable, than the main extrusion use. Thus, we also recommend the use of a small quantity of environmentally friendly chemicals, not only to improve the yield of the pre-treatment in terms of sugar recovery, but also to reduce energy consumption by improving the rheology (viscosity) of the biomass while reducing torque and specific mechanical energy. If possible, these chemicals should be recovered and reused several times. When water-intensive pretreatments are involved in the combination (e.g. hydrothermal pretreatments), the water must be recycled. For the scale-up challenge, we recommend starting with the most reliable models on the market, as described in § 6.4, to save money and time. Nevertheless, practical trials should be carried out to identify potential operational problems. Although extrusion is a well-known piece of industrial equipment, extrusion pretreatment is not necessarily a technology designed for large-scale industrial pretreatment, precisely because the cost of such equipment will hamper the CAPEX of the entire biomass valorization process. It is suggested that a techno-economic study be carried out to determine the optimum scale for a more profitable valorization process. For example, in the perspective of biogas production, an extrusion-based combination could be used by an association of small farmers in the same region. In this scenario, the equipment will be on a pre-pilot scale, and investment and operating costs will be shared between the associated farmers.

Given that extrusion has a strong impact on biomass defibrillation while significantly reducing biomass particle size (increasing biomass specific surface area) in a short time (less energy consumption), it may be interesting to study extrusion in combination with fungi solid-state fermentation for delignification purposes. In fact, white rot fungi require substantial biomass defibrillation and high particle surface area for their enzymes to be effective in lignin decomposition. Such a combination of extrusion and solid fermentation for delignification could

maximize carbohydrate recovery and reduce the cost of pretreatment by also capitalizing on the valorization of ligninolytic enzymes produced during pretreatment. Despite solid-state fermentation is known as a low-cost technology, many important technical problems may be encountered when investigating this novel pretreatment approach. Biomass compaction and agitation are the two main problems. Biomass compaction in the bioreactor limits oxygen transfer. As for agitation, strong agitation may destroy the mycelium, and weak agitation may not be sufficient to mix the biomass properly and avoid compaction in the bioreactor. Studies are needed to assess the effectiveness and economic viability of this new approach.

4.9 Conclusion

Given the interesting advantages of extrusion, this technology now occupies an important place among lignocellulosic biomass pretreatments. Extrusion coupling with many types of pretreatments witnesses the interest for this technology. In general, four facts emerge from the study of existing combinations of pretreatment with extrusion:

- First of all, results in terms of sugar recovery yield are close or above 80%;
- Also, several aspects such as the scaling up and techno-economic analysis remain less explored;
- Moreover, extrusion mitigates the disadvantages of the second pretreatment but does not eliminate them. The specific challenge for second physical and physico-chemical pretreatment (LHW, steam explosion, etc.) is energy consumption. As for the chemical methods (ILs, DES, etc.), it is about the cost of the chemical compounds, their recycling, and the optimization of the water quantities used;
- Finally, there is a lack of information about extrusion and biological pretreatment combination for lignocellulosic biomass pretreatment.

5 TROISIÈME ARTICLE

Biodecomposition with *Phanerochaete chrysosporium*: A review

Biodécomposition avec *Phanerochaete chrysosporium* : Une reevue

Delon Konan ¹, Adama Ndao ¹, Ekoun Koffi ², Saïd Elkoun ³, Mathieu Robert ³, Denis Rodrigue ⁴, and Kokou Adjallé ^{1,*}

1. Laboratoire de Biotechnologies Environnementales, Institut National de la Recherche Scientifique (INRS), 2605, boulevard du Parc-Technologique, G1P 4S5, Québec (Québec), Canada.

2. Département de génie chimique, Université Laval, 1065 Avenue de la Médecine, G1V0A6, Québec (Québec), Canada.

3. Center for Innovation in Technological Ecodesign (CITE), University of Sherbrooke, Sherbrooke, QC, J1K 2R1, Canada

4. Département de génie mécanique et énergétique, Institut National Polytechnique Félix Houphouët Boigny (INPHB), Yamoussoukro, Côte d'Ivoire.

5. Département de génie mécanique, Université de Sherbrooke, 2500, boulevard de l'Université, Sherbrooke (Québec) J1K 2R1.

*Correspondence: kokou.adjalle@inrs.ca

***AIMS Microbiology*, 2024, Volume 10, Issue 4: 1068-1101.**

Received: 08 August 2024 / Revised: 24 October 2024 / Accepted: 19 November 2024
/ Published: 25 November 2024

DOI : <https://doi.org/10.3934/microbiol.2024046>

Contribution des auteurs :

Conceptualization, Writing-Original Draft: Delon Konan; Writing-Review & Editing: Adama Ndao, Ekoun Koffi, Denis Rodrigue, Saïd Elkoun, Mathieu Robert, Kokou Adjallé; Supervision: Kokou Adjallé.

5.1 Abstract

Phanerochaete chrysosporium is considered the model fungus for white rot fungi. It is the first basidiomycete whose genome has been completely sequenced. Its importance lies in the fact that its enzymatic system comprises the major enzymes involved in lignin degradation. Lignin is a complex and highly recalcitrant compound that very few living organisms are capable of degrading naturally. On the other hand, the enzymes produced by *P. chrysosporium* are also powerful agents for the mineralization into CO₂ and H₂O of a wide range of aromatic compounds. However, these aromatic compounds are largely xenobiotic compounds with documented toxic effects on the environment and health. While the economic and environmental benefits of biodegradation with *P. chrysosporium* are well established, a thorough understanding of *P. chrysosporium* and its biodegradation processes is essential for successful biodegradation. Our aim of this critical literature review is to provide a concise and comprehensive insight of biodecomposition of organic substrate by *P. chrysosporium*.

Keywords: *Phanerochaete chrysosporium*; biodecomposition; lignocellulosic biomass; lignin; xenobiotic aromatic compounds

Lien entre l'article ou les articles précédents et le suivant :

L'article précédent (Article 2) répondait à l'objectif 2 qui était d'identifier et d'analyser les couplages de prétraitement existants et impliquant l'extrusion afin de proposer une approche novatrice et adaptée de prétraitement. Il en est ressorti principalement que :

- Compte tenu des nombreux avantages qu'elle offre, l'extrusion a été couplée avec plus d'une dizaine de prétraitements.
- Ces couplages tiennent compte uniquement des avantages techniques de l'extrusion et pas des caractéristiques des extrudats.
- Les couplages réalisés jusque-là l'ont été avec des prétraitements chimiques, physiques ou physico-chimiques.

Sur la base de ces résultats, et au regard des caractéristiques générales des extrudats, il a été proposé le couplage de l'extrusion et de la biodégradation (cf. § 4.8). Le but de cet article qui répond à l'objectif 3, est donc d'explorer et comprendre la biodégradation par fermentation avec *Phanerochaete chrysosporium* ; le choix de cette souche ayant été fait lors d'une analyse bibliographique préliminaire.

5.2 Introduction

Biodecomposition, biodegradation, or biological decomposition are all the processes, procedures, and means that lead to the degradation of a compound using microorganisms (bacteria, yeast, fungi, etc.) (Mohanty & Swain, 2017). Biodecomposition is a field of expertise in its own, with its theories, methods, concepts, techniques, and tools. Its importance in research has grown with the development of industries. The development of this field is closely linked to that of industrial production. Indeed, the exploitation of industries and their diversification over the years has given rise to several major environmental problems, including water pollution (Adane *et al.*, 2021; Kordbacheh & Heidari, 2023). Industrial effluents and manufactured products are heavily laden with pollutants of many types. These pollutants find their way into natural environments and cause significant damage to flora and fauna; hence, the need to treat these effluents before they are discharged into the environment. Certain phenolic and aromatic compounds are persistent xenobiotic pollutants with serious consequences for the health of living organisms, including humans (Anku *et al.*, 2017). They are present in effluents of a variety of industries (pulp and paper, agrifood, textiles, pharmaceuticals, chemicals, ceramics, electronics, etc.). Their elimination or degradation has been the subject of several chemical wastewater pretreatment methods. However, the cost, ecological aspect and effectiveness of these chemical methods pose problems. Biodecomposition, as a wastewater treatment method, has been developed based on the ability of certain microorganisms to degrade, decompose and metabolize phenolic compounds. The most promising of these microorganisms are fungi, especially white rot fungi (WRF). They are naturally equipped to degrade phenolic compounds through a system of intra- and extracellular enzymes (Pointing, 2001). These organisms can thrive in both liquid and solid media. That also contributes to their suitability as site decontamination agents (Bumpus, 2021). They also have the reputation of being the most efficient organisms for the degradation of one of the most complex compounds in the living world: Lignin. Lignin is one of the major components of lignocellulosic biomasses (Phanthong *et al.*, 2018). It is the main obstacle to the development of second-generation biorefineries, which aim to convert the cellulose and hemicellulose contained in lignocellulosic biomasses into biofuels. Today, lignin is the focus of much attention in biotechnology and materials science. The reasons for this situation are manifold. At a socio-economical level, petroleum-derived products are increasingly the subject of bad press because of their environmental cost. Despite the petrochemical industry's efforts to green its reputation, the balance is increasingly tipped in the direction of a definitive and urgent move away from non-renewables. Yet, lignocellulosic biomass is the only renewable source of energy that is most similar in composition and application to fossil fuels (oil, coal, etc.) (Zoghalmi & Paës, 2019).

Moreover, this type of biomass is the first and largest reservoir of cellulose, a compound highly prized in the materials and biorefinery sectors (O'Neill *et al.*, 2022). Because of their unique ability to break down lignin and aromatic compounds, fungi, especially white rot fungi (WRF), are used in the treatment of lignocellulosic biomasses, industrial effluents, for decontamination, bioremediation, etc. *Phanerochaete chrysosporium* is by far the most popular WRF because its many applications. The aim of this literature review is to provide the reader with a fundamental and in-depth understanding of this fungi in the context of biodegradation, by investigating the latest knowledge on the subject.

5.3 Classification in the fungi kingdom

P. chrysosporium is a fungus of the phylum Basidiomycetes, of the class Agaricomycetes, of the Polyporales order, and of the Phanerochaetaceae family. Basidiomycetes are the second most numerous phylum in the fungi kingdom, after Ascomycetes. They are estimated to contain over 40,000 different species of fungi (He *et al.*, 2022). Basidiomycetes are mainly characterized by the shape of their spore-producing organs, called basidia, which are reminiscent of a club or club-like shape with spores at the ends. In some species of basidiomycetes organized in hyphae, the hyphae is septate; i.e. the nuclei of the hyphae are separated from each other by septa (Naranjo-Ortiz & Gabaldón, 2019). Basidiomycetes are made up of three (or four, depending on the author) classes, the broadest of which is the Agaricomycetes. Most Agaricomycetes are saprophytic fungi (Yuan *et al.*, 2023). They are found in environments rich in organic matter. They play a crucial role in ecosystems, mineralizing nutrients and making them available to other growing plant and animal organisms. This group includes white and brown rot fungi. They are also pathogens when they target living organisms. The Agaricomycetes are highly diversified in terms of morphology and also include a large proportion of well-known edible fungi such as the popular commercial mushroom (*Agaricus bisporus*), the oyster mushroom (*Pleurotus oestratus*), and the Shiitake (*Lentinula edodes*) (Hibbett *et al.*, 2014). The Polyporales order of Agaricomycetes essentially contains ligninolytic fungi (capable of degrading lignin). Some fungi in this order can parasitize the roots of certain plants or form mycorrhizal associations with orchids. Polyporales are frequently isolated from woody tissues and plant roots (endophytes) (Cao *et al.*, 2021). As for the Phanerochaetaceae family, it is frequently subject to rearrangements or additions of genera based on new species discoveries or phylogenetic reclassification of existing ones (Miettinen *et al.*, 2016). However, the *Phanerochaete* genus in the Phanerochaetaceae family is stable. It groups together fungi that cause white rot on wood. Their fruiting structure is a monomitic septate hypha (composed of a single type of hypha). To date, the international Catalogue Of Life (COL)

database contains 105 species of Phanerochaetes. Few data exist in the literature on the *Phanerochaete* genus, but one of its species is the focus of much attention. This is *P. chrysosporium*. Other well-known Phanerochaetes include *Phanerochaete velutina* for bioremediation, and *Phanerochaete sordida* for biotransformation (Corredor *et al.*, 2024; Mori *et al.*, 2024).

5.4 Genetic identity

The *P. chrysosporium* genome was the first of the white rot fungi (and basidiomycetes in general) to be completely sequenced. The number of chromosomes can vary considerably from one strain to another (e.g. 10 chromosomes for *P. chrysosporium* BKMF-1767 and 11 for *P. chrysosporium* ME-446 (Reddy & D'Souza, 1994), but the genome is composed of almost 30 million base pairs. Today, research is focused on identifying the functions of the constituent genes (Kato *et al.*, 2024; Martinez *et al.*, 2004). Genes encoding the production of lignolytic enzymes have a prominent place in this research. The lignolytic enzymes of interest are manganese peroxidase, laccase, lignin peroxidase, and the cytochrome P450 family. By analyzing the genes responsible for manganese peroxidase (MnP) production, Kuppuraj *et al.* (2021) identified five (5) different manganese peroxidases produced by *P. chrysosporium*, ranging in size from 32 to 62 kDa and consisting of around 380 amino acids each. The genes encoding these enzymes comprise short chains of 6 or 7 introns (Gold & Alic, 1993). Expression of these genes occurs late in the life cycle, practically during the mature phase of the fungi. Moreover, manganese peroxidase secretion is triggered only under conditions of thermal stress and when the environment contains specific cofactors such as MnO₂ and hydrogen peroxide (H₂O₂). The quantity and quality of enzymes produced depend on these exogenous factors. According to Emami *et al.* (2020), heterogeneous iron oxide (Fe₂O₃) (containing alginate) significantly boosts MnP production by almost 70%.

The production of laccase in *P. chrysosporium* is highly controversial. Indeed, analysis of the *P. chrysosporium* genome has failed to reveal any genome regions coding for laccases known to date (Coconi-Linares *et al.*, 2015). However, some studies have demonstrated laccase production by *P. chrysosporium* (Singh *et al.*, 2020; Srinivasan *et al.*, 1995). Indeed, in the 90s, it was unclear whether *P. chrysosporium* production was dependent on environmental factors, or whether *P. chrysosporium* was genetically deficient in laccase production (Rodríguez *et al.*, 1997; Thurston, 1994). To date, although there is very little information concerning the genes responsible for laccase production in *P. chrysosporium*, it is nevertheless accepted that, like MnPs, laccase is produced as a result of environmental conditions and copper (Cu²⁺)-containing inducers such as

copper sulfate (Gnanamani *et al.*, 2006). Laccase production has been observed in the presence of high levels of nitrogen, glucose and copper (Dittmer *et al.*, 1997). Production can be even higher when co-cultured with *Trametes versicolor* or in the presence of manganese IV oxide (Rodríguez *et al.*, 1997; Singh *et al.*, 2020). The addition of veratryl alcohol, 2,5-xylidine, fructose (more than 100-fold in certain basidiomycetes), glucose, and cellobiose to the culture medium has been reported to significantly increase laccase production (Kunamneni *et al.*, 2007). Laccase is reported to play the dual role of depolymerizing lignin and repolymerizing quinones and phenols (products of lignin degradation), with the aim of preserving fungi from these compounds which, once released into the environment, become toxic to fungi (Rodríguez *et al.*, 1997). The production of laccase in white rot fungi would therefore appear to be a defense mechanism resulting from adaptation. However, studies have demonstrated the ability of recombinant strains of *P. chrysosporium* to produce laccase using genes from other white rot fungi strains well known for laccase production, such as *Trametes versicolor* and *Pleurotus eryngii* (Coconi-Linares *et al.*, 2015; Coconi Linares *et al.*, 2018). Laccase transcription has been reported to be mediated by different genes, but gene sequences range from 515 to 619 amino acids.

The lignin peroxidase family comprises several isoenzymes. These enzymes are synthesized from clustered genes separated by 8 or 9 short intron chains (Gold & Alic, 1993). Each isoenzyme is encoded by a different gene of 343 to 344 amino acids. The genes encoding these enzymes have been located on 5 of the 10 chromosomes of *P. chrysosporium* BKM-1767 and on 4 of the 11 chromosomes of *P. chrysosporium* ME-446. Like manganese peroxidases and laccases, LiP expression is influenced by the nutrient composition of the medium. Excess nitrogen and carbon in the medium leads to non-secretion of LiP and MnP, while excess Mn(II) boosts MnP production but suppresses LiP expression (Holzbaur & Tien, 1988; Reddy & D'Souza, 1994). A total of 154 genes encoding P450somes have been identified in the *P. chrysosporium* genome, constituting around 1% of the genome (Kato *et al.*, 2024). Research into cytochromes P450s (CYPs) is more recent than the other three enzyme types discussed. Furthermore, cytochromes are secondary metabolites. They are a family of enzymes produced by many microorganisms, including human cells. They play several roles, such as elimination of toxic substances, and are involved in fatty acid metabolism in human cells (Sarparast *et al.*, 2020). In *P. chrysosporium*, they are also involved in the degradation of phenolic compounds (Matsuzaki & Wariishi, 2004; Ning & Wang, 2012). Analysis of the *P. chrysosporium* genome has identified over 150 genes encoding P450somes, covering more than 12 families and 23 subfamilies. This is one of the largest numbers of genes encoding P450somes ever identified in a fungal genome. The cytochrome P450 family includes CYP51, CYP53, CYP61, CYP63, CYP505, CYP5158A1, and CYP5144C8

(Ichinose *et al.*, 2022; Ning *et al.*, 2010; Yadav *et al.*, 2006). All 150 genes have been shown to be expressed regardless of the conditions under which *P. chrysosporium* is grown: Lignolytic (low nitrogen content) or non-lignolytic (high nitrogen content). However, 23 of these genes are upregulated in the presence of high nitrogen levels and 4 are upregulated in the opposite case; i.e., when there is a low level of nitrogen (Subramanian & Yadav, 2008).

Since the earliest days of the research into the genetic identity of *P. chrysosporium* in the 1980s, researchers have been interested in gene cloning, using a variety of techniques available at the time. In 1989, Alic *et al.* (1989) successfully carried out the first genetic transformation of an adenine auxotrophic strain of *P. chrysosporium*. This involved introducing into the DNA sequence of the adenine deficient *Phanerochaete* strain, the corresponding *ade2* gene isolated from another fungus strain (*Schizophyllum commune*). After this study, several others followed with genetic transformations involving several other genes. In 1998, the genetic transformation of *P. chrysosporium* took another step forward with the introduction of the λ YES expression vector, enabling the construction of a complementary DNA library for *P. chrysosporium* (Schick Zapanta *et al.*, 1998). When the genome of *P. chrysosporium* was finally completely sequenced in 2004 by Martinez *et al.* (2004), in 2006 Sharma *et al.* (2006) proposed a less costly and rather efficient approach to genetic transformation of *P. chrysosporium*. This approach, used in other contexts with other microorganisms, involved co-culturing pellets of the auxotrophic strain with pellets of the virulent strain containing the gene to be cloned. In 2012, Suzuki *et al.* (2012)'s comparative study of the genomes of *P. chrysosporium* and *P. chrysosporium* provided a better understanding of the genome of *P. chrysosporium*, and the genetic reasons for their natural tendency to colonize hardwood more than softwood. While gene cloning in *P. chrysosporium* continues to be the subject of research in recent years, primacy is given to genes encoding enzymes of the ligninolytic enzyme system, certainly because of the potential of these enzymes for various cutting-edge applications and their future economic value.

5.5 Natural habitat

While some studies restrict the presence of *P. chrysosporium* to North America and Africa, the fact is that it can be found in woodland and temperate ecosystems throughout the world (Lim *et al.*, 2007). It proliferates particularly on dead wood (branches, stems, leaves, etc.), but also evolves in various soil and water environments and even on animals. For example, Vivekanandhan *et al.* (2021), Liu *et al.* (2016b), Dahiya *et al.* (2001), and Zhao *et al.* (1995) isolated it in India from the effluent of a sago food processing plant, in China from mountain trees,

in Canada from the soil of a sugar factory landfill, and in South Africa from an indigenous forest. In general, *P. chrysosporium* prefers humid environments with temperatures close to 40°C.

5.6 Isolation technique and natural substrate

Most of the *P. chrysosporium* strains used in research come from biotechnology companies, associations, or institutes such as the American Type Culture Collection (ATCC) in the USA, the Deutsche Sammlung von Mikroorganismen und Zellkulturen (DSMZ) in Germany and the National Collection of Yeast Cultures (NCYC) in the UK. The advantage of using strains from biotechnology organizations is the time saved and the reliability of the *Phanerochaete* strain used. This is particularly useful in research to compare results with those in the literature. In addition, these companies offer genetically modified strains of *P. chrysosporium* for specialized applications. To date, several different strains of *P. chrysosporium* are commercially available and can be identified by an alphanumeric code following the species name. For example, *P. chrysosporium* B-22 is effective for parasitizing nematode species (Bin *et al.*, 2019). However, for one reason or another, it may be useful to isolate one or more strains of *P. chrysosporium* from its natural environment. In this case, isolation involves a series of steps that can be summarized in four consecutive stages: (i) in-situ sampling of a portion of the natural environment, (ii) inoculation onto a suitable synthetic medium, (iii) strain identification, and (iv) subculture of the desired strain. The first step consists in identifying an environment suited to the development of the desired strain, and a time of year when its activity is likely to be at its peak. This could be, for example, damp dead wood in a state of advanced decomposition during hot periods of the year; or damp soil covered by a high concentration of woody debris (Yang, 2005). Better still, if fructification of the strain is visible, the first step can be completed by directly sampling the carpophore with a portion of its medium to recover the underlying mycelium. The sampling step should preferably be conducted in a sterile tube or container, to avoid external contamination of the sample and make the third step less difficult. The culture medium may or may not be selective but should contain at least the nutrients required for strain development (see § 8). The agar culture is then incubated at 25 to 40 °C for 48 to 72 hours to allow sufficient time for the microorganism species to develop. Once colonies and mycelia are clearly visible, identification can begin. This is a tedious and sometimes frustrating stage. It consists of morphological identification (Khalil *et al.*, 2021; Zhao *et al.*, 1995). *P. chrysosporium* presents different morphologies depending on the environment and conditions in which it is found. When grown in petri dishes, it develops a beautiful, white, filamentous radial mycelium that is densely reticulated after 48 hours (Figure 5.1). Under certain conditions, not yet fully understood, small tufts of fluffy, whitish cotton-like fuzz form on the

mycelium. On dead wood, *P. chrysosporium* develops a mycelium with the appearance of a smooth and uniform concretion of plank paint (Liu *et al.*, 2020a). Open-access online databases are available to help identify fungus species. These databases provide information on each species listed, with supporting photos for some of them. Among the best known are Mushroom Observer, MycoBank, Catalogue of Life and Index Fungorum (Bánki *et al.*, 2024). However, *P. chrysosporium* can easily be confused with *Phanerochaete velutina*, *Phanerochaete sordida*, *Phanerochaete laevis*, *Phanerochaete tuberculata*, and *Phanerochaete bubalina*, as their appearance are very similar. For this reason, in addition to morphological evaluation, further identification may be required through molecular and biochemical analyses targeting DNA. Franco-Duarte *et al.* (2019) present a useful overview of the essentials of these analytical techniques. Once the *Phanerochaete* strain has been identified, the next step is the cultivation of the organism in liquid medium or on agar for 24 to 48 hours. Samples of the liquid culture broth or strain mycelium (on agar) can then be stored at -4 °C for future use.

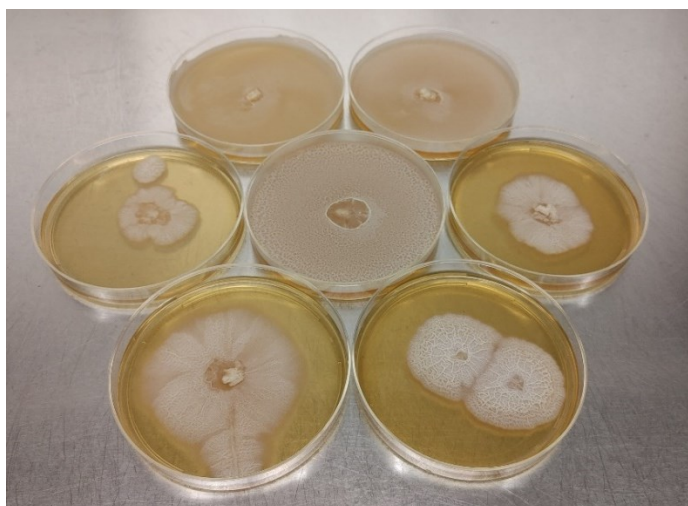


Figure 5.1 *P. chrysosporium* on petri dish started with a piece of mycelium as inoculum.

(Incubation temperature was 30 °C and culture media was Yeast Broth BD 271120.)

Lignin is the natural substratum of *P. chrysosporium*, which it degrades to find carbon sources and food. Lignin is the most abundant natural aromatic polymer on earth (Calvo-Flores & Dobado, 2010). It is found in plant cell walls, where it plays a structural role, as well as a protective role against physical, chemical and biological aggressions external to the plant (Liu *et al.*, 2018). Lignin is extremely ramified and is composed of three monomers: p-coumaryl alcohol, coniferyl alcohol, and sinapyl alcohol. Its chemical structure is highly irregular, differs within the same species, and

depends on factors such as: The plant's stage of development, environmental conditions, and the part of the plant concerned (trunk, stem, straw, branch, etc.). These factors exert a major influence on the monomeric composition of lignin and affect its structure. Lignin is the second main constituent of lignocellulosic biomasses (wood and agricultural residues) after cellulose and before hemicellulose. In lignocellulose microfibrils, i.e., lignin acts as a binder and barrier to cellulose and hemicellulose (**Figure 5.2**) (Konan *et al.*, 2022a). This is a major obstacle to the conversion of lignocellulosic biomasses into biofuels by recovering the carbohydrates (cellulose and hemicellulose) contained in these biomasses. Despite lignin's complex structure, white rot fungi such as *P. chrysosporium* have acquired the ability to degrade it, its derivatives and a wide range of aromatic compounds, including pesticides, environmental pollutants, dyes and toxic waste (Rosa *et al.*, 2024). They achieve this through a complex system of extracellular enzymes they secrete. It is this particular ability of WRFs to degrade such complex compounds that is attracting research attention. As for *P. chrysosporium*, it is considered the model WRF (Lundell *et al.*, 2014). It possesses one of the most complete enzyme systems, encompassing the major lignolytic enzymes known to date. This gives it a significant efficiency in the degradation of woody and aromatic compounds. Lignin degradation leaves cellulose virtually intact in lignocellulosic biomass and gives the white color to wood degraded by *P. chrysosporium*.

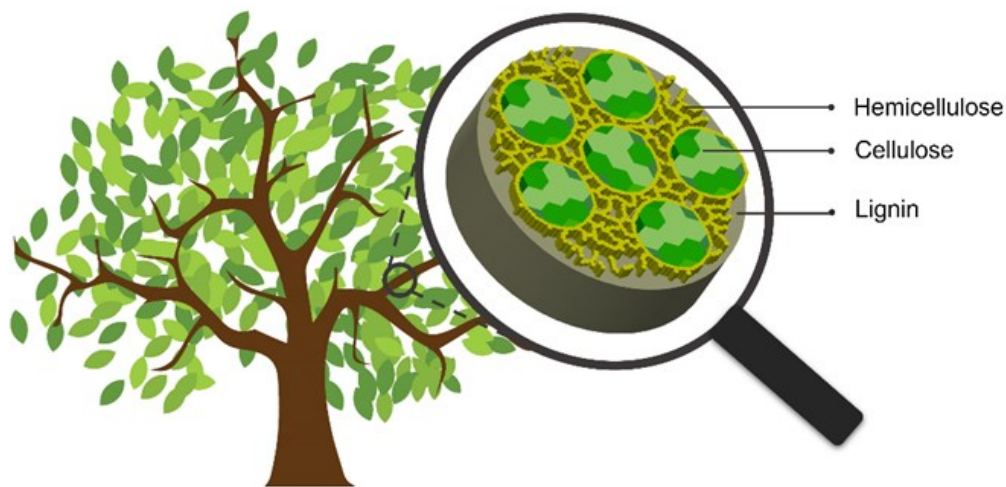


Figure 5.2 Structure of a lignocellulose microfibril.

5.7 Enzymatic system

Most white rot fungi can degrade lignin and lignin-like compounds using a non-substrate specific enzyme system. This system generally consists of one or two enzyme groups. Only a handful of species can secrete a complete ligninolytic enzyme system, that is, the three key groups namely laccases, manganese peroxidases and lignin peroxidases. *P. chrysosporium* and *Trametes versicolor* are two such species. However, the former remains one of the most widely used fungi, certainly because it was one of the first to be studied in the laboratory, and because the complete genome sequence is now available.

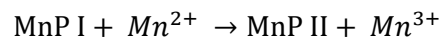
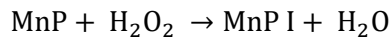
5.7.1 Key enzyme

P. chrysosporium is a heterotrophic organism that obtains its nutrients from the decomposition of woody plant matter and aromatic compounds in its environment. When nutrients are not directly available, extracellular enzymes are secreted to degrade these compounds. Only a handful of microorganisms are capable of this task. These are essentially fungi. They are grouped together under the name of rot fungi. There are three main types: brown rot fungi (BRF), soft rot fungi (SRF) and white rot fungi (WRF), in reference to their respective color/aspect on the wood they colonize. SRF degrade cellulose and leave lignin untouched, while WRF degrade lignin and leave cellulose intact. SRFs do the same as WRFs, degrading lignin and leaving only carbohydrates, but do so less efficiently in terms of degradation yield (Yang et al., 2024). The lignolytic enzyme system of *P. chrysosporium* is recognized as the most complete of all enzyme complexes produced by other lignolytic fungi. This is one of the main reasons why *P. chrysosporium* is considered the model strain for lignolytic activity (Singh & Chen, 2008). *P. chrysosporium* has a system composed of three main enzymes that work in concert to degrade lignin, phenolics, aromatics and similar compounds. These are laccase, lignin peroxidase, and manganese peroxidase; which are oxidoreductases. Apart from these enzymes, *P. chrysosporium* also produces several other enzymes such as methanol oxidase, 1,4-benzoquinone reductase, methyltransferase and cytochrome P450s (Larrondo et al., 2005). Some enzymes of the P450 family are thought to be involved in the xenobiotic activity of *P. chrysosporium* through O-demethylation at the ring break of aromatic compounds such as Methoxyhydroquinone (MHQ) (Kato et al., 2024).

5.7.2 Manganese peroxidases

MnPs (EC 1.11.1.13) are a group of enzymes using Mn^{2+} as a substrate. This enzyme was first purified and characterized by Jeffrey K. Glen and Michael in 1985 from *P. chrysosporium* (Glenn & Gold, 2022). They are acid glycoproteins with pH 4.5 and a molecular weight of around 45 kDa. MnPs are hemoproteins; i.e., they consist of two parts: (i) a protein part and (ii) a prosthetic group, the heme containing the iron cofactor (Fe^{3+}). The heme is the enzyme's active site. There are more than a dozen MnPs. Their role is to oxidize Mn^{2+} to Mn^{3+} . This catalysis takes place in three stages, according to Équation 5.2. **Figure 5.3** illustrates the transformation mechanism. The MnP enzyme binds with hydrogen peroxide (or other peroxide) at the heme to form a first complex. In this complex, the iron of the heme enters into a bond with one of the oxygen atoms of the peroxide. The oxygen-oxygen bond in the peroxide is then cleaved by the transfer of two electrons from the heme to the peroxide. This results in the production of a water molecule and a Fe^{4+} -oxo-porphyrin radical called MnP I complex. The MnP I complex in turn oxidizes Mn^{2+} to Mn^{3+} . This electron gain leads to a second radical compound, MnP II, which in turn oxidizes another Mn^{2+} ion to Mn^{3+} . This second electron obtained by MnP II during this operation enables the release of the oxygen atom attached to the heme, with the formation of a water molecule, a return to the initial enzyme and a second Mn^{3+} ion. In this way, MnP enables one molecule of peroxide and two Mn^{2+} ions to be converted into 2 molecules of water and 2 Mn^{3+} ions (Glenn & Gold, 2022; Hofrichter, 2002; Sundaramoorthy et al., 2005).

Équation 5.1 – Reactions cycle of manganese peroxidase.



Mn^{3+} ions are highly reactive. They react rapidly with chelating agents produced by the fungus such as oxalic acid to stabilize. The resulting low-molecular-weight compound is a powerful redox mediator capable of radicalizing the phenolic structures of lignin. The radicals created in the lignin structure trigger the spontaneous disintegration of lignin. The principle of degradation remains broadly the same with phenolic compounds other than lignin. MnPs are sensitive to peroxide concentration. Too much peroxide leads to inactivation of the enzyme (Emami et al., 2020).

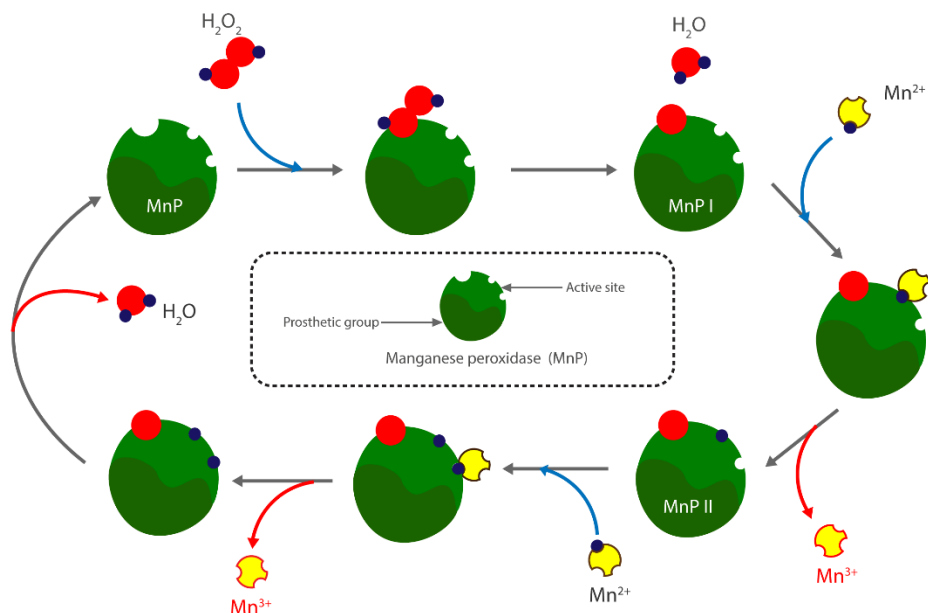


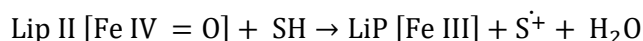
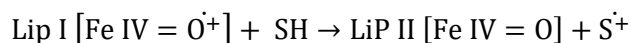
Figure 5.3 Transformation mechanism of Mn²⁺ into Mn³⁺ by manganese peroxidases structure of a lignocellulose microfiber.

5.7.3 Lignin peroxidases

LiPs isoenzymes are globular or helical glycoproteins of 40 kDa, consisting of 343 or 344 amino acids and typically fit into a volume of 50 x 40 x 40 Å (Falade *et al.*, 2017). LiPs (EC 1.11.1.14) are also heme enzymes. They have an optimal pH of 3. They feature among the highest redox potentials of peroxidases ($E_o = 1.2$ V at pH 3); significantly higher than MnPs and Laccases, both of which display 0.8 V at their optimal pH (pH 4.5 and pH 5.5, respectively) (Pollegioni *et al.*, 2015). This property confers on LiP the ability to catalyze the oxidation of non-phenolic aromatic compounds even in the absence of mediators. Two calcium ions (Ca²⁺) are present in their structure, as well as numerous N- and O-glycosylation sites. The LiP heme is embedded within the protein, with a narrow opening to the external environment. The default substrate for LiP is the 3,4-dimethoxybenzyl alcohol known as veratryl alcohol. Like hydrogen peroxide, veratryl alcohol is a secondary metabolite produced by *P. chrysosporium*. The reaction chain produced by LiP is similar to that of MnP, except that instead of Mn, LiP uses veratryl alcohol as a substrate. It begins with the oxidation of Fe³⁺ from heme to form the first LiP I complex, with the production of a water molecule. LiP I is an oxo-ferryl intermediate deficient in the two electrons it has surrendered to the peroxide to form the water molecule. LiP I is then transformed into a second intermediate LiP II by reaction with veratryl alcohol, which acts as an electron donor. The LiP II compound is therefore electron deficient. The cycle is completed when another veratryl alcohol

molecule reacts with LiP II to yield an electron (Pollegioni *et al.*, 2015). The enzyme returns to its initial state (LiP) and the cycle can resume as many times, as long as substrates are available and pH and temperature conditions are favorable. Équation 5.2 summarizes the reactions. The intermediate compounds LiP I and LiP II are highly reactive forms of LiP (Koduri & Tien, 1994). Apart from veratryl alcohol, they can react with numerous other phenolic and non-phenolic compounds, including lignin monomers and their derivatives (guaiacol, syringic acid, catechol, vanillyl alcohol, etc.), attacking β - O - 4, C - C, C - O - C bonds and side chains. LiP I and II are also capable of inducing demethylation, intramolecular addition, rearrangement, hydroxylation, and other reactions in their substrates, leading to substrate disintegration. However, in the prolonged absence of the substrate to be reduced, LiP II reacts with peroxide to form a LiP III compound, leading to irreversible inactivation of the enzyme. The role of veratryl alcohol, produced naturally by *P. chrysosporium*, would therefore be to preserve enzyme inactivation when there is no or no longer any substrate to oxidize in the medium (Falade *et al.*, 2017; Koduri & Tien, 1995; Pollegioni *et al.*, 2015; Singh *et al.*, 2015).

Équation 5.2 – Reactions cycle of lignin peroxidase.



5.7.4 Laccases

Laccases are a large group of isoenzymes with molecular weights ranging from 50 to 100 kDa, partly because they can be highly glycosylated. The carbons in the side chains account for 10 to 40% of the enzyme's molecular weight. Glycosylation of laccases is thought to play a role in their extracellular secretion, thermal stability, and retention of copper atoms. Over a hundred laccases have been discovered. They are produced not only by fungi, but also by other organisms (plants, insects, bacteria, etc.). However, those produced by fungi have a higher redox potential (+800 mV) than those produced by insects and plants. Unlike the previous two enzymes, laccase does not catalyze reactions involving hydrogen peroxide (Rivera-Hoyos *et al.*, 2013). They are "blue multicopper oxidases" and oxidize a wide range of aromatic and non-aromatic compounds by producing two molecules of water resulting from the reduction of two oxygen atoms. These substrates are transformed into free radicals depending on their structure and the reaction conditions. Laccase production tends to be low when the fungi evolve in a liquid rather than a

solid medium. However, the concentration of aromatic compounds such as 2,5-xylidine seems to have a positive effect on laccase production. Laccases have 4 copper atoms in their structure. One of them is located at the T1 site. This atom, in its oxidized state, is responsible for the blue-green color of the medium. T1 is the binding site for the substrate to be reduced. The other three atoms are grouped at sites T2/T3. These sites catalyze the reduction of molecular oxygen to water. Laccases are not substrate-specific but are capable of oxidizing a wide variety of compounds. There are, however, differences in substrate preference from one isoenzyme to another. Among laccase substrates, we find ortho and paradiphenols, methoxy-substituted phenols, polyphenols, aromatic amines, benzenthols, hydroxindols, 1-naphthol and syringaldazine (Kunamneni *et al.*, 2007; Rivera-Hoyos *et al.*, 2013). Laccase uses over 100 different mediators. ABTS (2,2'-azino-bis(3-ethylbenzothiazoline-6-sulfonic acid) and HBT (1-hydroxybenzotriazole) are the most commonly used. These mediators are low-molecular-weight compounds with a higher redox potential (>900 mV) than laccase. They are oxidized by the enzyme to give highly reactive radicals. The radicals formed can attack substrates with molecular weights too large to bind to the enzyme's catalytic sites. In the case of ABTS, laccase performs electron transfer to this mediator. The optimum temperature for laccases is between 30 and 60 °C. Laccase activity is inhibited in the presence of compounds capable of binding to the T2 and T3 sites without producing radicals, including metal ions and fatty acids.

5.8 Culture in solid fermentation

5.8.1 Inoculum preparation

Inoculum preparation usually begins with a concentrated suspension of spores obtained from a commercial retailer or on request from research organizations. It is also possible to prepare an inoculum after isolating the strain in its natural environment. The concentrated spore suspension is obtained by harvesting spores from the surface of a mycelium agar culture. Between the 3rd and 5th day of mycelium culture in a 100 mm x 15 mm petri dish, 20 ml of distilled water is poured onto the surface of the mycelium and gently scraped with a sterile rod to release the spores. The obtained suspension is then collected in a sterile tube and diluted to obtain a spore concentration close to 1×10^6 spores/ml (Gao *et al.*, 2023).

Spores can easily be counted using a microscope and a hemacytometer (Zhang *et al.*, 2021a). Determining the absorbance of the desired suspension can help to speed up the process in cases where it is necessary to prepare several suspensions at once, as spore counting can be a slow and tedious task (Li *et al.*, 2024b). Once the spore concentration of the suspension is achieved,

1 to 2 ml of the suspension is added per 100 ml of culture medium. The composition of the culture medium may vary from strain to strain and according to the strain supplier's instructions, but it always includes one or more sources of carbon, nitrogen, vitamins, and nutrients essential to the strain's primary metabolism, plus water. For example, for *P. chrysosporium* strain A-381 (ATCC 48746), the culture medium consists of (per 1000 ml) of yeast extract (3.0 g), malt extract (3.0 g), dextrose (10.0 g) and peptone (5.0 g) and water (1000 ml). For *P. chrysosporium* BKMF-1767 (CCTCC AF96007), the culture medium consists of glucose (10g), of ammonium tartrate (0.206 g), KH_2PO_4 (2 g), MgSO_4 (0.5 g), $\text{FeSO}_4 \cdot 7\text{H}_2\text{O}$ (0.115 g), CaCl_2 (0.1g), $\text{ZnSO}_4 \cdot 7\text{H}_2\text{O}$ (0.089 g), $\text{CuSO}_4 \cdot 5\text{H}_2\text{O}$ (0.05 g), and vitamin B1 (0.001 g) dissolved in sodium tartrate buffer (20 mM, pH = 4.5). The culture medium is autoclaved at 121 °C for 20 min, then cooled before inoculation with the prepared spore suspension. This is then placed in a shaker incubator at 30 °C and 180 rpm for several days (3 to 5 days) (Chen *et al.*, 2021b).

5.8.2 Solid fermentation

Solid-state fermentation (SSF) is defined as the growth of microorganisms on a moist, solid substrate in the absence or near absence of free liquid (usually water). The substrate serves both as a growth medium and as a nutrient source. This is an old technique. Egyptian bread-making (2600 BC) and Asian Koji sauce are two of the oldest documented applications. It is also used in the production of enzymes, pigments, flavors, antibiotics, biosurfactants, enriched proteins, and organic acids (Mitchell *et al.*, 2011). For fungi cultivation, SSF is the type of fermentation that best approximates their natural environment. SSF for fungi cultivation has many advantages over submerged fermentation (SmF). It takes less volume because it uses less water for the same substrate. The risk of contamination disturbance is lower, thanks to the fungi's ability to grow in a heterogeneous environment. Oxygen transfer is maximized and optimized in stirred reactors. There is little or no effluent to treat at the end of fermentation. Little or no chemicals are used. Fermentation products are not diluted as in liquid fermentation, but rather concentrated. Energy consumption is low. In addition, operating costs for solid fermentation are significantly lower compared to liquid fermentation (Machado de Castro *et al.*, 2018). However, major difficulties yet remain challenges for solid-state fermentation, notably the transition from a small to a full-scale (industrial) operation. In SSF, heat transfer is provided by air and is therefore poor. As volume increases, substrate compaction also becomes a problem. Another drawback is the high risk of dead zones (where there is no activity) in the substrate, even with agitation. The design of bioreactors for solid-state fermentation remains one of the major challenges for scaling up the process to date, due to the poor heat and oxygen transfer. To date, there are bioreactors well

known for their advantages, but which also suffer from drawbacks that often disqualify them from certain small or large-scale applications. Bioreactors are generally classified according to their aeration system. A distinction is made between free aeration bioreactors and forced aeration bioreactors. The former include laboratory glassware, plate chambers, rotating drums, and stirred drums, while the latter include fixed-bed and fluidized-bed reactors.

5.8.3 Bioreactors

5.8.3.1 Laboratory glassware

At a laboratory scale, solid fermentation can be carried out in wide-mouth Erlenmeyer, jars or flasks (Durand, 2003). These types of reactors have the advantage of being easily accessible, and solid fermentation is simple to operate. The biomass is introduced into the container and inoculated with the strain. The container can remain at room temperature or be kept in an incubator at the desired temperature (Figure 5.4). The pH can be adjusted according to fermentation conditions (water activity, etc.). Oxygen transfer and biomass homogeneity are improved by gentle mixing to avoid destroying the mycelium. Fermentation can be batch or fed-batch. In the latter case, the risk of contamination is higher. However, this type of fermentation is particularly suitable for screening fungi or biomass, or for rapidly testing cultivation conditions. The amount of substrate is small; in the gram range. Above a kilogram, the material becomes compacted, and aeration and oxygen transfer become a problem.

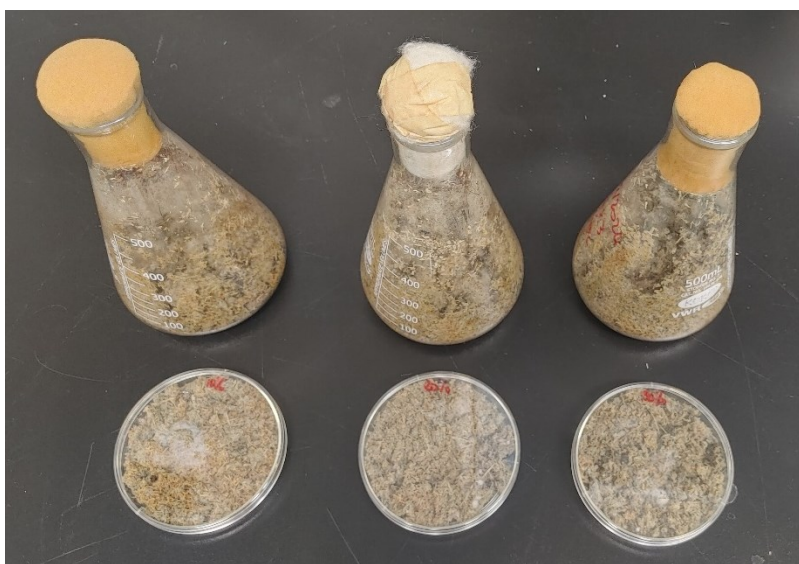


Figure 5.4 Solid state fermentation with *P. chrysosporium* on corn stover and black spruce chips in flasks and petri dishes.

5.8.3.2 Tray bed reactor - Incubator

The use of tray chambers goes back as far as the first traditional Koji fermentations in Asia. The biomass is laid out in layers (of varying thickness, between 5 and 15 cm) on perforated benches (also called trays) made of wood, aluminum, plastic, or other materials. The upper part of the biomass is in free contact with the air, while the lower part receives air through perforations in the benches. The benches are arranged on several levels and installed in an enclosure (reactor) or room (hall) in which the temperature is controlled (**Figure 5.5**) ([Krishania et al., 2018](#)). Tray chambers are well known and mastered as they present a rather basic design and because they have been used for a long time. However, heat accumulation in the biomass is one of the major drawbacks of this type of reactor. The biomass can be stirred manually from time to time, not only to dissipate the metabolic heat produced, but also to improve aeration. Otherwise, a significant temperature gradient is formed within the biomass ([Wang & Yang, 2007](#)). Moreover, sometimes, the substrate concretes, causing mixing to be impossible. Several trays may be lost in this case. It is also possible to install a sprinkler system to control room humidity. The other major drawback with tray chambers is the space (volume, surface area) they require. It is an extensive technique. Scaling up involves increasing the number and/or surface area of trays ([Arora et al., 2018](#)).



Tray bed reactors

- ① Temperature control panel
- ② Inside incubator
- ③ Glass door and hermetic door
- ④ Tray beds
- ⑤ Tray beds support
- ⑥ Bottom support with heating holes for temperature control inside the incubator

Figure 5.5 Tray bed reactors in an incubator.

5.8.3.3 Fixed, rotating or stirred reactors

Fixed reactors are vertical glass tanks specially designed for solid fermentations. They feature aeration, temperature control and aeration systems, and are generally equipped with a control panel (**Figure 5.6**). These reactors are available for small volumes (less than 10 L), because of the compaction problems that arise with larger volumes. Rotary or agitated drums, on the other hand, are better suited to large volumes. Rotary drums are horizontal (**Figure 5.6**) or vertical cylindrical enclosures half-filled with inoculated biomass and fitted with an air inlet and outlet. These drums rotate around an axis either mechanically or automatically, entraining the substrate in their movement. The drums are often fitted with fixed or mobile mixers (known as agitated rotary drums). The result is improved oxygen and CO₂ transfer within the biomass ([Webb, 2017](#)). Mycelium growth is faster and more uniform in drums than with tray chambers ([Robinson & Nigam, 2003](#)). However, drum rotation speed has been shown to be inversely correlated with mycelium growth. Rotating drums also offer the advantage of batch, fed-batch or continuous

operation. On the other hand, temperature control is a major challenge, even on a small scale (Nava *et al.*, 2011).

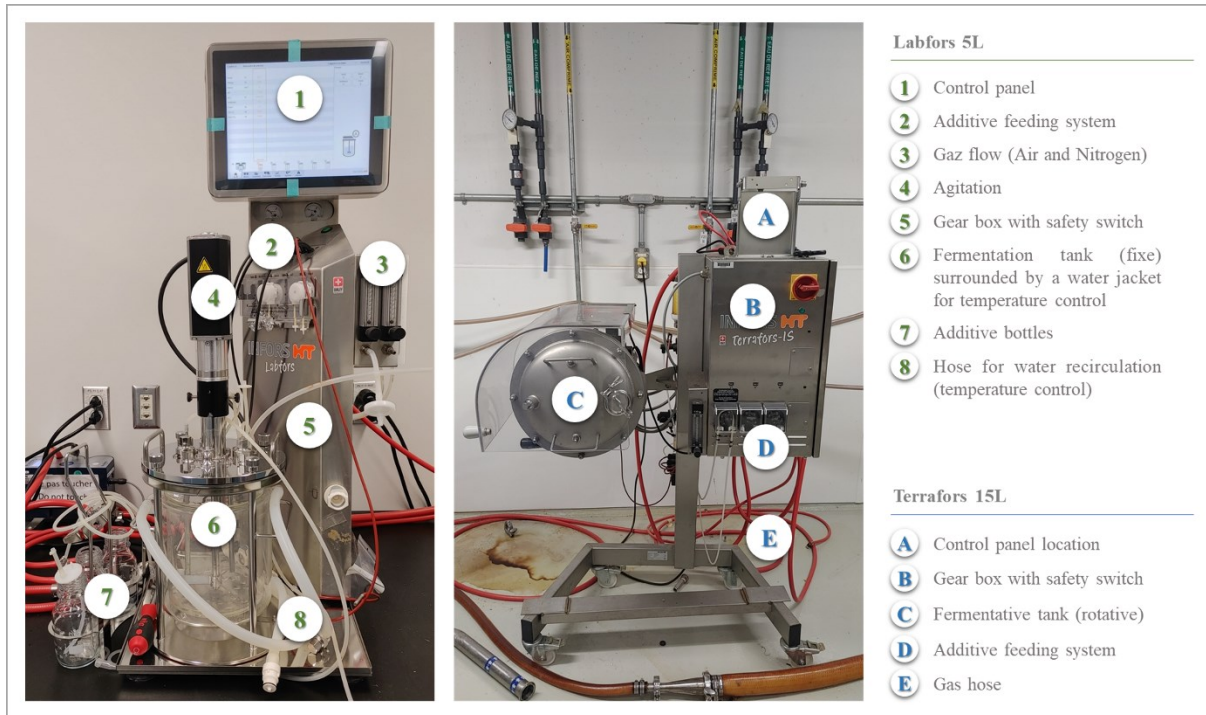


Figure 5.6 Fixe reactor LABFORS (5 L) and Rotative drum TERRAFORS (15 L).

5.8.3.4 Fixed-bed reactor

The fixed-bed reactor is a column with a perforated bench or tray. Aeration is forced upwards through the perforations. The reactor is placed vertically, but can be horizontal or inclined (Ge *et al.*, 2017). The inoculated biomass is deposited in varying thicknesses on the bench. Temperature is controlled using a water bath in the laboratory model, or by means of a jacket of water maintained at the desired temperature and in direct contact with the reactor wall (Lonsane *et al.*, 1985). Humidity is maintained in the column by injecting water-saturated air. The major problems with this type of reactor are the risk of biomass compaction, the creation of privileged aeration channels within the biomass, the difficulty of removing heat when the biomass is very thick, and the pressure drop in the column; hence, the difficulty of using it on a large scale. On the other hand, in a scale model, forced aeration with agitation is quite effective in preventing heat build-up and pressure drop (Arora *et al.*, 2018).

5.8.3.5 Fluidized-bed reactor

The fluidized-bed reactor is similar to the vertical fixed-bed reactor, but with this type of reactor, biomass particles are kept in suspension thanks to a continuous flow of gas (from bottom to top). The flow must be just sufficient to prevent biomass particles from settling on the perforated bed or accumulating on the top of the reactor. In the former case, the perforations in the bed through which the air flows would clog up, and in the latter, the gas outlet would get obstructed. The fluidized-bed reactor is particularly suitable for small and light particles (Ge *et al.*, 2017). Occasionally, during operation, these particles agglomerate, fall and then accumulate on the perforated bench. An agitator can be installed in the reactor column not only to prevent particles from accumulating on the bench, but also to break down the agglomerates. In the laboratory model, i.e., for a volume of just a few liters, temperature control is as simple as in the fixed-bed reactor (water bath or water jacket), and oxygen transfer is maximal. The difficulty of fluidization and temperature control arises with larger volumes (Werther, 2007). Particles are more likely to agglomerate. Using larger agitators would damage the mycelium, slowing down fungal growth and process efficiency.

5.8.4 Solid state fermentation parameters

5.8.4.1 Water activity

Water activity (a_w) is a dimensionless parameter. It reflects consistency in terms of the water content of a system, body, or matrix. In SSF, it is defined as the proportion of water available in a system for biochemical reactions. Water activity is, for a given temperature, the ratio of the system's vapor pressure to the reference vapor pressure; the reference pressure being that of pure distilled water, taken equal to 1 (Fernández, 2011). Every microorganism has a water activity threshold below which it is unable to maintain itself alive or even in a vegetative state. Most bacteria are unable to grow in environments with a water activity below 0.91. The threshold for fungi is 0.6 (V, 2018). Water activity also influences the quality and spectrum of products that can be obtained. It changes throughout the fermentation process, depending on temperature, growth, aeration, agitation, and other conditions. Water plays three major roles in biological systems: (i) A structural role; i.e., it is involved in the constitution (composition) of cell walls; (ii) a solvent role, enabling biochemical reactions; and (iii) a transport role (heat and oxygen). The last two roles are an advantage for liquid fermentation and a challenge for solid fermentation. In solid fermentation, the continuity of the medium is ensured by the gas phase than the liquid (aqueous) phase as in

liquid fermentation. As a result, there is a significant risk of temperature gradient formation, heterogeneity in biomass decomposition and aeration.

5.8.4.2 Influence of pH

Controlling pH is a difficult operation in solid-state fermentation. Indeed, pH varies throughout fermentation and seems to be practically difficult to measure due to the absence of free water and the heterogeneity of the matrix (gas-liquid-solid) (do Nascimento *et al.*, 2021; Teixeira *et al.*, 2019). The pH can only be measured locally and is therefore not representative of the medium as a whole. In semi-solid fermentation, on the other hand, pH measurement remains the same as in liquid fermentation, given the continuity of the medium provided by free water. In this case, pH becomes an input parameter. However, it is now well documented that fungi are tolerant of pH variation. Indeed, most fungi grow at pH levels between 4 and 9, but require a pH close to 7 for optimal sporulation (Sala *et al.*, 2019; Suryadi *et al.*, 2022).

5.8.4.3 Influence of temperature

Temperature is one of the most important parameters in solid fermentation. According to Manpreet *et al.* (2005), during solid fermentation, 100 to 300 kJ of heat is released per kilogram of substrate. This heat comes mainly from the catabolic reactions of the micro-organisms, the synthesis of compounds used by their primary metabolism and the enzymatic reactions of lignin degradation (Rosenberg & Zilber-Rosenberg, 2016). The heat produced may vary significantly from one species to another, depending on growth rate or substrate type (Liu *et al.*, 2022; Wu *et al.*, 2020). However, in the absence of appropriate agitation and aeration systems, a temperature gradient is frequently created in the substrate. A gradient of 3 °C/cm thickness has been reported in a fermenter only 6.5 cm high (de Reu *et al.*, 1993). Yet many white rot fungi used in solid fermentation have growth temperatures between 25°C and 40°C, and sometimes 50 °C for certain species (Azad *et al.*, 2013; Bhati, 2019; Ouahiba *et al.*, 2021). However, this temperature range remains narrow in view of the metabolic heat released. Temperature control is therefore a key issue. This is one of the serious issues in reactor design. Manufactured bioreactors are now equipped with aeration and agitation systems, temperature sensors and a water jacket combined with a chiller to regulate the temperature inside the fermentation tank.

5.8.4.4 Influence of aeration

The type of aeration is related to the choice of reactor. The gas composition and the aeration rate are crucial. Gas composition is a key factor in fermentation, especially in solid fermentation. Investigating different proportions of O₂ and CO₂ in the aeration gas, [Villegas et al. \(1993\)](#) demonstrated that the qualitative (type of gas) and quantitative (relative proportion) composition of the gas has a strong influence on fungal growth, sugar consumption, pressure drop, and metabolic CO₂ production. Indeed, the role of aeration is not only to supply oxygen, but also to regulate water activity (by water-saturated gas), to evacuate heat, CO₂ and all the other volatile organic compounds produced by the metabolism of micro-organisms, which can inhibit biological activity once accumulated. Metabolic CO₂, on the other hand, is characteristic of each species and reflects the growth rate of the mycelium. It is often used as an indicator of the stage of fermentation ([Cruz-Cordova et al., 1999](#)). Aeration rate is another important factor to consider, particularly in forced aeration reactors. High aeration rates have been reported to destroy the mycelium and disrupt enzymatic activity. However, while it is clear that high levels are harmful, there are no general rules on the impact of moderate and low levels. For example, in the case of lactone production by solid fermentation, a very low aeration rate inhibits Acetyl-Coenzyme A activity and when the aeration rate increases, the enzyme's activity decreases ([Try, 2018](#)). In contrast, for lignolytic enzyme production with *Trametes versicolor*, [Montoya et al. \(2021\)](#) tested all three aeration regimes: low, moderate and high. The highest laccase production was recorded under the lowest aeration rate. Thus, aeration must be optimized according to the microorganism, reactor type, fermentation conditions, and desired products.

5.8.4.5 Influence of agitation

Substrate compaction and particle agglomeration limit fungi's access to the substrate. They also make heat evacuation difficult and limit the efficiency of aeration (oxygen transfer, etc.). The main role of agitation is to overcome these difficulties. Agitation can be continuous or intermittent (semi-continuous), and automatic or manual. Each of these modes has its advantages and disadvantages, and is highly dependent on the type of reactor, the type of substrate, the type of microorganism (mycelium) and the fermentation conditions. However, literature regularly mentions an optimum agitation speed of around 30 rpm. Agitation efficiency is not only dependent on agitation speed, but also on agitation duration. Vigorous agitation, however, even for a relatively short time, would lead to destruction of the mycelium and a reduction in enzyme production ([Teixeira et al., 2019](#)). For forced aeration reactors, aeration can be a way of

maintaining agitation. In pilot or industrial-scale fermenters, the limits of this practice quickly become apparent. Given the large substrate masses used in this type of fermenter, the risks of settling and particle agglomeration are much greater, and increasing the aeration flow is ineffective at the risk of causing the biomass to settle on the opposite wall to the direction of aeration.

5.8.4.6 Fermentation duration

The duration of fermentation depends on the desired product (type and quantity), the capacity of the fungus(es), the inoculum (quantity), the substrate (type, quantity and quality) and the fermentation conditions (optimal or not). It can range from a few hours to several days or even months (Kwanga *et al.*, 2022; Mardawati *et al.*, 2020; Naeimi *et al.*, 2020). In general, metabolite production is low in the first few days and increases fairly rapidly until it reaches a production peak (Tai *et al.*, 2019; Wu *et al.*, 2018). Without monitoring, production slowly declines until it fades. The first part of the curve is directly correlated with the growth phase of the mycelium, while the decline in production is linked to various limiting factors such as the amount of nutrients available in the medium, the oxygen, and CO₂ levels, and the presence and accumulation of inhibitors in the medium. Fermentation can continue as long as all optimal conditions are met.

5.9 Applications

P. chrysosporium has a wide range of applications which cannot be covered exhaustively in this review. The applications alone could be the subject of a dedicated review article. We present only four of the classic applications, namely biodelignification, decolorization, bioremediation of polyaromatic hydrocarbons and ligninolytic enzyme production. However, the following Tableau 5.1 gives an overview of the diversity of *P. chrysosporium* applications.

Tableau 5.1 Application of *Phanerochaete chrysosporium* for biodecomposition in diverse industries.

Industry	Substrate	Application	Conditions	Main result	References
Distillery industry	Vinasse (Colored recalcitrant wastewater)	Vinasse degradation	32 days, 39°C	Decrease of phenolic concentration and color: 59.41%	(Yuan <i>et al.</i> , 2023)
Textile dyeing industry	Wastewater	Decolorization	6 days, pH 4.5, 180 rpm, 39°C, Glucose supplement	84% decolorization	
Circuit printing industry	Copper from waste printed circuit	Leaching	14 days, 30°C, 150 rpm	60,96 % leaching of copper	(Liu <i>et al.</i> , 2020b)
Drugs	Sulfamethazine (SMT) and Cadmium	Biotransformation	48 hours, 30°C, 120 rpm	49% biotransformation for Cd and 62.9% for SMT	(Guo <i>et al.</i> , 2018)
Fuel	Anthracene	Degradation	2 days, 37°C, 80 rpm	Residual anthracene concentration was 16% at the end	Mohammadi and Nasernejad (2009)
Textile industry	Azo dyes	Decolorization and detoxification	10 days, Concentration of 50 mg/L, 28°C, 180 rpm, in the dark	82% Direct Yellow (DY27), 89% Reactive Black 5 (RB5), and 94 % Reactive Red 120 (RR120) but increase of phytotoxicity	(de Almeida <i>et al.</i> , 2021)
Papermill industry	Pentachlorophenol (PCP)	Removal	3 days, 0.23% lignisulfonate, 2% glucose supplement	75% PCP removed	Aiken and Logan (1996)
Agriculture	Olive mill effluent	Bioremediation	10 days, 135 rpm, 26°C	59 % soluble COD removal 70% colour removal 30% phenyl content removal	(Díaz <i>et al.</i> , 2021)
Pulp and paper industry	Kraft Black Liquor effluent	Treatment	10 days, 25°C, 150 rpm, Glucose supplement (3g/L), pH 6	Removal of 65% COD, 37% colour and 56% phenolic compounds	(Díaz <i>et al.</i> , 2022)
Civil and military industry	2,4,6-trinitrotoluene (TNT)	Removal	72 hours, 30 mg/L, 28°C	82% removal	(Ibbini <i>et al.</i> , 2024)
Plastic industry	Poly(lactic acid) (PLA) Polystyrene (PS)	Degradation	35 days	34.35% degradation for PLA and 19.7% for PS	(Wu <i>et al.</i> , 2023a)
Textile industry	Dye	Decolorization	24 hours, 37°C, Succinate buffer	100 % decolorization of acid red 88, reactive black 5 and reactive orange 16	(Ghasemi <i>et al.</i> , 2010)

5.9.1 Biodelignification

Biodelignification refers to the removal of lignin from lignocellulosic biomasses using microorganisms competent to perform this task. These are essentially white rot fungi (WRF). Biodelignification was the very first application of *P. chrysosporium*. Today, the subject remains relevant, especially in the context of climate change and the exploration of sustainable alternatives to fossil fuels. Lignocellulosic biomass is a renewable source for bioethanol production, but it remains under-utilized. Global production of lignocellulosic biomass is estimated at 181.5 billion tons per year, of which only 8.2 billion are used, or just 4.5% billion tons (Mujtaba *et al.*, 2023). Although the processes for converting cellulose into bioethanol are now well established, the difficulty with lignocellulosic biomass lies in the difficulty of accessing cellulose because of the lignin, which hinders recovery of this compound. To date, the delignification stage remains the limiting step in the valorization of lignocellulosic biomasses into bioethanol, due to the recalcitrance of lignin (Hoang *et al.*, 2021; Zhang *et al.*, 2021). This step is estimated to account for 40% of bioethanol production costs with lignocellulosic biomasses (Sindhu *et al.*, 2016). Existing chemical, physical and physico-chemical methods often create more environmental issues than they solve. While many strategic advantages are associated with biodelignification, it is, however, criticized for the slowness of the process and problems of scale-up as highlighted above. Lignin is *P. chrysosporium*'s natural substrate, but the enzymatic system it secretes is effective only on destructured lignin or lignin with a relatively low molecular weight. Consequently, some authors suggest coupling biodelignification with other treatment processes such as reactive extrusion (Gupta *et al.*, 2023a; Gupta *et al.*, 2023b; Konan *et al.*, 2024b). Reactive extrusion is a fast, environmentally-friendly technique known for its ability to destructure the lignocellulosic complex, followed by an increase in the specific surface area of the particles. This preliminary action boosts the speed and yield of delignification by *P. chrysosporium*. Further research into pre-treatment methods involving biodelignification is required to make second-generation bioethanol production profitable on an industrial scale.

Tableau 5.2 Some results of biodelignification with *P. chrysosporium*.

Biomass	Particle	Reactor	Inoculum	Mass	Temp.	Time	Results	Reference
Apple pomace	20–60 mesh size	Petri dish	Spore suspension (1 ml)	5 g	28 °C	7 days	19.8% delignification	(Chen <i>et al.</i> , 2024)
Corn cobs	30 mesh size	Shake flask	Spore suspension (1×10^8 spores/mL)	2.5 g	40 °C	3 days	78% delignification	(Reddy <i>et al.</i> , 2024)
Coffee pulp	1 – 2 mm	-	Semi solid medium on biomass	-	35 °C	50 days	50.2% delignification	Phuong and Nguyen (2024)
Paddy straw and pine needles	-	Bags	25 mL of water-washed mycelia	100 g	28 °C	28 days	Decrease of lignin from 27.11% to 14.11%	(Gupta <i>et al.</i> , 2023a)
Camelina straw and Switchgrass	10 mm	Vented bags	Malt extract broth	20 g	28 °C	35 days	24.08 %, and 25.02% delignification for Camelina straw and switchgrass	(Dao <i>et al.</i> , 2023)
Wheat straw	-	Flask	4 agar discs per flask	2.5 g	28 °C	15 days	45.6% delignification	Shrivastava and Sharma (2023)
Olive pulp (25%) and wheat straw (75%)	2 to 5 mm for Olive pulp and 0.5 to 1.5 cm for wheat straw	Petri dishes	Colonized sorghum grains (1 g)	10 g	28 °C	84 days	60 % delignification	(Benaddou <i>et al.</i> , 2023)
Cotton stalks	Ground to pass through a 3 mm screen	Flask	Spore inoculation 1 ml (5×10^6 spores/ml)	Solid loadin g was 5% w/v	39 °C	14 days	20.7% delignification	(Shi <i>et al.</i> , 2009)
Switchgrass	1.6 mm	Vented bag	Malt extract broth (10 ml)	20 g	28 °C	21 days	23.6% delignification	(Onu Olughu <i>et al.</i> , 2022)

5.9.2 Decolorization

There are over 100,000 different dyes on the market, for a production of around 700,000 tons per year (Kalra & Gupta, 2021; McMullan *et al.*, 2001). Most of this production ends up in polluted waters every year. The impact of colorants on the environment and human health is manifold. They are essentially complex and dangerous aromatic and heterocyclic compounds. Apart from the direct impact of this type of compound on human health (cancer, genetic mutation, coughing, diarrhea, eye and skin irritation, gastrointestinal infection, etc.), even at low concentrations (1 mg/l), these dyes affect water transparency, contribute a substantial organic load to the

environment, significantly disrupt biological processes such as photosynthesis and destroy the survival conditions of organisms in their ecosystem (Ganaie *et al.*, 2023; Kalra & Gupta, 2021). Moreover, they can undergo reactions with other molecules in the environment, resulting in even more dangerous compounds. Dyes found in the environment originate for the most part from the textile industry, but are also produced in a large number of industries such as cosmetics, ink production, pulp and paper, leather tanning, plastics and printing (Kalra & Gupta, 2021). Yet dyes are persistent contaminants for which conventional water treatment processes are ineffective. Several chemical and physical methods have been developed, but remain either ineffective, energy-intensive, or expensive to deploy on an industrial scale. Because of their natural ability to degrade complex cyclic compounds, white rot fungi are being experimentally explored for the decolorization of industrial wastewater (usually from the textile industry) prior to discharge into the environment. Here again, *P. chrysosporium* is one of the fungi most frequently used in these processes. Some authors have reported promising results. Senthilkumar *et al.* (2014) highlighted the decolorization capacity of *P. chrysosporium* on azo dyes in submerged fermentation. When glucose, manganese, and ammonium salt were supplied at 0.5%, 0.1%, and 0.5% respectively, the rate of dye degradation by *P. chrysosporium* was close to 98% on the third day of culture. A few years earlier, Radha *et al.* (2005) had investigated the efficiency of *P. chrysosporium* in stationary phase on seven other different types of dye (Methyl violet, Congo red, Acid orange, Acid red 114, Vat magenta, Methylene blue and Acid green) and showed that decolorization efficiency depended on the initial dye concentration. The best results (> 95%) were obtained with an initial concentration of 0.05 g/l (35 °C, pH = 4.5). Similarly, for Gugel *et al.* (2024), results were equally conclusive for the five dyes investigated, namely Orange II, Red 8BLP, Direct black 80, Direct yellow 11, Basic brown 1. By the end of the seventh day of culture, all solutions containing the dyes appeared almost completely decolorized. Thus, *P. chrysosporium* is a promising decolorizing agent.

5.9.3 PAH Biomemediation

The concept of using *P. chrysosporium* in bioremediation is also based on the ability of the enzymatic system (including cytochrome P450 (Li *et al.*, 2023) of *P. chrysosporium* to mineralize polyaromatic hydrocarbons (PAHs), chlorinated aromatic hydrocarbons (CAHs), and a wide range of aromatic organopollutants, including pesticides, explosives, etc., into CO₂ and H₂O. Compounds in this group are known to pose significant environmental pollution problems (Fulekar *et al.*, 2013). For a long time, fungi were neglected in bioremediation in favor of bacteria, until their susceptibility to mineralize aromatic contaminants was highlighted by Bumpus *et al.* in their work

on 22 different PAHs (Bumpus, 1989; Bumpus, 2021). Bacteria are often ineffective in environments saturated with aromatic compounds. PAHs originate mainly from anthropogenic sources, but can also come from natural sources (volcanic eruptions, bush fires, tree exudates, etc.) (Lee *et al.*, 2020). They come from the incomplete combustion of fossil fuels, exhaust smoke, tobacco smoke, etc. and are classified as Persistent Organic Pollutants (POPs) (Venkatraman *et al.*, 2024).

Their derivatives are equally or more toxic. A simple dehydration reaction can lead to carcinogenic or mutagenic compounds. PAHs are found in all matrices (soil, air and water). The efficiency of *P. chrysosporium* in mineralizing PAHs has been studied in a number of studies. Abo-State *et al.* (2021) demonstrated that *P. chrysosporium* is able to completely (100%) or almost completely (>90%) degrade pyrene, acenaphthene, anthracene, fluoranthene, and phenanthrene in CO₂ and H₂O within seven (7) days at room temperature (25 °C), under different MnSO₄ conditions (600 µM and 2000 µM) in agitated and non-agitated cultures. By comparing the ionization energies of 9 and 12 PAHs, respectively, Hammel *et al.* (1986) and Bogan and Lamar (1995) demonstrated that PAHs suitable for degradation by LiP from *P. chrysosporium* have ionization potentials of 7.55 eV or less. Wang *et al.* (2009) identified LiP and MnP as the main enzymes in the *P. chrysosporium* system responsible for the degradation of PAHs in soils. These two enzymes were responsible for over 70% of phenanthrene degradation after 19 days of treatment. It has been identified that solubility is a key limiting factor for PAH degradation in soils. PAHs with low molecular weights are therefore easily degraded by *P. chrysosporium* than those with higher molecular weights (Wang *et al.*, 2009; Zheng & Obbard, 2002). In aqueous media, phenanthrene and pyrene degradation approaches 100% in 60 days when the medium is nitrogen-poor and carbon-rich (Ding *et al.*, 2013).

5.9.4 Production of ligninolytic enzymes

Enzymes are valuable chemical compounds, especially in the food sector. According to Grand View Research, in 2021, the global enzyme market was worth 11.47 billion US dollars, and the forecast for 2028 is 17.88 billion, with an annual growth rate of 6.5% (Research, 2021). Amylases and then cellulases are the leading carbohydratases in demand to date (Siqueira *et al.*, 2020). With the development of second-generation biorefineries, there is a growing demand for ligninolytic enzymes (Niladevi, 2009). Alginolytic enzymes refer to enzymes capable of degrading the lignin contained in lignocellulosic biomasses, thereby making cellulose and hemicellulose accessible. There are three major types of ligninolytic enzymes: manganese peroxidase (MnP),

lignin peroxidase (LiP) and laccase. Solid fermentation attempts to reproduce the natural (but controlled) environment in which white rot fungi naturally produce ligninolytic enzymes. White rot fungi are grown in the presence of lignocellulosic material such as forest residues, agricultural residues, or any other type of lignocellulosic residue. Broadly the production of ligninolytic enzymes under solid fermentation proceeds as follows: Biomass is sterilized and introduced into the bioreactor, then inoculated with either fungal spores or pre-cultured mycelium. Fungi grow under specific conditions (pH, temperature, agitation, etc.) depending on the fungi species, substrate type and bioreactor. A few hours or days after inoculation, the mycelium adsorbs and grows on biomass particles, degrading the lignin by means of ligninolytic enzymes it produces. Lignin degradation is accompanied by the utilization of part of the sugars released (cellulose and hemicellulose) by the fungi to ensure their vital needs and growth (primary metabolism). The enzymes produced can then be recovered and purified for other applications. Enzyme production by solid fermentation has been proven to be in general more advantageous than liquid fermentation (Fujian *et al.*, 2001). For example, Wang and Yang (2007) reported that cellulase production in liquid media is \$20/kg, whereas it is only \$0.2/kg biomass in solid fermentation in comparison.

5.10 Perspectives

Considering the potential of *P. chrysosporium* to secrete powerful enzymes capable of degrading one of the most recalcitrant compounds in lignocellulosic biomasses; considering lignin to be the main cause of difficulties in the valorization of lignocellulosic biomasses for biorefineries, *P. chrysosporium* could play an important role in second-generation biorefineries by contributing to the biodelignification of lignocellulosic biomasses in order to increase their enzymatic digestibility during the enzymatic hydrolysis stage. Yet, in the specific context of lignocellulosic residues, given the rigidity of these biomasses, the use of *P. chrysosporium* on these residues should ideally be preceded by mechanical pre-treatment. Mechanical treatment should have the effect of disorganizing the structure of these biomasses and increasing the specific surface area of biomass particles to enable maximum efficiency of ligninolytic enzymes during the fermentation step. The challenges associated with this approach are manifold and include selecting the most suitable mechanical technology and its optimization without the formation of inhibitors; optimization of the conditions for growth and delignification of *P. chrysosporium* in solid or semi-solid fermentation; and minimization of pre-treatment costs to ensure the economic viability of the process.

5.11 Conclusion

P. chrysosporium has an excellent potential for a wide range of applications. The great interest in this fungus is linked to its ability to secrete several of the major enzymes involved in the natural degradation of lignin, but also of a broad range of aromatic compounds. Its importance is reinforced, on the one hand, by the fact that very few living organisms are capable of this exploit. On the other hand, *P. chrysosporium* is one of the few WRFs whose genome has been completely sequenced and has the advantage of being one of the most used WRF. Furthermore, given the development of bioengineering and the important role played by aromatic compounds in modern society (dyes, textiles, paint, food, energy, construction, automobiles, printing, pulp and paper, etc.), in contrast with their toxicity, and their increasingly alarming accumulation, the development of technologies using *P. chrysosporium* has just begun.

5.12 Acknowledgement

This work was supported by Institut National de la Recherche Scientifique (INRS) and the Natural Sciences and Engineering Research Council of Canada (NSERC).

6 QUATRIÈME ARTICLE

Optimization of biomass delignification by extrusion and analysis of extrudate characteristics

Optimisation de la délignification de la biomasse lignocellulosique par extrusion et analyse des caractéristiques des extrudats

Delon Konan ¹, Adama Ndao ¹, Ekoun Koffi ², Saïd Elkoun ³, Mathieu Robert ³, Denis Rodrigue ⁴, and Kokou Adjallé ^{1,*}

1. Laboratoire de Biotechnologies Environnementales, Institut National de la Recherche Scientifique (INRS), 2605, boulevard du Parc-Technologique, G1P 4S5, Québec (Québec), Canada.

2. Département de génie chimique, Université Laval, 1065 Avenue de la Médecine, G1V0A6, Québec (Québec), Canada.

3. Center for Innovation in Technological Ecodesign (CITE), University of Sherbrooke, Sherbrooke, QC, J1K 2R1, Canada

4. Département de génie mécanique et énergétique, Institut National Polytechnique Félix Houphouët Boigny (INPHB), Yamoussoukro, Côte d'Ivoire.

5. Département de génie mécanique, Université de Sherbrooke, 2500, boulevard de l'Université, Sherbrooke (Québec) J1K 2R1.

*Correspondence: kokou.adjalle@inrs.ca

Waste, 2025, Volume 3, Issue 2, 12.

Received: 27 January 2025 / Revised: 14 March 2025 / Accepted: 20 March 2025 / Published: 25 March 2025

DOI : <https://doi.org/10.3390/waste3020012>

Contribution des auteurs :

Conceptualization, Writing - Original Draft: Delon Konan; Writing - Review & Editing: Adama Ndao, Ekoun Koffi, Denis Rodrigue, Saïd Elkoun, Mathieu Robert, Kokou Adjallé; Funding Acquisition, Supervision: Kokou Adjallé.

6.1 Abstract

Pretreatment of lignocellulosic biomass remains the primary obstacle to the profitable use of this type of biomass in biorefineries. The challenge lies in the recalcitrance of the lignin-carbohydrate complex to pretreatment, especially the difficulty in removing the lignin to access the carbohydrates (cellulose and hemicellulose). This study had two objectives: (i) to investigate the effect of reactive extrusion on lignocellulosic biomass in terms of delignification percentage and the structural characteristics of the resulting extrudates, and (ii) to propose a novel pretreatment approach involving extrusion technology based on the results of the first objective. Two types of biomasses were used: agricultural residue (corn stover) and forest residue (black spruce chips). By optimizing the extrusion conditions via response surface analysis (RSA), the delignification percentages were significantly improved. For corn stover, the delignification yield increased from 2.3% to 27.4%, while increasing from 1% to 25.3% for black spruce chips. The highest percentage were achieved without the use of sodium hydroxide and for temperatures below 65 °C. Furthermore, the optimized extrudates exhibited important structural changes without any formation of p-cresol, furfural and 5-hydroxymethylfurfural (HMF) (enzymes and microbial growth-inhibiting compounds). The structural changes included the disorganization of the most recalcitrant functional groups, reduction of particle sizes, increase of specific surface areas, and the appearance of microscopic roughness on the particles. Analyzing all the data led to propose a new promising approach to the pretreatment of lignocellulosic biomasses. This approach involves combining extrusion and biodelignification with white rot fungi to improve the enzymatic hydrolysis of carbohydrates.

Keywords: Biomass pretreatment; Extrusion; Pretreatment optimization; Response surface methodology; Biodelignification.

Lien entre l'article ou les articles précédents et le suivant :

L'article 1 identifiait les paramètres les plus importants du prétraitement à l'extrusion et mettait en lumière l'importance de l'optimisation de ces paramètres pour un prétraitement adéquat. L'article

2 proposait le couplage de l'extrusion et de la biodélicnification après analyse des prétraitements existants et des caractéristiques des extrudats. L'article 3 étudiait la biodélicnification et mettait en lumière la complémentarité de celle-ci et de l'extrusion. Le but de l'article 4 est : (i) d'optimiser les paramètres de prétraitement de deux biomasses lignocellulosiques (un résidu agricole et un résidu forestier) par extrusion et (ii) d'analyser les caractéristiques des extrudats optimisés. Les résultats de cet article serviront de point de départ pour l'article 5 (biodélicnification à partir des extrudats optimisés).

6.2 Introduction

The biorefinery sector plays a crucial role in energy transition as it uses technologies to convert lignocellulosic biomass (LCB), once considered as waste, into renewable fuels. Lignocellulosic biomasses are mainly composed of agricultural and forest residues, but the main challenge in using lignocellulosic residues as raw materials is the need for a pretreatment step (Ab Rasid *et al.*, 2021; Chakraborty *et al.*, 2024). This step is the most energy-intensive stage and accounts for more than 40% of the total production cost, while 30 – 50% is for the total equipment cost and 20 – 25% for the operational cost when lignocellulosic biomass is converted into biofuels such as bioethanol (Audibert *et al.*, 2025; Kordala *et al.*, 2024). The high cost is due to the difficulty of breaking down the lignocellulose complex during the pretreatment. Lignocellulose (lignin, cellulose and hemicellulose), which is the main component of plant cell walls, acts as the plant's natural defense system against various forms of aggression and also provides rigidity to plant cells (Delmer *et al.*, 2024). In particular, lignin plays a crucial role in binding cellulose and hemicellulose together, but also prevents access to carbohydrates, making the pretreatment more difficult.

Various technologies for lignocellulosic biomass pretreatment have been developed with varying degrees of success. However, when integrated for the conversion of lignocellulosic biomasses into biofuels, these technologies fail to ensure the economic viability of the valorization. In other words, the cost per liter of the obtained biofuel remains higher than the market price, allowing fossil fuels to be maintain a monopoly position (Wang & Zhao, 2018; Watson *et al.*, 2024). In comparison, the cost of bioethanol production from sugar or starch-based feedstock (which is first-generation bioethanol) is a 43% lower compared to ethanol production from lignocellulosic biomasses (second-generation bioethanol) (Iram *et al.*, 2022). Nevertheless, 1G bioethanol is still less competitive compared to fossil fuels in general (Stafford *et al.*, 2019), although 2G bioethanol represents less than 5% of the global bioethanol production (Sharma *et al.*, 2020) and numerous

technical and economic analyses have identified the pretreatment stage as the limiting factor in the valorization of lignocellulosic biomass (Caporusso *et al.*, 2022; Ong & Wu, 2020b). This is why investigations on promising pretreatment methods are still ongoing. Reactive extrusion is one of these technologies (Gallego-García *et al.*, 2023). Extrusion is a well-known thermomechanical process used in the plastics industry to mix and shape polymers. It was recently used as a physical pretreatment for lignocellulosic biomasses, especially using twin-screw extruders for good mixing conditions (materials uniformity) (Guiao *et al.*, 2022a; Han *et al.*, 2020). The biomass is fed into the extruder, where it undergoes high shear forces as it is conveyed from one end of the screws to the other. The shear is maximized through the design of the screw modules and temperature control. Some extruders are equipped with liquid injection ports, which are useful for materials with unsuitable rheological behavior, such as lignocellulosic biomasses (reactive extrusion) (Chevalier *et al.*, 2023). Extrusion is considered an attractive alternative to traditional pretreatment methods due to several advantages including high pretreatment speed, low operating and energy costs, low water consumption, non-selectivity of the biomasses, absence of inhibitor generation, and flexibility (Akobi *et al.*, 2016; Shukla *et al.*, 2023). However, the success of extrusion strongly depends on choosing the right extrusion conditions, which presents a challenge due to the numerous parameters involved.

Extrusion conditions can be classified into three categories: intrinsic extruder parameters, biomass-related parameters, and operating parameters. Intrinsic extruder parameters include the number, size, type, configuration, and length of the screws, as well as the presence or absence of a die, and the die shape (metal channels imparting a specific cross-sectional shape to a polymer stream) (Konan *et al.*, 2022b). Biomass-related parameters are the type of biomass, lignocellulosic composition, particle size, and moisture content. As for the operating parameters, they include temperature, screw rotation speed, biomass feed rate, biomass residence time, and recirculation. When a liquid chemical is injected during extrusion, a fourth category of parameters must be considered. These are the type of additive, the concentration, the injection rate, and the injection location along the extruder barrel. Optimizing all these extrusion parameters is crucial to maximize the process performance.

This study had two consecutive objectives: (i) The optimization of the extrusion pretreatment for maximum delignification, and (ii) the analysis of the characteristics of the extrudates, to propose either a complementary pretreatment coupling for further delignification for LCB valorization into cost-effective bioethanol production, or the proposition of possible biocomposite materials based on the results of the analysis. The study investigated the effects of reactive extrusion on

lignocellulosic biomasses in terms of delignification percentage and structural characteristics of the resulting extrudate. Corn stover (agricultural residue) and black spruce residues (forestry residues) were selected as feedstocks for this study. Corn is the primary crop in Quebec province (Canada) and black spruce is one of the main tree species. According to the last report of the Ministry of Energy and Natural Resources of Quebec, about 6.8 million tons/year of wood and 549 000 tons/year of agricultural residues are available in the province for bioenergy production ([WSP, 2021b](#)).

6.3 Materials and methods

6.3.1 Raw biomasses and characterization

One forest residue and one agricultural residue were used in this work: black spruce (*Picea mariana*) and corn stover (*Zea mays*). Black spruce chips (BS) were provided by Savard et Fils sawmill (Quebec, Canada), and dry corn stover (CS) was provided by Agrosphere Inc. (Quebec, Canada). BS consisted exclusively of chips from the tree trunk, while CS consisted of a mixture of leaves, stalks, and cobs. Upon receipt, BS and CS had particle sizes between 2 and 5 mm. They were ground into 1 mm and 1.5 mm (for extrusion trials) using a Pulverisette 15 (Frisch, Germany) and stored at room temperature. A sample of each biomass was ground with a small grinder (Magic Bullet, Canada), and particle size below 0.2 mm was collected for characterization, especially to determine the biomass composition in terms of cellulose, hemicellulose, lignin, and extractives. Extractives and hemicellulose were determined using NDF (Neutral Detergent Fiber) and ADF (Acid Detergent Fiber) method respectively, using an ANKOM fiber analyzer (ANKOM, USA) ([Van Soest et al., 1991b](#)). Finally, the lignin content was evaluated using the Klason Lignin method, while cellulose content was calculated by mass comparison ([Sluiter et al., 2008](#)).

6.3.2 Parameter screening

Pretreatment parameters were screened by: (i) extensive literature reviews summarized in Konan et al. ([Konan et al., 2022a](#); [Konan et al., 2022b](#)), (ii) through preliminary extrusion trials, and (iii) operation constrains. Table S1 (Supplementary material) presents the details of the parameter's selection.

6.3.3 Reactive extrusion

The reactive extrusion steps were performed using a Process 11 extruder (Thermo Scientific, USA) equipped with twin co-rotating screws (11 mm diameter each). The standard screw

configuration was used for all extrusions. It consisted of four (4) forward screw zones and three (3) kneading element zones as shown in [Figure 6.1](#). Before to extrusion, some amounts of each biomass were mixed with sodium hydroxide according to the experimental plan (§ 2.3). The trials of the experimental plan were randomly performed. For each trial, 20 g of extrudates were collected only when the conditions (temperature, screw speed, and torque) were stable. Daily extrusion trials were preceded and followed by cleaning (purging) the extruder with low-density polyethylene (LDPE).

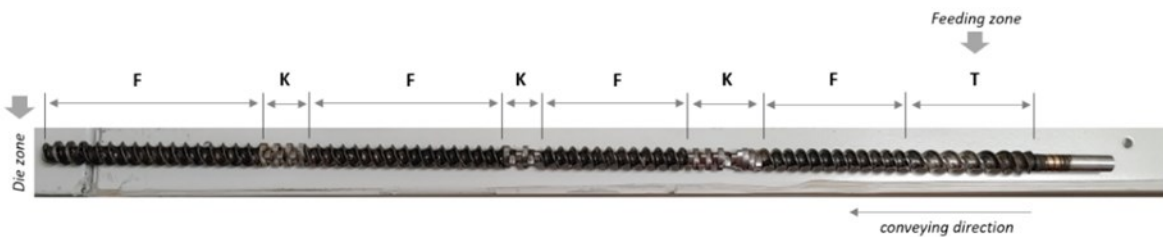


Figure 6.1 Screw configuration for the extrusion step (T = transport zone, F = forward screw element and K = kneading elements block).

6.3.4 Experimental plan

Prior to build the experimental plan, multiple series of trials were run in different extreme conditions of temperature, rotation speed, particle size, biomass moisture, biomass/NaOH ratio, biomass feeding throughput, extruder die configuration, feeding ratio, and biomass recirculation to determine the experimental space. This resulted in different experimental spaces for BS and CS as shown in [Tableau 6.1](#). Then, a faced central composite design (CCD) was designed with Design Expert 13 software to build the experimental plan for each biomass. The central composite design was chosen for its flexibility (ex: more trials can be added if needed) and robustness to estimate complex interactions and non-linear effects between parameters which was expected with biomass extrusion and confirmed by this study. However, the choice of the faced-centered central composite design (FCCCD) instead of the rotatable central composite design (RCCD) was dictated by preliminary experiments. It was not possible to extrudate the biomasses beyond the experimental space (ex: screw speed < 150 rpm or > 300 rpm) so α (the distance of axial points from the center) was equal to 1. The experimental plan for each biomass is composed of 34 runs including 6 center points ([Tableau 6.2](#)).

Tableau 6.1 Experimental space for the extrusion conditions.

	Black spruce chips (BS)				Corn stover (CS)			
	Screw speed	Temp	NaOH	Particle size	Screw speed	Temp	NaOH	Particle size
Type	Numeric	Numeric	Numeric	Categoric	Numeric	Numeric	Numeric	Categoric
Unit	rpm	°C	%	mm	rpm	°C	%	mm
Low level (-1)	150	50	0	1	80	40	0	1
High level (+1)	300	100	15	1.5	300	110	15	1.5
- alpha	150	50	0	1	80	40	0	1
+ alpha	300	100	15	1.5	300	110	15	1.5

Tableau 6.2 Experimental trials for black spruce chips (BS) and corn stover (CS).

Run	Black spruce chips					Corn stover				
	Space type	Screw speed (rpm)	Temp (°C)	NaOH ¹ (%)	Particle size (mm)	Space type	Screw speed (rpm)	Temp (°C)	NaOH (%)	Particle size (mm)
1	Factorial	300	100	0	1	Center	190	80	7.5	1.5
2	Axial	225	50	7.5	1	Axial	190	80	15	1.5
3	Factorial	150	100	0	1.5	Axial	190	80	15	1
4	Factorial	300	50	0	1.5	Factorial	80	110	0	1.5
5	Factorial	150	50	15	1.5	Factorial	300	50	0	1.5
6	Axial	300	75	7.5	1.5	Axial	190	80	0	1
7	Axial	150	75	7.5	1	Axial	80	80	7.5	1.5
8	Axial	225	50	7.5	1.5	Factorial	80	110	0	1
9	Factorial	150	50	0	1	Center	190	80	7.5	1
10	Factorial	300	100	0	1.5	Axial	80	80	7.5	1
11	Center	225	75	7.5	1	Axial	300	80	7.5	1
12	Factorial	300	50	0	1	Factorial	80	50	15	1.5
13	Center	225	75	7.5	1	Factorial	80	50	15	1
14	Factorial	150	50	15	1	Factorial	300	50	0	1
15	Factorial	150	100	0	1	Axial	190	50	7.5	1.5
16	Center	225	75	7.5	1.5	Axial	190	110	7.5	1.5

Black spruce chips						Corn stover				
Run	Space type	Screw speed (rpm)	Temp (°C)	NaOH ¹ (%)	Particle size (mm)	Space type	Screw speed (rpm)	Temp (°C)	NaOH (%)	Particle size (mm)
17	Factorial	300	50	15	1	Factorial	300	110	15	1
18	Axial	225	100	7.5	1	Center	190	80	7.5	1
19	Factorial	300	100	15	1.5	Factorial	80	110	15	1
20	Factorial	300	50	15	1.5	Factorial	300	110	0	1.5
21	Axial	225	75	0	1	Factorial	80	50	0	1.5
22	Factorial	300	100	15	1	Center	190	80	7.5	1.5
23	Axial	225	75	0	1.5	Factorial	300	110	15	1.5
24	Axial	300	75	7.5	1	Factorial	300	50	15	1
25	Factorial	150	100	15	1.5	Factorial	300	110	0	1
26	Axial	225	75	15	1.5	Center	190	80	7.5	1.5
27	Center	225	75	7.5	1.5	Factorial	300	50	15	1.5
28	Factorial	150	50	0	1.5	Axial	190	50	7.5	1
29	Center	225	75	7.5	1	Factorial	80	50	0	1
30	Axial	150	75	7.5	1.5	Center	190	80	7.5	1
31	Axial	225	75	15	1	Factorial	80	110	15	1.5
32	Factorial	150	100	15	1	Axial	190	80	0	1.5
33	Center	225	75	7.5	1.5	Axial	190	110	7.5	1
34	Axial	225	100	7.5	1.5	Axial	300	80	7.5	1.5

6.3.5 Preparation of biomass

The additive used was sodium hydroxide (NaOH) 98% purity purchased from Thermo Scientific (USA). The NaOH solutions were mixed with the biomass just before extrusion with an additive ratio of 2:1 (w/w). For instance, 500 g of biomass was mixed with 250 g of water or NaOH solution (7.5% or 15% w/w NaOH) according to the experimental plan (Tableau 6.2).

6.3.6 Moisture content

The moisture content of the extrudates was determined using a moisture analyzer HR83 Halogen (Mettler Toledo, USA) as follows: 0.5 g of the extrudate was placed in the apparatus and heated to 105 °C until the mass of the sample remained constant (5 – 10 min). The moisture content was then calculated as:

Équation 6.1 – Moisture.

$$\text{Moisture} = 100 \times \frac{(0.5 - m_{105})}{0.5}$$

where m_{105} is the constant mass of biomass when heated at 105 °C.

6.3.7 Particle size and specific surface

Particle size distribution and specific surface of the extrudates and the raw materials were measured using a laser scattering analyzer Horiba LA-950 (Horiba Ltd., Japan).

6.3.8 Delignification percentage

Before delignification analysis, the extrudates were filtered with hot water several times till neutral pH in order to remove sodium hydroxide, and the soluble products of lignin degradation. The filtered extrudates were then oven-dried at 50 °C. The insoluble lignin composition of the biomass was determined by the Klason method. In a 100 ml beaker, 0.5 g of biomass was added along with 20 ml of 72% sulfuric acid (H₂SO₄) solution prepared from 98% H₂SO₄ (Fisher Chemicals). The content of the beaker was stirred at regular intervals for 1 h and 20 min. Afterward, the mixture was transferred to a 320 ml round-bottomed cylindrical tube and 290 ml of distilled water was added to obtain a 3% H₂SO₄ solution. The tube was then placed in a digester and heated to 185 °C for 3 h. The content was filtered and washed with 200 ml of distilled water using a filter device and Whatman 45 µm paper. The solid fraction on the Whatman paper was placed in a 100 ml beaker and dried overnight at 105 °C. Once dried, the beaker was weighed, and the dry mass of insoluble lignin (biomass dry solid fraction) was calculated by subtracting the weight of the filter paper and the beaker (which were weighed beforehand). The delignification percentage was calculated by comparing the mass of lignin in the raw biomass to the mass of lignin in the extrudate. The equation for the delignification percentage is:

Équation 6.2 – Delignification percentage.

$$\gamma = \frac{mL_{\text{raw}} - mL_{\text{ext}}}{mL_{\text{raw}}} \times 100$$

where mL_{raw} represents the mass of lignin in the raw biomass, while mL_{ext} represents the mass of lignin in the extrudate.

6.3.9 Optimization

BS and CS were optimized separately due to their different experimental space. The optimizations were performed by using the response surface methodology (RSM). RSM uses mathematical and statistical methods to predict a dependent variable based on a set of independent variables and a regression equation (Équation 6.3). The extrusion conditions were mathematically modeled into a regression equation to match their respective results. Then by calculating appropriate statistical tests, such as the variance ratio (F) and the associated p value (probability), the analysis of variances (ANOVA) was used to determine by iteration the effect of each term on the final response. The terms that did not meet the significance thresholds were removed from the model to refine it. Once the model was obtained, it was possible to identify the best response that could be achieved within the defined experimental space. The input parameters in this study were the particle size (mm), screw rotation speed (rpm), temperature (°C), and sodium hydroxide concentration (% w/w). The main response investigated was the delignification percentage, while the secondary responses were the specific surface area and the particle size of the extrudates. The general equation for a quadratic model with n independent variables is provided by:

Équation 6.3 – General equation for a quadratic model with n independent variables.

$$y = \beta_0 + \beta_1 X_1 + \beta_2 X_2 + \dots + \beta_n X_n + \beta_{11} X_1^2 + \beta_{22} X_2^2 + \dots + \beta_{nn} X_n^2 + \beta_{12} X_1 X_2 + \dots + \beta_{1n} X_1 X_n + \beta_{2n} X_2 X_n + \varepsilon$$

where y is the response, X_1, X_2, \dots, X_n represent the independent variables, β_0 represents the intercept term, $\beta_1, \beta_2, \dots, \beta_n$ are the coefficients of the linear terms, $\beta_{11}, \beta_{22}, \dots, \beta_{nn}$ are the coefficients of the squared (quadratic) terms, $\beta_{12}, \beta_{13}, \dots, \beta_{1n}, \beta_{2n}$ are the interaction coefficients, and ε represents the experimental error.

6.3.10 Scanning Electron Microscopy (SEM)

The morphology of the biomass was examined before and after extrusion using scanning electron microscopy (SEM) (Zeiss EVO® 50 smart SEM, Germany). Different magnifications (Mag) and working distances (WD) were used, along with a secondary electrode 1 (SE 1) detector and an Extra High Tension (EHT) of 10 kV. Prior to SEM testing, all the samples were coated with a fine platinum layer using a High Vacuum Sputter Coater (Leica Microsystems, Canada).

6.3.11 Fourier Transformed Infrared Spectroscopy (FTIR) analysis

FTIR spectra for the raw and extruded biomasses were recorded with a Nicolet iS50 FT-IR spectrophotometer equipped with a standard ATR crystal cell detector (Thermo Scientific, USA). The wavelength range was from 400 to 4000 cm^{-1} . Each spectrum was acquired by the average of 16 scans with 4 cm^{-1} resolution.

6.3.12 Gas chromatography/mass spectrometry (GC/MS)

After optimizing the extrusion conditions, 2 g of biomass was sampled from the extrudate and blended with 40 g of deionized water into a 250 ml beaker. The mixture was thoroughly mixed and slightly heated for 5 min on a heated plate equipped with magnetic stirring. After 5 min, the mixture was filtered with a 45 μm Whatman paper. The filtrate was collected and injected in a Clarus 500 gas chromatography/mass spectrometry (Perkin Elmer, USA). Sample injection was performed in splitless mode, with an injector temperature of 250°C, a splitless time of 0.75 min, and an injection volume of 0.7 μL . Water was used as the rinsing solvent for both injectors A and B. Chromatographic separation was carried out on a RTX-WAX column (30 m \times 0.25 mm \times 0.25 μm), with a constant helium flow rate of 1.5 mL/min as the carrier gas. The initial oven temperature was set to 70°C. Detection of the compounds was performed in SCAN mode with a mass range of 35-350 m/z, a transfer line temperature of 250°C, and an ion source temperature of 260°C.

6.4 Results and discussion

6.4.1 Biomass characteristics

Figure 6.2 displays the elemental compositions of raw BS and raw CS in terms of carbon (C), hydrogen (H), nitrogen (N) and sulfur (S). These two biomasses have similar compositions, in terms of the relative proportion of each four chemical elements and in terms of the CHNS percentage. Sulfur in both biomasses was too low to be detected as well as nitrogen in BS. CHNS

represents 53.7% of the total mass of BS and 50.3% of CS. The relative proportion of each element influences the calorific value of the biomass. Theoretically, BS and CS have similar calorific values. Based on Équation 6.4 given by [Sheng and Azevedo \(2005\)](#) they have respectively a calorific value of 19.3 MJ/kg and 18.7 MJ/kg. However, in terms of cellulose, hemicellulose, lignin, extractives, and ash composition, both biomasses exhibit different compositions ([Figure 6.3](#)). The relative proportion of these compounds is more balanced in CS than in BS, meaning that the variance in BS components is significantly higher than in CS (resp. 264.3 and 90.1). The lignin content of BS is $28.9 \pm 0.7\%$, which is 1.5 times higher than the lignin content of CS ($18.9 \pm 0.7\%$). Similarly, BS contains almost twice the of cellulose amount in CS but less than half its hemicellulose quantity. The high level of extractives in CS is explained by the mixed composition of these residues. They consist of various parts of the plant, including peduncles, spathes, stigmas, panicles, stems, and leaves. These parts contain varying amounts of crude protein and starch, known as non-structural components (NSC) ([Liu et al., 2016a](#)). NSCs can be up to 30% in corn stover ([Zhang et al., 2018](#)). NSC are soluble in neutral detergent. They are all removed at the NDF (Neutral Detergent Fiber) stage in the Van Soest method and accounted as extractives ([Mustafa et al., 2004; Zhang et al., 2021d](#)). These characterization results are coherent with those of [Fang et al. \(2011\)](#) for BS and [Zhang et al. \(2018\)](#) for CS.

Équation 6.4 – Calorific energy.

$$CV = -1.3675 + 0.3137 C + 0.7009 H + 0.0318 O^*$$

where CV: calorific value (MJ/kg), C: Carbon proportion (%), H: Hydrogen (%) and O*: $O = 100 - C - H - \text{Ash}$.

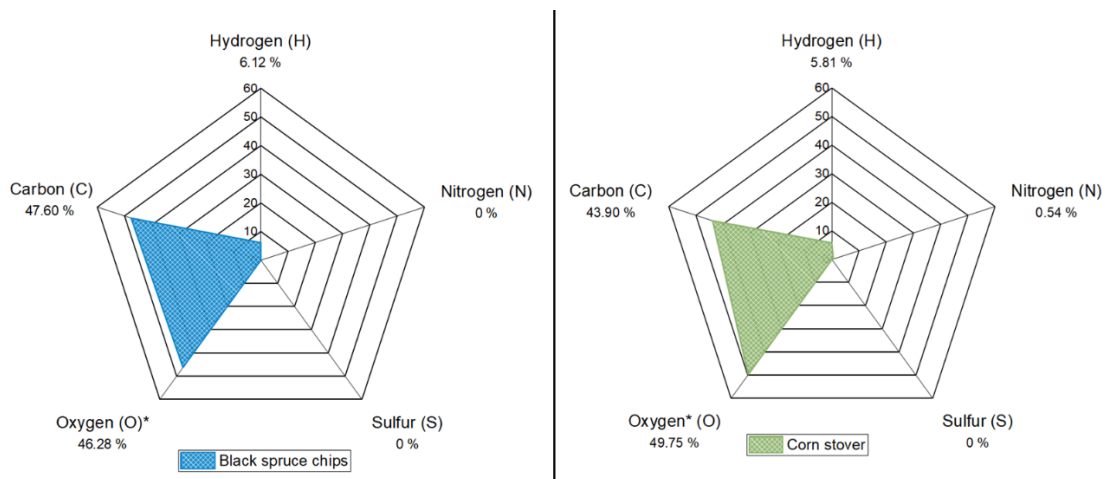


Figure 6.2 Elemental composition of black spruce chips and corn stover.

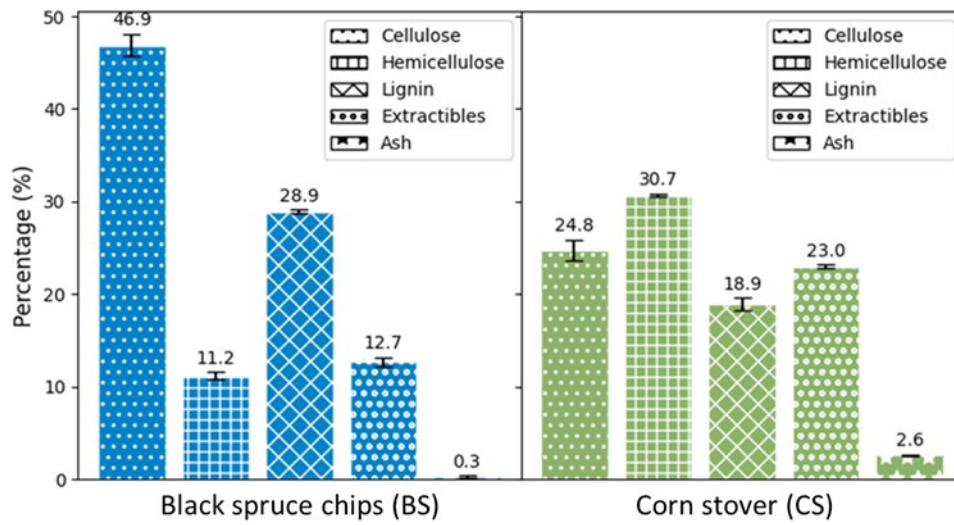


Figure 6.3 Black spruce chips (BS) and corn stover (CS) characterization.

6.4.2 Extrusion conditions

Screw configuration is an important parameter for an efficient pretreatment of lignocellulosic biomass by extrusion. The screw configuration used in this study was based on previous literature data (Konan *et al.*, 2022b). It consisted of three kneading zones (K), four forward conveying zones (F), and one transport zone (T) (also the biomass feeding zone) (Figure 6.1). No reverse screw elements were included in the configuration to avoid excessive pressure in the extruder, pore blocking, and lignin redistribution in the biomass, as observed by Zheng *et al.* (2015).

Biomass structural compositions (lignin, cellulose, and hemicellulose) do have an impact on extrusion conditions. Preliminary tests conducted to determine the experimental space led to different temperature and rotation speed conditions for BS and CS (Tableau 6.3). Trials were initially conducted with two dies of different sizes (diameters of 1 mm and 3 mm) to maximize the back pressure in the barrel but were later repeated without them. The dies obstructed the extrudates from exiting properly and the extrudates were compacted by the screw behind the die. This was then often followed by the jamming of the screws. The compaction behind the die was especially fast when the extrusion trials involved sodium hydroxide solution such as in runs 2, 5 and 6 (Figure 6.4). Sodium hydroxide is a strong alkaline agent that depolymerizes lignin in the biomass, making the fibers more susceptible to deformation and stretching (Long *et al.*, 2015). Under pressure and elevated temperature, sodium hydroxide becomes viscous and easily mixes with the biomass. However, the change in temperature and pressure at the extruder outlet

solidified it, causing the NaOH to function as a binder, holding the CS particles together. As for BS, extrusions with dies were impossible due to extruder jamming. Using a die may also affect the cost and energy balance of the pretreatment, as it requires an additional grinding step of the extrudate before subsequent processing steps such as washing or enzymatic hydrolysis. In line with these results, all the 68 trials (34 x 2) were performed without dies.

The minimum screw rotation speed for BS was 150 rpm, and 80 rpm for CS (Tableau 6.3). CS are more compressible than BS which has more rigid particles. Below 150 rpm for BS and 80 rpm for CS, the torque required to set the screws in motion exceeds the extruder's capacity, causing the screws to stop. On the other hand, above 300 rpm for both biomasses, the speed was too high and created an instability in the rotation of the screws. This instability caused the co-rotation to become less synchronous and the screws to jam. There are two main reasons for this instability. First, the rheological behavior of biomasses, unlike chemical polymers, is random due to the irregular shape of their particles. Secondly, the biomass is discontinuous along the screws because most of the load is blocked in the kneading zones. In fact, at higher speeds, the residence time of the extrudate in the mixing element where the kneading occurs and where the shear forces are maximal is shortened. Therefore, the particle sizes are not sufficiently reduced to be conveyed from the first mixing element to the next element while new biomass loads are pushed into the mixing zone by the previous screw elements. This creates a load difference between the mixing zones and instability in the twin-screw synchronous rotation. These results indicate that the type and composition of biomass can significantly affect extrusion conditions, specifically screw rotation speed. Therefore, it is crucial to conduct preliminary extrusion tests for each new biomass. Regarding the difference in temperature range, it was greater with CS than with BS. It is attributed to the hygroscopic properties of agricultural residues. Agricultural residues tend to absorb more moisture internally compared to forest residues. The internal moisture content affects the biomass thermal behavior during processing. The higher the moisture content, the more significant the biomass compression and the effect of hot water on the fibers. It has also been observed that water evaporated during extrusion, even though the boiling point of water is beyond the barrel temperature due to high pressure. This phenomenon is governed by [Équation 6.5](#) the Clausius-Clapeyron equation, which describes the relationship between vapor pressure and temperature ([Velasco et al., 2009](#)). In the mixing zones, the real-time temperature was higher than the setpoint temperature due to the high shear forces occurring there. Under these conditions, the water vapor pressure also increases, resulting in a sudden release of water molecules in steam form.

Équation 6.5 – Clausius-Clapeyron equation.

$$\ln\left(\frac{P_1}{P_2}\right) = -\frac{\Delta H_{vap}}{R} \left(\frac{1}{T_1} - \frac{1}{T_2}\right)$$

where P_1 : vapor pressure at temperature T_1 ; P_2 : vapor pressure at temperature T_2 ; ΔH_{vap} : enthalpy of vaporization of the substance; R : ideal gas constant (8.314 J/mol K).

Tableau 6.3 Extrusion experimental space codes.

Parameters	Black spruce chips		Corn stover	
	Low level (-1)	High level (+1)	Low level (-1)	High level (+1)
Screw speed (rpm)	150	300	80	300
Temperature (°C)	50	100	40	110
NaOH (% w/w)	0	15	0	15
Particle size (mm)	1	1.5	1	1.5

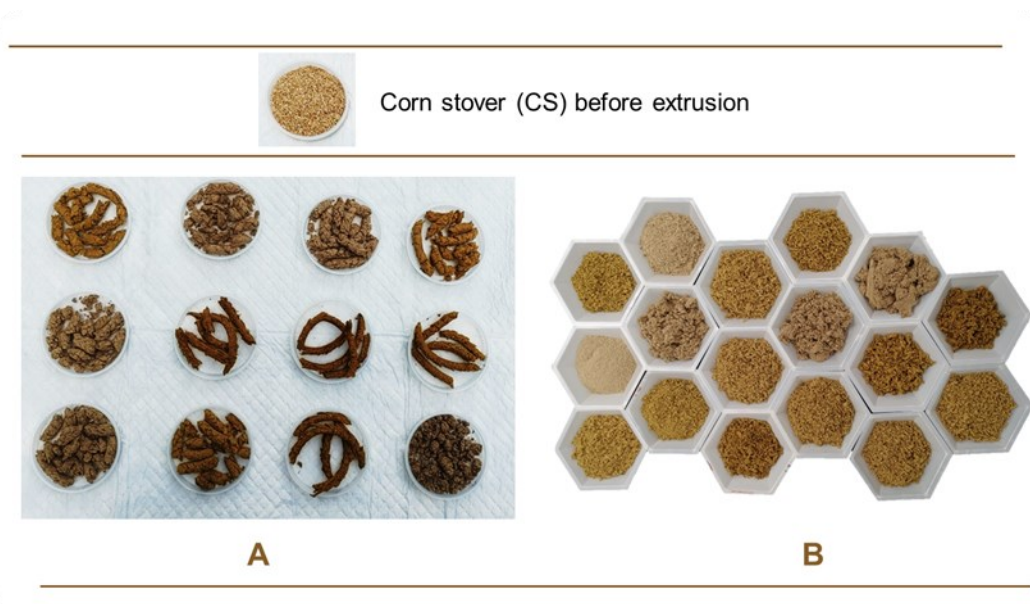


Figure 6.4 Corn stover of 1 mm particle size extruded: (A) with a 3 mm die in different conditions of temperature and screw speed, and (B) without a 3 mm die in different conditions of temperature and screw speed.

6.4.3 Extrudate characteristics

After each extrusion trial (68 in total), the delignification percentage, moisture, particle size, and specific surface area of the extrudates were measured. These parameters represent the four responses (S1 to S4) for BS and (R1 to R4) for CS (Tableau 6.4).

Moisture is an important parameter not only for operational reasons as it allows a steady flow (stability) of the extrusion, but is also important for the reduction of water consumption during downstream processes; higher moisture is better. However, the moisture of the trials varied widely, ranging from 23.6% to 59.2% for R2 and from 5.4% to 34.8% for S2. These results indicate that BS retains moisture better during extrusion compared to CS although they absorb less comparatively, as reported in § 3.2. Pearson coefficient analysis was performed to assess the relationship between the parameters (Chang & Ng, 2011; Gu *et al.*, 2019). Table 6.5 presents the correlation matrix. For black spruce extrudates (BSE), there is no statistical evidence supporting a correlation between the extrusion temperature and the extrudate moisture ($r = -0.283$, $p > 0.05$) or between the screw speed and the extrudate moisture ($r = -0.021$, $p > 0.05$). However, the sodium hydroxide concentration and the extrudate moisture are positively related ($r = 0.349$, $p < 0.05$). Lower moisture seems to be influenced by a combination of both temperature and NaOH concentration. On the other hand, for corn stover extrudates (CSE), the significant moisture loss was negatively correlated with the extrusion temperature ($r = -0.719$, $p < 0.05$), as well as with the specific surface area ($r = -0.753$, $p < 0.05$). The higher the temperature, the higher the specific surface and the lower the moisture. In addition, particle size and specific surface area are negatively correlated ($r = -0.849$, $p < 0.05$). This can be explained by the fact that CSE particles agglomerate with moisture, resulting in larger particles and reduced specific surface area.

The particle sizes of all extrudates ranged from 68 to 205 μm for BSE (S3) and from 116 to 1204 μm for CSE (R3). Raw BS particle sizes (1 mm and 1.5 mm) did not have a significant effect on their extrudate particle sizes (Figure 6.5). On the contrary, for CS, there was an important size difference between the initial particle sizes and their resulting CSE particles. The median CSE particle sizes were 328 μm and 713 μm respectively for CS 1 mm and CS 1.5 mm, which were much higher than those of BSE (122 μm and 148 μm). The extrudate particle size distribution with raw residues grounded with a fine grinder (Magic Bullet, Canada) was also done to investigate the difference in size reduction between extrusion and grinding. Figure 6.6 A and B present the results on logarithmic scales. With grinding, it was not possible to achieve more particle size reduction even after several cycles and/or for a longer duration than the extruder takes. This is because the shear forces in the kneading zones are responsible for the mechanical reduction in

particle size. In this zone, intensive grinding occurs under pressure in a confined space (with a clearance in the microns range), which is not the case in a grinder. For particle size reduction, extrusion has the advantage to being very fast as it takes between a few seconds to 2 min for biomass to move from the feeding zone to the die exit.

Tableau 6.4 Summary of the responses.

Response	Parameter	Units	Observation	Minimum	Maximum	Mean	Std. dev.	Ratio
Corn stover								
R1	Delignification	%	34	2.2	24.4	12.7	6.1	10.9
R2	Moisture	%	34	5.4	34.8	25.1	8.3	6.4
R3	Particle size	µm	34	115	1203	565	324	10.4
R4	Specific surface	cm ² /cm ³	34	174	1183	462	271	6.8
Black spruce chips								
S1	Delignification	%	34	0.9	25.2	12.6	4.5	25.8
S2	Moisture	%	34	23.6	59.2	31.8	5.6	2.5
S3	Particle size	µm	34	68.2	204	135	29	3.0
S4	Specific surface	cm ² /cm ³	34	646	1569	955	203	2.4

Tableau 6.5 Pearson correlation coefficients.

Corn stover								
	S.S	T°C	[NaOH]	P.S*	D%	M%	S.S.A	E.P.S
Screw speed (S.S)	1.000	0.000	0.000	n.a	0.037	0.027	-0.007	0.022
Temperature (T°C)		1.000	0.000	n.a	-0.144	-0.719*	0.298	-0.145
[NaOH]			1.000	n.a	0.070	0.078	-0.312	0.577*
Particle size (P.S)				n.a	n.a	n.a	n.a	n.a
Delignification (D%)					1.000	-0.029	0.134	-0.013
Moisture (M%)						1.000	-0.753*	0.548*
Specific surface area (S.S.A)							1.000	-0.849*
Extrudate particle size (E.P.S)								1.000
Black spruce								
	S.S	T°C	[NaOH]	P.S	D%	M%	S.S.A	E.P.S
Screw speed (S.S)	1.00	0.00	0.000	n.a*	0.302	-0.021	-0.285	0.285
Temperature (T°C)		1.00	0.000	n.a	-0.015	-0.283	-0.027	-0.053
[NaOH]			1.000	n.a	0.314	-0.349*	-0.106	0.200
Particle size (P.S)				n.a	n.a	n.a	n.a	n.a
Delignification (D%)					1.00	-0.105	-0.076	0.191

Moisture (M%)	1.00	0.120	-0.190
Specific surface area (S.S.A)		1.00	-0.957*
Extrudate particle size (E.P.S)			1.00

+ categoric parameter, * p-value inferior to 0.05

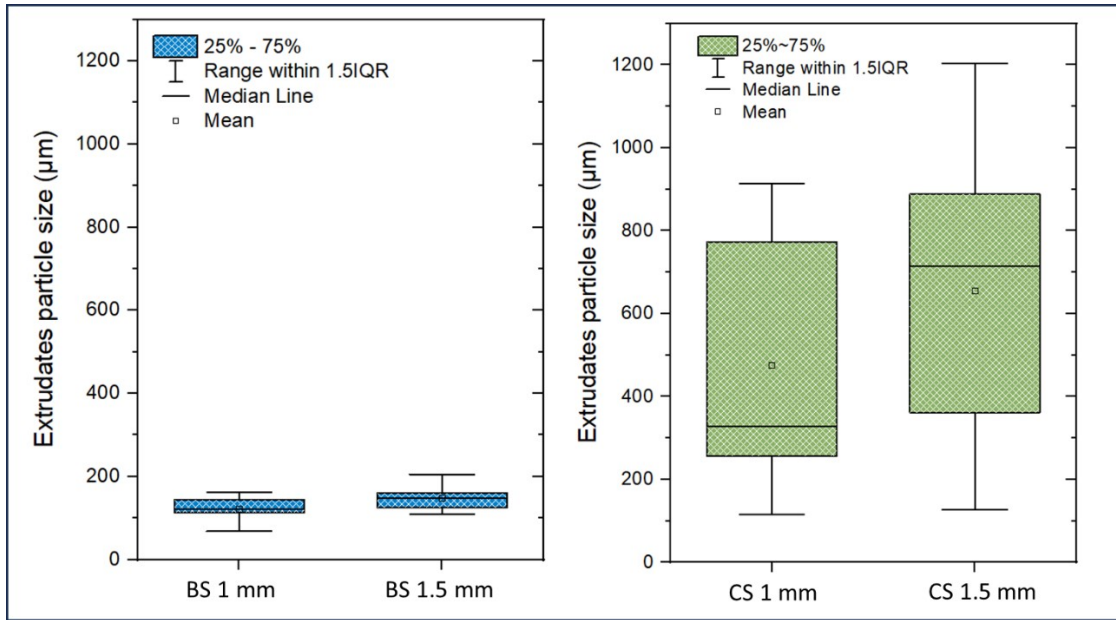


Figure 6.5 Distribution of the extrudate particle size (black spruce chips and corn stover).

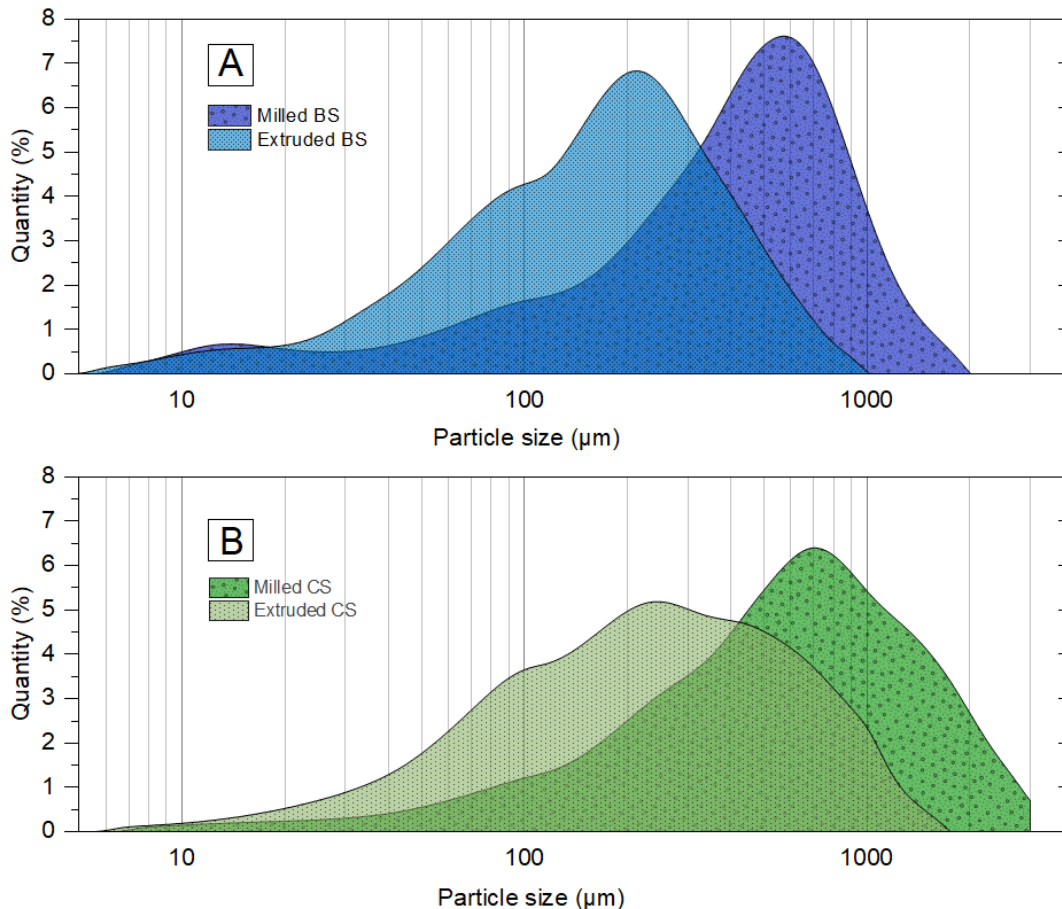


Figure 6.6 Comparison of the particle size distribution between the extrudates and milled raw biomasses: A) Black spruce chips (BS), and B) Corn stover (CS).

6.4.4 Statistical analysis

A design of experiments is used to model a phenomenon, process, procedure, or response reliably and robustly, based on a reduced number of trials. The benefit is that it saves time, energy, and money (Román-Ramírez & Marco, 2022). A design of experiments is generally used for one of three purposes: (i) comparison or characterization, (ii) screening, and (iii) optimization. A comparison or characterization design is used to confirm the importance of a parameter on the response, independently of their important parameters. Screening is used to identify which parameters have the highest influence on the response (NIST, 2024). Optimization is by far the most widespread of all, it is used to determine the optimal configuration(s) of parameters according to the desired level of response. In practice, optimization is often preceded by screening, which can also be a literature review validated by experimental data, such as in this study (Konan *et al.*, 2022b).

The objective of this study was to optimize the pretreatment conditions of lignocellulosic biomass to achieve the highest possible delignification percentage. Therefore, delignification was the main response. Tableau 6.6 reports the delignification percentages for each extrusion run. It ranges between 2.2% and 23.5% for S1 and from 1% to 25.3% for R1. These significant variations in delignification percentage justified the need for an optimization of the extrusion conditions. Tableau 6.6 also includes six center points per biomass (three center points for 1 mm residues and three for 1.5 mm residues). A center point refers to a point at the center of the experimental space, which is repeated multiple times independently under the same conditions to validate the reproducibility of the results. The highest standard deviation recorded for delignification percentages at center points was 1.2% (CS with 1 mm). This result suggests that the accuracy of the delignification data in the table is $\pm 1.2\%$, which is very good considering the complex situation analyzed. The best delignification achieved with BS was with BS 1 mm, extruded at 225 rpm, without sodium hydroxide, and at 75 °C. For CS, the best percentage was obtained with CS 1 mm, extruded at 300 rpm, without sodium hydroxide, and at 50 °C. So, the best conditions seem to be obtained with small particle sizes, high screw rotation speeds, low temperatures, and without NaOH. These results partially differ from our expectations, especially for the effect of sodium hydroxide. It was expected that its presence would help the delignification step of the biomass due to its ability to depolymerize lignin and break lignin-hemicellulose bonds (Augustina *et al.*, 2022; Jung *et al.*, 2018). The assumption was supported by the 2nd best results (22.3% for BS and 23.7% for CS), but not for the optimum results. The 2nd best results was obtained when the biomasses were extruded with a 15% w/w NaOH solution. However, these results could be explained by the fact that lignin can recondense or form a pseudo-lignin complex under harsh alkaline conditions and high temperatures (Yang *et al.*, 2021). Komatsu and Yokoyama (2021) also observed lignin recondensation above 130 °C, which is likely to occur during extrusion due to the shear forces locally increasing the thermal energy (viscous dissipation) in the biomass.

The results in Tableau 6.6 were used to determine the regression equations to model the delignification percentages of both biomass ($Y_1 = \text{BS}$ and $Y_2 = \text{CS}$) as a function of the parameters studied (A = screw rotation speed, B = temperature, C = NaOH concentration, and D = particle size). Equations (6) and (7) respectively model the delignification responses of black spruce chips (S1) and corn stover (R1) as:

Équation 6.6 - Regression equation of delignification percentage for black spruce

$$Y_1 = 12.09 + 1.77 * A - 1.04 * AC - 1.47 * AD - 2.24 * BC + 4.17 * BD + 2.14 * CD + 4.99 * C^2 + 0.5813 * ABC + 1.01 * ABD - 0.5725 * BCD + 2.38 * A^2C - 1.39 * A^2D - 1.2 * B^2D - 5.75 * C^2D + 0.585 * ABCD - 4.98 * A^2B^2 - 5.16 * A^2BD - 1.89 * A^2CD - 1.89 * A^2CD + 9.29 * A^2B^2D$$

Équation 6.7 - Regression equation of delignification percentage for corn stover

$$Y_2 = 11.51 + 4.62 * A + 1.57 * B - 2.41 * C + 1.94 * D - 2.01 * AB + 0.8169 * AC + 4.41 * CD - 1.75 * B^2 + 3.81 * C^2 + 1.12 * ABC - 2.37 * ABD - 1.33 * BCD - 3.38 * A^2B + 3.71 * A^2C - 6.71 * A^2D - 5.41 * AB^2 + 2.86 * B^2D - 2.9 * ABCD + 3.25 * A^2BD - 2.92 * A^2CD$$

For each model, an analysis of variance (ANOVA) was performed to evaluate its significance. [Tableau 6.7](#) summarizes the test results. Both models successfully passed the p -values significance test ($p < 0.05$). The lack of fit is a measure of how well a model fits the data. In both cases, the p -values of the lack of fit did not pass the significance test ($p > 0.05$ for BS and CS). This indicates that both models fit well their respective data. A lack of fit less than 0.05 would indicate that the model predictions are significantly different from the observations ([Huang & Ma, 2019](#)). To confirm the statistical tests, the delignification percentages predicted by the models were compared with the experimental delignification percentages ([Figure 6.7](#)). The predicted and experimental data fit well ($R^2 = 0.9865$ for the BS model and $R^2 = 0.9660$ for the CS model).

Tableau 6.6 Responses of the statistical analyses.

Run	Corn stover				Black spruce chips			
	Delign. (%)	Moisture (%)	Spec. surf. (cm ² /cm ³)	Particle size (µm)	Delign. (%)	Moisture (%)	Spec. surf. (cm ² /cm ³)	Particle size (µm)
1	14.6	29.4	208.0	739.3	15.0	29.6	845.3	151.7
2	17.9	29.8	228.2	1104.7	18.3	33.0	1495.6	72.9
3	8.9	25.8	281.7	902.7	11.0	35.0	981.0	121.5
4	16.4	7.2	1023.3	126.9	10.1	35.0	866.0	148.4
5	6.3	34.8	767.4	227.4	22.2	28.8	646.7	204.9
6	22.5	29.4	537.1	268.0	10.0	31.2	872.3	153.8
7	2.2	31.8	245.8	766.9	9.7	31.2	1569.1	68.2
8	13.8	5.4	1111.1	115.6	7.6	34.2	1030.9	121.9
9	8.2	29.6	231.9	772.2	0.9	31.4	809.4	152.5
10	12.7	28.4	341.8	441.2	13.6	23.6	870.9	148.8

Run	Corn stover				Black spruce chips			
	Delign. (%)	Moisture (%)	Spec. surf. (cm ² /cm ³)	Particle size (µm)	Delign. (%)	Moisture (%)	Spec. surf. (cm ² /cm ³)	Particle size (µm)
11	21.5	31.0	185.4	911.7	11.4	31.6	1145.7	108.1
12	7.7	32.0	229.5	888.5	11.4	35.0	938.5	127.9
13	23.7	23.8	723.3	257.4	13.2	31.6	1050.7	119.6
14	24.4	30.2	513.8	328.5	10.5	30.2	1059.3	112.8
15	13.2	32.4	322.7	589.1	8.5	27.8	1038.3	115.2
16	16.3	11.4	710.0	214.9	11.9	31.6	1012.9	125.8
17	15.2	9.2	1183.3	133.1	17.0	31.8	782.6	160.9
18	8.0	29.4	174.6	914.1	8.2	30.6	922.8	124.8
19	7.3	20.2	348.4	828.4	13.5	26.4	671.1	186.9
20	6.8	7.0	689.1	190.1	16.5	32.2	703.2	183.6
21	5.5	32.4	487.5	361.1	25.2	33.0	900.4	143.7
22	13.1	31.6	304.4	679.1	13.9	24.6	772.5	162.0
23	8.7	23.2	439.2	713.7	9.5	59.2	1010.5	117.1
24	14.0	21.8	657.7	326.5	16.0	32.0	976.7	126.9
25	4.5	19.0	626.1	197.1	10.4	29.0	763.6	157.1
26	14.6	29.4	266.4	734.9	13.1	29.6	775.3	159.8
27	21.0	30.8	187.5	1203.9	12.5	31.2	1113.6	109.3
28	4.1	30.2	324.2	665.7	6.8	32.6	755.2	163.0
29	19.1	27.8	652.7	230.9	12.2	31.6	1097.3	112.6
30	6.0	29.6	364.5	487.7	10.1	33.8	923.6	144.9
31	20.0	22.8	312.8	1040.5	20.37	34.4	1039.8	121.9
32	13.9	29.6	357.9	548.3	11.45	24.6	1246.9	92.8
33	7.2	17.0	498.9	308.7	13.43	32.4	965.0	128.4
34	11.8	30.6	179.6	1010.9	14.23	32.0	835.4	147.4

Tableau 6.7 Summary of the ANOVA analysis for BS and CS.

Source	Sum of squares	df	Mean square	F-value	p-value	Significance
Black spruce chips						
Model	679.35	19	35.76	53.87	< 0.0001	Significant
Residual	9.29	14	0.6637			
Lack of Fit	6.43	10	0.6426	0.8972	0.5977	Not significant
Pure Error	2.86	4	0.7162			
Cor Total	688.64	33				

Source	Sum of squares	df	Mean square	F-value	p-value	Significance
Corn stover						
Model	1206.48	20	60.32	18.49	< 0.0001	Significant
Residual	42.40	13	3.26			
Lack of Fit	38.03	9	4.23	3.87	0.1028	Not significant
Pure Error	4.37	4	1.09			
Cor Total	1248.88	33				

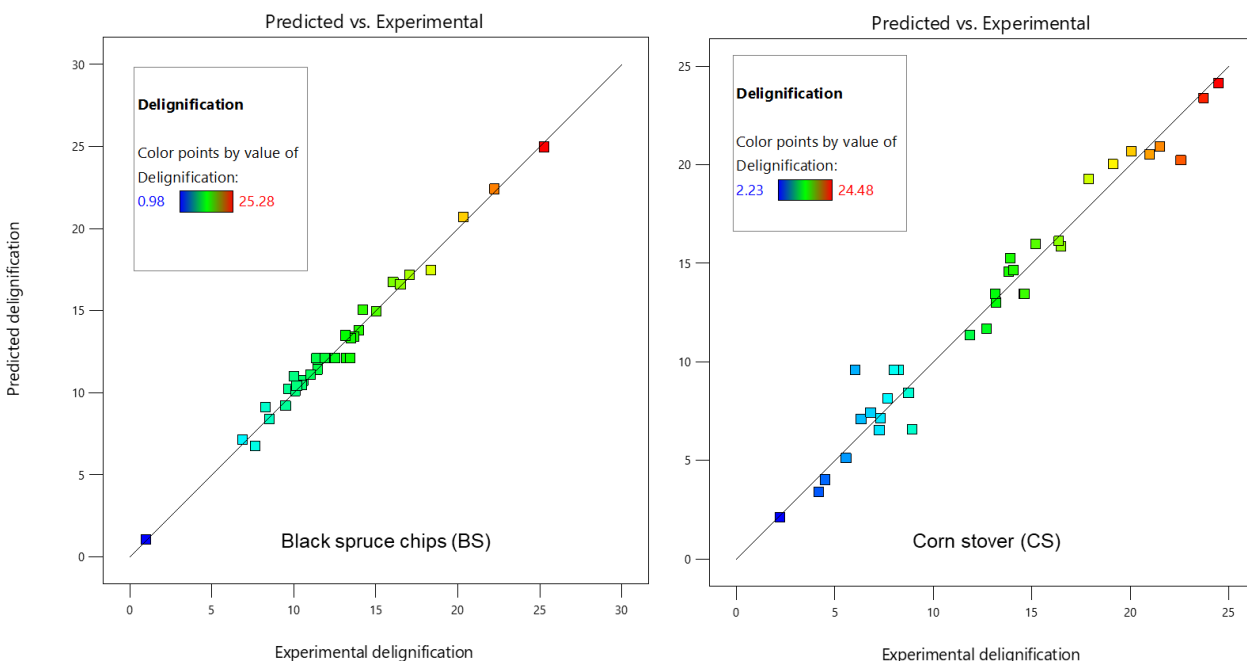


Figure 6.7 Model predictions as a function of the experimental delignification percentage.

6.4.5 Effect of the parameters on delignification percentage

Figure 6.8 shows the 2D and 3D response surfaces for the two best delignification conditions for BS and **Figure 6.9** the same results for the two best delignification conditions for CS. For BS, the space delimited by the highest delignification percentages (in red) is larger than that of CS. The boundary conditions of temperature and rotation speed have a very significant effect on the delignification percentages of BS, which is not the case for CS. The highest delignification percentages for BS are in the 50 – 90 °C and 200 - 300 rpm range. For CS, a concentration of higher delignification percentages is observed in smaller zones delimited by 60 – 95 °C and 290 - 300 rpm. On the 2D plots for both biomasses and conditions, the screw rotation speeds is the parameter with the highest influence on delignification percentages, at least more important than

the temperature. Below 190 rpm, the probability of obtaining delignification percentages higher than 20% becomes lower. However, in practice, higher speeds can lead to process instability, especially with biomass containing high lignin contents (above 25%).

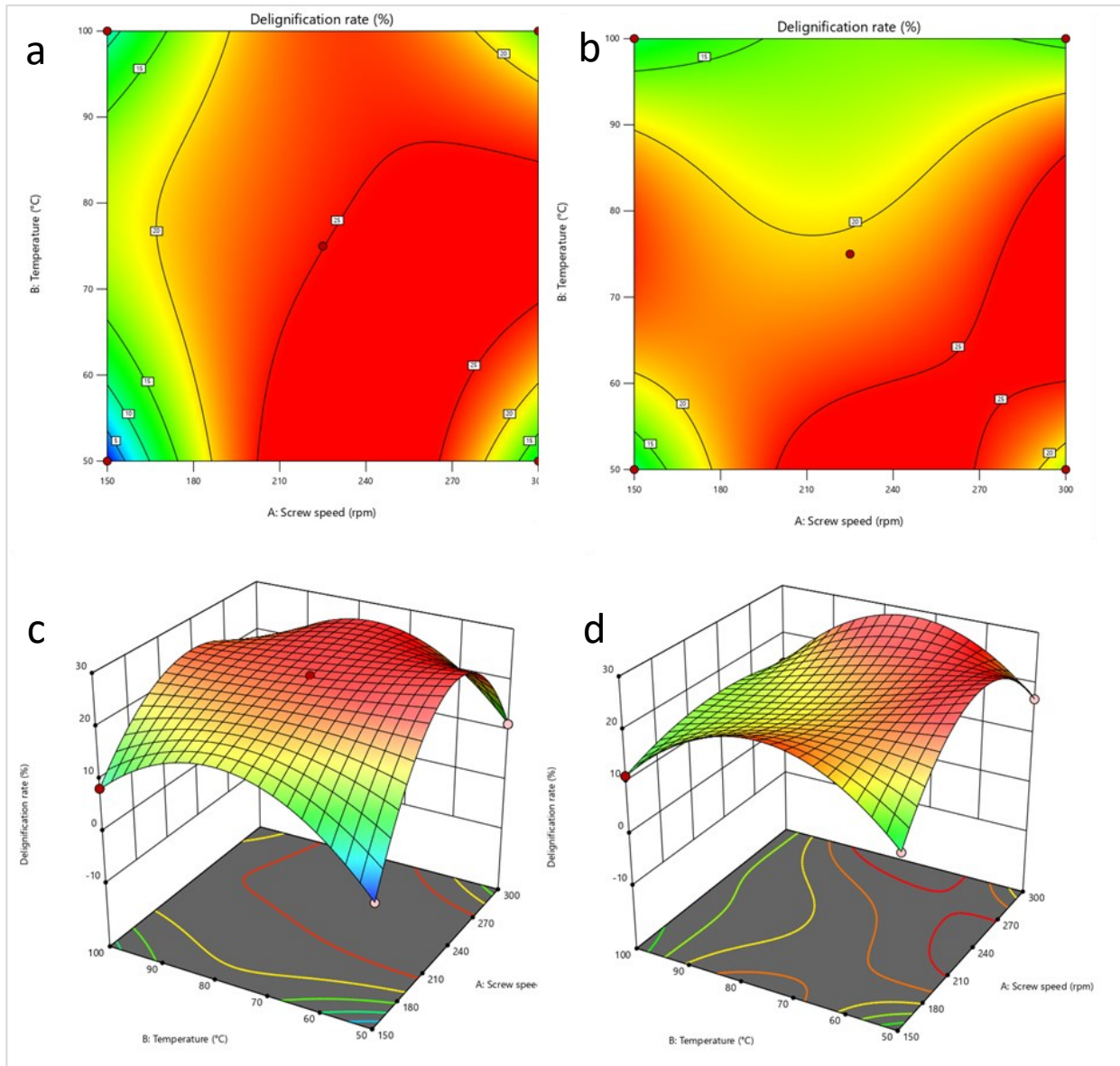


Figure 6.8 2D and 3D response surface of the optimum extrusion conditions for black spruce chips (a and c: 0% NaOH; b and d: 15% NaOH).

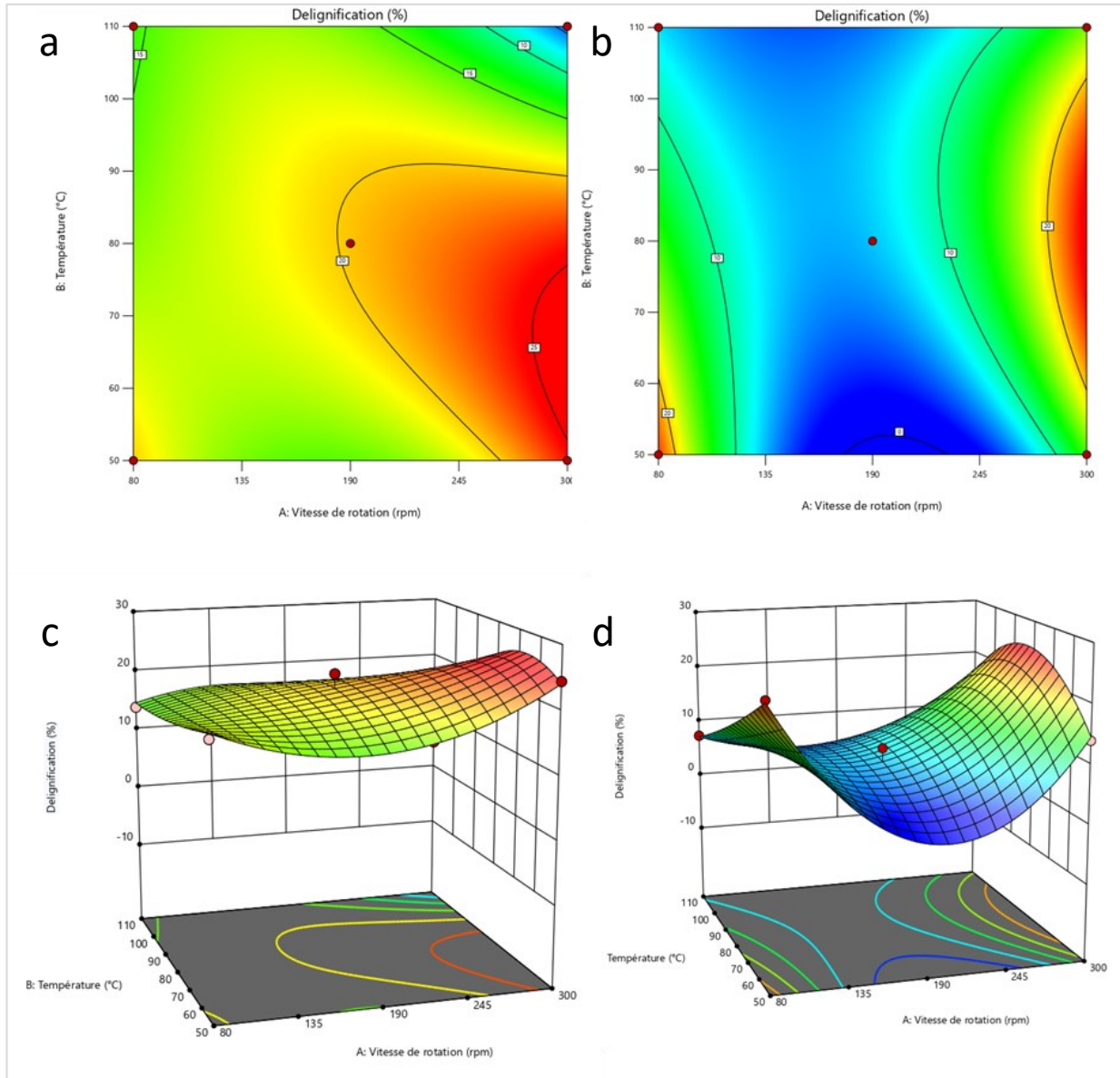


Figure 6.9 2D and 3D response surface of the optimum extrusion conditions for black spruce chips and corn stover (a and c: 0%NaOH; b and d: 15%NaOH).

6.4.6 Response optimization

Extrusion optimization consisted of finding the parameters that led to the best delignification percentages for each biomass. It was based on the analysis of the response surfaces with Design Expert 13. The optimization constraints were: (i) minimize NaOH concentration to reduce pretreatment costs and chemical usage, (ii) minimize raw biomass particle size to avoid extruding under unstable conditions and damaging the equipment over time, (iii) minimize rotation speed to avoid extruder instability and reduce specific mechanical energy, (iv) minimize extrusion

temperature to reduce costs and retain more biomass moisture during extrusion, and (v) ensure that the delignification percentage is above 20% as reported in the literature ([Calcio Gaudino et al., 2022b](#)).

Tableau 6.8 presents the relative importance of each constraint. The optimization was conducted numerically using the Y_1 and Y_2 equations (Équation 6.6 and Équation 6.7) and the Design Expert software integrated solver. With these constraints, the solutions were under the following conditions:

For Y_1 (28.9%): A = 233 rpm, B = 50 °C, C = 0%, and D = 1 mm.

For Y_2 (26.6%): A = 300 rpm, B = 65 °C, C = 0%, and D = 1 mm.

To verify the reliability of the optimization (model validation), the biomasses were extruded under these conditions. The experimental delignification percentage obtained for CS (Y_2) was 27.4%, which is only 0.8% higher than the predicted delignification. The particle size was 204.6 μm , and the specific surface was 597.9 cm^2/cm^3 . The central composite design for CS improved the delignification percentage by 22%, and the response surface method improved it by 5%. For BS, Y_1 was 22.5% compared to 28.9% (prediction), resulting in a difference of 6.5%. The extrudate took the form of a fine powder (55 μm), with a very high specific surface area (2402 cm^2/cm^3). Under these conditions, the spaces between the particles are very small. It leads to high electrostatic and van der Waals forces and limits good mixing between the extrudate and the sulfuric acid during the Klason lignin analysis, resulting in the formation of agglomerated particles ([Feng & Hays, 2003](#)). This explains the lower delignification percentage obtained (more than 5%). Nevertheless, both optimizations were successful as the delignification percentages obtained from both optimization models are significantly higher than without their use. Additionally, they involved very low temperatures (50 °C and 65 °C instead of 190 °C), while no chemicals were necessary, and the screw rotation speed was low to achieve stable extrusion conditions.

Tableau 6.8 Optimization constraints imposed of the models.

Criteria	Unit	Limit	Goal	Reason	Relative importance (1 to 5)
Particle size	mm	1 – 1.5	Minimize	Reduce the energy needed to mill the biomasses prior to extrusion	+++ (3)
Screw rotation speed	rpm	190 – 300	Minimize	Lower electrical energy consumption	+ (1)
NaOH concentration	w/w	0 – 15	Minimize	Reduce the use of chemical	++ (2)
Temperature	°C	50 – 90	Minimize	Reduce energy consumption	+ (1)
Delignification	% (w/w)	> 20	Maximize	Enhance the enzymatic digestibility of the biomasses	+++++ (5)

6.4.7 Effect of extrusion on the biomass structure

Scanning electron microscopy (SEM) images before and after treatment were used to visualize the effect of extrusion on the structural organization of the processed biomass (Figure 6.10). Images of the raw biomasses show a compact and ordered structure, with larger parts and small fragments of residues. Macrofibers are organized side by side. In some places, the pieces are crumbling, with peels (small plates) more or less detached from the rest of the structure. These peelings are the result of the milling blades used to reduce the particle sizes from 2-5 mm to 1 mm. In contrast, the images of the extruded biomasses present a different morphology. Extrusion has a defibrillation effect on the biomass. The microfibers in the extrudates are shortened and detached from each other. They are twisted, interlocked, and chaotically disorganized. Their appearance is much rougher and more irregular than the raw biomass. Nodules can be observed, which are actually microfibers agglomerated under the action of shear forces (kneading screw elements). The extrudates also become a micropore-filled structure, with the micropores being created by the spaces left between the macro- and microfibers. The result is a significant increase of the specific surface area of the BSE and CSE. These observations were confirmed by analyzing the specific surface areas of the extrudates. Raw CS (ground to 0.5 mm) and BS (ground to 0.5 mm) had specific surface areas of 398.9 cm²/cm³ and 511.5 cm²/cm³, respectively. On the other hand, their respective optimized extrudates had 1183.3 cm²/cm³ and 1569.1 cm²/cm³, respectively. This represents a four-times increase in the specific surface area of over the raw residues. According to Mosier *et al.* (2005), the disruption of the ordered structure of the raw biomass increases the specific surface area accessible to the enzymes in the microfibers, thus enhancing the enzymatic digestibility. Furthermore, extrusion does not change the elemental composition of the biomass in terms of carbon, hydrogen, nitrogen and sulfur. The CHNS analysis of the optimized BSE and CSE gave the same relative proportion compared to their respective raw biomass. However, comparing the FTIR spectra of the raw biomasses and their optimized

extrudates, it was clear that extrusion significantly changed the molecular organization of BS, but not so much for CS (Figure 6.11). The spectra show the absorption of infrared radiation by the biomass samples, with peaks corresponding to the vibrational frequencies of different functional groups. In the raw biomasses, the functional groups are ordered and engaged in several types of bonds. They have less freedom to vibrate or stretch, consequently displaying lower absorbance. For BSE, the peaks are clearly marked and distinguishable from one another. This indicates that the extrusion processing was able to de-structure the lignocellulose complex by efficiently breaking multiple bonds. Several key functional groups were affected (Tableau 6.9), but the most important were those at 1024, 2897, and 3335 cm^{-1} attributed respectively to C-O stretching in hemicellulose, H-C-H stretching in cellulose, and phenols ring vibration in lignin (Ahmed *et al.*, 2021; Goncalves *et al.*, 2021; Kurian *et al.*, 2015; Silvestre *et al.*, 2018). The 2358 cm^{-1} peak, it is present in the extrudates but absent from the spectra of the raw biomasses. This peak corresponds to carbon dioxide (CO_2) which might be formed from the thermal degradation (oxidation/combustion) of the biomass in the extruder, although the optimum extrusions were performed at low temperatures: 50 °C for BS and 65 °C for CS. This information confirms the hypothesis that higher temperatures can occur locally within the biomass during the extrusion step due to high shear forces (friction) in the confined space between the screws and the barrel.

GC/MS analysis of BSE and CSE was performed to detect the formation of non-desirable compounds in the extrudates, especially furfural and 5-hydroxymethylfurfural (HMF), but none of them was detected (Appendixes A and B). Furfural and HMF are pentoses (C5) and hexose (C6) derivatives usually generated from the dehydration of furan and pyran rings. Xylose, the main hemicellulose component, is the main source of furfural, while glucose, the monomer of cellulose, is the main source of HMF. Furfural and HMF usually appear under harsh chemical or thermal pretreatment conditions and are inhibitors of enzymatic activity (Koopman *et al.*, 2010). Although furfural and HMF have an important market value, when the pretreatment is related to bioethanol production (Mittal *et al.*, 2020; Yong *et al.*, 2022), their formation is not desired. Chemical and hydrothermal pretreatments, such as ionic liquid, deep eutectic solvent, steam explosion, and liquid hot water, are generally confronted with the problem of inhibitor formation (Behera *et al.*, 2014; Ilanidis *et al.*, 2021; Ko *et al.*, 2015). Acetic acid was detected in CSE. Although acetic acid has limited inhibitory effect on the activity of cellulases (Jing *et al.*, 2009; Ko *et al.*, 2015), depending on the concentration, it may affect the yeast's enzymatic activity during ethanol production (Ko *et al.*, 2015). For example, while investigating the effect of acetic acid on the growth of a strain of the most used ethanol-production yeast (*Saccharomyces cerevisiae*), Narendranath *et al.* (Narendranath *et al.*, 2001) reported a minimum inhibitory concentration (MIC)

of 0.6% w/v (100 mM) for acetic acid to affect the development of the yeast. Inhibitor formation is one of the primary concerns of lignocellulosic biomass pretreatment for second-generation bioethanol production. Many studies investigated and proposed innovative approaches to remove such compounds or to improve the ethanol yield. Kumar et al. (Kumar et al., 2020) presented an interesting overview of strategies and trending methods for inhibitors removal including biological methods, such as microbial electrochemical cells and recombinant *Escherichia coli*. Wimalasena et al. (Wimalasena et al., 2014), looking for an inhibitor-tolerant ethanol yeast strain. They screened 90 strains of *Saccharomyces spp.* and found *S. cerevisiae* strain, YPS 606, as a general tolerant strain to inhibitors. The ethanolic fermentation with *S. cerevisiae* strain, YPS 606, was not affected by the presence of inhibitors (10 mM acetic acid, 5 mM formic acid, 5 mM levulinic acid, 5 mM HMF, 5 mM furfural and 5 mM vanillin in combination). As for Khan et al. Khan et al. (2024), they proposed a different approach for ethanol yield enhancement: the dewaxing of the biomass before the pretreatment, combined with a post-pretreatment washing. This technique was used successfully with acid (sulfuric acid, 2.95 wt.%) and alkaline (sodium hydroxide, 2.17 M) pretreatments to convert tobacco residues into bioethanol. The sugar yield was improved by more than 23% when the biomass was dewaxed before the pretreatments compared to pretreatments without the dewaxing step. As for the ethanol production, the dewaxed alkali pretreated biomass improved the yield by 34% compared to the un-dewaxed alkali biomass. The drawback of this method is however the additional steps, energy and water consumption associated to this approach. To be viable, the economic profitability of the ethanol yield enhancement must outweigh the drawbacks.

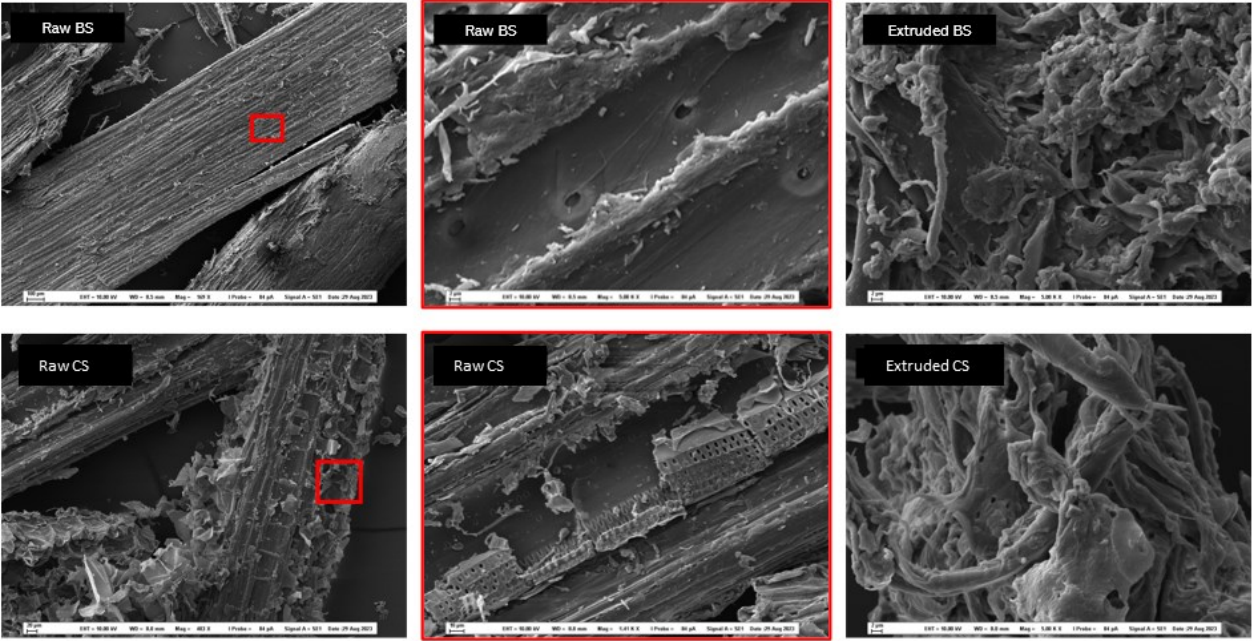


Figure 6.10 Scanning electron microscope images of black spruce chips (BS) and corn stover (CS) before and after extrusion.

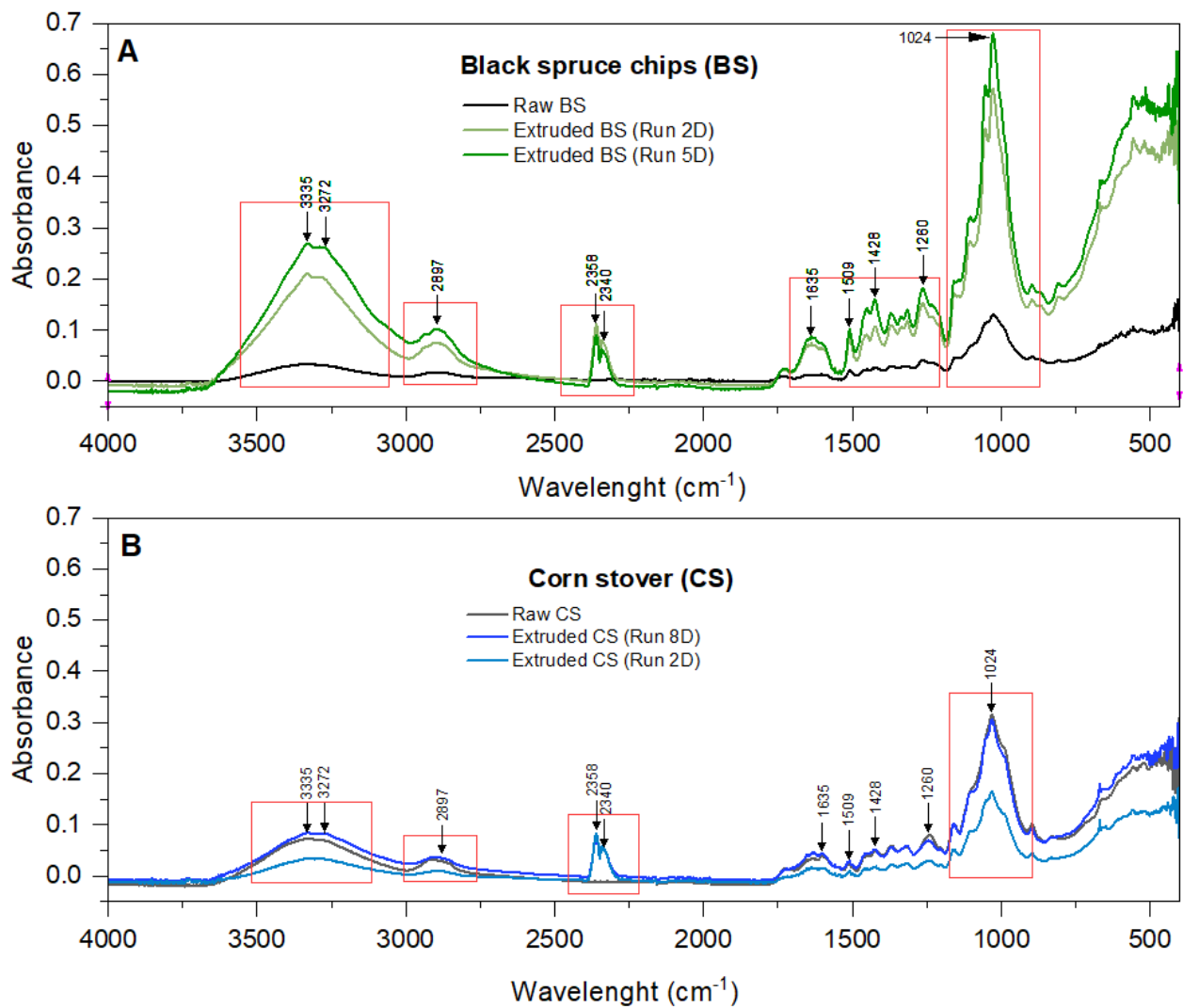


Figure 6.11 FTIR spectra of black spruce chips (A) and corn stover (B) before and after extrusion.

Tableau 6.9 Functional groups detected in the biomass samples by FTIR spectroscopy.

adapted from (Ahmed et al., 2021; Goncalves et al., 2021; Kurian et al., 2015; Silvestre et al., 2018).

Wavelength (cm ⁻¹)	Functional group
838	Aromatic C-H out of plane bending vibration
896	C-O, C=C, and C-C-O in hemicellulose
1024	C-O stretching in hemicellulose, C=C, C-C-O vibrational stretching
1260	Esters or ethers, C-O of guaïacyl rings in lignin
1428	Aromatic C-C stretching, deformation of C-H, CH ₂ scissoring in cellulose
1599	Aromatic skeletal vibration
1635	C=O stretching in lignin
2340- 2358	CO ₂ stretching
2897	Alkanes/primary amines or alkanes and acids/aliphatic H-C-H stretching cellulose

6.4.8 Energy consumption and pretreatment cost

Energy consumption and the associated costs of biomass pretreatment are of significant importance for large scale (commercial/industrial) production. Some pretreatments having high enzymatic hydrolysis rates are not suitable for industrial use due to their high costs. This is especially true for chemical pretreatments such as Organosolv, ionic liquid, and ozonolysis, where the cost of the chemicals remains high (Sidana & Yadav, 2022). In terms of mechanical pretreatment, the main challenge is energy consumption. One of the advantages of extrusion technology is its low electrical energy consumption. The mini-extruder (11 mm) used in this study had specifications of 16 A and 230 V. Under the optimized conditions of this study, the pretreatment flow rate was 1.5 g/min of biomass, resulting in an energy consumption of 40 kWh/kg of biomass. To this consumption must be added the biomass grinding step to reduce the chips or stover size to 1 mm before extrusion. The electrical specifications of the cutting mill (Pulverisette 15) used in this study were: 100-120 V/1~, 60 Hz, 1900 W, 3 Nm with 2.1 kW (drive). It took about 45 min to grind 1 kg of black spruce from 2 – 5 mm to 1 mm, and about 25 min to grind 1 kg of corn stover from 2 – 5 mm to 1 mm. The energy consumption was 1.43 kWh/kg of ground black spruce and 0.8 kWh of ground corn stover. In the province of Quebec (Canada), the energy consumption cost is 6.704¢/kWh for the first 40 kWh of the day and 10.342¢/kWh for each kWh after. Pretreating 1 kg of black spruce with the 11 mm mini-extruder would theoretically cost 1.97 \$ USD (2.83 \$ CAD), while pretreating 1 kg of corn stover would cost 1.92 \$ USD (2.76 \$ CAD)

(HydroQuébec, 2023). Energy savings could be even better with larger extruders able to process several tons of biomass. In the province of Quebec (Canada), pretreating 1 kg of biomass with the 11 mm mini-extruder would theoretically cost 1.92 USD at a rate of 0.06509 CAD/kWh for the first 40 kWh (HydroQuébec, 2023). Energy savings could be even better with larger extruders able of processing several tons of biomass. For example, Hjorth *et al.* (2011) used a large twin-screw extruder (Model MSZ B55e; Lehmann Maschinenbau GmbH, Germany) with an energy consumption of only 4 to 10 kWh/ton of biomass. Additionally, they included 150 kWh/ton of biomass for heating the extruder from 20 °C to 150 °C, resulting in a total consumption of 160 kWh/ton of biomass to start the extrusion, and similar values when the desired temperature is reached. By optimizing the extrusion process using a design of experiment, the extrusion temperature can be significantly reduced, as reported in this study for BS (50 °C) and CS (65 °C). Nevertheless, calculations must be done for each specific equipment, biomass, and conditions.

6.4.9 Perspective for future work

The results discussed above highlighted important facts about BS and CS extrusion. They showed that extrudates with very small particle sizes and large specific surface areas can be obtained from raw CS and BS larger than 1 mm in size. This is achieved through the strong effect of the extruder screws on the morphology of the biomasses, which is highly desirable for enzymatic activity (larger specific surface area). Additionally, over 20% delignification was achieved without the use of chemicals (NaOH) and low extrusion temperatures. These conditions suggested that the energy consumption for extrusion and heating can be significantly reduced on a larger scale. Furthermore, extrusion is a technology generating no enzyme inhibitors such as furfural or 5-hydroxymethylfurfural, as confirmed by GC/MS analyses. Extrusion does not require post-washing operations prior to enzymatic hydrolysis for the recovery of sugars (glucose, xylose, etc.) (Duque *et al.*, 2017). Considering the elemental composition of the biomasses studied, they both have high carbon content (47.6% for BS and 43.9% for CS) and CS as a high C/N (carbon/nitrogen) ratio of 81:1. These elemental compositions were not changed by the extrusion process. All these characteristics make BSE and CSE excellent candidates for biodelignification by white rot fungi (WRF). White rot fungi can effectively delignify lignocellulosic biomasses under favorable conditions, including a nitrogen/carbon ratio of 50:1 - 122:1, temperature range of 25 °C – 40 °C, particle size range of mm to µm, large specific surface area, agitation, pH range of 4 - 9, and low water activity (Montoya *et al.*, 2021; Sala *et al.*, 2019; V, 2018). The biodelignification is achieved through an enzyme system mainly consisting of three lignolytic enzymes: lignin peroxidase, manganese peroxidase, and laccase, which are known to break carbon-carbon

bonds to mineralize lignin. Depending on the strain and enzyme system, part of the holocellulose (cellulose and hemicellulose) may be consumed during fermentation (Millati *et al.*, 2011). However, the recovery of the enzymes produced, and the efficiency of the pretreatment would offset the loss of this portion. Solid-state fermentation is known for its energy efficiency and strategic advantages, such as low volume and water usage, lower contamination risk, concentration of fermentation products, minimal use of chemicals, and low operating costs (Machado de Castro *et al.*, 2018). Therefore, the proposed pretreatment involves coupling extrusion and biodelignification technology in solid fermentation with fungal strains. To the best of our knowledge, this approach has never been attempted before. The extrusion process would enable a minimum preliminary delignification of 20% while reducing the rigidity of the carbohydrate-lignin complex structure. This extrusion action would enhance fungal activity during biodelignification to ensure complete biomass delignification. The development of this new pretreatment approach should be conducted in two stages: (i) evaluate delignification percentage in a laboratory model, and (ii) conduct a technical-economic analysis. The extrusion-biodelignification pretreatment approach could be integrated into the production of second-generation biofuels, with the simultaneous production of commercial ligninolytic enzymes (Manganese peroxidase, lignin peroxidase and laccase) and the manufacture of biobased composite materials. This is the subject of a forthcoming study.

6.4.10 Conclusion

The analysis and optimization of black spruce chips (BS) and corn stover (CS), through an experimental design, increased their delignification percentage from 2.3% to 27.4% and from 1% to 25.3%, respectively. The delignification percentages were reproducible with a low standard deviation of 1.2% maximum. The two mathematical models developed for BS and CS were strong (p -value < 0.0001) to successfully predict the maximum delignification possible with an error margin of 0.8% for CS and less than 3% (theoretically) for BS. The analysis of extrudate characteristics showed that extrusion reduced particle size from 1000 μm to 55 μm for BS and from 1000 μm to 204 μm for CS. It multiplied by more than 4 times BS specific surface area (512 to 2402 cm^2/cm^3) and increased CS specific surface area by 200 cm^2/cm^3 (399 to 597 cm^2/cm^3). Extrusion also created desirable roughness on the particles, generated no inhibitor and was able to profoundly de-structure the lignocellulosic complex. These results led to the proposition of the development of a new approach to lignocellulosic biomass pretreatment. The novel approach involves combining extrusion and biodelignification in solid fermentation. The outcomes expected from the approach are: (i) a low-cost pretreatment, (ii) complete delignification of biomass from

the pretreatment stage, (iii) a significant increase in enzymatic digestibility, and (iv) a substantial improvement in the profitability of lignocellulosic biomass valorization.

6.4.11 Acknowledgement

This work was supported by Institut National de la Recherche Scientifique (INRS) and the Natural Sciences and Engineering Research Council of Canada (NSERC).

6.4.1 Supplementary material

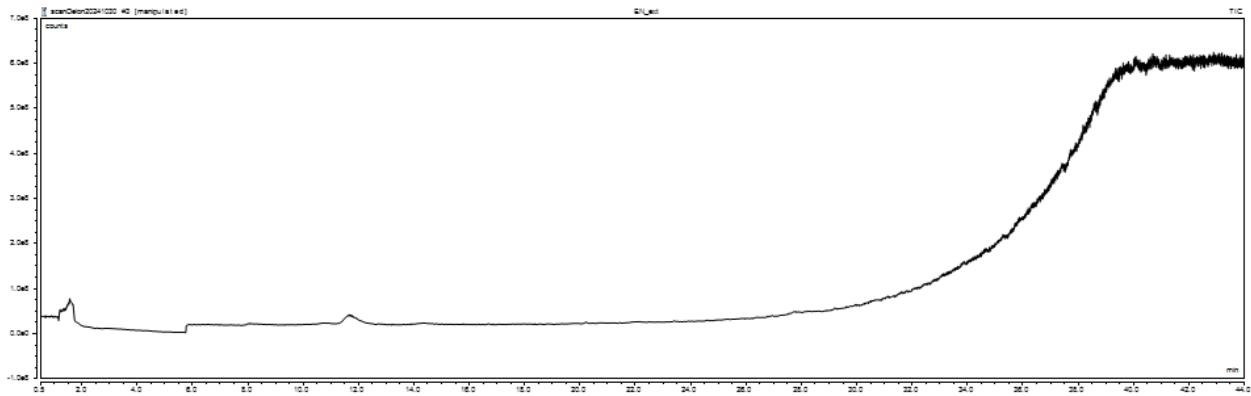
Supplementary materials 1. Parameter screening.

N°	Parameters	Justification	References
Extruder			
1	Screw type	Modulated Screw (MoS) gives more flexibility than One-Piece Screw (OPS). Their screw element can be rearranged according to the desire screw configuration. The Process 11 extruder used in this study is a MoS.	(Gatt <i>et al.</i> , 2018; Kelly <i>et al.</i> , 2006; Konan <i>et al.</i> , 2022a; Senturk-Ozer <i>et al.</i> , 2011)
		Intermeshing co-rotating extruders provide better mixing than counter-rotative extruders. The Process 11 extruder used in this study has co-rotative screws.	(Gupta, 2004; Konan <i>et al.</i> , 2022a)
2	Screw geometry	Cylindrical screws are common for MoS. They are relatively less difficult to design and manufacture compared for example to conical screws. This type of shape gives additional freedom in the screw configuration because the screw modules (elements) have the same socket diameter. So it is possible to arrange them in several different ways to obtain different layouts. The Process 11 extruder used in this study has two cylindrical screws.	(Gu <i>et al.</i> , 2019; Konan <i>et al.</i> , 2022a; Liu <i>et al.</i> , 2013; Vandebossche <i>et al.</i> , 2014; Zheng <i>et al.</i> , 2016)
3	Screw elements	All the screw elements for biomass extrusion were used (forward screw element (F), transport screw element (T), and mixing screw element (M)) except reverse screw element (R) to avoid excessive back pressure in the barrel.	(Konan <i>et al.</i> , 2022a)
4	Shaft configuration	Screw configuration is crucial in biomass extrusion. It has been reported to play a role in biomass pretreatment and influence SME, torque, pressure, inner temperature, and biomass residence time. The typical screw configuration for biomass extrusion is F-T-M-R-M-R-M-T given by Gatt <i>et al.</i> (2018). However, the R elements were replaced by T elements as suggested in (Konan <i>et al.</i> , 2022a) to reduce the back pressure building in the Process 11 extruder used in this study.	(Duque <i>et al.</i> , 2014; Gatt <i>et al.</i> , 2018; Kelly <i>et al.</i> , 2006; Konan <i>et al.</i> , 2022a; Wahid <i>et al.</i> , 2015)
5	Screw diameter	The Process 11 extruder used in this study is a 11 mm laboratory scale extruder with all the main	(Konan <i>et al.</i> , 2022a)

N°	Parameters	Justification	References
	and L/D ratio	characteristics of pilot-scale extruders (16 mm, 18 mm and 25 mm). The length to diameter ratio is 40.	
6	Screw speed	Since the early stage of extrusion as a pretreatment of lignocellulosic biomass, screw speed has been considered as an important parameter. It influences the shear forces, the biomass residence time, the torque, the internal biomass temperature, etc. Screw speed for most biomass extrusion ranges between 30 – 400 rpm.	(Duque <i>et al.</i> , 2017; Han <i>et al.</i> , 2020; Konan <i>et al.</i> , 2022a; Kuster Moro <i>et al.</i> , 2017; Negro <i>et al.</i> , 2015)
7	Die size and shape	The extruder was used without a die. The biomass extrusions was impossible to run with a die because of frequent jamming of the screw during the preliminary trials.	
8	Temperature	Temperature is one of the most important extrusion parameters. Lignocellulosic biomass extrusion usually ranges between 50°C and 200°C.	(Gu <i>et al.</i> , 2019; Karunanithy <i>et al.</i> , 2012a; Konan <i>et al.</i> , 2022a; Merci <i>et al.</i> , 2015)
9	Pressure	Pressure is an output parameter. It was used to assess the boundary limits during the preliminary trials.	(Konan <i>et al.</i> , 2022a)
10	Torque	Torque is an output parameter. It was used to assess the boundary limits during the preliminary trials.	(Konan <i>et al.</i> , 2022a)
Biomass			
11	Biomass type	Corn stover and black spruce chips were used in this study for two main reason: 1. Corn in the primary crop in Quebec province (Canada) and black spruce one of the main wood species in Quebec forest. Both biomasses generate high lignocellulosic residues which are still underexploited. 2. Corn stovers are agricultural residues and black spruce chips are forest residues. Both agricultural and forest residues have different biomass composition and rheological behavior in extrusion.	(WSP, 2021b)
12	Particles size	Biomass particle size is an important parameter. It has an influence on the rheological properties of the biomass in the extruder barrel. Particle size must be suitable for the extruder for the screws to have maximal impact of the particles via shear forces. The preliminary trials showed that biomass particle size over 1.5 mm was too big for the Process 11 extruder, while particle size under 1 mm was too fine to be properly extruded.	(Chundawat <i>et al.</i> , 2007; Karunanithy & Muthukumarappan, 2011b; Kim <i>et al.</i> , 2002; Konan <i>et al.</i> , 2022a; Yang <i>et al.</i> , 2008)
Additive			
13	Additive type	Sodium hydroxide was used as an additives in this study for future scaling up purposes. Compared to most over alternative, such as organic or acid solvent, NaOH is more accessible, less costly, and recoverable if required, as well as being effective to solubilize lignin.	(Choi & Oh, 2012b; Duque <i>et al.</i> , 2014; Konan <i>et al.</i> , 2022a; Kuster Moro <i>et al.</i> , 2017; Montiel <i>et al.</i> , 2016; Zhang <i>et al.</i> , 2012c)

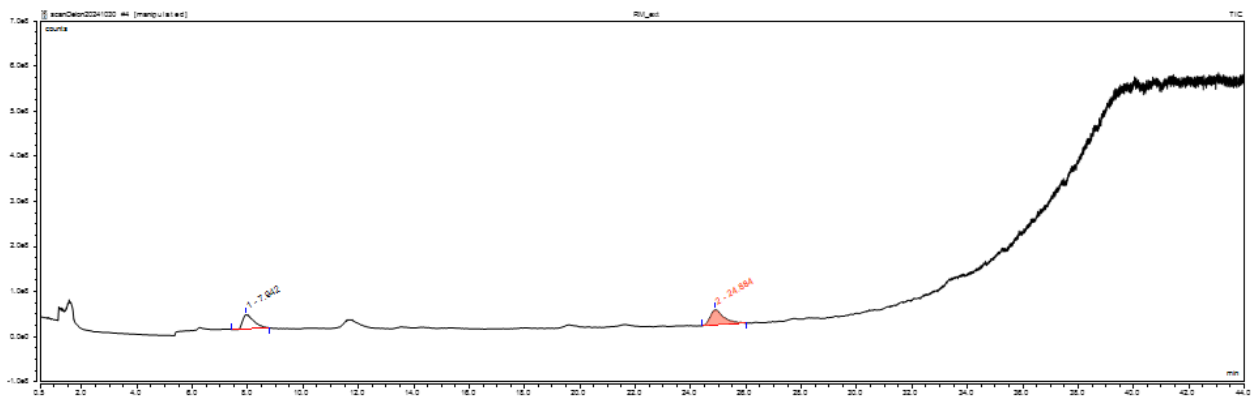
6.4.2 Appendixes

Appendix A. Gas chromatography/mass spectrometry (GC/MS) results of black spruce extrudate.



Peak No.	Ret. Time min	1st Hit SI	Library Compound	Area counts*min	CAS Number
TIC	TIC	TIC	TIC	TIC	TIC
1	-	-	-	-	-

Appendix B. Gas chromatography/mass spectrometry (GC/MS) results of corn stover extrudate.



Peak No.	Ret. Time min	1st Hit SI	Library Compound	Area counts*min	CAS Number
TIC	TIC	TIC	TIC	TIC	TIC
1	7.94	948	Acetic acid	14845990.4	64-19-7
2	24.88	738	Benzofuran, 2,3-dihydro-	19141586.9	496-16-2

7 CINQUIÈME ARTICLE

Extrusion-Biodelignification Approach for Biomass Pretreatment

Approche Extrusion-Biodelignification pour le prétraitement des biomasses

Delon Konan ¹, Adama Ndao ¹, Ekoun Koffi ², Saïd Elkoun ³, Mathieu Robert ³, Denis Rodrigue ⁴, and Kokou Adjallé ^{1,*}

1. Laboratoire de Biotechnologies Environnementales, Institut National de la Recherche Scientifique (INRS), 2605, boulevard du Parc-Technologique, G1P 4S5, Québec (Québec), Canada.

2. Département de génie chimique, Université Laval, 1065 Avenue de la Médecine, G1V0A6, Québec (Québec), Canada.

3. Center for Innovation in Technological Ecodesign (CITE), University of Sherbrooke, Sherbrooke, QC, J1K 2R1, Canada

4. Département de génie mécanique et énergétique, Institut National Polytechnique Félix Houphouët Boigny (INPHB), Yamoussoukro, Côte d'Ivoire.

5. Département de génie mécanique, Université de Sherbrooke, 2500, boulevard de l'Université, Sherbrooke (Québec) J1K 2R1.

*Correspondence: kokou.adjalle@inrs.ca

Waste, 2025, Volume 3, Issue 3, 21.

Received: 30 April 2025 / Revised: 13 June 2025 / Accepted: 17 June 2025 / Published: 26 June 2025.

DOI : <https://doi.org/10.3390/waste3030021>

Contribution des auteurs:

Conceptualization, Writing - Original Draft: Delon Konan; Writing - Review & Editing: Adama Ndao, Ekoun Koffi, Denis Rodrigue, Saïd Elkoun, Mathieu Robert, Kokou Adjallé; Funding Acquisition, Supervision: Kokou Adjallé.

7.1 Abstract

This work presents a new approach for lignocellulosic biomass pretreatment. The process is a sequential combination of extrusion (Ex) and semi solid fermentation (SSF). To assess the Ex-SSF pretreatment efficiency, black spruce chips (wood residues) and corn stover (crop residues) were subjected to the process. The negative controls were the pretreatment of both residues with SSF alone without extrusion. Lignin peroxidase was the main ligninolytic enzyme contributing to the delignification in the negative controls. High lignin peroxide (LiP) activities were recorded for raw black spruce (53.7 ± 2.7 U/l) and corn stover (16.4 ± 0.8 U/l) compared to the Ex-SSF pretreated biomasses where the highest LiP activity recorded was 6.0 ± 0.3 U/l (corn residues). However, with the negative controls, only a maximum of 17% delignification was achieved for both biomasses. As for the Ex-SSF process, the pretreatments were preceded by the optimization of the extrusion (Ex) step and the semi solid fermentation (SSF) step via experimental designs. The Ex-SSF pretreatments led to interesting results and offered significant cost-effective advantages compared to existing pretreatments. Biomass delignification reached 59.1% and 65.4% for black spruce and corn stover, respectively. For the analyses performed, it was found that manganese peroxidase (MnP) was the main contributor for delignification during the SSF step. MnP activity was up to 13.8 U/l ± 0.7 for Ex-SSF pretreated black spruce, and 32.0 ± 1.6 U/l for Ex-SSF pretreated corn stover, while the maximum MnP recorded in the negative controls was 1.4 ± 0.1 U/l. Ex-SSF pretreatment was also found to increase the cellulose crystallinity index (CrI) by 13% for black spruce and 4% for corn stover. But enzymatic digestibility of the Ex-SSF pretreated biomasses, with 0.25 ml/g of enzyme led to 7.6 mg/l sugar recovery for black spruce, which is 2.3 times the raw biomass yield. The Ex-SSF pretreated corn stover led to 17.0 mg/l sugar recovery, which is a 44% improvement of sugar concentration compared to raw corn stover. But increasing the enzyme content from 0.25 ml/g to 0.50 mg/l and 0.75 mg/l generated lower hydrolysis efficiency (the sugar recovery decreased). Finally, the study presents the cost-effective advantages of the Ex-SSF technology.

Keywords: Bidelignification; *Phanerochaete chrysosporium*; biomass pretreatment; fungi; extrusion; solid fermentation.

Lien entre l'article ou les articles précédents et le suivant :

L'article précédent (article 4) a démontré : (i) l'importance et l'efficacité de l'optimisation des paramètres d'extrusion et (ii) les caractéristiques intéressantes des extrudats pour la biodégradation. Dans le présent article, les biomasses prétraitées et optimisées à l'extrusion sont soumises à la biodégradation (objectif 5), puis à l'hydrolyse enzymatique (objectif 6).

7.2 Introduction

Automotive and aviation industries are trying to reinvent themselves thanks to new decarbonized energy perspectives. Promising options are available today, but they have yet to be fully developed. For a long time, electric cars and their superpowered batteries have been gradually developed. Today, electric vehicles (EV) have the same, and sometimes even better autonomy, than a full tank of gasoline of conventional vehicles. EV production has surged in recent years since all the major automakers are now offering EV models. Some have made it their niche market with trucks, sport utility vehicle (SUV) or electric sports cars. This is why the demand for EV is constantly growing (IEA, 2024). Nevertheless, subsidies, discounts, promotions, payment by instalment, loans and other forms of incentive are all part of the EV boom. At the same time, the cost of petrol at the pump is still increasing, often by several tens of cents per liter within a few days. The reasons include geopolitical crises affecting both fuel transport costs and financial markets, resulting in excessively high costs at the pump (Zhao *et al.*, 2023). So the modern society needs a paradigm shift in energy consumption. The aim is both to reduce energy consumption and to find decarbonized, economically viable alternatives. A sustainable lifestyle without burdening ecosystems through the indiscriminate extraction of fossil fuels would be a good step forward. However, electric batteries remain a major environmental problem, both in terms of their production (mining of the rare-earth elements) and their end-of-life (recycling) (Das *et al.*, 2024; Råde & Andersson, 2001). Fortunately, a new generation of batteries with bio-sourced electrodes is under development. Another point is that the most realistic forecasts for the future predict a mix of several energies cohabiting with a preponderance towards renewable energy, rather than a sudden and definitive end to the use of fossil fuels (Hassan *et al.*, 2024). But the race for electrification of transport has somewhat blurred the importance of biofuels, which are vital to the energy transition.

In 2024, about 1.475 billion cars worldwide with 4 or more wheels were present on the road, with the following order: 543 million in Asia, 413 million in Europe and 358 million in North America. Of all these vehicles, only 19% were electric; i.e. around 280 million vehicles, and they are

concentrated in wealthy countries (Company, 2024). This means that 81% of all cars are combustion-powered by mostly fossil fuels or renewable fuels. The advantage of biofuels is that they can be used by internal combustion vehicles without any mechanical modification to the engine below. An example is a maximum of 10% bioethanol in the blend (E10) (Abdulkadir *et al.*, 2024). But in the 10-20% range, only a modification of the engine or fuel system is required. This places biofuels, and bioethanol in particular, in a very good position.

Bioethanol production is not a new concept. The principles are known for many decades and the basic idea is the ethanolic fermentation of simple sugars such as glucose. But different sources of glucose must be found and available. The first bioethanol developments considered sources such as sugarcane, beet and corn. Then, the biorefinery industry took a major step forward with the use of “energy crops”: the first-generation biorefinery (Jain & Kumar, 2024), which has been successful to this day.

As over 8 billion people are on the planet, the use of crops for energy production rather than for human consumption poses a problem. Most of these energy crops are cereals, which are the primary source of food for many people. According to the United Nations, 733 million people faced hunger in 2023, this is equivalent to one in eleven people globally (WHO, 2024). Instead of using energy crops, their residues combined with forestry residues can be used as valuable alternative sources of sugars since lignocellulosic residues are made up of lignin (5 - 40%), cellulose (20 - 50%) and hemicellulose (5 - 35%). Cellulose is a glucose polymer based on a glucose chain, while hemicellulose is mainly a xylose polymer and lignin is an aromatic polymer of p-coumaryl, coniferyl and sinapyl alcohols.

To use agricultural and forestry residues, removing lignin to access cellulose and hemicellulose is mandatory. This step is referred to as the pretreatment. However, lignocellulose is highly recalcitrant to pretreatment as lignin is the main obstacle. Several pretreatments have been proposed, but most of them are either not economical (too expensive) or not efficient (low delignification level) depending on the raw biomass selected.

So the main objective for this work is to propose a novel approach for lignocellulosic biomass pretreatment to improve the enzymatic digestibility and the profitability of the pretreatment. In particular, this approach is based on extrusion and biodelignification (semi solid fermentation) being sequentially performed.

7.3 Materials and methods

7.3.1 Raw biomass

Two lignocellulosic residues were used in this study. First, black spruce chips (BS) were supplied by Savard et Fils sawmill (Quebec, Canada), while the second was corn stover (CS) provided by Agrosphere Inc (Quebec, Canada). CS was a mixture of stalks, cobs and leaves. The residues had an initial particle size between 2 and 5 mm as received. They were then ground to 1 mm particle size according to 6.3.1 with a Pulverisette 15 (Frisch, Germany). Their elemental composition in terms of carbon, nitrogen, hydrogen and sulfur was analyzed using a Flash 2000 CHNS/O analyzer (Thermo Scientific, USA). Their relative proportions of cellulose, hemicellulose, lignin, extractives and ashes were determined as described in 6.3.1.

7.3.2 Extrusion

The extrusion step was carried out using a Process 11 extruder (Thermo Scientific, USA) with the specifications presented in Tableau 7.1. BS and CS were extruded under their respective optimized delignification conditions as reported in a previous study 6.4.6. The conditions for BS were 50 °C, 233 rpm (screw speed) and a biomass/water ratio of 1:1 w/w. For CS, the conditions were 65 °C, 300 rpm and 1:1 w/w biomass/water ratio.

Tableau 7.1 Process 11 extruder specifications.

Parameter	Setup
Extruder type	Twin-screw
Screw type	Fully segmented, co-rotating
Screw diameter	11 mm
Max speed	1000 rpm
Torque per shaft	6 Nm
Max temperature	350 °C
Barrel zone	7 x 5 L/D electrical heated
Length (L)	82 cm
Barrel Length L/D	40
Die	3 mm die*
Output	20 g to 2.5 kg/h

**All extrusion in this study was conducted without the die (it was removed to avoid clogging and excessive pressure in the barrel).*

7.3.3 Substrate for semi solid fermentations

The extrudates (residues obtained following the extrusion step) were used directly as substrates for the semi solid fermentation (SSF). As for the negative control, raw black spruce and raw corn stover were used for SSF without extrusion.

7.3.4 Fungal strains, inoculum and maintenance

The white rot fungus strain *Phanerochaete chrysosporium* A-381 (ATCC 48746) was used as a biodelignification (SSF) agent for its ability to synthesize a ligninolytic enzyme system able of uncoupling lignin from the lignocellulosic complex. The strain was grown under sterile conditions on solid culture medium in petri dishes (100 x 15 mm polycarbonate) for 3 days at 35 °C. The culture medium was BD 271210 composed of yeast extract (3 g), malt extract (3 g), dextrose (10 g), peptone (5 g), agar (20 g) and deionized water (1000 ml). The mycelium was harvested under sterile conditions by gently scraping the surface of the solid medium from the petri dishes using a glass rod. The harvested mycelium was used to inoculate 50 ml of a liquid culture medium (BD 271210 without agar) contained in a 250 ml Erlenmeyer flask. This medium was placed in a shaker incubator (INFORS HT Multitron Standard, INFORS, Switzerland) at 180 rpm and 35 °C for 96 h. The resulting broth was used as inoculum for both the flask fermentations (250 ml) and the 5 L fermentations.

7.3.5 Flask fermentations (250 ml)

Fermentations in flask were conducted to assess the growth conditions of the *Phanerochaete chrysosporium* strain on BS extrudates (BSE) and CS extrudate (CSE) prior to 5 L fermentations. The fermentations were carried out in 250 ml Erlenmeyer flasks. An experimental plan was design for each biomass as reported in Tableau 7.2 and Tableau 7.3. The experimental space was determined by preliminary trials and errors. The parameters selected were based on previous literature review: temperature (°C), inoculum content (ml/g biomass) and nitrogen concentration (w/w biomass) (5.8.4). The nitrogen source was ammonium chloride (NH₄Cl) and the biomass:additive ratio was set at 1:3.

The biomasses were thoroughly mixed with the additive before being placed in the autoclave. For each run, 5.0 ± 0.5 g of the autoclaved biomass were introduced into a 250 ml flask with the corresponding amount of additive and inoculum, and gently mixed with a glass rod. The flask was then incubated at the selected temperature. The experimental plan was a randomized central composite design (CCD) using the software Design Expert 13. A total 30 runs were carried out:

15 for BS and 15 for CS. During the fermentations, oxygen was supplied by free diffusion of air into the Erlenmeyer flasks through a foam; the role of the foam also being to prevent contamination. The pH was not monitored.

Tableau 7.2 Experimental space selected for the study.

Parameter	Black spruce			Corn stover		
	T	Inoculum	[NH ₄ Cl]	T	Inoculum	[NH ₄ Cl]
Unit	°C	ml/g	w/w (%)	°C	ml/g	w/w (%)
- alpha	26.6	0.16	0	26.6	0.16	0
Low level (- 1)	30	0.5	2	30	0.5	2
High level (+1)	40	1.5	8	40	1.5	8
+ alpha	43.4	1.84	10	43.4	1.84	10

Tableau 7.3 Experimental conditions for corn stover and black spruce.

Std	Run	Space type	Temperature (°C)	Inoculum (ml/g)	[NH ₄ Cl] w/w (%)
2	1	Factorial	40	0.5	0.5
3	2	Factorial	30	1.5	0.5
13	3	Axial	35	1	0
5	4	Factorial	30	0.5	2
14	5	Axial	35	1	2.5
10	6	Axial	43.4	1	1.25
8	7	Factorial	40	1.5	2
7	8	Factorial	30	1.5	2
15	9	Center	35	1	1.25
9	10	Axial	26.6	1	1.25
1	11	Factorial	30	0.5	0.5
6	12	Factorial	40	0.5	2
12	13	Axial	35	1.8	1.25
11	14	Axial	35	0.16	1.25
4	15	Factorial	40	1.5	0.5

7.3.6 Bioreactor fermentations (5 L glass tank)

Six solid fermentations were carried out in 5 L glass tanks, following the results of the 30 previous fermentations in flask. The six fermentations are: three for BS including one fermentation with raw BS (control) and two with BSE produced under different fermentation conditions. The same was done for CS.

For each fermentation, 200 g of biomass was placed in the tank and autoclaved for sterilization. Then, 600 ml of ammonium chloride solution (0.5% or 2.5% w/w) was added with additional nutrients. The nutrients for 1 L consist of KH_2PO_4 (0.6 g), $\text{MgSO}_4 \cdot 7 \text{H}_2\text{O}$ (0.5 g), $\text{CaCl}_2 \cdot \text{H}_2\text{O}$ (0.74 g), $\text{NH}_4\text{H}_2\text{PO}_4$ (2.32 g), yeast extract (1 g), veratryl alcohol (1 ml), $\text{CaCl} \cdot 7 \text{H}_2\text{O}$ (0.2 g), $\text{ZnSO}_4 \cdot 7 \text{H}_2\text{O}$ (0.14 g), $\text{FeSO}_4 \cdot 7 \text{H}_2\text{O}$ (0.5 g), $\text{MnSO}_4 \cdot \text{H}_2\text{O}_2$ (0.16 g) and $\text{CuSO}_4 \cdot \text{H}_2\text{O}_2$ (0.16 g). The batch started with the addition of the 4 days old inoculum to the fermentation medium (300 ml or 200 ml). The substrate was stirred after colonization of the biomass by the fungus (4 days) and then about every 3 days thereafter. Aeration was ensured by a foam cap on top of the tank. Two of the 6 fermentations were controls (one for each raw biomass). Samples of each batch were taken every 3 days in 50 ml sterile vials for analysis. The fermentations were stopped after 24 days except for each control which were stopped after 18 days.

7.3.7 Enzyme extraction

Enzyme extraction was carried out with the samples taken from the 5 L fermentations. A total of 42 samples (8 sample for each batch) were taken. Then, 5 g of the fermented substrate was transferred to a 250 ml flask with 35 ml of distilled water and placed in a shaker incubator at 37°C and 180 rpm for 24 h. The contents were filtered with a Whatman 45 μm paper filtration device and then centrifuged at 3,000 rpm and 10°C for 10 min in a centrifuge (Allegra 6R Centrifuge, Beckman Coulter, USA). The supernatant was then filtered through 22 μm PVDF syringe filters (Foxy Life Sciences, NH, USA), for enzymatic assays.

7.3.8 Enzymatic assays

Enzyme assays were carried out for the three main enzymes of the *Phanerochaete chrysosporium* ligninolytic system: manganese peroxidase (MnP), lignin peroxidase (LiP) and laccase (Lac). All analyses (42 x 3 = 126) were carried out at room temperature (25 °C) using a UV-visible spectrophotometer (Nicolet IS50 FTIR Spectrometer). The substrate used for MnP was N,N,N',N'-tetramethyl-1,4-phenylenediamine (TMPD). Analysis of MnP activity using TMPD relies on the ability of MnP to oxidize this substrate in the presence of hydrogen peroxide (H_2O_2) and manganese (Mn^{2+}) (Kameshwar & Qin, 2017; Oliveira *et al.*, 2009). Absorbance of oxidized TMPD is maximal at 611 nm. For spectrophotometric measurements, 1 ml TMPD (1 mM), 0.5 ml MnSO_4 (1 mM), 1 ml H_2O_2 (1 mM) and 0.3 ml enzyme extract were added to 2 ml 0.5 M sodium tartrate (pH 5). Readings were taken continuously every minute for 10 min. LiP activity was measured with veratryl alcohol at 310 nm. It is based on the oxidation of veratryl alcohol to

veratraldehyde by LiP in the presence of H₂O₂ (Arora & Gill, 2001; Kameshwar & Qin, 2017; Tien & Kirk, 1988). For spectrophotometric measurements, 115 µl veratryl alcohol (2 mM), 22 µl H₂O₂ (0.4 mM) and 50 µl enzyme extract were added to 2.86 ml D-tartaric acid (50 mM at pH 2.5). Laccase enzymatic activity was assayed using ABTS (2,2'-azino-bis(3-ethylbenzothiazoline-6-sulfonic acid)). ABTS is oxidized by laccase to form an intense blue-green cationic radical with maximum absorbance at 420 nm (Kameshwar & Qin, 2017; Park & Park, 2008). For spectrophotometric reading, 100 µl of enzyme extract was added to 2.8 ml of sodium acetate buffer solution at pH 4.5, and 100 µl of ABTS solution (5 mM). The readings were taken continuously (every minute) for 5 min. All the tests were performed in duplicate. The enzymatic activity was calculated as (Yan, 2023):

Équation 7.1 – Enzymatic activity.

$$Activity (U/l) = \frac{\Delta Abs \times V_{total}}{\epsilon_{wavelength} \times \Delta t \times V_{enzyme}} \times 10^6$$

where ΔAbs is the absorbance variation during a time Δt ; V_{total} is the total volume in ml of reaction medium for which V_{enzyme} in (ml) was added; $\epsilon_{wavelength}$ is the extinction coefficient (M⁻¹.cm⁻¹) of the enzyme substrate at the wavelength at which the absorbance is measured (Beer-Lambert law). The values are: 12200 M⁻¹cm⁻¹ for TMPD at 611 nm, 9300 M⁻¹cm⁻¹ for alcohol veratryl at 310 nm, and 36000 M⁻¹cm⁻¹ for ABTS at 420 nm.

7.3.9 Delignification

Fermented samples at three days interval were oven-dried at 60 °C for 4 h before being subjected to a Soxhlet extraction process for 12 cycles to eliminate the mycelium. The solvent used was ethanol:benzene (2:1 v/v). The solid fraction after extraction was left at room temperature for drying and to evaporate the solvent. The biomass was then washed with hot tap water by filtration to remove the remaining solvent. Subsequently, 0.5 g of biomass was subjected to Klason lignin analysis. For the corn residues, an additional grinding step using a small kitchen grinder was necessary to break up the agglomerates formed during the extraction stage prior to Klason analysis. Then, 20 ml of 72% sulfuric acid was poured on 0.5 g of biomass and stirred regularly for 80 min. The resulting mixture was diluted to 3% H₂SO₄ with distilled water and then transferred to a digester (Digester 2006 Tecator™ Technology, FOSS, Denmark) for 3 h. The mixture was filtered using a Whatman 45 µm paper filtration device and the solid fraction (Klason lignin) was rinsed several times with hot tap water until neutral pH (6 - 8) before being oven dried at 105 °C

and weighed. All the analyses were carried out in duplicate. The delignification rate was calculated as:

Équation 7.2 – Delignification percentage.

$$\gamma = \frac{mL_{\text{raw}} - mL_{\text{ext}}}{mL_{\text{raw}}} \times 100$$

where mL_{raw} represents the mass of lignin in the raw biomass and mL_{ext} represents the mass of lignin in the extrudate.

7.3.10 Fourier Transform Infrared Spectroscopy (FTIR)

Samples of raw and pretreated BS and CS were scanned with a FTIR device to investigate the effect of the pretreatment on the molecular structure of the biomasses, especially for the crystallinity index (CrI) measurement via the lateral order index (LOI) (Darim *et al.*, 2018; Hřčka *et al.*, 2020). The measurements were done on a Nicolet IS50 FTIR Spectrometer (Thermo Scientific, USA) equipped with a standard ATR (attenuation total reflection) crystal cell detector. Each recorded spectrum was an average of 16 consecutive scans of 4 cm⁻¹ resolution from 700 to 1500 cm⁻¹.

7.3.11 Enzymatic hydrolysis

Enzymatic hydrolysis tests were carried out on the raw biomasses and all the biomasses subjected to extrusion followed by fermentation (Ex-SSF) after 24 days. The enzymatic hydrolysis protocol was based on Danisco Us Inc (Danisco, 2007) and Miller (1959a). A total of 15 g of biomass was oven-dried at 50°C for 24 h to obtain a dryness over 95%. The enzyme was the Accellerase Duet enzyme cocktail. Then, 12.5 g of biomass was placed in a 50 ml flask, covered with 100 ml citric buffer (0.05 M) pH 4.8, tetracycline (10 g/l in 70% ethanol) and cycloheximide (10 g/l). The mixture was placed in an incubator-agitator at 55°C and 180 rpm for 96 h. An aliquot was taken every 24 h and placed in hot water for 5 min to stop the enzymatic reactions. The sample was then filtered and centrifuged at 3,000 rpm for 10 min at 10 °C. The reducing sugars were analyzed in the supernatant using DNS (dinitrosalicylic acid) solution and a spectrophotometer (Miller, 1959b).

7.4 Results and discussion

7.4.1 Lignocellulosic biomass recalcitrance

Lignocellulose biomass is the complex formed by cellulose, hemicellulose, and lignin in the cell-wall of biomass such as woods and agricultural residues. The amount of lignocellulose and the relative proportion of its component vary from one biomass to another (softwood, hardwood, agricultural residues, grass, etc.). Lignin is the constituent limiting the enzymatic digestibility of cellulose and hemicellulose embedded in lignocellulosic biomass (Wang *et al.*, 2018b).

The pretreatment approach developed in this study was carried out on black spruce chips (BS) and corn stover (CS). **Figure 7.1** shows the relative proportion of cellulose, hemicellulose, and lignin in both raw biomasses. BS has $60.1 \pm 1.6\%$ of holocellulose (cellulose and hemicellulose) and $28.9 \pm 0.2\%$ of lignin, while CS has $55.5 \pm 1.2\%$ of holocellulose and $18.9 \pm 0.7\%$ of lignin. Fang *et al.* (2011) found similar results for black spruce chips with 29% of lignin and 59.7% of holocellulose (glucan, xylan, mannan, galactan and arabinan). For CS, the results are in agreement with Zhang *et al.* (2018) who found 56.4% of holocellulose and 15.3% of lignin in corn residues (bark). Although the holocellulose content is higher in BS than in CS, its accessibility by enzymatic hydrolysis is technically more difficult because of its higher lignin content. There is another layer of complexity associated to the lignin recalcitrance of BS compared to CS as the former is a softwood while the latter is an agricultural residue. Softwoods have thicker cell wall and their lignins are structurally different from agricultural residues lignins. Lignin is an aromatic polymer mainly composed of two or three units called monolignols and connected by ether (C-O-C) or carbon-carbon (C-C) bonds. These monolignols are: guaiacyl (G unit), syringyl (S unit) and p-hydroxyphenyl (H unit) (Jiang *et al.*, 2023). Softwood lignin is mainly composed of G unit, while agricultural residues are mainly composed by S and H units. The G units are more recalcitrant because they are linked by strong covalent C-C bonds instead of the more cleavable β -O-4 bonds present in the other units. The S/G ratio in biomass is used as an indicator of biomass susceptibility to enzymatic hydrolysis. The lower the S/G ratio (higher G unit) is, the more difficult is the enzymatic hydrolysis. In the literature, a S/G ratio of 0.014 for spruce and 0.64 for corn stover were reported (Anderson *et al.*, 2016; Wang *et al.*, 2018b). This is in contrast with hardwoods having S/G ratios up to 2.7 (Sequeiros & Labidi, 2017). In both cases, BS and CS are technically though biomass to use directly in biorefineries. This is why softwood and agricultural residues are usually taken as model biomasses to assess the efficiency of pretreatments.

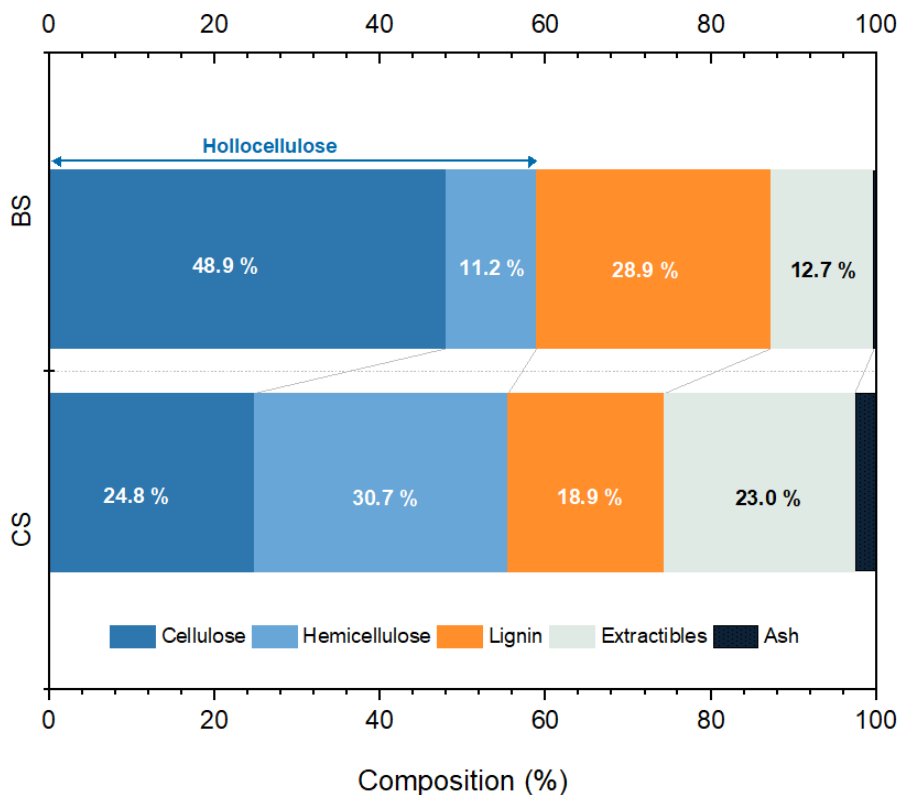


Figure 7.1 Composition of the raw black spruce chips (BS) and raw corn stover (CS).

7.4.2 Extrusion

Previous investigations on extrusion technology as a pretreatment for BS and CS confirmed that this method is very effective to de-structure lignocellulosic biomass and increase the particles specific surface area (666.3.7). The analysis of the extruded biomasses gave 25.3% delignification and 1183.3 cm²/cm³ of specific surface for BS, and 27.4% delignification and 1569.1 cm²/cm³ of specific surface for CS. These extrudate were used in this study for further biodelignification with white rot fungi to enhance the enzymatic saccharification of cellulose and hemicellulose into reducing sugars. Extrusion, unlike other pretreatments, is compatible with biodelignification because it does not generate inhibitors of microbiological activities such as furfural and hydroxymethyl furfural (Karunanithy *et al.*, 2012b). Furfural and hydroxymethyl furfural are compounds which are more likely to appear during most physico-chemical pretreatment due to frequent unexpected degradation of the C5 and C6 carbohydrates. In addition, the extrudates feature disrupted structures and highly increased particles specific surface. These characteristics are well suited for ligninolytic enzyme activities.

7.4.3 Flask fermentations (250 ml)

Biodelignification consists of the removal of lignin in lignocellulosic biomass by micro-organism through ligninolytic enzymes. Only a handful of microorganisms are able of this feature. The most remarkable ones lie in the heterogenous white rot fungi (WRF) group which are responsible of wood-decaying in nature. *Phanerochaete chrysosporium* is one of the most emblematic of this group. However, WRF in general, and *Phanerochaete chrysosporium* in particular, requires specific conditions for growth and activate their enzymatic activities (Singh & Chen, 2008).

Flask fermentations were conducted to determine the growth conditions of *Phanerochaete chrysosporium* on extruded BS (BSE) and extruded CS (CSE). Tableau 7.4 shows the growth assessment results. Of the 15 runs carried out for each biomass, only 2 runs for corn residues (CS) and 6 runs for black spruce (BS) showed growth of the strain. These were Run 2 and 8 for corn residues, and Runs 2, 3, 4, 5, 10 and 13 for black spruce residues. As for the other runs, no microbial development was observed over two weeks of cultivation. However, growth rates varied from one run to the next. Strain growth on corn residues was higher and better developed than on black spruce residues (Figure 7.2). Strain growth on residues took the form of greenish colonization of the biomass. For corn residues, the strain was more sensitive to temperature and inoculum size, and more tolerant the amount of additive. The only two growth conditions observed were at 30°C and 1.5 ml/g inoculum. The amount of additive was 0.5 for the highest growth (Run 2) and 2.0 for Run 8. Thus, less additive leads to higher strain growth on the biomass residues at 30°C and 1.5 ml/g inoculum. Additive tolerance observed here is because CSE contain their own source of nitrogen. Elemental analysis of the corn residues yielded a C/N (carbon/nitrogen) ratio of 88:1. This ratio is sufficient to induce and maintain strain growth. Huang *et al.* (2020) studied the effect of four C/N ratios (122:1, 50:1, 26:1 and 14:1) on the dry weight of *Phanerochaete chrysosporium* mycelium. Their results showed similar mycelial growth with these different ratios, but the best growth was observed at 50:1. On BSE, the strain's growth conditions were more diversified. Growth occurred between 26.6 and 35 °C; between 0.5 and 1.8 ml/g inoculum and between 0 and 2.5% ammonium chloride concentration. No growth was observed at 40 °C and above neither for BSE nor for CSE no matter the inoculum load or the ammonium chloride concentration. Yet, *Phanerochaete chrysosporium* can grow at temperature as high as 40 °C (Caizán Juanarena *et al.*, 2016; Hofsten & Rydéean, 1975). The water activity (a_w) is responsible for the growth absence. In fact, a_w is crucial for *Phanerochaete chrysosporium* development. Its cells are not able of active internal water transport (Gervais & Molin, 2003). Each cell gets its required supply directly from the immediate extracellular environment. Under solid state

fermentation, there is little to no free water between the biomass particles. However, in semi solid fermentations conditions, cells use the capillary and hygroscopic water in the biomass (Figure 7.3). At 40 °C and 46.6 °C, the capillary water evaporated after 4 to 6 h and the hygroscopic water after 6 to 9 h. So, in less than 10 h of incubation, the cells no longer have access to water and their development is stopped, while below 37 °C the small amount of water available in the environment is sufficient to trigger lignin degradation which produces additional water (H₂O) and carbon dioxide (CO₂). This explains why (i) there is still a growth at the lowest temperature tested (26.6 °C); and (ii) the optimum temperature is 30 °C, as the best growth conditions occurred at this temperature for both biomasses.

Tableau 7.4 Growth assessment of Phanerochaete chrysosporium on extruded black spruces chips (BSE) and corn stover (CSE).

Run	Conditions			BSE growth	CSE growth
	Temp. (°C)	Inoculum (ml/g)	[NH ₄ Cl] w/w (%)		
1	40	0.5	0.5	-	-
2	30	1.5	0.5	+++	+++
3	35	1	0	+	-
4	30	0.5	2	++	-
5	35	1	2.5	+	-
6	43.4	1	1.25	-	-
7	40	1.5	2	-	-
8	30	1.5	2	-	++
9	35	1	1.25	-	-
10	26.6	1	1.25	+	-
11	30	0.5	0.5	-	-
12	40	0.5	2	-	-
13	35	1.8	1.25	+	-
14	35	0.16	1.25	-	-
15	40	1.5	0.5	-	-

+++ Intense growth ++ Medium growth + Low growth - No growth

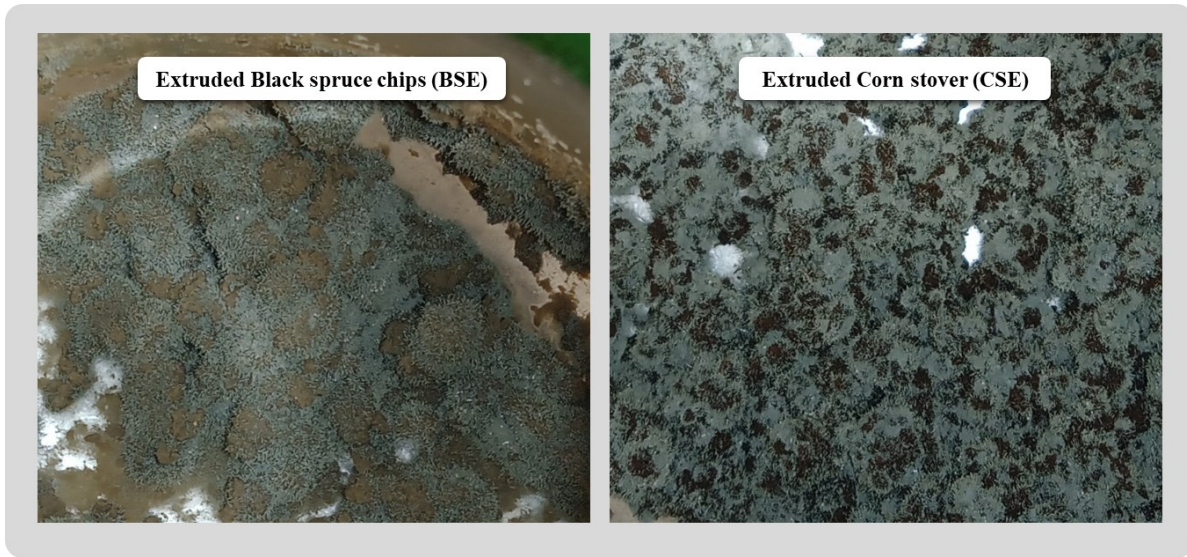


Figure 7.2 Colonization of extruded black spruce chips (BSE) and corn stover (CSE) by *Phanerochaete chrysosporium* during flask solid state fermentation.

(Both BSE and CSE colonization took place under Run 2 conditions: 30 °C, 1.5 ml/g inoculum and 0.5 w/w (%) ammonium chloride).

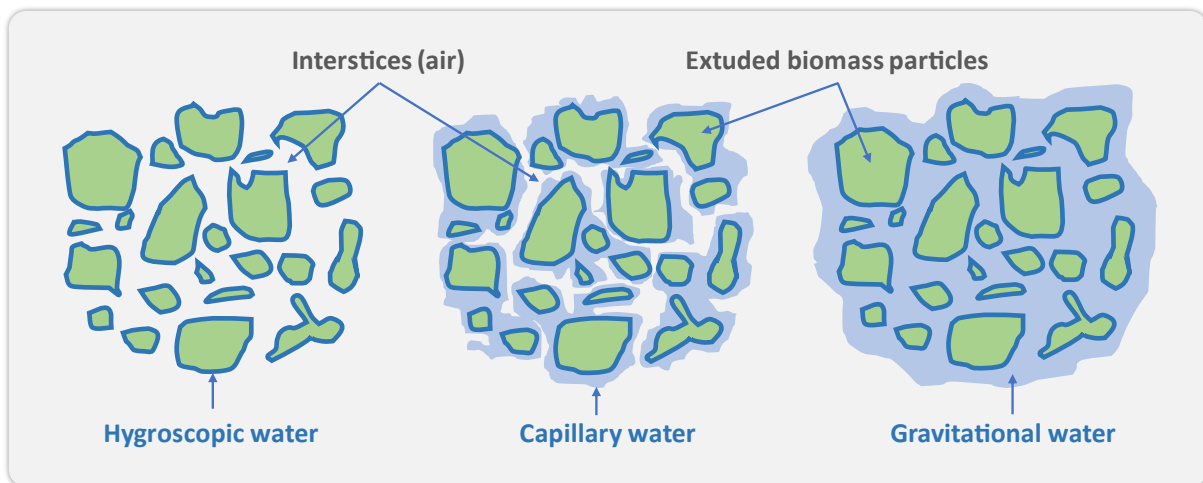


Figure 7.3 Type of water supply available in biomass for microbial development.

(Hygroscopic water (solid fermentation), capillary water (solid and semi solid fermentation), and gravitational water (submerged fermentation)).

7.4.4 Bioreactor fermentations (5 L glass tank)

Based on the flask fermentation results, two conditions for BSE and two conditions for CSE were selected for a fermentation scale-up (40X: from 5 g to 200 g). The fermentations were performed in 5 L glass tanks. The selected conditions were those of the best growth condition obtain in flask, except for BSE where Run 4 was replaced by Run 5 (Tableau 7.2). Although Run 4 had higher mycelium development than Run 5, the analysis of biomass delignification gave 38.4% for Run 5 and 11.2% for Run 4. This is why Run 2 and Run 5 were selected for 5 L fermentation of BSE, while Run 2 and Run 8 were selected for CSE. But one fermentation of raw BS and one fermentation of raw CS were performed as controls. Based on the water activity issues, to maximize fermentability over 24 days, the biomass/water ratio was adjusted to 0.23 ± 0.02 in the 5 L instead of 0.33 used during the flask fermentation. Under these conditions, the fermentations were more semi solid fermentations (SSF) than solid state fermentations. In addition, basal medium components were added as nutrient in each fermentation to support rapid mycelium proliferation during the first days of fermentation. The nutrient concentration was 0.0241 g/g of biomass.

7.4.5 Effect of Ex-SSF pretreatment

The goal of the bioreactor fermentation was to study the effect of the extrusion-biodelignification pretreatment on BS and CS. The focus was on the effect of different pretreatment conditions on (i) *Phanerochaete chrysosporium*'s enzymatic system, (ii) delignification rate, (iii) cellulose crystallinity, (iv) enzymatic digestibility and (v) the role of enzyme load on enzymatic digestibility.

7.4.5.1 Ligninolytic enzyme production

Delignification of ligneous biomass by fungi is possible due to ligninolytic enzymes attacking lignin in the fibrous biomass. These enzymes are mainly laccases (Lac), manganese peroxidase (MnP) and lignin peroxidases (LiP). Contrary to most of the microbial degrading agent, *Phanerochaete chrysosporium* can release these three main enzymes. However, their secretion and relative proportion depend on the environment. **Figure 7.4** presents the evolution of the Lac, MnP and LiP activities for 24 days semi solid fermentation (SSF) of extruded black spruce chips (BS) and corn stover (CS). All three enzymes were expressed in the controls and the extruded biomasses.

Laccase activities was very low and ranged between 0.1 and 0.2 U/l. There was no significant difference between the controls and the extruded biomasses. Laccase secretion by *Phanerochaete chrysosporium* is directly linked to the presence of copper (Cu) in the medium.

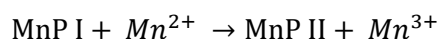
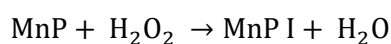
Cu is not only an inducer of laccase production, but also an element of laccase structure. Laccases have 4 copper atoms in their structure, which are important active sites for ligninolytic actions. It has been reported that for biomass with low copper content, there is little to none laccase activity from *Phanerochaete chrysosporium* (Dittmer *et al.*, 1997). The copper source in all the 6 fermentations was from CuSO₄ which was at very low concentration (0.48 mg/g of biomass). So, the lack of sufficient copper supply was responsible for the low laccase production observed in the fermentations. Copper is certainly essential in laccase production, but co-culture and supplementation of manganese oxide (IV) can also trigger laccase production. Singh *et al.* (2020) showed that laccase production was 8.2 times enhanced by co-culturing *Phanerochaete chrysosporium* and *Trametes versicolor* in presence of azo dyes. In this case, the production was the result of *Phanerochaete chrysosporium* hyphal modification and its synergistic interaction with *Trametes versicolor*. As for Mn supplementation, Rodríguez *et al.* (1997) reported a 16-fold increase of laccase production when *Phanerochaete chrysosporium* was cultured on barley straw. Although techniques or additives can be used to trigger and enhance the laccase activity, economic viability must be considered.

For manganese peroxidase activities, there is a distinctive difference between both raw materials: BSE (2 and 5) and CSE (2 and 8). MnP activity were very low. Their maximum MnP activity was 1.4 U/l for CSE recorded at the end of the 24th day. However, BSE (Run 2 and 5) and CSE (Run 2 and 8) MnP activities were consistently high from the 3rd day to the end, with maximum activity respectively of 13.8 ± 0.7 U/l (BSE 5) at day 18th, and 32.0 ± 1.6 U/l (CSE 2) at day 21. These are 28-fold and 21-fold the enzyme activity of their respective raw biomass in less than 21 days. In general, 4 phases or trends can be distinguished for BSE and CSE between the 1st and 24th day. During the first days (1-3), there was a relatively important MnP activity going on followed by a slight decline between the 3rd and 12th day. The reason is that MnP production started in the inoculum medium before inoculation and continued until reaching a peak at the 3rd day where limited free nutrient occurred. This resulted in a decline in MnP activity. At the same time, new production of MnP was triggered by *Phanerochaete chrysosporium* to degrade lignin and find nutrients. The stress conditions brought by the limited nutrient significantly increased the MnP production (Govender, 2011). This explains the consistent increase of MnP activity from the 9th day at a rate of 0.9 U/l per day for BSE and from the 12th day at a rate of 2.5 U/l per day for CSE. After the 18th day for BSE and the 21st days for CSE, the slight decrease observed is related to two phenomena. First, as the delignification takes place in the medium thanks to the accumulation of enzymatic activity, phenolic compounds are released in the medium. These compounds from the degraded lignin are inhibitors of ligninolytic enzyme activity. Secondly, as the SSF was

performed, a continuous drop in water activity occurred because no additional water was added during fermentation. Additionally, a decrease of available nutrients or carbon source in the medium due to rapid consumption can increase the effect of both phenomena. These observations and explanations are consistent with the delignification rate (§ 3.5.2).

Several studies reported different ways to enhance MnP production from *P. chrysosporium*. Ürek and Pazarlioğlu (2005) obtained up to 421 U/l of MnP activity with the strain *Phanerochaete chrysosporium* BKM-F-1767 (ATCC 24725) by adding Mn²⁺ solution (174 µM) and Tween 80 (0.05%, v/v) to the medium. In fact, MnP uses Mn²⁺ as mediator substrate in their mechanism of lignin degradation. Mn²⁺ is oxidized into Mn³⁺ by MnP through a series of reactions (Équation 7.3). Mn³⁺ reacts with chelating agents to form powerful redox mediators able of lignin disintegration by attacking phenolic structures. Mn²⁺ was also found to be an inducer of laccase activity in *P. chrysosporium* through a mechanism not yet fully understood. This was observed by Chen *et al.* (2021b) during a study of an antibiotic degradation (norfloxacin) with the strain BKM-F-1767 (CCTCC AF96007). In another setup, ligninolytic enzymes (including MnP) were overexpressed by 2.6 to 4-fold compared to the control activity. This setup involved a recombinant *P. chrysosporium* obtained by shock wave-induced acoustic cavitation (Coconi Linares *et al.*, 2018). The method requires a power source for the acoustic wave generator which adds steps, complexity and costs to the process. The reactions involved are:

Équation 7.3 – Reactions cycle of manganese peroxidase.



Lignin peroxidase activity evolution was also investigated. Similar to MnP activities, a clear trend between the raw and the extruded biomass can be observed. However, contrary to MnP, the raw biomasses had important LiP activities compared to the extruded biomass. The highest activities recorded was 53.7±2.7 U/l at day 18 for CS, and 16.4±0.8 U/l at day 9 for BS. On the other hand, the maximum LiP activity recorded with the extrudates was 6.0±0.3 U/l from CSE 8 and 13.9±0.7 for BSE 2. This result highlights two facts: (i) raw CS were more suited for LiP production than raw BS and, (ii) the extruded biomasses did not favor the production of LiP contrary to the raw biomasses. A possible explanation about the difference between LiP in raw CS and raw BS lies in the different lignin content of these two biomasses. LiP has a specific ability to cleave β-O-4 linkages between lignin monomers (Chowdhary *et al.*, 2019). β-O-4 linkages are abundant in

biomass with high S/G ratio such as CS. So, LiP production is expected to be high in such environment compared to high G lignin environment where C–C links prevails. LiP is dependent on nitrogen concentration and is expressed in nitrogen-limited environment. Yet, extrusion did not modify the C/N ratio. A previous elemental analysis of raw corn stover, black spruce chips and their respective extruded biomasses revealed that extrusion does not change the C/N ratio of the biomass (6.4.3). The low LiP activity in both extruded biomasses is possibly attributed to a lower content of rigid ether linkage and higher specific surface area of the extrudates particles. These combinations may significantly lower the enzymatic energy required for breaking down lignin compared to the raw biomasses where lignocellulose is intact at the beginning of the fermentation. This explanation is supported by the FTIR profile of the raw and extruded biomasses (

Figure 7.6). The vibration and stretching of the functional groups including the ether groups around 1260 cm^{-1} , as well as aromatic C–O around 1024 cm^{-1} , were globally more pronounced in the extruded biomasses compared to the raw biomasses. Extrusion also significantly increased the surface potentially accessible by the enzymes: 1.5-fold (CS) and 4-fold (BSE) compared to their respective raw biomass.

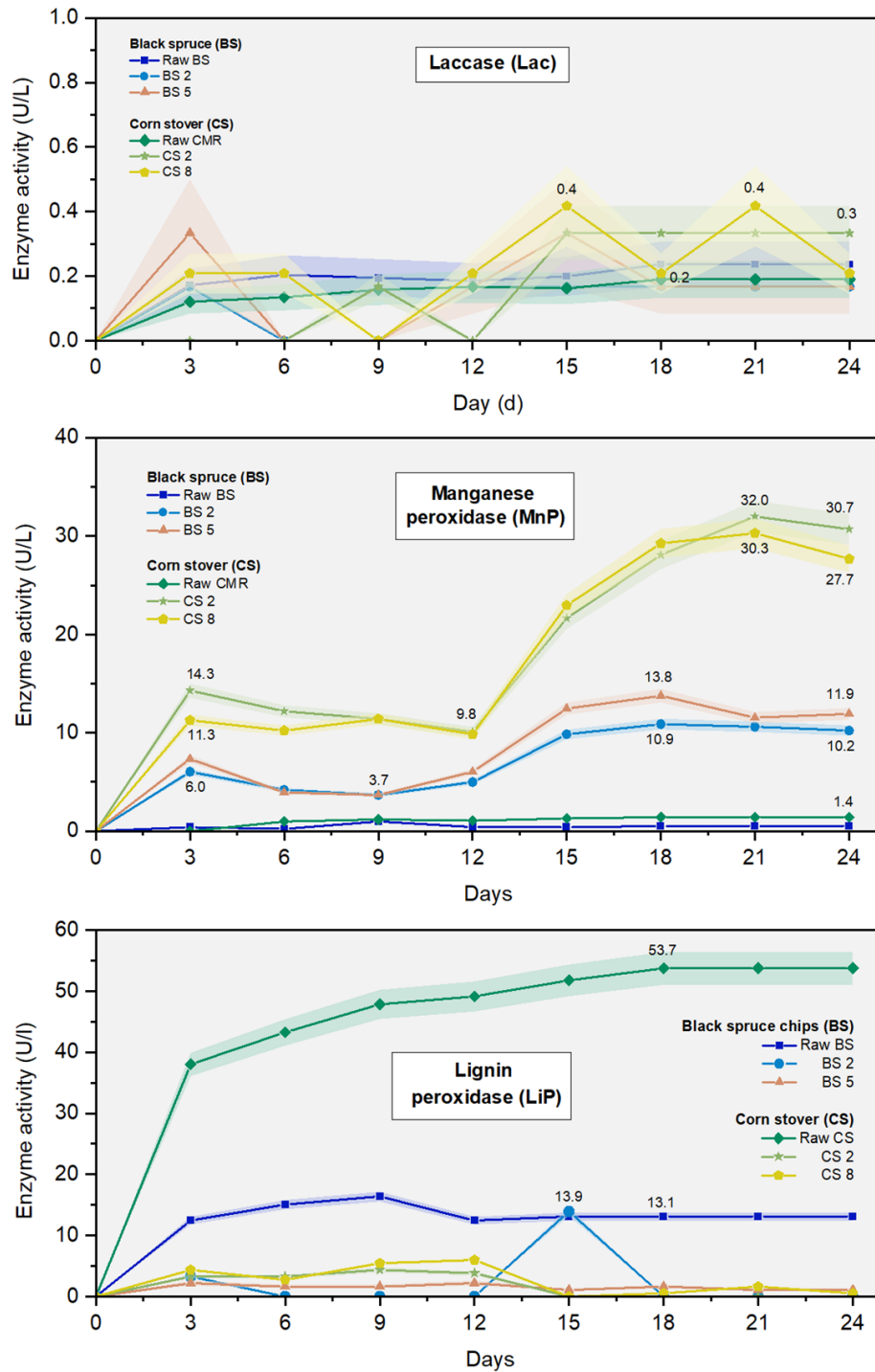


Figure 7.4 Evolution of laccase, manganese peroxidase and lignin peroxidase activities during 24 days of semi solid fermentation (SSF) with extruded black spruce chips (BS) and corn stover (CS).

7.4.5.2 Delignification rate

Biomass delignification is one of the most important parameters contributing to the improvement of biomass enzymatic digestibility for sugar recovery (Laureano-Perez *et al.*, 2005; Mikulski & Kłosowski, 2022). The biomass delignification rate was evaluated every three days during the bioreactor fermentations. **Figure 7.5** presents the results of delignification rates determined by the Klason lignin method. Based on experimental data, theoretical delignifications were assessed where Soxhlet extraction (benzene/alcohol) was less efficient on mycelium removal to accurately evaluate the experimental delignification. For some samples, the effect of mycelium presence on Klason lignin evaluation were combined with a reaction between residual benzene on the mycelium and the 20 ml of 72% sulfuric acid in presence of water and residual ethanol. The result was the sulfonation of benzene by H₂SO₄ evidenced by the whitish reaction in the medium. The relationship between biodelignification with *Phanerochaete chrysosporium* and time (in days) is a sigmoidal-like function (Zhang *et al.*, 2012b). The first phase of the curve is very slow with an almost steady evolution of the delignification rate: this is the latency phase. No significant delignification is performed since the nutrient brought by the inoculum medium is still available as carbon source for the fungi. The second phase is a rapid increase of the delignification rate where lignin becomes the target for carbon source. This phase is followed by a third phase with slight/negligible increase of the rate for various reasons including aging of fungal cells, CO₂ accumulation in the medium, and water activity drops especially if the biomass/water ratio is not adjusted over time. The Langevin function was used to build a model for BSE 2, BSE 5, CSE 2 and CSE 8 delignification evolution over time. The data, parameters, function expression and results for each model is available in Annex 1212. When raw black spruce chips (BS) were subjected to fermentation without extrusion, a maximum delignification of 14.7 ± 0.7% was recorded after 15 days with 12.5% delignification during the first 3 days and limited increase from the 3rd to the 15th day. As for the raw corn stover (CS) control, no delignification took place during the same period. On the other hand, when black spruce was extruded before fermentation (BSE 2 and BSE 5), the experimental delignification reached 59.1±3.0% for BSE after 15 days and 65.4 ± 3.4% for CS after 18 days of fermentation. The extrusion steps contributed for 25.3% of delignification for BSE 2 and BSE 5, while 27.4% of delignification for CSE 2 and CSE 8. Globally the first phase took place within 6 days, except for CSE 2 which was shorter (3 to 4 days). The second phase lasted 6 days in all models, followed by the third phase beginning at day 12, except for CSE 2 at day 9. Similarly, the slope in the second phase were 0.23 ± 0.02 except for CSE (0.33). Based on our information, there is no previous study on Ex-SSF pretreatment for biomass

delignification for enzymatic digestibility, and much less with black spruce chips and corn stover. However these results are similar to Zhang *et al.* (2012b) on rice straw using steam explosion. The authors pretreated rice straw by steam explosion followed by solid fermentation with *P. chrysosporium*. The delignification results were a sigmoidal function with a 0.25 slope and a maximum delignification of 58% after 12 days under optimized condition including supplementation of 0.3% of Tween 80.

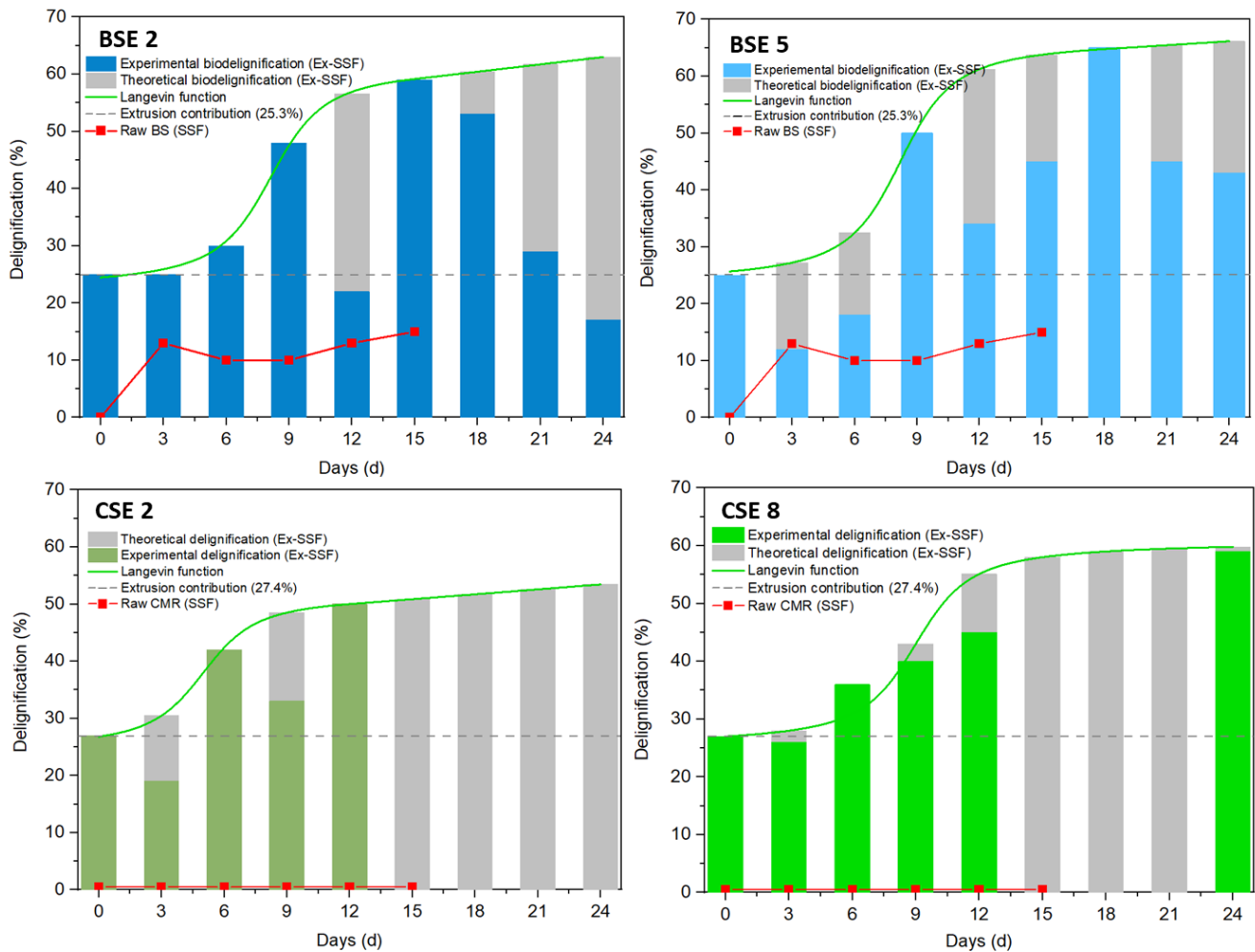


Figure 7.5 Biomass delignification rate during the tank fermentation of black spruce chips and corn stover.

(BSE 2 and BSE 5 are the plots for fermentations with respectively extruded biomass in Run 2 and Run 5 conditions. The red line with square symbol on both plots is the control fermentation with raw black spruce chips without extrusion (BS). Idem for CSE 2 and CSE 8 which are the plots for fermentations with respectively extruded biomass in Run 2 and Run 8 conditions. The red line with square symbol on both plot is the control fermentation with raw corn stover without extrusion (CS)).

7.4.5.3 Crystallinity index

Fourier transform infrared spectroscopy (FTIR) is widely used to determine the crystallinity index (CrI) in biomass since the early work of [Vydrina et al. \(2023\)](#). It is based on the method proposed by [Hurtubise and Krassig \(1960\)](#) and [Nelson and O'Connor \(1964\)](#) on lateral order index (LOI) taken equivalent to CrI. CrI is calculated as the ratio of the peaks recorded at 1427 cm^{-1} (A_{1427}) and 898 cm^{-1} (A_{898}). CrI, similar to biomass delignification, plays a major role in enzymatic saccharification. Theoretically, amorphous regions gives better accessibility to enzymes for saccharification ([Zhang et al., 2019b](#)). In the literature, the crystallinity index is usually defined as the ratio of crystalline cellulose to amorphous cellulose. If this is true for pure cellulose, it is not the case for lignocellulose. Actually, the amorphous region measured by the A_{898} peak is not only available for amorphous cellulose, but also for hemicellulose and lignin ([Karimi & Taherzadeh, 2016](#)).

Figure 7.6 shows the A_{1427} and A_{898} peak location for the raw biomasses (untreated and pretreated by the Ex-SSF approach), while **Tableau 7.5** presents the crystallinity index. Untreated black spruce had 54.8%, while untreated corn stover had 46.9% of crystallinity index. Black spruce contained almost twice the cellulose amount in corn stover (48.9% vs. 24.8%) and was expected to have a higher CrI than CS. However, the results show that the Ex-SSF pretreatment significantly increased the CrI for BS by 13.0% (BS2) and 9.8% (BS5) compared to CS with only 4.0% (CSE 2) and 2.7% (CSE 8). These results suggest that a decrease of the amorphous region in the biomass occurred. When considering the high delignification discussed previously, the CrI increase can be explained by the fact that lignin removal reduced the amorphous region absorbance peak (A_{898}). CrI increases after pretreatment has been reported by several studies ([Chinwatpaiboon et al., 2020](#); [Choudhary et al., 2022](#); [Fatriasari et al., 2016](#); [Kundu et al., 2021](#); [Wang et al., 2016](#)). For example, [Fatriasari et al. \(2016\)](#) pretreated bamboo by microwave followed by fungus (*Trametes versicolor*). For all the pretreatment conditions, they recorded a LOI increase from 1.2 to 3.2%. [Chinwatpaiboon et al. \(2020\)](#) pretreated Napier grass by *Clostridium beijerinckii* JCM 8026 and recorded a 38% crystallinity index increase after acid pretreatment with H_2SO_4 and 41% increase after alkali pretreatment with NaOH. The high intensity of the bands in the pretreated BS biomass compared to the raw biomass confirms the disruptive effect of the Ex-SSF pretreatment on BS as the functional groups could vibrate and stretch more freely than in the rigid structure of the raw biomass.

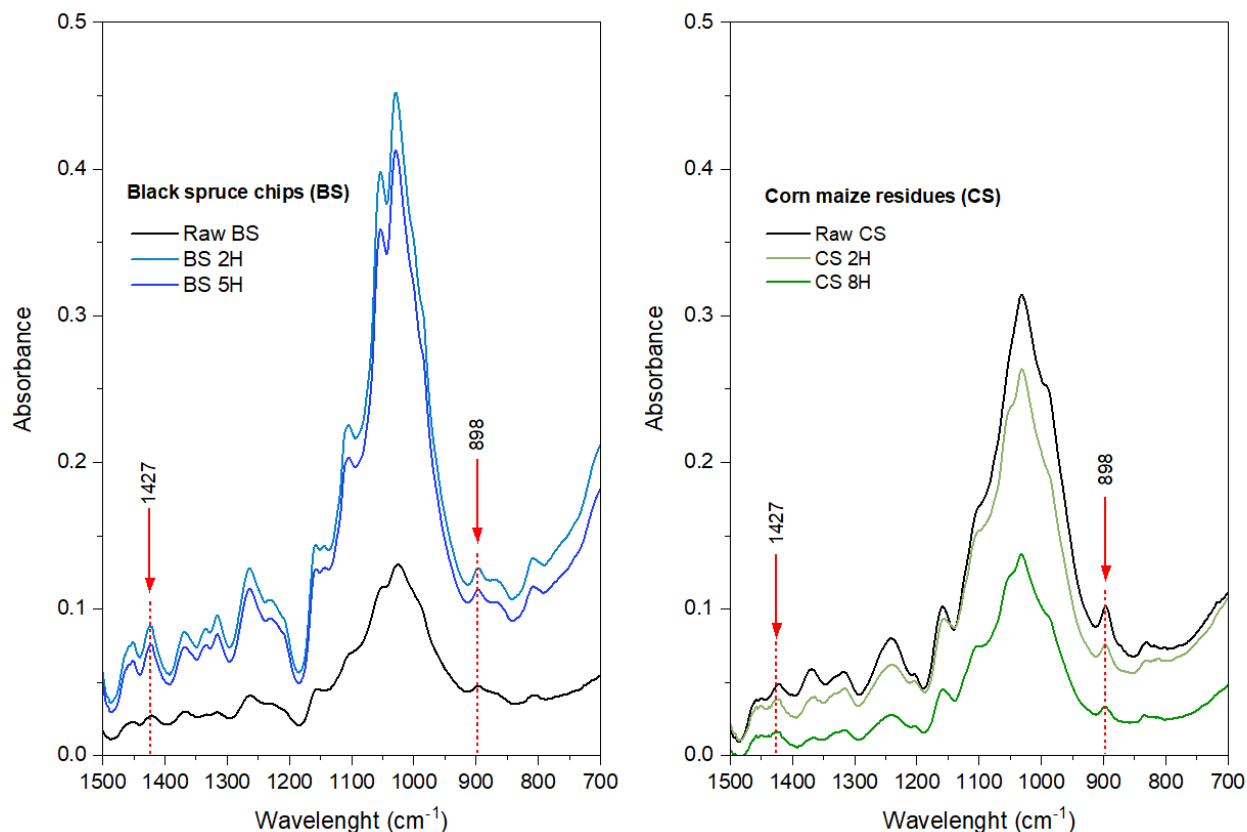


Figure 7.6 FTIR spectra of the raw and Ex-SSF pretreated black spruce chips (BS) and corn stover (CS).

Tableau 7.5 Crystallinity index of the samples.

Parameter	Black spruce chips (BS)			Corn stover (CS)		
	Raw BS	BSE 2	BSE 5	Raw CS	CSE 2	CSE 8
A_{1427}	0.02599	0.08621	0.07261	0.04692	0.03778	0.01599
A_{893}	0.04744	0.12715	0.11247	0.10006	0.07431	0.03226
Cri (%)	54.7%	67.8%	64.5%	46.8%	50.8%	49.5%

7.4.6 Enzymatic digestibility

The effect of the Ex-SSF pretreatment on decreasing the sugar yield after enzymatic hydrolysis was investigated over a period of 96 h for black spruce chips and corn stover. **Figure 7.7** presents the evolution of the sugar concentration (glucose, xylose, galactose, etc.) as a function of time. After 96 h, the sugar concentration was reduced by more than 2 times for BS pretreated with Ex-SSF compared to the untreated BS. The sugar concentration was 7.6 ± 0.4 g/l for BSE 2 and

7.1±0.4 g/l for BSE 5, while the raw BS had 3.3±0.2 g/l. For CS, the Ex-SSF pretreatment improved the saccharification by 44% (CSE 2) and 36% (CSE 8). The trend of the pre-treated biomasses curves suggests that the enzymatic saccharification was still in progress and better yield could be obtained if the tests were not stopped. Run 2 gave the best sugar concentration for both biomass (BS and CS). The conditions were 30 °C for fermentation, 0.5 ml/g for inoculum and 0.5% (w/w) for ammonium chloride. This result is in agreement with the observations during flask fermentation where Run 2 gave the best mycelium development for both BS and CS (Tableau 7.4 and **Figure 7.2**). Additionally, BSE 5 and BSE 2 had similar sugar concentration reduction, as well as CSE 8 and CSE 2. This is consistent with their delignification rate and crystallinity index: two key parameters of enzymatic hydrolysis ([Agarwal et al., 2013](#)). BSE 5 and BSE 2 had only 3.2% difference in biodelignification (models) and 3.2% difference in CrI. The same conclusion applies for CSE 2 and CSE 8 with respectively 6.4% biodelignification (models) and 1.3% CrI difference. However, enzymatic hydrolysis with corn stover (pretreated or not) gave 2.2 times higher sugar reduction than black spruce hydrolysis even if CS had 2 times less cellulose content. In fact, reducing sugar are from holocellulose (cellulose + hemicellulose). When considering the holocellulose content in both biomass, BS and CS have close holocellulose content with 60.1% and 55.5%, respectively. However, black spruce has almost twice the lignin content (29.8%) than corn stover (18.9%) (**Figure 7.1**). Therefore, the sugar reduction recorded for both biomasses is aligned with the predictions and confirms that lignin is the main obstacle to enzymatic hydrolysis efficiency. This also justifies the relevance of the Ex-SSF pretreatment.

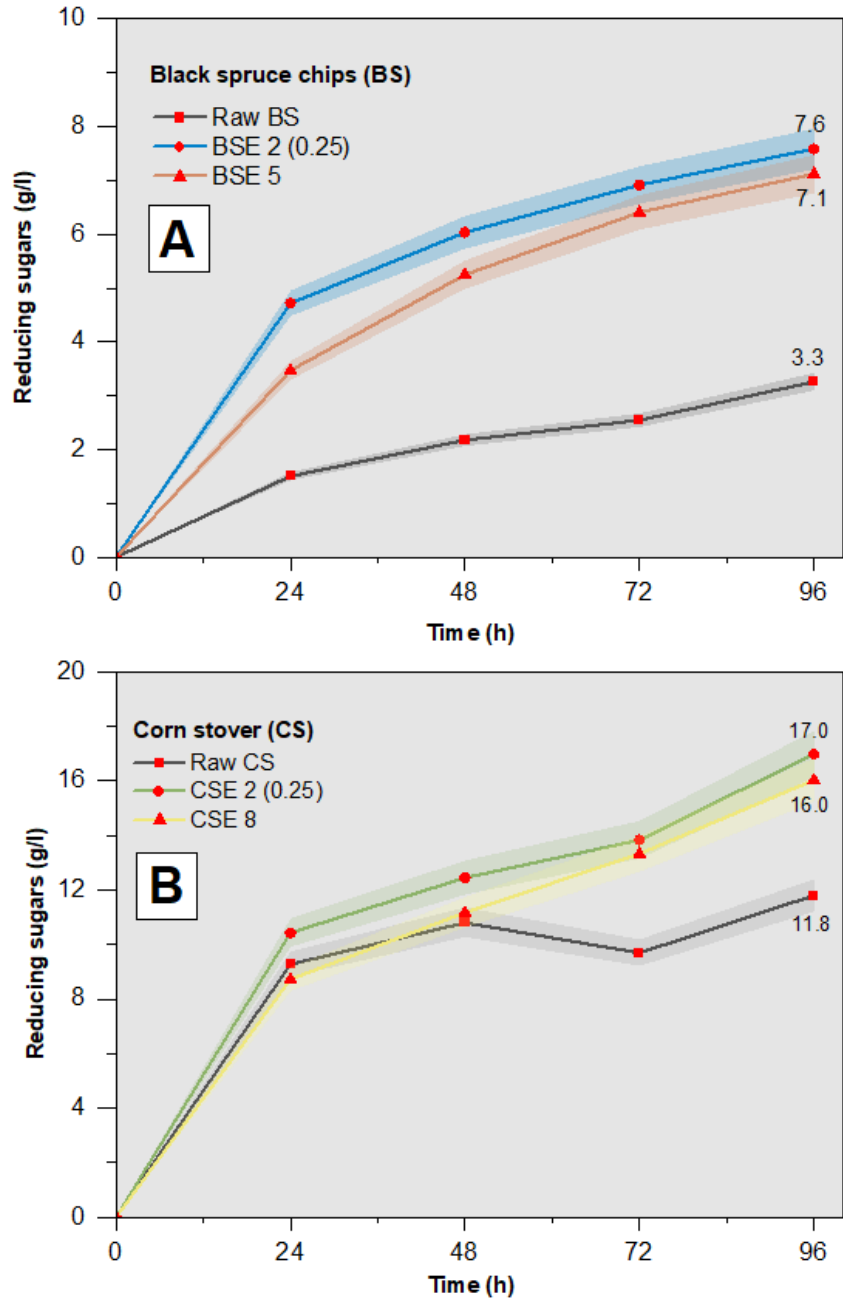


Figure 7.7 Reducing sugar concentration as a function of hydrolysis time with an enzyme content of 0.25 ml/g of biomass.

(A presents the results for raw black spruce (BS) and black spruce pretreated in Run 2 (BSE 2) and Run 5 (BSE 5), while B presents the results for raw corn stover (CS) and pretreated corn stover in Run 2 (CSE 2) and Run 8 (CSE 8)).

7.4.7 Effect of enzyme load on enzyme digestibility

Several studies investigated the effect of biomass load on enzymatic hydrolysis of pretreated biomass. It was shown that increasing the biomass content led to lower efficiency of the enzymatic digestibility. The reasons are many folds: poor mass transfer of cellulolytic enzymes, formed sugar inhibition effect, higher substrate viscosity, etc. (Ioelovich & Morag, 2012; Kristensen *et al.*, 2009; Weiss *et al.*, 2019). To optimize the enzymatic hydrolysis in this study, the enzyme content was increased from 0.25 ml/g of biomass to 0.5 ml/g and 0.75 ml/g. For this investigation, BSE 2 and CSE 2 were selected as they gave the best hydrolysis yield with 0.25 ml/g load. Raw biomass of black spruce and corn stover was also subjected to 0.5 ml/g and 0.75 ml/g enzyme content for the controls. The sugar reduction was again recorded for 96 h and **Figure 7.8** presents the results. No significant increase in raw BS sugar reduction yield (0.7% increase) occurred. On the other hand, increasing the enzyme content negatively affected the sugar yield of the Ex-SSF pretreated black spruce (BSE 2) as the concentration dropped from 7.6 g/l with 0.25 ml/g enzyme to 5.9 g/l and 5.1 g/l for 0.50 ml/g and 0.75 ml/g, respectively (33% reduction). The same trend is observed for raw corn stover (CS) and pretreated corn stover (CSE 2). A 47.5% reduction for raw CS was recorded and up to 70.6% for CSE 2. No significant difference between the 0.5 ml/g and 0.75 ml/g values were observed. Contrary to BS where the pretreated biomass had higher sugar reduction concentration compared to the raw biomass, the pretreated corn stover (CSE 2) exhibited less sugar yield than the raw biomass (raw CS). This result suggests that the enzyme content is very important to maximize the enzymatic hydrolysis. For this conclusion, it can be assumed that better hydrolysis yield than those of 0.25 ml/g enzyme content can be obtained if the enzyme content is optimized. But it was not the case in this study. The reduction of sugar concentration is not the result of end-product inhibition in which case, the sugar accumulation would have been rapid during the first 24 h followed by a rapid stagnation (plateau). But the results suggest an enzyme saturation effect.

Accellerase Duet is a consortium of different enzymes including endoglucanase, β -glucosidase, and xylanase (Ramchandran *et al.*, 2013). Each of them has a particular substrate and attack site in the biomass. When the enzyme content is high, the accessibility of a particular enzyme to its preferred site is reduced, as the access is limited by other enzymes. For example, endoglucanase needs access to the amorphous region in cellulose, β -glucosidase is only efficient on oligosaccharides and xylanase is specific to Xylan (Anoop Kumar *et al.*, 2019; Prade, 1996). Limited access to these sites can lead to disorganization of the enzyme synergy and a significant drop in enzymatic hydrolysis efficiency (Hu *et al.*, 2011)

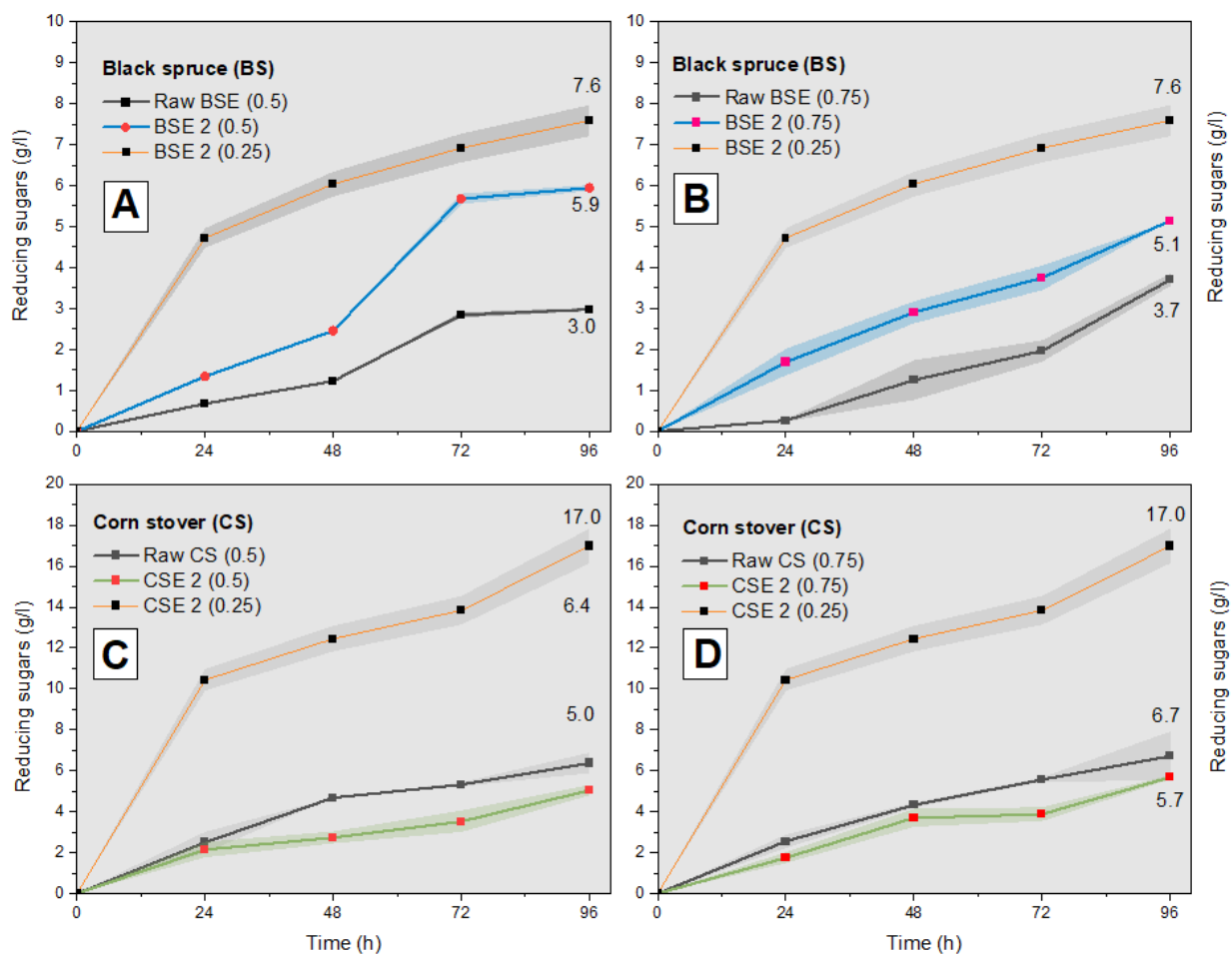


Figure 7.8 Sugar concentration reduction as a function of hydrolysis time with an enzyme content of 0.50 and 0.75 ml/g of biomass.

(A and B present the evolution of sugar concentration for raw BS and pretreated black spruce in Run 2 (BSE 2): A for 0.50 ml/g and B for 0.75 ml/g, while C and D present the evolution of sugar concentration for raw CS and pretreated CS in Run 2 (CSE 2) with C for 0.50 ml/g and D for 0.75 ml/g).

7.4.8 Overview of Ex-SSF techno-economic potential

Pretreatment is a key step for lignocellulosic biomass valorization, especially for applications in the biorefinery industry. Biomass pretreatment represents about 40% of the total valorization cost of 2nd generation bioethanol production (Ahmed *et al.*, 2022). Conventional biomass pretreatment, such as steam explosion, acid pretreatment, alkali pretreatment, microwave, ionic liquids (IL), ammonia fiber explosion (AFEX), ozonolysis, and organosolv have failed to lower the pretreatment costs to make bioethanol production not only economically viable, but also more attractive and competitive compared to fossil fuels or first-generation bioethanol (Ahmed *et al.*,

2022; Alvira *et al.*, 2010; Rezania *et al.*, 2020). The Ex-SSF approach provides major advantages compared to existing technologies. As evidenced in this study with black spruce and corn stover, Ex-SSF pretreatment led to interesting sugar recovery yields, similar to the most efficient conventional methods. However, the competitive advantage of the Ex-SSF pretreatment lies in: (i) the important cost reduction of the pretreatment, (ii) the substantial secondary revenues opportunities that Ex-SSF offers and, (iii) the scalability of the pretreatment as described next.

First, Ex-SSF is a sequential pretreatment starting with extrusion and followed by semi solid fermentation. Extrusion is a very fast pretreatment with low energy consumption. The mini-extruder (11 mm) used in this study had a pretreatment flow rate of about 1 kg/h with an energy consumption of 40 kWh/kg, but the energy consumption with regular pilot scale extruders (36 mm and higher) can easily drop to 10 kWh/kg (Hjorth *et al.*, 2011) and process up to 200 kg/h (Liu *et al.*, 2013). Important economy of scale can be made by upscaling. Additionally, Ex-SSF does not use additives neither during the extrusion step nor during the fermentations. This is a key advantage over most chemical and physico-chemical pretreatment and one less expenditure. No sophisticated reactor is required as SSF can be carried out in simple tanks. SSF can be operated in batch, fed-batch or continuous mode in combination with the feed coming from the extruder. As for the strain, *Phanerochaete chrysosporium* is a widely available fungi which can be isolated in the environment on decaying wood (Suzuki *et al.*, 2012). It has the advantage to flourish in less sterile condition in SSF contrary to bacteria in submerged fermentation (SmF). *P. chrysosporium* in SSF has a low optimum temperature (30 °C). The Ex-SSF technology also involves very little water consumption, just enough to ensure a steady flow in the barrel for extrusion and to maintain the fungal growth for SSF. Another advantage is that SSF does not required a day-to-day monitoring. Only intermittent mixing is necessary to evenly distribute the fungal colonization to avoid dead zones. About secondary revenues opportunities, several options are possible. For example, according to the results, Ex-SSF produced a relatively important amount of manganese peroxide (MnP). MnP could be extracted (eventually purified) and used for diverse purposes such as bioextrusion or commercialization. Furthermore, the residual biomass after enzymatic hydrolysis could be used as an input to produce composite materials with the extruder for construction and packaging industries (Madhankumar & Viswanathan, 2024; Rowell, 2007b). So, the extruder in the Ex-SSF approach has a double function: pretreatment and reactor to make materials. Composite materials are an important field of materials science and demand for biosourced materials is growing (Weyhrich *et al.*, 2023). Finally, extrusion and semi solid fermentation are both scalable technologies which is not always the case with conventional

technologies. Today several different sizes of extruder exist on the market, as well as larger than 2000 L vessels for SSF.

Taking everything into account, Ex-SSF is promising for a pilot or industrial scale valorization of lignocellulosic biomass, especially black spruce and corn stover as presented here. However, a complete techno-economic analysis is required to confirm the viability of the Ex-SSF technology, for example in a specific context such as biomass valorization in Quebec (Canada). This will be the focus of a future investigation.

7.5 Conclusion

The novel pretreatment approach developed in this study displayed interesting results and potential cost-effective advantages compared to existing pretreatment approaches. Manganese peroxidase (MnP) mainly responsible for the delignification was up to 13.8 U/l for Ex-SSF pre-treated black spruce (BSE) and 32.0 U/l for Ex-SSF pre-treated corn stover (CSE). This resulted in 59.1% and 65.4% biodelignification rate, respectively. The extrusion step contributed to 25.3% and 27.4%, respectively. A high lignin peroxidase (LiP) activity was recorded in raw BS and CS compared to their extruded biomasses. However, less than 17% biodelignification was recorded for the raw biomasses. The Ex-SSF pretreatment increased the cellulose crystallinity (CrI) by 13% for BSE and 4% for CSE. However, enzymatic digestibility of the Ex-SSF pretreated biomass with 0.25 ml/g enzyme led to 7.6 g/l of sugar recovery (glucose, xylose, galactose, etc.) for black spruce, which is 2.3 times the raw biomass yield. As for Ex-SSF pre-treated biomass, up to 17.0 g/l was recorded, which is 44% higher sugar concentration than the raw corn stover. Increasing the enzyme load from 0.25 ml/g to 0.50 mg/l and 0.75 mg/l did not improve the results.

7.6 Acknowledgement

This work was supported by Institut National de la Recherche Scientifique (INRS) and the Natural Sciences and Engineering Research Council of Canada (NSERC).

8 SIXIÈME ARTICLE

A concise techno-economic analysis of 2G bioethanol production integrating extrusion-biodelignification pretreatment

Analyse technico-économique préliminaire de la production de bioéthanol 2G intégrant le prétraitement par extrusion-biodélicnification

Delon Konan ¹, Adama Ndao ¹, Ekoun Koffi ², Saïd Elkoun ³, Mathieu Robert ³, Denis Rodrigue ⁴, and Kokou Adjallé ^{1,*}

1. Laboratoire de Biotechnologies Environnementales, Institut National de la Recherche Scientifique (INRS), 2605, boulevard du Parc-Technologique, G1P 4S5, Québec (Québec), Canada.

2. Département de génie chimique, Université Laval, 1065 Avenue de la Médecine, G1V0A6, Québec (Québec), Canada.

3. Center for Innovation in Technological Ecodesign (CITE), University of Sherbrooke, Sherbrooke, QC, J1K 2R1, Canada

4. Département de génie mécanique et énergétique, Institut National Polytechnique Félix Houphouët Boigny (INPHB), Yamoussoukro, Côte d'Ivoire.

5. Département de génie mécanique, Université de Sherbrooke, 2500, boulevard de l'Université, Sherbrooke (Québec) J1K 2R1.

*Correspondence: kokou.adjalle@inrs.ca

Contribution des auteurs :

Conceptualization, Writing - Original Draft: Delon Konan; Writing - Review & Editing: Adama Ndao, Ekoun Koffi, Denis Rodrigue, Saïd Elkoun, Mathieu Robert, Kokou Adjallé; Funding Acquisition, Supervision: Kokou Adjallé.

8.1 Abstract

The pretreatment is crucial stage in second-generation biorefinery. Recently, a novel pretreatment approach was developed. It consisted of a sequential coupling of extrusion and semi solid

fermentation (Ex-SSF). This study presented a concise assessment of 2G bioethanol production integrating the Ex-SSF pretreatment. Three preliminary scenarios S1, S2 and S3 were analyzed in the context of Quebec province (Canada). The CAPEX per plant capacity was 1154 \$/t, 825 \$/t, and 739 \$/t respectively for S1, S2 and S3, while the OPEX per feedstock was 57.7 \$/t for S1, 41.3 \$/t for S2 and 151.6 \$/t for S3. A 56% increase was observed when the plant capacity tripled. These metrics were used to determine two minimum profitability scenarios (M1 and M2). Simulations of M1 and M2 suggested that 2G bioethanol production from corn stover and black spruce incorporating Ex-SSF pretreatment is most appropriate for farmland larger than 400 ha, or a combination of medium-sized farmland (113 ha).

Keywords: Techno-economic analysis, lignocellulosic biomass, Ex-SSF, extrusion, solid fermentation, *Phanerochaete chrysosporium*, corn stover, black spruce.

Lien entre l'article ou les articles précédents et le suivant :

Cet article répond à l'objectif 7. C'est une analyse technico-économique préliminaire du procédé développé dans cette thèse à savoir le couplage extrusion-biodélicnification. Cette analyse s'appuie sur les résultats de prétraitement et d'hydrolyse enzymatique de l'article précédent (Article 5).

8.2 Introduction

Second-generation biorefinery in general lacks techno-economic studies to evaluate the technologies developed. Yet, technologies designed to offer an ecological alternative to fossil fuels must demonstrate economic viability if they are to be implemented. Techno-economic analysis is therefore a key requirement at the end of a technology development. Biotechnologies or process in general, while intended to be environmentally friendly, can often require important capital investment (Gallego-García *et al.*, 2023). In this case, a techno-economic analysis (even preliminary), is justified by the need to place the technology in a precise regulatory and legislative context. Such an analysis could also lead to the identification of profitability conditions and new opportunities to be explored. This remains true for second-generation biorefineries; i.e. transformation of lignocellulosic biomasses into biofuels.

Lignocellulosic biomasses (LCBs) have great potential but are under-exploited (Diwan *et al.*, 2020). Among all the available energy sources, they are the only ones that can replace fossil fuels for both energy and petrochemical applications. The main constituents of BLCs - carbohydrates

(cellulose and hemicellulose) and lignin - make them a genuine “gold mine”. Cellulose and hemicellulose, which make up between 50 and 80% of these biomasses, are prized for the sugars that can be extracted from them by enzymatic hydrolysis. Cellulose is a predominantly crystalline polymer of glucose, while hemicellulose is a heterogeneous polymer made up of D-pentoses (C5 sugars), the most common of which is Xylose (Narisetty *et al.*, 2022). Recently, a novel approach of lignocellulosic biomass pretreatment has been developed to increase enzymatic digestibility of the carbohydrates and enhance the sugar recovery (cf. § 7). The pretreatment is the sequential coupling of extrusion and semi-solid fermentation known as the (Ex-SSF) process. The present study is a concise techno-economic analysis of the integration of Ex-SSF pretreatment into 2G bioethanol production in the province of Quebec, Canada. This analysis is based on the NREL (National Renewable Energy Laboratory) report NREL/TP-510-32438 about technical-economic analysis of 2nd generation ethanol design and process (Aden *et al.*, 2002).

8.3 Materiel and methods

8.3.1 Context

Canada is the second largest country in the world after Russia and before the US. It covers 9.985 million km² of land. Its forest area is 347 million hectares which represents nearly 10% of the world total forest area. Except in the northern region of Nunavut, the forest is abundant and cover all the province and territories from Yukon territory and British Columbia in the west coast (Pacific Ocean) to Nova Scotia and Newfoundland and Labrador in the east coast (Atlantic Ocean) (CCFM, 2025). Boreal forest represents 80% of the forest land and is the main forest type in Québec province. The predominant trees are black spruce, white spruce, balsam fir, jack pine, white birch, trembling aspen, tamarack and willow (NRCan, 2025a). Canada land also serve for agriculture needs. Over the last 50 years, with the agriculture modernization in Canada, the average farm size almost doubled. In 2023, the country had 189,874 farms and covered 62.2 million hectares. Farms in Canada employed up to 247,200 workers and generate as much as 31.7 billion Canadian dollars (approximately 22.5 billion USD). These farms are mainly located in Québec province and in the southern Ontario (NRCan, 2025b). In Quebec province, corn is the main crop cultivated with 41% of crop lands. The seeded area was 430 000 ha in 2024 (Québec, 2025). The last estimation of the average farm size in Quebec was 107 ha (2021) (UPA, 2024). While Canadian forest and agricultural product have interesting market demand locally and internationally, Canadian forest and agriculture residues are largely underexploited. However, there is a growing interest in Quebec (as well as in Ontario) for the use of forest and agricultural

residues to produce value added byproducts such as second-generation bioethanol (Calvert & Mabee, 2014; Canuel *et al.*, 2023; Krigstin *et al.*, 2016; Levin *et al.*, 2011; Locoh *et al.*, 2022; WSP, 2021a). Quebec government has launched programs (Programme Bioénergies, Programme Technoclimat) to develop this niche market opportunities and reach key environmental objectives such as carbon emission reduction (Government, 2025a; Government, 2025c).

8.3.2 Study background

Lignocellulosic biomass potential has been established over the years. However, second generation biorefinery struggle to find a path in the energy industry. The pretreatment is a major concern. It is estimated up to 40% of the total valorization cost of lignocellulosic biomasses. Investigations of the literature and exploration of many pretreatment technologies, led to the proposition of novel pretreatment approach: the Ex-SSF approach (Konan *et al.*, 2022a; Konan *et al.*, 2024a; Konan *et al.*, 2024b). This approach was developed in Article 5 and was a sequential combination of extrusion (Ex) and biodelignification in semi-solid fermentation (SSF). Ex-SSF presented interesting results in terms of biomass delignification (65.4%), lignolytic enzymes production (up to 32.0 U/l), and most importantly the enhancement of reducing sugar recovery (up to 17.0 mg/l). Ex-SSF pretreatment offered key cost-effective advantages that may significantly enhance the overall profitability of the lignocellulosic biomass valorization. These advantages were among others, the flexibility of extrusion for many different uses with biomass, the low handling requirement for SSF and, the scalability of Ex-SSF technology.

8.3.3 Feedstocks

This analysis focused on two feedstocks: corn stover for agricultural residues and black spruce chips for forest residues. Corn (*Zea mays*) is the main crop produced in Quebec and Black spruce (*Picea mariana*) is one of main tree species in Quebec boreal forest.

8.3.4 Scenarios

Techno-economic analysis may strongly depend on many parameters. So, in order to investigate the biomass valorization process in different setups, three scenarios were identified to reflect Quebec province context. All the scenarios can be located in Montérégie region, or Centre-du-Québec region. These regions have the highest concentration of farmland. They are the two

principals crop production region with respectively 42% and 14% of the province crop land ([Government, 2025b](#)).

Scenario 1 (S1): A medium-sized corn farm. The cultivated land is 80% of farmland; assuming that 20% of the land is not used. The farm has no other specialized equipment and product than those required for the regular farming activities (soil preparation, seeding, irrigation, fertilization, pest and weed control, pollination, harvest, transportation storage, etc.). The farm is supposed to dispose of at least 100 m² of unaffected land for plant installation.

Scenario 2 (S2): An association of 3 medium-sized corn farms within 10 km radius. Each farm. The total farmland is three times the average farm size. The cultivated land is 80% of the farmlands. The total ([UPA, 2024](#)). Each farm possesses the basic equipment and materials for regular corn farming activities like in the first scenario. One of the farms as at least 150 m² of unaffected land.

Scenario 3 (S3): An independent entrepreneur decides to transform corn stover and black spruce residues into bioethanol. He has 3 farm suppliers for corn stover feedstock, and one forestry supplier for black spruce residues. The total corn stover feedstock is the same as in scenario 2. The black spruce supply is one third of the stover feedstock. The plant in this case is located at less than 10 km of corn stover suppliers.

8.3.5 Ex-SSF model

[Figure 8.1](#) presents the flow diagram of plant integrating the Ex-SSF (Extrusion-Semi solid fermentation) pretreatment. Biomass residues are collected and transported to the plant where a shredder reduces the residues size into smaller size (< 2 mm). The biomass is conveyed into an extruder for extensive disruption of the lignocellulose complex, size reduction and specific surface improvement. Extrudates are then subjected to semi-solid fermentation in silo for 96 hours. The liquid fraction is collected for enzymatic hydrolysis and ethanolic fermentation. Bioethanol is recovered by distillation and dehydration. The solid fraction from the SSF step is collected and conveyed to the wastewater treatment where biogas is produced to supply electricity or steam generation. Biomass pelletization, biocomposite material fabrication, enzyme valorization, carbon certificates, and others significant revenues sources associated with the use of the Ex-SSF pretreatment, were not considering in this study for conciseness and to focus only on 2G bioethanol production.

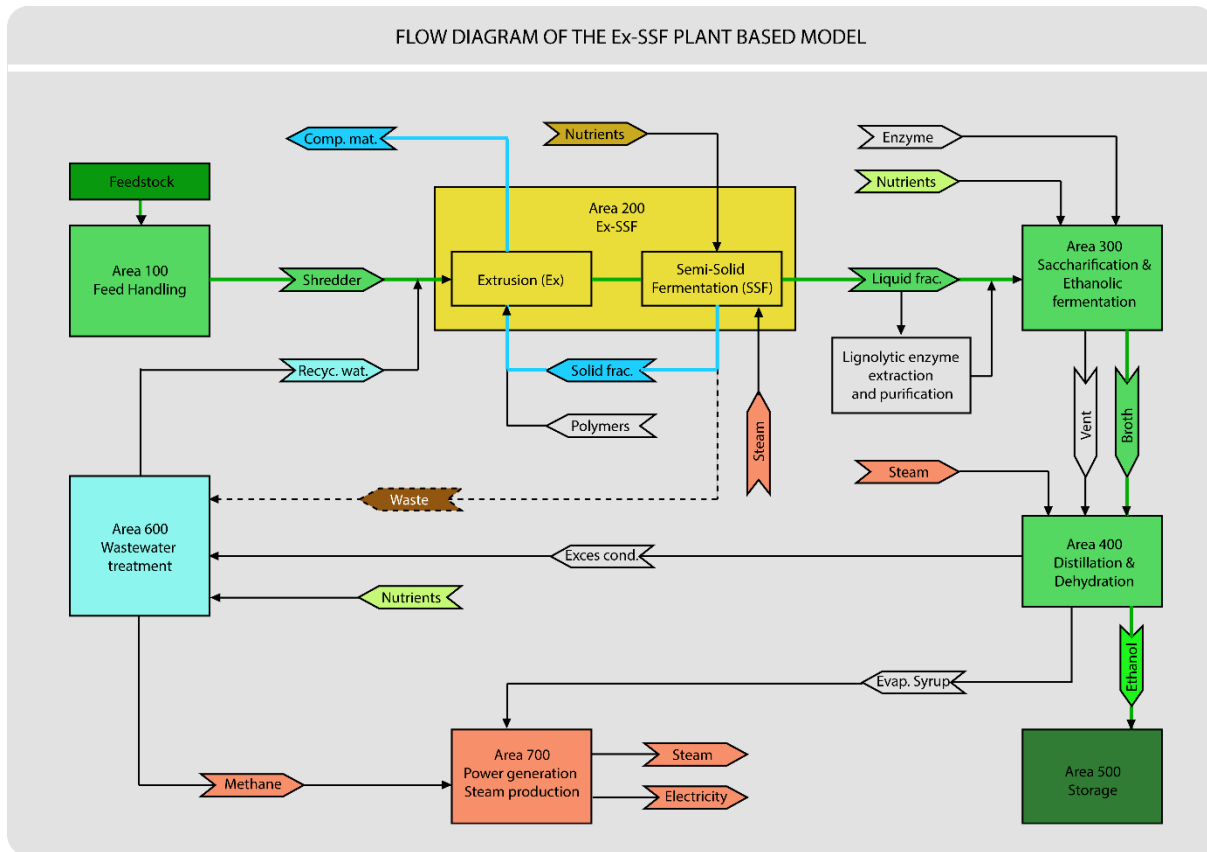


Figure 8.1 Overall process of the Ex-SSF plant based model.

8.3.6 Process technical design

8.3.6.1 Plant size, feedstock quantity and transportation

Biomass residues are collected from the field. It requires a second passage on the field with a windrower and a bale wrapper after crop harvest. The residues are then baled and directly stored in Area 100 (scenario S1) or transported over 10 km maximum to the plant facility before being stored in Area 100 (scenarios S2 and S3). Plant size in terms of effective capacity is an important decision as it may affect the overall cost of the products. It is a function of feedstock quantity (M) and can be related to transportation distance to the plant. For each scenario, the plant size was calculated based on equations given by [Nguyen and Prince \(1996\)](#) about the estimation of the optimum plant capacity (Équation 8.1, Équation 8.2, Équation 8.3).

Équation 8.1 – Plant capacity (P)

$$P = M/y$$

Équation 8.2 – Feedstock quantity (M)

$$M = \pi a Y x^2$$

Where P is the plant size in metric tons per year (Mt/y); M is the feedstock quantity to a distance x ; y is the fractional feedstock yield from the raw biomass; a is the fraction of useful land, Y is the agricultural yield per unit area (in ton per ha). The total transportation cost to the distance x is given as follow:

Équation 8.3 – Transportation cost (T)

$$T = \frac{2}{3} \pi Y a k b x^3$$

where k is the transportation cost per unit distance and unit mass, and b is the circuitry factor (a constant for the ratio of actual road length to direct distance) equal to 1.3 in Canada (Ballou *et al.*, 2002).

8.3.6.2 Feedstock handling and storage: Area 100

Upon receipt, the feedstock is inspected, sieved and eventually soaked into recycled water to remove dirt. It is then passed through a shredder to reduce the biomass size into smaller size less than 2 mm. The list of equipment is presented in Annex II with their estimated cost.

8.3.6.3 Ex-SSF pretreatment: Area 200

Area 200 is where the Ex-SSF pretreatment approach take place. This area is equipped with a co-rotative twin screw extruder and one or multiple tanks for semi-solid fermentation depending on the scenarios. The extruder has no die at the end of the barrel. The SSF stage is processed in fed-batch. The total tank volume (V_t) for SSF in each scenario and the number of tanks required (N) were determined by [Équation 8.4](#) and [Équation 8.5](#) respectively. V_t was considered as constrained by the number of available operators instead of a function of the plant capacity to minimize additional cost related to extra employment needs. The working conditions for corn stover and black spruce are based on the results of Article 4 (cf. § 6) and Article 5 (cf. § 7) ([Tableau 8.1](#)).

Équation 8.4 – Total volume of the semi solid fermentation tanks (V_t)

$$V_t = n \times \alpha$$

Équation 8.5 – Number of tanks (N)

$$N = \frac{0.6 P}{8 \alpha (m + 1)}$$

where V_t is the total volume of SSF tanks, n is the number of operators, α is the capacity of one operator in term of batch volume an individual can handle for 1 batch; N is the number of tanks required, P is the plant capacity (kg), and m the number of months for feedstocks collection.

Tableau 8.1 Ex-SSF working condition for corn stover and black spruce chips.

Parameters	Unit	Black spruce chips	Corn stover
Extrusion (Ex)			
Particle size	mm	< 2	< 5
Temperature	°C	50	65
Screw speed	rpm	233	300
Biomass/water	w/w	1	1
Semi-solid fermentation (SSF)			
Strain	-	<i>Phanerochaete chrysosporium</i>	<i>Phanerochaete chrysosporium</i>
Temperature	°C	30	30
Inoculum	ml/g	1.5	1.5
[NH ₄ Cl]	w/w (%)	0.5	0.5
Water activity	-	0.22	0.25
[Nutrients]*	mg/g	24	24

*The nutrient for 1 L of SSF volume consisted of KH₂PO₄ (0.6), MgSO₄ · 7 H₂O (0.5 g), CaCl₂ · H₂O (0.74 g), NH₄H₂PO₄ (2.32 g), yeast extract (1 g), veratryl alcohol (1 ml), CaCl · 7 H₂O (0.2 g), ZnSO₄ · 7 H₂O (0.14 g), FeSO₄ · 7 H₂O (0.5 g), MnSO₄ · H₂O (0.16 g) et CuSO₄ – H₂O (0.16 g).

After Ex-SSF, the substrate is diluted up to 20% total solid and transferred to Area 300 for simultaneous saccharification and ethanol production.

8.3.6.4 Saccharification and ethanolic fermentation: Area 300

Simultaneous saccharification and ethanol production were envisaged for cost effectiveness related to investment costs (suppression of additional separate ethanolic fermentation tank, installation, heating, and monitoring time). This setup has been proven effective for bioethanol production on various residues including lignocellulosic biomasses (Althuri *et al.*, 2018; Kádár *et al.*, 2004). The operations are in fed-batch. The computation of total vessel volume is given by

Équation 8.6 assuming a cylinder with a conical base. The working volume is taken 70% of the total volume. *Saccharomyces cerevisiae* is used as the methanogen agent for its ability to convert glucose and xylose into bioethanol. Tableau 8.2 presents the working conditions. Bioethanol production yield from *Saccharomyces cerevisiae* is estimated to be 0.46 g per g of sugar (glucose and xylose). The total bioethanol production was calculated by Équation 8.7 and is based on the results of enzymatic hydrolysis during Ex-SSF development (Article 5).

Équation 8.6 – Total volume of the vessel (V_{tsf})

$$V_{tsf} = \pi r^2 \left(h + \frac{1}{3} h_c \right)$$

Where V_{Tsf} is the total volume of the vessel, r is the radius of the cone at the bottom of the vessel ($r = \frac{1}{12}h$), h is the height of the cylinder, h_c is the height of the cone (h_c is 10% of h).

Équation 8.7 – Total volume of bioethanol (V_{EtOH})

$$V_{EtOH} = 0.46 \times V_{reducing\ sugar}$$

where V_{EtOH} is the volume of bioethanol and $V_{reducing\ sugar}$ the volume of reducing sugar.

Tableau 8.2 Simultaneous saccharification and fermentation conditions

Parameters	Unit	Black spruce chips	Corn stover
Total solid	%	40	20
Cellulases	-	Accellerase Duet	Accellerase Duet
Enzyme load	°C	0.25	0.25
Strain	-	<i>Saccharomyces cerevisiae</i>	<i>Saccharomyces cerevisiae</i>
Inoculum	%	10	10
Residence time	h	36	36
Temperature	°C	65	65

8.3.6.5 Distillation, dehydration: Area 400

This area is where the bioethanol is recovered. It starts with the filtration of the broth to retain the aqueous fraction containing the bioethanol and the dissolved CO₂. The bioethanol is then separate from water and CO₂ molecules. The azeotropic bioethanol (95% ethanol - 5% water) is further dehydrated by adsorption. This process take place into conventional distillation columns available commercially. The solid fraction is collected and used as feedstock for energy production (biogas) in area 600 or steam generation in area 700.

8.3.6.6 Product storage: Area 500

Bioethanol from Area 400 is stored into a carbon steel tank. The tank volume is calculated to accommodate one the annual bioethanol production at full capacity, plus 25% of this volume as a security margin (Équation 8.8).

Équation 8.8 – Total volume of the storage (V_{st})

$$V_{st} = 1.25 \times V_{EtOH}$$

where V_{st} is the total volume of the storage, and V_{EtOH} is the total volume of ethanol.

8.3.6.7 Waste pretreatment: Area 600

One of the advantages of the Ex-SSF pretreatment and the chosen downstream process is the low water consumption and wastewater generation. Wastewater essentially come from Area 300 and is composed of the filtrate (from which the azeotropic bioethanol has been removed), and the unused solid fraction from the broth filtration. The waste treatment setup is a digester for biogas production operated in fed-batch with a residence time of 7 days. The volume of the digester correspond to the total volume of the waste generated for 7 days of full bioethanol production. The waste quantity is estimated by Équation 8.9.

Équation 8.9 – Total volume of the digester ($V_{digester}$)

$$V_{digester} = 1.3 \times V_{wst} = 1.3 \times (V_{tsf} - V_{iEtOH})$$

Where $V_{digester}$ is the total volume of the digester, V_{wst} is total volume of waste produced per one batch of full bioethanol production, V_{tsf} is the total volume of Area 300 vessel, and V_{iEtOH} is the volume of ethanol for one batch in Area 300.

8.3.6.8 Energy generation: Area 700

The energy supplied for power, heating, steam generation is produced by the biogas from the digester. Area 700 is equipped with a cogeneration unit and a steam generator. Biogas production is estimated by Boyle's equation of methane yield estimation from biomass elemental composition ($C_e H_f O_g N_i S_j$) Équation 8.10. The corresponding power generation was calculated according to the specifications of the cogeneration unit using (Équation 8.11)(Sowunmi et al., 2016).

Équation 8.10 – Biomethane production (V_{CH_4})

$$V_{CH_4} = \frac{22.4 \times \left(\frac{e}{2} + \frac{f}{8} - \frac{g}{4} - \frac{3i}{8} - \frac{j}{4} \right)}{12.017e + 1.0079f + 15.999g + 14.0067i + 32.065j}$$

Where V_{CH_4} (ml CH_4 gVS⁻¹) is the theoretical biomethane production and e, f, g, i, j are the stoichiometric indices.

Équation 8.11 – Electricity production from biomethane (E)

$$E = V_{CH_4} \times E_{ch_4} \times \eta_E \times \eta_{TD}$$

where E (Wh) is the net potential electricity supply from biomethane, V_{CH_4} is the theoretical biomethane production, η_E is the electrical conversion efficiency of the co-generator, and η_{TD} is the transmission and distribution efficiency.

8.3.7 Project economics

The currency used for the evaluation was the Canadian dollars (referred to as \$). The economics of the project were divided into plant site development costs, equipment costs, installation costs, operation and maintenance costs, and product revenues. Plant site development cost, equipment cost, and installation cost represented the capital expenditure (CAPEX) while the operation and maintenance cost represented the operation expenditure (OPEX). Equipment cost (C_{Equip}) was calculated by aggregating the individual equipment cost, and the CAPEX was determined by [Équation 8.12](#). The installation (C_{Inst}) cost was estimated to 30% of the equipment cost [Équation 8.13](#). ANNEXE II present the detailed list of equipment per Area with their respective estimated price. These prices were obtained through diverse online catalog and platforms.

Équation 8.12 – Capital expenditure (CAPEX)

$$CAPEX = C_{Dev} + C_{Equip} + C_{Inst} = C_{Dev} + \sum C_{iEquip} + C_{Inst}$$

where $CAPEX$ is the total investment cost, C_{Dev} is the total cost of plant site development, C_{Equip} is the total equipment cost and C_{iEqu} is the cost of each individual equipment.

Équation 8.13 – Installation cost (C_{Inst})

$$C_{Inst} = 0.3 \times C_{Equip}$$

where C_{Inst} is the total installation cost, and C_{Equip} is the total equipment cost.

The operation expenditure (OPEX) was composed of the feedstock cost and the operation and maintenance cost (O&M) of the plant. Annual O&M is generally assumed to be 4% of the CAPEX and comprised chemical supplied, labor, energy consumption and by-product disposal (Santhakumar *et al.*, 2024). OPEX was calculated according to the following formula:

Équation 8.14 – Operation expenditure (OPEX)

$$OPEX = C_{Feed} + O\&M = C_{Feed} + 0.04 \times CAPEX$$

where $OPEX$ is the annual operation expenditure cost, C_{Feed} is the annual feedstock cost, $O\&M$ is the annual operation and maintenance cost, and $CAPEX$ is the capital expenditure cost.

The feedstock cost was based on the price reported by the last report of the Ministry of Energy and Natural Resources of Quebec province (Canada) on the inventory of available biomasses in the province for bioenergy production (WSP, 2021b). The feedstock cost was given by Équation 8.15.

Équation 8.15 – Feedstock cost (C_{Feed})

$$C_{Feed} = T + C_{Feed. Aquis.} = T + c \times M_{corn\ residues} + b \times M_{black\ spruce\ residues}$$

where C_{Feed} (\$/year) is the feedstock cost, T is the transportation cost (\$/year), $C_{Feed. Aquis.}$ is the feedstock acquisition cost (\$/year), c is the price of corn residues (in \$/Mt), $M_{corn\ residues}$ is the corn residues quantity (Mt/year), b is the price of black spruce chips (\$/Mt) and $M_{black\ spruce\ residues}$ is the black spruce chips quantity (Mt/year).

8.4 Results and discussion

8.4.1 Scenarios implications

Scenario 1 (S1), 2 (S2) and 3 (S3) have some technical and economic implications in term of feedstock supply, transportation, equipment, and workload. A corn field produces around 8.9 t/ha of lignocellulosic residues (García-Condado *et al.*, 2019). Between 1951 and 2016 in Quebec province, the number of farmers decreased by 21.8%. However, on the same period of time, the average farm size has been constantly growing from 51 ha (1951) to 113 ha (2006) (113 ha) before a stabilization over 10 years, and a decline during the pandemic's years (Fig. 8.2). No data was available for post-pandemic years (starting at 2022). The pre-pandemic average farm size (113 ha) was used as the average farmland size. This represents 804.6 t/year of corn stover in S1, 2413 t/year in S2 and the same quantity for the corn residues fraction of the S3 feedstock.

Although S1 beneficiaries of the lowest transportation cost because of the proximity of the feedstock to the plant (1 Km), it misses the benefit of economic of scale associated with collaboration of farmers (S2). S2 particularly could benefit from risk and cost share of equipment and workload between the associated farmers. On this matter for S1 and S3, the farmer and the entrepreneur bear all the risks and cost of their respective projects but with an additional issue for S3: The distance between the plant and the location of the feedstocks to be collected could be of critical concern. Regarding the environmental aspect, S1 is expected to be more sustainable in terms of CO₂ emission associated with transportation than S2 and S3.

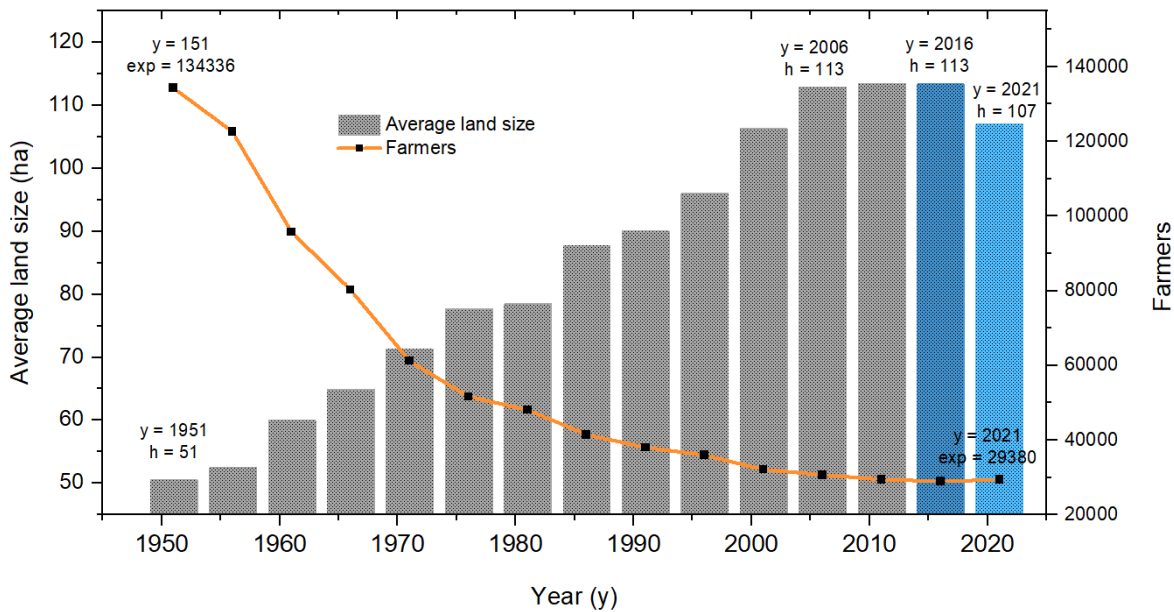


Figure 8.2 Evolution of the average farmland size (ha) and the number of farms from 1951 to 2021. Data source (Canada, 2021).

8.4.2 Capital expenditure comparison

Assuming that all the harvested residues are effectively used as feedstock ($y=1$ in Equation 8.1), the Plant capacity (P) equals the total potential residues production from the field. It was 1005.7 Mt/y in scenario S1, 3015 Mt/y in scenario S2 and 3,821 Mt/y in scenario S3. The plant capacity was used to assess the key specification of the equipment in each scenario. Tableau 8.3 shows the cost of installed equipment per area and the total equipment cost (C_{Equip}). For detailed cost estimation see Annex II and Annex III adapted from Appendix B of the NREL guide (Aden et al., 2002). Although the plan capacity of S2 and S3 were respectively 3 times and 3.8 times of the plan capacity of S1, their total equipment cost (C_{Equip}) were only 2.2 and 2.5 times the total cost

of S1. By increasing the plant capacity, an average economy of 186 000 \$ was achieved per each 1000 Mt/y (or 113 ha of corn land) added. This represented 474 000 \$ economy in S2, and 814 400 \$ economy in S3 relative to S1. For all scenarios, Area 2 (Ex-SSF pretreatment) was the heaviest budget item. It accounts for 40% of the total equipment cost in S1, 37% in S2 and 33% in S3. The extruder was the main item in Area 200 and represented between 75% and 80% of the total Area 200 cost. Although extruder might be an expensive item, it is an asset. Its advantage lies in its diversity of application. Extruders are used for diverse applications with lignocellulosic biomass including biomass pelletization and materials fabrication (Dittrich *et al.*, 2024; Pereira *et al.*, 2024; Raza *et al.*, 2024). All these applications could be significant revenue sources for the plant (using the solid waste from Area 200 after the SSF process) but was not included in this study. Area 100 was the least expansive of all areas. It accounted for 5% in all scenarios. This is one of the key advantages of the Ex-SSF pretreatment. Only biomass size reduction and humidity adjustment are required before the Ex-SSF pretreatment. Size reduction can easily be achieved on corn stover and black spruce chips with any average entry-model biomass shredder; and the humidity adjustment by simply mixing biomass and water in a 3:1 (w/w) ratio according to § 76.3.5. Installation cost was proportionated to equipment cost. It was 186 900 \$ for S1, 418 500 \$ for S2 and 465 900 \$ for S3. Additionally, to the equipment and the installation costs, pre-construction costs were also estimated for all scenarios. These were warehouse construction costs, site development costs, administrative costs, field expenses, office costs, and other non-identified costs (See Annex 2 for detailed pre-construction estimation). S1 and S2 had a cost advantage over S3 for the site development because it the land is at least cleared and graded in S1 and S2, but in S3. However, this site advantage was not significant enough to minimize the proportion of the pre-construction cost in the CAPEX. S1, S2 and S3 had respectively 1 160 550 \$, 2 490 750 \$, and 2 826 250 \$ of CAPEX, but the pre-construction cost accounted in each scenario for 30.2%, 27.2% and 28.6%. Furthermore, in term of plant capacity, the CAPEX investment was 1153.9 \$/Mt in S1, while it was 825.5 \$/Mt in S2 and 739.5 \$/Mt. The more was the plan capacity the less was the capital investment per metric ton. This metric was valuable to simulate the minimum economic profitability scenarios (§ 3.5).

Tableau 8.3 Total installed equipment costs per Area.

Process Area	Scenario 1	Scenario 2	Scenario 3
Area 100 Feedstock handling and storage	35 000 \$	80 000 \$	85 000 \$
Area 200 Ex-SSF pretreatment	250 000 \$	515 000 \$	525 000 \$
Area 300 Saccharification and fermentation	70 000 \$	190 000 \$	250 000 \$
Area 400 Distillation, dehydration	80 000 \$	205 000 \$	225 000 \$
Area 500 Product storage	42 000 \$	85 000 \$	118 000 \$
Area 600 Waste treatment	90 000 \$	200 000 \$	230 000 \$
Area 700 Energy generation	56 000 \$	120 000 \$	120 000 \$
Total equipment cost (C_{Equip})	623 000 \$	1 395 000 \$	1 553 000 \$

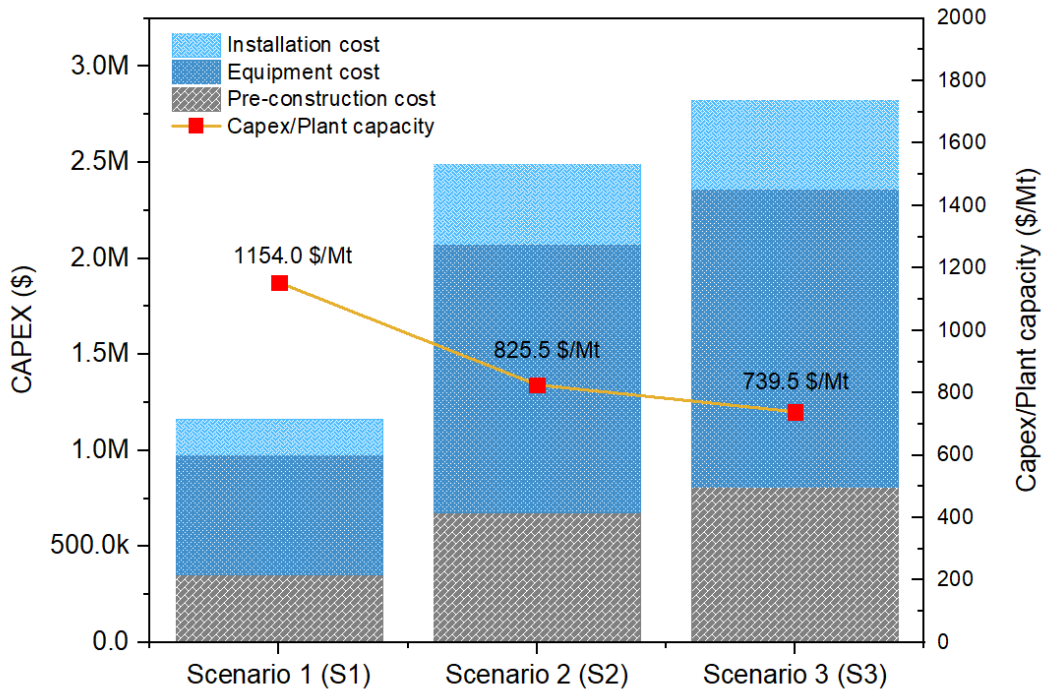


Figure 8.3 CAPEX composition and CAPEX/Plant capacity.

8.4.3 Operation expenditure comparison

The annual electricity supply generated by biogas from 600 in S1, S2 and S3 was 1250, 3751, and 5239 KWh respectively. This supply is only sufficient enough to cover the basic power need of the plant such as the lighting, and the household appliances. It was not included in the operation

expenditure estimation. The OPEX was the aggregation of the expenses related to the annual operation of the plant (chemicals, energy, labor, etc.). Its calculation was based on feedstock cost and the operation and maintenance cost. The feedstock cost was composed by the feedstock acquisition (selling) cost and the transportation cost. In S1 and S2, the acquisition cost was assumed to be zero as the farmer own the feedstock. In these cases, the feedstock cost was only composed by the transportation cost. As for S3, the acquisition cost was calculated according to the estimated price of the agricultural residues and forestry residues feedstock in Canada. Corn stover was 122 \$/t and black spruce was 100 \$/t (Government, 2024; WSP, 2021b).

Tableau 8.4 present the result of Équation 8.1 to Équation 8.15. The transportation cost in all scenarios was calculated based on the distance from moving the residues from the field to the plant. The cost per unit distance and unit mass (k) for small biorefineries is 0.63\$/m³/km (Shadbahr *et al.*, 2021). However, corn residues and black spruce chips have different density – 130 kg/m³ and 396 kg/m³ respectively (Li *et al.*, 2011; Viamajala *et al.*, 2006) – so the total feedstock cost was 439 \$/year for S1, 13 179 \$/year for S2, and 374 931 \$/year for S3. The relative high residues selling cost in S3 had drastically raised the feedstock cost in this scenario by more than 20 times compared for example to the similar crop quantity (3218.2 Mt/year) in a S2 setup (association of farmers). The OPEX followed the same trend. Figure 8.4 present the OPEX composition per scenario. OPEX computation for S1 and S2 resulted respectively in 46 861 \$/year and 112 809 \$/year while for S3 it was 487 981 \$/year. OPEX in S3 was significantly higher than in S1 and S2. When comparing the OPEX per ton of biomass, S2 was more advantageous over S3 and S1. S2 benefited the most the economy of scale due to it high feedstock quantity (M) and relatively low feedstock cost (C_{feed}). The OPEX per ton of biomass dropped from 58.2 \$/Mt to 46.7 \$/Mt; i.e. 20% reduction of the operation expenditure per metric ton of biomass, while S2 biomass quantity was only 3 times the S1 quantity. So, in similar S2 setup, increasing the biomass could benefit the economics of the plant by lowering the OPEX per ton of biomass by 6.7 \$ for each 113 ha added. These metrics can be used to determine the optimum crop quantity (and plant size) required to maximize the benefit margin of the bioethanol production process.

Tableau 8.4 Results of equations 8.1 to 8.15

Equation	Parameter	Annotation	Unit	Scenario S1	Scenario S2	Scenario S3
Eq. 1	Plant capacity	P	Mt/year	1005.7	3017.1	3821.7
Eq. 2	Feedstock quantity	M	Mt/year	804.6	2413.7	3218.2
Eq. 3	Transportation cost	T	cad	439.3	13178.8	17571.4
Eq. 4	Total volume of SSF tanks	V_t	m ³	10	30	50
Eq. 5	Number of tanks required	N	-	2	6	5
Eq. 6	Volume of the saccharification vessel	V_{tsf}	m ³	5	15	25
Eq. 7	Volume of bioethanol*	V_{EtOH}	m ³	79.75	239.23	274.88
Eq. 8	Volume of the storage	V_{st}	m ³	100	300	350
Eq. 9	Volume of the digester	$V_{digester}$	m ³	5.5	16	26
Eq. 10	Theoretical biomethane production	V_{CH_4}	m ³	337.9	1013.8	1416.1
Eq. 11	Potential biomethane electricity supply	E	KWh	1250.2	3751.1	5239.6
Eq. 12	Capital expenditure	$CAPEX$	\$	1 160 550	2 490 750	2 826 250
Eq. 13	Equipment cost	C_{Inst}	\$/year	623 000 \$	1 395 000 \$	1 553 000 \$
Eq. 14	Operation expenditure	$OPEX$	\$/year	46861	112809	487981
Eq. 15	Feedstock cost	C_{Feed}	\$/year	439	13 179	374 931

* $V_{reducing\ sugar} = 0.17\ g.g^{-1}$ of corn stover and $0.076\ g.g^{-1}$ of black spruce chips.

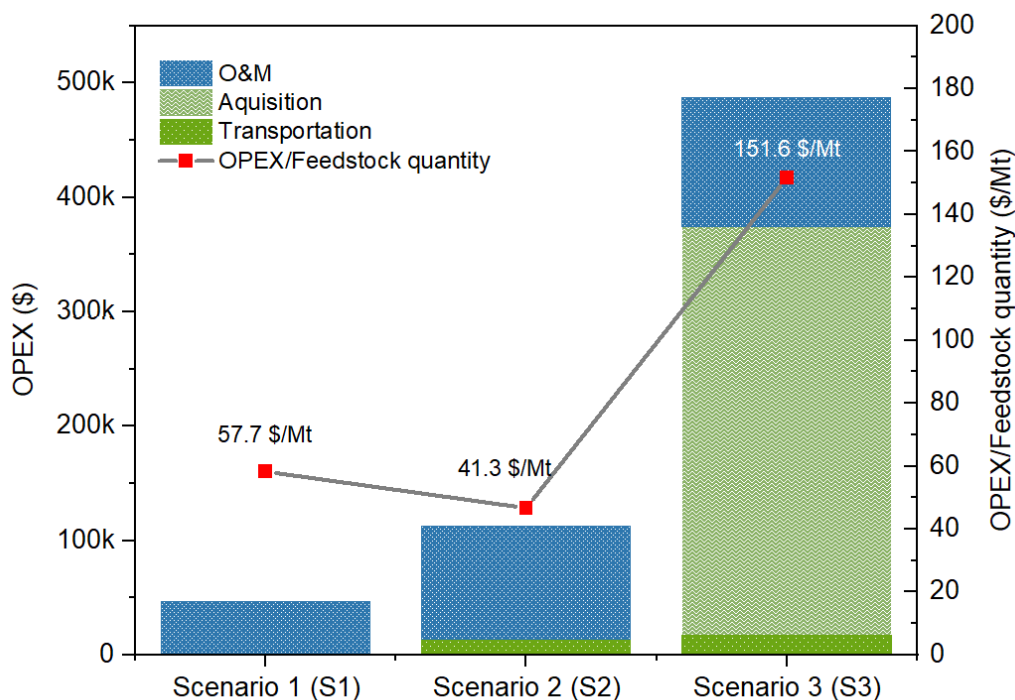


Figure 8.4 OPEX composition and OPEX/Feedstock quantity.

8.4.4 Product value comparison

The product in all scenarios was bioethanol. Biomass pellets, biogas, ligninolytic enzymes and biocomposite materials was not considered. The bioethanol value was calculated to assess the annual profitability of the plants. Bioethanol production in S1, S2 and S3 was respectively 79 750 l/year, 239 230 l/year and 274 880 l/year. Over the past five years, ethanol price fluctuated between 0.84 and 3.45 USD/Gal with a mean of 1.9937 USD/Gal (e.g. 0.38 \$/l). For S1, with a OPEX of 46 861 \$/year, the total bioethanol value was estimated at 30 305 \$/year which create a deficit of 16 556 \$. In order for the plant in S1 to be profitable (regarding only the OPEX), the bioethanol must be sold at 0.58 \$/l. For S2, with an OPEX of 112 809 \$/year, the total bioethanol value is estimated to be 90 907.4 \$/year which is 21 700 \$ less than the OPEX. However, compared to S1, the loss per farm in S2 is reduced from 16 556 \$ to 7300 \$. The primary contributor for this reduction was the plan capacity (P). This meant that by tripling the plan capacity, 56% loss reduction were achieved. More reduction could be reach by reducing the transportation cost in S2. As for S3, with an OPEX of 487 981 \$/year, the total bioethanol value was estimated to be 104 454 \$/year which is only 25% of the OPEX. The biomass acquisition cost was the principal responsible of the loss and critically affected the viability of such scenario.

8.4.5 Economic profitability scenario

Based on the previous results in scenario S1, S2 and S3, two minimum profitability scenarios (M1 and M2) were determined. **Tableau 8.5** presents the economics of the minimum profitability scenario for a single farm (Scenario M1) and, for an association of farms (Scenario M2). The ratios CAPEX/Plant capacity of S2 and S3 were the references for the ratio estimation of M1 and M2. In scenario M1, the residues are located close to the farm, which resulted in lower transport costs (1342 \$/year) instead of 13618 \$/year if multiples farms were associated like in scenario S2. The minimum feedstock quantity required in M1 was 2458.32 Mt/year, which represent 345.3 ha of corn land equivalent; i.e. 3.1 times the average farmland size in Quebec. The annual break-even point was 92 596 \$, while it was 132 659 \$ in M2. However, M2 had a lower CAPEX/Plant capacity ratio compared to M1 (644.1 \$/Mt and 742.4 \$/Mt respectively). M2 required more feedstock (1063Mt/year) than M1 to be economically viable. This resulted in 495 ha; i.e. 4.4 time the average farmland size in Quebec. The results suggested that the production of 2G bioethanol from corn stover and black spruce incorporating Ex-SSF pretreatment is more appropriate for above average farm (> 400 ha) or an association of average farms (113 ha).

Tableau 8.5 Economics of the minimum profitability scenarios

Parameter	Minimum viable scenario	
	Single farm (M1)	Association of farmers (M2)
Plan capacity	3072.9 Mt/year	4402.4 Mt/year
Feedstock quantity	2458.32 Mt/year	3521.92 Mt/year
Farmland*	345.3 ha	494.7 ha
CAPEX/plant capacity	742.4 \$/Mt	644.1 \$/Mt
Transportation	1342 \$/year	19230 \$/year
O&M	91 254 \$/year	113 429 \$/year
OPEX	92 596 \$/year	132 659 \$/year
Bioethanol volume	243 675 liters/year	349 102 liters/year
Annual revenue	92 596 \$/year	132 659 \$/year

*corn farm

8.4.6 Conclusion

A concise evaluation of the profitability conditions of the Ex-SSF process for upgrading corn stover and black spruce residues into bioethanol highlighted a number of key points: (i) the process is

suitable for large farms or medium-sized farm associations, but not for small farms; (ii) the annual operating costs are relatively low; i.e. less than 150,000 \$. However, too important fluctuation in the cost per liter of bioethanol can affect the profitability, if this is not taken into account in the economic analysis of the biorefinery; (iii) the most important compressible budget item is the pre-construction costs, which represented around 30% of the CAPEX and depended directly on the specific characteristics and conditions of the construction site. Implementing the Ex-SSF biorefinery process for a specific farm or an association of farms should enable a more detailed and specific assessment of profitability conditions.

9 DISCUSSION GÉNÉRALE, CONCLUSION, RECOMMANDATIONS

9.1 Discussion générale

La recherche menée dans le cadre de cette thèse a servi à développer une nouvelle approche de prétraitement des biomasses lignocellulosiques pour augmenter la digestibilité enzymatique des carbohydrates. Cette approche consistait au couplage séquentiel des procédés d'extrusion (réactive) et de la biodégradation par fermentation solide. La **Figure 9.1** présente la démarche adoptée pour atteindre les objectifs spécifiques de cette thèse (cf. § 1.5.4).

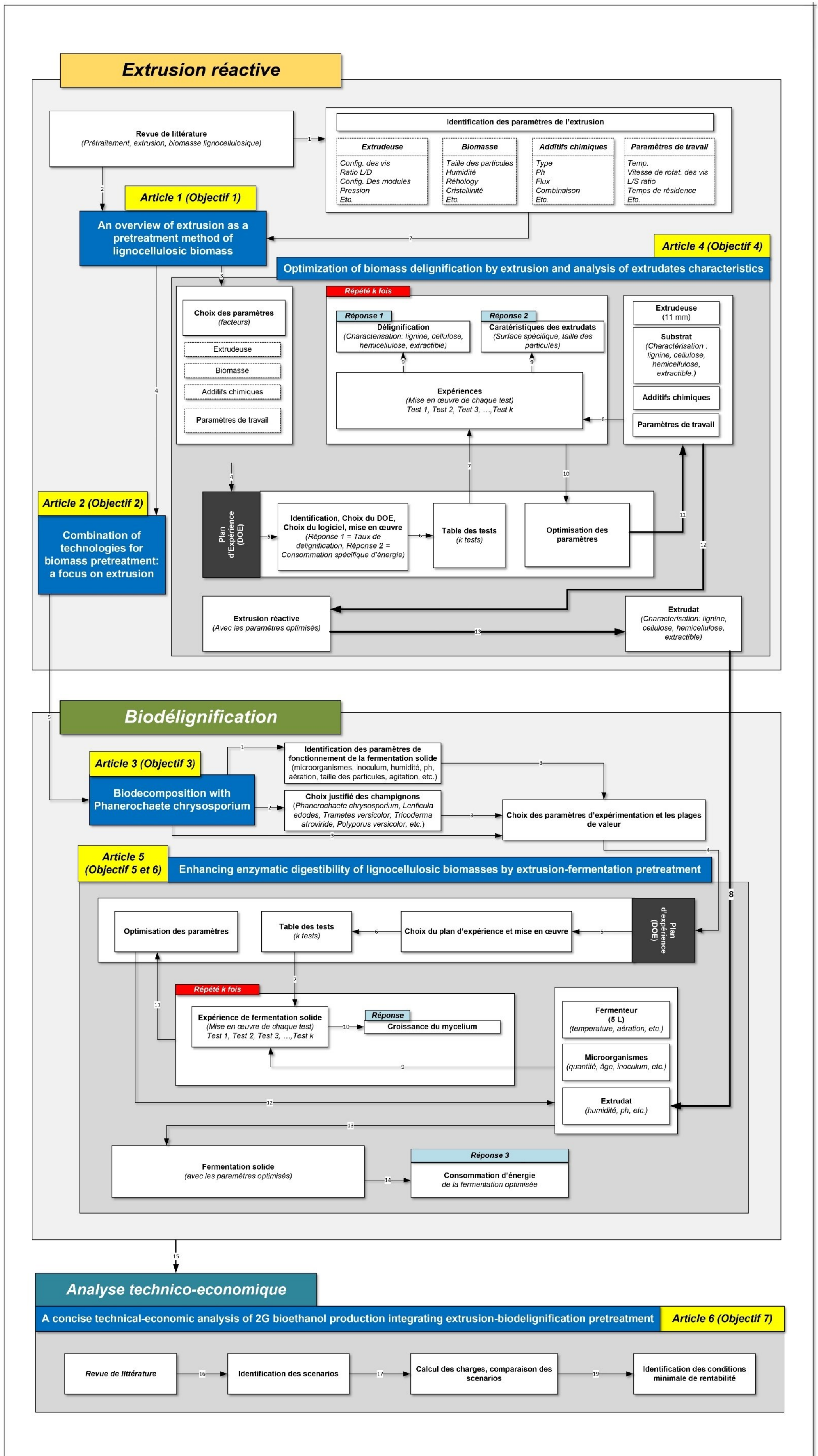


Figure 9.1 Cheminement de la thèse.

9.1.1 Évaluation du potentiel de l'extrusion et détermination des principaux paramètres de prétraitement

Explorer l'extrusion en évaluant son potentiel, ses paramètres et leurs relations permet d'identifier les paramètres les plus importants et de planifier une meilleure optimisation de l'extrusion.

9.1.1.1 Potentiel de l'extrusion

Le **potentiel** de l'extrusion comme technologie de prétraitement des biomasses lignocellulosiques a été investigué sur 20 travaux de référence présentés dans le tableau en [ANNEXE I](#). Le tableau présente, pour chacune de ces études, les caractéristiques de l'extrudeuse utilisée, les conditions de prétraitement, les biomasses prétraitées et les meilleurs taux de récupération de sucres obtenus. Les taux de récupération varient significativement entre les études (ex : 40,2 % – 78,4 % pour le glucose et 11,8 % – 43,5 % pour la xylose) et dépendent des conditions d'extrusion. Ce constat est en accord avec de précédentes études qui suggéraient que l'efficacité de l'extrusion serait liée aux paramètres d'extrusion ([Duque et al., 2013](#); [Karunanithy & Muthukumarappan, 2010](#)). En effet, en prétraitant à l'extrusion le millet vivace (*Panicum virgatum*) et la spartine pectinée (*Spartina pectinata*), [Karunanithy and Muthukumarappan \(2010\)](#) ont observé des variations plus ou moins importante dans le rendement d'hydrolyses en variant le ratio de compression des vis, la température d'extrusion et la vitesse de rotation des vis. [Duque et al. \(2013\)](#) ont observé également des différences significatives d'hydrolyses lorsque les pailles d'orges étaient prétraitées à l'extrusion et que le ratio biomasse/NaOH et la température d'extrusion variaient. Or les paramètres susceptibles d'influencer l'extrusion sont multiples ([Konan et al., 2022a](#)).

9.1.1.2 Paramètres d'extrusion

Plus d'une vingtaine de paramètres susceptibles d'influencer l'extrusion ont été investigués dans le [chapitre 3](#) et l'[ANNEXE I](#). Les paramètres les plus importants étaient : la **taille des particules** de biomasse, la **configuration des vis** de l'extrudeuse, la **vitesse de rotation** des vis de l'extrudeuse, la **température** d'extrusion, le **produit chimique** utilisé (additif) et la **concentration** de ce produit ([Konan et al., 2022b](#)).

La **taille des particules** de biomasse variait entre 0,2 – 2 mm pour les extrudeuses de moins de 20 mm de diamètre, c'est-à-dire pour les extrudeuses de 15 mm, 16 mm, 18 mm et de 20 mm ; et entre 1 – 6 mm pour les extrudeuses de plus de 25 mm, notamment celles de 25 mm, 45 mm

et 55 mm. La taille des particules de biomasse influençait le comportement rhéologique de la biomasse dans les extrudeuses. En effet, lorsque les tailles de particules de biomasse ne sont pas adaptées à la taille des vis de l'extrudeuse (ex : 5 mm de taille de particule pour une extrudeuse de 16 mm de diamètre de vis), il se crée une instabilité dans la rotation des vis. De plus, les biomasses de taille de particules supérieure à 2 mm engendrent généralement une augmentation du **torque** et de la **consommation spécifique d'énergie** (SME) (Gu *et al.*, 2019).

Les **configurations des vis** étaient constituées de quatre types d'éléments de vis ayant des fonctions différentes. Il s'agissait d'éléments de vis de transport avant (F et T), d'éléments de vis de pétrissage (M) et d'éléments de vis de transport retour (R) (cf. § 3.5.3). Leur agencement (enchaînement) les uns à la suite des autres définissait la configuration des vis. La configuration standard pour le prétraitement de biomasses lignocellulosiques était celle proposée par (Gatt *et al.*, 2018). Il s'agit de l'agencement F-T-M-R-M-R-M-T. Cet enchaînement capitalise sur la séquence M-R, sur laquelle une tendance avait été observée dans plusieurs études. Lorsqu'un élément de transport retour (R) est placé après un élément de vis de pétrissage (M), il est observé une augmentation du taux de récupération de sucre (Kuster Moro *et al.*, 2017; Negro *et al.*, 2015). En effet, lors du passage de la biomasse dans la zone M, elle est mastiquée puis convoyée à l'élément R qui la renvoie à nouveau dans la zone M. Ce cycle se poursuit jusqu'à ce que la biomasse soit suffisamment fine (voire pâteuse) pour traverser la zone R. Toutefois, il s'en suit un risque majeur qui est l'accumulation de matériel et l'augmentation de la **pression** dans le baril de l'extrudeuse. Cette pression résulte de l'accumulation de biomasse dans la zone de transport avant (T) qui précède les zones M-R (Vandenbossche *et al.*, 2015).

La **vitesse de rotation des vis** était inversement proportionnelle au temps de résidence des biomasses dans l'extrudeuse. Cependant, même avec des vitesses de rotation relativement élevées, c'est-à-dire comprises entre 120 - 300 rpm, il était possible de recirculer les extrudats plusieurs fois, ou d'augmenter la longueur des vis et accroître le temps de résidence. La première option était la plus raisonnable pour la réduction de la **consommation d'énergie**. Cependant, après la première recirculation, celles d'après n'amélioreraient pas significativement le taux de récupération de sucre obtenu au premier passage (Da Silva *et al.*, 2013b; Duque *et al.*, 2018b; Kuster Moro *et al.*, 2017). Ces résultats pourraient s'expliquer par le fait que le **torque** de l'extrudeuse et les **forces de cisaillement** qui en résultent seraient positivement corrélées à la rigidité du substrat extrudé. Plus le substrat est rigide (c'est-à-dire fibreux dans le cas des BLC), plus haut est le torque requis pour entraîner les vis et plus importante est l'intensité des forces de cisaillement générées par les frottements. Or, la biomasse est beaucoup plus fibreuse lors du

premier passage que lors des passages suivants parce qu'elle est brute et n'a subi aucun traitement préalable.

La **température** variait beaucoup d'une étude à une autre : entre 50 °C et 200 °C. Pour le même type de résidus de maïs par exemple, [Zhang et al. \(2014c\)](#) avaient obtenu leur meilleur résultat en utilisant uniformément 99 °C sur les vis de l'extrudeuse. Wang ([Wang et al., 2020](#)) avait utilisé uniformément 120 °C et Duque ([Duque et al., 2021](#)) avait utilisé une combinaison de différentes températures (50 °C, 100 °C, etc.). Le rôle de la température est d'améliorer la déstructuration de la lignocellulose en apportant l'énergie d'activation nécessaire aux molécules et aux liaisons chimiques contenus dans la biomasse. En effet, pour la cellulose par exemple, lorsque la température interne de la biomasse est supérieure à 200 °C, on observe la rupture des liaisons hydrogène, puis s'en suit une reconfiguration des zones cristallines de la cellulose en zones amorphes ([Wada et al., 2003](#)). Cette reconfiguration participe à la désorganisation du complexe lignocellulosique et à la fragilisation des liaisons (hydrogènes et covalentes) entre les principaux composants de la biomasse. Cela a pour conséquence de réduire l'énergie mécanique nécessaire à l'extrusion de cette biomasse. Dans le but de maximiser cet effet, certaines études utilisent également des **additifs chimiques** durant l'extrusion : on parle d'extrusion réactive ([Calcio Gaudino et al., 2022a](#)).

Les **additifs chimiques** utilisés pour prétraiter les BLC par extrusion réactive étaient des catalyseurs, des solvants ou des enzymes. Des produits chimiques particuliers, tels que les liquides ioniques et les solvants eutectiques profonds, étaient aussi employés ([Ai et al., 2020](#); [Han et al., 2020](#)). L'emploi des additifs chimiques vise la rupture des liaisons chimiques entre les composants de la biomasse (cellulose, hémicellulose, lignine) et à l'intérieur de leur structure respective. L'hydroxyde de sodium (NaOH) est le plus commun pour son accessibilité, son faible coût et sa faible toxicité comparés à la plupart des autres produits, mais aussi pour son efficacité à désorganiser la structure chimique des BLC. Lorsqu'il est solubilisé en présence de BLC (charge <10 % w/w), l'hydroxyde de sodium attaque les liaisons éther-éther (R – O – R') dans l'hémicellulose et la lignine, les liaisons éther et carbone-carbone (C – C) dans la lignine. Il possède ainsi une capacité de dé-acétylation (CH₃ – CO–) de la biomasse ([Modenbach & Nokes, 2014](#)). Son efficacité sur ces liaisons peut être améliorée par l'augmentation de la température entre 25 °C et 150 °C.

9.1.1.3 Conclusion

Ces recherches démontrent d'une part que l'extrusion est une méthode de prétraitement non sélective, c'est-à-dire qui peut être utilisée sur divers types de biomasses lignocellulosiques. D'autre part, l'extrusion possède des paramètres clés et dont l'optimisation est essentielle pour maximiser l'efficacité de l'extrusion. Enfin, ces résultats suggèrent que l'extrusion pourrait être un excellent premier traitement dans le cadre d'un couplage de technologie de prétraitement.

9.1.2 Analyse des couplages de prétraitement impliquant l'extrusion et proposition d'une nouvelle approche de prétraitement.

Analyser les couplages existants permet de proposer une approche prometteuse de prétraitement des biomasses sur la base des résultats de travaux antérieurs.

9.1.2.1 Nature des couplages existants

Le [chapitre 4](#) explore les couplages de prétraitement impliquant l'extrusion. Les couplages existants sont des associations de l'extrusion avec des prétraitements physiques, des prétraitements physico-chimiques et des prétraitements chimiques. Les prétraitements physiques employés consistent essentiellement au prétraitement au microonde et à l'ultrasonication. Les prétraitements physico-chimiques concernés sont entre autres, l'explosion à la vapeur, le prétraitement à l'eau chaude et l'explosion des fibres ammoniac (AFEX). Quant aux prétraitements chimiques, ils incluent l'organosolvation, les solvants eutectiques profonds (DES) et les liquides ioniques (ILs). Si plusieurs de ces couplages offrent des avantages intéressants du point de vue de l'amélioration de l'hydrolyse enzymatique des biomasses prétraitées, ils possèdent cependant des inconvénients qui limitent leur implémentation dans les procédés biotechnologiques de deuxième génération ([Konan et al., 2024b](#)).

9.1.2.2 Analyse des couplages existants

Le [Tableau 9.1](#) présente le potentiel des différents couplages et les défis qui limitent leur exploitation. Quoique la plupart de ces couplages permettent d'atteindre plus de 90 % de taux de récupération de sucres, de nombreuses difficultés cependant entravent l'utilisation de ces couplages à grande échelle. La **consommation d'eau** demeure un problème majeur. D'importantes quantités d'eau sont utilisées pendant le prétraitement pour déstructurer les BLC avec des charges solides inférieures à 15 % p/p, ce qui entraîne la génération de grandes

quantités d'eau usées dont le traitement ou la récupération nécessitent de l'énergie et des intrants chimiques. L'eau est aussi utilisée après le prétraitement pour séparer (lavage) les produits chimiques des BLC avant la phase d'hydrolyse enzymatique (Nakasu *et al.*, 2021). Ainsi, Zhang (Zhang *et al.*, 2023) préconise l'utilisation de prétraitements à fortes charges solides dans les procédés de bioraffinerie pour diminuer la consommation d'eau et d'énergie. L'extrusion à elle seule ne nécessite pas d'utilisation d'eau puisqu'une humidité de 50 à 80 % de la biomasse est suffisante pour procéder à l'extrusion. C'est aussi une technologie à faible **consommation d'énergie** par quantité de biomasse prétraitée (Gu *et al.*, 2018). Cependant, cet avantage est mitigé lorsque l'extrusion est couplée aux prétraitements physiques. Ces prétraitements nécessitent une forte puissance électrique pour produire des ondes de hautes fréquences comprises entre 16 kHz et 2,5 GHz. L'efficacité de ces traitements sur les BLC repose sur la capacité des ondes à engendrer la cavitation des molécules d'eau au contact des BLC et à augmenter la température interne des composants de la biomasse (Kerboua *et al.*, 2022). De telles opérations peuvent prendre entre 30 min et plusieurs heures pour atteindre l'efficacité des méthodes de prétraitement chimique par exemple. Les puissances requises dans ces prétraitements affectent le bilan énergétique des couplages avec l'extrusion. En plus des défis de consommation d'eau et d'énergie, la **mise à l'échelle** des couplages existants est un enjeu technique important. Dans le cas du couplage avec des prétraitements physiques, le **transfert de chaleur** est le principal problème (Flores *et al.*, 2021; Ong & Wu, 2020a). L'énergie thermique est produite lorsque le champ électromagnétique créé par les ondes à haute fréquence fait vibrer les molécules polaires dans la biomasse (principalement les molécules d'eau). Cette énergie se propage ensuite dans la biomasse par conduction, c'est-à-dire de proche en proche, par contact. Le problème du transfert de chaleur se pose lorsque les quantités importantes de BLC sont traitées. En effet, les BLC sont des milieux discontinus constitués de particules de tailles différentes. Les particules sont séparées par l'air, qui est un très mauvais conducteur thermique. À titre de comparaison, la conductivité thermique de l'air à 25 °C et à la pression atmosphérique est d'environ 0,025 W/m·K, tandis qu'elle est de 0,597 W/m·K pour l'eau à température et pression égales (Singh & Heldman, 2014). En l'absence de fluide approprié (eau, solvant, etc.), il se crée des zones mortes dans la partie intérieure de la biomasse dues au tassement des particules de biomasse. Des zones chaudes aussi apparaissent dans la partie extérieure de la biomasse où s'accumule la chaleur. Pour les prétraitements chimiques, les **coûts de prétraitement** constituent les défis majeurs. Cette difficulté est inhérente aux produits chimiques. La lignocellulose est un composé complexe et récalcitrant. Les produits chimiques utilisés pour désorganiser sa structure chimique nécessitent une certaine agressivité. Les liquides ioniques,

les solvants eutectiques et l'ammonium sont assez efficaces pour rompre les liaisons β (1 – 4), C – C et hydrogènes de la biomasse. Ce sont néanmoins des produits dispendieux, peu biodégradable et écotoxiques (Baaqel *et al.*, 2020; Flieger & Flieger, 2020; Vaidya *et al.*, 2022). Les liquides ioniques aprotique, qui sont les plus couramment utilisés pour le prétraitement de BLC, coûtent entre 2,50 et 50 \$USD/kg comparé à 0,45 \$USD/kg pour des solvant conventionnels comme l'éthanol (Ovejero-Pérez *et al.*, 2024). Ces difficultés limitent l'utilisation à grande échelle des couplages extrusion-prétraitement chimique. Quant aux prétraitements physico-chimiques, les difficultés rencontrées dans la mise à l'échelle se situent au niveau du **design des réacteurs**. Les prétraitements physico-chimiques consomment d'importants volumes d'eau et nécessitent conséquemment des réacteurs de grande taille pour prétraiter de faibles quantités de biomasses. De plus, ce sont des prétraitements très corrosifs pour les métaux et les alliages (Chen *et al.*, 2022b; Ruiz *et al.*, 2020). En effet, les cycles de prétraitement font intervenir des températures élevées allant de 130 à 400 °C, de hautes pressions pouvant atteindre 5 MPa et des catalyseurs chimiques dont les propriétés corrosives sont augmentées par ces températures et pressions. Les catalyseurs habituels sont l'acide sulfurique (H₂SO₄), l'oxyde de soufre (SO₂) et le dioxyde de carbone (CO₂). La difficulté ici réside à optimiser le design des réacteurs et les équipements post-traitement de manière à minimiser l'énergie et les volumes d'eau utilisés, ainsi que de réduire les coûts liés au design des équipements. Ceci demeure à ce jour une entreprise à risque technique et financier élevés.

9.1.2.3 Proposition d'une nouvelle approche de prétraitement

D'une part, les couplages existants échouent à être implémentés pour des raisons qui sont intrinsèques à la nature de ces couplages. D'autre part, le constat général est que les couplages existants emploient l'extrusion comme un moyen rapide de réduction des tailles de particules des BLC, sans capitaliser sur les caractéristiques des extrudats. Les BLC prétraités à l'extrusion présentent des caractéristiques uniques de défibrillation, de réduction des tailles de particules et d'augmentation des surfaces spécifiques des particules. Au regard des résultats qui précèdent, il a été proposé une approche biologique de prétraitement des BLC (biodélicnification en fermentation solide) en combinaison avec l'extrusion. Les caractéristiques et avantages liés à la biodélicnification en fermentation solide sont présentés dans le [Chapitre 5](#). L'approche Ex-SSF (Extrusion – biodélicnification en fermentation solide) consiste au prétraitement de la biomasse brute par extrusion suivie de la biodélicnification des extrudats en fermentation solide avec *Phanerochaete chrysosporium*. En effet, les champignons de la pourriture blanche, tel que

Phanerochaete chrysosporium, sont naturellement capables de dégrader la lignine grâce à un puissant système d'enzymes lignolitiques constitués de MnP, de LiP et de Lacasse. Toutefois, la performance de *P. chrysosporium* requiert une défibrillation importante de la biomasse et une grande surface spécifique pour les particules de biomasse (Konan *et al.*, 2024a). Le **Tableau 9.1** présente une comparaison des systèmes étudiés.

Tableau 9.1 Potentiel des couplages et défis associés à leur implémentation.

Pretreatment	Biomass	Results	References
Extrusion - Liquid hot water	Eucalyptus, aspen wood (Tian <i>et al.</i> , 2019)	Xylans conversion: 54% for eucalyptus and 38.1% for aspen wood; Cellulose hydrolysis: 79.6% for eucalyptus and 100% for aspen wood	Reactor design, kinetic model, heat transfer model, reactor corrosion, water consumption, energy consumption, large scale studies, continuous reactor.
Extrusion - Steam explosion	Corn cob (Zhang <i>et al.</i> , 2014a)	Hemicellulose conversion: 90%	(Chen <i>et al.</i> , 2022b; Heidari <i>et al.</i> , 2019; Li <i>et al.</i> , 2013; Pavlovic <i>et al.</i> , 2013; Ruiz <i>et al.</i> , 2020)
	Corn stover (Chen <i>et al.</i> , 2014)	Sugar recovery yield: 89%	
	Hazelnut skin (Oliva, 2017)	Lignin reduction from 35% to 29.4%; methane production 310.6 ml CH ₄ /g VS	
Extrusion - Ultrasonication	Rice hull (Zhang <i>et al.</i> , 2020)	Carbohydrates conversion: 77.7%; Sugar reducing yield: 381.59 mg/g (sugar), 291.59 mg/g (glucose), and 88.87 mg/g (xylose) of rice hull	Energy waste, optimization of energy consumption, reactor design, economic profitability, uniformity of cavitation activity. (Flores <i>et al.</i> , 2021; Ong & Wu, 2020a)
	Miscanthus sacchariflorus (Byun <i>et al.</i> , 2020)	Sugar recovery: 83.1%	
Extrusion - Microwave	Switchgrass (SG) and Big bluestem (BB) (Karunanithy <i>et al.</i> , 2014)	Sugar recovery: 59.2% (SG) and 68.1% (BB); glucose recovery: 52.6% (SG), 83.2%; xylose recovery: 75.5% (SG), 92.1% (BB)	Fundamental understanding of microwaves heating system, the penetration depth of the waves inside the biomass, dielectric properties of different biomass, uneven distribution of microwave energy, inhomogeneity of reaction temperature, missing technical information for commercial design and development, need for electrical energy, risk of overheating (degradation of compounds). (Kostas <i>et al.</i> , 2017; Mitani, 2018; Puligundla <i>et al.</i> , 2016; Robinson <i>et al.</i> , 2022)
Extrusion - Ionic liquid	Wood powder of pussy willow (Han <i>et al.</i> , 2020)	Glucose yield: 99%; xylose yield: 99.5%	Toxicity, stability, moisture sensibility, high viscosity, solvent regeneration and recycling, reaction kinetic and parameters, development of biobased ILs, costliness, lack of scale-up studies. (Amini <i>et al.</i> , 2021; Asim <i>et al.</i> , 2019; Badgujar <i>et al.</i> , 2019; Chen <i>et al.</i> , 2022a; Zhang <i>et al.</i> , 2021b)
	Sugarcane bagasse (Da Silva <i>et al.</i> , 2013b)	Glucose yield: 92.2%; xylose yield: 85.9%	
Extrusion - Deep eutectic solvent	Sorghum bagasse (Ai <i>et al.</i> , 2020)	Glucose yield: 87.0%; xylose yield: 86.5%	Thermal stability, high viscosity, lack of life cycle analysis and techno-economic studies, inhibitor generation, contaminant

Pretreatment	Biomass	Results	References
			susceptibility, recycling, clarifying reaction mechanism, thermodynamic models, computer simulation, the influence of water molecule in DES. (Chen <i>et al.</i> , 2021a; Chen <i>et al.</i> ; Florindo <i>et al.</i> , 2019; Sattlewal <i>et al.</i> , 2018; Tang <i>et al.</i> , 2017)
Extrusion - Organosolv	Prairie cordgrass (Brudecki <i>et al.</i> , 2013)	Glucose yield: 92%; lignin removal: 87% xylan removal: 95%	Corrosivity, high volatility, flammability, toxicity, large amount of water used in the process, high process cost, energy consumption, compounds recovery (solvent and catalyst), high temperature, continuous organosolv process. (Vaidya <i>et al.</i> , 2022; Wei Kit Chin <i>et al.</i> , 2020; Zhang <i>et al.</i> , 2022; Zhao <i>et al.</i> , 2022)
	Wheat straw (Beisl <i>et al.</i> , 2017)	Lignin extraction: 22.3%	
Extrusion - AFEX	Corn stover (Dale <i>et al.</i> , 1999)	Enzymatic hydrolysis increased by 3.5 times compare to untreated	High temperature and pressure, energy consumption, environment pollution, partial lignin removal, ineffective on high-lignin biomass, cost of ammonia. (Wagle <i>et al.</i> , 2022; Zhao <i>et al.</i> , 2022)

9.1.3 Optimisation des paramètres d'extrusion et analyse des caractéristiques des extrudats

Les paramètres d'extrusion ont été investigués et optimisés pour le prétraitement de résidus de maïs (RMA) et de résidus d'épinette noire (REN). Les RMA et les REN sont des biomasses abondantes au Canada et particulièrement dans la province de Québec. On estime à 549 000 tonnes la quantité annuelle de biomasses agricoles disponibles pour produire de la bioénergie et à 762 000 tonnes la quantité annuelle de résidus forestiers disponibles pour produire de la bioénergie (WSP, 2021b). Le maïs est la principale céréale cultivée au Québec et l'épinette noire est l'une des principales essences de bois des vastes forêts boréales que compte la province (NRCan, 2025a) (Québec, 2025).

9.1.3.1 Biomasses lignocellulosiques étudiées

Les RMA utilisés dans cette étude étaient constitués de différentes parties non comestibles de la plante (pédoncules, spathes, stigmates, etc.). Quant aux REN, il s'agissait de copeaux du tronc de l'arbre sans l'écorce. L'holocellulose (cellulose et hémicellulose) représentait $55,5 \pm 1,2\%$ des RMA et $60,1 \pm 1,6\%$ des REN. Cependant, les REN comptaient deux fois plus de lignine que les RMA. Ces résultats de caractérisation sont cohérents avec ceux de Zhang *et al.* (2018) et de Fang *et al.* (2011). La lignine joue un rôle de structure plus important chez les plantes gymnospermes (épinette noire) que chez les herbacés (maïs). L'épinette noire possède des

adaptations anatomiques et physiologiques dans les climats froids. Pour éviter l'embolie due au gel des nutriments dans son système vasculaire, elle possède de petites trachéides avec des parois épaisses, ce qui a pour conséquence d'augmenter la densité du bois et sa teneur en lignine (Krause *et al.*, 2010; Puchi *et al.*, 2020).

9.1.3.2 Conditions d'extrusion

Les conditions d'extrusion des RMA et des REN avant optimisation étaient basées sur les résultats de (Konan *et al.*, 2022a) (cf. § 9.1.1). Les **tailles des particules** investiguées étaient 1 mm et 1,5 mm. La **configuration des vis** consistait en 4 zones de transport avant (F et T) et 3 zones de pétrissages (K) de différentes longueurs. La séquence d'agencement était T-K-F-K-F-K-F-T. Les éléments de vis retour (R) dans la configuration standard ont été remplacés par des éléments de vis de transport pour prévenir une accumulation trop importante de matériel et une élévation de la pression dans le baril de l'extrudeuse vu le faible diamètre des vis (11 mm) (Gatt *et al.*, 2018). La **vitesse de rotation** des vis allait de 80 à 300 rpm. Les **températures** d'extrusion étaient comprises entre 40 et 110°C. L'**additif** utilisé était l'hydroxyde de sodium entre 15 % p/p et 0 % p/p (eau). Le plan central composite a permis de générer une série de 30 tests d'extrusion par biomasse.

Bien que le ratio biomasse:additif ait été ajusté à 3:1 pour les deux biomasses avec une siccité de départ égale (>95 %), l'**humidité** des extrudats variait entre 5,4 % et 34,8 % pour les résidus de maïs, ainsi que 23,6 % et 59,2 % pour les résidus d'épinette noire. Ces résultats suggèrent que les résidus d'épinette noire conservent mieux l'humidité lors de leur passage dans l'extrudeuse que les résidus de maïs, avec des différences significatives d'un test à l'autre pour la même biomasse. Une perte trop importante d'humidité des biomasses augmente non seulement le risque de carbonisation de la biomasse dans l'extrudeuse, mais aussi le risque de bourrage des vis. Ce phénomène peut être important si les vis ne parviennent pas à briser la rigidité de la biomasse.

Les **tailles de particules** des extrudats ont été analysées. Elles étaient comprises entre 68 et 205 µm pour les REN et entre 115 à 1203 µm pour les RMA. Ces résultats montrent que les forces de cisaillement générées par les vis ont été suffisamment importantes pour réduire les tailles des particules de biomasse brutes. Les différences de tailles de particules observées entre les REN et les RMA peuvent s'expliquer par la différence de comportement mécanique des deux biomasses. Les REN sont cassants, c'est à dire peu résistants à la déformation, contrairement aux résidus de maïs qui sont plus flexibles compte tenu de leur basse teneur en lignine. Le module

d'élasticité est de l'ordre de 100 – 140 MPa pour les résidus de maïs contre 60 – 70 MPa pour l'épinette (Mohite *et al.*, 2022; TWD, 2025). L'analyse de la **Figure 6.5** démontre cependant que la taille des particules de départ n'a pas d'influence significative sur la taille des particules des extrudats. La taille des particules des extrudats dépend premièrement du type de biomasse puis d'une combinaison de l'humidité, de la température et de la vitesse de rotation des vis. En comparant les tailles de particules après extrusion avec des résidus bruts passés au broyage, il a été démontré que le broyage, même après plusieurs passages, ne permettait pas d'approcher les résultats obtenus avec l'extrusion (**Figure 6.6**). En effet, la diversité de forme, de taille, d'inclinaison et d'agencement des éléments de vis d'une extrudeuse confèrent à l'extrusion un avantage unique pour déstructurer la biomasse.

9.1.3.3 Taux de délignification

Les **taux de délignification** des tests d'extrusion ont été analysés dans le but de déterminer les meilleures conditions de prétraitement avant l'optimisation des paramètres d'extrusion. Les taux de délignification variant entre 2,2 % et 23,5 % pour les REN et entre 1 % et 25,3 % pour les RMA. La précision enregistrée sur les taux était inférieure à 1,2 %. Ce qui équivaut à une bonne estimation sachant que la méthode Klason est une méthode d'analyse gravimétrique. Le meilleur taux de délignification pour les REN a été obtenu avec de la biomasse de 1 mm de taille de particule extrudée à 225 rpm à 75°C avec 0% de NaOH (eau). Celui des RMA a été obtenu également avec des biomasses de 1 mm extrudé seulement avec de l'eau (0% NaOH), mais à 300 rpm et 50 °C. L'hypothèse de départ prévoyait que les tests avec 7,5 % p/p et 15 % p/p NaOH permettraient d'obtenir de meilleurs taux qu'avec 0 % NaOH (eau). Ce ne fut pas le cas. En revanche, les deuxièmes meilleurs résultats (22,3 % pour les REN et 23,7 % pour les RMA) confirmaient cette hypothèse. Ce résultat s'expliquerait par le fait qu'en condition alcaline et à haute température, la lignine ait tendance à se recondenser pour former un complexe pseudo-lignine (Yang *et al.*, 2021). Or, même si la température d'extrusion est réglée qu'à 75 °C pour REN et 50 °C pour RMA, localement dans la biomasse, par contre, les frictions entre les vis de l'extrudeuse et les particules de biomasse peuvent accroître significativement la température interne de la biomasse.

9.1.3.4 Modélisation des extrusions

L'**analyse ANOVA** des résultats des tests d'extrusion a été réalisée dans le but de modéliser le taux de délignification en fonction des paramètres de prétraitement clés que sont la vitesse de

rotation des vis (A), la température d'extrusion (B), la concentration de NaOH (C) et la taille des biomasses brutes (D) (Cf. § 6.4.4). Les modèles numériques des RMA et des REN est donné respectivement par les équations de régression Y_1 et Y_2 (Équation 6.6 et Équation 6.7). Le modèle des RMA démontre que la vitesse de rotation des vis (A) est le seul paramètre constituant l'effet principal. Les trois autres paramètres, quant à eux, participent essentiellement aux effets d'interaction à 2 variables et plus (ex : BC, ABCD, A^2BD). Ceci signifie que la vitesse de rotation des vis a une influence directe sur le taux de délignification des RMA, contrairement aux autres paramètres qui influencent la délignification par l'entremise d'effets d'interactions entre les paramètres. Pour ce qui est du modèle pour les REN, tous les paramètres participent de manière indépendante aux effets principaux et aux effets d'interaction.

9.1.3.5 Optimisation des modèles d'extrusion

Les modèles Y_1 et Y_2 ont permis d'optimiser les conditions d'extrusion pour maximiser le taux de délignification. Le solveur intégré au logiciel Design Expert a été utilisé à cet effet. Les contraintes d'optimisation imposées sont présentées dans le tableau ci-dessous (**Tableau 9.2**). Les résultats d'optimisation indiquaient un maximum de délignification de 26,6 % pour les RMA dans les conditions suivantes : Vitesse de rotation des vis = 233 rpm, température d'extrusion = 50 °C, concentration de NaOH = 0%, et la taille des particules de biomasses brutes = 1 mm. Les résultats expérimentaux confirment les prédictions du modèle d'optimisation à +0.8 % près, soit 27.4 %. Ces conditions présentent plusieurs avantages majeurs. D'abord, 233 rpm est une vitesse relativement faible pour l'extrudeuse utilisée ($v_{\max} = 1000$ rpm). À cette vitesse, l'extrusion des biomasses est stable. Ensuite, une faible température d'extrusion optimale (50 °C) est avantageuse pour minimiser la consommation d'énergie de l'extrudeuse. En effet, les températures habituelles d'extrusion de biomasse sont comprises entre 100 et 150 °C (Konan *et al.*, 2022a). Enfin, ces conditions suggèrent l'utilisation de l'eau (0% p/p NaOH) plutôt qu'une solution d'hydroxyde de sodium. Cela supprime non seulement les coûts liés à l'achat de produit chimique, mais aussi l'étape de lavage des extrudats, donc moins d'utilisation d'eau et d'énergie, et un gain de temps dans l'étape de post-extrusion. Pour ce qui est de l'optimisation des REN, le modèle prédisait un maximum de 28,9 % de taux de délignification dans les conditions suivantes : vitesse de rotation des vis = 300 rpm, température d'extrusion = 65 °C, concentration de NaOH = 0 % et la taille des particules de biomasses brutes = 1 mm. Ces conditions sont similaires aux conditions de REN et offrent les mêmes avantages. Toutefois, les résultats expérimentaux enregistrés diffèrent de -6.5 % des taux prédits. Cette situation s'interprète en examinant les

caractéristiques des extrudats de REN (cf. § 9.1.3.6). Dans les deux cas, l'optimisation a été un succès car elle a permis d'obtenir de meilleurs taux de délignification comparés aux extrusions non optimisées.

Tableau 9.2 Optimization constraints imposed of the models

Criteria	Unit	Limit	Goal	Relative importance (1 to 5)
Particle size	mm	1 – 1.5	Minimize	+++ (3)
Screw rotation speed	rpm	190 – 300	Minimize	+ (1)
NaOH concentration	w/w	0 – 15	Minimize	++ (2)
Temperature	°C	50 – 90	Minimize	+ (1)
Delignification	% (w/w)	> 20	Maximize	+++++ (5)

9.1.3.6 Caractérisation des extrudats

Les **caractéristiques des extrudats** ont été analysées. Il s'agissait de la taille des particules, de la surface spécifique, de l'aspect des particules à échelle nanométrique, de la présence d'inhibiteur de croissance de microorganismes et de la composition élémentaire des extrudats. La **taille des particules** des extrudats de RMA était de 204 μm contre 55 μm pour les REN. La tendance est la même pour les surfaces spécifiques. La **surface spécifique** moyenne des particules extrudats de RMA était de 597,9 cm^2/cm^3 contre 2402 cm^2/cm^3 pour les REN. Les extrudats de REN paraissent sous la forme de très fines particules. Lors de l'analyse des taux de délignification par la méthode Klason, les forces électrostatiques et de van der Waals générés par les particules empêchent la solubilisation complète des biomasses dans la solution d'acide sulfurique à 72% (Feng & Hays, 2003). Ceci expliquerait la différence de taux observés sur les résultats prédits par le modèle d'optimisation des REN. De manière générale, les résultats de surfaces spécifiques des REN et des RMA démontrent que l'extrusion permet de réduire de plus de 3 fois la surface spécifique des biomasses brutes avec un seul passage de biomasse. Le **temps de résidence** de la biomasse dans l'extrudeuse est d'environ 90 s dans les conditions d'optimisation présentées au paragraphe précédent. Cela confirme la capacité de l'extrusion à augmenter significativement la surface spécifique des particules, ce qui est d'un atout majeur pour l'étape suivante : la biodélignification. De plus, l'analyse au microscope électronique à balayage (MEB) des extrudats optimisés a mis en évidence une défibrillation intensive des biomasses. Les biomasses extrudées présentent toutes des **structures très désorganisées** à l'échelle nanométrique (Figure 6.10). L'analyse au GC/MS a démontré qu'aucun **inhibiteur** de

type furfural ou hydroxyméthylfurfural n'a été généré par l'extrusion. Le **rapport C/N** des extrudats n'a pas été altéré par l'extrusion.

Ces résultats confirment l'éligibilité des extrudats optimisés pour la biodégradation en fermentation solide avec *Phanerochaete chrysosporium*.

9.1.4 Optimisation des conditions de biodégradation par fermentation solide des biomasses prétraitées par extrusion et hydrolyse enzymatique des préhydrolysats.

9.1.4.1 Biomasses/extrudats et conditions de croissance de *P. chrysosporium*

Les résidus de maïs et d'épINETTE noire ont été extrudés selon leurs conditions respectives d'extrusion déterminées au [chapitre 4](#). Le tableau ci-dessous présente ces conditions d'extrusion.

Tableau 9.3 Conditions optimisées d'extrusion

Conditions	Résidus d'épINETTE noire	Résidus de maïs
Taille des particules de biomasse brute	1 mm	1 mm
Configuration des vis	F-K-F-K-F-K-F-T	F-K-F-K-F-K-F-T
Vitesse de rotation des vis	233 rpm	300 rpm
Température	50 °C	65 °C
Concentration NaOH	0 %	0 %

Les extrudats optimisés de RMA et de REN ont été soumis à la fermentation solide sous différentes conditions dans des fioles de 250 ml pour déterminer les conditions optimales de croissance de l'agent de biodégradation utilisé. Il s'agissait de la souche *Phanerochaete chrysosporium* A-381 (ATCC 48746). *P. chrysosporium* est un organisme hétérotrophe et sensible à l'environnement dans lequel il évolue. La température, la concentration de l'inoculum et le ratio C/N sont des paramètres clés de la fermentation solide avec *P. chrysosporium*. **La température** joue un rôle clé dans la croissance du mycélium et dans l'activité des enzymes lignolitiques. En deçà de 25 °C et au-delà de 45 °C, *P. chrysosporium* est incapable de se développer (Konan *et al.*, 2024a) ; la croissance du mycélium est stoppée. Le mycélium meurt progressivement et la maturité des spores est figée en attendant des conditions adéquates de température. De même, les enzymes lignolitiques requièrent des températures optimales

comprises entre 25 et 40 °C pour délignifier les BLC. Plusieurs études montrent que la **concentration de l'inoculum** est un paramètre important pour maintenir la croissance du mycélium de *P. chrysosporium*. Il est généralement recommandé entre 10⁵ et 10⁶ spores/ml (Gao *et al.*, 2023). Lorsque l'inoculum est moins concentré, le temps de colonisation de la biomasse est lent. Dans le cas inverse, il y a une compétition entre les spores ce qui peut conduire à un déséquilibre du ratio C/N. Le **ratio C/N** est également un paramètre crucial en fermentation solide. Le carbone est utilisé comme source d'énergie et l'azote dans la synthèse des acides nucléiques, des enzymes et des protéines (Debbarma *et al.*, 2023). La quantité d'azote varie beaucoup d'une biomasse à une autre et le ratio C/N doit être ajusté en conséquence avec des sources d'azote minérales (ex : sels d'ammonium) ou organiques (ex : urée). *P. chrysosporium* tolère toutefois une plage relativement importante de ratio C/N (de 14:1 à 112:1) (Huang *et al.*, 2020).

9.1.4.2 Optimisation des conditions de biodégradation et production d'enzymes lignolitiques

Les données précédentes couplées à des essais préliminaires de fermentation ont permis de déterminer les **conditions** limites de **croissance** de la souche de *P. chrysosporium* utilisée. La **température** était comprise entre 26 °C et 43 °C ; la **concentration de l'inoculum** (ml/g de biomasse) entre 0,1 ml/g et 1,8 ml/g et la **concentration de sel d'ammonium** [NH₄Cl] (% m/m) entre 0 % et 2,5 %. Sur les 30 fermentations réalisées selon le plan d'expérience, 8 ont montré une croissance de mycélium dont 6 pour les REN et 2 pour les RMA. Toutefois, le meilleur développement de la souche a été observé dans les mêmes conditions pour les REN et que pour les RAM. Il s'agissait de l'essai 2 (Run 2) avec une température de 30 °C, une concentration d'inoculum de 1,5 ml/g et de 0,5 % m/m. Le deuxième meilleur développement de mycélium observé pour l'épinette noire était l'essai 5 (Run 5) avec 35 °C, 1 ml/g et 2,5 %. Quant aux résidus de maïs, le deuxième meilleur développement de mycélium s'est observé dans les conditions de l'essai 8 (Run 8), c'est-à-dire 30 °C, 1,5 ml/g et 2 %. Ces résultats suggèrent que l'apport de sel d'ammonium est indispensable au développement de *P. chrysosporium*. Ceci s'explique par la faible teneur en azote des RMA et des REN. L'analyse CHNS des biomasses (cf. § 6.4.1) montre que les RAM possèdent 0,54 % en teneur d'azote, tandis qu'elle est inférieure à 0,1% dans les REN. Ces teneurs auraient été insuffisantes pour assurer le maintien des fonctions métaboliques de base de *P. chrysosporium* et maintenir sa croissance. Ces résultats démontrent que le mycélium prolifère avec un inoculum de 1,5 ml/g, mais encore mieux lorsque la température est inférieure à 35 °C et la concentration de sel d'ammonium à 0,5 %. Les quatre conditions ont été

retenues pour passer des réacteurs de 250 ml avec 5 g de biomasse à des bioréacteurs de 5 litres avec 200 g de biomasse, soit une échelle de 40X. Pour chaque type de biomasse, un contrôle négatif avec des biomasses brutes non extrudées a été soumis aux conditions de fermentation de l'essai 2 (Run 2) (30 °C, 1,5 ml/g et 0,5 % m/m). L'impact des conditions de biodégradation des extrudats dans les bioréacteurs de 5 litres a été analysé sur la **production d'enzymes lignolitiques**, le **taux de dégradation** et la **crystallinité** des biomasses prétraitées. La lignine peroxydase était la principale enzyme sécrétée dans les contrôles négatifs avec $53,7 \pm 2,7$ U/l et $16,4 \pm 0,8$ U/l respectivement pour le contrôle des REN et pour le contrôle des RMA. Toutefois, le maximum de dégradation enregistré n'était que de 17 %. En ce qui concerne la biodégradation avec les résidus extrudés, les taux de dégradation étaient de 59,1 % et 65,4 % respectivement pour les REN dans les conditions de l'essai 5 (Run 5), ainsi que les RMA dans les conditions de l'essai 8 (Run 8). Les principales enzymes responsables de la dégradation étaient les manganèses peroxydase avec 13,8 U/l pour les REN et 32,0 U/l pour les RMA. Ces résultats démontrent que l'extrusion améliore significativement l'efficacité de la biodégradation et promeut principalement la production de MnP. Cependant, il a été enregistré une augmentation de la cristallinité de la biomasse de 13 % pour les REN et de 4 % pour les RMA après l'étape de fermentation. Ce phénomène pourrait être la conséquence de la dégradation. En effet, en dehors de la cellulose qui est majoritairement cristalline dans la biomasse, l'hémicellulose et la lignine sont des polymères amorphes (Goldstein, 2018). Ainsi, lorsque la lignine est dégradée, la cristallinité globale de la biomasse augmente si la cristallinité de la cellulose est conservée durant le prétraitement.

9.1.4.3 Hydrolyse enzymatique

Les biomasses fermentées dans les 4 conditions précédemment présentées ont été soumises à hydrolyse enzymatique dans le but d'évaluer la récupération des sucres après le prétraitement Ex-SSF. La concentration d'enzyme était de 0,25 ml/g de biomasse. L'hydrolyse enzymatique sur les résidus d'épinette noire fermentés dans les conditions de l'essai 2 (Run 2) a conduit à une production de 7,6 mg/l de sucres et 7,1 mg/l dans les conditions de l'essai 5 (Run 5). Ceci représente 2,3 fois la quantité de sucre récupérée avec le contrôle négatif (3,3 mg/l). Quant à l'hydrolyse sur les résidus de maïs fermenté dans les conditions de l'essai 2 (Run 2), elle a conduit à une récupération de 17 mg/l de sucres et 16 mg/l de sucre dans les conditions de l'essai 8 (Run 8). Ceci représente 44 % d'amélioration de la récupération des sucres comparée au contrôle négatif (11,8 mg/l). En d'autres termes, ces résultats démontrent que la dégradation des

biomasses par le procédé Ex-SSF permet d'améliorer significativement la digestibilité enzymatique des REN et des RMA. Le prétraitement Ex-SSF a permis de récupérer dans les RMA plus du double des sucres récupérés dans les REN. Deux raisons peuvent expliquer la différence de résultat observée. D'une part, la différence de teneur en lignine de REN et RAM serait responsable de cette différence. La lignine est l'un des principaux obstacles à l'efficacité de l'étape d'hydrolyse enzymatique (Wu *et al.*, 2023b). Dans le cadre de cette thèse, la durée de fermentation des RAM et des REN était la même (soit 24 jours). Or, les REN contiennent deux fois plus de lignine que les RMA. D'autre part, la cristallinité des REN fermentés serait co-responsable de cet écart. La cristallinité des biomasses est un facteur susceptible de limiter l'efficacité de l'hydrolyse enzymatique (Xu *et al.*, 2019). Or, elle a augmenté de 13 % dans les REN comparé à 4 % pour les RMA. Ces deux hypothèses explicatives suggèrent qu'il faudrait une durée de fermentation plus grande des REN que celle des RMA pour obtenir des quantités de sucres similaires.

9.1.5 Analyse technico-économique de la production de bioéthanol 2G avec le prétraitement Ex-SSF

La production de bioéthanol 2G intégrant le prétraitement Ex-SSF a fait l'objet d'une analyse technico-économique préliminaire basée sur le guide NREL (Aden *et al.*, 2002).

9.1.5.1 Scénarios initiaux

L'analyse était circonscrite à la province de Québec (Canada) et identifiait 3 différents scénarios de départ à savoir S1, S2 et S3. S1 était une exploitation agricole de maïs de taille moyenne, c'est-à-dire 113 ha avec une capacité totale de production (P) de résidus lignocellulosiques équivalente à 1005,7 t/an (cf. Équation 8.1). S2 était une association de 3 exploitations agricoles de maïs de taille moyenne, soit une capacité de production (P) de 3017,1 t/an. Quant à S3, il s'agissait d'un particulier ayant 4 fournisseurs de biomasses lignocellulosiques dont 3 fournisseurs de résidus de maïs (provenant chacune d'exploitation de taille moyenne) et 1 fournisseur de résidus d'épinette noire (1/3 de la quantité totale de résidus de maïs). La capacité (P) de S3 était de 3821,7 t/an. La **Figure 8.1** présente le modèle d'intégration du prétraitement Ex-SSF dans le processus de production de bioéthanol. Il se situe en amont du procédé de bioraffinage et précède la phase de réduction des biomasses en copeaux.

9.1.5.2 Comparaison des coûts entre scénarios

Les capacités P des scénarios S1, S2 et S3 ont été utilisées pour identifier les spécifications des équipements nécessaires dans chaque zone identifiée dans le modèle de bioraffinerie (Area 100, 200, 300, etc.). L'13ANNEXE III présentent le détail des équipements et leur coût estimatif. Les scénarios ont été comparés selon leur capital d'investissement (CAPEX), leur dépense d'exploitation (OPEX) et la valeur économique du bioéthanol produit. Le CAPEX incluait les coûts de pré-construction, le coût des équipements et le coût d'installation des équipements. L'OPEX couvrait tous les coûts liés au fonctionnement de la bioraffinerie dont le coût d'acquisition de la biomasse, le coût du transport, le coût des produits chimiques et d'énergie. Rapporté à la capacité P, le CAPEX de S1 était supérieur à celui de S2 et S3. Il était de 1154.0 \$/t pour S1, 825.5 \$/t pour S2 et 739.5 \$/t pour S3. Ainsi, le coût d'investissement par tonne de résidus de biomasse diminue avec l'augmentation de la capacité (P) de la bioraffinerie. Il s'agit d'une économie d'échelle réalisée sur le coût des équipements. Dans le cas des OPEX, la tendance est différente. S1 avait un coût d'exploitation de 57.7 \$/t, ceux de S2 et S3 étaient respectivement de 41.3 \$/t et 151.6 \$/t. Les coûts d'exploitation dans le scénario S3 représentent presque le triple de celui de S1 ou S2. En effet, le CAPEX de S3 est affecté par le coût d'acquisition et le transport de la biomasse qui représente plus de 75 % de l'OPEX. Cette difficulté pourrait affecter significativement la rentabilité du scénario 3. Le prix moyen du bioéthanol sur les cinq dernières années est de 0,38 \$/l ([Economics, 2025](#)). Pour S1 avec un OPEX de 46 861 \$/an, le revenu annuel est de 30 305 \$/an, soit un déficit de 16 556 \$. Pour S2 avec un OPEX de 112 809 \$/an, le revenu annuel est de 90 907 \$/an, soit un déficit de 7 300 \$ par exploitation agricole. On observe cependant une augmentation de 56 % des revenus de la bioraffinerie en triplant sa capacité P.

9.1.5.3 Scénario finaux et conditions minimale de rentabilité

Les résultats ont permis de calculer les conditions minimales de rentabilité. Deux scénarios (M1 et M2) ont été identifiés. M1 est celui d'une seule exploitation et M2 est celui d'une association d'exploitation. Le [Tableau 8.5](#) présente les résultats des simulations. Dans le scénario M1, la quantité minimale de biomasses lignocellulosiques devrait être de 2458 t/an, soit une superficie de 345,3 ha d'exploitation. Dans le scénario M2, la quantité minimale de biomasses lignocellulosiques devrait être de 3521 t/an, soit une superficie totale de 494,7 ha. M1 et M2 suggèrent que la production de bioéthanol 2G intégrant le prétraitement Ex-SSF est plus adaptée

pour les exploitations agricoles individuelles de plus de 400 ha, ainsi que pour les associations d'exploitations moyennes dont les superficies totales sont supérieures à 500 ha.

9.2 Conclusion générale

Cette thèse a eu pour objectif de développer une approche novatrice de prétraitement des biomasses lignocellulosiques pour augmenter leur digestibilité enzymatique.

- A.) Les recherches bibliographiques ont abouti à la proposition du couplage Extrusion – Biodélicnification (Ex-SSF) comme méthode prometteuse de prétraitement des biomasses lignocellulosiques. Il s'agissait d'un couplage séquentiel de deux technologies prometteuses : l'extrusion (Ex) et la biodélicnification (SSF). L'approche Ex-SSF a été développée sur des résidus de maïs et sur des résidus d'épinette noire. Les données expérimentales ont permis de démontrer la capacité du procédé Ex-SSF à augmenter significativement la digestibilité des résidus de maïs et des résidus d'épinette noire.
- B.) En optimisant les conditions d'extrusion par analyse de surfaces de réponse (RSA), les taux de délicnification augmentent de 2,3 % à 27,4 % pour les résidus de maïs, ainsi que de 1 % à 25,3 % pour les résidus d'épinette noire avec une reproductibilité des résultats de $\pm 1,2$ %. Les modèles d'optimisation développés pour les résidus d'épinette noire et de maïs sont robustes pour prédire les résultats de délicnification avec une précision de 0,8 % pour les résidus de maïs et de 3 % pour les résidus d'épinette noire. Les avantages de l'optimisation se situent également au niveau des températures et des caractéristiques des extrudats. Les températures d'extrusion optimisées sont basses (< 65 °C), ce qui a pour effet de réduire la consommation énergétique de l'extrudeuse. Les extrudats ont des tailles significativement réduites comparées à leurs biomasses brutes. Les copeaux d'épinette noire de 1 mm de taille de particules passent à 55 μm après le passage à l'extrusion dans les conditions optimisées, tandis que leur surface spécifique augmente d'environ 50 % (399 à 597 cm^2/cm^3). Le constat est encore plus intéressant avec les résidus de maïs. Les particules initiales de 1 mm sont réduites à 204 μm après extrusion et la surface spécifique est multipliée par 4, passant de 512 à 2402 cm^2/cm^3 . De plus, l'étape d'extrusion ne génère pas d'inhibiteurs du type furfural ou hydroxyméthylfurfural.
- C.) Lorsque les biomasses brutes sont soumises à la biodélicnification en fermentation semi-solide avec *Phanerochaete chrysosporium*, moins de 17 % de délicnification sont atteints

après 21 jours de prétraitement. La lignine peroxyase est l'enzyme lignolitique la plus active dans ces conditions avec $53,7 \pm 2,7$ U/l et $16,4 \pm 0,8$ U/l respectivement pour l'épinette noire et les résidus de maïs. En contraste avec les biomasses brutes, lorsque les extrudats sont prétraités en fermentation solide avec *Phanerochaete chrysosporium*, on obtient jusqu'à 59,1 % de délignification totale avec les résidus d'épinette noire et 65,4% avec les résidus de maïs. La manganèse peroxydase est la principale enzyme responsable de la biodélignification sur les extrudats. Elle possède la plus importante activité lignolytique avec 13,8 U/l et 32,0 U/l respectivement pour résidus d'épinette noire et les résidus de maïs. L'hydrolyse enzymatique des extrudats prétraités à la fermentation permet de récupérer 7,6 mg/l de sucre avec les résidus d'épinette noire, c'est-à-dire 2,3 fois de plus la quantité obtenue avec leurs résidus brutes. Quant aux extrudats de maïs, le prétraitement des extrudats à la fermentation permet de récupérer 17,0 mg/l de sucre, soit une amélioration de 44 % par rapport aux résidus bruts.

D.) Le prétraitement développé dans cette thèse est adapté pour les exploitations agricoles qui envisagent la production de bioéthanol 2G avec les résidus lignocellulosiques de leurs exploitations. Dans le cas d'une exploitation unique, la rentabilité du procédé commence à partir de 2 458 tonnes de biomasses par an, soit l'équivalent de la production de résidus lignocellulosiques de 345 ha de culture de maïs. Dans le cas d'une association d'exploitants agricoles, il s'agissait d'une capacité totale de 3 522 tonnes de biomasse par an, soit l'équivalent de la production de résidus lignocellulosiques de 495 ha de culture de maïs.

Les contributions de cette thèse à l'avancement des connaissances dans le domaine du prétraitement des biomasses lignocellulosiques sont multiples. Il s'agit entre autres de :

- Le développement d'une approche novatrice de prétraitement des BLC ;
- L'analyse approfondie des paramètres de l'extrusion pour le prétraitement des biomasses;
- La compréhension des relations entre les différents paramètres et leur influence sur le taux de délignification ;
- La proposition d'un modèle d'optimisation de l'extrusion des biomasses lignocellulosiques;
- L'analyse approfondie de tous les couplages technologiques de prétraitement incluant l'extrusion ;

- Une synthèse critique de l'emploi de *Phanerochaete chrysosporium* en tant qu'agent de biodégradation pour le traitement des biomasses ;
- La détermination des conditions de rentabilité d'une bioraffinerie intégrant le prétraitement Ex-SSF.

9.3 Recommandations

Sur la base des travaux réalisés et de l'expérience acquise, nous recommandons pour la suite des travaux de :

- **Normaliser l'analyse des taux de dégradation après fermentation**

L'analyse du taux de dégradation sur les biomasses prétraitées par fermentation requiert de séparer le mycélium de la biomasse. Ceci peut se faire en utilisant des solvants ou des mélanges de solvants dans un procédé d'extraction Soxhlet. Toutefois, l'efficacité de cette approche est très variable. Il est recommandé d'explorer d'autres options ou d'autres solvants que le mélange éthanol:benzène (2:1 v/v). Parmi les alternatives prometteuses, l'utilisation du mélange éthanol:toluène (2:1) constitue une option moins toxique que le benzène, tout en offrant une capacité d'extraction comparable pour les composés organiques non liés à la lignine. De même, des solvants plus sélectifs tels que l'acétone pure, ou des mélanges dioxane:eau (9:1) peuvent être évalués, sous réserve de tests de compatibilité avec les fractions lignocellulosiques. Il est également recommandé d'envisager des méthodes de séparation non solvantées ou moins destructives, qui préservent l'intégrité des structures lignocellulosiques. Ce sont par exemple :

- ❖ Le lavage alcalin doux : Un traitement avec une solution diluée de NaOH (0,1 à 0,5 N) permet de solubiliser le mycélium sans entraîner une dégradation significative de la cellulose ou de l'hémicellulose. Cette méthode est simple, économique, et peut être suivie d'un rinçage à l'eau distillée pour éliminer les résidus.
- ❖ Le traitement enzymatique sélectif : L'application d'enzymes ciblant les composants fongiques, comme la chitinase ou la glucanase, peut permettre la lyse spécifique du mycélium sans attaquer les parois végétales. Cette approche nécessite un ajustement précis des conditions de pH et de température, mais représente une voie très prometteuse pour une séparation douce et contrôlée.
- ❖ La centrifugation différentielle couplée à des lavages successifs : Une série de centrifugations à différentes vitesses, suivies de lavages à l'éthanol ou à l'eau

tiède, peut favoriser la séparation physique du mycélium en fonction de la densité, tout en limitant les pertes de matière lignocellulosique.

Nous recommandons donc de valider expérimentalement plusieurs de ces approches, afin d'identifier celle qui offre le meilleur compromis entre efficacité de séparation et préservation des structures lignocellulosiques.

- **Développement des protocoles de récupération et de purification des enzymes lignolitiques**

Lors de l'étape de biodégradation, des enzymes lignolitiques (MnP, LiP et Lac) sont produites par l'agent de biodégradation utilisé (ici *Phanerochaete chrysosporium*). D'une part, l'efficacité de la biodégradation pourrait être davantage améliorée si ces enzymes étaient récupérées à la fin des fermentations et réutilisées pour les fermentations subséquentes. Dans ce cas, la purification des enzymes ne serait pas nécessaire ; la simple récupération des enzymes brutes suffirait. D'autre part, les enzymes lignolitiques pourraient être purifiées et utilisées pour d'autres applications. En effet, les manganèse peroxidases, les lignines peroxydases et les laccases trouvent des applications intéressantes dans de nombreux autres domaines de recherche. Il est recommandé d'explorer ces deux alternatives séparément.

- **Concevoir des matériaux composites avec les résidus de prétraitement**

Après l'hydrolyse enzymatique des résidus prétraités au procédé Ex-SSF, il reste une fraction solide de biomasse qui peut être valorisée en matériaux biosourcés. En effet, l'extrudeuse offre cet unique avantage d'outil de prétraitement et d'outil de conception de matériaux. Il est recommandé de sécher à l'étuve (50 °C) la fraction solide après hydrolyse, puis de l'analyser à la TGA (Thermogravimetric Analysis) et au DSC (Differential Scanning Calorimetry).

10 BIBLIOGRAPHIE

- Ab Rasiid N. S., Shamjuddin A., Abdul R. A. Z., Amin N. A. S. (2021). Recent advances in green pre-treatment methods of lignocellulosic biomass for enhanced biofuel production. *Journal of Cleaner Production* 321:129038. <https://doi.org/10.1016/j.jclepro.2021.129038>
- Abbas T., Issa M., Ilinca A. (2020). Biomass cogeneration technologies: A review. *Journal of Sustainable Bioenergy Systems* 10(1):1-15. <https://doi.org/10.4236/jsbs.2020.101001>
- Abdulkadir L. N., Abioye A. M., Adisa B. A., Abdulkadir M. (2024). Characterization and SI engine testing of gasoline and blends of gasoline and bioethanol produced from co-fermented watermelon and pineapple wastes. *Nigerian Journal of Tropical Engineering* 18(2). <https://doi.org/10.59081/njte.18.2.008>
- Abeykoon C., Kelly A. L., Brown E. C., Coates P. D. (2016). The effect of materials, process settings and screw geometry on energy consumption and melt temperature in single screw extrusion. *Applied energy* 180:880-894. <https://doi.org/10.1016/j.apenergy.2016.07.014>
- Abo-State M. A. M., Osman M. E., Khattab O. H., El-Kelani T. A., Abdel-Rahman Z. M. (2021). Degradative pathways of polycyclic aromatic hydrocarbons (PAHs) by *Phanerochaete chrysosporium* under optimum conditions. *Journal of Radiation Research and Applied Sciences* 14(1):507-520. <https://doi.org/10.1080/16878507.2021.2001247>
- Acharya S., Hu Y., Abidi N. (2021). Cellulose Dissolution in Ionic Liquid under Mild Conditions: Effect of Hydrolysis and Temperature. *Fibers* 9(1):5. <https://doi.org/10.3390/fib9010005>
- Adane T., Adugna A. T., Alemayehu E. (2021). Textile industry effluent treatment techniques. *Journal of Chemistry* 2021(1):5314404. <https://doi.org/10.1155/2021/5314404>
- Aden A., Ruth M., Ibsen K., Jechura J., Neeves K., Sheehan J., Wallace B., Montague L., Slayton A., Lukas J. (2002). *Lignocellulosic biomass to ethanol process design and economics utilizing co-current dilute acid prehydrolysis and enzymatic hydrolysis for corn stover*. National Renewable Energy Lab.(NREL), Golden, CO (United States). 154 p. <https://doi.org/10.2172/15001119>
- Adhikari S., Nam H., Chakraborty J. P. (2018). Conversion of Solid Wastes to Fuels and Chemicals Through Pyrolysis. *Waste Biorefinery* :239-263. <https://doi.org/10.1016/b978-0-444-63992-9.00008-2>
- Agarwal U. P., Zhu J. Y., Ralph S. A. (2013). Enzymatic hydrolysis of loblolly pine: effects of cellulose crystallinity and delignification. 67(4):371-377. <https://doi.org/10.1515/hf-2012-0116>
- Agbor V. B., Cicek N., Sparling R., Berlin A., Levin D. B. (2011a). Biomass pretreatment: Fundamentals toward application. *Biotechnology Advances* 29(6):675-685. <https://doi.org/10.1016/j.biotechadv.2011.05.005>
- Agbor V. B., Cicek N., Sparling R., Berlin A., Levin D. B. (2011b). Biomass pretreatment: fundamentals toward application. *Biotechnol Adv* 29(6):675-685. <https://doi.org/10.1016/j.biotechadv.2011.05.005>
- Aguilar-Reynosa A., Romaní A., Ma. Rodríguez-Jasso R., Aguilar C. N., Garrote G., Ruiz H. A. (2017). Microwave heating processing as alternative of pretreatment in second-generation biorefinery: An overview. *Energy Conversion and Management* 136:50-65. <https://doi.org/10.1016/j.enconman.2017.01.004>

- Ahiduzzaman M. & Islam A. S. (2013). Development of biomass stove for heating up die barrel of rice husk briquette machine. *Procedia Engineering* 56:777-781. <https://doi.org/10.1016/j.proeng.2013.03.194>
- Ahmad E. & Pant K. K. (2018). Lignin Conversion: A Key to the Concept of Lignocellulosic Biomass-Based Integrated Biorefinery. *Waste Biorefinery*. p 409-444. <https://doi.org/10.1016/b978-0-444-63992-9.00014-8>
- Ahmed A., Bakar M. S. A., Razzaq A., Hidayat S., Jamil F., Amin M. N., Sukri R. S., Shah N. S., Park Y.-K. (2021). Characterization and Thermal Behavior Study of Biomass from Invasive *Acacia mangium* Species in Brunei Preceding Thermochemical Conversion. *Sustainability* 13(9). <https://doi.org/10.3390/su13095249>
- Ahmed S. F., Mofijur M., Chowdhury S. N., Nahrin M., Rafa N., Chowdhury A. T., Nuzhat S., Ong H. C. (2022). Pathways of lignocellulosic biomass deconstruction for biofuel and value-added products production. *Fuel* 318:123618. <https://doi.org/10.1016/j.fuel.2022.123618>
- Ahvazi B., Wojciechowicz O., Ton-That T. M., Hawari J. (2011). Preparation of lignopolyols from wheat straw soda lignin. *J Agric Food Chem* 59(19):10505-10516. <https://doi.org/10.1021/jf202452m>
- Ai B., Li W., Woomeer J., Li M., Pu Y., Sheng Z., Zheng L., Adedeji A., Ragauskas A. J., Shi J. (2020). Natural deep eutectic solvent mediated extrusion for continuous high-solid pretreatment of lignocellulosic biomass. *Green chemistry* 22(19):6372-6383. <https://doi.org/10.1039/d0gc01560a>
- Aiken B. S. & Logan B. E. (1996). Degradation of pentachlorophenol by the white rot fungus *Phanerochaete chrysosporium* grown in ammonium lignosulphonate media. *Biodegradation* 7(3):175-182. <https://doi.org/10.1007/BF00058177>
- Akdogan H. (1996). Pressure, torque, and energy responses of a twin screw extruder at high moisture contents. *Food Research International* 29(5-6):423-429. [https://doi.org/10.1016/s0963-9969\(96\)00036-1](https://doi.org/10.1016/s0963-9969(96)00036-1)
- Akobi C., Yeo H., Hafez H., Nakhla G. (2016). Single-stage and two-stage anaerobic digestion of extruded lignocellulosic biomass. *Applied energy* 184:548-559. <https://doi.org/10.1016/j.apenergy.2016.10.039>
- Akram H. A., Imran M., Javid A., Latif S., Rizvi N. B., Jesionowski T., Bilal M. (2023). Pretreatment and catalytic conversion of lignocellulosic and algal biomass into biofuels by metal organic frameworks. *Molecular Catalysis* 539:112893. <https://doi.org/10.1016/j.mcat.2022.112893>
- Al-Samhan M., Al-Fadhli J., Al-Otaibi A. M., Al-Attar F., Bouresli R., Rana M. S. (2022). Prospects of refinery switching from conventional to integrated: An opportunity for sustainable investment in the petrochemical industry. *Fuel* 310. <https://doi.org/10.1016/j.fuel.2021.122161>
- Alic M., Kornegay Janet R., Pribnow D., Gold Michael H. (1989). Transformation by Complementation of an Adenine Auxotroph of the Lignin-Degrading Basidiomycete *Phanerochaete chrysosporium*. *Applied and Environmental Microbiology* 55(2):406-411. <https://doi.org/10.1128/aem.55.2.406-411.1989>
- Alio M. A., Tugui O. C., Vial C., Pons A. (2019). Microwave-assisted Organosolv pretreatment of a sawmill mixed feedstock for bioethanol production in a wood biorefinery. *Bioresour Technol* 276:170-176. <https://doi.org/10.1016/j.biortech.2018.12.078>

- Althuri A., Chintagunta A. D., Sherpa K. C., Banerjee R. (2018). Simultaneous Saccharification and Fermentation of Lignocellulosic Biomass. *Biorefining of Biomass to Biofuels: Opportunities and Perception*, Kumar S & Sani RK (Édit.) Springer International Publishing, Cham. p 265-285. https://doi.org/10.1007/978-3-319-67678-4_12
- Alvira P., Tomás-Pejó E., Ballesteros M., Negro M. J. (2010). Pretreatment technologies for an efficient bioethanol production process based on enzymatic hydrolysis: a review. *Bioresource technology* 101(13):4851-4861. <https://doi.org/10.1016/j.biortech.2009.11.093>
- Amin F. R., Khalid H., Zhang H., Rahman S. U., Zhang R., Liu G., Chen C. (2017). Pretreatment methods of lignocellulosic biomass for anaerobic digestion. *AMB Express* 7(1):72. <https://doi.org/10.1186/s13568-017-0375-4>
- Amini E., Valls C., Roncero M. B. (2021). Ionic liquid-assisted bioconversion of lignocellulosic biomass for the development of value-added products. *Journal of Cleaner Production* 326:129275. <https://doi.org/10.1016/j.jclepro.2021.129275>
- An Y. X., Zong M. H., Wu H., Li N. (2015). Pretreatment of lignocellulosic biomass with renewable cholinium ionic liquids: Biomass fractionation, enzymatic digestion and ionic liquid reuse. *Bioresour Technol* 192:165-171. <https://doi.org/10.1016/j.biortech.2015.05.064>
- Anderson E. M., Katahira R., Reed M., Resch M. G., Karp E. M., Beckham G. T., Román-Leshkov Y. (2016). Reductive Catalytic Fractionation of Corn Stover Lignin. *ACS Sustainable Chemistry & Engineering* 4(12):6940-6950. <https://doi.org/10.1021/acssuschemeng.6b01858>
- Anku W. W., Mamo M. A., Govender P. P. (2017). Phenolic compounds in water: sources, reactivity, toxicity and treatment methods. *Phenolic compounds-natural sources, importance and applications* :419-443. <https://doi.org/10.5772/66927>
- Anoop Kumar V., Suresh Chandra Kurup R., Snishamol C., Nagendra Prabhu G. (2019). Role of Cellulases in Food, Feed, and Beverage Industries. *Green Bio-processes: Enzymes in Industrial Food Processing*, Parameswaran B, Varjani S, Raveendran S (Édit.) Springer Singapore, Singapore. p 323-343. https://doi.org/10.1007/978-981-13-3263-0_17
- Ansell M. P. & Mwaikambo L. Y. (2009). The structure of cotton and other plant fibres. *Handbook of Textile Fibre Structure*. p 62-94. <https://doi.org/10.1533/9781845697310.1.62>
- Antar M., Lyu D., Nazari M., Shah A., Zhou X., Smith D. L. (2021). Biomass for a sustainable bioeconomy: An overview of world biomass production and utilization. *Renewable and Sustainable Energy Reviews* 139. <https://doi.org/10.1016/j.rser.2020.110691>
- Appels L., Degreve J., Van der Bruggen B., Van Impe J., Dewil R. (2010). Influence of low temperature thermal pre-treatment on sludge solubilisation, heavy metal release and anaerobic digestion. *Bioresour Technol* 101(15):5743-5748. <https://doi.org/10.1016/j.biortech.2010.02.068>
- Arora A., Nandal P., Singh J., Verma M. L. (2020). Nanobiotechnological advancements in lignocellulosic biomass pretreatment. *Materials Science for Energy Technologies* 3:308-318. <https://doi.org/10.1016/j.mset.2019.12.003>
- Arora D. S. & Gill P. K. (2001). Comparison of two assay procedures for lignin peroxidase. *Enzyme and Microbial Technology* 28(7-8):602-605. [https://doi.org/10.1016/S0141-0229\(01\)00302-7](https://doi.org/10.1016/S0141-0229(01)00302-7)

- Arora S., Rani R., Ghosh S. (2018). Bioreactors in solid state fermentation technology: Design, applications and engineering aspects. *Journal of Biotechnology* 269:16-34. <https://doi.org/10.1016/j.jbiotec.2018.01.010>
- Asim A. M., Uroos M., Naz S., Sultan M., Griffin G., Muhammad N., Khan A. S. (2019). Acidic ionic liquids: Promising and cost-effective solvents for processing of lignocellulosic biomass. *Journal of Molecular Liquids* 287:110943. <https://doi.org/10.1016/j.molliq.2019.110943>
- Audibert E., Floret J., Quintero A., Martel F., Rémond C., Paës G. (2025). Determination of trade-offs between 2G bioethanol production yields and pretreatment costs for industrially steam exploded woody biomass. *Applied energy* 380:125028. <https://doi.org/10.1016/j.apenergy.2024.125028>
- Augustina S., Wahyudi I., Dwianto W., Darmawan T. (2022). Effect of Sodium Hydroxide, Succinic Acid and Their Combination on Densified Wood Properties. *Forests* 13(2). <https://doi.org/10.3390/f13020293>
- Azad K., Halim M. A., Hossain F. (2013). Optimization Of Culture Conditions For The Production Of Xylanase By Two Thermophilic Fungi Under Solid State Fermentation. *Journal of the Asiatic Society of Bangladesh, Science* 39(1):43-51. <https://doi.org/10.3329/jasbs.v39i1.16032>
- Baaqel H., Tulus V., Chachuat B., Guillén-Gosálbez G., Hallett J. (2020). Uncovering the True Cost of Ionic Liquids using Monetization. *Computer Aided Chemical Engineering*, Pierucci S, Manenti F, Bozzano GL, Manca D (Édit.) Elsevier, Vol 48. p 1825-1830. <https://doi.org/10.1016/B978-0-12-823377-1.50305-0>
- Badgujar K. C. & Bhanage B. M. (2018). Dedicated and Waste Feedstocks for Biorefinery: An Approach to Develop a Sustainable Society. *Waste Biorefinery*. p 3-38. <https://doi.org/10.1016/b978-0-444-63992-9.00001-x>
- Badgujar K. C., Wilson L. D., Bhanage B. M. (2019). Recent advances for sustainable production of levulinic acid in ionic liquids from biomass: Current scenario, opportunities and challenges. *Renewable and Sustainable Energy Reviews* 102:266-284. <https://doi.org/10.1016/j.rser.2018.12.007>
- Bajwa D. S., Peterson T., Sharma N., Shojaeiarani J., Bajwa S. G. (2018). A review of densified solid biomass for energy production. *Renewable and Sustainable Energy Reviews* 96:296-305. <https://doi.org/10.1016/j.rser.2018.07.040>
- Baksi S., Saha D., Saha S., Sarkar U., Basu D., Kuniyal J. C. (2023). Pre-treatment of lignocellulosic biomass: review of various physico-chemical and biological methods influencing the extent of biomass depolymerization. *International Journal of Environmental Science and Technology* 20(12):13895-13922. <https://doi.org/10.1007/s13762-023-04838-4>
- Balakrishnan M., Jeevarathinam G., Kumar S. K. S., Muniraj I., Uthandi S. (2021). Optimization and scale-up of α -amylase production by *Aspergillus oryzae* using solid-state fermentation of edible oil cakes. *BMC Biotechnology* 21(1):33. <https://doi.org/10.1186/s12896-021-00686-7>
- Ballou R. H., Rahardja H., Sakai N. (2002). Selected country circuitry factors for road travel distance estimation. *Transportation Research Part A: Policy and Practice* 36(9):843-848. [https://doi.org/10.1016/S0965-8564\(01\)00044-1](https://doi.org/10.1016/S0965-8564(01)00044-1)

- Bals B., Rogers C., Jin M., Balan V., Dale B. (2010). Evaluation of ammonia fibre expansion (AFEX) pretreatment for enzymatic hydrolysis of switchgrass harvested in different seasons and locations. *Biotechnology for Biofuels* 3(1):1. <https://doi.org/10.1186/1754-6834-3-1>
- Bandyopadhyay-Ghosh S., Ghosh S. B., Sain M. (2015). The use of biobased nanofibres in composites. *Biofiber reinforcements in composite materials* :571-647. <https://doi.org/10.1533/9781782421276.5.571>
- Bánki O., Roskov Y., Döring M., Ower G., Hernández Robles D. R., Plata Corredor C. A., Stjernegaard Jeppesen T., Örn A., Vandepitte L., Hobern D., Schalk P., DeWalt R. E., Ma K., Miller J., Orrell T., Aalbu R., Abbott J., Adlard R., Aedo C. (2024). Catalogue Of Life checklist (Version 2024-03-26). in *Catalogue of Life*. <https://doi.org/10.48580/dfz8d>
- Banu J R., Sugitha S., Kavitha S., Kannah R Y., Merrylin J., Kumar G. (2021). Lignocellulosic Biomass Pretreatment for Enhanced Bioenergy Recovery: Effect of Lignocelluloses Recalcitrance and Enhancement Strategies. *Frontiers in Energy Research* 9. <https://doi.org/10.3389/fenrg.2021.646057>
- Behera S., Arora R., Nandhagopal N., Kumar S. (2014). Importance of chemical pretreatment for bioconversion of lignocellulosic biomass. *Renewable and Sustainable Energy Reviews* 36:91-106. <https://doi.org/10.1016/j.rser.2014.04.047>
- Beisl S., Biermair F., Friedl A., Mundigler N., Miltner A. (2017). Sequential Extrusion and Organosolv Pretreatment for Wheat Straw Valorization. *Chemical Engineering Transactions* 61:853-858. <https://doi.org/10.3303/CET1761140>
- Benaddou M., Hajjaj H., Diouri M. (2023). Fungal Treatment and Wheat Straw Blend for Enhanced Animal Feed from Olive Pulp. *Journal of Ecological Engineering* 24(12):187-200. <https://doi.org/10.12911/22998993/172423>
- Bernal B., Jara A. G., Chacon F. J., Belleville M. P., Lozano P. (2014) A two-steps sustainable process for enzymatic saccharification of ionic liquid-pretreated lignocellulosic biomass. *4th International Congress on Green Process Engineering-GPE2014*. <https://doi.org/10.13140/RG.2.2.31649.63842>
- Bhargava N., Mor R. S., Kumar K., Sharanagat V. S. (2021). Advances in application of ultrasound in food processing: A review. *Ultrasonics Sonochemistry* 70:105293. <https://doi.org/10.1016/j.ultsonch.2020.105293>
- Bhati P. (2019). Effect of temperatures on the growth of floral waste degrading fungi. *Fungal Territory* 2(2):12-15. <https://doi.org/10.36547/ft.2019.2.2.12-15>
- Bhutto A. W., Qureshi K., Harijan K., Abro R., Abbas T., Bazmi A. A., Karim S., Yu G. (2017). Insight into progress in pre-treatment of lignocellulosic biomass. *Energy* 122:724-745. <https://doi.org/10.1016/j.energy.2017.01.005>
- Bin D., Yumei X., Hailong D., Li Y., Jianming W. (2019). Phanerochaete chrysosporium strain B-22, a parasitic fungus infecting *Meloidogyne incognita*. *bioRxiv* :622472. <https://doi.org/10.1101/622472>
- Blanchette R. A. (1991). Delignification by wood-decay fungi. *Annual review of phytopathology* 29(1):381-403. <https://doi.org/10.1146/annurev.py.29.090191.002121>
- Bogan B. W. & Lamar R. T. (1995). One-electron oxidation in the degradation of creosote polycyclic aromatic hydrocarbons by *Phanerochaete chrysosporium*. *Applied and*

- Environmental Microbiology* 61(7):2631-2635. <https://doi.org/10.1128/aem.61.7.2631-2635.1995>
- Bohre A., Dutta S., Saha B., Abu-Omar M. M. (2015). Upgrading Furfurals to Drop-in Biofuels: An Overview. *ACS Sustainable Chemistry & Engineering* 3(7):1263-1277. <https://doi.org/10.1021/acssuschemeng.5b00271>
- Braga A. & Faria N. (2022). Biotechnological production of specialty aromatic and aromatic-derivative compounds. *World Journal of Microbiology and Biotechnology* 38(5). <https://doi.org/10.1007/s11274-022-03263-y>
- Brudecki G., Cybulska I., Rosentrater K. (2013). Integration of extrusion and clean fractionation processes as a pre-treatment technology for prairie cordgrass. *Bioresour Technol* 135:672-682. <https://doi.org/10.1016/j.biortech.2012.10.132>
- Bumpus J. A. (1989). Biodegradation of polycyclic hydrocarbons by *Phanerochaete chrysosporium*. *Applied and Environmental Microbiology* 55(1):154-158. <https://doi.org/10.1128/aem.55.1.154-158.1989>
- Bumpus J. A. (2021). White rot fungi and their potential use in soil bioremediation processes. *Soil biochemistry* :65-100. <https://doi.org/10.1201/9781003208884-2>
- Byun J., Cha Y.-L., Park S.-M., Kim K.-S., Lee J.-E., Kang Y.-G. (2020). Lignocellulose Pretreatment Combining Continuous Alkaline Single-Screw Extrusion and Ultrasonication to Enhance Biosugar Production. *Energies* 13(21). <https://doi.org/10.3390/en13215636>
- Caizán Juanarena L., Ter Heijne A., Buisman C. J. N., van der Wal A. (2016). Wood Degradation by Thermotolerant and Thermophilic Fungi for Sustainable Heat Production. *ACS Sustainable Chemistry & Engineering* 4(12):6355-6361. <https://doi.org/10.1021/acssuschemeng.6b00914>
- Calcio Gaudino E., Grillo G., Manzoli M., Tabasso S., Maccagnan S., Cravotto G. (2022a). Mechanochemical Applications of Reactive Extrusion from Organic Synthesis to Catalytic and Active Materials. *Molecules* 27(2):449. <https://www.mdpi.com/1420-3049/27/2/449>
- Calcio Gaudino E., Grillo G., Manzoli M., Tabasso S., Maccagnan S., Cravotto G. (2022b). Mechanochemical Applications of Reactive Extrusion from Organic Synthesis to Catalytic and Active Materials. *Molecules* 27(2). <https://doi.org/10.3390/molecules27020449>
- Calvert K. & Mabee W. (2014). Spatial Analysis of Biomass Resources within a Socio-Ecologically Heterogeneous Region: Identifying Opportunities for a Mixed Feedstock Stream. *ISPRS International Journal of Geo-Information* 3(1):209-232. <https://doi.org/10.3390/ijgi3010209>
- Calvo-Flores F. G. & Dobado J. A. (2010). Lignin as renewable raw material. *ChemSusChem* 3(11):1227-1235. <https://doi.org/10.1002/cssc.201000157>
- Canada S. (2021). Table 32-10-0228-01 Land tenure, Census of Agriculture historical data.). <https://doi.org/10.25318/3210022801-eng>
- Cantine O. (2017). PEO hot melt extrudates for controlled drug delivery. :145. <https://theses.hal.science/tel-01540630v1>
- Canuel C.-M., Thiffault E., Locoh A., Thiffault N. (2023). La bioénergie forestière pour lutter contre les changements climatiques : quelles implications dans la transition énergétique du Québec (Canada)? *The Forestry Chronicle* 99(1):11-24. <https://doi.org/10.5558/tfc2023-004>

- Cao B., Haelewaters D., Schoutteten N., Begerow D., Boekhout T., Giachini A. J., Gorjón S. P., Gunde-Cimerman N., Hyde K. D., Kemler M., Li G.-J., Liu D.-M., Liu X.-Z., Nuytinck J., Papp V., Savchenko A., Savchenko K., Tedersoo L., Theelen B., Thines M., Tomšovský M., Toome-Heller M., Urón J. P., Verbeken A., Vizzini A., Yurkov A. M., Zamora J. C., Zhao R.-L. (2021). Delimiting species in Basidiomycota: a review. *Fungal Diversity* 109(1):181-237. <https://doi.org/10.1007/s13225-021-00479-5>
- Caporusso A., Giuliano A., Liuzzi F., De Bari I. (2022). Techno-economic analysis of a lignocellulosic biorefinery producing microbial oils by oleaginous yeasts. *Chemical Engineering Transactions* 92:637-642. <https://doi.org/10.3303/CET2292107>
- Caposciutti G., Antonelli M., Barontini F., Galletti C., Tognotti L., Desideri U. (2022). An Experimental Investigation on the Effect of Exhaust Gas Recirculation in a Small-scale Fixed Bed Biomass Boiler. *Chemical Engineering Transactions* 92:397-402. <https://doi.org/10.3303/CET2292067>
- CCFM (2025). *Vast and abundant forests*. <https://www.ccfm.org/healthy-forests/vast-and-abundant-forests/> (Consulté le 06/01/2025)
- Cha Y.-L., Yang J., Seo S.-i., An G. H., Moon Y.-H., You G.-D., Lee J.-E., Ahn J.-W., Lee K.-B. (2016). Alkaline twin-screw extrusion pretreatment of Miscanthus with recycled black liquor at the pilot scale. *Fuel* 164:322-328. <https://doi.org/10.1016/j.fuel.2015.10.006>
- Chakraborty P., Kumar R., Chakraborty S., Saha S., Chattaraj S., Roy S., Banerjee A., Tripathy S. K., Kumar Ghosh A., Jeon B.-H. (2024). Technological advancements in the pretreatment of lignocellulosic biomass for effective valorization: A review of challenges and prospects. *Journal of Industrial and Engineering Chemistry* 137:29-60. <https://doi.org/10.1016/j.jiec.2024.03.025>
- Chang Y. H. & Ng P. K. W. (2011). Effects of Extrusion Process Variables on Quality Properties of Wheat-Ginseng Extrudates. *International Journal of Food Properties* 14(4):914-925. <https://doi.org/10.1080/10942910903491173>
- Chen B., Peng Z., Li C., Feng Y., Sun Y., Tang X., Zeng X., Lin L. (2021a). Catalytic Conversion of Biomass to Furanic Derivatives with Deep Eutectic Solvents. *ChemSusChem* 14(6):1496-1506. <https://doi.org/10.1002/cssc.202100001>
- Chen J., Adjallé K., Lai T. T., Barnabé S., Perrier M., Paris J. (2019). Effect of Mechanical Pretreatment for Enzymatic Hydrolysis of Woody Residues, Corn Stover and Alfalfa. *Waste and Biomass Valorization* 11(11):5847-5856. <https://doi.org/10.1007/s12649-019-00856-x>
- Chen J., Zhang W., Zhang H., Zhang Q., Huang H. (2014). Screw extrude steam explosion: A promising pretreatment of corn stover to enhance enzymatic hydrolysis. *Bioresource technology* 161:230-235. <https://doi.org/10.1016/j.biortech.2014.02.043>
- Chen J., Zhou J., Yuan R., Shao X., Lu Y., Sun W., Cao X. (2024). Mild Pretreatment Combined with Fed-Batch Strategy to Improve the Enzymatic Efficiency of Apple Pomace at High-Solids Content. *BioEnergy Research*. <https://doi.org/10.1007/s12155-024-10719-6>
- Chen L. F., Xiong Y. H., Qin H., Qi Z. W. (Advances of Ionic Liquids and Deep Eutectic Solvents in Green Processes of Biomass-Derived 5-Hydroxymethylfurfural. *ChemSusChem* :20. <https://doi.org/10.1002/cssc.202102635>
- Chen L. F., Xiong Y. H., Qin H., Qi Z. W. (2022a). Advances of Ionic Liquids and Deep Eutectic Solvents in Green Processes of Biomass-Derived 5-Hydroxymethylfurfural. *ChemSusChem* :20. <https://doi.org/10.1002/cssc.202102635>

- Chen W. H., Nizetic S., Sirohi R., Huang Z., Luque R., A M. P., Sakthivel R., Phuong Nguyen X., Tuan Hoang A. (2022b). Liquid hot water as sustainable biomass pretreatment technique for bioenergy production: A review. *Bioresour Technol* 344(Pt A):126207. <https://doi.org/10.1016/j.biortech.2021.126207>
- Chen W. H., Xu Y. Y., Hwang W. S., Wang J. B. (2011). Pretreatment of rice straw using an extrusion/extraction process at bench-scale for producing cellulosic ethanol. *Bioresour Technol* 102(22):10451-10458. <https://doi.org/10.1016/j.biortech.2011.08.118>
- Chen Z., Li N., Lan Q., Zhang X., Wu L., Liu J., Yang R. (2021b). Laccase inducer Mn²⁺ inhibited the intracellular degradation of norfloxacin by *Phanerochaete chrysosporium*. *International Biodeterioration & Biodegradation* 164:105300. <https://doi.org/10.1016/j.ibiod.2021.105300>
- Chevalier A., Evon P., Monlau F., Vandenbossche V., Sambusiti C. (2023). Twin-Screw Extrusion Mechanical Pretreatment for Enhancing Biomethane Production from Agro-Industrial, Agricultural and Catch Crop Biomasses. *Waste* 1(2):497-514. <https://doi.org/10.3390/waste1020030>
- Chinwatpaiboon P., Doolayagovit I., Boonsombuti A., Savarajara A., Luengnaruemitchai A. (2020). Comparison of acid-, alkaline-, and ionic liquid-treated Napier grass as an immobilization carrier for butanol production by *Clostridium beijerinckii* JCM 8026. *Biomass Conversion and Biorefinery* 10(4):1071-1082. <https://doi.org/10.1007/s13399-019-00491-5>
- Choi C. H. & Oh K. K. (2012a). Application of a continuous twin screw-driven process for dilute acid pretreatment of rape straw. *Bioresource technology* 110:349-354. <https://doi.org/10.1016/j.biortech.2012.01.075>
- Choi C. H. & Oh K. K. (2012b). Application of a continuous twin screw-driven process for dilute acid pretreatment of rape straw. *Bioresour Technol* 110:349-354. <https://doi.org/10.1016/j.biortech.2012.01.075>
- Choi W.-I., Oh K.-K., Park J.-Y., Lee J.-S. (2014). Continuous sodium hydroxide-catalyzed pretreatment of empty fruit bunches (EFB) by continuous twin-screw-driven reactor (CTSR). *Journal of Chemical Technology & Biotechnology* 89(2):290-296. <https://doi.org/10.1002/jctb.4119>
- Choudhary H., Simmons B. A., Gladden J. M. (2022). Comparative Study on the Pretreatment of Aspen and Maple With 1-Ethyl-3-methylimidazolium Acetate and Cholinium Lysinate. *Frontiers in Energy Research* 10. <https://doi.org/10.3389/fenrg.2022.868181>
- Choudhury G. S. & Gautam A. (1999). Screw Configuration Effects on Macroscopic Characteristics of Extrudates Produced by Twin-screw Extrusion of Rice Flour. *Journal of Food Science* 64(3):479-487. <https://doi.org/10.1111/j.1365-2621.1999.tb15067.x>
- Chowdhary P., More N., Yadav A., Bharagava R. N. (2019). Chapter 12 - Ligninolytic Enzymes: An Introduction and Applications in the Food Industry. *Enzymes in Food Biotechnology*, Kuddus M (Édit.) Academic Press. p 181-195. <https://doi.org/10.1016/B978-0-12-813280-7.00012-8>
- Chundawat S. P., Venkatesh B., Dale B. E. (2007). Effect of particle size based separation of milled corn stover on AFEX pretreatment and enzymatic digestibility. *Biotechnol Bioeng* 96(2):219-231. <https://doi.org/10.1002/bit.21132>

- Chundawat S. P. S., Balan V., Sousa L. D. c., Dale B. E. (2010). Thermochemical pretreatment of lignocellulosic biomass. *Bioalcohol Production*. p 24-72. <https://doi.org/10.1533/9781845699611.1.24>
- Chung C. I. (1975). Maximum pressure developed by solid conveying force in screw extruders. *Polymer Engineering and Science* 15(1):29-34. <https://doi.org/10.1002/pen.760150105>
- Chung H. & Washburn N. R. (2016). Extraction and Types of Lignin. *Lignin in Polymer Composites*. p 13-25. <https://doi.org/10.1016/b978-0-323-35565-0.00002-3>
- Clark J. & Deswarte F. (2015). The Biorefinery Concept. *Introduction to Chemicals from Biomass*. p 1-29. <https://doi.org/10.1002/9781118714478.ch1>
- Coconi-Linares N., Ortiz-Vázquez E., Fernández F., Loske A. M., Gómez-Lim M. A. (2015). Recombinant expression of four oxidoreductases in *Phanerochaete chrysosporium* improves degradation of phenolic and non-phenolic substrates. *Journal of Biotechnology* 209:76-84. <https://doi.org/10.1016/j.jbiotec.2015.06.401>
- Coconi Linares N., Fernández F., Loske A. M., Gómez-Lim M. A. (2018). Enhanced delignification of lignocellulosic biomass by recombinant fungus *Phanerochaete chrysosporium* overexpressing laccases and peroxidases. *Journal of Molecular Microbiology and Biotechnology* 28(1):1-13. <https://doi.org/10.1159/000485976>
- Coconi Linares N., Fernández F., Loske Achim M., Gómez-Lim Miguel A. (2018). Enhanced Delignification of Lignocellulosic Biomass by Recombinant Fungus *Phanerochaete chrysosporium* Overexpressing Laccases and Peroxidases. *Journal of Molecular Microbiology and Biotechnology* 28(1):1-13. <https://doi.org/10.1159/000485976>
- Coimbra M. C., Duque A., Saéz F., Manzanares P., Garcia-Cruz C. H., Ballesteros M. (2016). Sugar production from wheat straw biomass by alkaline extrusion and enzymatic hydrolysis. *Renewable Energy* 86:1060-1068. <https://doi.org/10.1016/j.renene.2015.09.026>
- Company H. (2024). *How Many Cars Are There In The World in 2024?* Online, <https://hedgescompany.com/blog/2021/06/how-many-cars-are-there-in-the-world/#:~:text=CLICK%20TO%20ENLARGE%3A%20This%20graphic,vehicles%20on%20Earth%20in%202023> (Consulté le 08/11/2024)
- Corredor D., Duchicela J., Flores F. J., Maya M., Guerron E. (2024). Review of Explosive Contamination and Bioremediation: Insights from Microbial and Bio-Omic Approaches. *Toxics* 12(4):249. <https://doi.org/10.3390/toxics12040249>
- Cruz-Cordova T., Roldán-Carrillo T., Diaz-Cervantes D., Ortega-López J., Saucedo-Castañeda G., Tomasini-Campocoso A., Rodríguez-Vázquez R. (1999). CO₂ evolution and ligninolytic and proteolytic activities of *Phanerochaete chrysosporium* grown in solid state fermentation. *Resources, Conservation and Recycling* 27(1-2):3-7. [https://doi.org/10.1016/S0921-3449\(98\)00080-9](https://doi.org/10.1016/S0921-3449(98)00080-9)
- da Silva A. S., Sobral Teixeira R. S., Oliveira R. d., Santana V., de Barros R. d. R. O., Antonieta M., da Silva Bo E. P. (2013a). Sugarcane and Woody Biomass Pretreatments for Ethanol Production. *Sustainable Degradation of Lignocellulosic Biomass - Techniques, Applications and Commercialization*. <https://doi.org/10.5772/53378>
- Da Silva A. S. A., Teixeira R. S. S., Endo T., Bon E. P. S., Lee S.-H. (2013b). Continuous pretreatment of sugarcane bagasse at high loading in an ionic liquid using a twin-screw extruder. *Green chemistry* 15(7):1991. <https://doi.org/10.1039/c3gc40352a>

- Dahiya J., Singh D., Nigam P. (2001). Decolourisation of synthetic and spentwash melanoidins using the white-rot fungus *Phanerochaete chrysosporium* JAG-40. *Bioresource technology* 78(1):95-98. [https://doi.org/10.1016/S0960-8524\(00\)00119-X](https://doi.org/10.1016/S0960-8524(00)00119-X)
- Dahmen N., Lewandowski I., Zibek S., Weidtmann A. (2019). Integrated lignocellulosic value chains in a growing bioeconomy: Status quo and perspectives. *GCB Bioenergy* 11(1):107-117. <https://doi.org/10.1111/gcbb.12586>
- Dale B. E., Weaver J., Byers F. M. (1999). Extrusion Processing for Ammonia Fiber Explosion (AFEX). *Appl Biochem Biotechnol* 77(1-3):35-46. <https://doi.org/10.1385/abab:77:1-3:35>
- Danisco (2007). Accelerase 1000 – Cellulase enzyme complex for lignocellulosic biomass hydrolysis – Technical bulletin no.1 : saccharification.
- Dao C. N., Tabil L. G., Mupondwa E., Dumonceaux T. (2023). Microbial pretreatment of camelina straw and switchgrass by *Trametes versicolor* and *Phanerochaete chrysosporium* to improve physical quality and enhance enzymatic digestibility of solid biofuel pellets. *Renewable Energy* 217:119147. <https://doi.org/10.1016/j.renene.2023.119147>
- Darim R. A., Azizan A., Salihon J. (2018) Study of crystallinity index (CrI) of oil palm frond pretreatment using aqueous [EMIM][OAc] in a closed system. *IOP Conference Series: Materials Science and Engineering*. IOP Publishing, p 012007. <https://doi.org/10.1088/1757-899X/358/1/012007>
- Das P. K., Bhat M. Y., Sajith S. (2024). Life cycle assessment of electric vehicles: a systematic review of literature. *Environmental Science and Pollution Research* 31(1):73-89. <https://doi.org/10.1007/s11356-023-30999-3>
- de Almeida A. P., Macrae A., Ribeiro B. D., do Nascimento R. P. (2021). Decolorization and detoxification of different azo dyes by *Phanerochaete chrysosporium* ME-446 under submerged fermentation. *Brazilian Journal of Microbiology* 52(2):727-738. <https://doi.org/10.1007/s42770-021-00458-7>
- de Reu J. C., Zwietering M. H., Rombouts F. M., Nout M. J. R. (1993). Temperature control in solid substrate fermentation through discontinuous rotation. *Applied Microbiology and Biotechnology* 40(2):261-265. <https://doi.org/10.1007/BF00170377>
- Debbarma R., Singh S. K., Waikhom G., Biswas P., Meena D. K., Choudhary B. K. (2023). Chapter 12 - Biofloc technology: a strategic way to waste recycling in aquaculture. *Organic Farming (Second Edition)*, Sarathchandran, M.R U, Thomas S, Meena DK (Édit.) Woodhead Publishing. p 395-419. <https://doi.org/10.1016/B978-0-323-99145-2.00017-3>
- Debiagi F., Faria-Tischer P. C. S., Mali S. (2019). Nanofibrillated cellulose obtained from soybean hull using simple and eco-friendly processes based on reactive extrusion. *Cellulose* 27(4):1975-1988. <https://doi.org/10.1007/s10570-019-02893-0>
- Debiagi F., Faria-Tischer P. C. S., Mali S. (2021). A Green Approach Based on Reactive Extrusion to Produce Nanofibrillated Cellulose from Oat Hull. *Waste and Biomass Valorization* 12(2):1051-1060. <https://doi.org/10.1007/s12649-020-01025-1>
- Dedes G., Karnaouri A., Topakas E. (2020). Novel Routes in Transformation of Lignocellulosic Biomass to Furan Platform Chemicals: From Pretreatment to Enzyme Catalysis. *Catalysts* 10(7). <https://doi.org/10.3390/catal10070743>
- Delmer D., Dixon R. A., Keegstra K., Mohnen D. (2024). The plant cell wall—dynamic, strong, and adaptable—is a natural shapeshifter. *The Plant Cell* 36(5):1257-1311. <https://doi.org/10.1093/plcell/koad325>

- Díaz A. I., Ibañez M., Laca A., Díaz M. (2021). Biodegradation of Olive Mill Effluent by White-Rot Fungi. *Applied Sciences* 11(21). <https://doi.org/10.3390/app11219930>
- Díaz A. I., Laca A., Lima N., Díaz M. (2022). Treatment of kraft black liquor using basidiomycete and ascomycete fungi. *Process Safety and Environmental Protection* 168:67-76. <https://doi.org/10.1016/j.psep.2022.09.065>
- Ding J., Chen B., Zhu L. (2013). Biosorption and biodegradation of polycyclic aromatic hydrocarbons by *Phanerochaete chrysosporium* in aqueous solution. *Chinese Science Bulletin* 58(6):613-621. <https://doi.org/10.1007/s11434-012-5411-9>
- Dittmer J. K., Patel N. J., Dhawale S. W., Dhawale S. S. (1997). Production of multiple laccase isoforms by *Phanerochaete chrysosporium* grown under nutrient sufficiency. *FEMS Microbiology Letters* 149(1):65-70. <https://doi.org/10.1111/j.1574-6968.1997.tb10309.x>
- Dittrich C., Pecenka R., Selge B., Zacharias M., Kruggel-Emden H. (2024). Production and investigation of water absorbent fibre pellets from unutilised lignocellulosic biomass pre-processed in a twin-screw extruder. *Industrial Crops and Products* 214:118525. <https://doi.org/10.1016/j.indcrop.2024.118525>
- Diwan B., Mukhopadhyay D., Gupta P. (2020). Chapter 11 - Recent trends in biorefinery-based valorisation of lignocellulosic biomass. *Biovalorisation of Wastes to Renewable Chemicals and Biofuels*, Krishnaraj Rathinam N & Sani RK (Édit.) Elsevier. p 219-242. <https://doi.org/10.1016/B978-0-12-817951-2.00011-0>
- Djuric D. & Kleinebudde P. (2008). Impact of screw elements on continuous granulation with a twin-screw extruder. *J Pharm Sci* 97(11):4934-4942. <https://doi.org/10.1002/jps.21339>
- do Nascimento F. V., de Castro A. M., Secchi A. R., Coelho M. A. Z. (2021). Insights into media supplementation in solid-state fermentation of soybean hulls by *Yarrowia lipolytica*: Impact on lipase production in tray and insulated packed-bed bioreactors. *Biochemical Engineering Journal* 166:107866. <https://doi.org/10.1016/j.bej.2020.107866>
- Doménech P., Duque A., Higuera I., Iglesias R., Manzanares P. (2020). Biorefinery of the Olive Tree—Production of Sugars from Enzymatic Hydrolysis of Olive Stone Pretreated by Alkaline Extrusion. *Energies* 13(17):4517. <https://doi.org/10.3390/en13174517>
- Dong Y., Tian B., Guo F., Du S., Zhan Y., Zhou H., Qian L. (2021). Application of low-cost Fe-based catalysts in the microwave-assisted pyrolysis of macroalgae and lignocellulosic biomass for the upgradation of bio-oil. *Fuel* 300. <https://doi.org/10.1016/j.fuel.2021.120944>
- Dulie N. W., Woldeyes B., Demsash H. D., Jabasingh A. S. (2021). An Insight into the Valorization of Hemicellulose Fraction of Biomass into Furfural: Catalytic Conversion and Product Separation. *Waste and Biomass Valorization* 12(2):531-552. <https://doi.org/10.1007/s12649-020-00946-1>
- Duque A., Álvarez C., Doménech P., Manzanares P., Moreno A. D. (2021). Advanced Bioethanol Production: From Novel Raw Materials to Integrated Biorefineries. *Processes* 9(2):206. <https://doi.org/10.3390/pr9020206>
- Duque A., Doménech P., Álvarez C., Ballesteros M., Manzanares P. (2020). Study of the bioprocess conditions to produce bioethanol from barley straw pretreated by combined soda and enzyme-catalyzed extrusion. *Renewable Energy* 158:263-270. <https://doi.org/10.1016/j.renene.2020.05.130>
- Duque A., Manzanares P., Ballesteros I., Negro M. J., Oliva J. M., Gonzalez A., Ballesteros M. (2014). Sugar production from barley straw biomass pretreated by combined alkali and

- enzymatic extrusion. *Bioresour Technol* 158:262-268. <https://doi.org/10.1016/j.biortech.2014.02.041>
- Duque A., Manzanares P., Ballesteros I., Negro M. J., Oliva J. M., Saez F., Ballesteros M. (2013). Optimization of integrated alkaline–extrusion pretreatment of barley straw for sugar production by enzymatic hydrolysis. *Process Biochemistry* 48(5-6):775-781. <https://doi.org/10.1016/j.procbio.2013.03.003>
- Duque A., Manzanares P., Ballesteros M. (2017). Extrusion as a pretreatment for lignocellulosic biomass: Fundamentals and applications. *Renewable Energy* 114:1427-1441. <https://doi.org/10.1016/j.renene.2017.06.050>
- Duque A., Manzanares P., González A., Ballesteros M. (2018a). Study of the Application of Alkaline Extrusion to the Pretreatment of Eucalyptus Biomass as First Step in a Bioethanol Production Process. *Energies* 11(11). <https://doi.org/10.3390/en11112961>
- Duque A., Manzanares P., González A., Ballesteros M. (2018b). Study of the Application of Alkaline Extrusion to the Pretreatment of Eucalyptus Biomass as First Step in a Bioethanol Production Process. *Energies* 11(11):2961. <https://doi.org/doi:10.3390/en11112961>
- Durand A. (2003). Bioreactor designs for solid state fermentation. *Biochemical Engineering Journal* 13(2-3):113-125. [https://doi.org/10.1016/s1369-703x\(02\)00124-9](https://doi.org/10.1016/s1369-703x(02)00124-9)
- Easwaran S. N., Mohanakrishnan A. S., Santharam L., Adimoolam S. R., Mahadevan S. (2022). Metabolic heat responses of *Kluyveromyces marxianus* and *Saccharomyces cerevisiae* during Carboxypeptidase Y Enzyme production. *Process Biochemistry* 112:71-79. <https://doi.org/10.1016/j.procbio.2021.11.015>
- Economics T. (2025). *Ethanol*. <https://tradingeconomics.com/commodity/ethanol> (Consulté le 07/01/2025)
- Ejaz U. & Sohail M. (2021). Chapter 1 - Sugarcane bagasse: A promising substrate for solid-state fermentation. *Green Sustainable Process for Chemical and Environmental Engineering and Science*, Inamuddin, Boddula R, Asiri AM, Rahman MM (Édit.) Elsevier. p 1-13. <https://doi.org/10.1016/B978-0-12-819720-2.00001-1>
- Elgharbawy A. A. M., Hayyan M., Hayyan A., Basirun W. J., Salleh H. M., Mirghani M. E. S. (2020). A grand avenue to integrate deep eutectic solvents into biomass processing. *Biomass and Bioenergy* 137:105550. <https://doi.org/10.1016/j.biombioe.2020.105550>
- Emami E., Zolfaghari P., Golizadeh M., Karimi A., Lau A., Ghiasi B., Ansari Z. (2020). Effects of stabilizers on sustainability, activity and decolorization performance of Manganese Peroxidase enzyme produced by *Phanerochaete chrysosporium*. *Journal of Environmental Chemical Engineering* 8(6):104459. <https://doi.org/10.1016/j.jece.2020.104459>
- Endersen P. G. (2012). Co-rotating fully intermeshing twin-screw compounding: advancements for improved performance and productivity. <https://doi.org/10.1002/j.1941-9635.2013.tb00988.x>
- Espert A., de las Heras L. A., Karlsson S. (2005). Emission of possible odourous low molecular weight compounds in recycled biofibre/polypropylene composites monitored by head-space SPME-GC–MS. *Polymer Degradation and Stability* 90(3):555-562. <https://doi.org/10.1016/j.polymdegradstab.2005.03.009>
- Falade A. O., Nwodo U. U., Iweriebor B. C., Green E., Mabinya L. V., Okoh A. I. (2017). Lignin peroxidase functionalities and prospective applications. *MicrobiologyOpen* 6(1):e00394. <https://doi.org/10.1002/mbo3.394>

- Fang H., Deng J., Zhang T. (2011). Dilute Acid Pretreatment of Black Spruce Using Continuous Steam Explosion System. *Applied Biochemistry and Biotechnology* 163(4):547-557. <https://doi.org/10.1007/s12010-010-9061-6>
- Fatriasari W., Syafii W., Wistara N., Syamsu K., Prasetya B., Anita S. H., Risanto L. (2016). Fiber Disruption of Betung Bamboo (*Dendrocalamus asper*) by Combined Fungal and Microwave Pretreatment. *BIOTROPIA* 22(2):81-94. <https://doi.org/10.11598/btb.2015.22.2.363>
- Feng J. Q. & Hays D. A. (2003). Relative importance of electrostatic forces on powder particles. *Powder Technology* 135-136:65-75. <https://doi.org/10.1016/j.powtec.2003.08.005>
- Feng Y. H., Lei B., Liang Y., Zhong H. T., Yin X. C., Qu J. P., He H. Z. (2016). Changes in the Microstructure and Components of *Eulaliopsis binata* Treated by Continuous Screw Extrusion Steam Explosion. *BioResources* 11(4):9455-9466. <https://doi.org/10.15376/biores.11.4.9455-9466>
- Fernández-Rodríguez J., Erdocia X., Sánchez C., González Alriols M., Labidi J. (2017). Lignin depolymerization for phenolic monomers production by sustainable processes. *Journal of Energy Chemistry* 26(4):622-631. <https://doi.org/10.1016/j.jechem.2017.02.007>
- Fernández V. M. (2011). Water Activity. *Encyclopedia of Astrobiology*, Gargaud M, Amils R, Quintanilla JC, Cleaves HJ, Irvine WM, Pinti DL, Viso M (Édit.) Springer Berlin Heidelberg, Berlin, Heidelberg. p 1763-1764. https://doi.org/10.1007/978-3-642-11274-4_1678
- Flieger J. & Flieger M. (2020). Ionic Liquids Toxicity—Benefits and Threats. *International Journal of Molecular Sciences* 21(17):6267. <https://doi.org/10.3390/ijms21176267>
- Flores E. M. M., Cravotto G., Bizzi C. A., Santos D., Iop G. D. (2021). Ultrasound-assisted biomass valorization to industrial interesting products: state-of-the-art, perspectives and challenges. *Ultrason Sonochem* 72:105455. <https://doi.org/10.1016/j.ultsonch.2020.105455>
- Florindo C., Lima F., Ribeiro B. D., Marrucho I. M. (2019). Deep eutectic solvents: overcoming 21st century challenges. *Current Opinion in Green and Sustainable Chemistry* 18:31-36. <https://doi.org/10.1016/j.cogsc.2018.12.003>
- Formela K., Wołosiak M., Klein M., Wang S. (2016). Characterization of volatile compounds, structural, thermal and physico-mechanical properties of cross-linked polyethylene foams degraded thermo-mechanically at variable times. *Polymer Degradation and Stability* 134:383-393. <https://doi.org/10.1016/j.polymdegradstab.2016.11.011>
- Formela K., Zedler L., Hejna A., Tercjak A. (2018). Reactive extrusion of bio-based polymer blends and composites – Current trends and future developments. *Express Polymer Letters* 12(1):24-57. <https://doi.org/10.3144/expresspolymlett.2018.4>
- Franco-Duarte R., Černáková L., Kadam S., S. Kaushik K., Salehi B., Bevilacqua A., Corbo M. R., Antolak H., Dybka-Stępień K., Leszczewicz M. (2019). Advances in chemical and biological methods to identify microorganisms—from past to present. *Microorganisms* 7(5):130. <https://doi.org/10.3390/microorganisms7050130>
- Fu Y., Gu B.-J., Wang J., Gao J., Ganjyal G. M., Wolcott M. P. (2018). Novel micronized woody biomass process for production of cost-effective clean fermentable sugars. *Bioresour technol* 260:311-320. <https://doi.org/10.1016/j.biortech.2018.03.096>
- Fujian X., Hongzhang C., Zuohu L. (2001). Solid-state production of lignin peroxidase (LiP) and manganese peroxidase (MnP) by *Phanerochaete chrysosporium* using steam-exploded

- straw as substrate. *Bioresource technology* 80(2):149-151. [https://doi.org/10.1016/S0960-8524\(01\)00082-7](https://doi.org/10.1016/S0960-8524(01)00082-7)
- Fulekar M. H., Pathak B., Fulekar J., Godambe T. (2013). Bioremediation of Organic Pollutants Using *Phanerochaete chrysosporium*. *Fungi as Bioremediators*, Goltapeh EM, Danesh YR, Varma A (Édit.) Springer Berlin Heidelberg, Berlin, Heidelberg. p 135-157. https://doi.org/10.1007/978-3-642-33811-3_6
- Fülöp G., Domokos A., Galata D., Szabó E., Gyürkés M., Szabó B., Farkas A., Madarász L., Démuth B., Lendér T., Nagy T., Kovács-Kiss D., Van Der Gucht F., Marosi G., Nagy Z. K. (2021). Integrated twin-screw wet granulation, continuous vibrational fluid drying and milling: A fully continuous powder to granule line. *International Journal of Pharmaceutics* 594:120126. <https://doi.org/10.1016/j.ijpharm.2020.120126>
- Gabhane J., William S. P. M. P., Vaidya A. N., Anand D., Wate S. (2014). Pretreatment of garden biomass by alkali-assisted ultrasonication: effects on enzymatic hydrolysis and ultrastructural changes. *Journal of Environmental Health Science and Engineering* 12(1):76. <https://doi.org/10.1186/2052-336X-12-76>
- Galbe M. & Zacchi G. (2007). Pretreatment of lignocellulosic materials for efficient bioethanol production. *Adv Biochem Eng Biotechnol* 108:41-65. https://doi.org/10.1007/10_2007_070
- Gallego-García M., Moreno A. D., Manzanares P., Negro M. J., Duque A. (2023). Recent advances on physical technologies for the pretreatment of food waste and lignocellulosic residues. *Bioresource technology* 369:128397. <https://doi.org/10.1016/j.biortech.2022.128397>
- Ganaie R. J., Rafiq S., Sharma A. (2023) Recent advances in physico-chemical methods for removal of dye from wastewater. *IOP Conference Series: Earth and Environmental Science*. IOP Publishing, p 012040. <https://doi.org/10.1088/1755-1315/1110/1/012040>
- Gao L., Huang D., Cheng M., Yan M., Wei Z., Xiao R., Du L., Wang G., Li R., Chen S., Yin L. (2023). Effect of *Phanerochaete chrysosporium* inoculation on manganese passivation and microbial community succession during electrical manganese residue composting. *Bioresource technology* 370:128497. <https://doi.org/10.1016/j.biortech.2022.128497>
- García-Condado S., López-Lozano R., Panarello L., Cerrani I., Nisini L., Zucchini A., Van der Velde M., Baruth B. (2019). Assessing lignocellulosic biomass production from crop residues in the European Union: Modelling, analysis of the current scenario and drivers of interannual variability. *GCB Bioenergy* 11(6):809-831. <https://doi.org/10.1111/gcbb.12604>
- Garlapati V. K., Chandel A. K., Kumar S. P. J., Sharma S., Sevda S., Ingle A. P., Pant D. (2020). Circular economy aspects of lignin: Towards a lignocellulose biorefinery. *Renewable and Sustainable Energy Reviews* 130. <https://doi.org/10.1016/j.rser.2020.109977>
- Gatt E., Rigal L., Vandenbossche V. (2018). Biomass pretreatment with reactive extrusion using enzymes: A review. *Industrial Crops and Products* 122:329-339. <https://doi.org/10.1016/j.indcrop.2018.05.069>
- Ge X., Vasco-Correa J., Li Y. (2017). 13 - Solid-State Fermentation Bioreactors and Fundamentals. *Current Developments in Biotechnology and Bioengineering*, Larroche C, Sanromán MÁ, Du G, Pandey A (Édit.) Elsevier. p 381-402. <https://doi.org/10.1016/B978-0-444-63663-8.00013-6>

- George A., Brandt A., Tran K., Zahari S. M. S. N. S., Klein-Marcuschamer D., Sun N., Sathitsuksanoh N., Shi J., Stavila V., Parthasarathi R., Singh S., Holmes B. M., Welton T., Simmons B. A., Hallett J. P. (2015). Design of low-cost ionic liquids for lignocellulosic biomass pretreatment. *Green chemistry* 17(3):1728-1734. <https://doi.org/10.1039/c4gc01208a>
- Gervais P. & Molin P. (2003). The role of water in solid-state fermentation. *Biochemical Engineering Journal* 13(2-3):85-101. [https://doi.org/10.1016/S1369-703X\(02\)00122-5](https://doi.org/10.1016/S1369-703X(02)00122-5)
- Ghaemi F., Abdullah L. C., Ariffin H. (2019). Lignocellulose Structure and the Effect on Nanocellulose Production. *Lignocellulose for Future Bioeconomy*. p 17-30. <https://doi.org/10.1016/b978-0-12-816354-2.00002-5>
- Ghandi K. (2014). A Review of Ionic Liquids, Their Limits and Applications. *Green and Sustainable Chemistry* 04(01):44-53. <https://doi.org/10.4236/gsc.2014.41008>
- Ghasemi F., Tabandeh F., Bambai B., Rao K. R. S. S. (2010). Decolorization of different azo dyes by *Phanerochaete chrysosporium* RP78 under optimal condition. *International Journal of Environmental Science & Technology* 7(3):457-464. <https://doi.org/10.1007/bf03326155>
- Glenn J. K. & Gold M. H. (2022). Reprint of: Purification and Characterization of an Extracellular Mn (II)-Dependent Peroxidase from the Lignin-Degrading Basidiomycete, *Phanerochaete chrysosporium*. *Archives of Biochemistry and Biophysics* 726:109251. [https://doi.org/10.1016/0003-9861\(85\)90217-6](https://doi.org/10.1016/0003-9861(85)90217-6)
- Gnanamani A., Jayaprakashvel M., Arulmani M., Sadulla S. (2006). Effect of inducers and culturing processes on laccase synthesis in *Phanerochaete chrysosporium* NCIM 1197 and the constitutive expression of laccase isozymes. *Enzyme and Microbial Technology* 38(7):1017-1021. <https://doi.org/10.1016/j.enzmictec.2006.01.004>
- Godavarti S. & Karwe M. V. (1997). Determination of Specific Mechanical Energy Distribution on a Twin-Screw Extruder. *Journal of Agricultural Engineering Research* 67(4):277-287. <https://doi.org/10.1006/jaer.1997.0172>
- Godswill A. C. (2017). Sugar alcohols: chemistry, production, health concerns and nutritional importance of mannitol, sorbitol, xylitol, and erythritol. *Int. J. Adv. Acad. Res* 3:31-66. <http://hdl.handle.net/20.500.12306/1286>
- Gogoi B. K., Oswalt A. J., Choudhury G. S. (1996). Reverse Screw Element(s) and Feed Composition Effects during Twin-Screw Extrusion of Rice Flour and Fish Muscle Blends. *Journal of Food Science* 61(3):590-595. <https://doi.org/10.1111/j.1365-2621.1996.tb13165.x>
- Gold M. H. & Alic M. (1993). Molecular biology of the lignin-degrading basidiomycete *Phanerochaete chrysosporium*. *Microbiological reviews* 57(3):605-622. <https://doi.org/10.1128/mr.57.3.605-622.1993>
- Goldstein I. (2018). Composition of Biomass. p 9-18. <https://doi.org/10.1201/9781351075251-2>
- Goncalves D., Orišková S., Matos S., Machado H., Vieira S., Bastos D., Gaspar D., Paiva R., Bordado J. C., Rodrigues A., Galhano dos Santos R. (2021). Thermochemical Liquefaction as a Cleaner and Efficient Route for Valuing Pinewood Residues from Forest Fires. *Molecules* 26(23). <https://doi.org/10.3390/molecules26237156>
- Govender S. (2011). Biofilm productivity and concomitant cell autolysis in a membrane bioreactor. *Biotechnology Letters* 33:263-271. <https://doi.org/10.1007/s10529-010-0443-1>

- Government O. (2024). *Alternative feeds for beef cattle*. Ministère de l'Agriculture, de l'Alimentation et de l'Agroentreprise et ministère de Affaires rurales, <https://www.ontario.ca/page/alternative-feeds-beef-cattle> (Consulté le 24/12/2024)
- Government Q. (2025a). *Bioénergies*. <https://transitionenergetique.gouv.qc.ca/en/affaires/programmes/bioenergies> (Consulté le 08/01/2025)
- Government Q. (2025b). *Culture des grains (céréales et oléagineux)*. <https://www.quebec.ca/agriculture-environnement-et-ressources-naturelles/agriculture/industrie-agricole-au-quebec/productions-agricoles/culture-grains-cereales-oleagineux> (Consulté le 08/01/2025)
- Government Q. (2025c). *Technoclimat*. <https://transitionenergetique.gouv.qc.ca/innovation/programme/technoclimat> (Consulté le 08/01/2025)
- Groff D., George A., Sun N., Sathitsuksanoh N., Bokinsky G., Simmons B. A., Holmes B. M., Keasling J. D. (2013). Acid enhanced ionic liquid pretreatment of biomass. *Green chemistry* 15(5). <https://doi.org/10.1039/c3gc37086k>
- Gu B.-J., Wolcott M. P., Ganjyal G. M. (2018). Pretreatment with lower feed moisture and lower extrusion temperatures aids in the increase in the fermentable sugar yields from fine-milled Douglas-fir. *Bioresource technology* 269:262-268. <https://doi.org/10.1016/j.biortech.2018.08.109>
- Gu B. J., Dhumal G. S., Wolcott M. P., Ganjyal G. M. (2019). Disruption of lignocellulosic biomass along the length of the screws with different screw elements in a twin-screw extruder. *Bioresour Technol* 275:266-271. <https://doi.org/10.1016/j.biortech.2018.12.033>
- Gugel I., Summa D., Costa S., Manfredini S., Vertuani S., Marchetti F., Tamburini E. (2024). Mycoremediation of Synthetic Azo Dyes by White-Rot Fungi Grown on Dairy Waste: A Step toward Sustainable and Circular Bioeconomy. *Fermentation* 10(2). <https://doi.org/10.3390/fermentation10020080>
- Guha M., Ali S. Z., Bhattacharya S. (1997). Twin-screw extrusion of rice flour without a die: Effect of barrel temperature and screw speed on extrusion and extrudate characteristics. *Journal of Food Engineering* 32(3):251-267. [https://doi.org/10.1016/s0260-8774\(97\)00028-9](https://doi.org/10.1016/s0260-8774(97)00028-9)
- Guião K. S., Gupta A., Tzoganakis C., Mekonnen T. H. (2022a). Reactive extrusion as a sustainable alternative for the processing and valorization of biomass components. *Journal of Cleaner Production* 355:131840. <https://doi.org/10.1016/j.jclepro.2022.131840>
- Guião K. S., Tzoganakis C., Mekonnen T. H. (2022b). Green mechano-chemical processing of lignocellulosic biomass for lignin recovery. *Chemosphere* 293:133647. <https://doi.org/10.1016/j.chemosphere.2022.133647>
- Guimarães J. L., Frollini E., da Silva C. G., Wypych F., Satyanarayana K. G. (2009). Characterization of banana, sugarcane bagasse and sponge gourd fibers of Brazil. *Industrial Crops and Products* 30(3):407-415. <https://doi.org/10.1016/j.indcrop.2009.07.013>
- Guleria A., Kumari G., Saravanamurugan S. (2020). Chapter 17 - Cellulose valorization to potential platform chemicals. *Biomass, Biofuels, Biochemicals*, Saravanamurugan S, Pandey A, Li H, Riisager A (Édit.) Elsevier. p 433-457. <https://doi.org/10.1016/B978-0-444-64307-0.00017-2>

- Guo X., Peng Z., Huang D., Xu P., Zeng G., Zhou S., Gong X., Cheng M., Deng R., Yi H., Luo H., Yan X., Li T. (2018). Biotransformation of cadmium-sulfamethazine combined pollutant in aqueous environments: *Phanerochaete chrysosporium* bring cautious optimism. *Chemical Engineering Journal* 347:74-83. <https://doi.org/10.1016/j.cej.2018.04.089>
- Guo Y. & Chung C. I. (1989). Dependence of melt temperature on screw speed and size in extrusion. *Polymer Engineering and Science* 29(6):415-419. <https://doi.org/10.1002/pen.760290610>
- Gupta A., Preetam A., Ghosh P., Arora K., Sharma S., Kumar V., Kumar M. (2023a). A novel combinatorial approach for cleaner production of biodegradable sheets from the combination of paddy straw and pine needle waste. *Journal of Cleaner Production* 421:138440. <https://doi.org/10.1016/j.jclepro.2023.138440>
- Gupta A., Tiwari A., Ghosh P., Arora K., Sharma S. (2023b). Enhanced lignin degradation of paddy straw and pine needle biomass by combinatorial approach of chemical treatment and fungal enzymes for pulp making. *Bioresource technology* 368:128314. <https://doi.org/10.1016/j.biortech.2022.128314>
- Gupta A. S. a. M. (2004). Comparison of the flow in co-rotating and counter-rotating twinscrew extruders. *ANTEC* :5. https://plasticflow.com/papers/ANTEC04_twinscrews.pdf
- Gupta R., Sharma M., Jangir V., Gautam A. K., Chandra A., Arya R. K. (2022). A theoretical and mathematical study on the importance of petroleum derivatives in the production of sanitizer based products. *Materials Today: Proceedings*. <https://doi.org/10.1016/j.matpr.2021.12.423>
- Guthrie F. (2010). LII. On eutexia. *The London, Edinburgh, and Dublin Philosophical Magazine and Journal of Science* 17(108):462-482. <https://doi.org/10.1080/14786448408627543>
- Hadj Saadoun J., Bertani G., Levante A., Vezzosi F., Ricci A., Bernini V., Lazzi C. (2021). Fermentation of Agri-Food Waste: A Promising Route for the Production of Aroma Compounds. *Foods* 10(4):707. <https://www.mdpi.com/2304-8158/10/4/707>
- Haghighi Mood S., Hossein Golfeshan A., Tabatabaei M., Salehi Jouzani G., Najafi G. H., Gholami M., Ardjmand M. (2013). Lignocellulosic biomass to bioethanol, a comprehensive review with a focus on pretreatment. *Renewable and Sustainable Energy Reviews* 27:77-93. <https://doi.org/10.1016/j.rser.2013.06.033>
- Hamawand I., Seneweera S., Kumarasinghe P., Bundschuh J. (2020). Nanoparticle technology for separation of cellulose, hemicellulose and lignin nanoparticles from lignocellulose biomass: A short review. *Nano-Structures & Nano-Objects* 24:100601. <https://doi.org/10.1016/j.nanoso.2020.100601>
- Hammel K. E., Kalyanaraman B., Kirk T. K. (1986). Oxidation of polycyclic aromatic hydrocarbons and dibenzo[p]-dioxins by *Phanerochaete chrysosporium* ligninase. *Journal of Biological Chemistry* 261(36):16948-16952. [https://doi.org/10.1016/S0021-9258\(19\)75982-1](https://doi.org/10.1016/S0021-9258(19)75982-1)
- Han S.-Y., Park C.-W., Endo T., Febrianto F., Kim N.-H., Lee S.-H. (2020). Extrusion process to enhance the pretreatment effect of ionic liquid for improving enzymatic hydrolysis of lignocellulosic biomass. *Wood Science and Technology* 54(3):599-613. <https://doi.org/10.1007/s00226-020-01170-9>
- Harmann D. V. & Harper J. M. (1973). Effect of Extruder Geometry on Torque and Flow. *Transactions of the ASAE* 16(6):1175-1178. <https://doi.org/10.13031/2013.37727>
- Hassan Q., Viktor P., J. Al-Musawi T., Mahmood Ali B., Algburi S., Alzoubi H. M., Khudhair Al-Jiboory A., Zuhair Sameen A., Salman H. M., Jaszczur M. (2024). The renewable energy

- role in the global energy Transformations. *Renewable Energy Focus* 48:100545. <https://doi.org/10.1016/j.ref.2024.100545>
- Hassan S. S., Williams G. A., Jaiswal A. K. (2018). Emerging technologies for the pretreatment of lignocellulosic biomass. *Bioresource technology* 262:310-318. <https://doi.org/10.1016/j.biortech.2018.04.099>
- He M.-Q., Zhao R.-L., Liu D.-M., Denchev T. T., Begerow D., Yurkov A., Kemler M., Millanes A. M., Wedin M., McTaggart A. R., Shivas R. G., Buyck B., Chen J., Vizzini A., Papp V., Zmitrovich I. V., Davoodian N., Hyde K. D. (2022). Species diversity of Basidiomycota. *Fungal Diversity* 114(1):281-325. <https://doi.org/10.1007/s13225-021-00497-3>
- He O., Zhang Y., Wang P., Liu L., Wang Q., Yang N., Li W., Champagne P., Yu H. (2021). Experimental and Kinetic Study on the Production of Furfural and HMF from Glucose. *Catalysts* 11(1). <https://doi.org/10.3390/catal11010011>
- He Z., Wang Z., Zhao Z., Yi S., Mu J., Wang X. (2017). Influence of ultrasound pretreatment on wood physiochemical structure. *Ultrasonics Sonochemistry* 34:136-141. <https://doi.org/10.1016/j.ultsonch.2016.05.035>
- Heidari M., Dutta A., Acharya B., Mahmud S. (2019). A review of the current knowledge and challenges of hydrothermal carbonization for biomass conversion. *Journal of the Energy Institute* 92(6):1779-1799. <https://doi.org/10.1016/j.joei.2018.12.003>
- Heltberg R. (2003). *Household energy use in developing countries: a multicountry study*. World Bank Group, (27588) p. <http://documents.worldbank.org/curated/en/560761468780297294/Household-energy-use-in-developing-countries-a-multicountry-study>
- Hennessy K., Lawrence J., Mackey B. (2022). IPCC Sixth Assessment Report (AR6): Climate Change 2022-Impacts, Adaptation and Vulnerability: Regional Factsheet Australasia. <https://coilink.org/20.500.12592/7f1fm4>
- Heredia-Olea E., Pérez-Carrillo E., Serna-Saldívar S. O. (2015). Effect of extrusion conditions and hydrolysis with fiber-degrading enzymes on the production of C5 and C6 sugars from brewers' spent grain for bioethanol production. *Biofuel Research Journal* :203-208. <https://doi.org/10.18331/brj2015.2.1.6>
- Hibbett D. S., Bauer R., Binder M., Giachini A. J., Hosaka K., Justo A., Larsson E., Larsson K. H., Lawrey J. D., Miettinen O., Nagy L. G., Nilsson R. H., Weiss M., Thorn R. G. (2014). 14 Agaricomycetes. *Systematics and Evolution: Part A*, Mclaughlin DJ & Spatafora JW (Edit.) Springer Berlin Heidelberg, Berlin, Heidelberg. p 373-429. https://doi.org/10.1007/978-3-642-55318-9_14
- Hjorth M., Gränitz K., Adamsen A. P. S., Møller H. B. (2011). Extrusion as a pretreatment to increase biogas production. *Bioresource technology* 102(8):4989-4994. <https://doi.org/10.1016/j.biortech.2010.11.128>
- Hoang A. T., Nguyen X. P., Duong X. Q., Ağbulut Ü., Len C., Nguyen P. Q. P., Kchaou M., Chen W.-H. (2023). Steam explosion as sustainable biomass pretreatment technique for biofuel production: Characteristics and challenges. *Bioresource technology* 385:129398. <https://doi.org/10.1016/j.biortech.2023.129398>
- Hoang A. T., Nizetic S., Ong H. C., Mofijur M., Ahmed S. F., Ashok B., Bui V. T. V., Chau M. Q. (2021). Insight into the recent advances of microwave pretreatment technologies for the conversion of lignocellulosic biomass into sustainable biofuel. *Chemosphere* 281:130878. <https://doi.org/10.1016/j.chemosphere.2021.130878>

- Hofrichter M. (2002). Review: lignin conversion by manganese peroxidase (MnP). *Enzyme and Microbial Technology* 30(4):454-466. [https://doi.org/10.1016/S0141-0229\(01\)00528-2](https://doi.org/10.1016/S0141-0229(01)00528-2)
- Hofsten B. V. & Rydéan A.-L. (1975). Submerged cultivation of a thermotolerant basidiomycete on cereal flours and other substrates. *Biotechnology and Bioengineering* 17(8):1183-1197. <https://doi.org/10.1002/bit.260170807>
- Holzbaur E. L. F. & Tien M. (1988). Structure and regulation of a lignin peroxidase gene from *Phanerochaete chrysosporium*. *Biochemical and Biophysical Research Communications* 155(2):626-633. [https://doi.org/10.1016/S0006-291X\(88\)80541-2](https://doi.org/10.1016/S0006-291X(88)80541-2)
- Hrčka R., Kučerová V., Hýrošová T., Hönl V. (2020). Cell Wall Saturation Limit and Selected Properties of Thermally Modified Oak Wood and Cellulose. *Forests* 11(6). <https://doi.org/10.3390/f11060640>
- Hu J., Arantes V., Saddler J. N. (2011). The enhancement of enzymatic hydrolysis of lignocellulosic substrates by the addition of accessory enzymes such as xylanase: is it an additive or synergistic effect? *Biotechnology for Biofuels* 4(1):36. <https://doi.org/10.1186/1754-6834-4-36>
- Hu X. & Gholizadeh M. (2020). Progress of the applications of bio-oil. *Renewable and Sustainable Energy Reviews* 134:110124. <https://doi.org/10.1016/j.rser.2020.110124>
- Huang S., Huang D., Wu Q., Hou M., Tang X., Zhou J. (2020). Effect of environmental C/N ratio on activities of lignin-degrading enzymes produced by *Phanerochaete chrysosporium*. *Pedosphere* 30(2):285-292. [https://doi.org/10.1016/S1002-0160\(17\)60391-6](https://doi.org/10.1016/S1002-0160(17)60391-6)
- Huang T., Qin H., Wang R., Cheng H., Chen L., Qi Z. (2021). Liquid-Liquid Equilibrium for the Esterification System of Acrylic Acid with n-Butanol Catalyzed by Ionic Liquid [BMIm][HSO₄] at Atmospheric Pressure. *Journal of Chemical & Engineering Data*. <https://doi.org/10.1021/acs.jced.1c00170>
- Huang Y.-F., Chiueh P.-T., Kuan W.-H., Lo S.-L. (2016). Microwave pyrolysis of lignocellulosic biomass: Heating performance and reaction kinetics. *Energy* 100:137-144. <https://doi.org/10.1016/j.energy.2016.01.088>
- Huang Y. L. & Ma Y. S. (2019). Optimization of the extrusion process for preparation of soluble dietary fiber-enriched calamondin pomace and its influence on the properties of bread. *J Food Sci Technol* 56(12):5444-5453. <https://doi.org/10.1007/s13197-019-04015-x>
- Hurtubise F. G. & Krassig H. (1960). Classification of fine structural characteristics in cellulose by infrared spectroscopy. Use of potassium bromide pellet technique. *Analytical Chemistry* 32(2):177-181. <https://doi.org/10.1021/ac60158a010>
- HydroQuébec (2023). 2023 Tarif d'électricité. (Bibliothèque et Archives nationales du Québec, 2023). <https://www.hydroquebec.com/data/documents-donnees/pdf/tarifs-electricite.pdf?v=20230401>
- Ibbini J., Al-Kofahi S., Davis L. C., Alrousan D., Elshebli M. (2024). Investigating the Potential of *Fusarium solani* and *Phanerochaete chrysosporium* in the Removal of 2,4,6-TNT. *Applied Biochemistry and Biotechnology* 196(5):2713-2727. <https://doi.org/10.1007/s12010-023-04735-z>
- Ichinose H., Ukeba S., Kitaoka T. (2022). Latent potentials of the white-rot basidiomycete *Phanerochaete chrysosporium* responsible for sesquiterpene metabolism: CYP5158A1 and CYP5144C8 decorate (E)- α -bisabolene. *Enzyme and Microbial Technology* 158:110037. <https://doi.org/10.1016/j.enzmictec.2022.110037>

- IEA (2022). *Global Energy Review: CO2 Emissions in 2021*. IEA, Paris p.<https://www.iea.org/reports/global-energy-review-co2-emissions-in-2021-2>
- IEA (2024). *Global EV Outlook 2024*. <https://www.iea.org/reports/global-ev-outlook-2024>
- Ilanidis D., Stage S., Jönsson L. J., Martín C. (2021). Hydrothermal Pretreatment of Wheat Straw: Effects of Temperature and Acidity on Byproduct Formation and Inhibition of Enzymatic Hydrolysis and Ethanol Fermentation. *Agronomy* 11(3). <https://doi.org/10.3390/agronomy11030487>
- Ioelovich M. & Morag E. (2012). Study of enzymatic hydrolysis of pretreated biomass at increased solids loading. *BioResources* 7(4). <https://doi.org/10.15376/biores.7.4.4672-4682>
- Ippolito J., Lentz R., Novak J., Spokas K., Collins H., Streubel J. (2011) Biochar usage: Pros and cons. *Western Nutrient Management Conference Proceedings, March 3-4, 2011, Reno, Nevada*. p 93-98. <https://eprints.nwisrl.ars.usda.gov/id/eprint/1522>
- Iram A., Cekmecelioglu D., Demirci A. (2022). Integrating 1G with 2G Bioethanol Production by Using Distillers' Dried Grains with Solubles (DDGS) as the Feedstock for Lignocellulosytic Enzyme Production. *Fermentation* 8(12). <https://doi.org/10.3390/fermentation8120705>
- Jain S. & Kumar S. (2024). A comprehensive review of bioethanol production from diverse feedstocks: Current advancements and economic perspectives. *Energy* 296:131130. <https://doi.org/10.1016/j.energy.2024.131130>
- Jędrzejczyk M., Soszka E., Czapnik M., Ruppert A. M., Grams J. (2019). Chapter 6 - Physical and chemical pretreatment of lignocellulosic biomass. *Second and Third Generation of Feedstocks*, Basile A & Dalena F (Édit.) Elsevier. p 143-196. <https://doi.org/10.1016/B978-0-12-815162-4.00006-9>
- Jiang B., Jiao H., Guo X., Chen G., Guo J., Wu W., Jin Y., Cao G., Liang Z. (2023). Lignin-Based Materials for Additive Manufacturing: Chemistry, Processing, Structures, Properties, and Applications. *Advanced Science* 10(9):2206055. <https://doi.org/10.1002/advs.202206055>
- Jin M. & Dale B. E. (2024). AFEX™ Pretreatment-Based Biorefinery Technologies. *Handbook of Biorefinery Research and Technology: Biomass Logistics to Saccharification*, Bisaria V (Édit.) Springer Netherlands, Dordrecht. p 457-472. https://doi.org/10.1007/978-94-007-6308-1_2
- Jing X., Zhang X., Bao J. (2009). Inhibition Performance of Lignocellulose Degradation Products on Industrial Cellulase Enzymes During Cellulose Hydrolysis. *Applied Biochemistry and Biotechnology* 159(3):696-707. <https://doi.org/10.1007/s12010-009-8525-z>
- Joseph P., Opedal M. T., Moe S. T. (2021). The O-factor: using the H-factor concept to predict the outcome of organosolv pretreatment. *Biomass Conversion and Biorefinery*. <https://doi.org/10.1007/s13399-021-01667-8>
- Jung W., Savithri D., Sharma-Shivappa R., Kolar P. (2018). Changes in Lignin Chemistry of Switchgrass due to Delignification by Sodium Hydroxide Pretreatment. *Energies* 11(2). <https://doi.org/10.3390/en11020376>
- Kádár Z., Szengyel Z., Réczey K. (2004). Simultaneous saccharification and fermentation (SSF) of industrial wastes for the production of ethanol. *Industrial Crops and Products* 20(1):103-110. <https://doi.org/10.1016/j.indcrop.2003.12.015>
- Kalhor P. & Ghandi K. (2019). Deep Eutectic Solvents for Pretreatment, Extraction, and Catalysis of Biomass and Food Waste. *Molecules* 24(22). <https://doi.org/10.3390/molecules24224012>

- Kalra A. & Gupta A. (2021). Recent advances in decolourization of dyes using iron nanoparticles: A mini review. *Materials Today: Proceedings* 36:689-696. <https://doi.org/10.1016/j.matpr.2020.04.677>
- Kameshwar A. K. S. & Qin W. (2017). Qualitative and quantitative methods for isolation and characterization of lignin-modifying enzymes secreted by microorganisms. *BioEnergy Research* 10:248-266. <https://doi.org/10.1007/s12155-016-9784-5>
- Kang K. E., Han M., Moon S.-K., Kang H.-W., Kim Y., Cha Y.-L., Choi G.-W. (2013). Optimization of alkali-extrusion pretreatment with twin-screw for bioethanol production from Miscanthus. *Fuel* 109:520-526. <https://doi.org/10.1016/j.fuel.2013.03.026>
- Kapoor M., Semwal S., Gaur R., Kumar R., Gupta R. P., Puri S. K. (2018). The Pretreatment Technologies for Deconstruction of Lignocellulosic Biomass. Springer Singapore. p 395-421. https://doi.org/10.1007/978-981-10-7431-8_17
- Karimi F., Mazaheri D., Saei Moghaddam M., Mataei Moghaddam A., Sanati A. L., Orooji Y. (2021). Solid-state fermentation as an alternative technology for cost-effective production of bioethanol as useful renewable energy: a review. *Biomass Conversion and Biorefinery*. <https://doi.org/10.1007/s13399-021-01875-2>
- Karimi K. & Taherzadeh M. J. (2016). A critical review of analytical methods in pretreatment of lignocelluloses: Composition, imaging, and crystallinity. *Bioresour technol* 200:1008-1018. <https://doi.org/10.1016/j.biortech.2015.11.022>
- Karunanithy C. & Muthukumarappan K. (2010). Effect of extruder parameters and moisture content of switchgrass, prairie cord grass on sugar recovery from enzymatic hydrolysis. *Appl Biochem Biotechnol* 162(6):1785-1803. <https://doi.org/10.1007/s12010-010-8959-3>
- Karunanithy C. & Muthukumarappan K. (2011a). Influence of extruder and feedstock variables on torque requirement during pretreatment of different types of biomass – A response surface analysis. *Biosystems Engineering* 109(1):37-51. <https://doi.org/10.1016/j.biosystemseng.2011.02.001>
- Karunanithy C. & Muthukumarappan K. (2011b). Optimization of switchgrass and extruder parameters for enzymatic hydrolysis using response surface methodology. *Industrial Crops and Products* 33(1):188-199. <https://doi.org/10.1016/j.indcrop.2010.10.008>
- Karunanithy C. & Muthukumarappan K. (2013). Thermo-Mechanical Pretreatment of Feedstocks. *Green Biomass Pretreatment for Biofuels Production*, Gu T (Édit.) Springer Netherlands, Dordrecht. p 31-65. https://doi.org/10.1007/978-94-007-6052-3_2
- Karunanithy C., Muthukumarappan K., Gibbons W. R. (2012a). Extrusion pretreatment of pine wood chips. *Appl Biochem Biotechnol* 167(1):81-99. <https://doi.org/10.1007/s12010-012-9662-3>
- Karunanithy C., Muthukumarappan K., Gibbons W. R. (2012b). Extrusion Pretreatment of Pine Wood Chips. *Applied Biochemistry and Biotechnology* 167(1):81-99. <https://doi.org/10.1007/s12010-012-9662-3>
- Karunanithy C., Muthukumarappan K., Gibbons W. R. (2014). Sequential extrusion-microwave pretreatment of switchgrass and big bluestem. *Bioresour Technol* 153:393-398. <https://doi.org/10.1016/j.biortech.2013.12.032>
- Kato H., Takahashi Y., Suzuki H., Ohashi K., Kawashima R., Nakamura K., Sakai K., Hori C., Takasuka Taichi E., Kato M., Shimizu M. (2024). Identification and characterization of methoxy- and dimethoxyhydroquinone 1,2-dioxygenase from *Phanerochaete*

- chryso sporium. *Applied and Environmental Microbiology* 90(2):e01753-01723. <https://doi.org/10.1128/aem.01753-23>
- Kazi F. K., Fortman J. A., Anex R. P., Hsu D. D., Aden A., Dutta A., Kothandaraman G. (2010). Techno-economic comparison of process technologies for biochemical ethanol production from corn stover. *Fuel* 89:S20-S28. <https://doi.org/10.1016/j.fuel.2010.01.001>
- Kelly A. L., Brown E. C., Coates P. D. (2006). The effect of screw geometry on melt temperature profile in single screw extrusion. *Polymer Engineering & Science* 46(12):1706-1714. <https://doi.org/10.1002/pen.20657>
- Kempa K., Moslener U., Schenker O. (2021). The cost of debt of renewable and non-renewable energy firms. *Nature Energy* 6(2):135-142. <https://doi.org/10.1038/s41560-020-00745-x>
- Kerboua K., Mazouz D., Hasaounia I. (2022). Single acoustic cavitation bubble and energy concentration concept. *Energy Aspects of Acoustic Cavitation and Sonochemistry*, Elsevier. p 3-23. <https://doi.org/10.1016/B978-0-323-91937-1.00020-7>
- Keskin T., Nalakath Abubackar H., Arslan K., Azbar N. (2019). Biohydrogen Production From Solid Wastes. *Biohydrogen*. p 321-346. <https://doi.org/10.1016/b978-0-444-64203-5.00012-5>
- Khalil H., Legin E., Kurek B., Perre P., Taidi B. (2021). Morphological growth pattern of Phanerochaete chryso sporium cultivated on different Miscanthus x giganteus biomass fractions. *BMC Microbiology* 21(1):318. <https://doi.org/10.1186/s12866-021-02350-8>
- Khan M. A. K. M. A., Panakkal E. J., Sriariyanun M., Gundupalli M. P., Roddecha S., Katam K., Jayaprakash J., Cheenkachorn K. (2024). Dewaxing and Post-Pretreatment Washing: Impact on Sugar and Ethanol Yields from Tobacco Residue. *Applied Science and Engineering Progress* 17(4):7495-7495. <https://doi.org/10.14416/j.asep.2024.07.010>
- Kim S. K., Park P. J., Kim J. B., Shahidi F. (2002). Purification and characterization of a collagenolytic protease from the filefish, *Novodon modestrus*. *J Biochem Mol Biol* 35(2):165-171. <https://doi.org/10.5483/bmbrep.2002.35.2.165>
- Ko J. K., Um Y., Park Y.-C., Seo J.-H., Kim K. H. (2015). Compounds inhibiting the bioconversion of hydrothermally pretreated lignocellulose. *Applied Microbiology and Biotechnology* 99(10):4201-4212. <https://doi.org/10.1007/s00253-015-6595-0>
- Kobayashi M. (2021). Chapter 1 - Introduction. *Dry Syngas Purification Processes for Coal Gasification Systems*, Kobayashi M (Édit.) Elsevier. p 1-49. <https://doi.org/10.1016/B978-0-12-818866-8.00001-X>
- Koduri R. S. & Tien M. (1994). Kinetic Analysis of Lignin Peroxidase: Explanation for the Mediation Phenomenon by Veratryl Alcohol. *Biochemistry* 33(14):4225-4230. <https://doi.org/10.1021/bi00180a016>
- Koduri R. S. & Tien M. (1995). Oxidation of Guaiacol by Lignin Peroxidase: ROLE OF VERATRYL ALCOHOL (∗). *Journal of Biological Chemistry* 270(38):22254-22258. <https://doi.org/10.1074/jbc.270.38.22254>
- Kohlgrüber K., Ullrich M., Hepperle J., Rudolf R., König T., Liesenfelder U., Bierdel M., Kirchhoff J., Lechner F., Sämann H.-J., Wiedmann W., Heidemeyer P., Wuttke R., Christ H., Davids R., Weller U. (2008). Co-rotating twin-screw extruders fundamentals, technology, and applications. <https://doi.org/10.3139/9783446433410>
- Komatsu T. & Yokoyama T. (2021). Revisiting the condensation reaction of lignin in alkaline pulping with quantitativity part I: the simplest condensation between vanillyl alcohol and

- creosol under soda cooking conditions. *Journal of Wood Science* 67(1):45. <https://doi.org/10.1186/s10086-021-01978-4>
- Konan D., Koffi E., Ndao A., Peterson E. C., Rodrigue D., Adjallé K. (2022a). An Overview of Extrusion as a Pretreatment Method of Lignocellulosic Biomass. *Energies* 15(9). <https://doi.org/10.3390/en15093002>
- Konan D., Koffi E., Ndao A., Peterson E. C., Rodrigue D., Adjallé K. (2022b). An Overview of Extrusion as a Pretreatment Method of Lignocellulosic Biomass. *Energies* 15(9):3002. <https://doi.org/10.3390/en15093002>
- Konan D., Ndao A., Koffi E., Elkoun S., Robert M., Rodrigue D., Adjallé K. (2024a). Biodecomposition with *Phanerochaete chrysosporium*: A review. *AIMS Microbiology* 10(4):1068-1101. <https://doi.org/10.3934/microbiol.2024046>
- Konan D., Rodrigue D., Koffi E., Elkoun S., Ndao A., Adjallé K. (2024b). Combination of Technologies for Biomass Pretreatment: A Focus on Extrusion. *Waste and Biomass Valorization*. <https://doi.org/10.1007/s12649-024-02472-w>
- Koopman F., Wierckx N., de Winde J. H., Ruijsenaars H. J. (2010). Identification and characterization of the furfural and 5-(hydroxymethyl) furfural degradation pathways of *Cupriavidus basilensis* HMF14. *Proceedings of the National Academy of Sciences* 107(11):4919-4924. <https://doi.org/10.1073/pnas.0913039107>
- Kordala N., Walter M., Brzozowski B., Lewandowska M. (2024). 2G-biofuel ethanol: an overview of crucial operations, advances and limitations. *Biomass Conversion and Biorefinery* 14(3):2983-3006. <https://doi.org/10.1007/s13399-022-02861-y>
- Kordbacheh F. & Heidari G. (2023). Water pollutants and approaches for their removal. *Materials Chemistry Horizons* 2(2):139-153. <https://doi.org/10.22128/mch.2023.684.1039>
- Kostas E. T., Beneroso D., Robinson J. P. (2017). The application of microwave heating in bioenergy: A review on the microwave pre-treatment and upgrading technologies for biomass. *Renewable and Sustainable Energy Reviews* 77:12-27. <https://doi.org/10.1016/j.rser.2017.03.135>
- Krause C., Rossi S., Thibeault-Martel M., Plourde P. Y. (2010). Relationships of climate and cell features in stems and roots of black spruce and balsam fir. *Annals of Forest Science* 67(4):402-402. <https://doi.org/10.1051/forest/2009122>
- Krigstin S., Wetzel S., Mabee W., Stadnyk S. (2016). Can woody biomass support a pellet industry in southeastern Ontario: A case study. *The Forestry Chronicle* 92:189-199. <https://doi.org/10.5558/tfc2016-038>
- Krishania M., Sindhu R., Binod P., Ahluwalia V., Kumar V., Sangwan R. S., Pandey A. (2018). Design of Bioreactors in Solid-State Fermentation. *Current Developments in Biotechnology and Bioengineering*. p 83-96. <https://doi.org/10.1016/b978-0-444-63990-5.00005-0>
- Kristensen J. B., Felby C., Jørgensen H. (2009). Yield-determining factors in high-solids enzymatic hydrolysis of lignocellulose. *Biotechnology for Biofuels* 2(1):11. <https://doi.org/10.1186/1754-6834-2-11>
- Kumar D. & Singh V. (2019). Bioethanol Production From Corn. *Corn*. p 615-631. <https://doi.org/10.1016/b978-0-12-811971-6.00022-x>

- Kumar P., Barrett D. M., Delwiche M. J., Stroeve P. (2009). Methods for Pretreatment of Lignocellulosic Biomass for Efficient Hydrolysis and Biofuel Production. *Industrial & engineering chemistry research* 48(8):3713-3729. <https://doi.org/10.1021/ie801542g>
- Kumar V., Yadav S. K., Kumar J., Ahluwalia V. (2020). A critical review on current strategies and trends employed for removal of inhibitors and toxic materials generated during biomass pretreatment. *Bioresource technology* 299:122633. <https://doi.org/10.1016/j.biortech.2019.122633>
- Kunamneni A., Ballesteros A., Plou F. J., Alcalde M. (2007). Fungal laccase—a versatile enzyme for biotechnological applications. *Communicating current research and educational topics and trends in applied microbiology* 1:233-245. https://doi.org/10.1007/978-3-030-10480-1_13
- Kundu C., Samudrala S. P., Kibria M. A., Bhattacharya S. (2021). One-step peracetic acid pretreatment of hardwood and softwood biomass for platform chemicals production. *Scientific Reports* 11(1):11183. <https://doi.org/10.1038/s41598-021-90667-9>
- Kuppuraj S. P., Venkidasamy B., Selvaraj D., Ramalingam S. (2021). Comprehensive in silico and gene expression profiles of MnP family genes in Phanerochaete chrysosporium towards lignin biodegradation. *International Biodeterioration & Biodegradation* 157:105143. <https://doi.org/10.1016/j.ibiod.2020.105143>
- Kurian J. K., Garipey Y., Orsat V., Raghavan G. S. V. (2015). Microwave-assisted lime treatment and recovery of lignin from hydrothermally treated sweet sorghum bagasse. *Biofuels* 6(5-6):341-355. <https://doi.org/10.1080/17597269.2015.1110775>
- Kuster Moro M., Sposina Sobral Teixeira R., Sant'Ana da Silva A., Duarte Fujimoto M., Albuquerque Melo P., Resende Secchi A., Pinto da Silva Bon E. (2017). Continuous pretreatment of sugarcane biomass using a twin-screw extruder. *Industrial Crops and Products* 97:509-517. <https://doi.org/10.1016/j.indcrop.2016.12.051>
- Kwanga S. N., Djuffo D. T., Boum A. T., Anoh F. A., Dongmo P. M. J. (2022). Effect of Solid-State Fermentation on the Essential Oil Yield of Curcuma longa Residues. *Waste and Biomass Valorization*. <https://doi.org/10.1007/s12649-022-01817-7>
- La Fuente C. I. A., do Val Siqueira L., Augusto P. E. D., Tadini C. C. (2022). Casting and extrusion processes to produce bio-based plastics using cassava starch modified by the dry heat treatment (DHT). *Innovative Food Science & Emerging Technologies* 75:102906. <https://doi.org/10.1016/j.ifset.2021.102906>
- Ladisch M. R., Kohlman K. L., Westgate P. L., Weil J. R., Yang Y. (1998). *Processes for treating cellulosic material*. Transfer PRFOOT, 08/273,417, (United States) Attribué.
- Lam S. S., Liew R. K., Jusoh A., Chong C. T., Ani F. N., Chase H. A. (2016). Progress in waste oil to sustainable energy, with emphasis on pyrolysis techniques. *Renewable and Sustainable Energy Reviews* 53:741-753. <https://doi.org/10.1016/j.rser.2015.09.005>
- Lamsal B., Yoo J., Brijwani K., Alavi S. (2010). Extrusion as a thermo-mechanical pre-treatment for lignocellulosic ethanol. *Biomass and Bioenergy* 34(12):1703-1710. <https://doi.org/10.1016/j.biombioe.2010.06.009>
- Larrondo L. F., Vicuña R., Cullen D. (2005). 14 - Phanerochaete chrysosporium Genomics. *Applied Mycology and Biotechnology*, Arora DK & Berka RM (Édit.) Elsevier, Vol 5. p 315-352. [https://doi.org/10.1016/S1874-5334\(05\)80016-4](https://doi.org/10.1016/S1874-5334(05)80016-4)
- Laureano-Perez L., Teymouri F., Alizadeh H., Dale B. E. (2005). Understanding Factors that Limit Enzymatic Hydrolysis of Biomass: Characterization of Pretreated Corn Stover. *Applied*

- Lee A. H., Lee H., Heo Y. M., Lim Y. W., Kim C.-M., Kim G.-H., Chang W., Kim J.-J. (2020). A proposed stepwise screening framework for the selection of polycyclic aromatic hydrocarbon (PAH)-degrading white rot fungi. *Bioprocess and Biosystems Engineering* 43(5):767-783. <https://doi.org/10.1007/s00449-019-02272-w>
- Lee S. H., Teramoto Y., Endo T. (2009). Enzymatic saccharification of woody biomass micro/nanofibrillated by continuous extrusion process I--effect of additives with cellulose affinity. *Bioresour Technol* 100(1):275-279. <https://doi.org/10.1016/j.biortech.2008.05.051>
- Lei H., Fulcher R. G., Ruan R., van Lengerich B. (2005). Empirical Modeling of Die Pressure, Shaft Torque, SME, and Product Temperature of Rice Flour in a Corotating Twin-Screw Extruder. *Cereal Chemistry Journal* 82(5):582-587. <https://doi.org/10.1094/cc-82-0582>
- Lei Z., Chen B., Koo Y. M., MacFarlane D. R. (2017). Introduction: Ionic Liquids. *Chem Rev* 117(10):6633-6635. <https://doi.org/10.1021/acs.chemrev.7b00246>
- Leng J., Wu J., Chen N., Xu X., Zhang J. (2019). The development of a conical screw-based extrusion deposition system and its application in fused deposition modeling with thermoplastic polyurethane. *Rapid Prototyping Journal* 26(2):409-417. <https://doi.org/10.1108/rpj-05-2019-0139>
- Levin R., Krigstin S., Wetzel S. (2011). Biomass availability in eastern Ontario for bioenergy and wood pellet initiatives. *The Forestry Chronicle* 87(1):33-41. <https://doi.org/10.5558/tfc87033-1>
- Li B., Li H., Zha Q., Bandekar R., Alsaggaf A., Ni Y. (2011). Effects of wood quality and refining process on TMP pulp and paper quality. *BioResources* 6(3). <http://dx.doi.org/10.15376/biores.6.3.3569-3584>
- Li C., Knierim B., Manisseri C., Arora R., Scheller H. V., Auer M., Vogel K. P., Simmons B. A., Singh S. (2010). Comparison of dilute acid and ionic liquid pretreatment of switchgrass: Biomass recalcitrance, delignification and enzymatic saccharification. *Bioresour Technol* 101(13):4900-4906. <https://doi.org/10.1016/j.biortech.2009.10.066>
- Li D., Wu R., Zhang S., Liu Z., Wei P., Hu X., Huang L., Shen X., Jiang J., Wang L. (2024a). Sulfite Pretreatment Enhances Tobacco Stalk Deconstruction for Cellulose Saccharification and Lignin Pyrolysis. *Catalysts* 14(12):889. <https://doi.org/10.3390/catal14120889>
- Li H. Q., Li C. L., Sang T., Xu J. (2013). Pretreatment on Miscanthus lutarioriparius by liquid hot water for efficient ethanol production. *Biotechnol Biofuels* 6(1):76. <https://doi.org/10.1186/1754-6834-6-76>
- Li M., Cao S., Meng X., Studer M., Wyman C. E., Ragauskas A. J., Pu Y. (2017). The effect of liquid hot water pretreatment on the chemical-structural alteration and the reduced recalcitrance in poplar. *Biotechnol Biofuels* 10:237. <https://doi.org/10.1186/s13068-017-0926-6>
- Li N., Yu J., Wang X., Chen L., Jiang H., Zhang W. (2024b). Growth, Oxidative Stress and Ability to Degrade Tetrabromobisphenol A of Phanerochaete chrysosporium in the Presence of Different Nano Iron Oxides. *Water* 16(4). <https://doi.org/10.3390/w16040567>
- Li Q., Wang J., Wang Z., Zhang W., Zhan H., Xiao T., Yu X., Zheng Y. (2023). Surfactants double the biodegradation rate of persistent polycyclic aromatic hydrocarbons (PAHs) by a white-

- rot fungus *Phanerochaete sordida*. *Environmental Earth Sciences* 82(12):285. <https://doi.org/10.1007/s12665-023-10970-8>
- Li Q., Zhou Z., Zhang D., Wang Z., Cong W. (2020). Lipid extraction from *Nannochloropsis oceanica* biomass after extrusion pretreatment with twin-screw extruder: optimization of processing parameters and comparison of lipid quality. *Bioprocess and Biosystems Engineering* 43(4):655-662. <https://doi.org/10.1007/s00449-019-02263-x>
- Li T., Chen C., Brozena A. H., Zhu J. Y., Xu L., Driemeier C., Dai J., Rojas O. J., Isogai A., Wagberg L., Hu L. (2021). Developing fibrillated cellulose as a sustainable technological material. *Nature* 590(7844):47-56. <https://doi.org/10.1038/s41586-020-03167-7>
- Li T., Cui L., Song X., Cui X., Wei Y., Tang L., Mu Y., Xu Z. (2022). Wood decay fungi: an analysis of worldwide research. *Journal of Soils and Sediments* 22(6):1688-1702. <https://doi.org/10.1007/s11368-022-03225-9>
- Liang Y., Lei B., Zhong H.-T., Feng Y.-H., Qu J.-P. (2016). A promising screw-extrusion steam explosion pretreatment process: effects on the morphological and structural features of *Eucalyptus* woodchips. *RSC Advances* 6(111):109657-109663. <https://doi.org/10.1039/c6ra24639g>
- Lim Y.-W., Baik K.-S., Chun J.-S., Lee K.-H., Jung W.-J., Bae K.-S. (2007). Accurate delimitation of *Phanerochaete chrysosporium* and *Phanerochaete sordida* by specific PCR primers and cultural approach. *Journal of microbiology and biotechnology* 17(3):468-473. <https://koreascience.kr/article/JAKO200714539087214.pdf>
- Liu C., Chen G., Zhou Y., Yue L., Liu W. (2022). Investigation on compression and mildew of mixed and separated maize. *Food Science & Nutrition*. <https://doi.org/10.1002/fsn3.2985>
- Liu C., Van Der Heide E., Wang H., Li B., Yu G., Mu X. (2013). Alkaline twin-screw extrusion pretreatment for fermentable sugar production. *Biotechnology for Biofuels* 6(1):97. 10.1186/1754-6834-6-97
- Liu K.-X., Li H.-Q., Zhang J., Zhang Z.-G., Xu J. (2016a). The effect of non-structural components and lignin on hemicellulose extraction. *Bioresource technology* 214:755-760. <https://doi.org/10.1016/j.biortech.2016.05.036>
- Liu K., Du H., Zheng T., Liu H., Zhang M., Zhang R., Li H., Xie H., Zhang X., Ma M., Si C. (2021). Recent advances in cellulose and its derivatives for oilfield applications. *Carbohydrate Polymers* 259:117740. <https://doi.org/10.1016/j.carbpol.2021.117740>
- Liu L., Li H., Liu Y., Li Y., Wang H. (2020a). Whole Transcriptome Analysis Provides Insights Into the Molecular Mechanisms of Chlamydospore-Like Cell Formation in *Phanerochaete chrysosporium*. *Frontiers in Microbiology* 11. <https://doi.org/10.3389/fmicb.2020.527389>
- Liu L., Qin Y., Li P., Li Y., Wang Y., Wang G., Wang H. (2016b). Improvement in continuous cropping of cut chrysanthemum by *phanerochaete chrysosporium*. *Pak. J. Bot* 48(4):1453-1457. <https://inis.iaea.org/records/2n1zz-b4921>
- Liu Q., Bai J.-f., Gu W.-h., Peng S.-j., Wang L.-c., Wang J.-w., Li H.-x. (2020b). Leaching of copper from waste printed circuit boards using *Phanerochaete chrysosporium* fungi. *Hydrometallurgy* 196:105427. <https://doi.org/10.1016/j.hydromet.2020.105427>
- Liu Q., Luo L., Zheng L. (2018). Lignins: biosynthesis and biological functions in plants. *International Journal of Molecular Sciences* 19(2):335. <https://doi.org/10.3390/ijms19020335>

- Liu Y., Nie Y., Lu X., Zhang X., He H., Pan F., Zhou L., Liu X., Ji X., Zhang S. (2019). Cascade utilization of lignocellulosic biomass to high-value products. *Green chemistry* 21(13):3499-3535. <https://doi.org/10.1039/c9gc00473d>
- Lo S.-L., Huang Y.-F., Chiueh P.-T., Kuan W.-H. (2017). Microwave Pyrolysis of Lignocellulosic Biomass. *Energy Procedia* 105:41-46. <https://doi.org/10.1016/j.egypro.2017.03.277>
- Locoh A., Thiffault É., Barnabé S. (2022). Sustainability Impact Assessment of Forest Bioenergy Value Chains in Quebec (Canada)—A ToSIA Approach. *Energies* 15(18). <https://doi.org/10.3390/en15186676>
- Long J., Xu Y., Wang T., Yuan Z., Shu R., Zhang Q., Ma L. (2015). Efficient base-catalyzed decomposition and in situ hydrogenolysis process for lignin depolymerization and char elimination. *Applied energy* 141:70-79. <https://doi.org/10.1016/j.apenergy.2014.12.025>
- Lonsane B. K., Ghildyal N. P., Budiartman S., Ramakrishna S. V. (1985). Engineering aspects of solid state fermentation. *Enzyme and Microbial Technology* 7(6):258-265. [https://doi.org/10.1016/0141-0229\(85\)90083-3](https://doi.org/10.1016/0141-0229(85)90083-3)
- Lundell T. K., Mäkelä M. R., de Vries R. P., Hildén K. S. (2014). Chapter Eleven - Genomics, Lifestyles and Future Prospects of Wood-Decay and Litter-Decomposing Basidiomycota. *Advances in Botanical Research*, Martin FM (Édit.) Academic Press, Vol 70. p 329-370. <https://doi.org/10.1016/B978-0-12-397940-7.00011-2>
- Luo J., Fang Z., Smith R. L. (2014). Ultrasound-enhanced conversion of biomass to biofuels. *Progress in energy and combustion science* 41:56-93. <https://doi.org/10.1016/j.pecs.2013.11.001>
- Luzzi S. C., Artifon W., Piovesan B., Tozetto E., Mulinari J., Kuhn G. d. O., Mazutti M. A., Priamo W. L., Mossi A. J., Silva M. F., Golunski S. M., Treichel H., Bender J. P. (2017). Pretreatment of lignocellulosic biomass using ultrasound aiming at obtaining fermentable sugar. *Biocatalysis and Biotransformation* 35(3):161-167. <https://doi.org/10.1080/10242422.2017.1310206>
- MacFarlane D. R., Tachikawa N., Forsyth M., Pringle J. M., Howlett P. C., Elliott G. D., Davis J. H., Watanabe M., Simon P., Angell C. A. (2014). Energy applications of ionic liquids. *Energy Environ. Sci.* 7(1):232-250. <https://doi.org/10.1039/c3ee42099j>
- Machado de Castro A., Fragoso dos Santos A., Kachrimanidou V., Koutinas A. A., Freire D. M. G. (2018). Chapter 10 - Solid-State Fermentation for the Production of Proteases and Amylases and Their Application in Nutrient Medium Production. *Current Developments in Biotechnology and Bioengineering*, Pandey A, Larroche C, Soccol CR (Édit.) Elsevier. p 185-210. <https://doi.org/10.1016/B978-0-444-63990-5.00010-4>
- Madhankumar S. & Viswanathan K. (2024). 4 - A review of the utilization of biomass-based materials in food packaging. *Plant Biomass Applications*, Jawaid M, Khan A, Ahmed Asiri AM (Édit.) Academic Press. p 77-108. <https://doi.org/10.1016/B978-0-443-15465-2.00006-9>
- Mankar A. R., Pandey A., Modak A., Pant K. K. (2021). Pretreatment of lignocellulosic biomass: A review on recent advances. *Bioresource technology* 334:125235. <https://doi.org/10.1016/j.biortech.2021.125235>
- Manpreet S., Sawraj S., Sachin D., Pankaj S., Banerjee U. (2005). Influence of process parameters on the production of metabolites in solid-state fermentation. *Malaysian Journal of Microbiology* 2(1):1-9. <http://dx.doi.org/10.21161/mjm.120501>

- Mardawati E., Sinurat Y., Yuliana T., Iop (2020). Production of Crude Xylanase From *Trichoderma* sp. Using *Reutealis trisperma* Exocarp Substrate in Solid State Fermentation. in *INTERNATIONAL CONFERENCE OF SUSTAINABILITY AGRICULTURE AND BIOSYSTEM*). <https://doi.org/10.1088/1755-1315/515/1/012024>
- Marianou A. A., Michailof C. C., Ipsakis D., Triantafyllidis K., Lappas A. A. (2019). Cellulose conversion into lactic acid over supported HPA catalysts. *Green chemistry* 21(22):6161-6178. <https://doi.org/10.1039/C9GC02622C>
- Marone A., Trably E., Carrère H., Prompsy P., Guillon F., Joseph-Aimé M., Barakat A., Fayoud N., Bernet N., Escudié R. (2018). Enhancement of corn stover conversion to carboxylates by extrusion and biotic triggers in solid-state fermentation. *Applied Microbiology and Biotechnology* 103(1):489-503. <https://doi.org/10.1007/s00253-018-9463-x>
- Martínez-Avila O., Llenas L., Ponsá S. (2022). Sustainable polyhydroxyalkanoates production via solid-state fermentation: Influence of the operational parameters and scaling up of the process. *Food and Bioproducts Processing* 132:13-22. <https://doi.org/10.1016/j.fbp.2021.12.002>
- Martinez D., Larrondo L. F., Putnam N., Gelpke M. D. S., Huang K., Chapman J., Helfenbein K. G., Ramaiya P., Detter J. C., Larimer F., Coutinho P. M., Henrissat B., Berka R., Cullen D., Rokhsar D. (2004). Genome sequence of the lignocellulose degrading fungus *Phanerochaete chrysosporium* strain RP78. *Nature Biotechnology* 22(6):695-700. <https://doi.org/10.1038/nbt967>
- Mason W. H. (1926). Process and apparatus for disintegration of wood and the like. (Google Patents).
- Matsuzaki F. & Wariishi H. (2004). Functional diversity of cytochrome P450s of the white-rot fungus *Phanerochaete chrysosporium*. *Biochemical and Biophysical Research Communications* 324(1):387-393. <https://doi.org/10.1016/j.bbrc.2004.09.062>
- McKendry P. (2002). Energy production from biomass (part 2): conversion technologies. *Bioresource technology* 83(1):47-54. [https://doi.org/10.1016/S0960-8524\(01\)00119-5](https://doi.org/10.1016/S0960-8524(01)00119-5)
- McMullan G., Meehan C., Conneely A., Kirby N., Robinson T., Nigam P., Banat I. M., Marchant R., Smyth W. F. (2001). Microbial decolourisation and degradation of textile dyes. *Applied Microbiology and Biotechnology* 56(1-2):81-87. <https://doi.org/10.1007/s002530000587>
- Mehta M. J., Kulshrestha A., Sharma S., Kumar A. (2021). Room temperature depolymerization of lignin using a protic and metal based ionic liquid system: an efficient method of catalytic conversion and value addition. *Green chemistry* 23(3):1240-1247. <https://doi.org/10.1039/d0gc03463k>
- Merci A., Urbano A., Grossmann M. V. E., Tischer C. A., Mali S. (2015). Properties of microcrystalline cellulose extracted from soybean hulls by reactive extrusion. *Food Research International* 73:38-43. <https://doi.org/10.1016/j.foodres.2015.03.020>
- Merklein K., Fong S. S., Deng Y. (2016). Chapter 11 - Biomass Utilization. *Biotechnology for Biofuel Production and Optimization*, Eckert CA & Trinh CT (Édit.) Elsevier, Amsterdam. p 291-324. <https://doi.org/10.1016/B978-0-444-63475-7.00011-X>
- Mesa-Stonestreet N., Alavi S., Gwirtz J. (2012). Extrusion-enzyme liquefaction as a method for producing sorghum protein concentrates. *Journal of Food Engineering* 108:365–375. <https://doi.org/10.1016/j.jfoodeng.2011.07.024>

- Methrath Liyakathali N. A., Muley P. D., Aita G., Boldor D. (2016). Effect of frequency and reaction time in focused ultrasonic pretreatment of energy cane bagasse for bioethanol production. *Bioresource technology* 200:262-271. <https://doi.org/10.1016/j.biortech.2015.10.028>
- Miettinen O., Spirin V., Vlasák J., Rivoire B., Stenroos S., Hibbett D. (2016). Polypores and genus concepts in Phanerochaetaceae (Polyporales, Basidiomycota). *MycKeys* 17:1-46. <https://doi.org/10.3897/mycokeys.17.10153>
- Mikulandrić R., Vermeulen B., Nicolai B., Saeys W. (2016). Modelling of thermal processes during extrusion based densification of agricultural biomass residues. *Applied energy* 184:1316-1331. <https://doi.org/10.1016/j.apenergy.2016.03.067>
- Mikulski D. & Kłosowski G. (2022). Delignification efficiency of various types of biomass using microwave-assisted hydrotropic pretreatment. *Scientific Reports* 12(1):4561. <https://doi.org/10.1038/s41598-022-08717-9>
- Millati R., Syamsiah S., Niklasson C., Cahyanto M. N., Ludquist K., Taherzadeh M. J. (2011). Biological pretreatment of lignocelluloses with white-rot fungi and its applications: a review. *BioResources* 6(4):5224-5259. <http://dx.doi.org/10.15376/biores.6.4.Isroi>
- Miller G. (1959a). Determination of reducing sugar by DNS method. *Anal chem* 31(3):426-428.
- Miller G. L. (1959b). Use of Dinitrosalicylic Acid Reagent for Determination of Reducing Sugar. *Analytical Chemistry* 31(3):426-428. <https://doi.org/10.1021/ac60147a030>
- Mitani T. (2018). Recent Progress on Microwave Processing of Biomass for Bioenergy Production. *Journal of the Japan Petroleum Institute* 61(2):113-120. <https://doi.org/10.1627/jpi.61.113>
- Mitchell D. A., de Lima Luz L. F., Krieger N., Berovič M. (2011). Bioreactors for Solid-State Fermentation. *Comprehensive Biotechnology*. p 347-360. <https://doi.org/10.1016/b978-0-08-088504-9.00107-0>
- Mittal A., Pilath H. M., Johnson D. K. (2020). Direct Conversion of Biomass Carbohydrates to Platform Chemicals: 5-Hydroxymethylfurfural (HMF) and Furfural. *Energy & Fuels* 34(3):3284-3293. <https://doi.org/10.1021/acs.energyfuels.9b04047>
- Modenbach A. A. & Nokes S. E. (2014). Effects of sodium hydroxide pretreatment on structural components of biomass. *Transactions of the ASABE* 57(4):1187-1198. <https://doi.org/10.13031/trans.57.10046>
- Mohammadi A. & Nasernejad B. (2009). Enzymatic degradation of anthracene by the white rot fungus Phanerochaete chrysosporium immobilized on sugarcane bagasse. *Journal of Hazardous Materials* 161(1):534-537. <https://doi.org/10.1016/j.jhazmat.2008.03.132>
- Mohanty F. & Swain S. K. (2017). Chapter 18 - Bionanocomposites for Food Packaging Applications. *Nanotechnology Applications in Food*, Oprea AE & Grumezescu AM (Édit.) Academic Press. p 363-379. <https://doi.org/10.1016/B978-0-12-811942-6.00018-2>
- Mohite A. S., Jagtap A. R., Avhad M. S., More A. P. (2022). Recycling of major agriculture crop residues and its application in polymer industry: A review in the context of waste to energy nexus. *Energy Nexus* 7:100134. <https://doi.org/10.1016/j.nexus.2022.100134>
- Molino A., Chianese S., Musmarra D. (2016). Biomass gasification technology: The state of the art overview. *Journal of Energy Chemistry* 25(1):10-25. <https://doi.org/10.1016/j.jechem.2015.11.005>
- Montiel C., Hernández-Meléndez O., Vivaldo-Lima E., Hernández-Luna M., Bárzana E. (2016). Enhanced Bioethanol Production from Blue Agave Bagasse in a Combined Extrusion–

- Montoya S., Patiño A., Sánchez Ó. J. (2021). Production of Lignocellulolytic Enzymes and Biomass of *Trametes versicolor* from Agro-Industrial Residues in a Novel Fixed-Bed Bioreactor with Natural Convection and Forced Aeration at Pilot Scale. *Processes* 9(2):397. <https://doi.org/doi:10.3390/pr9020397>
- Morales-Huerta J. C., Hernández-Meléndez O., Hernández-Luna M. G., Manero O., Bárzana E., Vivaldo-Lima E. (2021). An Experimental and Modeling Study on the Pretreatment and Alkaline Hydrolysis of Blue Agave Bagasse in Twin-Screw Extruders. *Industrial & engineering chemistry research* 60(34):12449-12460. <https://doi.org/10.1021/acs.iecr.1c02175>
- Morales-Huerta J. C., Jaramillo-Soto G., Manero O., Bárzana E., Vivaldo-Lima E. (2020). Modeling of Pretreatment and Acid/Alkaline Hydrolyses of Lignocellulosic Biomasses in Twin-Screw Extruders. *Industrial & engineering chemistry research* 59(25):11389-11401. <https://doi.org/10.1021/acs.iecr.0c01737>
- Mori T., Sugimoto S., Ishii S., Wu J., Nakamura A., Dohra H., Nagai K., Kawagishi H., Hirai H. (2024). Biotransformation and detoxification of tetrabromobisphenol A by white-rot fungus *Phanerochaete sordida* YK-624. *Journal of Hazardous Materials* 465:133469. <https://doi.org/10.1016/j.jhazmat.2024.133469>
- Mosier N., Hendrickson R., Ho N., Sedlak M., Ladisch M. R. (2005). Optimization of pH controlled liquid hot water pretreatment of corn stover. *Bioresour Technol* 96(18):1986-1993. <https://doi.org/10.1016/j.biortech.2005.01.013>
- Mota T. R., Oliveira D. M., Simister R., Whitehead C., Lanot A., Dos Santos W. D., Rezende C. A., McQueen-Mason S. J., Gomez L. D. (2021). Design of experiments driven optimization of alkaline pretreatment and saccharification for sugarcane bagasse. *Bioresour Technol* 321:124499. <https://doi.org/10.1016/j.biortech.2020.124499>
- Mujtaba M., Fernandes Fraceto L., Fazeli M., Mukherjee S., Savassa S. M., Araujo de Medeiros G., do Espírito Santo Pereira A., Mancini S. D., Lipponen J., Vilaplana F. (2023). Lignocellulosic biomass from agricultural waste to the circular economy: a review with focus on biofuels, biocomposites and bioplastics. *Journal of Cleaner Production* 402:136815. <https://doi.org/10.1016/j.jclepro.2023.136815>
- Mustafa A. F., Hassanat F., Berthiaume R. R. (2004). In situ forestomach and intestinal nutrient digestibilities of sweet corn residues. *Animal Feed Science and Technology* 114(1):287-293. <https://doi.org/10.1016/j.anifeedsci.2003.08.013>
- Naeimi S., Khosravi V., Varga A., Vagvolgyi C., Kredics L. (2020). Screening of Organic Substrates for Solid-State Fermentation, Viability and Bioefficacy of *Trichoderma harzianum* AS12-2, a Biocontrol Strain Against Rice Sheath Blight Disease. *AGRONOMY-BASEL* 10(9). <https://doi.org/10.3390/agronomy10091258>
- Nakasu P. Y. S., Ienczak J. L., Rabelo S. C., Costa A. C. (2021). The water consumption of sugarcane bagasse post-washing after protic ionic liquid pretreatment and its impact on 2G ethanol production. *Industrial Crops and Products* 169:113642. <https://doi.org/10.1016/j.indcrop.2021.113642>
- Naqvi M. & Yan J. (2015). First-Generation Biofuels. *Handbook of Clean Energy Systems*. p 1-18. <https://doi.org/10.1002/9781118991978.hces207>

- Naranjo-Ortiz M. A. & Gabaldón T. (2019). Fungal evolution: diversity, taxonomy and phylogeny of the Fungi. *Biological Reviews* 94(6):2101-2137. <https://doi.org/10.1111/brv.12550>
- Narendranath N. V., Thomas K. C., Ingledew W. M. (2001). Effects of acetic acid and lactic acid on the growth of *Saccharomyces cerevisiae* in a minimal medium. *Journal of Industrial Microbiology and Biotechnology* 26(3):171-177. <https://doi.org/10.1038/sj.jim.7000090>
- Narisetty V., Cox R., Bommareddy R., Agrawal D., Ahmad E., Pant K. K., Chandel A. K., Bhatia S. K., Kumar D., Binod P., Gupta V. K., Kumar V. (2022). Valorisation of xylose to renewable fuels and chemicals, an essential step in augmenting the commercial viability of lignocellulosic biorefineries. *Sustainable Energy & Fuels* 6(1):29-65. <https://doi.org/10.1039/d1se00927c>
- Nastaj A. & Wilczyński K. (2021). Optimization and Scale-Up for Polymer Extrusion. *Polymers (Basel)* 13(10):1547. <https://doi.org/10.3390/polym13101547>
- Nava I., Favela-Torres E., Saucedo-Castaneda G. (2011). Effect of mixing on the solid-state fermentation of coffee pulp with *Aspergillus tamarii*. *Food Technology and Biotechnology* 49:391-395. <https://link.gale.com/apps/doc/A267610448/AONE?u=anon~5c8aaf34&sid=googleScholar&xid=d28bfbd9>
- Negro M. J., Duque A., Manzanares P., Sáez F., Oliva J. M., Ballesteros I., Ballesteros M. (2015). Alkaline twin-screw extrusion fractionation of olive-tree pruning biomass. *Industrial Crops and Products* 74:336-341. <https://doi.org/10.1016/j.indcrop.2015.05.018>
- Nelson M. L. & O'Connor R. T. (1964). Relation of certain infrared bands to cellulose crystallinity and crystal latticed type. Part I. Spectra of lattice types I, II, III and of amorphous cellulose. *Journal of Applied Polymer Science* 8(3):1311-1324. <https://doi.org/10.1002/app.1964.070080322>
- Nguyen M. H. & Prince R. G. H. (1996). A simple rule for bioenergy conversion plant size optimisation: Bioethanol from sugar cane and sweet sorghum. *Biomass and Bioenergy* 10(5):361-365. [https://doi.org/10.1016/0961-9534\(96\)00003-7](https://doi.org/10.1016/0961-9534(96)00003-7)
- Nieder-Heitmann M., Haigh K., Louw J., Görgens J. F. (2019). Economic evaluation and comparison of succinic acid and electricity co-production from sugarcane bagasse and trash lignocelluloses in a biorefinery, using different pretreatment methods: dilute acid (H₂SO₄), alkaline (NaOH), organosolv, ammonia fibre expansion (AFEX™), steam explosion (STEX), and wet oxidation. *Biofuels, Bioproducts and Biorefining* 14(1):55-77. <https://doi.org/10.1002/bbb.2020>
- Niladevi K. N. (2009). Ligninolytic Enzymes. *Biotechnology for Agro-Industrial Residues Utilisation: Utilisation of Agro-Residues*, Singh Nee' Nigam P & Pandey A (Édit.) Springer Netherlands, Dordrecht. p 397-414. https://doi.org/10.1007/978-1-4020-9942-7_22
- Ning D. & Wang H. (2012). Involvement of Cytochrome P450 in Pentachlorophenol Transformation in a White Rot Fungus *Phanerochaete chrysosporium*. *PLOS ONE* 7(9):e45887. <https://doi.org/10.1371/journal.pone.0045887>
- Ning D., Wang H., Zhuang Y. (2010). Induction of functional cytochrome P450 and its involvement in degradation of benzoic acid by *Phanerochaete chrysosporium*. *Biodegradation* 21(2):297-308. <https://doi.org/10.1007/s10532-009-9301-z>
- Nishimura H., Kamiya A., Nagata T., Katahira M., Watanabe T. (2018). Direct evidence for α ether linkage between lignin and carbohydrates in wood cell walls. *Scientific Reports* 8(1). <https://doi.org/10.1038/s41598-018-24328-9>

- NIST (2024). *Engineering statistics handbook*. National Institute of Standards and Technology, <https://www.itl.nist.gov/div898/handbook/pri/pri.htm> (Consulté le 2024-10-31)
- Niu N., Feng L., Lin Y., Li X., Zhang D., Yao S. (2020). The sources of Dechlorane Plus (DP) in surface sediment from Bohai Sea and the northern part of the Yellow Sea, China: Evidence from the fractional abundance of anti-DP (fanti) combined with lignin biomarker. *Regional Studies in Marine Science* 39. <https://doi.org/10.1016/j.rsma.2020.101437>
- NRCan (2025a). *Forest classification*. <https://natural-resources.canada.ca/our-natural-resources/forests/sustainable-forest-management/measuring-and-reporting/forest-classification/13179> (Consulté le 07/01/2025)
- NRCan (2025b). *Overview of Canada's agriculture and agri-food sector*. <https://europepmc.org/article/nbk/nbk579971> (Consulté le 07/01/2025)
- O'Neill M. A., Moon R. J., York W. S., Darvill A. G., Godula K., Urbanowicz B., Mohnen D. (2022). Glycans in Bioenergy and Materials Science. *Essentials of Glycobiology*, Varki A, Cummings RD, Esko JD, Stanley P, Hart GW, Aebi M, Mohnen D, Kinoshita T, Packer NH, Prestegard JH, Schnaar RL, Seeberger PH (Édit.) Cold Spring Harbor Laboratory Press. <https://doi.org/10.1101/glycobiology.4e.59>
- Copyright © 2022 The Consortium of Glycobiology Editors, La Jolla, California; published by Cold Spring Harbor Laboratory Press; doi:10.1101/glycobiology.4e.59. All rights reserved., Cold Spring Harbor (NY). p 797-804. <https://doi.org/10.1101/glycobiology.4e.59>
- Oliva J. M. (2017). A Sequential Steam Explosion and Reactive Extrusion Pretreatment for Lignocellulosic Biomass Conversion within a Fermentation-Based Biorefinery Perspective. *Fermentation* 3(2). <https://doi.org/10.3390/fermentation3020015>
- Oliveira P. L. d., Duarte M. C. T., Ponezi A. N., Durrant L. R. (2009). Purification and Partial characterization of manganese peroxidase from *Bacillus pumilus* AND *Paenibacillus* sp. *Brazilian Journal of Microbiology* 40:818-826. <https://doi.org/10.1590/S1517-838220090004000012>
- Ong V. Z. & Wu T. Y. (2020a). An application of ultrasonication in lignocellulosic biomass valorisation into bio-energy and bio-based products. *Renewable and Sustainable Energy Reviews* 132. <https://doi.org/10.1016/j.rser.2020.109924>
- Ong V. Z. & Wu T. Y. (2020b). An application of ultrasonication in lignocellulosic biomass valorisation into bio-energy and bio-based products. *Renewable and Sustainable Energy Reviews* 132:109924. <https://doi.org/10.1016/j.rser.2020.109924>
- Onu Olughu O., Tabil L. G., Dumonceaux T., Mupondwa E., Cree D. (2022). Optimization of Solid-State Fermentation of Switchgrass Using White-Rot Fungi for Biofuel Production. *Fuels* 3(4):730-752. <https://doi.org/10.3390/fuels3040043>
- Ouahiba G., Yasmina S., Azzeddine B., Zahra A., Nouari S. (2021). Optimization of endoglucanase production from *Sarocladium kiliense* strain BbV1 under solid state fermentation, using response surface methodology. *PONTE International Journal of Science and Research* 77(4). <http://dx.doi.org/10.21506/j.ponte.2021.4.3>
- Ovejero-Pérez A., Ayuso M., Rigual V., Domínguez J. C., García J., Alonso M. V., Oliet M., Rodríguez F. (2021). Technoeconomic Assessment of a Biomass Pretreatment + Ionic Liquid Recovery Process with Aprotic and Choline Derived Ionic Liquids. *ACS Sustainable Chemistry & Engineering* 9(25):8467-8476. <https://doi.org/10.1021/acssuschemeng.1c01361>

- Ovejero-Pérez A., Nakasu P. Y. S., Hopson C., Costa J. M., Hallett J. P. (2024). Challenges and opportunities on the utilisation of ionic liquid for biomass pretreatment and valorisation. *npj Materials Sustainability* 2(1):7. <https://doi.org/10.1038/s44296-024-00015-x>
- Paiva A., Craveiro R., Aroso I., Martins M., Reis R. L., Duarte A. R. C. (2014). Natural Deep Eutectic Solvents – Solvents for the 21st Century. *ACS Sustainable Chemistry & Engineering* 2(5):1063-1071. <https://doi.org/10.1021/sc500096j>
- Pan-Utai W. & lamtham S. (2019). Physical extraction and extrusion entrapment of C-phycocyanin from *Arthrospira platensis*. *Journal of King Saud University - Science* 31(4):1535-1542. <https://doi.org/10.1016/j.jksus.2018.05.026>
- Park K.-M. & Park S.-S. (2008). Purification and characterization of laccase from basidiomycete *Fomitella fraxinea*. *Journal of microbiology and biotechnology* 18(4):670-675. <https://www.jmb.or.kr/submission/Journal/018/JMB018-04-09.pdf>
- Park S., Baker J. O., Himmel M. E., Parilla P. A., Johnson D. K. (2010). Cellulose crystallinity index: measurement techniques and their impact on interpreting cellulase performance. *Biotechnol Biofuels* 3:10. <https://doi.org/10.1186/1754-6834-3-10>
- Patel D. D. & Lee J. M. (2012). Applications of ionic liquids. *Chem Rec* 12(3):329-355. <https://doi.org/10.1002/tcr.201100036>
- Pathak P., Gupta A., Bhardwaj N. K., Goyal A., Moholkar V. S. (2020). Impact of mild and harsh conditions of formic acid-based organosolv pretreatment on biomass fractionation of sugarcane tops. *Biomass Conversion and Biorefinery* 11(5):2027-2040. <https://doi.org/10.1007/s13399-020-00629-w>
- Patil P. D., Feng J. J., Hatzikiriakos S. G. (2006). Constitutive modeling and flow simulation of polytetrafluoroethylene (PTFE) paste extrusion. *Journal of Non-Newtonian Fluid Mechanics* 139(1-2):44-53. <https://doi.org/10.1016/j.jnnfm.2006.05.013>
- Pavlovic I., Knez Z., Skerget M. (2013). Hydrothermal reactions of agricultural and food processing wastes in sub- and supercritical water: a review of fundamentals, mechanisms, and state of research. *J Agric Food Chem* 61(34):8003-8025. <https://doi.org/10.1021/jf401008a>
- Peralta R. M., da Silva B. P., Gomes Côrrea R. C., Kato C. G., Vicente Seixas F. A., Bracht A. (2017). Chapter 5 - Enzymes from Basidiomycetes—Peculiar and Efficient Tools for Biotechnology. *Biotechnology of Microbial Enzymes*, Brahmachari G (Édit.) Academic Press. p 119-149. <https://doi.org/10.1016/B978-0-12-803725-6.00005-4>
- Pereira J. F., Núñez E., Reyes A., Mali S., Lopez-Rubio A., Fabra M. J. (2024). On the use of lignocellulosic hemp fibers to produce biodegradable cost-efficient biocomposites. *Future Foods* 10:100507. <https://doi.org/10.1016/j.fufo.2024.100507>
- Pereira Marques F., Lima Soares A. K., Lomonaco D., Alexandre e Silva L. M., Tédde Santaella S., de Freitas Rosa M., Carrhá Leitão R. (2021). Steam explosion pretreatment improves acetic acid organosolv delignification of oil palm mesocarp fibers and sugarcane bagasse. *International Journal of Biological Macromolecules* 175:304-312. <https://doi.org/10.1016/j.ijbiomac.2021.01.174>
- Pérez-Rodríguez N., García-Bernet D., Domínguez J. M. (2017). Extrusion and enzymatic hydrolysis as pretreatments on corn cob for biogas production. *Renewable Energy* 107:597-603. <https://doi.org/10.1016/j.renene.2017.02.030>

- Peter S., Lyczko N., Gopakumar D., Maria H. J., Nzihou A., Thomas S. (2022). Nanocellulose and its derivative materials for energy and environmental applications. *Journal of Materials Science*. <https://doi.org/10.1007/s10853-022-07070-6>
- Phanthong P., Reubroycharoen P., Hao X., Xu G., Abudula A., Guan G. (2018). Nanocellulose: Extraction and application. *Carbon Resources Conversion* 1(1):32-43. <https://doi.org/10.1016/j.crcon.2018.05.004>
- Phuong D. & Nguyen L. (2024). Coffee pulp pretreatment methods: A comparative analysis of hydrolysis efficiency. *Food and raw materials* 12(1). <http://doi.org/10.21603/2308-4057-2024-1-594>
- Pointing S. (2001). Feasibility of bioremediation by white-rot fungi. *Applied Microbiology and Biotechnology* 57(1):20-33. <https://doi.org/10.1007/s002530100745>
- Pollegioni L., Tonin F., Rosini E. (2015). Lignin-degrading enzymes. *The FEBS Journal* 282(7):1190-1213. <https://doi.org/10.1111/febs.13224>
- Prade R. A. (1996). Xylanases: from Biology to BioTechnology. *Biotechnology and Genetic Engineering Reviews* 13(1):101-132. <https://doi.org/10.1080/02648725.1996.10647925>
- Prasad A., Sotenko M., Blenkinsopp T., Coles S. R. (2015). Life cycle assessment of lignocellulosic biomass pretreatment methods in biofuel production. *The International Journal of Life Cycle Assessment* 21(1):44-50. <https://doi.org/10.1007/s11367-015-0985-5>
- Puchi P. F., Castagneri D., Rossi S., Carrer M. (2020). Wood anatomical traits in black spruce reveal latent water constraints on the boreal forest. *Global Change Biology* 26(3):1767-1777. <https://doi.org/10.1111/gcb.14906>
- Puig-Arnavat M., Bruno J. C., Coronas A. (2010). Review and analysis of biomass gasification models. *Renewable and Sustainable Energy Reviews* 14(9):2841-2851. <https://doi.org/10.1016/j.rser.2010.07.030>
- Puligundla P., Oh S.-E., Mok C. (2016). Microwave-assisted pretreatment technologies for the conversion of lignocellulosic biomass to sugars and ethanol: a review. *Carbon letters* 17(1):1-10. <https://doi.org/10.5714/cl.2016.17.1.001>
- Québec I. d. I. S. d. (2025). *Area of field crops, yield per hectare and production, by combined administrative regions¹, Québec, 2007-2024 (in French only)*. <https://statistique.quebec.ca/en/produit/tableau/3786>
- Rackemann D. W. & Doherty W. O. (2011). The conversion of lignocellulosics to levulinic acid. *Biofuels, Bioproducts and Biorefining* 5(2):198-214. <https://doi.org/10.1002/bbb.267>
- Råde I. & Andersson B. A. (2001). Requirement for metals of electric vehicle batteries. *Journal of Power Sources* 93(1):55-71. [https://doi.org/10.1016/S0378-7753\(00\)00547-4](https://doi.org/10.1016/S0378-7753(00)00547-4)
- Radha K. V., Regupathi I., Arunagiri A., Murugesan T. (2005). Decolorization studies of synthetic dyes using *Phanerochaete chrysosporium* and their kinetics. *Process Biochemistry* 40(10):3337-3345. <https://doi.org/10.1016/j.procbio.2005.03.033>
- Ramchandran D., Rajagopalan N., Strathmann T. J., Singh V. (2013). Use of treated effluent water in ethanol production from cellulose. *Biomass and Bioenergy* 56:22-28. <https://doi.org/10.1016/j.biombioe.2013.04.003>
- Raquez J.-M., Narayan R., Dubois P. (2008). Recent Advances in Reactive Extrusion Processing of Biodegradable Polymer-Based Compositions. *Macromolecular Materials and Engineering* 293(6):447-470. <https://doi.org/10.1002/mame.200700395>

- Rashed G. I., Chong L., Zhiyuan S., Hongzhen F., Chen C., Junjie L., Qiao L., Jianhui D., Huazheng C., Hongmei W., Hongbo L., Qingze J., Yanhong F., Yongchun W., Kheshti M. (2021). Effect of a promising CSESE pretreatment on the morphological structure and properties of jute fibers. *E3S Web of Conferences* 252. <https://doi.org/10.1051/e3sconf/202125202049>
- Ravindran R. & Jaiswal A. K. (2016). Microbial Enzyme Production Using Lignocellulosic Food Industry Wastes as Feedstock: A Review. *Bioengineering (Basel, Switzerland)* 3(4):30. <https://doi.org/10.3390/bioengineering3040030>
- Raza M., Farhan A., Abu-Jdayil B. (2024). Lignocellulose-based insulation materials: A review of sustainable and biodegradable solutions for energy efficiency. *International Journal of Thermofluids* 24:100844. <https://doi.org/10.1016/j.ijft.2024.100844>
- Reddy C. A. & D'Souza T. M. (1994). Physiology and molecular biology of the lignin peroxidases of *Phanerochaete chrysosporium*. *FEMS Microbiology Reviews* 13(2-3):137-152. <https://doi.org/10.1111/j.1574-6976.1994.tb00040.x>
- Reddy K. T., Kocher G. S., Singh A. (2024). Pretreatment and saccharification of corn cobs using partially purified fungal ligninolytic enzymes. *Biofuels, Bioproducts and Biorefining*. <https://doi.org/10.1002/bbb.2661>
- Refaat A. A. (2012). Biofuels from Waste Materials. *Comprehensive Renewable Energy*. p 217-261. <https://doi.org/10.1016/b978-0-08-087872-0.00518-7>
- Research G. V. (2021). *Enzymes Market Size, Share & Trends Analysis Report By Type (Industrial, Specialty), By Product (Carbohydrase, Proteases), By Source (Microorganisms, Animals), By Region, And Segment Forecasts, 2021 - 2028*. Grand View Research (978-1-68038-022-4). 153 p. https://www.grandviewresearch.com/industry-analysis/enzymes-industry?utm_source=globenewswire&utm_medium=referral&utm_campaign=cmfe-9-mar-22&utm_term=enzymes-industry&utm_content=rd
- Reshmy R., Paulose T. A. P., Philip E., Thomas D., Madhavan A., Sirohi R., Binod P., Kumar Awasthi M., Pandey A., Sindhu R. (2022). Updates on high value products from cellulosic biorefinery. *Fuel* 308:122056. <https://doi.org/10.1016/j.fuel.2021.122056>
- Rezania S., Oryani B., Cho J., Talaiekhosani A., Sabbagh F., Hashemi B., Rupani P. F., Mohammadi A. A. (2020). Different pretreatment technologies of lignocellulosic biomass for bioethanol production: An overview. *Energy* 199:117457. <https://doi.org/10.1016/j.energy.2020.117457>
- Rivera-Hoyos C. M., Morales-Álvarez E. D., Poutou-Piñales R. A., Pedroza-Rodríguez A. M., Rodríguez-Vázquez R., Delgado-Boada J. M. (2013). Fungal laccases. *Fungal Biology Reviews* 27(3):67-82. <https://doi.org/10.1016/j.fbr.2013.07.001>
- Robinson J., Binner E., Vallejo D. B., Perez N. D., Al Mughairi K., Ryan J., Shepherd B., Adam M., Budarin V., Fan J., Gronnow M., Peneranda-Foix F. (2022). Unravelling the mechanisms of microwave pyrolysis of biomass. *Chemical Engineering Journal* 430:132975. <https://doi.org/10.1016/j.cej.2021.132975>
- Robinson T. & Nigam P. (2003). Bioreactor design for protein enrichment of agricultural residues by solid state fermentation. *Biochemical Engineering Journal* 13(2):197-203. [https://doi.org/10.1016/S1369-703X\(02\)00132-8](https://doi.org/10.1016/S1369-703X(02)00132-8)
- Rodrigue J.-P. (2020). The geography of transport systems. <https://doi.org/10.4324/9780429346323>

- Rodríguez C. S., Santoro R., Cameselle C., Sanroman A. (1997). Laccase production in semi-solid cultures of *Phanerochaete chrysosporium*. *Biotechnology Letters* 19(10):995-998. <https://doi.org/10.1023/A:1018495216946>
- Román-Ramírez L. A. & Marco J. (2022). Design of experiments applied to lithium-ion batteries: A literature review. *Applied energy* 320:119305. <https://doi.org/10.1016/j.apenergy.2022.119305>
- Rosa F. M., Mota T. F., Busso C., Arruda P. V., Brito P. E., Miranda J. P., Trentin A. B., Dekker R. F. H., Cunha M. A. (2024). Filamentous Fungi as Bioremediation Agents of Industrial Effluents: A Systematic Review. *Fermentation* 10(3). <https://doi.org/10.3390/fermentation10030143>
- Rosenberg E. & Zilber-Rosenberg I. (2016). Do microbiotas warm their hosts? *Gut Microbes* 7(4):283-285. <https://doi.org/10.1080/19490976.2016.1182294>
- Rowell R. M. (2007a). Challenges in Biomass–Thermoplastic Composites. *Journal of Polymers and the Environment* 15(4):229-235. <https://doi.org/10.1007/s10924-007-0069-0>
- Rowell R. M. (2007b). Composite Materials from Forest Biomass: A Review of Current Practices, Science, and Technology. in *ACS Symposium Series* (American Chemical Society), p 76-92. <https://doi.org/10.1021/bk-2007-0954.ch005>
- Ruiz H. A., Conrad M., Sun S. N., Sanchez A., Rocha G. J. M., Romani A., Castro E., Torres A., Rodriguez-Jasso R. M., Andrade L. P., Smirnova I., Sun R. C., Meyer A. S. (2020). Engineering aspects of hydrothermal pretreatment: From batch to continuous operation, scale-up and pilot reactor under biorefinery concept. *Bioresour Technol* 299:122685. <https://doi.org/10.1016/j.biortech.2019.122685>
- Sala A., Barrena R., Artola A., Sánchez A. (2019). Current developments in the production of fungal biological control agents by solid-state fermentation using organic solid waste. *CRITICAL REVIEWS IN ENVIRONMENTAL SCIENCE AND TECHNOLOGY* 49(8):655-694. <https://doi.org/10.1080/10643389.2018.1557497>
- Santhakumar S., Meerman H., Faaij A. (2024). Future costs of key emerging offshore renewable energy technologies. *Renewable Energy* 222:119875. <https://doi.org/10.1016/j.renene.2023.119875>
- Saratale G. D., Saratale R. G., Varjani S., Cho S.-K., Ghodake G. S., Kadam A., Mulla S. I., Bharagava R. N., Kim D.-S., Shin H. S. (2020). Development of ultrasound aided chemical pretreatment methods to enrich saccharification of wheat waste biomass for polyhydroxybutyrate production and its characterization. *Industrial Crops and Products* 150:112425. <https://doi.org/10.1016/j.indcrop.2020.112425>
- Sarker T. R., Azargohar R., Stobbs J., Karunakaran C., Meda V., Dalai A. K. (2022). Complementary effects of torrefaction and pelletization for the production of fuel pellets from agricultural residues: A comparative study. *Industrial Crops and Products* 181:114740. <https://doi.org/10.1016/j.indcrop.2022.114740>
- Sarparast M., Dattmore D., Alan J., Lee K. S. S. (2020). Cytochrome P450 metabolism of polyunsaturated fatty acids and neurodegeneration. *Nutrients* 12(11):3523. <https://doi.org/10.3390/nu12113523>
- Satlewal A., Agrawal R., Bhagia S., Sangoro J., Ragauskas A. J. (2018). Natural deep eutectic solvents for lignocellulosic biomass pretreatment: Recent developments, challenges and novel opportunities. *Biotechnology Advances* 36(8):2032-2050. <https://doi.org/10.1016/j.biotechadv.2018.08.009>

- Saville B. A., Griffin W. M., MacLean H. L. (2016). Ethanol Production Technologies in the US: Status and Future Developments. *Global Bioethanol*. p 163-180. <https://doi.org/10.1016/b978-0-12-803141-4.00007-1>
- Schick Zapanta L., Hattori T., Rzetskaya M., Tien M. (1998). Cloning of *Phanerochaete chrysosporium* leu2 by Complementation of Bacterial Auxotrophs and Transformation of Fungal Auxotrophs. *Applied and Environmental Microbiology* 64(7):2624-2629. <https://doi.org/10.1128/aem.64.7.2624-2629.1998>
- Seifert S. (2013). Comparison of parallel and conical twin screw extruders from the processing point of view. *Plastics, Rubber and Composites* 34(3):134-142. <https://doi.org/10.1179/174328905x55515>
- Senthilkumar S., Perumalsamy M., Janardhana Prabhu H. (2014). Decolourization potential of white-rot fungus *Phanerochaete chrysosporium* on synthetic dye bath effluent containing Amido black 10B. *Journal of Saudi Chemical Society* 18(6):845-853. <https://doi.org/10.1016/j.jscs.2011.10.010>
- Senturk-Ozer S., Gevgilili H., Kalyon D. M. (2011). Biomass pretreatment strategies via control of rheological behavior of biomass suspensions and reactive twin screw extrusion processing. *Bioresour Technol* 102(19):9068-9075. <https://doi.org/10.1016/j.biortech.2011.07.018>
- Sequeiros A. & Labidi J. (2017). Characterization and determination of the S/G ratio via Py-GC/MS of agricultural and industrial residues. *Industrial Crops and Products* 97:469-476. <https://doi.org/10.1016/j.indcrop.2016.12.056>
- Shadbahr J., Bensebaa F., Ebadian M. (2021). Impact of forest harvest intensity and transportation distance on biomass delivered costs within sustainable forest management - A case study in southeastern Canada. *Journal of environmental management* 284:112073. <https://doi.org/10.1016/j.jenvman.2021.112073>
- Sharma B., Larroche C., Dussap C.-G. (2020). Comprehensive assessment of 2G bioethanol production. *Bioresource technology* 313:123630. <https://doi.org/10.1016/j.biortech.2020.123630>
- Sharma K. K., Gupta S., Kuhad R. C. (2006). Agrobacterium-mediated delivery of marker genes to *Phanerochaete chrysosporium* mycelial pellets: a model transformation system for white-rot fungi. *Biotechnology and Applied Biochemistry* 43(3):181-186. <https://doi.org/10.1042/ba20050160>
- Sheng C. & Azevedo J. L. T. (2005). Estimating the higher heating value of biomass fuels from basic analysis data. *Biomass and Bioenergy* 28(5):499-507. <https://doi.org/10.1016/j.biombioe.2004.11.008>
- Shi J., Sharma-Shivappa R. R., Chinn M. S. (2009). Microbial pretreatment of cotton stalks by submerged cultivation of *Phanerochaete chrysosporium*. *Bioresource technology* 100(19):4388-4395. <https://doi.org/10.1016/j.biortech.2008.10.060>
- Shrivastava A. & Sharma R. K. (2023). Conversion of lignocellulosic biomass: Production of bioethanol and bioelectricity using wheat straw hydrolysate in electrochemical bioreactor. *Heliyon* 9(1):e12951. <https://doi.org/10.1016/j.heliyon.2023.e12951>
- Shrotri A., Kobayashi H., Fukuoka A. (2017). Catalytic Conversion of Structural Carbohydrates and Lignin to Chemicals. (Advances in Catalysis. p 59-123. <https://doi.org/10.1016/bs.acat.2017.09.002>

- Shukla A., Kumar D., Girdhar M., Kumar A., Goyal A., Malik T., Mohan A. (2023). Strategies of pretreatment of feedstocks for optimized bioethanol production: distinct and integrated approaches. *Biotechnology for Biofuels and Bioproducts* 16(1):44. <https://doi.org/10.1186/s13068-023-02295-2>
- Sidana A. & Yadav S. K. (2022). Recent developments in lignocellulosic biomass pretreatment with a focus on eco-friendly, non-conventional methods. *Journal of Cleaner Production* 335:130286. <https://doi.org/10.1016/j.jclepro.2021.130286>
- Silvestre W. P., Galafassi P. L., Ferreira S. D., Godinho M., Pauletti G. F., Baldasso C. (2018). Fodder radish seed cake biochar for soil amendment. *Environmental Science and Pollution Research* 25(25):25143-25154. <https://doi.org/10.1007/s11356-018-2571-4>
- Sindhu R., Binod P., Pandey A. (2016). Biological pretreatment of lignocellulosic biomass--An overview. *Bioresour Technol* 199:76-82. <https://doi.org/10.1016/j.biortech.2015.08.030>
- Singamneni S., Warnakula A., Smith D. A., Le Guen M. J. (2019). Biopolymer alternatives in pellet form for 3D printing by extrusion. *3D Printing and Additive Manufacturing* 6(4):217-226. <https://doi.org/10.1089/3dp.2018.0152>
- Singh D. & Chen S. (2008). The white-rot fungus *Phanerochaete chrysosporium*: conditions for the production of lignin-degrading enzymes. *Appl Microbiol Biotechnol* 81(3):399-417. <https://doi.org/10.1007/s00253-008-1706-9>
- Singh J., Das A., Yogalakshmi K. N. (2020). Enhanced laccase expression and azo dye decolorization during co-interaction of *Trametes versicolor* and *Phanerochaete chrysosporium*. *SN Applied Sciences* 2(6). <https://doi.org/10.1007/s42452-020-2832-y>
- Singh R. P. & Heldman D. R. (2014). Chapter 4 - Heat Transfer in Food Processing. *Introduction to Food Engineering (Fifth Edition)*, Singh RP & Heldman DR (Édit.) Academic Press, San Diego. p 265-419. <https://doi.org/10.1016/B978-0-12-398530-9.00004-8>
- Singh S., Cheng G., Sathitsuksanoh N., Wu D., Varanasi P., George A., Balan V., Gao X. D., Kumar R., Dale B. E., Wyman C. E., Simmons B. A. (2015). Comparison of different biomass pretreatment techniques and their impact on chemistry and structure. *Frontiers in Energy Research*. <https://doi.org/10.3389/fenrg.2014.00062>
- Singh S. K. & Savoy A. W. (2020). Ionic liquids synthesis and applications: An overview. *Journal of Molecular Liquids* 297. <https://doi.org/10.1016/j.molliq.2019.112038>
- Sinitsyn A. P. & Sinitsyna O. A. (2021). Bioconversion of Renewable Plant Biomass. Second-Generation Biofuels: Raw Materials, Biomass Pretreatment, Enzymes, Processes, and Cost Analysis. *Biochemistry (Moscow)* 86(S1):S166-S195. <https://doi.org/10.1134/s0006297921140121>
- Siqueira J. G. W., Rodrigues C., Vandenberghe L. P. d. S., Woiciechowski A. L., Soccol C. R. (2020). Current advances in on-site cellulase production and application on lignocellulosic biomass conversion to biofuels: A review. *Biomass and Bioenergy* 132:105419. <https://doi.org/10.1016/j.biombioe.2019.105419>
- Sluiter A., Hames B., Ruiz R., Scarlata C., Sluiter J., Templeton D., Crocker D. (2008). Determination of structural carbohydrates and lignin in biomass. *Laboratory analytical procedure* 1617(1):1-16. <https://www.nrel.gov/docs/gen/fy13/42618.pdf>
- Smith E. L., Abbott A. P., Ryder K. S. (2014). Deep eutectic solvents (DESs) and their applications. *Chem Rev* 114(21):11060-11082. <https://doi.org/10.1021/cr300162p>

- Sofokleous M., Christofi A., Malamis D., Mai S., Barampouti E. M. (2022). Bioethanol and biogas production: an alternative valorisation pathway for green waste. *Chemosphere* 296:133970. <https://doi.org/10.1016/j.chemosphere.2022.133970>
- Solano D., Vinyes P., Arranz P. (2016). The biomass briquetting process : A Guideline Report. <http://www.cedro-undp.org/content/uploads/publication/161124125247966~Briquettingreportforweb.pdf>
- Sowunmi A., Mamone R. M., Bastidas-Oyanedel J.-R., Schmidt J. E. (2016). Biogas potential for electricity generation in the Emirate of Abu Dhabi. *Biomass Conversion and Biorefinery* 6(1):39-47. <https://doi.org/10.1007/s13399-015-0182-6>
- Srinivasan C., Dsouza T., Boominathan K., Reddy C. (1995). Demonstration of laccase in the white rot basidiomycete *Phanerochaete chrysosporium* BKM-F1767. *Applied and Environmental Microbiology* 61(12):4274-4277. <https://doi.org/10.1128/aem.61.12.4274-4277.1995>
- Stafford W. H. L., Lotter G. A., von Maltitz G. P., Brent A. C. (2019). Biofuels technology development in Southern Africa. *Development Southern Africa* 36(2):155-174. <https://doi.org/10.1080/0376835X.2018.1481732>
- Stoklosa R. J., Del Pilar Orjuela A., Da Costa Sousa L., Uppugundla N., Williams D. L., Dale B. E., Hodge D. B., Balan V. (2017). Techno-economic comparison of centralized versus decentralized biorefineries for two alkaline pretreatment processes. *Bioresour. Technol.* 226:9-17. <https://doi.org/10.1016/j.biortech.2016.11.092>
- Subramanian V. & Yadav J. S. (2008). Regulation and heterologous expression of P450 enzyme system components of the white rot fungus *Phanerochaete chrysosporium*. *Enzyme and Microbial Technology* 43(2):205-213. <https://doi.org/10.1016/j.enzmictec.2007.09.001>
- Sugiarto S., Pong R. R., Tan Y. C., Leow Y., Sathasivam T., Zhu Q., Loh X. J., Kai D. (2022). Advances in sustainable polymeric materials from lignocellulosic biomass. *Materials Today Chemistry* 26:101022. <https://doi.org/10.1016/j.mtchem.2022.101022>
- Suhara H., Kodama S., Kamei I., Maekawa N., Meguro S. (2012). Screening of selective lignin-degrading basidiomycetes and biological pretreatment for enzymatic hydrolysis of bamboo culms. *International Biodeterioration & Biodegradation* 75:176-180. <https://doi.org/10.1016/j.ibiod.2012.05.042>
- Sun S.-C., Sun D., Li H.-Y., Cao X.-F., Sun S.-N., Wen J.-L. (2021). Revealing the topochemical and structural changes of poplar lignin during a two-step hydrothermal pretreatment combined with alkali extraction. *Industrial Crops and Products* 168. <https://doi.org/10.1016/j.indcrop.2021.113588>
- Sun S., De Angelis G., Bertella S., Jones M. J., Dick G. R., Amstad E., Luterbacher J. S. (2024). Integrated Conversion of Lignocellulosic Biomass to Bio-Based Amphiphiles using a Functionalization-Defunctionalization Approach. *Angewandte Chemie International Edition* 63(5):e202312823. <https://doi.org/10.1002/anie.202312823>
- Sundaramoorthy M., Youngs H. L., Gold M. H., Poulos T. L. (2005). High-Resolution Crystal Structure of Manganese Peroxidase: Substrate and Inhibitor Complexes. *Biochemistry* 44(17):6463-6470. <https://doi.org/10.1021/bi047318e>
- Suryadi H., Judono J. J., Putri M. R., Ecclesia A. D., Ulhaq J. M., Agustina D. N., Sumiati T. (2022). Biodelignification of lignocellulose using ligninolytic enzymes from white-rot fungi. *Heliyon* 8(2):e08865. <https://doi.org/10.1016/j.heliyon.2022.e08865>

- Suzuki H., MacDonald J., Syed K., Salamov A., Hori C., Aerts A., Henrissat B., Wiebenga A., vanKuyk P. A., Barry K., Lindquist E., LaButti K., Lapidus A., Lucas S., Coutinho P., Gong Y., Samejima M., Mahadevan R., Abou-Zaid M., de Vries R. P., Igarashi K., Yadav J. S., Grigoriev I. V., Master E. R. (2012). Comparative genomics of the white-rot fungi, *Phanerochaete carnososa* and *P. chrysosporium*, to elucidate the genetic basis of the distinct wood types they colonize. *BMC Genomics* 13(1):444. <https://doi.org/10.1186/1471-2164-13-444>
- Tadesse H. & Luque R. (2011). Advances on biomass pretreatment using ionic liquids: An overview. *Energy & Environmental Science* 4(10). <https://doi.org/10.1039/c0ee00667j>
- Taherzadeh M. J. & Karimi K. (2008). Pretreatment of lignocellulosic wastes to improve ethanol and biogas production: a review. *Int J Mol Sci* 9(9):1621-1651. <https://doi.org/10.3390/ijms9091621>
- Tai W. Y., Tan J. S., Lim V., Lee C. K. (2019). Comprehensive studies on optimization of cellulase and xylanase production by a local indigenous fungus strain via solid state fermentation using oil palm frond as substrate. *Biotechnology Progress* 35(3):e2781. <https://doi.org/10.1002/btpr.2781>
- Talebnia F., Karakashev D., Angelidaki I. (2010). Production of bioethanol from wheat straw: An overview on pretreatment, hydrolysis and fermentation. *Bioresour Technol* 101(13):4744-4753. <https://doi.org/10.1016/j.biortech.2009.11.080>
- Tang X., Zuo M., Li Z., Liu H., Xiong C., Zeng X., Sun Y., Hu L., Liu S., Lei T., Lin L. (2017). Green Processing of Lignocellulosic Biomass and Its Derivatives in Deep Eutectic Solvents. *ChemSusChem* 10(13):2696-2706. <https://doi.org/10.1002/cssc.201700457>
- Teixeira M. C. V., Alves E. H., de Oliveira F. P., Vaz L. S., Wiendl V. B. (2019). Automation of solid state fermentation reactor for enzymes synthesis. *Revista Univap* 25(49):1-12. <https://doi.org/10.18066/revistaunivap.v25i49.2015>
- Thurston C. F. (1994). The structure and function of fungal laccases. *Microbiology* 140(1):19-26. <https://doi.org/10.1099/13500872-140-1-19>
- Tian D., Shen F., Yang G., Deng S., Long L., He J., Zhang J., Huang C., Luo L. (2019). Liquid hot water extraction followed by mechanical extrusion as a chemical-free pretreatment approach for cellulosic ethanol production from rigid hardwood. *Fuel* 252:589-597. <https://doi.org/10.1016/j.fuel.2019.04.155>
- Tien M. & Kirk T. K. (1988). Lignin peroxidase of *Phanerochaete chrysosporium*. *Methods in Enzymology*, Academic Press, Vol 161. p 238-249. [https://doi.org/10.1016/0076-6879\(88\)61025-1](https://doi.org/10.1016/0076-6879(88)61025-1)
- Tomás-Pejó E., Alvira P., Ballesteros M., Negro M. J. (2011). Chapter 7 - Pretreatment Technologies for Lignocellulose-to-Bioethanol Conversion. *Biofuels*, Pandey A, Larroche C, Ricke SC, Dussap C-G, Gnansounou E (Édit.) Academic Press, Amsterdam. p 149-176. <https://doi.org/10.1016/B978-0-12-385099-7.00007-3>
- Try S. (2018). *Production d'arômes par fermentation en milieu solide*. (Université Bourgogne Franche-Comté).
- TWD (2025). *The wood database: Black Spruce*. <https://www.wood-database.com/black-spruce/> (Consulté le 07/02/2025)
- UPA (2024). *Terres agricoles : éviter la dépossession - Consultation nationale sur le territoire et les activités agricoles*. Québec. 14 p.

https://www.upa.qc.ca/fileadmin/01_UPA_provincial/Dossier_Consultations-nationales/MEM3_MAPAQ_Consultation_territoire_activites_agricoles_2024-02-15.pdf

- Ürek R. Ö. & Pazarlioğlu N. K. (2005). Production and stimulation of manganese peroxidase by immobilized Phanerochaete chrysosporium. *Process Biochemistry* 40(1):83-87. <https://doi.org/10.1016/j.procbio.2003.11.040>
- V A. J. L. (2018). Quality Control: Water Activity Considerations for Beyond-use Dates. *International Journal of Pharmaceutical Compounding* 22(4):288-293. <https://pubmed.ncbi.nlm.nih.gov/39405575/>
- Vaidya A. A., Gaugler M., Smith D. A. (2016). Green route to modification of wood waste, cellulose and hemicellulose using reactive extrusion. *Carbohydr Polym* 136:1238-1250. <https://doi.org/10.1016/j.carbpol.2015.10.033>
- Vaidya A. A., Murton K. D., Smith D. A., Dedual G. (2022). A review on organosolv pretreatment of softwood with a focus on enzymatic hydrolysis of cellulose. *Biomass Conversion and Biorefinery*. <https://doi.org/10.1007/s13399-022-02373-9>
- Van Soest P. J., Robertson J. B., Lewis B. A. (1991a). Methods for Dietary Fiber, Neutral Detergent Fiber, and Nonstarch Polysaccharides in Relation to Animal Nutrition. *Journal of Dairy Science* 74(10):3583-3597. [https://doi.org/10.3168/jds.S0022-0302\(91\)78551-2](https://doi.org/10.3168/jds.S0022-0302(91)78551-2)
- Van Soest P. v., Robertson J. B., Lewis B. A. (1991b). Methods for dietary fiber, neutral detergent fiber, and nonstarch polysaccharides in relation to animal nutrition. *Journal of Dairy Science* 74(10):3583-3597. [https://doi.org/10.3168/jds.S0022-0302\(91\)78551-2](https://doi.org/10.3168/jds.S0022-0302(91)78551-2)
- Vandenbossche V., Brault J., Hernandez-Melendez O., Evon P., Barzana E., Vilarem G., Rigal L. (2016). Suitability assessment of a continuous process combining thermo-mechano-chemical and bio-catalytic action in a single pilot-scale twin-screw extruder for six different biomass sources. *Bioresource technology* 211:146-153. <https://doi.org/10.1016/j.biortech.2016.03.072>
- Vandenbossche V., Brault J., Vilarem G., Hernández-Meléndez O., Vivaldo-Lima E., Hernández-Luna M., Barzana E., Duque A., Manzanares P., Ballesteros M., Mata J., Castellón E., Rigal L. (2014). A new lignocellulosic biomass deconstruction process combining thermo-mechano chemical action and bio-catalytic enzymatic hydrolysis in a twin-screw extruder. *Industrial Crops and Products* 55:258-266. <https://doi.org/10.1016/j.indcrop.2014.02.022>
- Vandenbossche V., Brault J., Vilarem G., Rigal L. (2015). Bio-catalytic action of twin-screw extruder enzymatic hydrolysis on the deconstruction of annual plant material: Case of sweet corn co-products. *Industrial Crops and Products* 67:239-248. <https://doi.org/10.1016/j.indcrop.2015.01.041>
- Velasco S., Román F. L., White J. A. (2009). On the Clausius–Clapeyron Vapor Pressure Equation. *Journal of Chemical Education* 86(1):106. <https://doi.org/10.1021/ed086p106>
- Venkatraman G., Giribabu N., Mohan P. S., Muttiah B., Govindarajan V. K., Alagiri M., Abdul Rahman P. S., Karsani S. A. (2024). Environmental impact and human health effects of polycyclic aromatic hydrocarbons and remedial strategies: A detailed review. *Chemosphere* 351:141227. <https://doi.org/10.1016/j.chemosphere.2024.141227>
- Vera-Sorroche J., Kelly A. L., Brown E. C., Gough T., Abeykoon C., Coates P. D., Deng J., Li K., Harkin-Jones E., Price M. (2014). The effect of melt viscosity on thermal efficiency for single screw extrusion of HDPE. *Chemical Engineering Research and Design* 92(11):2404-2412. <https://doi.org/10.1016/j.cherd.2013.12.025>

- Viamajala S., Selig M. J., Vinant T. B., Tucker M. P., Himmel M. E., McMillan J. D., Decker S. R. (2006). Catalyst transport in corn stover internodes. *Applied Biochemistry and Biotechnology* 130(1):509-527. <https://doi.org/10.1385/ABAB:130:1:509>
- Villegas E., Aubague S., Alcantara L., Auria R., Revah S. (1993). Solid state fermentation: Acid protease production in controlled CO₂ and O₂ environments. *Biotechnology Advances* 11(3):387-397. [https://doi.org/10.1016/0734-9750\(93\)90008-B](https://doi.org/10.1016/0734-9750(93)90008-B)
- Vivekanandhan K., Ayyappadas M. P., Abirami S. K. G., Devi R. R., Shobana M. F., Priya V. S., Mani V. M. (2021). Biodegradation of sago effluent by white-rot fungus *Phanerochaete chrysosporium*. *International Journal of Life Science and Pharma Research* 11(2):91-99. <https://doi.org/10.22376/ijpbs/lpr.2021.11.2.91-99>
- Vydrina I., Malkov A., Vashukova K., Tyshkunova I., Mayer L., Faleva A., Shestakov S., Novozhilov E., Chukhchin D. (2023). A new method for determination of lignocellulose crystallinity from XRD data using NMR calibration. *Carbohydrate Polymer Technologies and Applications* 5:100305. <https://doi.org/10.1016/j.carpta.2023.100305>
- Wada M., Kondo T., Okano T. (2003). Thermally Induced Crystal Transformation from Cellulose Ia to Ib. *Polymer Journal* 35(2):155-159. <https://doi.org/10.1295/polymj.35.155>
- Wagle A., Angove M. J., Mahara A., Wagle A., Mainali B., Martins M., Goldbeck R., Raj Paudel S. (2022). Multi-stage pre-treatment of lignocellulosic biomass for multi-product biorefinery: A review. *Sustainable Energy Technologies and Assessments* 49:101702. <https://doi.org/10.1016/j.seta.2021.101702>
- Wahid R., Hjorth M., Kristensen S., Møller H. B. (2015). Extrusion as Pretreatment for Boosting Methane Production: Effect of Screw Configurations. *Energy & Fuels* 29(7):4030-4037. <https://doi.org/10.1021/acs.energyfuels.5b00191>
- Wang C., Sun H., Li J., Li Y., Zhang Q. (2009). Enzyme activities during degradation of polycyclic aromatic hydrocarbons by white rot fungus *Phanerochaete chrysosporium* in soils. *Chemosphere* 77(6):733-738. <https://doi.org/10.1016/j.chemosphere.2009.08.028>
- Wang H., Pu Y., Ragauskas A., Yang B. (2019). From lignin to valuable products—strategies, challenges, and prospects. *Bioresource technology* 271:449-461. <https://doi.org/10.1016/j.biortech.2018.09.072>
- Wang J., Xin D., Hou X., Wu J., Fan X., Li K., Zhang J. (2016). Structural properties and hydrolysabilities of Chinese Pennisetum and Hybrid Pennisetum: Effect of aqueous ammonia pretreatment. *Bioresource technology* 199:211-219. <https://doi.org/10.1016/j.biortech.2015.08.046>
- Wang L. & Yang S.-T. (2007). Chapter 18 - Solid State Fermentation and Its Applications. *Bioprocessing for Value-Added Products from Renewable Resources*, Yang S.-T. (Édit.) Elsevier, Amsterdam. p 465-489. <https://doi.org/10.1016/B978-044452114-9/50019-0>
- Wang L. J., Liu X. L., Weng M. L., Wu F. S., Li Z. J., Wang S. F. (2013). Extraction of Hemicellulose from Sugarcane Bagasse under Microwave Radiation. *Advanced Materials Research* 634-638:975-980. <https://doi.org/10.4028/www.scientific.net/AMR.634-638.975>
- Wang M. & Zhao J. (2018). Are renewable energy policies climate friendly? The role of capacity constraints and market power. *Journal of Environmental Economics and Management* 90:41-60. <https://doi.org/10.1016/j.jeem.2018.05.003>

- Wang S., Shuai L., Saha B., Vlachos D. G., Epps T. H., III (2018a). From Tree to Tape: Direct Synthesis of Pressure Sensitive Adhesives from Depolymerized Raw Lignocellulosic Biomass. *ACS Central Science* 4(6):701-708. <https://doi.org/10.1021/acscentsci.8b00140>
- Wang Y., Akbarzadeh A., Chong L., Du J., Tahir N., Awasthi M. K. (2022). Catalytic pyrolysis of lignocellulosic biomass for bio-oil production: A review. *Chemosphere* 297:134181. <https://doi.org/10.1016/j.chemosphere.2022.134181>
- Wang Z., He X., Yan L., Wang J., Hu X., Sun Q., Zhang H. (2020). Enhancing enzymatic hydrolysis of corn stover by twin-screw extrusion pretreatment. *Industrial Crops and Products* 143:111960. <https://doi.org/10.1016/j.indcrop.2019.111960>
- Wang Z., Lin X., Li P., Zhang J., Wang S., Ma H. (2012). Effects of low intensity ultrasound on cellulase pretreatment. *Bioresource technology* 117:222-227. <https://doi.org/10.1016/j.biortech.2012.04.015>
- Wang Z., Winstrand S., Gillgren T., Jönsson L. J. (2018b). Chemical and structural factors influencing enzymatic saccharification of wood from aspen, birch and spruce. *Biomass and Bioenergy* 109:125-134. <https://doi.org/10.1016/j.biombioe.2017.12.020>
- Watson M. J., Machado P. G., da Silva A. V., Saltar Y., Ribeiro C. O., Nascimento C. A. O., Dowling A. W. (2024). Sustainable aviation fuel technologies, costs, emissions, policies, and markets: A critical review. *Journal of Cleaner Production* 449:141472. <https://doi.org/10.1016/j.jclepro.2024.141472>
- Webb C. (2017). Design Aspects of Solid State Fermentation as Applied to Microbial Bioprocessing. *Journal of Applied Biotechnology & Bioengineering* 4(1). <https://doi.org/10.15406/jabb.2017.04.00094>
- Wei Kit Chin D., Lim S., Pang Y. L., Lam M. K. (2020). Fundamental review of organosolv pretreatment and its challenges in emerging consolidated bioprocessing. *Biofuels, Bioproducts and Biorefining* 14(4):808-829. <https://doi.org/10.1002/bbb.2096>
- Weiss N. D., Felby C., Thygesen L. G. (2019). Enzymatic hydrolysis is limited by biomass–water interactions at high-solids: improved performance through substrate modifications. *Biotechnology for Biofuels* 12(1):3. <https://doi.org/10.1186/s13068-018-1339-x>
- Werther J. (2007). Fluidized-Bed Reactors. *Ullmann's Encyclopedia of Industrial Chemistry*. https://doi.org/10.1002/14356007.b04_239.pub2
- Wesholowski J., Hoppe K., Nickel K., Muehlenfeld C., Thommes M. (2019). Scale-Up of pharmaceutical Hot-Melt-Extrusion: Process optimization and transfer. *European Journal of Pharmaceutics and Biopharmaceutics* 142:396-404. <https://doi.org/10.1016/j.ejpb.2019.07.009>
- Weyhrich C. W., Petrova S. P., Edgar K. J., Long T. E. (2023). Renewed interest in biopolymer composites: incorporation of renewable, plant-sourced fibers. *Green chemistry* 25(1):106-129. <https://doi.org/10.1039/D2GC03384D>
- WHO (2024). *Hunger numbers stubbornly high for three consecutive years as global crises deepen: UN report*. <https://www.who.int/news/item/24-07-2024-hunger-numbers-stubbornly-high-for-three-consecutive-years-as-global-crises-deepen--un-report>
- Wimalasena T. T., Greetham D., Marvin M. E., Liti G., Chandelia Y., Hart A., Louis E. J., Phister T. G., Tucker G. A., Smart K. A. (2014). Phenotypic characterisation of *Saccharomyces* spp. yeast for tolerance to stresses encountered during fermentation of lignocellulosic residues to produce bioethanol. *Microbial Cell Factories* 13(1):47. <https://doi.org/10.1186/1475-2859-13-47>

- WSP (2021a). *Inventaire de la biomasse disponible pour produire de la bioénergie et portrait de la production de la bioénergie sur le territoire québécois* Ministère de l'énergie et des ressources naturelles. 277 p. <https://mrnf.gouv.qc.ca/wp-content/uploads/WSP-Canada-Inventaire-biomasse-production-bioenergies-quebec-03-2021.pdf>
- WSP (2021b). *Inventaire de la biomasse disponible pour produire de la bioénergie et portrait de la production de la bioénergie sur le territoire québécois. Rapport réalisé par WSP Canada Inc., pour le compte du Ministère de l'Énergie et des Ressources naturelles.* . Ministère de l'énergie et des ressources naturelles, (Réf. WSP : 201-03354-00). 277 p. <https://mrnf.gouv.qc.ca/wp-content/uploads/WSP-Canada-Inventaire-biomasse-production-bioenergies-quebec-03-2021.pdf>
- Wu C., Zhang F., Li L., Jiang Z., Ni H., Xiao A. (2018). Novel optimization strategy for tannase production through a modified solid-state fermentation system. *Biotechnology for Biofuels* 11(1):92. <https://doi.org/10.1186/s13068-018-1093-0>
- Wu F., Guo Z., Cui K., Dong D., Yang X., Li J., Wu Z., Li L., Dai Y., Pan T. (2023a). Insights into characteristics of white rot fungus during environmental plastics adhesion and degradation mechanism of plastics. *Journal of Hazardous Materials* 448:130878. <https://doi.org/10.1016/j.jhazmat.2023.130878>
- Wu G., Liu Y., Liu G., Hu R., Gao G. (2021). Characterizing the electronic structure of ionic liquid/benzene catalysts for the isobutane alkylation. *Journal of Molecular Liquids* 328:115411. <https://doi.org/10.1016/j.molliq.2021.115411>
- Wu W., Li P., Huang L., Wei Y., Li J., Zhang L., Jin Y. (2023b). The Role of Lignin Structure on Cellulase Adsorption and Enzymatic Hydrolysis. *Biomass* 3(1):96-107. <https://www.mdpi.com/2673-8783/3/1/7>
- Wu Z. D., Zhang Q., Yin J., Wang X. M., Zhang Z. J., Wu W. F., Li F. J. (2020). Interactions of Multiple Biological Fields in Stored Grain Ecosystems. *Scientific Reports* 10(1):9302. <https://doi.org/10.1038/s41598-020-66130-6>
- Xin Y., Zhu X., Wang T. (2020). Mixing Characteristics of Polymer Melt in Triple Screw Extruders with Combined Screws using Finite Element Method. *IOP Conference Series: Materials Science and Engineering* 768(2):022068. <https://doi.org/10.1088/1757-899x/768/2/022068>
- Xu C., Paone E., Rodríguez-Padrón D., Luque R., Mauriello F. (2020a). Recent catalytic routes for the preparation and the upgrading of biomass derived furfural and 5-hydroxymethylfurfural. *Chemical Society Reviews* 49(13):4273-4306. <https://doi.org/10.1039/D0CS00041H>
- Xu E., Wu Z., Jin Z., Campanella O. H. (2018). Bioextrusion of Broken Rice in the Presence of Divalent Metal Salts: Effects on Starch Microstructure and Phenolics Compounds. *ACS Sustainable Chemistry & Engineering* 6(1):1162-1171. <https://doi.org/10.1021/acssuschemeng.7b03459>
- Xu H., Che X., Ding Y., Kong Y., Li B., Tian W. (2019). Effect of crystallinity on pretreatment and enzymatic hydrolysis of lignocellulosic biomass based on multivariate analysis. *Bioresour Technol* 279:271-280. <https://doi.org/10.1016/j.biortech.2018.12.096>
- Xu H., Kong Y., Peng J., Song X., Liu Y., Su Z., Li B., Gao C., Tian W. (2021). Comprehensive analysis of important parameters of choline chloride-based deep eutectic solvent pretreatment of lignocellulosic biomass. *Bioresour Technol* 319:124209. <https://doi.org/10.1016/j.biortech.2020.124209>

- Xu H., Peng J., Kong Y., Liu Y., Su Z., Li B., Song X., Liu S., Tian W. (2020b). Key process parameters for deep eutectic solvents pretreatment of lignocellulosic biomass materials: A review. *Bioresource technology* 310:123416. <https://doi.org/10.1016/j.biortech.2020.123416>
- Xu J. & Cheng J. J. (2011). Pretreatment of switchgrass for sugar production with the combination of sodium hydroxide and lime. *Bioresource technology* 102(4):3861-3868. <https://doi.org/10.1016/j.biortech.2010.12.038>
- Xue B., He H. Z., Liu B. D., Xue F., Zhu Z. W., Liu S. M., Chen M., Wang G. Z., Zhan Z. M., Chen Q.-H., Chen D.-L. (2018). Study on the Morphology, Mechanical, Thermal Stability Properties of Poly(Lactic-Acid)/Poly(Ether-Block-Amide) Blends Prepared by Triple-Single Screw Extruder. *Key Engineering Materials* 783:51-55. <https://doi.org/10.4028/www.scientific.net/KEM.783.51>
- Yadav J., Doddapaneni H., Subramanian V. (2006). P450ome of the white rot fungus *Phanerochaete chrysosporium*: structure, evolution and regulation of expression of genomic P450 clusters. (Portland Press Ltd.). <https://doi.org/10.1042/bst0341165>
- Yağcı S., Sutay Kocabaş D., Çalışkan R., Özbek H. N. (2022a). Statistical investigation of the bioprocess conditions of alkali combined twin-screw extrusion pretreatment to enhance fractionation and enzymatic hydrolysis of bulgur bran. *Journal of the Science of Food and Agriculture* 102(11):4770-4779. <https://doi.org/10.1002/jsfa.11837>
- Yağcı S., Sutay Kocabaş D., Çalışkan R., Özbek H. N. (2022b). Statistical investigation of the bioprocess conditions of alkali combined twin-screw extrusion pretreatment to enhance fractionation and enzymatic hydrolysis of bulgur bran. *Journal of the Science of Food and Agriculture*. <https://doi.org/10.1002/jsfa.11837>
- Yan X., Wang Z., Zhang K., Si M., Liu M., Chai L., Liu X., Shi Y. (2017). Bacteria-enhanced dilute acid pretreatment of lignocellulosic biomass. *Bioresource technology* 245:419-425. <https://doi.org/10.1016/j.biortech.2017.08.037>
- Yan X. J., Hu; Hongpeng, Yang; Sheng, Que; Litong, Ban; Ning, Sun; Yiting, Li (2023). Determination method of manganese peroxidase during straw degradation. *J Microbiol Modern Tech* 7(1):101. <https://www.annepublishers.com/articles/JMC/7101-Determination-Method-of-Manganese.pdf>
- Yang C., Qin J., Sun S., Gao D., Fang Y., Chen G., Tian C., Bao C., Zhang S. (2024). Progress in developing methods for lignin depolymerization and elucidating the associated mechanisms. *European Polymer Journal* 210:112995. <https://doi.org/10.1016/j.eurpolymj.2024.112995>
- Yang C., Shen Z., Yu G., Wang J. (2008). Effect and aftereffect of gamma radiation pretreatment on enzymatic hydrolysis of wheat straw. *Bioresour Technol* 99(14):6240-6245. <https://doi.org/10.1016/j.biortech.2007.12.008>
- Yang D.-Q. (2005). Isolation of wood-inhabiting fungi from Canadian hardwood logs. *Canadian journal of microbiology* 51(1):1-6. <https://doi.org/10.1139/w04-104>
- Yang H., Shi Z., Xu G., Qin Y., Deng J., Yang J. (2019). Bioethanol production from bamboo with alkali-catalyzed liquid hot water pretreatment. *Bioresour Technol* 274:261-266. <https://doi.org/10.1016/j.biortech.2018.11.088>
- Yang J., Sun M., Jiao L., Dai H. (2021). Molecular Weight Distribution and Dissolution Behavior of Lignin in Alkaline Solutions. *Polymers* 13(23). <https://doi.org/10.3390/polym13234166>

- Yang S., Shi L., Zhou Q., Qian B., De Girolamo A., Zhang L. (2022). Elucidating the synergistic interaction and reaction pathway between the individual lignocellulosic components during flash pyrolysis. *Chemical Engineering Journal* 432:134372. <https://doi.org/10.1016/j.cej.2021.134372>
- Yao A., Choudhary H., Mohan M., Rodriguez A., Magurudeniya H., Pelton J. G., George A., Simmons B. A., Gladden J. M. (2021). Can Multiple Ions in an Ionic Liquid Improve the Biomass Pretreatment Efficacy? *ACS Sustainable Chemistry & Engineering* 9(12):4371-4376. <https://doi.org/10.1021/acssuschemeng.0c09330>
- Yogalakshmi K., Poornima Devi K., Sivashanmugam P., Kavitha S., Yukesh Kannah R., Varjani S., AdishKumar S., Kumar G., Rajesh Banu J. (2022). Lignocellulosic biomass-based pyrolysis: A comprehensive review. *Chemosphere* 286:131824. <https://doi.org/10.1016/j.chemosphere.2021.131824>
- Yong K. J., Wu T. Y., Lee C. B. T. L., Lee Z. J., Liu Q., Jahim J. M., Zhou Q., Zhang L. (2022). Furfural production from biomass residues: Current technologies, challenges and future prospects. *Biomass and Bioenergy* 161:106458. <https://doi.org/10.1016/j.biombioe.2022.106458>
- Yoo J. (2011). *Technical and economical assessment of thermo-mechanical extrusion pretreatment for cellulosic ethanol production*. PhD (Kansas State University).
- Yoo J., Alavi S., Vadlani P., Amanor-Boadu V. (2011). Thermo-mechanical extrusion pretreatment for conversion of soybean hulls to fermentable sugars. *Bioresource technology* 102(16):7583-7590. <https://doi.org/10.1016/j.biortech.2011.04.092>
- Yuan Y., Bian L.-S., Wu Y.-D., Chen J.-J., Wu F., Liu H.-G., Zeng G.-Y., Dai Y.-C. (2023). Species diversity of pathogenic wood-rotting fungi (Agaricomycetes, Basidiomycota) in China. *Mycology* 14(3):204-226. <https://doi.org/10.1080/21501203.2023.2238779>
- Zabed H. M., Akter S., Yun J., Zhang G., Awad F. N., Qi X., Sahu J. N. (2019). Recent advances in biological pretreatment of microalgae and lignocellulosic biomass for biofuel production. *Renewable and Sustainable Energy Reviews* 105:105-128. <https://doi.org/10.1016/j.rser.2019.01.048>
- Zhang B., Liu X., Bao J. (2023). High solids loading pretreatment: The core of lignocellulose biorefinery as an industrial technology – An overview. *Bioresource technology* 369:128334. <https://doi.org/10.1016/j.biortech.2022.128334>
- Zhang H.-J., Fan X.-G., Qiu X.-L., Zhang Q.-X., Wang W.-Y., Li S.-X., Deng L.-H., Koffas M. A. G., Wei D.-S., Yuan Q.-P. (2014a). A novel cleaning process for industrial production of xylose in pilot scale from corncob by using screw-steam-explosive extruder. *Bioprocess and Biosystems Engineering* 37(12):2425-2436. <https://doi.org/10.1007/s00449-014-1219-0>
- Zhang H., Xu X., Tan L., Liang Z., Cao R., Wan Q., Xu H., Wang J., Huang T., Wen G. (2021a). The aggregation of Aspergillus spores and the impact on their inactivation by chlorine-based disinfectants. *Water research* 204:117629. <https://doi.org/10.1016/j.watres.2021.117629>
- Zhang H., Yang W., Roslan I. I., Jaenicke S., Chuah G.-K. (2019a). A combo Zr-HY and Al-HY zeolite catalysts for the one-pot cascade transformation of biomass-derived furfural to γ -valerolactone. *Journal of catalysis* 375:56-67. <https://doi.org/10.1016/j.jcat.2019.05.020>

- Zhang J., Wang Y.-H., Qu Y.-S., Wei Q.-Y., Li H.-Q. (2018). Effect of the organizational difference of corn stalk on hemicellulose extraction and enzymatic hydrolysis. *Industrial Crops and Products* 112:698-704. <https://doi.org/10.1016/j.indcrop.2018.01.007>
- Zhang J., Zhang X., Yang M., Singh S., Cheng G. (2021b). Transforming lignocellulosic biomass into biofuels enabled by ionic liquid pretreatment. *Bioresource technology* 322:124522. <https://doi.org/10.1016/j.biortech.2020.124522>
- Zhang J., Zou D., Singh S., Cheng G. (2021c). Recent developments in ionic liquid pretreatment of lignocellulosic biomass for enhanced bioconversion. *Sustainable Energy & Fuels* 5(6):1655-1667. <https://doi.org/10.1039/d0se01802c>
- Zhang P., Yuan J., Fellingner T.-P., Antonietti M., Li H., Wang Y. (2013). Improving Hydrothermal Carbonization by Using Poly(ionic liquid)s. *Angewandte Chemie International Edition* 52(23):6028-6032. <https://doi.org/10.1002/anie.201301069>
- Zhang Q., De Oliveira Vigier K., Royer S., Jerome F. (2012a). Deep eutectic solvents: syntheses, properties and applications. *Chem Soc Rev* 41(21):7108-7146. <https://doi.org/10.1039/c2cs35178a>
- Zhang R., Ma S., Li L., Zhang M., Tian S., Wang D., Liu K., Liu H., Zhu W., Wang X. (2021d). Comprehensive utilization of corn starch processing by-products: A review. *Grain & Oil Science and Technology* 4(3):89-107. <https://doi.org/10.1016/j.gaost.2021.08.003>
- Zhang S., Jiang M., Zhou Z., Zhao M., Li Y. (2012b). Selective removal of lignin in steam-exploded rice straw by Phanerochaete chrysosporium. *International Biodeterioration & Biodegradation* 75:89-95. <https://doi.org/10.1016/j.ibiod.2012.09.003>
- Zhang S., Keshwani D. R., Xu Y., Hanna M. A. (2012c). Alkali combined extrusion pretreatment of corn stover to enhance enzyme saccharification. *Industrial Crops and Products* 37(1):352-357. <https://doi.org/10.1016/j.indcrop.2011.12.001>
- Zhang S., Xu Y., Hanna M. A. (2012d). Pretreatment of Corn Stover with Twin-Screw Extrusion Followed by Enzymatic Saccharification. *Applied Biochemistry and Biotechnology* 166(2):458-469. <https://doi.org/10.1007/s12010-011-9441-6>
- Zhang X., Zhang W., Su J., Wang M., Lu C. (2014b). Preparation, characterization, and properties of polyethylene composites highly filled with calcium carbonate through co-rotating conical twin-screw extrusion. *Journal of Vinyl and Additive Technology* 20(2):108-115. <https://doi.org/10.1002/vnl.21345>
- Zhang Y., Hou T., Li B., Liu C., Mu X., Wang H. (2014c). Acetone-butanol-ethanol production from corn stover pretreated by alkaline twin-screw extrusion pretreatment. *Bioprocess Biosyst Eng* 37(5):913-921. <https://doi.org/10.1007/s00449-013-1063-7>
- Zhang Y., Huang M., Su J., Hu H., Yang M., Huang Z., Chen D., Wu J., Feng Z. (2019b). Overcoming biomass recalcitrance by synergistic pretreatment of mechanical activation and metal salt for enhancing enzymatic conversion of lignocellulose. *Biotechnology for Biofuels* 12(1). <https://doi.org/10.1186/s13068-019-1354-6>
- Zhang Y., Li T., Shen Y., Wang L., Zhang H., Qian H., Qi X. (2020). Extrusion followed by ultrasound as a chemical-free pretreatment method to enhance enzymatic hydrolysis of rice hull for fermentable sugars production. *Industrial Crops and Products* 149:112356. <https://doi.org/10.1016/j.indcrop.2020.112356>
- Zhang Y., Ni S., Wu R., Fu Y., Qin M., Willför S., Xu C. (2022). Green fractionation approaches for isolation of biopolymers and the critical technical challenges. *Industrial Crops and Products* 177:114451. <https://doi.org/10.1016/j.indcrop.2021.114451>

- Zhang Z., Harrison M. D., Rackemann D. W., Doherty W. O. S., O'Hara I. M. (2016). Organosolv pretreatment of plant biomass for enhanced enzymatic saccharification. *Green chemistry* 18(2):360-381. <https://doi.org/10.1039/c5gc02034d>
- Zhao C., Shao Q., Chundawat S. P. S. (2020). Recent advances on ammonia-based pretreatments of lignocellulosic biomass. *Bioresource technology* 298:122446. <https://doi.org/10.1016/j.biortech.2019.122446>
- Zhao J., de Koker T. H., Janse B. J. H. (1995). First report of the white rotting fungus *Phanerochaete chrysosporium* in South Africa. *South African Journal of Botany* 61(3):167-168. [https://doi.org/10.1016/S0254-6299\(15\)30503-2](https://doi.org/10.1016/S0254-6299(15)30503-2)
- Zhao J., Wang B., Dong K., Shahbaz M., Ni G. (2023). How do energy price shocks affect global economic stability? Reflection on geopolitical conflicts. *Energy Economics* 126:107014. <https://doi.org/10.1016/j.eneco.2023.107014>
- Zhao L., Sun Z.-F., Zhang C.-C., Nan J., Ren N.-Q., Lee D.-J., Chen C. (2022). Advances in pretreatment of lignocellulosic biomass for bioenergy production: Challenges and perspectives. *Bioresour Technol* 343:126123. <https://doi.org/10.1016/j.biortech.2021.126123>
- Zhao Q. & Anderson J. L. (2012). 2.11 - Ionic Liquids. *Comprehensive Sampling and Sample Preparation*, Pawliszyn J (Édit.) Academic Press, Oxford. p 213-242. <https://doi.org/10.1016/B978-0-12-381373-2.00053-3>
- Zhao X., Cheng K., Liu D. (2009). Organosolv pretreatment of lignocellulosic biomass for enzymatic hydrolysis. *Appl Microbiol Biotechnol* 82(5):815-827. <https://doi.org/10.1007/s00253-009-1883-1>
- Zhao X., Zhang L., Liu D. (2012). Biomass recalcitrance. Part I: the chemical compositions and physical structures affecting the enzymatic hydrolysis of lignocellulose. *Biofuels, Bioproducts and Biorefining* 6(4):465-482. <https://doi.org/10.1002/bbb.1331>
- Zhao Z., Jiang J., Zheng M., Wang F. (2021). Advancing development of biochemicals through the comprehensive evaluation of bio-ethylene glycol. *Chemical Engineering Journal* 411. <https://doi.org/10.1016/j.cej.2021.128516>
- Zheng J., Choo K., Rehmann L. (2015). The effects of screw elements on enzymatic digestibility of corncobs after pretreatment in a twin-screw extruder. *Biomass and Bioenergy* 74:224-232. <https://doi.org/10.1016/j.biombioe.2015.01.022>
- Zheng J., Choo K., Rehmann L. (2016). Xylose removal from lignocellulosic biomass via a twin-screw extruder: The effects of screw configurations and operating conditions. *Biomass and Bioenergy* 88:10-16. <https://doi.org/10.1016/j.biombioe.2016.03.012>
- Zheng J. & Rehmann L. (2014). Extrusion pretreatment of lignocellulosic biomass: a review. *Int J Mol Sci* 15(10):18967-18984. <https://doi.org/10.3390/ijms151018967>
- Zheng Z. & Obbard J. P. (2002). Oxidation of polycyclic aromatic hydrocarbons (PAH) by the white rot fungus, *Phanerochaete chrysosporium*. *Enzyme and Microbial Technology* 31(1):3-9. [https://doi.org/10.1016/S0141-0229\(02\)00091-1](https://doi.org/10.1016/S0141-0229(02)00091-1)
- Zhou Z., Lei F., Li P., Jiang J. (2018). Lignocellulosic biomass to biofuels and biochemicals: A comprehensive review with a focus on ethanol organosolv pretreatment technology. *Biotechnology and Bioengineering* 115(11):2683-2702. <https://doi.org/10.1002/bit.26788>

- Zhu X. Z., Tong Y., Hu Y. X. (2018). Chaotic Manifold Analysis of Four-Screw Extruders Based on Lagrangian Coherent Structures. *Materials* 11(11).
<https://doi.org/10.3390/ma11112272>
- Zoghalmi A. & Paës G. (2019). Lignocellulosic biomass: understanding recalcitrance and predicting hydrolysis. *Frontiers in Chemistry* 7:874.
<https://doi.org/10.3389/fchem.2019.00874>

Tableau 11.1 Revue sur les extrusions de biomasse lignocellulosiques

N°	Auteurs	Diamètre	Caractéristiques	Extrudeuse		Type	Biomasse	Méthode de caractérisation des carbohydrates	Inhibiteurs dans l'extrudat	Meilleurs résultats
				Additifs	Enzymes durant l'extrusion					
1	Mariana Kuster Moro et al., 2017	16 mm	<ul style="list-style-type: none"> - Bi-vis - Modèle : HAAKE PolyLab OS - Ratio L/D = 25 - Vis de transport (avant et arrière) et vis de pétrissage - 50 °C (avec eau) et 85 °C (avec glycérol) - 30 rpm (avec eau) et 85 rpm (avec glycérol) 	<ul style="list-style-type: none"> - Eau - Glycérol - Éthylène glycol - Polysorbate 80 	Aucune	<ul style="list-style-type: none"> - Bagasse de canne à sucre - Paille de canne à sucre 	<ul style="list-style-type: none"> - Taille : 0,20 mm à 2,00 mm - Cellulose : 44,7 % - Hémicellulose : 30,8 % - Lignine : 20,8 % - Taille : 0,20 mm à 2,00 mm - Cellulose : 36,9 % - Hémicellulose : 26,6 % - Lignine : 21,4 % 	Chromatographie Liquide à Haute Performance (HPLC)	Aucun	<p>Conditions : Eau, modification config des vis Glucose : 59,1 % de MS</p> <p>Condition : Glycérol, modification config des vis Glucose : 68,2 % de MS</p>
2	Maria José Negro et al., 2015	25 mm	<ul style="list-style-type: none"> - Bi-vis à 6 modules - Modèle : Clextral Processing Platform Evolum® 25 A110 - Ratio L/D = 24 - Vis de transport (avant et arrière) et vis de pétrissage - 70, 90 et 110 °C - 70 rpm et 150 rpm 	- NaOH et eau	Aucune	Taille de bois d'olivier	<ul style="list-style-type: none"> - Taille : 1 mm à 4 mm - Glucose+Glucose : 29,9 % - Hémicellulose : 17,5 % - Lignine : 17,8 % - Extractibles : 24,5 % - Cendre : 4,1 % - Groupe acétyle : 2,3 % 	Chromatographie Liquide à Haute Performance (HPLC)	Acide formique Acide acétique Phénols	<p>Conditions : 150 rpm, 110 °C, 5 g NaOH/100 g substrat</p> <ul style="list-style-type: none"> - Glucose : 42,95 % - Hémicellulose : 31 % - Lignine : 28,95 %
3	Arleta Duque et al., 2014	25 mm	<ul style="list-style-type: none"> - Bi-vis à 6 modules - Modèle : Clextral Processing Platform Evolum® 25 A110 - Ratio L/D = 24 - Vis de transport (avant et arrière) et vis de pétrissage - 68 °C pour la 1^{ère} extrusion puis 50 °C pour la 2^{ème} (bioextrusion) - Nombre rpm : assisté par un logiciel 	- NaOH - H ₃ PO ₄	Cellulases et hemicellulases Novozymes A/S (Danemark)	Paille de blé	<ul style="list-style-type: none"> - Taille : 5 mm - Cellulose : 39,1 % - Hémicellulose : 25,7 % - Lignine : 15,2 % - Extractibles : 10,2 % - Groupe acétyle : 1,8 % - Cendre : 6,8 % 	Méthodes d'analyse de la biomasse en laboratoire de la National Renewable Energy Laboratory (NREL, CO) laboratory analytical procedures (LAP)	Le furfural et l'hydroxyméthyl furfural n'ont pas été détectés	<ul style="list-style-type: none"> - Glucose : 47,4 % - Xylose : 24,5 % - Galactose : 1,3 % - Arabinose : 3,1 % - Lignine : 17,6 % - Cendre : 4,9 %
4	Juhyun Yoo et al., 2011	18 mm	<ul style="list-style-type: none"> - Bis-vis à 6 modules - Modèle : Micro-18, American Leistritz, Somerville, NJ - Ratio L/D = 30 - Vis de transport (avant seulement) et vis de pétrissage - 80, 110 et 140 °C - 240 à 420 rpm 	<ul style="list-style-type: none"> - Éthylène glycol (solvant) - H₂SO₄ (avant extrusion) - NaOH (avant extrusion) 	Combinaison de - Cellulase (Cellulast 1.L) - β-glucosidase (Novozym 188) - Complexe enzymatique (Viscozyme L)	Coque de soja	<ul style="list-style-type: none"> - Taille : 1041 μm - Cellulose : 35,35 % - Hémicellulose : 17,21 % - Lignine : 2,33 % 	<ul style="list-style-type: none"> - La ANKOM Fiber Analyzer (ANKOM Technology, NY) - La méthode 920.40; AOAC, 2010 pour l'amidon 	Aucun	<p>Conditions : Traitement au NaOH avant l'extrusion, 80 °C et 350 rpm</p> <ul style="list-style-type: none"> - Cellulose : 66,72 % - Hémicellulose : 14,59 % - Lignine : 11,66 %
5	Kyeong Eop Kang et al., 2012	28 mm	<ul style="list-style-type: none"> - Bis-vis - Modèle : ChangHae Ethanol Multi ExTruder (CHEMET) Changhae Ethanol Co., Ltd., Jeonju, KoreaPlasticorder Extruder Model PL 2000, Hackensack, NJ - Vis de transport (avant et arrière) et vis de pétrissage - Ratio L/D = 36 - 0 à 200 °C (contrôlée par ordinateur) - 150 rpm 	- NaOH	Aucune	Miscanthus	<ul style="list-style-type: none"> - Taille : moins de 2 mm - Glucose : 45,3 % - Hémicellulose : 21,2 % - Lignine : 25,1 % - Cendre : 1,5 % 	Méthode de laboratoire d'analyse des matières lignocellulosiques de la NREL (National Renewable Energy Laboratory) in Golden, CO., 2008	Aucun	<ul style="list-style-type: none"> - Cellulose : 62 % - Xylose : 20,7 % - Lignine : 13,0 % - Cendre : 0,3 %
6	Michelle Cardoso Coimbra et al., 2016	25 mm	<ul style="list-style-type: none"> - Bi-vis à 6 modules - Modèle : Clextral Processing Platform Evolum® 25 A110 - Ratio L/D = 24 - Vis de transport (avant et arrière) et vis de pétrissage - 70 °C - 150 rpm - Temps de résidence : 2 min 	- NaOH	Aucune	Paille de blé	<ul style="list-style-type: none"> - Taille : 5 mm - Humidité : 6 % - Glucose : 37,8 % - Hémicellulose : 28,2 % - Lignine : 19,8 % - Extractive : 7,1 % - Groupe acétyle : 2,5 % - Cendre : 3,7 % 	Laboratory Analytical Procedures (LAP) for biomass analysis de la National Renewable Energy Laboratory (NREL, CO, USA)	Aucun	<ul style="list-style-type: none"> - Glucose : 46,9 % - Hémicellulose : 28,7 % - Lignine : 17,4 % - Extractive : 6,7 % - Groupe acétyle : 2,5 % - Cendre : 3,3 %
7	Pérez-Rodríguez et al., 2017	16 mm	<ul style="list-style-type: none"> - Bi-vis - Modèle : HAAKE Rheomex™ PTW OS, Fisher, France - Ratio L/D = 25 - Vis de transport (avant et arrière) et vis de pétrissage - Température ambiante - Temps de résidence : 55 s et 35 s - Nombre rpm : assisté par ordinateur 	- NaOH (0,4% w/v)	Aucune	Épi de maïs	<ul style="list-style-type: none"> - Taille : inférieure à 2 mm - Humidité : n.c. - Cellulose (glucose) : 42 % - Hémicellulose : 45,9 % - Lignine : 2,8 % - NDS (Neutral Detergent Soluble compound) : 9,1 % 	La méthode Van Soest fiber analysis	Aucun	<p>Condition : 35 secondes d'extrusion</p> <ul style="list-style-type: none"> - Cellulose (glucose) : 37,6 % - Hémicellulose : 39,4 % - Lignine : 5,9 % - NDS (Neutral Detergent Soluble compound) : 17,1 %
8	Shujing Zhang et al., 2012	20 mm	<ul style="list-style-type: none"> - Bi-vis à 16 modules ou segments (S) - Modèle : C.W. Brabender co-rotating twin screw extruder (TSE 20) - Ratio L/D = 20 - Vis de transport (avant et arrière) et vis de pétrissage - 50 °C de S1 à S13 et 140 °C de S14 à S16 - 40, 60, 80, 100 rpm - Temps de résidence : 27 min 	- NaOH (1, 3, 5 et 14 % m/m) avant extrusion	Aucune	Tige de maïs	<ul style="list-style-type: none"> - Taille : inférieure à 2 mm - Humidité : 50 % pour 100 g de substrat - Cellulose (glucanes) : 33,15 % - Hémicellulose : 21,97 % - Lignine : 14,9 % - Extractives : 12,9 % - Cendre : 10,91 % - Protéines : 4,00 % - Autres : 2,2 % 	Les procédures standard de la NREL	Aucun	<p>Conditions : 14% de NaOH et 80 rpm</p> <ul style="list-style-type: none"> - Glucose : 78,4 % - Xylose : 43,5 %
9	Song-Yi Han et al., 2020	15 mm	<ul style="list-style-type: none"> - Bi-vis - Modèle : 2D15W, Toyo Seiki Seisaku-sho, Ltd., Tokyo, Japan - Ratio L/D = 17 - Vis de transport (avant et arrière) et vis de pétrissage - 140 et 160 °C - 2, 5 et 15 rpm 	<ul style="list-style-type: none"> - Avant extrusion - [EMIM]Ac pure - DMSO pure - Mélange de DMSO et [EMIM]Ac 	Aucune	Les saules	<ul style="list-style-type: none"> - Taille : inférieure à 0,42 mm - Cellulose : 47,2 % - Hémicellulose : 26,4 % - Lignine : 25,1 % - Extractibles : 5,6 % 	Les procédures standard de la NREL (2008)	Aucun	<p>Conditions : 100% [EMIM]Ac, 25% DMSO, 140 °C et 5 rpm</p> <ul style="list-style-type: none"> - Glycan : 40,2 % - Xylane : 11,8 % - Lignine : 26,4 %
10	Virginie Vandebossche et al., 2015	45 mm (BC 45) 21 mm (BC 21)	<ul style="list-style-type: none"> - Bis-vis de 7 modules chacun - Modèle 1 : Clextral BC 45 twin-screw extruder - Modèle 2 : Clextral BC 21 twin-screw extruder - Ratio L/D BC 45 : 31 - Ratio L/D BC 21 : 33 	- NaOH (0,8 kg/h) - H ₃ PO ₄ (0,9 kg/h)	<ul style="list-style-type: none"> - Endoglucanase - Xylanase - β-glucosidase 	Co-produits de maïs doux déshydraté	<ul style="list-style-type: none"> - Taille : 6 mm - Humidité : 20 % - Cellulose : 39 % - Hémicellulose : 36 % - Lignine : 4 % - Cendre : 4 % 	Méthode ADF-NDF method de Van Soest and Wine (1967, 1968).	Aucun	<ul style="list-style-type: none"> - Glucose : 54,4 % - Xylose : 22,3 % - Arabinose : 3 % - Galactose : 0,7 % - Mannose : 0,1 % - Lignine : 4,8 %

N°	Auteurs	Extrudeuse			Enzymes durant l'extrusion	Type	Biomasse		Méthode de caractérisation des carbohydrates	Inhibiteurs dans l'extrudat	Meilleurs résultats
		Diamètre	Caractéristiques	Additifs			Caractéristiques				
			<ul style="list-style-type: none"> - Vis de transport (avant et arrière) et vis de pétrissage (BC 45) - Vis de transport (avant uniquement) et vis de pétrissage (BC 41) - 100 °C (BC 45) - 50 °C (BC 21) - 110 rpm (BC 45) - 200 rpm (BC 21) - Temps de résidence : environ 2 min 								
11	Youwei Zhang et al., 2020	56 mm	<ul style="list-style-type: none"> - Bi-vis - Modèle : DS56-X, JINAN SAIXIN MACHINERY CO., LTD, Shandong Province, China - Ratio L/D = 25 - Vis de transport (avant et arrière) et vis de pétrissage - 143 °C - 350 rpm 	- Aucun	- Aucune	Coque de riz	<ul style="list-style-type: none"> - Taille : inférieure à 0,250 mm (60 mesh) - Humidité : 29 % - Cellulose : 35,56 % - Hémicellulose : 13,68 % - Lignine : 19,21 % - Cendre : 18,05 % 	Procédure standard de l'Association of Official Analytical Chemists (AOAC, 2005)	Aucun	<ul style="list-style-type: none"> - Cellulose : 33,26 % - Hémicellulose : 10,12 % - Lignine : 21,21 % - Cendre : 20,05 % 	
12	Shujing Zhang et al., 2016	20 mm	<ul style="list-style-type: none"> - Bi-vis à 16 modules - Modèle : TSE 20/40 made by C. W. Brabender - Ratio L/D = 20 - Vis de transport (avant et arrière) et vis de pétrissage - 50 °C (zone 1) et 140 °C (zone 2) - 40 rpm à 140 rpm avec des pas de 20 rpm 	- Aucun	- Aucune	Tige de maïs	<ul style="list-style-type: none"> - Taille : inférieure à 2 mm - Humidité : 22,5 % ; 25 % et 27,5 % - Glucane : 33,15 % - Xylane : 19,16 % - Arabinane : 2,80 % - Lignine : 14,9 % - Extractibles : 12,96 % - Cendre : 10,91 % - Protéines : 4 % - Autres : 2,2 % 	Méthode NREL/TP-510-42618 (Sluiter, 2008)	Aucun	<ul style="list-style-type: none"> Condition : 27,5 % d'humidité et 80 rpm - Glucose : 48,79 % - Xylose : 24,98 % 	
13	Young-Lok Cha et al., 2016	50 mm	<ul style="list-style-type: none"> - Bi-vis à 49 modules/vis - Modèle : issue de la collaboration avec Changhae Engineering Co., Ltd. (Corée) - Ratio L/D = 43 - Vis de transport (avant et arrière) et vis de pétrissage - 100 °C - 80 rpm - Temps de résidence : 8 min 	- NaOH (0,6 M)	- Aucune	Miscanthus	<ul style="list-style-type: none"> - Taille : inférieure à 3 mm - Humidité : 7 % - Cellulose : 40,3 % (wt) - Hémicellulose : 24,1 % (wt) - Lignine : 24,1 % (wt) 	Méthode NREL/TP-510-42618 (Sluiter, 2006)	Aucun	<ul style="list-style-type: none"> - Cellulose : 58,9 % wt - Hémicellulose : 26,1 % wt - Lignine : 12,6 % wt 	
14	Aleta Duque et al., 2021	25 mm	<ul style="list-style-type: none"> - Bi-vis à 6 modules - Modèle : Clextal Processing Platform Evolum® 25 A110, Clextal, France - Ratio L/D = 24 - Vis de transport (avant et arrière) et vis de pétrissage - 50 °C et 100 °C dans la partie #3 et #4 - 120 rpm - Temps de résidence : 3 heures 	<ul style="list-style-type: none"> - NaOH (7,2 % w/v) - H₂SO₄ (2,5 % w/v) 	- Commercial cellulolytic cocktail, Cellic CTec2 (Novozymes A/S, Denmark (5 ; 7,5 et 10 FPU/g))	Paille d'orge	<ul style="list-style-type: none"> - Taille : inférieure à 2 mm - Humidité : 11,4 % (extrusion réactive) et 55 % (bioextrusion) - Glucan : 32,9 % - Hémicellulose : 26,1 % - Lignine : 18,8 % - Extractibles : 10,4 % - Groupe acétyle : 1,7 % - Cendre : 3,9 % 	Méthode LAP de la National Renewable Energy Laboratory (NREL, CO) 2007	Aucun	<ul style="list-style-type: none"> Condition : 5 FPU/g - Glucose : 36,13 % - Xylose : 18,49 % - Arabinose : 3,33 % - Galactose : 1,29 % - Lignine : 15,71 % - Cendre : 2,17 % 	
15	Etienne Gatt et al., 2019	27 mm	<ul style="list-style-type: none"> - Bi-vis à 24 modules - Modèle : Entek, OR, US - Ratio L/D = ? - Vis de transport (avant et arrière) et vis de pétrissage - 50 °C - 125 rpm - Temps de résidence : 5 min 	- NaOH (Avant extrusion) 12 %/g	- ACCELLERASE® DUET cocktail from DuPont Industrial Biosciences in a citrate buffer (50 mM, pH 4.5).	Résidus de maïs (épi, feuille et tige)	<ul style="list-style-type: none"> - Taille : inférieure à 5 mm - Cellulose : 44 % - Hémicellulose : 22 % - Lignine : 14 % - Extractibles : 19 % 	High Performance Liquid Chromatography (HPLC)	Aucun	<ul style="list-style-type: none"> Condition: Ratio S/L = 14% - Glucose : 52 % 	
16	Zichao Wang et al., 2020	11 mm	<ul style="list-style-type: none"> - Bi-vis - Modèle : Process 11, Thermo Fisher Scientific, Waltham, MA, USA - Ratio L/D=40 - Vis de transport (avant et arrière) et vis de pétrissage - 120 °C - 100 rpm 	<ul style="list-style-type: none"> - Eau distillée - Glycerol (2 %) - NaHCO₃ (1 g/L) 	Aucune	Tige de maïs	<ul style="list-style-type: none"> - Taille : ? - Humidité : 25 % et 23 % - Cellulose : 32,75 % - Hémicellulose : 31,08 % - Lignine : 10,07 % - Glucide : 2,16 % - Protéine : 0,95 % - Cendre : 4,08 % 	Fibertec™ 2010 automatic fiber analyzer (FOSS, Denmark) according the Van-Soest method (Le et al., 2017). Et high performance liquid chromatography (HPLC)	Aucun	<ul style="list-style-type: none"> Condition : combinaison Eau distillée, Glycérol et NaHCO₃ - Cellulose : 35,03 % - Hémicellulose : 28,85 % - Lignine : 10,01 % - Glucide : 1,95 % - Protéine : 5,06 % - Cendre : 3,76 % 	
17	Yuedong Zhang et al., 2013	n.c.	<ul style="list-style-type: none"> - Bi-vis - Modèle : Extrudeuse hors-série faisant l'objet de brevet - Ratio L/D = n.c. - Vis de transport (avant et arrière) - 99 °C - 350 rpm - Temps de résidence : ? 	- NaOH (8 %)	Aucune	Tige de maïs	<ul style="list-style-type: none"> - Taille : 2 < t < 5 mm - Humidité : 10,75 % - Glucane : 32,31 % - Xylane : 16,78 % - Arabinane : 1,94 % - Lignine : 23,03 % - Acetyl : 2,98 % - Extractibles : 18,45 % - Cendres : 7,44 % 	NREL analytical procedure	Aucun	<ul style="list-style-type: none"> - Glucane : 53,87 % - Xylane : 20,19 % - Arabinane : 1,29 % - Lignine : 23,03 % - Acétyle : 0,36 % - Extractibles : - - Cendres : - 	
18	Ayla Sant'Ana da Silva et al., 2013	15 mm	<ul style="list-style-type: none"> - Bi-vis à 16 modules - Modèle : 2D15W, Toyo Seiki, Tokyo, Japan - Ratio L/D = 17 - Vis de transport (avant et arrière) et vis de pétrissage - 140 °C - 15 rpm - Temps de résidence : 4 min 	- [Emin] Ac	Aucune	Bagasse de canne à sucre	<ul style="list-style-type: none"> - Taille : 0,425 - 1,000 mm - Humidité : 11,1 % ; 16,6 % ; 25 % ; 50 % - Glucane : 41,9 % - Xylane : 25,0 % - Lignine : 22,7 % 	Laboratory Analytical Procedure, NREL/TP-510-42628, 2012	Aucun	<ul style="list-style-type: none"> Condition : 50%, 3 passages, - Glucane : 41,9 % - Xylane : 25,0 % - Lignine : 22,7 % 	
19	T. de Vrije et al., 2002	55 mm	<ul style="list-style-type: none"> - Bi-vis - Modèle : Clextal BC45 corotating twin-screw extruder (Clextal, Firminy, France) - Ratio L/D=23 - Vis de transport (avant et arrière) et vis de pétrissage - 50, 70 et 90 °C - 100 rpm - Temps de résidence : ? 	NaOH (12 % m/m)	Aucune	Miscanthus	<ul style="list-style-type: none"> - Taille 0,22 mm et 17 µm - Humidité : Entre 86 % et 90 % - Cellulose : 32,8 % - Hémicellulose : 24,3 % - Lignine : 25 % - Protéines : 1,3 % - Extractibles : 5,6 % - Cendre : 2,0 % 	Méthode de la Technical Association of the Pulp and Paper Industry (TAPPI)	Aucun	<ul style="list-style-type: none"> Conditions : 90 °C - Glucane : 52,9 % - Lignine : 9,6 % 	
20	Juhyun Yoo et al., 2011	18 mm	<ul style="list-style-type: none"> - Bi-vis à 18 modules - Modèle : Micro-18; American Leistritz, Somerville, NJ - Ratio L/D=30 - 40 °C à 80 °C (gradient dans l'extrudeuse) - 280 rpm ; 350 rpm et 420 rpm - Temps de résidence : ?? 	- Aucun	Aucune	Coque de soja	<ul style="list-style-type: none"> - Taille : <1041 µm - Humidité : 40 % ; 45 % ; 50 % - Cellulose : 36,2 % - Hémicellulose : 17,7 % - Lignine : 2,0 % - Amidon : 0,83 % 	ANKOM Fiber Analyzer (ANKOM Technology, NY) et AOAC 979.10 standard glucoamylase method for starch	<ul style="list-style-type: none"> - Furfural - Acide acétique - Glycérol - HMF 	<ul style="list-style-type: none"> - Cellulose : n.d. - Hémicellulose : n.d. - Lignine : n.d. - Amidon : n.d. 	

12 ANNEXE II

Tableau 12.1 Delignification model results for Ex-SSF pre-treated black spruce chips.

Days	Black spruce Run 2 (BSE 2)			Black spruce Run 5 (BSE 5)		
	Experimental delignification (%)	Langevin reference point	Theoretical delignification (%)	Experimental delignification (%)	Langevin reference point	Theoretical delignification (%)
0	25	25	24.5	25	25	25.7
3	25	-	25.9	12	-	27.2
6	30	30	30.9	18	-	32.5
9	48	48	47.4	50	50	50.3
12	22	-	56.9	34	-	61.3
15	59	59	59.2	45	-	63.7
18	53	-	60.5	65	65	64.7
21	29	-	61.7	45	-	65.4
24	17	-	62.9	43	-	66.1
Function	$Z = x-xc; \coth(z) = \cosh(z)/\sinh(z); y = y_0 + C (\coth(z) - 1/z);$					
Parameters	y0 = 42.0 xc = 8.13 C = 20.0			y0 = 45.0 xc = 8.2 C = 22.0		

Tableau 12.2 Delignification model results for Ex-SSF pre-treated corn stover.

Days	Corn maize residues Run 2 (CS 2)			Corn maize residues Run 8 (CS 8)		
	Experimental delignification (%)	Langevin reference point	Theoretical delignification (%)	Experimental delignification (%)	Langevin reference point	Theoretical delignification (%)
0	27	27	27.0	27	27	27.0
3	19	-	30.5	26	-	28.0
6	42	42	42.0	36	37	37.0
9	33	-	48.5	40	-	43.0
12	50	50	50.0	45	-	55.1
15	n.d.	-	50.9	n.d.	-	58.0
18	n.d.	-	51.7	n.d.	-	59.0
21	n.d.	-	52.6	n.d.	-	59.5
24	n.d.	-	53.4	59	59.8	59.8
Function	$z = x-xc; \coth(z) = \cosh(z)/\sinh(z); y = y_0 + C (\coth(z) - 1/z);$					
Parameters	y0 = 38.0 xc = 5.00 C = 14.0			y0 = 43.0 xc = 9.00 C = 18.0		

13 ANNEXE III

Tableau 13.1 List of equipment per Area and their respective estimated cost adapted from Aden et al. (2002).

Equipments	Scenario 1			Scenario 2			Scenario 3		
	Key parameter	Qt	Total cost (\$)	Key parameter	Qt	Total cost (\$)	Key parameter	Qt	Total cost (\$)
Area 100:									
Shredder	3-5 t/h	1	30 000	10-15 t/h	1	80 000	10-15 t/h	1	80 000
Belt Conveyor	5 m	1	10 000	15 m	1	30 000	15 m	1	30 000
Cooling Tower System	1000 l	1	10 000	3000 l	1	30 000	4000 l	1	40 000
Plant Air Compressor	20-50 m ³ /min	1	50 000	50-150 m ³ /min	1	80 000	50-150 m ³ /min	1	80 000
Cooling Water Pump	10 -20 m ³ /h	1	10 000	50-100 m ³ /h	1	30 000	50-100 m ³ /h	1	30 000
Make-up Water Pump	10 -20 m ³ /h	1	5 000	50-100 m ³ /h	1	15 000	50-100 m ³ /h	1	15 000
Process Water Circulating Pump	10 -20 m ³ /h	1	15000	50-100 m ³ /h	1	30 000	50-100 m ³ /h	1	30 000
Instrument Air Dryer	10-20 m ³ /min	1	15000	10-20 m ³ /min	2	30 000	10-20 m ³ /min	2	30 000
Product Recovery Filter Air Receiver	5-15 m ³	1	20 000	15-50 m ³	1	30 000	5-15 m ³	2	30 000
Process Water Tank	50 m ³	1	25 000	200 m ³	1	75 000	250 m ³	1	80 000
Subtotal			190 000			430 000			445 000
Area 200:									
Extruder	1000-1500 kg/h	1	300 000	3000-5000 kg/h	1	600 000	3000-5000 kg/h	1	600 000
Gravimetric feeders	1000-1500 kg/h	1	12 000	3000-5000 kg/h	1	20 000	3000-5000 kg/h	1	20 000
Feeding hopper	2-5 m ³	1	8 000	10-15 m ³	1	20 000	10-15 m ³	1	20 000
Cooling system	5 – 10 m ³ /h	1	25 000	20 – 50 m ³ /h	1	60 000	20 – 50 m ³ /h	1	60 000
Conveyor	500-2000 kg/h	1	10 000	2000-5000 kg/h	1	30 000	2000-5000 kg/h	1	30 000
Automation system	PLC or SCADA	1	40 000	PLC or SCADA	1	100 000	PLC or SCADA	1	100 000
Tooling set	-	1	10 000	-	1	30 000		1	30 000
Exhaust gas treatment system	10 m ³ /h	1	50 000	30 m ³ /h	1	150 000	30 m ³ /h	1	150 000
Semi-Solid fermentation Tank	10 m ³	2	20 000	30 m ³	2	50 000	50 m ³	2	60 000
SSF tank Agitator	10-50 kW	2	8 000	50 - 100 kW	2	15 000	50 - 100 kW	2	15 000
Aeration system	1-5 m ³ /min	1	25 000	5-15 m ³ /min	1	75 000	5-15 m ³ /min	1	75 000
Temperature control system	20-90 °C	1	15 000	20-90 °C	2	30 000	20-90 °C	2	30 000
Feeding system	500-1500 kg/h	2	10 000	4000-5000 kg/h	1	30 000	4000-5000 kg/h	1	30 000
Sensors and probes	Precision : ±1 %	4	5 000	Precision : ±1 %	12	15 000	Precision : ±1 %	12	15 000
CIP (Clean-In-Place) system	Close system	1	15 000	Close system	1	15 000	Close system	1	15 000
Discharge system	500-1000 kg/h	1	10 000	3000-5000 kg/h	1	25 000	3000-5000 kg/h	1	25 000
Subtotal			563 000			1 265 000			1 275 000
Area 300:									
Ethanol Fermentor Agitator	-	1	10 000	-	1	20 000	-	1	20 000
Saccharification Tank Agitator	-	1	10 000	-	1	20 000	-	1	20 000
Ethanol Fermentor	5 m ³	1	100 000	15 m ³	1	200 000	25 m ³	1	250 000
Fermentation Cooler	1 m ³ /h	1	20 000	3 m ³ /h	1	50 000	5 m ³ /h	1	60 000
Hydrolyzate Heater	1 m ³ /h	1	15 000	3 m ³ /h	1	25 000	5 m ³ /h	1	30 000

		Scenario 1			Scenario 2			Scenario 3		
Equipments		Key parameter	Qt	Total cost (\$)	Key parameter	Qt	Total cost (\$)	Key parameter	Qt	Total cost (\$)
	Saccharified Slurry Cooler	1 m ³ /h	1	15 000	3 m ³ /h	1	25 000	5 m ³ /h	1	30 000
	Fermentation Recirc/Transfer Pump	5 m ³	1	8 000	15 m ³	1	15 000	15 m ³	1	15 000
	Transfer Pump	1 m ³ /h	2	8 000	3 m ³ /h	2	15 000	5 m ³ /h	2	15 000
	Storage Tank	50 m ³	1	60 000	150 m ³	1	120 000	200 m ³	1	150 000
Subtotal				246 000		490 000				590 000
Area 400:										
	Bulk Column	3-5 m	2	20 000	10-15 m	2	50 000	10-15 m	2	50 000
	Column Reboiler	25 – 50 kW	2	15 000	100 – 150 kW	2	50 000	100 – 200 kW	2	70 000
	Column Condenser	1 m ³ /h	2	10 000	3 m ³ /h	2	30 000	5 m ³ /h	2	50 000
	Molecular Sieve	-	1	20 000	-	2	40 000	-	2	40 000
	Column Bottoms Pump	1 - 2 m ³ /h	2	8 000	5 - 10 m ³ /h	2	15 000	10 - 15 m ³ /h	2	20 000
	Column Reflux Pump	1 - 2 m ³ /h	2	8 000	5 - 10 m ³ /h	2	15 000	10 - 15 m ³ /h	2	15 000
	Evaporator Condensate Pump	1 - 2 m ³ /h	1	8 000	5 - 10 m ³ /h	1	15 000	10 - 15 m ³ /h	1	15 000
	Scrubber Bottoms Pump	1 - 2 m ³ /h	1	8 000	5 - 10 m ³ /h	1	15 000	5 - 10 m ³ /h	1	15 000
	Recycled Water Pump	5 m ³ /h	1	8 000	10 m ³ /h	1	15 000	10 m ³ /h	1	15 000
	Pneumapress Filter	1 - 2 m ³ /h	1	10 000	5 - 10 m ³ /h	1	30 000	10 - 15 m ³ /h	1	30 000
	Column Reflux Drum	1 - 2 m ³ /h	1	5 000	5 - 10 m ³ /h	1	15 000	10 - 15 m ³ /h	1	15 000
	Vent Scrubber	1 - 2 m ³ /h	1	5 000	5 - 10 m ³ /h	1	15 000	10 - 15 m ³ /h	1	15 000
	Evaporator Condensate Drum	1 - 2 m ³ /h	1	5 000	5 - 10 m ³ /h	1	15 000	10 - 15 m ³ /h	1	15 000
	Recycled Water Tank	1 - 2 m ³ /h	2	2 000	5 - 10 m ³ /h	2	5 000	10 - 15 m ³ /h	2	5 000
Subtotal				132 000		325 000				370 000
Area 500: Storage										
	Ethanol Product Pump	5 m ³ /h	2	4 000	15 m ³ /h	2	12 000	20 m ³ /h	2	15 000
	Firewater Pump	10 m ³ /h	1	3 000	30 m ³ /h	1	8 000	30 m ³ /h	1	12 000
	Cellulase Pump	1 - 2 m ³ /h	1	2 000	5 - 10 m ³ /h	1	5 000	15 - 20 m ³ /h	1	8 000
	Ethanol Product Storage Tank	100 m ³	1	100 000	300 m ³	1	200 000	400 m ³	1	250 000
	Firewater storage Tank	50 m ³	1	5 000	150 m ³	1	15 000	200 m ³	1	20 000
	Nutrient storage Tank	1 m ³	2	5 000	3 m ³	2	15 000	5 m ³	2	20 000
Subtotal				119 000		255 000				325 000
Area 600: Waste treatment										
	Anaerobic agitator	15-50 kW	1	10 000	15-50 kW	2	20 000	15-50 kW	2	20 000
	Anaerobic Digester Feed Cooler	5 m ³ /h	1	15 000	15 m ³ /h	1	20 000	20 m ³ /h	1	20 000
	Nutrient Feed System	1 m ³ /h	1	10 000	3 m ³ /h	1	30 000	5 m ³ /h	1	40 000
	Biogas Emergency Flare	50 kW/h	1	10 000	150 kW/h	1	25 000	150 kW/h	1	25 000
	Anaerobic Reactor Feed Pump	1 m ³ /h	1	5 000	3 m ³ /h	1	15 000	5 m ³ /h	1	20 000
	Sludge Filtrate Recycle Pump	5 m ³ /h	2	5 000	15 m ³ /h	2	15 000	20 m ³ /h	2	15 000
	Treated Water Pump	10 m ³ /h	1	5 000	30 m ³ /h	1	15 000	50 m ³ /h	1	20 000
	Anaerobic Digester	6 m ³	1	30 000	16 m ³	1	60 000	26 m ³	1	70 000
Subtotal				90 000		200 000				230 000
Area 700: Energy generation										
	Burner Combustion Air Preheater	1 m ³ /h	2	15 000	3 m ³ /h	2	30 000	5 m ³ /h	2	40 000
	BFW Preheater	100-250 °C	1	30 000	100-250 °C	2	50 000	100-250 °C	2	50 000
	Combustion Gas Baghouse	10 m ³ /h	1	10 000	30 m ³ /h	1	30 000	30 m ³ /h	1	30 000
	Turbine/Generator	10 m ³ /h	1	15 000	30 m ³ /h	1	30 000	30 m ³ /h	1	30 000
	Turbine Condensate Pump	10 m ³ /h	1	5 000	30 m ³ /h	1	15 000	30 m ³ /h	1	15 000
	Deaerator Feed Pump	10 m ³ /h	1	5 000	30 m ³ /h	1	15 000	30 m ³ /h	1	15 000
	BFW Pump	10 m ³ /h	1	8 000	30 m ³ /h	1	15 000	30 m ³ /h	1	15 000

Equipments	Scenario 1			Scenario 2			Scenario 3		
	Key parameter	Qt	Total cost (\$)	Key parameter	Qt	Total cost (\$)	Key parameter	Qt	Total cost (\$)
Blowdown Pump	5 m ³ /h	1	8 000	15 m ³ /h	1	15 000	15 m ³ /h	1	15 000
Condensate Collection Tank	10 m ³ /h	1	8 000	30 m ³ /h	1	15 000	30 m ³ /h	1	15 000
Condensate Surge Drum	5 m ³	1	10 000	15 m ³	1	15 000	15 m ³	1	15 000
Deaerator	1 m ³ /h	1	7 000	3 m ³ /h	1	12 000	3 m ³ /h	1	12 000
Blowdown Flash Drum	1 m ³	1	10 000	3 m ³	1	30 000	3 m ³	1	30 000
Subtotal			131 000			272 000			282 000
Total equipment cost (C_{Equip})			1 471 000			3 237 000			3 517 000

Tableau 13.2 Estimated pre-construction and utilities costs adapted from Aden et al. (2002).

Item	Description	Scenario 1		Scenario 2		Scenario 3	
		% C_{Equip}	Cost	% C_{Equip}	Cost	% C_{Equip}	Cost
Warehouse	Building of the warehouse where the plant will be located	15	93 450 \$	15	209 250 \$	15	232 950 \$
Site development	Preparation of the site for construction (land clearing, excavation, grading, etc.)	05*	21750 \$	05*	49 500 \$	10*	108 500 \$
Administrative costs	Fringe benefits, burdens, and insurance of the construction contractor	10	62 300 \$	10	139 500 \$	10	155 300 \$
Field expenses	Consumables, small tool equip., field services, etc.	5	31 150 \$	5	69 750 \$	5	77 650 \$
Offices	Engineering plus incidentals, purchasing, and construction	5	31 150 \$	5	69 750 \$	5	77 650 \$
Other Costs	All other non-identified or non-budgeted cost	10	62 300 \$	10	139 500 \$	10	155 300 \$
Total cost			350 650 \$		677 250 \$		807 350 \$

* % of the installed cost of process equip in areas A100, A200, A300, and A400.

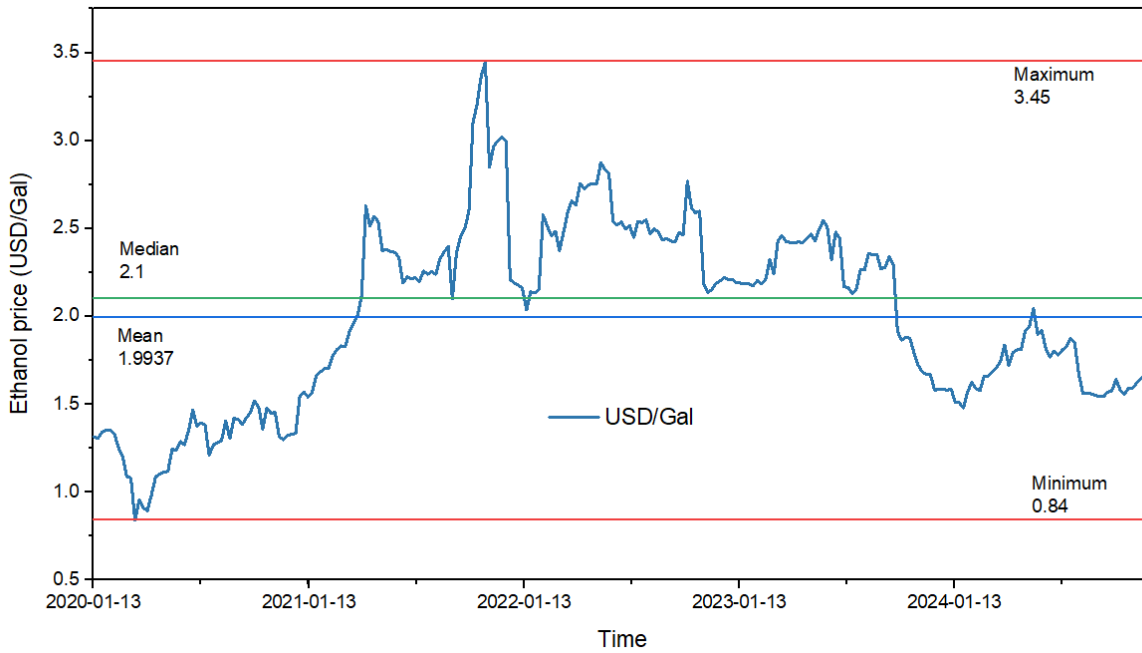


Figure 13.1 Ethanol price evolution over the past five year (Jan 2020 to Dec 2024) from (Economics, 2025).